MODELS TO STUDY MALARIA PARASITE-HOST CELL INTERACTIONS AND PATHOGENESIS

EDITED BY: Alister Craig, Andrea L. Conroy, Laurent Rénia and Maria Bernabeu

PUBLISHED IN: Frontiers in Cellular and Infection Microbiology

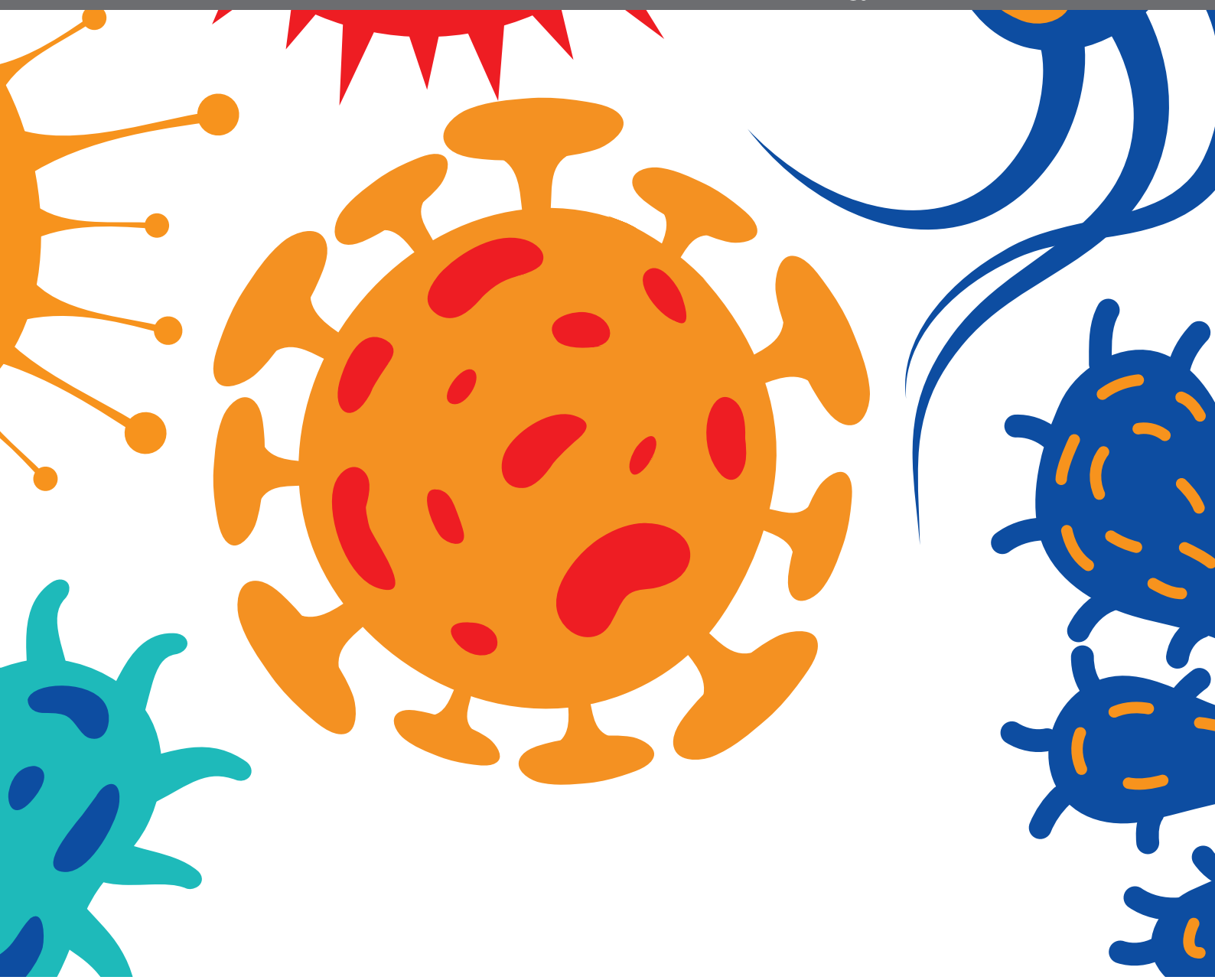

frontiers Research Topics

frontiers

ISSN 1664-8714
ISBN 978-2-83250-415-4
DOI 10.3389/978-2-83250-415-4

About Frontiers

Frontiers is more than just an open-access publisher of scholarly articles: it is a pioneering approach to the world of academia, radically improving the way scholarly research is managed. The grand vision of Frontiers is a world where all people have an equal opportunity to seek, share and generate knowledge. Frontiers provides immediate and permanent online open access to all its publications, but this alone is not enough to realize our grand goals.

Frontiers Journal Series

The Frontiers Journal Series is a multi-tier and interdisciplinary set of open-access, online journals, promising a paradigm shift from the current review, selection and dissemination processes in academic publishing. All Frontiers journals are driven by researchers for researchers; therefore, they constitute a service to the scholarly community. At the same time, the Frontiers Journal Series operates on a revolutionary invention, the tiered publishing system, initially addressing specific communities of scholars, and gradually climbing up to broader public understanding, thus serving the interests of the lay society, too.

Dedication to Quality

Each Frontiers article is a landmark of the highest quality, thanks to genuinely collaborative interactions between authors and review editors, who include some of the world's best academicians. Research must be certified by peers before entering a stream of knowledge that may eventually reach the public - and shape society; therefore, Frontiers only applies the most rigorous and unbiased reviews.
Frontiers revolutionizes research publishing by freely delivering the most outstanding research, evaluated with no bias from both the academic and social point of view. By applying the most advanced information technologies, Frontiers is catapulting scholarly publishing into a new generation.

What are Frontiers Research Topics?

Frontiers Research Topics are very popular trademarks of the Frontiers Journals Series: they are collections of at least ten articles, all centered on a particular subject. With their unique mix of varied contributions from Original Research to Review Articles, Frontiers Research Topics unify the most influential researchers, the latest key findings and historical advances in a hot research area! Find out more on how to host your own Frontiers Research Topic or contribute to one as an author by contacting the Frontiers Editorial Office: frontiersin.org/about/contact

MODELS TO STUDY MALARIA PARASITE-HOST CELL INTERACTIONS AND PATHOGENESIS

Topic Editors:
Alister Craig, Liverpool School of Tropical Medicine, United Kingdom
Andrea L. Conroy, Indiana University, United States
Laurent Rénia, Nanyang Technological University, Singapore
Maria Bernabeu, European Molecular Biology Laboratory, Spain

Citation: Craig, A., Conroy, A. L., Rénia, L., Bernabeu, M., eds. (2022). Models to Study Malaria Parasite-Host Cell Interactions and Pathogenesis. Lausanne: Frontiers Media SA. doi: 10.3389/978-2-83250-415-4

Table of Contents

04 ***Editorial: Models to Study Malaria Parasite-Host Interactions and Pathogenesis***
Maria Bernabeu, Andrea L. Conroy, Alister G. Craig and Laurent Renia

07 ***Harnessing the Potential of miRNAs in Malaria Diagnostic and Prevention***
Himanshu Gupta and Samuel C. Wassmer

20 ***Elucidating Spatially-Resolved Changes in Host Signaling During* Plasmodium *Liver-Stage Infection***
Elizabeth K. K. Glennon, Tinotenda Tongogara, Veronica I. Primavera, Sophia M. Reeder, Ling Wei and Alexis Kaushansky

32 **Plasmodium falciparum *Parasite Lines Expressing DC8 and Group A PfEMP1 Bind to Brain, Intestinal, and Kidney Endothelial Cells***
Luana S. Ortolan, Marion Avril, Jun Xue, Karl B. Seydel, Ying Zheng and Joseph D. Smith

42 ***Malaria Related Neurocognitive Deficits and Behavioral Alterations***
Pamela Rosa-Gonçalves, Flávia Lima Ribeiro-Gomes and Cláudio Tadeu Daniel-Ribeiro

51 ***Experimental Models to Study the Pathogenesis of Malaria-Associated Acute Respiratory Distress Syndrome***
Samantha Yee Teng Nguee, José Wandilson Barboza Duarte Júnior, Sabrina Epiphanio, Laurent Rénia and Carla Claser

74 ***Uncovering a Cryptic Site of Malaria Pathogenesis: Models to Study Interactions Between* Plasmodium *and the Bone Marrow***
Tamar P. Feldman and Elizabeth S. Egan

84 ***Differential Trafficking and Expression of PIR Proteins in Acute and Chronic* Plasmodium *Infections***
Maria Giorgalli, Deirdre A. Cunningham, Malgorzata Broncel, Aaron Sait, Thomas E. Harrison, Caroline Hosking, Audrey Vandomme, Sarah I. Amis, Ana Antonello, Lauren Sullivan, Faith Uwadiae, Laura Torella, Matthew K. Higgins and Jean Langhorne

105 **Plasmodium knowlesi *Cytoadhesion Involves SICA Variant Proteins***
Mariko S. Peterson, Chester J. Joyner, Stacey A. Lapp, Jessica A. Brady, Jennifer S. Wood, Monica Cabrera-Mora, Celia L. Saney, Luis L. Fonseca, Wayne T. Cheng, Jianlin Jiang, Stephanie R. Soderberg, Mustafa V. Nural, Allison Hankus, Deepa Machiah, Ebru Karpuzoglu, Jeremy D. DeBarry, MaHPIC-Consortium, Rabindra Tirouvanziam, Jessica C. Kissinger, Alberto Moreno, Sanjeev Gumber, Eberhard O. Voit, Juan B. Gutierrez, Regina Joice Cordy and Mary R. Galinski

123 **Plasmodium *6-Cysteine Proteins: Functional Diversity, Transmission-Blocking Antibodies and Structural Scaffolds***
Frankie M. T. Lyons, Mikha Gabriela, Wai-Hong Tham and Melanie H. Dietrich

143 ***Experimental Malaria-Associated Acute Kidney Injury is Independent of Parasite Sequestration and Resolves Upon Antimalarial Treatment***
Hendrik Possemiers, Emilie Pollenus, Fran Prenen, Sofie Knoops, Priyanka Koshy and Philippe E. Van den Steen

frontiers | Frontiers in Cellular and Infection Microbiology

TYPE Editorial
PUBLISHED 22 September 2022
DOI 10.3389/fcimb.2022.1039887

OPEN ACCESS

EDITED AND REVIEWED BY
Jeroen P. J. Saeij,
University of California, Davis,
United States

*CORRESPONDENCE
Alister G Craig
alister.craig@lstmed.ac.uk

SPECIALTY SECTION
This article was submitted to Parasite and Host, a section of the journal Frontiers in Cellular and Infection Microbiology

RECEIVED 08 September 2022
ACCEPTED 14 September 2022
PUBLISHED 22 September 2022

CITATION
Bernabeu M, Conroy AL, Craig AG and Renia L (2022) Editorial: Models to study malaria parasite-host interactions and pathogenesis. *Front. Cell. Infect. Microbiol.* 12:1039887.
doi: 10.3389/fcimb.2022.1039887

Editorial: Models to study malaria parasite-host interactions and pathogenesis

Maria Bernabeu[1], Andrea L. Conroy[2], Alister G. Craig[3]* and Laurent Renia[4]

[1]European Molecular Biology Laboratory (EMBL) Barcelona, Barcelona, Spain, [2]Ryan White Center for Paediatric Infectious Diseases and Global Health, Indiana University School of Medicine, Indianapolis, IN, United States, [3]Liverpool School of Tropical Medicine, Liverpool, United Kingdom, [4]Lee Kong Chian School of Medicine, Nanyang Technological University, Singapore, Singapore

KEYWORDS

malaria, model, pathogenesis, host - pathogen interactions, parasite biology

Editorial on the Research Topic

Models to study malaria parasite-host cell interactions and pathogenesis

In 1976 George Box, a British statistician, wrote "All models are wrong, some are useful" and malaria models are no exception. At times passions have run high over the rightfulness or otherwise of these models (Craig et al., 2012), but our ability to translate basic knowledge into mechanistic insights into malaria pathology depends to a large extent on models. The pathologies of malaria disease, in particular severe, life-threatening clinical syndromes are defined by the nature of the combination of the invading pathogen and the host environment that the pathogen encounters and subsequently modifies. Key areas that have been identified that influence disease processes include immunity, inflammation and cytoadherence, all of which can be represented to varying extents using existing models.

Indeed, our knowledge of the biology of the malaria parasite *Plasmodium* spp. has increased dramatically since the early 1970s through improvements in molecular and cellular biology technology and the use of models. However, translating this knowledge into an understanding of malaria pathology has been more of a challenge, not least because of the need to include the context of the host-parasite relationship in these studies. This Research Topic contains papers showing how models can be used to elucidate the complex relationships between host and parasite and to dissect the molecular mechanisms that underpin these processes.

Taken together, the Research Topic highlights several considerations of models:

Accessing the specific parasite-host material

Sourcing appropriate material from human infection is quite often impractical, and especially difficult is the obtention of tissue samples. Thus, Gupta and Wassmer review the use of miRNA as biomarkers of infection, host-pathogen interactions or severe disease. Other papers within this topic use animal and *in vitro* models as an alternative. Lyons et al used *in vitro* expression systems to produce proteins for functional and structural investigations, as well as generating antibodies as tools for research. Giorgalli et al. needed parasites from multiple stages of the rodent malaria parasites, *P. chabaudi chabaudi* to understand the complex expression patterns of PIR proteins throughout its lifecycle, and Glennon et al. faced a common issue of being able to focus on specific regions of interest of a tissue to remove the 'noise' from large areas of uninvolved cells, in this case to look at only the infected hepatocytes to understand the role of signalling in infection.

Matching the model to the study

One criticism of malaria models was that the model had become the whole story, rather than a tool to understand human disease (White et al., 2010). It does not seem unreasonable to investigate the fascinating biology of parasites in their hosts, however, if this research is done to understand human disease, then validating the model (or hypothesis generated) through comparison with clinical data is warranted. The most effective experimental animal models reproduce clinical findings to answer critical questions about disease pathogenesis. Comparison of clinical features is a good starting point, as seen with Possemiers et al. and their work on malaria-induced acute kidney injury. However, this can be taken further through an even deeper analysis of wider features of different models and their relationship to different aspects of human disease. Nguee et al. demonstrate this approach well in their review on models for acute respiratory syndrome, as does the work described by Rosa-Gonçalves et al, which through careful phenotypic evaluation, allows the complex clinical phenotype of neurocognitive deficits to be investigated.

Models can be simple or very complicated

Some models for research can be relatively simple, such as the primary human endothelial cells used by Ortolan et al. to show that specific PfEMP1 types can mediate cytoadherence to a range of tissues, which may indicate how multi-organ involvement takes place in severe malaria. However, even within cytoadherence research, the complexity of the model can step up significantly, such as the use of non-human primates (NHP) in revealing the role of SICA in *Plasmodium knowlesi* in mediating binding (Peterson et al). Recent advances in tissue engineering are increasing the complexity of *in vitro* models, including the development of 3D-microfluidic devices (Bernabeu et al., 2021) and organoids (Adams and Jensen, 2022), or stem cell approaches. For example, the extensive work done in developing cellular and *in vivo* models of erythropoiesis that have been adapted for malaria research on the effect of infection on anaemia and the behaviour of gametocytes in the bone marrow (Feldman and Egan). One of the issues of complicated models, either due to challenges in maintaining NHP appropriately or through the sheer complexity of the platform, is how to promote access across the research community.

The papers in this Research Topic show very clearly how the models that they employ can be used effectively to increase our knowledge about the biology of the host-parasite relationship and the pathology of disease. As we think about how to advance models to delineate pathways of disease in malaria, several themes emerge. First, there needs to be industry and government support so that scientists are able to establish, improve or modify existing models to adapt to the changing epidemiology of malaria and address changing research priorities. Models should be guided by clinical relevance and adapted to technology advancements and the needs of the research community over time. Partnerships should be guided by an ethical framework that supports and listens to the research priorities of scientists working in malaria endemic areas—and communities affected by malaria (Morton et al., 2022). Finally, there is a need for increased access to data sharing, common protocols, training platforms and open access publications to facilitate equitable access to the science.

Key issues

Models are really useful – they can elucidate complex biology, reveal the key pathological events in severe disease and down-select or validate potential therapies. So, what are some of the issues for the future?

- Supporting the development of refined or new models is important, but often not seen as innovative or moving the field forward. Supporting the development of new and better models needs investment and recognition.
- How do we support researchers who do not have access to clinical research sites so that they can test the hypotheses generated in their model systems? How do we make these partnerships equitable, including the development of the initial research questions?
- Having a variety of models can be useful but makes harmonisation of studies challenging. Can standardised models be implemented without stifling innovation and by sharing investment and access?

Author contributions

All authors acted as editors for manuscripts submitted for the Research Topic and contributed to the writing and revision of this editorial.

Acknowledgments

We would like to thank the authors who contributed their manuscripts to this Research Topic and who continue to support models in their research.

Conflict of interest

The authors declare that the research was conducted in the absence of any commercial or financial relationships that could be construed as a potential conflict of interest.

Publisher's note

All claims expressed in this article are solely those of the authors and do not necessarily represent those of their affiliated organizations, or those of the publisher, the editors and the reviewers. Any product that may be evaluated in this article, or claim that may be made by its manufacturer, is not guaranteed or endorsed by the publisher.

References

Adams, Y., and Jensen, A. R. (2022). Cerebral malaria - modelling interactions at the blood-brain barrier in vitro. *Dis. Model. Mech.* 15(7):dmm049410. doi: 10.1242/dmm.049410

Bernabeu, M., Howard, C., Zheng, Y., and Smith, J. D. (2021). Bioengineered 3D microvessels for investigating plasmodium falciparum pathogenesis. *Trends Parasitol.* 37, 401–413. doi: 10.1016/j.pt.2020.12.008

Craig, A. G., Grau, G. E., Janse, C., Kazura, J. W., Milner, D., Barnwell, J. W., et al. (2012). The role of animal models for research on severe malaria. *PloS Pathog.* 8, e1002401. doi: 10.1371/journal.ppat.1002401

Morton, B., Vercueil, A., Masekela, R., Heinz, E., Reimer, L., Saleh, S., et al. (2022). Consensus statement on measures to promote equitable authorship in the publication of research from international partnerships. *Anaesthesia* 77, 264–276. doi: 10.1111/anae.15597

White, N. J., Turner, G. D., Medana, I. M., Dondorp, A. M., and Day, N. P. (2010). The murine cerebral malaria phenomenon. *Trends Parasitol.* 26, 11–15. doi: 10.1016/j.pt.2009.10.007

frontiers in Cellular and Infection Microbiology

REVIEW
published: 16 December 2021
doi: 10.3389/fcimb.2021.793954

Harnessing the Potential of miRNAs in Malaria Diagnostic and Prevention

Himanshu Gupta and Samuel C. Wassmer**

Department of Infection Biology, London School of Hygiene and Tropical Medicine, London, United Kingdom

Despite encouraging progress over the past decade, malaria remains a major global health challenge. Its severe form accounts for the majority of malaria-related deaths, and early diagnosis is key for a positive outcome. However, this is hindered by the non-specific symptoms caused by malaria, which often overlap with those of other viral, bacterial and parasitic infections. In addition, current tools are unable to detect the nature and degree of vital organ dysfunction associated with severe malaria, as complications develop silently until the effective treatment window is closed. It is therefore crucial to identify cheap and reliable early biomarkers of this wide-spectrum disease. microRNAs (miRNAs), a class of small non-coding RNAs, are rapidly released into the blood circulation upon physiological changes, including infection and organ damage. The present review details our current knowledge of miRNAs as biomarkers of specific organ dysfunction in patients with malaria, and both promising candidates identified by pre-clinical models and important knowledge gaps are highlighted for future evaluation in humans. miRNAs associated with infected vectors are also described, with a view to expandind this rapidly growing field of research to malaria transmission and surveillance.

Keywords: miRNAs, malaria, *Plasmodium*, *Anopheles*, biomarkers, diagnosis

OPEN ACCESS

Edited by:
Alister Craig,
Liverpool School of Tropical Medicine, United Kingdom

Reviewed by:
Catherine A. Gordon,
The University of Queensland, Australia
Paulo J. G. Bettencourt,
Catholic University of Portugal, Portugal

***Correspondence:**
Himanshu Gupta
himanshu.gupta@lshtm.ac.uk
Samuel C. Wassmer
sam.wassmer@lshtm.ac.uk

Specialty section:
This article was submitted to Parasite and Host, a section of the journal Frontiers in Cellular and Infection Microbiology

Received: *12 October 2021*
Accepted: *09 November 2021*
Published: *16 December 2021*

Citation:
Gupta H and Wassmer SC (2021) Harnessing the Potential of miRNAs in Malaria Diagnostic and Prevention. Front. Cell. Infect. Microbiol. 11:793954. doi: 10.3389/fcimb.2021.793954

HIGHLIGHTS

- miRNAs have recently emerged as essential regulators of immunity against *Plasmodium* parasites both in mosquito vectors and human hosts
- Specific miRNAs have been associated with severe malaria and its associated life-threatening complications
- miRNAs present promising diagnostic/prognostic biomarkers of malaria disease and may also be targeted by therapeutic interventions

INTRODUCTION

Despite encouraging control progress over the past decade, malaria remains a major global health challenge. 409,000 malaria-associated deaths were reported in 2019, and 94% of these occurred in Africa (WHO, 2020). In addition to endemic countries, fatal cases are also reported in other parts of the world due to increasing imported infections (Zoller et al., 2009; Mischlinger et al., 2020). Malaria can be caused by several *Plasmodium* species in humans, including *Plasmodium falciparum* (*Pf*), *P. vivax* (*Pv*), *P. knowlesi* (*Pk*), *P. ovale* (*Po*), and *P. malariae* (*Pm*) (Garcia, 2010). Among these,

Pf and *Pv* are responsible for majority of cases worldwide (WHO, 2020), and *Pf* is considered the most lethal of the human malaria parasites. *Pf* cases can be classified into severe and uncomplicated malaria based on the World Health Organization (WHO) criteria (WHO, 2014). Severe *falciparum* malaria is characterized by multi-organ dysfunctions, which are triggered by the sequestration of infected erythrocytes (iEs) within the microvasculature of the host, combined with an exaggerated production of inflammatory mediators (White et al., 2013; Milner et al., 2014). In contrast, *Pv* infection has been perceived as relatively benign until recently, despite documented debilitating and potentially life-threatening complications (Gupta et al., 2015a; Gupta et al., 2016a; Anvikar et al., 2020). Severe malaria (SM) cases have also been reported in patients infected with *Pk* (Cox-Singh et al., 2010), *Po* (Kotepui et al., 2020a), and *Pm* (Kotepui et al., 2020b), although these remain anecdotal. There are distinct biochemical and morphological features across the different *Plasmodium* species, but the mechanisms underlying the development of SM are likely to be similar. They all involve inflammation caused by the release of *Plasmodium*-derived components (known as pathogen-associated molecular patterns), as well as host-derived components (or damage-associated molecular patterns) and sequestration of iEs in some specific species (Gazzinelli et al., 2014). *Plasmodium* spp. are transmitted by female *Anopheles* mosquitoes, which inject sporozoites into the subcutaneous tissue of the human host during their blood meal, triggering the host phase of the cycle (White, 2017).

The fundamental pathogenesis of SM is still poorly understood and treatments are currently precariously limited to antimalarial drugs and emergency supportive care (White et al., 2014). An early diagnosis is key for prompt and accurate treatment, resulting in positive outcomes. Unfortunately, this scenario remains rare as SM still have a fatality rate of 15-30% when patients are appropriately treated upon admission (Lucchi et al., 2011). The reasons are manifold and include *i)* late presentation to the hospital (the damage is already done); *ii*) generic symptoms such as a fever that overlaps with the presentation of viral, bacterial and parasitic infections (the infection is missed) (Rubio et al., 2016); and *iii*) out-of-criteria patients with laboratory parameters just below or above the hard WHO cut-offs for disease severity at the time of admission (the disease severity is increasing but unnoticed). For the latter category, patients treated for uncomplicated malaria (UM) have been reported to be ill enough to warrant hospitalization (Sahu et al., 2020), and could then progress to develop life-threatening SM. This suggests that complications may develop silently until it is too late (the damage is already done). A parallel study showed that UM patients with delayed treatment are highly likely to develop SM (Mousa et al., 2020). In view of these challenges, it is crucial to identify new biomarkers of early SM that can be then developed into cheap, reliable diagnostic and/or prognostic tools for clinicians to identify patients at risk.

microRNAs (miRNAs), a class of small non-coding RNAs (18-24 nt length), are rapidly released into the blood circulation upon physiological changes, including infection and organ damage (Cortez et al., 2011). They regulate gene expression endogenously at the post-transcriptional level, either through translation repression or mRNA degradation (Cortez et al., 2011). miRNAs can be secreted extracellularly as bound to lipoproteins or within cell-derived extracellular vesicles (Valadi et al., 2007; Arroyo et al., 2011; Nik Mohamed Kamal NNSB and Shahidan WNS 2020). These small molecules are highly stable and can be detected in a wide range of biological fluids, making them exceptionally promising non-invasive biomarkers (Rubio et al., 2016). Indeed, they can be potentially used to not only detect an infection, but also diagnose early-stage tissue or organ damage. This would represent a significant advantage over the standard methods currently being used to diagnose malaria, such as microscopic examination of blood smears (Fleischer, 2004), plasma antigen detection (Spencer et al., 1979), rapid diagnostic test (Moody and Chiodini, 2002) and molecular conventional and quantitative PCR assays (Snounou et al., 1993; Gupta et al., 2016b).

For these reasons, researchers using *in vitro* and mice models, as well as clinical samples have attempted to identify miRNA-based biomarkers of malarial disease in the last decade, with the hope to develop new diagnostic and prognostic tools. Remarkably, several miRNAs have also been discovered in *Pf*-infected Anopheles mosquitoes. Thus, specific profiles of miRNAs associated with different phases of the malaria life cycle have the potential to help control and elimination efforts by allowing the identification of *(i)* carrier mosquitoes, *(ii)* infected patients, symptomatic or not, and *(iii)* potential tailored treatment for the former category. The present review covers our current knowledge of miRNAs described across the malaria parasite life cycle, including both vector and host. Their potential as biomarkers of acute and chronic pathologies associated with malaria disease is discussed, as well as future research recommendations for this promising and rapidly growing field of research.

BUZZING AROUND: THE VECTOR PHASE

To complete the malaria parasite life cycle, gametocytes are ingested by female Anopheles mosquitoes from the blood of infected human hosts. Parasites then invade mosquito midgut, thereby eliciting a physiological response leading to variations in the expression and release of various miRNA. Studies of infected anopheline mosquitoes have identified several miRNAs (**Figure 1a**) that may alter mosquito immunity against *Plasmodium* infection. These miRNAs also have important roles in the development and maturation of the parasite within their vectors, and distinct expression patterns of miRNAs in specific tissues have been described (Winter et al., 2007; Mead and Tu, 2008; Jain et al., 2014; Dennison et al., 2015; Lampe et al., 2019; Dong et al., 2020). One study reported a reduction in the expression of aga-miR-34, aga-miR-1174 and aga-miR-1175 miRNAs in the midgut of *P. berghei*-infected *Anopheles gambiae* compared controls. In contrast, aga-miR-989 levels were significantly increased in the presence of the murine

malaria parasite *P. berghei*. aga-miR-989 levels decreased significantly in the rest of the body, suggesting the specificity of aga-miR-989 to the midgut of infected *Anopheles gambiae*. Additionally, knocking down Dicer1 and Ago1 mRNAs enhanced the vector's sensitivity to *Plasmodium* infection (Winter et al., 2007). Another study identified a series of differentially expressed *Anopheles gambiae* miRNAs induced by normal blood meal (miR-7, miR-92a, miR-317, and miR-N3) and infectious blood meal (miR-N3, miR-317, miR-2940, miR-N5, miR-N6 and miR-N4) (Biryukova et al., 2014). Similarly, elevated levels of aga-miR-989 and aga-miR-305 miRNAs were found in *Pf*-infected mosquito midgut tissue compared to naïve ones (**Figure 1a**). Furthermore, aga-miR-305 inhibition increased resistance to *Pf* infection (Dennison et al., 2015). Remarkably, bloodmeals have been shown to induce miR-276-5p levels in mosquito, which regulate the expression of branched-chain amino acid transferase to terminate the reproductive cycle. Inhibition of miR-276 elongated high rates of amino acid (AA) catabolism and increased female mosquito fertility, suggesting that timely termination of AA catabolism restricts both mosquito investment into reproduction and development of the transmissible sporozoite forms (Lampe et al., 2019). miRNAs (aga-miR-8, aga-miR-14, and aga-miR-305) were found to regulate mosquito immunity against parasite infection. Depletion of aga-miR-14 or aga-miR-305, but not aga-miR-8, increased mosquito resistance to both *P. berghei* and *Pf* infection by enhancing the expression of multiple immunity-related and anti-*Plasmodium* genes. This indicates a potential role for mosquito miRNAs in the development of malaria control through genetically engineered vectors (Dong et al., 2020). miRNA profiling revealed distinct expression patterns of miRNAs from early embryo to adult stages in *Anopheles stephensi*. miR-x2 was found associated with female reproduction, and constant miR-14 expression was indicative of its importance across all mosquito life stages (Mead and Tu, 2008). By applying next-generation sequencing (NGS) technology to whole vectors, differentially expressed miRNAs were reported post blood feeding (13 miRNAs) and parasite infection (16 miRNAs) in *Anopheles stephensi*. A set of miRNAs showed significant expression changes between 42h (midgut invasion) and 5 days (sporozoites release) post-infection, highlighting a stage-specific parasite influence on vector miRNAs. These miRNAs are known to target genes involved in several metabolic pathways including metabolic, redox homeostasis and protein processing machinery components. Specific miRNAs (miR-124, 305, and 309; **Figure 1a**) regulate multiple immune pathway genes (Jain et al., 2014). aan-miR-92a and aan-miR-275 levels were found upregulated and downregulated in blood-feeding and *Plasmodium* infection (**Figure 1a**), respectively, in the midgut of *Anopheles anthropophagus* compared to sugar-feeding mosquitoes (Liu et al., 2017). Collectively, these findings suggest that the expression of mosquito miRNAs changes in response to *Plasmodium* infection, and could therefore be used in molecular assays such as RT-qPCR to screen and identify parasite-carrying vectors. This would be done by comparing

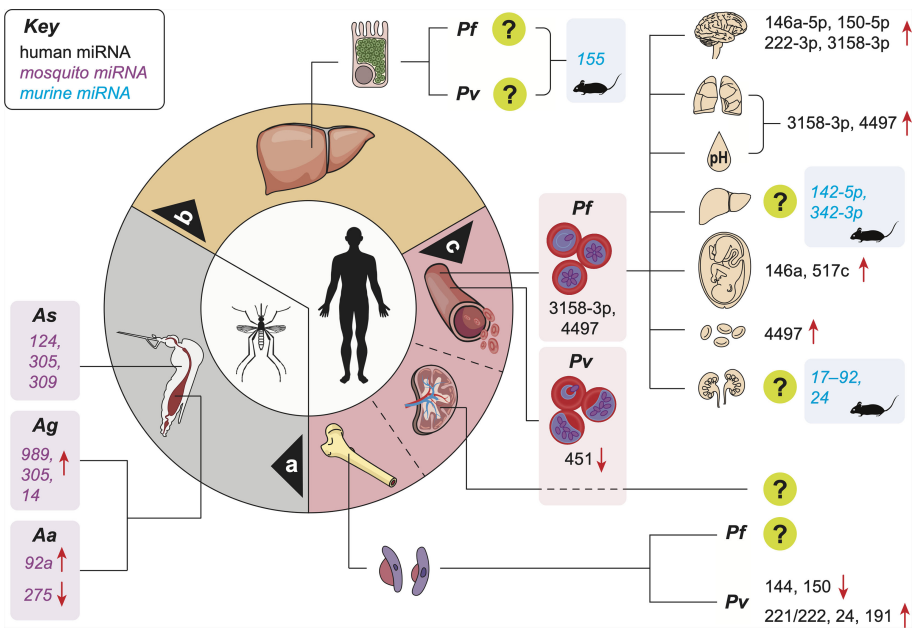

FIGURE 1 | Reported miRNA expression changes in the vector and host during malaria infection. miRNA level changes in the midgut of infected mosquitoes **a**; in animal models of the infection during the silent hepatic phase **b**; and in patients during the symptomatic erythrocytic phase **c**. Organ and metabolic dysfunctions represented in the upper right quadrant are, from top to bottom: brain (cerebral malaria), lungs (ARDS), acidosis (hyperlactatemia), liver (jaundice), placenta (PAM), decreased red blood cell count (anemia), kidneys (AKI). [upregulation (↑); downregulation (↓);?: human miRNAs not identified; *Pf*, *Plasmodium falciparum*; *Pv*, *Plasmodium vivax*; *Aa*, *Anopheles anthropophagus*; *Ag*, *Anopheles gambiae*; *As*, *Anopheles stephensi*].

their miRNA levels against a baseline from uninfected vectors of the same species. In turn, such approach could help estimating metrics of exposure and transmission intensity (Tusting et al., 2014). Epidemiological and ecological studies of malaria traditionally utilize detection of *Plasmodium* sporozoites in whole mosquitoes or salivary glands by microscopy (Habluetzel et al., 1992), or serological (Wirtz et al., 1987) or molecular assays (Echeverry et al., 2017; Calzetta et al., 2018). However, these methods are time-consuming, require skill and expertise, are labour-intensive, and can over- or underestimate mosquito transmission potential (Ramirez et al., 2019). Thus, there is a need for new technologies to improve mosquito surveillance programmes, and miRNA-based assays could accurately detect infected mosquitoes in a short period of time, with the potential to inform decision-making in the fight against malaria.

HIDE: THE ASYMPTOMATIC PRE-ERYTHROCYTIC PHASE

Upon the bite of an infected vector, sporozoites located in its salivary glands are injected into the subcutaneous vasculature of the host. Once in the bloodstream, they travel to the liver and infect hepatocytes, initiating the silent phase of the infection, during which each sporozoite develops into hundreds of merozoites. This pre-erythrocytic phase cannot currently be identified in infected patients, but represent a pivotal window of opportunity for diagnostic and treatment, since transmission does not start until the erythrocytic stage is initiated. Identifying infected individuals at this stage could revolutionize the active surveillance programme and represent a powerful tool in malaria control. A study of the murine model of malaria infection using *P. berghei* parasites identified several miRNA candidates associated with this pre-erythrocytic phase. Indeed, murine infection with genetically attenuated parasites (GAPs) that arrest in the liver and induce sterile immunity leads to the upregulation of miR-155 levels in the liver (**Figure 1b**), particularly in non-parenchymal cells including liver-resident macrophages, or Kupffer cells (Hentzschel et al., 2014). Additional studies are warranted to investigate plasma miRNA profiles specifically associated with this phase, which could be used in RT-qPCR-based assays for the early identification of silent infections.

AND SEEK: THE SYMPTOMATIC ERYTHROCYTIC PHASE

After release from infected hepatocytes, merozoites invade erythrocytes and mature from ring stages to trophozoites, and ultimately, to schizonts (**Figure 1c**). The burst of iEs to release daughter merozoites results in exponential growth of the parasite population, and some of these merozoites develop into sexual forms, or gametocytes. The clinical symptoms of malaria are mainly attributed to the rupture of schizont stage-iEs and the subsequent release of parasite-derived toxins, which stimulate innate immune cells to produce cytokines and inflammatory mediators causing periodic episodes of febrile illness (Oakley et al., 2011; Gazzinelli et al., 2014). Circulating cytokines also induce the upregulation of adhesion molecules by endothelial cells which, in turn, increase parasite sequestration (Gazzinelli et al., 2014). This phenomenon is mediated by *Pf* erythrocyte membrane protein 1 (PfEMP1), a family of proteins present on the surface of iEs and encoded by approximately 60 *var* genes (Hviid and Jensen, 2015). PfEMP-1 can bind to several host receptors on the surface of capillary endothelium, uninfected erythrocytes, placental syncytiotrophoblasts, and platelets (Rowe et al., 2009; Turner et al., 2013; Wassmer et al., 2015). Such receptors include intercellular adhesion molecule-1 (ICAM-1), CD36, endothelial protein C receptor (EPCR), gC1qR, chondroitin sulfate A (CSA), or complement receptor 1 (Jensen et al., 2020). By binding to the vessel walls, mature forms of *Pf* remove themselves from the circulation, thereby avoiding clearance by the spleen (Cranston et al., 1984; Buffet et al., 2011). However, the local accumulation of iEs disrupts or completely abrogates the blood flow, promotes clotting, triggers endothelial cell and blood-brain barrier disruption, potentially leading to the extravasation of vascular content in the parenchymal tissue and increased local inflammation. These mechanisms have all been linked to SM (Gazzinelli et al., 2014).

Cell-cell interactions, as well as the immune response of the host are highly likely to influence the expression of miRNAs during malaria infection. Remarkably, only human miRNAs are found in *Pf*-iEs (Rathjen et al., 2006; Xue et al., 2008), and it has been reported that human erythrocytes miRNAs could translocate and integrate into the parasite messenger RNAs to block their translation (LaMonte et al., 2012). In particular, miR-451 and let-7i were found abundant in sickle erythrocytes, and together with miR-223, reduced parasite growth (LaMonte et al., 2012).

A study using controlled human *Pf*-infection in adults identified a profile of 84 miRNAs associated with T cell and B cell activation, indicating a pivotal role of miRNAs in inter-individual variability in the immune response to falciparum malaria. Volunteers with increased levels of miR-15a-5p, miR-30c-5p, and miR-30e-5p had a higher frequency of activated and proliferating T cells and could control their *Pf* parasitemia more effectively after infection (Burel et al., 2017).

Similarly, host genetics can regulate *Pf* infection (Gupta et al., 2013; Gupta et al., 2015b; Gupta et al., 2017a), and the protective effect of rs114136945 minor allele on parasitemia mediated through miR-598-3p expression was recently reported (Dieng et al., 2020). In a study carried out in Thailand, the downregulation of both miR-451 and miR-16 was reported in 19 malaria patients compared to healthy individuals (Chamnanchanunt et al., 2015). Subsequent work on a smaller number of participants found 8 differentially expressed miRNAs between *Pf* malaria patients and healthy controls (Bertrams et al., 2021).

Severe Malaria: Multi-Organ and Physiological Dysfunctions

Severe *Pf* malaria is characterised by the sequestration of iEs in the microvasculature of the host (Miller et al., 2002). Combined

with an exacerbated production of inflammatory mediators, this accumulation leads to the dysfunction of peripheral organs, either alone or in combination, leading to severe complications. These include acute respiratory distress syndrome, (ARDS, affecting the lungs), jaundice (liver), acute kidney injury (AKI, kidneys) or cerebral malaria (CM, brain) (White et al., 2013; Milner et al., 2014). The hard WHO cut-offs for these severe complications at the time of admission exclude patients with parameters just above or below the defined threshold. Thus, determining direct or indirect markers of early and still progressing organ dysfunction in the context of SM could revolutionize its clinical management. A recent, large-scale study using a combination of *in vitro* models and plasma samples from Mozambican children infected with *Pf* and diagnosed with SM or UM demonstrated for the first time the association between both hsa-miR-3158-3p and hsa-miR-4497 with SM, its complications, and *Pf* biomass (**Figure 1c**) (Gupta et al., 2021a). These findings suggest that although unable to produce miRNAs (Xue et al., 2008), *Plasmodium* may manipulate the production of host miRNAs. In turn, these changes in small molecule levels have the potential to not only shed light on the molecular mechanisms involved in the pathogenesis of SM, but also be used as signatures associated with individual complications. As SM is a broad spectrum disease, such miRNA signatures may help identify complications and tailor treatment approaches to increase survival.

Neurological Changes: Cerebral Malaria (CM)

CM is an acute neurological complication and often lethal form of SM. It has a fatality rate up to 30% in treated patients (Wassmer et al., 2015), and neurocognitive sequelae are frequent in survivors (WHO, 2014). CM cases are predominantly seen in African children under five, as the high malaria transmission intensity in sub-Saharan Africa leads to the development antimalarial immunity during childhood. However, in South East Asia, where malaria transmission is seasonal and not intense enough to induce robust immunity, CM cases are mainly found in older children and adults (Sahu et al., 2015). In addition, while CM is mainly accompanied by severe anemia and/or metabolic acidosis in African children, it is very often reported in combination with other organ involvement such as lungs, liver and kidneys leading to ARDS, jaundice and AKI, respectively in Asian adults (Wassmer et al., 2015). The mechanisms behind these distinct clinical features between African children and South East Asian adults is still poorly understood.

In addition, CM is challenging to diagnose using the tools currently available. An autopsy study in Malawi demonstrated that up to 23% of children clinically diagnosed with CM had, in fact, another cause of death based on post-mortem examination (Taylor et al., 2004). Further work reported that CM was indeed overly misdiagnosed when assessed by parasite load alone; 38% *versus* only 1% who truly fulfilled WHO criteria (Makani et al., 2003). Over the past decade, neuroimaging studies in endemic areas have improved our understanding of CM (Mohanty et al., 2014). Distinct age-dependent brain changes identified by magnetic resonance imaging (MRI) on admission were recently linked to poor outcomes. In pediatric CM, severe brain swelling with brain stem herniation was associated with fatality (Seydel et al., 2015), a feature not observed in fatal adult cases (Mohanty et al., 2011; Maude et al., 2014). Our team demonstrated that in the latter group, global cerebral hypoxic injury was associated with mortality (Sahu et al., 2020). While the early identification of such features may prove critical to inform clinical management and improve survival in patients at risk, access to MRI facilities remains extremely limited in malaria endemic countries due to operational, logistical and financial challenges (Latourette et al., 2011). In addition, the occurrence of specific pathogenic features in different age groups may be difficult to detect and differentiate in adolescents or young adults. Therefore, alternative biomarkers of brain changes identified by MRI and validated in both age groups would represent a powerful prognosis tool to identify patients at risk of developing fatal disease, inform clinical management, and decrease mortality in CM. In view of these challenges, miRNAs found associated with defined MRI features could be helpful in CM diagnosis.

miR-155 was found to be an important player in the CM pathogenesis *via* negative regulation of blood-brain-barrier integrity and T cell function (Barker et al., 2017). In addition to miR-155, murine studies have yielded a series of biomarker candidates for CM, including miR-19a-3p, miR-540-5p, miR-223-3p, miR-142-3p, miR-19b-3p, let-7i, miR-27a, miR-150, miR-146a, miR-193b, miR-205, miR-215 and miR-467a (El-Assaad et al., 2011; Cohen et al., 2018; Martin-Alonso et al., 2018). These miRNAs are significantly involved in several pathways relevant to CM, including TGF-β, inflammation, TNF signaling, monocyte sequestration in cerebral microvessels, endocytosis (El-Assaad et al., 2011; Cohen et al., 2018; Martin-Alonso et al., 2018). Among the miRNA candidates identified, miR-146a-5p and miR-150-5p were also associated with CM in Indian patients (Gupta et al., 2021b), together with miR-222-3p and miR-3158-3p (**Figure 1c**). Upon further analysis, high miR-150-5p and miR-3158-3p levels were associated with fatal CM. miR-3158-3p levels decreased significantly in CM survivors at day 30 post-treatment, strongly suggesting the CM specificity of this miRNA. Lastly, miR-3158-3p levels were found correlated with hypoxia in the brain of adults, and negatively correlated with increased brain volume of children, both identified by MRI (Gupta et al., 2021b). This indicates that the production of miR-3158-3p is decreased in CM patients with high brain volume on admission, a feature associated with a poor outcome in children (Seydel et al., 2015; Sahu et al., 2020). Inversely, miR-3158-3p levels increased in patients with high hypoxia on admission, a hallmark of fatal adult CM (Sahu et al., 2020). While further validation of the association between miR-3158-3p levels and MRI features of poor outcomes in CM is needed, our findings support the potential use of miR-3158-3p for CM prognosis in children and adults in lieu of neuroimaging (Gupta et al., 2021b).

Liver Dysfunction

Several studies using the murine model of *P. chabaudi* infection identified differentially expressed miRNAs in the liver of infected

animals (Delic et al., 2011; Al-Quraishy et al., 2012; Dkhil et al., 2016). An upregulation of three and a downregulation of 16 miRNAs was reported in the mouse liver following infection. Remarkably, miRNA expression pattern persisted in immune mice even after re-infection, suggesting that the development of a protective immunity against *P. chabaudi* infection may be regulated in part by miRNAs (Delic et al., 2011). Another study reported 169 miRNAs downregulated in liver tissue obtained from *P. chabaudi*-infected mice, while miR-142-5p and miR-342-3p were found upregulated (**Figure 1c**) (Al-Quraishy et al., 2012). Similarly, a downregulation of 18 and upregulation of 14 miRNAs were reported in the liver during the acute phase of *P. chabaudi* infection (Dkhil et al., 2016).

Placenta: Pregnancy-Associated Malaria (PAM)

Pregnancy-associated malaria (PAM) is defined by the sequestration of iEs in the placental intervillous spaces. This sequestration is mediated by binding of VAR2CSA (Salanti et al., 2003) to chondroitin sulfate A (CSA) expressed at the surface of the placental syncytiotrophoblast (Zakama et al.; Fried and Duffy, 1996), contributing to inflammatory infiltrates and reduced nutrient transfer to the fetus (Rogerson et al., 2018), ultimately causing adverse outcomes including low birth weight, preterm birth, stillbirth, and miscarriage (Nosten et al., 2004). In addition, women who are pregnant for the first time generally lack immunity to antigenic variant presented by *Pf* parasites that accumulate selectively in the placenta, which put them at a higher risk of infection compared to non-pregnant women (Brabin et al., 2004; Gamain et al., 2007). The risk of infection decreases in the second trimester compared to first trimester in primigravid women. The infection risk also decreases after successive pregnancies (Gamain et al., 2007). Similarly to other organ-specific dysfunctions induced by *Pf*, increased levels of miR-517c (**Figure 1c**), an immunomodulator in pregnancy and tumorigenesis (Bullerdiek and Flor, 2012), were reported in mothers with PAM when compared to non-infected controls (Moro et al., 2016). miR-146a rs2910164 polymorphism was found to increases the odds of PAM occurrence in primigravid Ghanaian women, suggesting a role for miR-146a in this complication (van Loon et al., 2019). The authors of the study suggested that miR-146a is involved in protective malarial immunity, particularly its innate component.

Other Organ and Physiological Dysfunctions

A limited number of studies have been carried out to identify miRNAs associated with SM complications and organ dysfunction such as acidosis, severe anemia, ARDS, or AKI. Higher levels of miR-3158–3p were measured in Mozambican children who had acidosis or ARDS compared to UM children. In contrast, miR-4497 was associated with severe anemia and ARDS (**Figure 1c**) (Gupta et al., 2021a). A review suggested that miR-210; miR-125b and miR-181b; as well as miR 17–92 and miR-24 could be promising miRNA-based biomarkers of acidosis, ARDS and renal failure, respectively (**Figure 1c**) (Chamnanchanunt et al., 2017). However, miR-210-3p was not found associated with SM in a recent study conducted in India (Gupta et al., 2021b). Because this is still an emerging field, the data on biomarkers of malaria-associated organ dysfunction and severe complications remain limited. The resultant knowledge gap needs to be addressed to identify miRNAs associated with ARDS, AKI, acidosis and SA (**Figure 1c**). In turn, these tools will help researchers and clinicians to *i)* increase the granularity of the SM diagnosis and *ii)* determine pathogenetic pathways and potential therapeutic targets in SM (Wassmer et al., 2015). It is also noteworthy that grouping patients with single distinct SM complications is challenging. Indeed, acidosis, for example, is caused by the host anaerobic glycolysis due to tissue hypoxia following iE sequestration (Rubio et al., 2016) and develop in combination with other complications in most patients. Therefore, global or combination profiling may be an easier approach than identifying the profiles of miRNAs associated with specific dysfunction.

Thrombocytopenia is common in malaria (Lacerda et al., 2011; Anvikar et al., 2020) and has been associated with SM (Anvikar et al., 2020). The miRNA pair miR-4454/miR-7975 was found associated with low platelet counts (Santos et al., 2021). In addition, the roles of extracellular vesicles (EVs), small membrane-bound vesicles that can be classified based on their size, origin, and functions (EL Andaloussi et al., 2013), have recently emerged in the different stages of malaria life cycle, as well as in the pathogenesis of SM (Babatunde et al., 2020; Cheng et al., 2020). A high number of EVs can be found during pathological conditions (Combes et al., 2004; Nantakomol et al., 2011), and they can act as immunomodulators during *Plasmodium* infection either directly (Mantel and Marti, 2014) or *via* their miRNA cargo (Mantel et al., 2016; Wang et al., 2017). Indeed, EV contain miRNAs with regulatory functions, and those are protected from degradation by RNases (Cheng et al., 2014; Vojtech et al., 2014). A study reported that EV-derived miR-150-5p, miR-15b-5p and let-7a-5p were significantly up regulated in malaria patients compared to healthy individuals (Ketprasit et al., 2020). let-7a-5p miRNA was associated with falciparum malaria (Ketprasit et al., 2020), and miR-150-5p, miR-15b-5p and let-7a-5p with *Pv* infection (Ketprasit et al., 2020).

Chronic Malaria

In high transmission settings, intense exposure to malaria drives the development of anti-disease immunity, whereby individuals control their immune response to infection, ultimately resulting in asymptomatic malaria (AM) (Kimenyi et al., 2019). By definition, it is characterised by the lack of apparent clinical symptoms, and infected individuals do not seek treatment. They are missed by passive surveillance while remaining an important gametocytes reservoir, and such infections contribute to the persistence of malaria transmission (Galatas et al., 2016; Andolina et al., 2021). AM has been perceived as relatively benign until a study demonstrated that it was associated with recurrent episodes of symptomatic parasitemia, chronic anemia, maternal and neonatal mortality, co-infection with invasive bacterial disease, cognitive impairment, and continuous transmission (Chen et al., 2016). The authors proposed to rename the misleading AM to chronic malaria (Chen et al., 2016).

As a large proportion of AM infections are associated with low-density parasitemia, these individuals are also likely to be missed by conventional tests such as microscopy and rapid diagnostic tests, which have limited detection sensitivity (Okell et al., 2012; Bousema et al., 2014). New approaches are therefore needed for large scale populations screening. miR-3158-3p and miR-4497 were found associated with parasite biomass (Gupta et al., 2021a) so it could be postulated that these miRNAs are promising candidate to identify sub-patent infections. However, further investigations are warranted to determine the parasitemia detection threshold afforded by these miRNAs.

In a similar way, *Pv* has also been assumed to be unharmful due to relatively low parasitemia levels and high proportions of AM cases. However, evidence is mounting that vivax malaria is debilitating and potentially causes life-threatening complications similar to the ones reported in *Pf* infection (Gupta et al., 2015a; Gupta et al., 2016a; Anvikar et al., 2020). miR-451 and miR-16 levels were reported downregulated in *Pv* patients compared to controls (**Figure 1c**) (Chamnanchanunt et al., 2015). The miRNA pair miR-4454/miR-7975 was upregulated while miR-520f-3p, miR-150-5p and let-7b-5p were down regulated in patients with *Pv* infection (Santos et al., 2021). The miR-150-5p association with *Pv* infection has not been consistent in Thai and Brazilian populations (Ketprasit et al., 2020; Santos et al., 2021), suggesting the need for further validation. Another study found miR-7977, miR-28-3p, miR-378-5p, miR-194-5p and miR-3667-5p associated with *Pv* infection, and the authors postulated that miR-7977 exacerbated its pathology *via* the UBA52 or TGF-beta signalling pathways (Kaur et al., 2018). These results suggest that host miRNA levels are also influenced by the presence of *Pv* infection, which opens new avenues to identify miRNA-based biomarkers that can not only differentiate between malaria patients from healthy individuals but could also identify different *Plasmodium* species. To the best of our knowledge, this research field remains limited and only miR-451 levels were found differentially expressed between patients infected with *Pf* (n=3) and *Pv* (n=16) (Chamnanchanunt et al., 2015). However, the sample size for this comparison was small. Combined *Plasmodium* species-specific miRNA-based biomarkers could play an important in the context of malaria elimination programs to detect multi-species infections. Currently, these programs are mainly focusing on *Pf*, which can lead to the rise of other *Plasmodium* species.

Recent work demonstrated for the first time a large parasite biomass in the spleen of AM individuals compared to the peripheral circulation, which is likely to contribute to anemia (Kho et al., 2021a; Kho et al., 2021b). Both reticulocytes and asexual *Pv* parasites were observed in the splenic tissue, suggesting that the measure of the peripheral parasitemia alone vastly underestimates the *Pv* biomass in AM (Kho et al., 2021a). miR-4497 may play an important role in detecting hidden splenic parasites in AM individuals, as it was found associated with parasite biomass and SA (Gupta et al., 2021a). In addition, another study reported the downregulation of 25 miRNAs in the spleen obtained from mice infected with *P. chabaudi* (Al-Quraishy et al., 2012). However, additional validation work is needed to identify miRNA-based biomarkers with a potential to detect splenic parasites in individuals with AM. This approach will be crucial to identify and treat such cases in order to interrupt malaria transmission.

A hallmark of *Pv* is its ability to form dormant liver stages, or hypnozoites. These can reactivate, causing recurrent episodes of malaria (Dayananda et al., 2018). However, frequent episodes do not allow patients to recover from hematological damage, leading to severe anemia (Tjitra et al., 2008). Because current diagnostic tools cannot detect hypnozoites, a 14-day course of primaquine is recommended by the WHO for all patients who are not deficient in the glucose-6-phosphate dehydrogenase (G6PD) enzyme (WHO, 2015). In view of the challenges associated with the wide implementation of a long treatment course and practical pretreatment testing to identify G6PD-deficient individuals at risk of severe hemolysis (Baird et al., 2016), a screening tool to detect these hypnozoites may be key to reduce these bottlenecks. miRNA-based assays could fill this gap and support current elimination efforts.

Overall, miRNAs found associated with the symptomatic phase of the malaria life cycle in different studies, specifically miR-146a-5p, miR-150-5p, miR-3158-3p and miR-4497 have the potential to develop diagnostic and prognostic tools to identify malaria patients, organ dysfunction, and patients at the risk of developing SM associated life-threating complications, inform their clinical management, and decrease SM associated mortality.

READY FOR TAKE OFF: GAMETOCYTES

Gametocytes are sexual forms of the malaria parasite, which enable the establishment of infection in mosquitoes from its mammalian host, a crucial step in malaria transmission (Bousema and Drakeley, 2011). Similarly to mature asexual parasites in iEs, it has been postulated that immature gametocytes are "sequestered" away from the peripheral blood and the host immune cells. This process would ensure their safe maturation before they are released into the circulation (Bousema and Drakeley, 2011). Indeed, a high prevalence and abundance of early *Pf* sexual stages was identified in the bone marrow (BM), which was linked to both dyserythropoiesis and severe anemia (Aguilar et al., 2014). It is noteworthy that the presence of gametocytes in the BM leads to transcriptional changes of miRNAs expression involved in erythropoiesis. miR-221/222, miR-24 and miR-191 levels were all decreased in the BM during *Pv* infection, and returned to normal during convalescence (**Figure 1c**). In contrast, miR-144 and miR-150 levels were both upregulated during infection (**Figure 1c**) (Baro et al., 2017). However, these findings need further validation using *in vitro* models validated with clinical samples. Indeed, an *in vitro* model of tridimensional co-culture in a Matrigel scaffold with *Pf* gametocytes and self-assembling spheroids of human bone marrow mesenchymal cells (hBM-MSCs) was recently described (Messina et al., 2018), where the immature gametocytes adhered to hBM-MSCs *via* trypsin-sensitive parasite ligands exposed on the erythrocyte surface (Messina et al., 2018). This model could be used to identify altered miRNA expression by comparing the models

with and without gametocytes, prior to validating these findings in infected individuals.

OTHER RELEVANT CONSIDERATIONS

Age, Immunity, and miRNAs

Falciparum malaria-associated mortality is higher in children under five years of age, who lack immunity to the parasite (Streatfield et al., 2014). In contrast, adults in endemic areas have been exposed regularly, and have progressively built up an anti-disease immunity leading to sub-clinical infections (Schwartz et al., 2001). Because the development of such immunity depends on malaria exposure, SM cases are more often seen in African children as high malaria transmission intensity in sub-Saharan Africa leads to develop antimalarial immunity during childhood. However, in South East Asia, where malaria transmission is not sufficiently intense to induce robust immunity, SM mainly affects older children and adults (Sahu et al., 2015). Therefore, biomarkers of malaria infection validated in both age groups and transmission intensities would represent a powerful prognosis tool to identify patients at risk of SM fatality, inform their clinical management, and decrease SM associated mortality. In the context of miRNA-based biomarkers, miR-3158-3p is the only candidate that has been associated with SM and subcategories of SM in both Mozambican children (Gupta et al., 2021a), as well as Indian adults and children (Gupta et al., 2021b). Further validations and translational efforts are now needed, and the former may also help elucidating the mechanisms behind distinct the different clinical profiles of SM found in African children and South East Asian adults (Wassmer et al., 2015).

Technical Considerations

Studies investigating the potential diagnostic benefit of miRNA-based biomarkers in SM all used samples obtained patients in malaria endemic countries where co-infections are frequent. Because the symptoms of malaria infection are non-specific, they can easily overlap with concurrent infections, and one important consideration for future studies is to ensure that miRNAs candidates have been tested against non-malarial diseases. Indeed, the observed miRNA level changes in malaria patients can be influenced by inflammation due to the presence of other pathogens and samples obtained from patients with non-malarial diseases should be used as additional controls. There are several techniques available for the identification of miRNAs (recently reviewed in (Sempere et al.; Condrat et al., 2020) including classical and low-throughput methods such as northern blot and RNA protection assays, requiring large quantities of total RNA, and advanced methods such as microarray, nCounter Nanostring technology, NGS and reverse transcription quantitative PCR (RT-qPCR). Among these, microarray, nCounter Nanostring technology and NGS are usually used in the discovery phase or initial screening of the study, while RT-qPCR assays are used in the validation phase (Sempere et al.; Condrat et al., 2020). However, the use of RT-qPCRs can be limited due to the lack of appropriate normalizing controls. In our opinion, endogenous miRNA controls (ECs) should be disease-specific as ECs with stable expression in the case and control groups found suitable for cancer studies may not be appropriate for malaria samples. A study reported the combination of hsa-miR-30d-5p and hsa-miR-191–5p as the suitable ECs to normalize the miRNA RT-qPCRs data obtained using plasma from patients with malaria infection (Gupta et al., 2021a). The combination of ECs had a 0.044 NormFinder stability value. In addition, no differences were found in Ct values of the two ECs when compared between Mozambican patients with SM and UM (Gupta et al., 2021a), further confirming their stable expression in different malaria pathologies.

Future Directions

Lateral flow assays (LFA) developed to detect circulating miRNAs associated with different type of cancers are showing promising results. A gold nanoparticle-based LFA was able to detect a minimum concentration of 60 pM of miR-215 within 20 minutes in aqueous solutions and biological samples (Gao et al., 2014). Similarly, another LFA was able to detect miR-21, miR-155 and miR-210 with detection limits of 0.073, 0.061 and 0.085 nM, respectively (Zheng et al., 2018). Lastly a Gold@Silica nanocomposite-labeled LFA allowed the visual detection of miR-21 in cancer cells and human serum down to 1 pM (Dong et al., 2021). While these concentration thresholds are highly likely to afford the detection of candidates such as miR-3158-3p in SM, additional studies using plasma from different groups of infected individuals are needed to assess the sensitivity and reliability of such LFAs in malaria diagnosis. They could represent a game changer in the field, especially when the number of *pfhrp2* deletion reports are increasing (Gupta et al., 2017b; Gendrot et al., 2019; Galatas et al., 2020). PfHRP2-based rapid diagnostic tests (RDTs) are the most widely used diagnostic method across malaria endemic countries (Gendrot et al., 2019). The advantage of miRNA-based LFA is that they could be designed to detect multiple miRNAs (Zheng et al., 2018). This would not only further enhance the sensitivity and specificity of the assay, but also allow a higher granularity in clinical diagnosis.

In addition to their potential as diagnostic tools, miRNA may also open new therapeutic avenues in SM, by either mimicking or inhibiting specific miRNAs associated with its pathogenesis. In the former case, miRNA mimics aim to restore the expression of miRNA that was lost. Inversely, anti-miRNAs (antimiRs) are single stranded oligonucleotides, which are chemically designed to block the function of miRNA candidate overexpressed during the course of the disease (Rupaimoole and Slack, 2017). Attempts have been made using miRNA mimics and antimiRs for the therapeutic intervention in other diseases, including a mimic of the tumour suppressor miRNA miR-34, which reached phase I clinical trials for treating cancer, and antimiRs targeted at miR-122, which reached phase II trials for treating hepatitis (Rupaimoole and Slack, 2017; Hanna et al., 2019). Similarly, miR-16, miR-21, miR-29, miR-92 and miR-155 based therapeutics are also in phase I and II trials to test their efficacy to cure wound healing, heart failure, cancer and other

diseases (Hanna et al., 2019). While these approaches are not currently explored in malaria research, further investigations in the role of miR-3158-3p in regulating the genes associated with brain injury and processes relevant to SM may be promising. In addition, the WHO recently endorsed the RTS,S/AS01 (Mosquitix™) malaria vaccine for use among children in sub-Saharan Africa and in other regions with moderate to high falciparum malaria transmission. Several groups reported that vaccines could influence serum miRNA levels: a study demonstrated a change in miRNA expression levels in samples obtained from UK children who received vaccination against influenza (H1N1) (Drury et al., 2019). Using mice models, another study showed that vaccines associated with or without protection against respiratory syncytial virus led to different circulating miRNA profiles (Atherton et al., 2019). The roll-out of the Mosquitix™ vaccine will represent a great opportunity to investigate over-expressed or down-regulated miRNAs in protected vaccinated individuals. In turn, these could inform miRNA-based therapeutics against *Pf* infection.

CONCLUSIONS

Microscopy remains the gold standard for malaria diagnosis. However, no currently available methods can identify patients with parasite sequestration-associated tissue injury or predict their level of infection severity. There is a need for new tools and technologies easily implementable in malarious areas to improve diagnosis and increase survival. miRNAs, which are rapidly released in biofluids upon infection and organ damage, could serve as a measure of tissue injury and be used to accurately detect parasites not only in infected humans but also in mosquitoes, to contribute to malaria elimination efforts.

AUTHOR CONTRIBUTIONS

HG and SW designed and conceptualized the manuscript. HG carried out the literature search, and together with SW generated the first draft of the manuscript. Both authors reviewed and approved the final manuscript.

FUNDING

This work was supported by the National Institute of Allergy and Infectious Diseases of the National Institutes of Health under Award Numbers U19AI089676 and R21AI142472, and by the Medical Research Council, UK, under Award Number MR/S009450/1. The content is solely the responsibility of the authors and does not necessarily represent the official views of the funders.

ACKNOWLEDGMENTS

We would like to thank Benjamin Wassmer for drawing some of the beautiful artwork in **Figure 1**.

REFERENCES

Aguilar R., Magallon-Tejada A., Achtman A. H., Moraleda C., Joice R., Cistero P., et al. (2014). Molecular Evidence for the Localization of Plasmodium Falciparum Immature Gametocytes in Bone Marrow. *Blood* 123 (7), 959–966. doi: 10.1182/blood-2013-08-520767

Al-Quraishy S., Dkhil M. A., Delic D., Abdel-Baki A. A., and Wunderlich F. (2012). Organ-Specific Testosterone-Insensitive Response of miRNA Expression of C57BL/6 Mice to Plasmodium Chabaudi Malaria. *Parasitol. Res.* 111 (3), 1093–1101. doi: 10.1007/s00436-012-2937-3

Andolina C., Rek J. C., Briggs J., Okoth J., Musiime A., Ramjith J., et al. (2021). Sources of Persistent Malaria Transmission in a Setting With Effective Malaria Control in Eastern Uganda: A Longitudinal, Observational Cohort Study. *Lancet Infect. Dis.* 21 (11), 1568–1578. doi: 10.1016/S1473-3099(21)00072-4

Anvikar A. R., van Eijk A. M., Shah A., Upadhyay K. J., Sullivan S. A., Patel A. J., et al. (2020). Clinical and Epidemiological Characterization of Severe Plasmodium Vivax Malaria in Gujarat, India. *Virulence* 11 (1), 730–738. doi: 10.1080/21505594.2020.1773107

Arroyo J. D., Chevillet J. R., Kroh E. M., Ruf I. K., Pritchard C. C., Gibson D. F., et al. (2011). Argonaute2 Complexes Carry a Population of Circulating Microrna Independent of Vesicles in Human Plasma. *Proc. Natl. Acad. Sci. U. S. A.* 108 (12), 5003–5008. doi: 10.1073/pnas.1019055108

Atherton L. J., Jorquera P. A., Bakre A. A., and Tripp R. A. (2019). Determining Immune and MiRNA Biomarkers Related to Respiratory Syncytial Virus (RSV) Vaccine Types. *Front. Immunol.* 10, 2323. doi: 10.3389/fimmu.2019.02323

Babatunde K. A., Yesodha Subramanian B., Ahouidi A. D., Martinez Murillo P., Walch M., and Mantel P. Y. (2020). Role of Extracellular Vesicles in Cellular Cross Talk in Malaria. *Front. Immunol.* 11, 22. doi: 10.3389/fimmu.2020.00022

Baird J. K., Valecha N., Duparc S., White N. J., and Price R. N. (2016). Diagnosis and Treatment of Plasmodium Vivax Malaria. *Am. J. Trop. Med. Hyg.* 95 (6 Suppl), 35–51. doi: 10.4269/ajtmh.16-0171

Barker K. R., Lu Z., Kim H., Zheng Y., Chen J., Conroy A. L., et al. (2017). MiR-155 Modifies Inflammation, Endothelial Activation and Blood-Brain Barrier Dysfunction in Cerebral Malaria. *Mol. Med.* 23, 24–33. doi: 10.2119/molmed.2016.00139

Baro B., Deroost K., Raiol T., Brito M., Almeida A. C., De Menezes-Neto A., et al. (2017). Plasmodium Vivax Gametocytes in the Bone Marrow of an Acute Malaria Patient and Changes in the Erythroid Mirna Profile. *PloS Negl. Trop. Dis.* 11 (4), e0005365. doi: 10.1371/journal.pntd.0005365

Bertrams W., Griss K., Han M., Seidel K., Hippenstiel S., Suttorp N., et al. (2021). Transcriptional Analysis Identifies Potential Biomarkers and Molecular Regulators in Acute Malaria Infection. *Life Sci.* 270, 119158. doi: 10.1016/j.lfs.2021.119158

Biryukova I., Ye T., and Levashina E. (2014). Transcriptome-Wide Analysis of Microrna Expression in the Malaria Mosquito Anopheles Gambiae. *BMC Genomics* 15, 557. doi: 10.1186/1471-2164-15-557

Bousema T., and Drakeley C. (2011). Epidemiology and Infectivity of Plasmodium Falciparum and Plasmodium Vivax Gametocytes in Relation to Malaria Control and Elimination. *Clin. Microbiol. Rev.* 24 (2), 377–410. doi: 10.1128/CMR.00051-10

Bousema T., Okell L., Felger I., and Drakeley C. (2014). Asymptomatic Malaria Infections: Detectability, Transmissibility and Public Health Relevance. *Nat. Rev. Microbiol.* 12 (12), 833–840. doi: 10.1038/nrmicro3364

Brabin B. J., Romagosa C., Abdelgalil S., Menendez C., Verhoeff F. H., Mcgready R., et al. (2004). The Sick Placenta-The Role of Malaria. *Placenta* 25 (5), 359–378. doi: 10.1016/j.placenta.2003.10.019

Buffet P. A., Safeukui I., Deplaine G., Brousse V., Prendki V., Thellier M., et al. (2011). The Pathogenesis of Plasmodium Falciparum Malaria in Humans: Insights From Splenic Physiology. *Blood* 117 (2), 381–392. doi: 10.1182/blood-2010-04-202911

Bullerdiek J., and Flor I. (2012). Exosome-Delivered Micrornas of "Chromosome 19 MicroRNA Cluster" as Immunomodulators in Pregnancy and Tumorigenesis. *Mol. Cytogenet.* 5 (1), 27. doi: 10.1186/1755-8166-5-27

Burel J. G., Apte S. H., Groves P. L., Boyle M. J., Langer C., Beeson J. G., et al. (2017). Dichotomous MiR Expression and Immune Responses Following Primary Blood-Stage Malaria. *JCI Insight* 2 (15). doi: 10.1172/jci.insight.93434

Calzetta M., Perugini E., Seixas G., Sousa C. A., Guelbeogo W. M., Sagnon N., et al. (2018). A Novel Nested Polymerase Chain Reaction Assay Targeting Plasmodium Mitochondrial DNA in Field-Collected Anopheles Mosquitoes. *Med. Vet. Entomol.* 32 (3), 372–377. doi: 10.1111/mve.12293

Chamnanchanunt S., Fucharoen S., and Umemura T. (2017). Circulating MicroRNAs in Malaria Infection: Bench to Bedside. *Malar. J.* 16 (1), 334. doi: 10.1186/s12936-017-1990-x

Chamnanchanunt S., Kuroki C., Desakorn V., Enomoto M., Thanachartwet V., Sahassananda D., et al. (2015). Downregulation of Plasma MiR-451 and MiR-16 in Plasmodium Vivax Infection. *Exp. Parasitol.* 155, 19–25. doi: 10.1016/j.exppara.2015.04.013

Chen I., Clarke S. E., Gosling R., Hamainza B., Killeen G., Magill A., et al. (2016). "Asymptomatic" Malaria: A Chronic and Debilitating Infection That Should be Treated. *PloS Med.* 13 (1), e1001942. doi: 10.1371/journal.pmed.1001942

Cheng L., Sharples R. A., Scicluna B. J., and Hill A. F. (2014). Exosomes Provide a Protective and Enriched Source of Mirna for Biomarker Profiling Compared to Intracellular and Cell-Free Blood. *J. Extracell. Vesicles* 3. doi: 10.3402/jev.v3.23743

Cheng I. S., Sealy B. C., Tiberti N., and Combes V. (2020) Extracellular Vesicles, From Pathogenesis to Biomarkers: the Case for Cerebral Malaria. *Vessel Plus* 4, 17. doi: 10.20517/2574-1209.2020.08

Cohen A., Zinger A., Tiberti N., Grau G. E. R., and Combes V. (2018). Differential Plasma Microvesicle and Brain Profiles of MicroRNA in Experimental Cerebral Malaria. *Malar. J.* 17 (1), 192. doi: 10.1186/s12936-018-2330-5

Combes V., Taylor T. E., Juhan-Vague I., Mege J. L., Mwenechanya J., Tembo M., et al. (2004). Circulating Endothelial Microparticles in Malawian Children With Severe Falciparum Malaria Complicated With Coma. *JAMA* 291 (21), 2542–2544. doi: 10.1001/jama.291.21.2542-b

Condrat C. E., Thompson D. C., Barbu M. G., Bugnar O. L., Boboc A., Cretoiu D., et al. (2020). Mirnas as Biomarkers in Disease: Latest Findings Regarding Their Role in Diagnosis and Prognosis. *Cells* 9 (2). doi: 10.3390/cells9020276

Cortez M. A., Bueso-Ramos C., Ferdin J., Lopez-Berestein G., Sood A. K., and Calin G. A. (2011). MicroRNAs in Body Fluids–the Mix of Hormones and Biomarkers. *Nat. Rev. Clin. Oncol.* 8 (8), 467–477. doi: 10.1038/nrclinonc.2011.76

Cox-Singh J., Hiu J., Lucas S. B., Divis P. C., Zulkarnaen M., Chandran P., et al. (2010). Severe Malaria - a Case of Fatal Plasmodium Knowlesi Infection With Post-Mortem Findings: A Case Report. *Malar. J.* 9, 10. doi: 10.1186/1475-2875-9-10

Cranston H. A., Boylan C. W., Carroll G. L., Sutera S. P., Williamson J. R., Gluzman I. Y., et al. (1984). Plasmodium Falciparum Maturation Abolishes Physiologic Red Cell Deformability. *Science* 223 (4634), 400–403. doi: 10.1126/science.6362007

Dayananda K. K., Achur R. N., and Gowda D. C. (2018). Epidemiology, Drug Resistance, and Pathophysiology of Plasmodium Vivax Malaria. *J. Vector Borne Dis.* 55 (1), 1–8. doi: 10.4103/0972-9062.234620

Delic D., Dkhil M., Al-Quraishy S., and Wunderlich F. (2011). Hepatic MiRNA Expression Reprogrammed by Plasmodium Chabaudi Malaria. *Parasitol. Res.* 108 (5), 1111–1121. doi: 10.1007/s00436-010-2152-z

Dennison N. J., BenMarzouk-Hidalgo O. J., and Dimopoulos G. (2015). MicroRNA-Regulation of Anopheles Gambiae Immunity to Plasmodium Falciparum Infection and Midgut Microbiota. *Dev. Comp. Immunol.* 49 (1), 170–178. doi: 10.1016/j.dci.2014.10.016

Dieng M. M., Diawara A., Manikandan V., Tamim El Jarkass H., Serme S. S., Sombie S., et al. (2020). Integrative Genomic Analysis Reveals Mechanisms of Immune Evasion in P. Falciparum Malaria. *Nat. Commun.* 11 (1), 5093. doi: 10.1038/s41467-020-18915-6

Dkhil M. A., Al-Quraishy S. A., Abdel-Baki A. S., Delic D., and Wunderlich F. (2016). Differential MiRNA Expression in the Liver of Balb/C Mice Protected by Vaccination During Crisis of Plasmodium Chabaudi Blood-Stage Malaria. *Front. Microbiol.* 7, 2155. doi: 10.3389/fmicb.2016.02155

Dong S., Fu X., Dong Y., Simoes M. L., Zhu J., and Dimopoulos G. (2020). Broad Spectrum Immunomodulatory Effects of Anopheles Gambiae Micrornas and Their Use for Transgenic Suppression of Plasmodium. *PloS Pathog.* 16 (4), e1008453. doi: 10.1371/journal.ppat.1008453

Dong T., Yin R., Yu Q., Qiu W., Li K., Qian L., et al. (2021). Sensitive Detection of Microrna-21 in Cancer Cells and Human Serum With Au@Si Nanocomposite and Lateral Flow Assay. *Anal. Chim. Acta* 1147, 56–63. doi: 10.1016/j.aca.2020.12.042

Drury R. E., Pollard A. J., and O'Connor D. (2019). The Effect of H1N1 Vaccination on Serum MiRNA Expression in Children: A Tale of Caution for MicroRNA Microarray Studies. *PloS One* 14 (8), e0221143. doi: 10.1371/journal.pone.0221143

Echeverry D. F., Deason N. A., Makuru V., Davidson J., Xiao H., Niedbalski J., et al. (2017). Fast and Robust Single PCR for Plasmodium Sporozoite Detection in Mosquitoes Using the Cytochrome Oxidase I Gene. *Malar. J.* 16 (1), 230. doi: 10.1186/s12936-017-1881-1

EL Andaloussi S., Mager I., Breakefield X. O., and Wood M. J. (2013). Extracellular Vesicles: Biology and Emerging Therapeutic Opportunities. *Nat. Rev. Drug Discov.* 12 (5), 347–357. doi: 10.1038/nrd3978

El-Assaad F., Hempel C., Combes V., Mitchell A. J., Ball H. J., Kurtzhals J. A., et al. (2011). Differential MicroRNA Expression in Experimental Cerebral and Noncerebral Malaria. *Infect. Immun.* 79 (6), 2379–2384. doi: 10.1128/IAI.01136-10

Fleischer B. (2004). Editorial: 100 Years Ago: Giemsa's Solution for Staining of Plasmodia. *Trop. Med. Int. Health* 9 (7), 755–756. doi: 10.1111/j.1365-3156.2004.01278.x

Fried M., and Duffy P. E. (1996). Adherence of Plasmodium Falciparum to Chondroitin Sulfate a in the Human Placenta. *Science* 272 (5267), 1502–1504. doi: 10.1126/science.272.5267.1502

Galatas B., Bassat Q., and Mayor A. (2016). Malaria Parasites in the Asymptomatic: Looking for the Hay in the Haystack. *Trends Parasitol.* 32 (4), 296–308. doi: 10.1016/j.pt.2015.11.015

Galatas B., Mayor A., Gupta H., Balanza N., Jang I. K., Nhamussua L., et al. (2020). Field Performance of Ultrasensitive and Conventional Malaria Rapid Diagnostic Tests in Southern Mozambique. *Malar. J.* 19 (1), 451. doi: 10.1186/s12936-020-03526-9

Gamain B., Smith J. D., Viebig N. K., Gysin J., and Scherf A. (2007). Pregnancy-Associated Malaria: Parasite Binding, Natural Immunity and Vaccine Development. *Int. J. Parasitol.* 37 (3-4), 273–283. doi: 10.1016/j.ijpara.2006.11.011

Gao X., Xu H., Baloda M., Gurung A. S., Xu L. P., Wang T., et al. (2014). Visual Detection of Microrna With Lateral Flow Nucleic Acid Biosensor. *Biosens Bioelectron* 54, 578–584. doi: 10.1016/j.bios.2013.10.055

Garcia L. S. (2010). Malaria. *Clin. Lab. Med.* 30 (1), 93–129. doi: 10.1016/j.cll.2009.10.001

Gazzinelli R. T., Kalantari P., Fitzgerald K. A., and Golenbock D. T. (2014). Innate Sensing of Malaria Parasites. *Nat. Rev. Immunol.* 14 (11), 744–757. doi: 10.1038/nri3742

Gendrot M., Fawaz R., Dormoi J., Madamet M., and Pradines B. (2019). Genetic Diversity and Deletion of Plasmodium Falciparum Histidine-Rich Protein 2 and 3: A Threat to Diagnosis of P. Falciparum Malaria. *Clin. Microbiol. Infect.* 25 (5), 580–585. doi: 10.1016/j.cmi.2018.09.009

Gupta H., Afsal M. P., Shetty S. M., Satyamoorthy K., and Umakanth S. (2015a). Plasmodium Vivax Infection Causes Acute Respiratory Distress Syndrome: A Case Report. *J. Infect. Dev. Ctries.* 9 (8), 910–913. doi: 10.3855/jidc.6813

Gupta H., Chaudhari S., Rai A., Bhat S., Sahu P. K., Hande M. H., et al. (2017a). Genetic and Epigenetic Changes in Host ABCB1 Influences Malaria Susceptibility to Plasmodium Falciparum. *PloS One* 12 (4), e0175702. doi: 10.1371/journal.pone.0175702

Gupta H., Dhunputh P., Bhatt A. N., Satyamoorthy K., and Umakanth S. (2016a). Cerebral Malaria in a Man With Plasmodium Vivax Mono-Infection: A Case Report. *Trop. Doct.* 46 (4), 241–245. doi: 10.1177/0049475515624857

Gupta H., Jain A., Saadi A. V., Vasudevan T. G., Hande M. H., D'souza S. C., et al. (2015b). Categorical Complexities of Plasmodium Falciparum Malaria in Individuals Is Associated With Genetic Variations in ADORA2A and GRK5 Genes. *Infect. Genet. Evol.* 34, 188–199. doi: 10.1016/j.meegid.2015.06.010

Gupta H., Matambisso G., Galatas B., Cistero P., Nhamussua L., Simone W., et al. (2017b). Molecular Surveillance of Pfhrp2 and Pfhrp3 Deletions in Plasmodium Falciparum Isolates From Mozambique. *Malar. J.* 16 (1), 416. doi: 10.1186/s12936-017-2061-z

Gupta H., Rubio M., Sitoe A., Cistero P., Nhamussua L., Simone W., et al. (2021a). Plasma MicroRNA Profiling of Plasmodium Falciparum Biomass and

Association With Severity of Malaria Disease. *Emerg. Infect. Dis.* 27 (2), 430–442. doi: 10.3201/eid2702.191795

Gupta H., Sahu P. K., Pattnaik R., Mohanty A., Majhi M., Mohanty A. K., et al. (2021b). Plasma Levels of Hsa-MiR-3158-3p MicroRNA on Admission Correlate With MRI Findings and Predict Outcome in Cerebral Malaria. *Clin. Transl. Med.* 11 (6), e396. doi: 10.1002/ctm2.396

Gupta H., Sakharwade S. C., Angural A., Kotambail A., Bhat G. K., Hande M. H., et al. (2013). Evidence for Genetic Linkage Between a Polymorphism in the GNAS Gene and Malaria in South Indian Population. *Acta Trop.* 128 (3), 571–577. doi: 10.1016/j.actatropica.2013.08.005

Gupta H., Srivastava S., Chaudhari S., Vasudevan T. G., Hande M. H., D'souza S. C., et al. (2016b). New Molecular Detection Methods of Malaria Parasites With Multiple Genes From Genomes. *Acta Trop.* 160, 15–22. doi: 10.1016/j.actatropica.2016.04.013

Habluetzel A., Merzagora L., Jenni L., Betschart B., Rotigliano G., and Esposito F. (1992). Detecting Malaria Sporozoites in Live, Field-Collected Mosquitoes. *Trans. R Soc. Trop. Med. Hyg.* 86 (2), 138–140. doi: 10.1016/0035-9203(92)90542-K

Hanna J., Hossain G. S., and Kocerha J. (2019). The Potential for Microrna Therapeutics and Clinical Research. *Front. Genet.* 10, 478. doi: 10.3389/fgene.2019.00478

Hentzschel F., Hammerschmidt-Kamper C., Borner K., Heiss K., Knapp B., Sattler J. M., et al. (2014). AAV8-Mediated *In Vivo* Overexpression of MiR-155 Enhances the Protective Capacity of Genetically Attenuated Malarial Parasites. *Mol. Ther.* 22 (12), 2130–2141. doi: 10.1038/mt.2014.172

Hviid L., and Jensen A. T. (2015). Pfemp1 - a Parasite Protein Family of Key Importance in Plasmodium Falciparum Malaria Immunity and Pathogenesis. *Adv. Parasitol.* 88, 51–84. doi: 10.1016/bs.apar.2015.02.004

Jain S., Rana V., Shrinet J., Sharma A., Tridibes A., Sunil S., et al. (2014). Blood Feeding and Plasmodium Infection Alters the Mirnome of Anopheles Stephensi. *PloS One* 9 (5), e98402. doi: 10.1371/journal.pone.0098402

Jensen A. R., Adams Y., and Hviid L. (2020). Cerebral Plasmodium Falciparum Malaria: The Role of Pfemp1 in Its Pathogenesis and Immunity, and Pfemp1-Based Vaccines to Prevent it. *Immunol. Rev.* 293 (1), 230–252. doi: 10.1111/imr.12807

Kaur H., Sehgal R., Kumar A., Sehgal A., Bansal D., and Sultan A. A. (2018). Screening and Identification of Potential Novel Biomarker for Diagnosis of Complicated Plasmodium Vivax Malaria. *J. Transl. Med.* 16 (1), 272. doi: 10.1186/s12967-018-1646-9

Ketprasit N., Cheng I. S., Deutsch F., Tran N., Imwong M., Combes V., et al. (2020). The Characterization of Extracellular Vesicles-Derived MicroRNAs in Thai Malaria Patients. *Malar. J.* 19 (1), 285. doi: 10.1186/s12936-020-03360-z

Kho S., Qotrunnada L., Leonardo L., Andries B., Wardani P. a. I., Fricot A., et al. (2021a). Evaluation of Splenic Accumulation and Colocalization of Immature Reticulocytes and Plasmodium Vivax in Asymptomatic Malaria: A Prospective Human Splenectomy Study. *PloS Med.* 18 (5), e1003632. doi: 10.1371/journal.pmed.1003632

Kho S., Qotrunnada L., Leonardo L., Andries B., Wardani P. a. I., Fricot A., et al. (2021b). Hidden Biomass of Intact Malaria Parasites in the Human Spleen. *N. Engl. J. Med.* 384 (21), 2067–2069. doi: 10.1056/NEJMc2023884

Kimenyi K. M., Wamae K., and Ochola-Oyier L. I. (2019). Understanding P. Falciparum Asymptomatic Infections: A Proposition for a Transcriptomic Approach. *Front. Immunol.* 10, 2398. doi: 10.3389/fimmu.2019.02398

Kotepui M., Kotepui K. U., Milanez G. D., and Masangkay F. R. (2020a). Severity and Mortality of Severe Plasmodium Ovale Infection: A Systematic Review and Meta-Analysis. *PloS One* 15 (6), e0235014. doi: 10.1371/journal.pone.0235014

Kotepui M., Kotepui K. U., Milanez G. D., and Masangkay F. R. (2020b). Global Prevalence and Mortality of Severe Plasmodium Malariae Infection: A Systematic Review and Meta-Analysis. *Malar. J.* 19 (1), 274. doi: 10.1186/s12936-020-03344-z

Lacerda M. V., Mourao M. P., Coelho H. C., and Santos J. B. (2011). Thrombocytopenia in Malaria: Who Cares? *Mem. Inst. Oswaldo Cruz.* 106 Suppl 1, 52–63. doi: 10.1590/s0074-02762011000900007

LaMonte G., Philip N., Reardon J., Lacsina J. R., Majoros W., Chapman L., et al. (2012). Translocation of Sickle Cell Erythrocyte MicroRNAs Into Plasmodium Falciparum Inhibits Parasite Translation and Contributes to Malaria Resistance. *Cell Host Microbe* 12 (2), 187–199. doi: 10.1016/j.chom.2012.06.007

Lampe L., Jentzsch M., Kierszniowska S., and Levashina E. A. (2019). Metabolic Balancing by MiR-276 Shapes the Mosquito Reproductive Cycle and Plasmodium Falciparum Development. *Nat. Commun.* 10 (1), 5634. doi: 10.1038/s41467-019-13627-y

Latourette M. T., Siebert J. E., Barto R. J. Jr., Marable K. L., Muyepa A., Hammond C. A., et al. (2011). Magnetic Resonance Imaging Research in Sub-Saharan Africa: Challenges and Satellite-Based Networking Implementation. *J. Digit. Imaging* 24 (4), 729–738. doi: 10.1007/s10278-010-9323-4

Liu W., Hao Z., Huang L., Chen L., Wei Q., Cai L., et al. (2017). Comparative Expression Profile of Micrornas in Anopheles Anthropophagus Midgut After Blood-Feeding and Plasmodium Infection. *Parasit. Vectors* 10 (1), 86. doi: 10.1186/s13071-017-2027-6

Lucchi N. W., Jain V., Wilson N. O., Singh N., Udhayakumar V., and Stiles J. K. (2011). Potential Serological Biomarkers of Cerebral Malaria. *Dis. Markers* 31 (6), 327–335. doi: 10.1155/2011/345706

Makani J., Matuja W., Liyombo E., Snow R. W., Marsh K., and Warrell D. A. (2003). Admission Diagnosis of Cerebral Malaria in Adults in an Endemic Area of Tanzania: Implications and Clinical Description. *QJM* 96 (5), 355–362. doi: 10.1093/qjmed/hcg059

Mantel P. Y., Hjelmqvist D., Walch M., Kharoubi-Hess S., Nilsson S., Ravel D., et al. (2016). Infected Erythrocyte-Derived Extracellular Vesicles Alter Vascular Function *via* Regulatory Ago2-MiRNA Complexes in Malaria. *Nat. Commun.* 7, 12727. doi: 10.1038/ncomms12727

Mantel P. Y., and Marti M. (2014). The Role of Extracellular Vesicles in Plasmodium and Other Protozoan Parasites. *Cell Microbiol.* 16 (3), 344–354. doi: 10.1111/cmi.12259

Martin-Alonso A., Cohen A., Quispe-Ricalde M. A., Foronda P., Benito A., Berzosa P., et al. (2018). Differentially Expressed MicroRNAs in Experimental Cerebral Malaria and Their Involvement in Endocytosis, Adherens Junctions, Foxo and TGF-Beta Signalling Pathways. *Sci. Rep.* 8 (1), 11277. doi: 10.1038/s41598-018-29721-y

Maude R. J., Barkhof F., Hassan M. U., Ghose A., Hossain A., Abul Faiz M., et al. (2014). Magnetic Resonance Imaging of the Brain in Adults With Severe Falciparum Malaria. *Malar. J.* 13, 177. doi: 10.1186/1475-2875-13-177

Mead E. A., and Tu Z. (2008). Cloning, Characterization, and Expression of MicroRNAs From the Asian Malaria Mosquito, Anopheles Stephensi. *BMC Genomics* 9, 244. doi: 10.1186/1471-2164-9-244

Messina V., Valtieri M., Rubio M., Falchi M., Mancini F., Mayor A., et al. (2018). Gametocytes of the Malaria Parasite Plasmodium Falciparum Interact With and Stimulate Bone Marrow Mesenchymal Cells to Secrete Angiogenetic Factors. *Front. Cell. Infect. Microbiol.* 8, 50. doi: 10.3389/fcimb.2018.00050

Miller L. H., Baruch D. I., Marsh K., and Doumbo O. K. (2002). The Pathogenic Basis of Malaria. *Nature* 415 (6872), 673–679. doi: 10.1038/415673a

Milner D. A. Jr., Whitten R. O., Kamiza S., Carr R., Liomba G., Dzamalala C., et al. (2014). The Systemic Pathology of Cerebral Malaria in African Children. *Front. Cell. Infect. Microbiol.* 4, 104. doi: 10.3389/fcimb.2014.00104

Mischlinger J., Ronnberg C., Alvarez-Martinez M. J., Buhler S., Paul M., Schlagenhauf P., et al. (2020). Imported Malaria in Countries Where Malaria Is Not Endemic: A Comparison of Semi-Immune and Nonimmune Travelers. *Clin. Microbiol. Rev.* 33. doi: 10.1128/CMR.00104-19

Mohanty S., Mishra S. K., Patnaik R., Dutt A. K., Pradhan S., Das B., et al. (2011). Brain Swelling and Mannitol Therapy in Adult Cerebral Malaria: A Randomized Trial. *Clin. Infect. Dis.* 53 (4), 349–355. doi: 10.1093/cid/cir405

Mohanty S., Taylor T. E., Kampondeni S., Potchen M. J., Panda P., Majhi M., et al. (2014). Magnetic Resonance Imaging During Life: The Key to Unlock Cerebral Malaria Pathogenesis? *Malar. J.* 13, 276. doi: 10.1186/1475-2875-13-276

Moody A. H., and Chiodini P. L. (2002). Non-Microscopic Method for Malaria Diagnosis Using Optimal it, a Second-Generation Dipstick for Malaria Pldh Antigen Detection. *Br. J. BioMed. Sci.* 59 (4), 228–231. doi: 10.1080/09674845.2002.11783665

Moro L., Bardaji A., Macete E., Barrios D., Morales-Prieto D. M., Espana C., et al. (2016). Placental Microparticles and Micrornas in Pregnant Women With Plasmodium Falciparum or HIV Infection. *PloS One* 11 (1), e0146361. doi: 10.1371/journal.pone.0146361

Mousa A., Al-Taiar A., Anstey N. M., Badaut C., Barber B. E., Bassat Q., et al. (2020). The Impact of Delayed Treatment of Uncomplicated P. Falciparum Malaria on Progression to Severe Malaria: A Systematic Review and a Pooled

Multicentre Individual-Patient Meta-Analysis. *PloS Med.* 17 (10), e1003359. doi: 10.1371/journal.pmed.1003359

Nantakomol D., Dondorp A. M., Krudsood S., Udomsangpetch R., Pattanapanyasat K., Combes V., et al. (2011). Circulating Red Cell-Derived Microparticles in Human Malaria. *J. Infect. Dis.* 203 (5), 700–706. doi: 10.1093/infdis/jiq104

Nik Mohamed Kamal N., and Shahidan W. N. S. (2019). Non-Exosomal and Exosomal Circulatory MicroRNAs: Which Are More Valid as Biomarkers? *Front. Pharmacol.* 10, 1500. doi: 10.3389/fphar.2019.01500

Nosten F., Rogerson S. J., Beeson J. G., McGready R., Mutabingwa T. K., and Brabin B. (2004). Malaria in Pregnancy and the Endemicity Spectrum: What can We Learn? *Trends Parasitol.* 20 (9), 425–432. doi: 10.1016/j.pt.2004.06.007

Oakley M. S., Gerald N., McCutchan T. F., Aravind L., and Kumar S. (2011). Clinical and Molecular Aspects of Malaria Fever. *Trends Parasitol.* 27 (10), 442–449. doi: 10.1016/j.pt.2011.06.004

Okell L. C., Bousema T., Griffin J. T., Ouedraogo A. L., Ghani A. C., and Drakeley C. J. (2012). Factors Determining the Occurrence of Submicroscopic Malaria Infections and Their Relevance for Control. *Nat. Commun.* 3, 1237. doi: 10.1038/ncomms2241

Ramirez A. L., van den Hurk A. F., Mackay I. M., Yang A. S. P., Hewitson G. R., et al. (2019). Malaria Surveillance From Both Ends: Concurrent Detection of Plasmodium Falciparum in Saliva and Excreta Harvested From Anopheles Mosquitoes. *Parasit. Vectors* 12 (1), 355. doi: 10.1186/s13071-019-3610-9

Rathjen T., Nicol C., McConkey G., and Dalmay T. (2006). Analysis of Short Rnas in the Malaria Parasite and its Red Blood Cell Host. *FEBS Lett.* 580 (22), 5185–5188. doi: 10.1016/j.febslet.2006.08.063

Rogerson S. J., Desai M., Mayor A., Sicuri E., Taylor S. M., and van Eijk A. M. (2018). Burden, Pathology, and Costs of Malaria in Pregnancy: New Developments for an Old Problem. *Lancet Infect. Dis.* 18 (4), e107–e118. doi: 10.1016/S1473-3099(18)30066-5

Rowe J. A., Claessens A., Corrigan R. A., and Arman M. (2009). Adhesion of Plasmodium Falciparum-Infected Erythrocytes to Human Cells: Molecular Mechanisms and Therapeutic Implications. *Expert Rev. Mol. Med.* 11, e16. doi: 10.1017/S1462399409001082

Rubio M., Bassat Q., Estivill X., and Mayor A. (2016). Tying Malaria and MicroRNAs: From the Biology to Future Diagnostic Perspectives. *Malar. J.* 15, 167. doi: 10.1186/s12936-016-1222-9

Rupaimoole R., and Slack F. J. (2017). MicroRNA Therapeutics: Towards a New Era for the Management of Cancer and Other Diseases. *Nat. Rev. Drug Discov.* 16 (3), 203–222. doi: 10.1038/nrd.2016.246

Sahu P. K., Hoffmann A., Majhi M., Pattnaik R., Patterson C., Mahanta K. C., et al. (2020). Brain Magnetic Resonance Imaging Reveals Different Courses of Disease in Pediatric and Adult Cerebral Malaria. *Clin. Infect. Dis.* 73 (7), e2387–e2396. doi: 10.1093/cid/ciaa1647

Sahu P. K., Satpathi S., Behera P. K., Mishra S. K., Mohanty S., and Wassmer S. C. (2015). Pathogenesis of Cerebral Malaria: New Diagnostic Tools, Biomarkers, and Therapeutic Approaches. *Front. Cell Infect. Microbiol.* 5, 7.5. doi: 10.3389/fcimb.2015.00075

Salanti A., Staalsoe T., Lavstsen T., Jensen A. T., Sowa M. P., Arnot D. E., et al. (2003). Selective Upregulation of a Single Distinctly Structured Var Gene in Chondroitin Sulphate a-Adhering Plasmodium Falciparum Involved in Pregnancy-Associated Malaria. *Mol. Microbiol.* 49 (1), 179–191. doi: 10.1046/j.1365-2958.2003.03570.x

Santos M. L. S., Coimbra R. S., Sousa T. N., Guimaraes L. F. F., Gomes M. S., Amaral L. R., et al. (2021). The Interface Between Inflammatory Mediators and Micrornas in Plasmodium Vivax Severe Thrombocytopenia. *Front. Cell. Infect. Microbiol.* 11, 631333. doi: 10.3389/fcimb.2021.631333

Schwartz E., Sadetzki S., Murad H., and Raveh D. (2001). Age as a Risk Factor for Severe Plasmodium Falciparum Malaria in Nonimmune Patients. *Clin. Infect. Dis.* 33 (10), 1774–1777. doi: 10.1086/322522

Sempere L. F., Azmi A. S., and Moore A. (2021). Microrna-Based Diagnostic and Therapeutic Applications in Cancer Medicine. *Wiley Interdiscip. Rev. RNA.* 2021, e1662. doi: 10.1002/wrna.1662

Seydel K. B., Kampondeni S. D., Valim C., Potchen M. J., Milner D. A., Muwalo F. W., et al. (2015). Brain Swelling and Death in Children With Cerebral Malaria. *N. Engl. J. Med.* 372 (12), 1126–1137. doi: 10.1056/NEJMoa1400116

Snounou G., Viriyakosol S., Jarra W., Thaithong S., and Brown K. N. (1993). Identification of the Four Human Malaria Parasite Species in Field Samples by the Polymerase Chain Reaction and Detection of a High Prevalence of Mixed Infections. *Mol. Biochem. Parasitol.* 58 (2), 283–292. doi: 10.1016/0166-6851(93)90050-8

Spencer H. C., Collins W. E., Chin W., and Skinner J. C. (1979). The Enzyme-Linked Immunosorbent Assay (ELISA) for Malaria. I. The Use of *In Vitro*-Cultured Plasmodium Falciparum as Antigen. *Am. J. Trop. Med. Hyg.* 28 (6), 927–932. doi: 10.4269/ajtmh.1979.28.927

Streatfield P. K., Khan W. A., Bhuiya A., Hanifi S. M., Alam N., Diboulo E., et al. (2014). Malaria Mortality in Africa and Asia: Evidence From INDEPTH Health and Demographic Surveillance System Sites. *Glob Health Action* 7, 25369. doi: 10.3402/gha.v7.25369

Taylor T. E., Fu W. J., Carr R. A., Whitten R. O., Mueller J. S., Fosiko N. G., et al. (2004). Differentiating the Pathologies of Cerebral Malaria by Postmortem Parasite Counts. *Nat. Med.* 10 (2), 143–145. doi: 10.1038/nm986

Tjitra E., Anstey N. M., Sugiarto P., Warikar N., Kenangalem E., Karyana M., et al. (2008). Multidrug-Resistant Plasmodium Vivax Associated With Severe and Fatal Malaria: A Prospective Study in Papua, Indonesia. *PloS Med.* 5 (6), e128. doi: 10.1371/journal.pmed.0050128

Turner L., Lavstsen T., Berger S. S., Wang C. W., Petersen J. E., Avril M., et al. (2013). Severe Malaria Is Associated With Parasite Binding to Endothelial Protein C Receptor. *Nature* 498 (7455), 502–505. doi: 10.1038/nature12216

Tusting L. S., Bousema T., Smith D. L., and Drakeley C. (2014). Measuring Changes in Plasmodium Falciparum Transmission: Precision, Accuracy and Costs of Metrics. *Adv. Parasitol.* 84, 151–208. doi: 10.1016/B978-0-12-800099-1.00003-X

Valadi H., Ekstrom K., Bossios A., Sjostrand M., Lee J. J., and Lotvall J. O. (2007). Exosome-Mediated Transfer of Mrnas and MicroRNAs Is a Novel Mechanism of Genetic Exchange Between Cells. *Nat. Cell Biol.* 9 (6), 654–659. doi: 10.1038/ncb1596

van Loon W., Gai P. P., Hamann L., Bedu-Addo G., and Mockenhaupt F. P. (2019). MiRNA-146a Polymorphism Increases the Odds of Malaria in Pregnancy. *Malar. J.* 18 (1), 7. doi: 10.1186/s12936-019-2643-z

Vojtech L., Woo S., Hughes S., Levy C., Ballweber L., Sauteraud R. P., et al. (2014). Exosomes in Human Semen Carry a Distinctive Repertoire of Small non-Coding RNAs With Potential Regulatory Functions. *Nucleic Acids Res.* 42 (11), 7290–7304. doi: 10.1093/nar/gku347

Wang Z., Xi J., Hao X., Deng W., Liu J., Wei C., et al. (2017). Red Blood Cells Release Microparticles Containing Human Argonaute 2 and miRNAs to Target Genes of Plasmodium Falciparum. *Emerg. Microbes Infect.* 6 (8), e75. doi: 10.1038/emi.2017.63

Wassmer S. C., Taylor T. E., Rathod P. K., Mishra S. K., Mohanty S., Arevalo-Herrera M., et al. (2015). Investigating the Pathogenesis of Severe Malaria: A Multidisciplinary and Cross-Geographical Approach. *Am. J. Trop. Med. Hyg.* 93 (3 Suppl), 42–56. doi: 10.4269/ajtmh.14-0841

White N. J. (2017). Malaria Parasite Clearance. *Malar. J.* 16 (1), 88. doi: 10.1186/s12936-017-1731-1

White N. J., Pukrittayakamee S., Hien T. T., Faiz M. A., Mokuolu O. A., and Dondorp A. M. (2014). Malaria. *Lancet* 383 (9918), 723–735. doi: 10.1016/S0140-6736(13)60024-0

White N. J., Turner G. D., Day N. P., and Dondorp A. M. (2013). Lethal Malaria: Marchiafava and Bignami Were Right. *J. Infect. Dis.* 208 (2), 192–198. doi: 10.1093/infdis/jit116

WHO (2014). Severe Malaria. *Trop. Med. Int. Health* 19 (Suppl 1), 7–131. doi: 10.1111/tmi.12313_2

WHO (2020). *World Malaria Report 2020*. Available at: https://www.who.int/publications/i/item/9789240015791 (Accessed Accessed 09/03/2021).

WHO (2015) *Guidelines for the Treatment of Malaria - 3rd Edition* (Geneva: World Health Organization). Available at: https://apps.who.int/iris/handle/10665/162441 (Accessed Accessed 16/09/2021).

Winter F., Edaye S., Huttenhofer A., and Brunel C. (2007). Anopheles Gambiae Mirnas as Actors of Defence Reaction Against Plasmodium Invasion. *Nucleic Acids Res.* 35 (20), 6953–6962. doi: 10.1093/nar/gkm686

Wirtz R. A., Burkot T. R., Graves P. M., and Andre R. G. (1987). Field Evaluation of Enzyme-Linked Immunosorbent Assays for Plasmodium Falciparum and

Plasmodium Vivax Sporozoites in Mosquitoes (Diptera: Culicidae) From Papua New Guinea. *J. Med. Entomol.* 24 (4), 433–437. doi: 10.1093/jmedent/24.4.433

Xue X., Zhang Q., Huang Y., Feng L., and Pan W. (2008). No MiRNA Were Found in Plasmodium and the Ones Identified in Erythrocytes Could Not be Correlated With Infection. *Malar. J.* 7, 47. doi: 10.1186/1475-2875-7-47

Zakama A. K., Ozarslan N., and Gaw S. L. (2020). Placental Malaria. *Curr. Trop. Med. Rep.* 2020, 1–10. doi: 10.1007/s40475-020-00213-2

Zheng W., Yao L., Teng J., Yan C., Qin P., Liu G., et al. (2018). Lateral Flow Test for Visual Detection of Multiple Micrornas. *Sens Actuators B Chem.* 264, 320–326. doi: 10.1016/j.snb.2018.02.159

Zoller T., Naucke T. J., May J., Hoffmeister B., Flick H., Williams C. J., et al. (2009). Malaria Transmission in Non-Endemic Areas: Case Report, Review of the Literature and Implications for Public Health Management. *Malar. J.* 8, 71. doi: 10.1186/1475-2875-8-71

Conflict of Interest: The authors declare that the research was conducted in the absence of any commercial or financial relationships that could be construed as a potential conflict of interest.

Publisher's Note: All claims expressed in this article are solely those of the authors and do not necessarily represent those of their affiliated organizations, or those of the publisher, the editors and the reviewers. Any product that may be evaluated in this article, or claim that may be made by its manufacturer, is not guaranteed or endorsed by the publisher.

frontiers in Cellular and Infection Microbiology

ORIGINAL RESEARCH
published: 17 January 2022
doi: 10.3389/fcimb.2021.804186

Elucidating Spatially-Resolved Changes in Host Signaling During *Plasmodium* Liver-Stage Infection

Elizabeth K. K. Glennon[1], *Tinotenda Tongogara*[1,2], *Veronica I. Primavera*[1], *Sophia M. Reeder*[1], *Ling Wei*[1] *and Alexis Kaushansky*[1,3,4,5*]

[1] Seattle Children's Research Institute, Center for Global Infectious Disease Research, Seattle, WA, United States, [2] Grinnell College, Grinnell, IA, United States, [3] Department of Global Health, University of Washington, Seattle, WA, United States, [4] Department of Pediatrics, University of Washington, Seattle, WA, United States, [5] Brotman Baty Institute for Precision Medicine, Seattle, WA, United States

OPEN ACCESS

Edited by:
Maria Bernabeu,
European Molecular Biology Laboratory, Spain

Reviewed by:
Rebecca Tweedell,
St. Jude Children's Research Hospital, United States
Varadharajan Sundaramurthy,
National Centre for Biological Sciences, India

***Correspondence:**
Alexis Kaushansky
alexis.kaushansky@seattlechildrens.org

Specialty section:
This article was submitted to Parasite and Host, a section of the journal Frontiers in Cellular and Infection Microbiology

Received: 29 October 2021
Accepted: 21 December 2021
Published: 17 January 2022

Citation:
Glennon EKK, Tongogara T, Primavera VI, Reeder SM, Wei L and Kaushansky A (2022) Elucidating Spatially-Resolved Changes in Host Signaling During Plasmodium Liver-Stage Infection. Front. Cell. Infect. Microbiol. 11:804186. doi: 10.3389/fcimb.2021.804186

Upon transmission to the human host, *Plasmodium* sporozoites exit the skin, are taken up by the blood stream, and then travel to the liver where they infect and significantly modify a single hepatocyte. Low infection rates within the liver have made proteomic studies of infected hepatocytes challenging, particularly *in vivo*, and existing studies have been largely unable to consider how protein and phosphoprotein differences are altered at different spatial locations within the heterogeneous liver. Using digital spatial profiling, we characterized changes in host signaling during *Plasmodium yoelii* infection *in vivo* without disrupting the liver tissue. Moreover, we measured alterations in protein expression around infected hepatocytes and identified a subset of $CD163^{+}$ Kupffer cells that migrate towards infected cells during infection. These data offer the first insight into the heterogeneous microenvironment that surrounds the infected hepatocyte and provide insights into how the parasite may alter its milieu to influence its survival and modulate immunity.

Keywords: plasmodium, liver stage, mouse model, spatial profiling, kupffer cell

INTRODUCTION

Upon introduction to the human host by the bite of an infectious mosquito, *Plasmodium* parasites migrate to the liver where they invade a hepatocyte and proceed to develop and replicate. Once parasites complete their development within the liver, thousands of individual merozoites egress from the host hepatocyte and migrate to the bloodstream where they invade erythrocytes and initiate the symptomatic blood stage of infection. The liver is often discussed as a uniform organ, however, factors such as oxygen and nutrient gradients lead to diverse cellular phenotypes and the formation of niches within the tissue (Kietzmann, 2017; Gola et al., 2021). *Plasmodium* parasites traverse multiple hepatocytes before invading one (Mota et al., 2001; Coppi et al., 2007; Loubens et al., 2021) and preferentially invade both particular liver zones (Yang et al., 2021) and hepatocytes with specific phenotypes, such as high ploidy and particular surface receptor compositions (Austin et al., 2014; Kaushansky et al., 2015a). In addition to selecting particular hepatocytes for invasion,

parasites modify the host cell throughout their development within the liver, including cell size (Balasubramanian et al., 2019), microtubule and organelle organization (Vijayan et al., 2020), and signaling cascades (Kaushansky et al., 2013a; Glennon et al., 2019).

The liver stage (LS) is a substantial bottleneck in *Plasmodium* infection, making it an attractive point for intervention. Attrition in parasite numbers occurs between injection at the skin, invasion of hepatocytes, and completion of development within the liver (Amino et al., 2006). Heterogeneity among hepatocytes within and between individuals can exacerbate this attrition; susceptibility between even closely related mouse strains varies dramatically (Kaushansky et al., 2015b), and the ability of hepatocytes to support *Plasmodium falciparum* and *Plasmodium vivax* infection varied extensively between individual human donors (Roth et al., 2018). Experiments with genetically attenuated parasites demonstrated that parasites that successfully invade but die before completing LS infection can induce immunity and reduce susceptibility to subsequent infection (Vaughan and Kappe, 2017).

Several global studies have been conducted to understand alterations that occur during LS infection which may be important for the maintenance of infection. Transcriptomic studies have demonstrated extensive changes in host gene expression that vary over the course of infection, however concordance among these studies has been low, perhaps due to differences in hepatocyte origin and time needed to sort infected cells (Albuquerque et al., 2009; LaMonte et al., 2019). We used reverse phase protein array (RPPA) to evaluate changes in host protein and post-translational modifications in an *in vitro* model of *Plasmodium yoelii* infection (Kaushansky et al., 2013a), and to identify proteins that are expressed proteins that are expressed at different levels between hepatocyte populations of differential susceptibility to LS infection (Dembele et al., 2019; Glennon et al., 2019). Several proteins and processes that were identified as altered in infected cells were also found to be important for LS infection [reviewed in (Glennon et al., 2018)]. A small RPPA screen of infected hepatocytes revealed a suppression of p53 levels which was then found to be critical for maintenance of LS infection *in vitro* and *in vivo* (Kaushansky et al., 2013a; Kain et al., 2020). RNA-sequencing of infected hepatocytes revealed an increase in expression of aquaporin-3 (AQP3) and follow-up studies identified AQP3 as essential for infection and implicated it in nutrient acquisition (Posfai et al., 2018). Multiple approaches have been used to elucidate functional regulators of LS infection *in vitro*, including screens based on siRNA, CRISPR/Cas9, and kinase regression (Prudencio et al., 2008; Arang et al., 2017; Raphemot et al., 2019). However, large-scale proteomic studies of liver-stage infection, particularly *in vivo*, have been hindered by low infection rates, on the order of 1% *in vitro* and 0.01% *in vivo* (Prudencio et al., 2011). Additionally, *in vivo* studies traditionally involve sorting infected from uninfected cells and pooling all uninfected cells together, thereby losing the ability to link parasite biology to its microenvironment, or heterogeneity among uninfected cells to their spatial distribution within the liver and position relative to the infected cell.

RESULTS

To interrogate differences in host cell signaling in intact *Plasmodium*-infected liver tissue we used Digital Spatial Profiling (DSP). DSP interrogates levels of total and phosphorylated proteins in user-defined regions of fixed tissue (Beechem, 2020), thereby preserving spatial information and limiting sample processing that could induce artificial changes. To date, DSP has primarily been used to study heterogeneity within the tumor microenvironment, which has been strongly linked to disease progression and treatment outcomes (Stewart et al., 2020; Wang et al., 2021). Briefly, liver sections are scanned and regions of interest (ROIs) are selected based on staining with fluorescent markers. Slides are incubated with one of several panels of antibodies bound with a photocleavable linker to unique oligonucleotide barcode tags. UV light is shone on the defined ROIs, cleaving the oligo tags from bound antibodies which are collected and quantified using the nCounter system (**Figure 1A**). We infected BALB/c mice with 1 million *P. yoelii* sporozoites and allowed the infection to proceed for 44 hours. Liver sections (4 μm thick) from 7 infected and 8 uninfected mice were stained using an antibody directed against parasite protein *Py*HSP70 that had been covalently linked to Alexa Fluor 488. In parallel with fluorescent staining, liver sections were also incubated with a panel of 42 oligo-tagged antibodies against a variety of host proteins and/or post-translational modifications (**Table S1A**). Slides were imaged and pooled ROIs that encompassed five infected cells (~50 μm diameters) or corresponding uninfected regions were identified (**Figures 1A, B**). Oligos were cleaved and collected from ROIs using the GeoMx Digital Spatial Profiler for quantification. We observed host proteins/post-translational modifications that were both up- and down-regulated in infected regions compared to uninfected mice (**Figure 1C**), some of which have been previously identified as altered upon, or important for, infection (**Table S1A**) (Kaushansky et al., 2013a; Kaushansky et al., 2013b; Douglass et al., 2015; Boonhok et al., 2016; Arang et al., 2017; Glennon et al., 2019; Sharma et al., 2021). Because we conducted multiple DSP runs with tissues on multiple slides, we wanted to compare the reproducibility of our results and identify the contribution of run-to-run variation to the observed variability. Liver sections from infected and uninfected mice were evenly distributed across slides and runs. Comparisons of the fold change in protein levels (infected over uninfected) between two runs (**Figure S1A**), as well as between two slides within a single run (**Figure S1B**), all gave strong linear correlations, suggesting the data from multiple experiments are comparable. Interestingly, the slope of the line between two separate runs (**Figure S1A**) was greater than one, suggesting that comparisons of the magnitude of change between runs should be interpreted with caution.

We next asked if we could reliably detect changes in host protein levels in single infected cells by DSP. We hypothesized that the enlarged size of infected hepatocytes at 44hpi (approximately 50μm in diameter) might allow us to reliably detect changes in host proteins at the single cell level. The same panel of antibodies (**Table S1A**) was used to detect host protein levels in single infected-cell ROIs from a single infected mouse and in identical

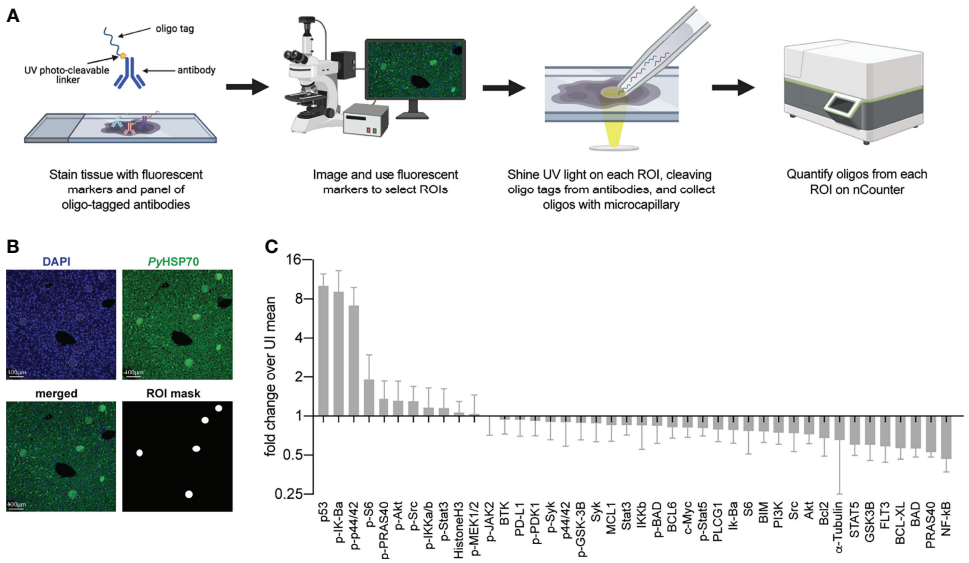

FIGURE 1 | Digital Spatial Profiling facilitates evaluation of proteins and post-translational modifications in *Plasmodium yoelii* infected tissue. **(A)** Schematic of DSP methodology. **(B)** Representative images of fluorescent staining of liver sections from uninfected or *P. yoelii*-infected mice at 44hpi. Parasites are stained with *Py*HSP70 in green and DAPI is shown in blue. Data were pooled from regions of interest indicated by white circles. **(C)** Signal from *P. yoelii*-infected mice normalized to ROI area and to the average signal from uninfected mice. Error bars indicate standard deviation. n = 7-8 mice per group with one pooled ROI measured from each mouse.

sized ROIs encompassing roughly 10 uninfected cells from a single uninfected mouse. Plotting the average of multiple infected single ROIs against the infected pooled ROI, for each antibody, gave a strong linear correlation (**Figure S1C**). The same was found for the comparable uninfected ROIs (**Figure S1D**), suggesting we have sufficient resolution to detect changes in host protein levels within single infected cells for these enlarged, infected cells. Upon examining the fold change between infected and uninfected single ROIs we observed a high degree of similarity between our pooled and single ROIs. The same top four proteins were seen in both pooled and single ROIs (**Figure 1A** and **Figure 2A**), suggesting that the increase detected in the pooled ROIs was not due to a small population of high-expressing cells but may in fact be a feature of multiple infected hepatocytes. As an orthologous approach, we used immunofluorescent microscopy to evaluate several proteins that exhibited differential levels in infected and uninfected cells. Patterns of changes in protein levels between infected and uninfected ROIs were comparable as measured by DSP and by single fluorescent antibody staining (**Figures 2B, C** and **Figure S1E**). We observed localization of multiple host proteins within the parasitophorous vacuole. One possible explanation is nonspecific binding to parasite proteins, which cannot be ruled out using this approach. Another is uptake of host cell cytosol by the parasite, as has been described in blood stage *Plasmodium* parasites and in multiple stages of the related apicomplexan parasite *Toxoplasma gondii* (Hanssen et al., 2012; Dou et al., 2014; Jonscher et al., 2019; Kannan et al., 2021). Distinguishing between these two possibilities, and further exploring the potential for cytosol uptake by the liver stage parasite, is an interesting area for future study.

We used the ability to make measurements in single infected cells to ask how host protein levels varied in single infected cells when compared to uninfected ROIs (**Figure 2D** and **Table S2**). We reasoned that proteins that exhibited substantially less variation between infected cells might represent features that are selected or tuned by the parasite to facilitate its survival and/or development. When examining the difference in variation between infected and uninfected ROIs for our panel of antibodies, we observed a trend towards increased variation in infected ROIs (**Figure 2D**). This is likely explained by the masking of single cell variation within the uninfected ROI, which encompasses roughly ten cells. Despite the skewedness of the data, several total and phosphorylated proteins (p-Src, NF-kB, IKKb, and p-Stat5) exhibited more variation in the uninfected ROI than in single infected cells (> 90th percentile) (**Figure 2D**). While data from more individual cells is required for a robust assessment of the distribution of given host signals, these data can be used for hypothesis generation. To investigate whether proteins with less variation in infected cells might act as part of a connected network, we reconstructed a phosphosignaling network using a database of known kinase target sequences (**Figure 2E**). Network reconstruction revealed that proteins with lower variation in infected cells can directly interact with each other *via* phosphorylation, suggesting they might regulate a common process important for infection and could be a target of parasite selection and/or manipulation. Of particular interest, the two kinases, Src and IKKb, were predicted to regulate LS infection; we have previously shown that shRNA-mediated knockdown of IKBKB reduces parasite numbers *in vitro* (Arang et al., 2017). Increased variation in infected cells could be due to

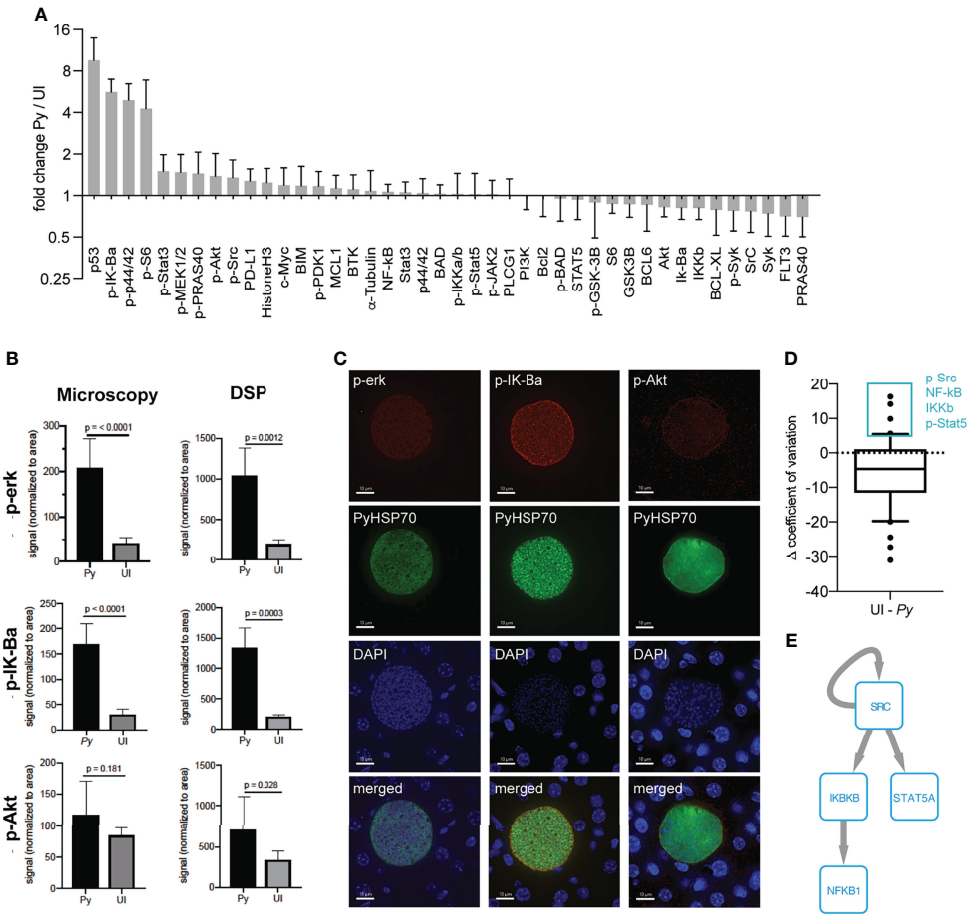

FIGURE 2 | Single infected hepatocytes produce sufficient signal for detection by DSP. **(A)** Signal from 9 infected cells from a single *P. yoelii*-infected mouse normalized to region of interest (ROI) area and to the average signal from 6 uninfected cell regions from a single uninfected mouse. Error bars indicate standard deviation. **(B)** ROI-area-normalized signal from single infected and uninfected ROIs as measured by DSP (from panel **A**) and single antibody staining fluorescent microscopy (n = 6 ROIs each from a single infected or uninfected mouse). **(C)** Representative images of infected cells were taken at a total magnification of 400x at 44hpi. **(D)** Difference in coefficient of variation between uninfected and single infected ROIs (from panel **A**) for each antibody. Box plot encompasses 10th-90th percentile. Antibodies within the 90th percentile which showed less variation in infected (*Py*) than in uninfected ROIs are boxed in blue. **(E)** Phosphosignaling network constructed from proteins with lower variation in infected ROIs. Arrows indicate direct phosphorylation events.

host cell and/or parasite-intrinsic heterogeneity, or due to the influence of different local microenvironments within the liver. These network-level hypotheses represent interesting areas for future investigation.

In addition to investigating signaling within the infected cells, we also asked how and if the environment that surrounds the parasite differed from more parasite-distal areas within the liver. Using concentric ring ROIs matched with each LS parasite, we measured protein levels in infected cells, proximal uninfected cells (Ring1), and distal uninfected cells (Ring2) surrounding each parasite (**Figure 3A**). In addition to the original antibody panel, we included a second panel encompassing proteins expressed on various immune cells (**Table S1B**). Protein levels in Ring1 and Ring2 were compared to those in their paired infected ROI and fell into clusters based on spatial patterns of relative expression (**Figures 3B, C** and **Table S3**). We were particularly interested in proteins with higher levels in Ring1 compared to Ring2 (**Table S4**) and theorized that these might be indicative of either (1) immune cell infiltration towards the infected hepatocyte, (2) selection of a cellular niche on a fine scale, or (3) neighboring cells responding to signals emanating out from the infected cell. Of the proteins with significantly higher levels in Ring1 compared to Ring2, several immune cell surface markers, all of which have been described on macrophages (PD-L1, B7-H3, CD68, CD163) (Krenkel and Tacke, 2017; Mao et al., 2017; Sun et al., 2018), were the most heavily upregulated (**Table S4**), leading us to investigate the distribution of macrophages around the parasite.

Macrophages populations within the liver can be resident or monocyte-derived. Kupffer cells, the resident liver macrophage, are the most prevalent non-parenchymal cell in the liver, making up about 35% of total cells (Wake et al., 1989). To investigate the distribution of Kupffer cells around infected hepatocytes, we stained liver sections with the Kupffer cell marker CLEC4F (Scott

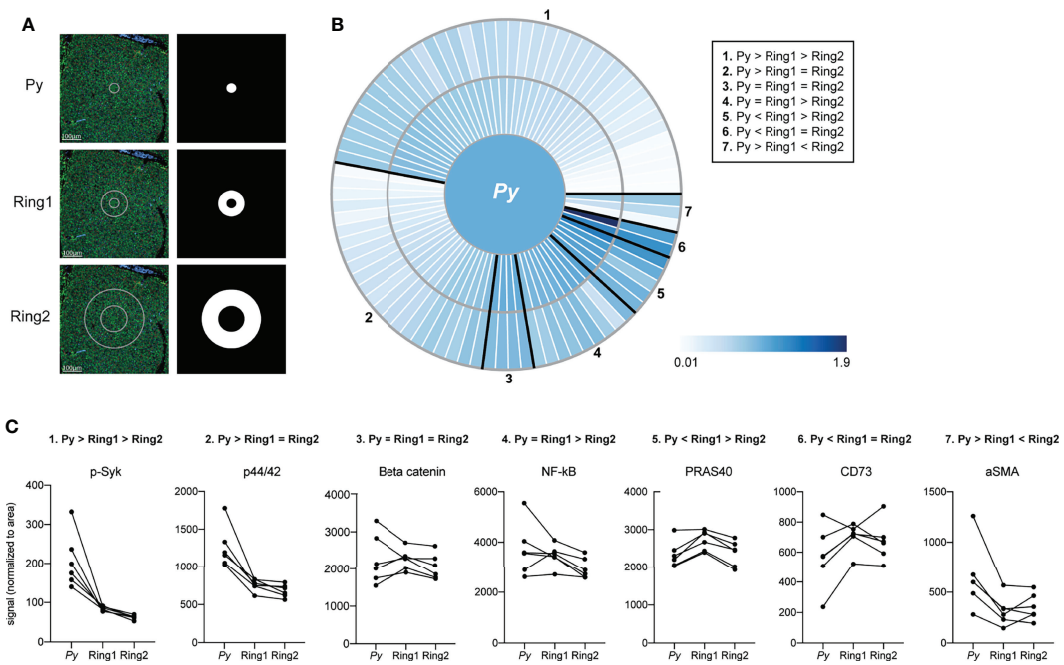

FIGURE 3 | Signals are altered in rings surrounding *Plasmodium*-infected hepatocytes. **(A)** Representative images of fluorescent staining of liver sections and region of interest (ROI) masks. **(B)** Heat maps showing fold change in protein levels between ring ROIs. Signal was normalized to ROI area and to the infected cell ROI, set at 1. Proteins showing similar relative patterns of expression across rings are grouped together and outlined in black. **(C)** Area normalized signal of antibodies illustrative of each spatial pattern. Lines connect matched infected cell and ring ROIs. n= 6 matched ROI sets from a single mouse.

et al., 2016; Krenkel and Tacke, 2017; Guillot and Tacke, 2019) and visualized liver stage parasites using DAPI (**Figures 4A–C**). We observed an increase in CLEC4F^{+} cells surrounding the parasite, with elevated density in Ring 1 compared to Ring 2, bystander cells within the same liver, and an identical-sized area of tissue within uninfected animals (**Figure 4D**). Interestingly, CLEC4F^{+} Kupffer cells often appear to wrap themselves around the LS-infected hepatocyte (**Figure 4B**). We then asked if high Kupffer cell density around infected cells at 44 hpi could be due to selection of an existing microenvironment at the time of hepatocyte invasion, or due to cells migrating to the site after infection had been established. Although often referred to as "resident", Kupffer cells have been shown to migrate along sinusoids within the liver (mean of 4.6μm/min) (MacPhee et al., 1992). When we quantified Kupffer cells around *P. yoelii* parasites in livers collected 24 hpi, we observed no statistically significant difference between the number of cells in Ring1 and Ring2 (**Figure 4E**). Because parasites are much smaller at 24hpi than 44hpi, with average diameters of 10μm and 45μm respectively, we also measured Kupffer cell distance from the parasite membrane. The most notable difference in distribution between 24 and 44hpi was the increase in Kupffer cell density within 40μm of the parasite membrane (**Figure 4F**). To further explore the hypothesis that the parasite is surrounded by Kupffer cells that have migrated to Ring 1 between 24 and 44hpi, rather than a shifting of cells due to the increase in hepatocyte mass that occurs as a result of LS growth, we compared the average number of Kupffer cells within 5μm from the membrane of the 44h parasite and 22.5μm from the membrane of the 24h parasite (55μm diameter ROIs) (**Figure S3**). Despite the increased potential area that could be occupied by Kupffer cells within the 24h ROI due to the smaller volume occupied by the parasite, there were ~4.4x more Kupffer cells within the 44h ROI. This difference was maintained when the ROI diameter was expanded to 65μm (**Figure S3**), indicating that the increase in Kupffer cell density at 44hpi is not due to the expansion of the parasite towards pre-existing cells within close proximity.

Finally, to evaluate if a Kupffer cell dense region was selected as part of the sporozoite traversal process that occurs prior to hepatocyte entry, we utilized the spect2- parasite strain. Wild type parasites enter the liver through a hepatocyte, Kupffer cell, or liver endothelial cell, and then traverse through several hepatocytes using a transient vacuole before finally invading a final hepatocyte within a parasitophorous vacuole (Mota et al., 2001; Frevert et al., 2005; Tavares et al., 2013). Spect2^{-} parasites that do not successfully invade are phagocytosed by Kupffer cells or fail to egress from their transient vacuole and are eliminated by host cell lysosomes (Ishino et al., 2005; Risco-Castillo et al., 2015; Yang et al., 2017). This inability to traverse multiple hepatocytes limits their ability to travel through many cells; this may impact the parasite's ability to select a particular local microenvironment. We infected mice with the spect2^{-} *P. yoelii* strain and measured Kupffer cell density at 44hpi. The pattern of Kupffer cell density around infected hepatocytes was maintained

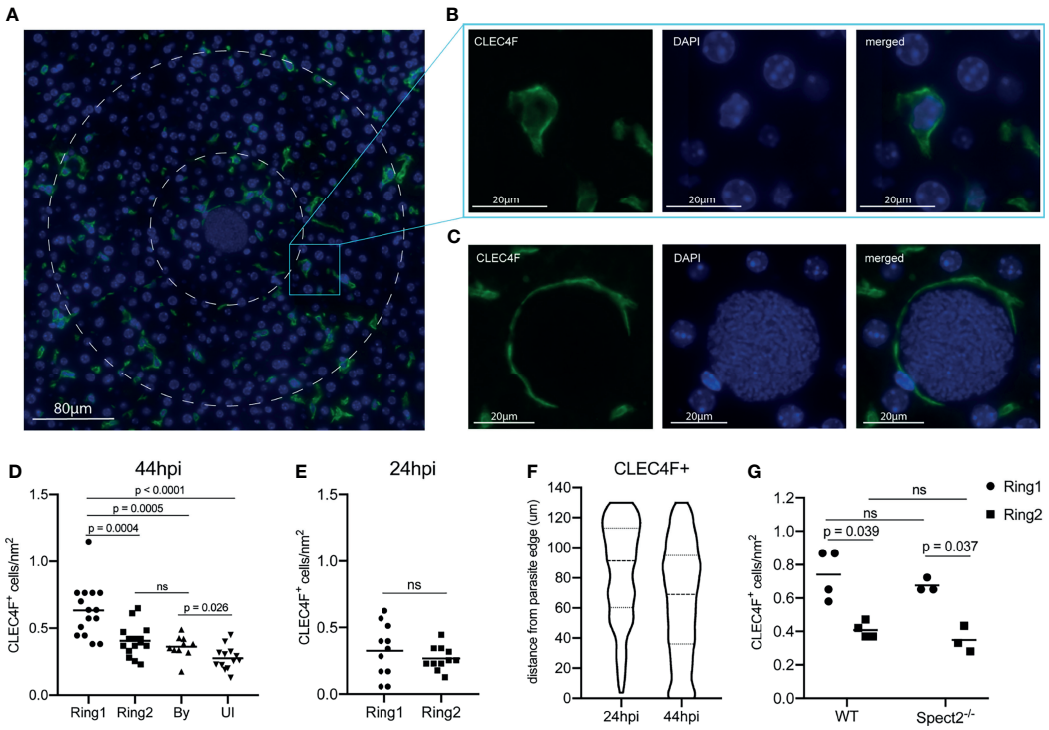

FIGURE 4 | A high density of macrophages surrounds *Plasmodium* infected hepatocytes. **(A)** Representative image of CLEC4F$^+$ staining within an infected liver. Nuclear DAPI staining is shown in blue, CLEC4F in green. Ring1 and Ring2 outer boundaries are indicated by dashed white circles. **(B)** CLEC4F staining of a single cell within Ring2 **(C)** Representative image of a CLEC4F$^+$ cell in close proximity to a parasite at 44hpi. **(D)** Number of CLEC4F$^+$ cells normalized by area in Ring1, Ring2, bystander (By) tissue, and uninfected (UI) tissue at 44hpi. 3-6 matched ROI sets were counted from each of three mice. **(E)** Number of CLEC4F$^+$ cells normalized by area in Ring1 and Ring2 at 24hpi. **(F)** Violin plot showing distribution of CLEC4F$^+$ cells binned by distance from parasite edge at 24 and 44hpi. **(G)** Levels of CLEC4F$^+$ cells in Ring1 and Ring2 around wild type (WT) and Spect2$^{-/-}$ parasites at 44hpi. ns, not significant.

for spect2$^-$ infected livers (**Figure 4G**), indicating that cell traversal does not influence Kupffer cell density around the infected cell.

We next sought to investigate the molecular characteristics of parasite-surrounding Kupffer cells. We revisited the DSP data (**Figure 3** and **Table S4**), and calculated pairwise Pearson's correlation coefficients between area normalized signal in Ring1 for all antibodies that were upregulated in Ring1 when compared to Ring2 (Groups 1,4 and 5, **Figure 3C**). We reasoned that if levels of two or more of these proteins correlated strongly with each other they might be linked to a particular cell type or process that distinguishes the microenvironment that surrounds infected hepatocytes. Using Pearson's correlation coefficients, we identified subsets of proteins that correlated with each other (**Figure S2**). The strongest correlations were between B7H3, CD163, and Src, all of which are expressed by Kupffer cells and have been linked to tolerogenic M2 polarization of macrophages, particularly within the tumor microenvironment (Sun et al., 2012; Kang et al., 2015; Mao et al., 2017; Ge and Ding, 2020).

We asked if the correlated proteins were expressed in overlapping populations of cells in Ring1 and Ring2. We found that CD163 was exclusively, and B7H3 almost exclusively, expressed on CLEC4F$^+$ cells (**Figures 5A, B**). We also stained for PD-L1, which was part of both antibody panels and consistently upregulated in Ring1 compared to Ring2 but did not correlate with B7H3 and CD163. Of note, though they showed similar trends when averaged across multiple ROIs (**Table S4**), the two PD-L1 antibodies did not correlate well with each other (**Figure S2**). This could be due to differences between the two tissue sections that were used for each antibody panel or to different binding efficiencies of the two antibodies which are not identical. PD-L1 was found on both CLECF4$^+$ and CLEC4F$^-$ cells within Ring 1, with over 60% of PD-L1$^+$ cells not expressing CLEC4F (**Figures 5A, B**). This is consistent with its lack of correlation with CD163 and B7H3, as well as published studies demonstrating PD-L1 expression on a variety of immune cell types (Wu et al., 2019). B7H3$^+$ and PD-L1$^+$ Kupffer cells were very rare, 1.6% and 2.9% of all CLEC4F$^+$ cells, respectively, however CD163$^+$ cells were abundant and represented a majority of CLEC4F$^+$ cells (**Figure 5C**).

Quantification of CD163$^+$ Kupffer cells revealed that more CD163$^+$CLEC4F$^+$, but not CD163$^-$CLEC4F$^+$, cells were present in Ring1 compared to Ring2, bystander, and uninfected tissue regions at 44hpi (**Figures 5D, E**). Interestingly, increased numbers of CD163$^+$ Kupffer cells were not found around *P. yoelii* parasites in livers collected 24 hpi (**Figure 5F**), but CLEC4F$^+$CD163$^-$ cells were slightly elevated in Ring1 compared to Ring2 (**Figure 5G**). Finally, we compared CD163 expression in Ring1 and Ring2 around WT

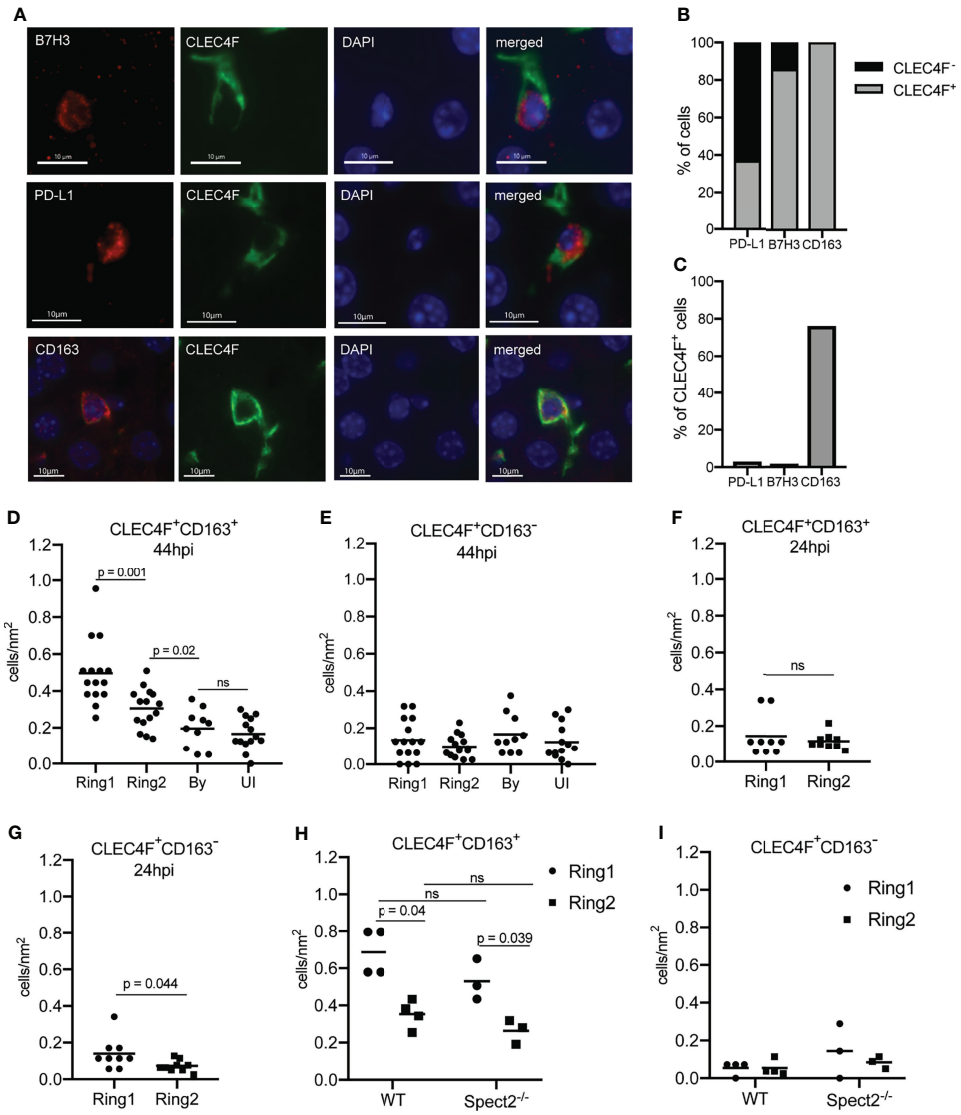

FIGURE 5 | Tolerogenic macrophages migrate to surround *Plasmodium* infected hepatocytes. **(A)** Representative images of fluorescent staining of infected tissue for B7H3, PD-L1, and CD163. **(B)** Proportion of PD-L1$^+$, B7H3$^+$, and CD163$^+$ cells within rings around infected cells that were CLEC4F$^+$ or CLEC4F$^-$. **(C)** Proportion of CLEC4F+ cells within rings around infected cells that were PD-L1$^+$, B7H3$^+$, or CD163$^+$. **(D)** Number of CD163$^+$CLEC4F$^+$ and **(E)** CD163$^-$CLEC4F$^+$ cells normalized by area in Ring1, Ring2, bystander (By) tissue, and uninfected (UI) tissue at 44hpi. 3-6 matched ROI sets were counted from each of three mice. **(F)** Number of CD163$^+$CLEC4F$^+$ and **(G)** CD163$^-$CLEC4F$^+$ cells normalized by area at 24hpi. **(H)** Number of CD163$^+$CLEC4F$^+$ and **(I)** CD163$^-$CLEC4F$^+$ cells normalized by area, in Ring1 and Ring2 around wild type (WT) and Spect2$^{-/-}$ parasites at 44hpi. ns, not significant.

and spect2– parasites. CLEC4F$^+$CD163$^+$ cells were present at a higher density in Ring1 compared to Ring2 in both WT and Spect2-infected livers, with no difference between parasite strains (**Figure 5H**). CLEC4F$^+$CD163$^-$ cell levels were not significantly different between rings or between parasite strains (**Figure 5I**).

DISCUSSION

In this study we utilized digital spatial profiling to characterize host total and phosphorylated proteins in and around *Plasmodium*-infected hepatocytes *in vivo*. Doing these analyses while preserving the tissue architecture allowed us to link a specific microenvironment to infected cells. Probing a large panel of proteins simultaneously in the same tissue regions allowed us to investigate the molecular characteristics of parasite-surrounding cells. Importantly, this is challenging to do with conventional approaches as it requires candidate-based investigation into specific candidate markers that may or may not be relevant for the cell type of interest. By measuring changes in host proteins in concentric rings around infected hepatocytes and correlations between these proteins we identified an influx of

$CD163^+$ Kupffer cells towards the parasite during the second half of liver stage infection.

Kupffer cells originate from fetal liver erythromyeloid progenitors and in the adult liver, under resting conditions, their populations are self-renewing independent of bone marrow-derived cells (Gomez Perdiguero et al., 2015). Upon Kupffer cell depletion, infiltrating circulating monocytes differentiate into Kupffer cells starting 96 hours post-depletion (Scott et al., 2016). Notably, monocyte-derived Kupffer cells do not begin expressing CLEC4F until between 72-96 hours post-depletion (Scott et al., 2016), indicating that the increase in $CLEC4F^+$ cells we observed near the parasite between 24 and 44hpi is highly unlikely to be due to differentiation of infiltrating monocytes. More likely, resident $CLEC4F^+$ cells that have migrated towards the parasite.

Macrophages exist along a continuum of states that are often described as ranging from pro-inflammatory (M1) to tolerogenic (M2) (Guillot and Tacke, 2019). Alterations of Kupffer cells upon sporozoite exposure are consistent with a model that parasites manipulate Kupffer cells to produce a tolerogenic environment for their development within the liver. Kupffer cell exposure to sporozoites has been shown to suppress respiratory burst (Usynin et al., 2007), suppress antigen presentation (Steers et al., 2005), and skew cytokine production upon pro-inflammatory stimulation towards an anti-inflammatory response (Klotz and Frevert, 2008). Co-culture of $CD8^+$ T cells with sporozoite-stimulated monocyte-derived macrophages also produced less IFNγ (Winkel et al., 2020). Most of these studies were conducted with prolonged co-incubation of sporozoites and macrophages *in vitro*. Several functional studies have been conducted in which Kupffer cells are depleted before sporozoite infection (Vreden et al., 1993; Baer et al., 2007), but the importance of these cells for infection maintenance are confounded by the effects of depletion on hepatocyte invasion.

CD163 is commonly utilized as a tolerogenic macrophage marker (Guillot and Tacke, 2019), however it may also play a functional role in maintenance of LS infection. CD163 is a scavenger receptor expressed on monocytes and macrophages that binds and facilitates the internalization and clearance of hemoglobin-haptoglobin (HbHp) complexes, thereby protecting the liver from oxidative damage (Van Gorp et al., 2010). Binding of HbHp complexes promotes the expression of heme oxygenase-1 (HO-1) which degrades the Hb heme subunit, producing biliverdin, iron, and carbon dioxide. Although not part of the panel we interrogated in this study, HO-1 has been shown to be upregulated in macrophages and hepatocytes during *Plasmodium* LS infection and to be critical for infection maintenance (Epiphanio et al., 2008). Of particular interest, HO-1 was not found to be essential for *Plasmodium* LS infection when hepatocytes are cultured alone *ex vivo*, suggesting its effect on nonparenchymal cells influences infection. Higher expression of CD163 on Kupffer cells has also been linked to greater phagocytic activity (He et al., 2009). Merozoite forms (often as 'packages' of parasites called merozomes) (Sturm et al., 2006) of the parasite exit the infected hepatocyte and enter the blood stream between 50-52 hpi. It is intriguing to speculate that the wrapping of Kupffer cells around infected hepatocytes (**Figure 4C**) late during infection could facilitate phagocytosis of the hepatocyte by Kupffer cells after merozoite exit. By regulating antigen presentation and inflammation around the infected cell microenvironment, Kupffer cells could be influencing the development of subsequent immunity. This could have long-reaching consequences not only for infection, but also for the development of whole parasite vaccines.

We are unable to determine from our data if $CD163^+$ Kupffer cells are infiltrating in towards the parasite, or if they begin expressing CD163 upon gaining their location near the infected cell, however the small increase in $CD163^-CLEC4F^+$ cells in Ring1 compared to Ring2 at 24 hpi (**Figure 5G**) supports the latter hypothesis. PD-L1 expression, which is increased in Ring1 compared to Ring2, has been shown to be induced in monocyte-derived macrophages in the skin upon exposure to *Plasmodium* sporozoites (Winkel et al., 2020). A portion of sporozoites are thought to cross and interact with Kupffer cells as they are entering the liver (Tavares et al., 2013), however, as no difference in $CD163^+$ Kupffer cell density was observed between WT parasites and $Spect2^-$ parasites, which are traversal deficient, we hypothesize that the increase in CD163 expression is not present prior to sporozoite invasion of hepatocytes.

By utilizing DSP we were able to measure host protein on a large scale in single infected hepatocytes *in vivo* without sorting cells and without dissociating cells from their microenvironment. While we cannot rule out non-specific binding of antibodies to parasite proteins, the minimal sample processing may better preserve the host cell condition compared to experiments that require hours of cell sorting, particularly in the case of post-translational modifications. Several of the proteins up-regulated in infected cells were phosphorylated, indicating increased activity: p-IK-Ba, p-S6, and p-Erk. Consistent with our results, Erk (MAPK1) activity was previously identified by our lab as important for maintenance of *P. yoelii* infection *in vitro* using a kinase inhibitor screen combined with a machine learning algorithm (Arang et al., 2017). Additionally, levels of p-S6 are higher in hepatocytes that are more susceptible to *Plasmodium* infection and in infected hepatocytes *in vitro*, although in the context of infection S6 phosphorylation is dysregulated from classical upstream activator p-Akt (Glennon et al., 2019). One surprising result was the increase seen in p53 levels in infected cells. *In vitro*, early during infection, P53 is suppressed in infected hepatocytes. Boosting levels of P53 efficiently eliminates liver stages parasites both *in vitro* and *in vivo*. The difference in time point (44h in this study, as opposed to 24h in previous *in vitro* studies) could explain the observed difference in p53 levels (Kaushansky et al., 2013a). It will be interesting to explore if the increase in p53 seen here at 44hpi represents a loss of regulation by the parasite as it shifts towards merozoite production and preparation for egress.

A very small number of parasites successfully invade hepatocytes and complete LS infection. This, and the extensive remodeling of infected hepatocytes, suggest *Plasmodium* parasites have substantial requirements of their host cells.

By identifying proteins/post-translational modifications that show very little variation among infected compared to uninfected cells, we may be able to identify specific targets or signaling nodes that are maintained within, or selected for, very narrow limits by the parasite. These factors could represent promising drug targets, as even small perturbations of these factors could have dire consequences for the developing LS parasite. Future studies might also explore the signaling perturbations that are altered in the context of liver stage parasites that do not complete development, as is the case with irradiated, drug-killed or genetically attenuated parasites. While this study is entirely focused on the rodent parasite *Plasmodium yoelii*, DSP is readily adaptable to the study of human-infectious species *Plasmodium falciparum* and *Plasmodium vivax* using a humanized mouse model (Vaughan et al., 2012; Mikolajczak et al., 2015) or other tissue models. Evaluating the spatially resolved host transcriptomic and proteomic responses that occur after infection, particularly in the context of the dormant *P. vivax* hypnozoite, may reveal novel biology regulating infection maintenance and development of immunity.

METHODS

Mosquito Rearing and Sporozoite Production

Female 6–8-week-old Swiss Webster mice (Envigo) were injected with blood stage *Plasmodium yoelii* 17XNL parasites. Infected mice were used to feed female *Anopheles stephensi* mosquitoes after gametocyte exflagellation was observed. Salivary gland sporozoites were isolated according to the standard procedures at days 14 or 15 post blood meal. Animal handling was conducted according to the Institutional Animal Care and Use Committee-approved protocols.

Mouse Infections

6-8-week-old female Balb/cAnN mice were purchased from Envigo. All mice were maintained in accordance with protocols approved by Seattle Children's Research Institute Institutional Animal Care and Use Committee (IACUC00502). Mice were infected by retro orbital injection with 100,000 or 1 million *P. yoelii* sporozoites. Livers from infected, or uninfected age-matched, mice were harvested at 24 or 44 hpi and fixed in 4% paraformaldehyde for 24 hours. Tissues were then paraffin embedded, cut into 4mm sections, and mounted on positively charged glass slides. Mounted liver slices were then used for digital spatial profiling or immunofluorescence staining.

Digital Spatial Profiling

Digital spatial profiling (DSP) was performed by NanoString Technologies using the GeoMx Digital Spatial profiler. For selecting regions of interest, slides were stained with DAPI and a fluorescent conjugated antibody against *Py*HSP70. Slides were simultaneously incubated with one of two pre-validated panels of 42-43 oligo-tagged antibodies (**Table S1**). Counts were normalized to an internal control (ERCC) and to ROI area. Data were not normalized to nucleus counts as *Plasmodium* parasites have been shown to preferentially invade highly polyploid hepatocytes (Austin et al., 2014). Traditional "housekeeping" proteins (RPS6, alpha-tubulin, histoneH3) within the antibody panels were also not used for normalization as they have either been previously identified to increase in infected cells, show cross-reactivity, or were upregulated in infected cells in our data (Mikolajczak et al., 2015; Glennon et al., 2019). Data normalized only to internal controls (ERCC) are available in **Tables S1**, **S3**. Data were analyzed by ANOVA with paired or unpaired multiple comparisons as appropriate. Our single infected-cell ROIs may encompass a portion of neighboring cells.

Immunofluorescence Staining

Slide-mounted liver slices were washed twice in xylene for 3 minutes followed by washes in 100%, 95%, 70% and 50% ethanol for 3 minutes each. Slides were then washed with DI water and heated to 90C for 30 minutes in 1% citrate-based antigen unmasking solution (Vector Laboratories) using a Biocare Medical Decloaking Chamber. Slides were washed with TBS-0.025% Tween (TBST) and then blocked for 4 hours in TBST containing 1.5% BSA and 15% goat serum (Sigma Aldrich). Slides were incubated in primary antibodies at 4C overnight. Following primary antibody staining, slides were washed with TBST and incubated with secondary antibodies and DAPI (1:3,000) for 1 hour at room temperature. Slides were washed with TBST and autofluorescence quenched using Vector TrueView (Vector Labs). Fluoromount G mounting media was used to preserve fluorescence signal. Primary antibodies were used at the following concentrations: *Py*Hsp70 1:1,000, *Py*CSP-488 1:500, p-p44/42 1:200 (Cell Signaling 4370), p-IK-Ba 1:200 (Cell Signaling 2850), p-Akt 1:100 (Cell Signaling 9271), CD163 1:500 (Proteintech 16646-1-AP), CLEC4F-647 1:100 (BioLegend 156804), PD-L1 1:200 (Cell Signaling 64988), B7H3 1:200 (Novus Bio NB600-1441). Secondary antibodies anti-mouse AlexaFluor-488, anti-rabbit AlexaFluor-594, and anti-rabbit AlexaFluor-647 (Invitrogen) were used at a 1:1,000 dilution.

Imaging and Quantification

Images (40X) were acquired using a DeltaVision Elite High Resolution Microscope. Z-stacks of 0.3μm thickness were taken for images encompassing infected and uninfected cells. For cell quantification within Ring ROIs 3x3 image panels were taken with a 60-pixel overlap. Images were stitched and deconvolved using the DeltaVision Softworx software and were visualized using Imaris software. ImageJ was used to quantify fluorescence intensity within defined ROIs. Distances from parasites to Kupffer cells were measured between nucleus centers, or from the parasite membrane to the Kupffer cell nucleus, using Imaris software. Only Kupffer cells with a visible, stained nucleus (DAPI) were included in counts.

The phosphosignaling network was reconstructed using PhosphoSitePlus®, a curated knowledgebase dedicated to

mammalian post-translational modifications (https://www.phosphosite.org) (Hornbeck et al., 2015).

DATA AVAILABILITY STATEMENT

The original contributions presented in the study are included in the article/**Supplementary Material**. Further inquiries can be directed to the corresponding author.

ETHICS STATEMENT

The animal study was reviewed and approved by Seattle Children's Research Institute Institutional Animal Care and Use Committee.

AUTHOR CONTRIBUTIONS

EG and AK designed experiments. EG, TT, and VP conducted experiments. Data analysis was done by EG, LW, TT, and SR. All authors contributed to writing and editing the manuscript.

FUNDING

This work was funded by grants R01GM101183, R21AI151344, and R01AI158719 from the National Institutes of Health to AK. SR is the recipient of T32 training grant 5T32HD007233-39 from the University of Washington and the National Institutes of Health.

ACKNOWLEDGMENTS

We would like to acknowledge Liuliu Pan and Yan Liang at NanoString Technologies for their assistance with our DSP runs. We thank Stefan Kappe for the gift of the PySpect2- parasite line.

SUPPLEMENTARY MATERIAL

The Supplementary Material for this article can be found online at: https://www.frontiersin.org/articles/10.3389/fcimb.2021.804186/full#supplementary-material

Supplementary Figure 1 | DSP results are reproducible across runs and between pooled and single ROIs. Average fold change between infected and uninfected ROIs for each antibody from **(A)** two independent DSP runs, and **(B)** two slides run at the same time. Data were analyzed by linear regression. **(C)** For each antibody the average area-normalized signal 9 single infected ROIs was plotted against that of one pooled infected ROI, all from the same mouse. **(D)** For each antibody the average area-normalized signal 9 single uninfected ROIs was plotted against that of one pooled uninfected ROI. Data were analyzed by linear regression. **(E)** Representative images of uninfected regions total magnification of 400x at 44hpi.

Supplementary Figure 2 | A subset of upregulated (phospho)proteins in proximity to *Plasmodium*-infected hepatocytes are correlated. **(A)** Heat map indicating the Pearson correlation coefficient for each pair of antibodies for those significantly upregulated in Ring1 compared to Ring2. Antibodies from multiple panels are identified as part of panel **(A)** or **(B)**. n = 6 matched ROI sets from a single mouse.

Supplementary Figure 3 | Growth of *Plasmodium* infected hepatocyte does not account for increased Kupffer cell density around cell. Kupffer cell density within circular ROIs of 55µm and 65µm around parasites at 24hpi and 44hpi. Parasites are shown as green circles. Length of lines is indicated in microns. Circles and rings are shown to scale. Kupffer cell density is shown as the mean from 3-4 parasites per mouse from 3 mice per time point.

REFERENCES

Albuquerque, S. S., Carret, C., Grosso, A. R., Tarun, A. S., Peng, X., Kappe, S. H., et al. (2009). Host Cell Transcriptional Profiling During Malaria Liver Stage Infection Reveals a Coordinated and Sequential Set of Biological Events. *BMC Genomics* 10, 270. doi: 10.1186/1471-2164-10-270

Amino, R., Thiberge, S., Martin, B., Celli, S., Shorte, S., Frischknecht, F., et al. (2006). Quantitative Imaging of Plasmodium Transmission From Mosquito to Mammal. *Nat. Med.* 12 (2), 220–224. doi: 10.1038/nm1350

Arang, N., Kain, H. S., Glennon, E. K., Bello, T., Dudgeon, D. R., Walter, E. N. F., et al. (2017). Identifying Host Regulators and Inhibitors of Liver Stage Malaria Infection Using Kinase Activity Profiles. *Nat. Commun.* 8 (1), 1232. doi: 10.1038/s41467-017-01345-2

Austin, L. S., Kaushansky, A., and Kappe, S. H. (2014). Susceptibility to Plasmodium Liver Stage Infection Is Altered by Hepatocyte Polyploidy. *Cell Microbiol.* 16 (5), 784–795. doi: 10.1111/cmi.12282

Baer, K., Roosevelt, M., Clarkson, A. B. Jr., van Rooijen, N., Schnieder, T., and Frevert, U. (2007). Kupffer Cells are Obligatory for Plasmodium Yoelii Sporozoite Infection of the Liver. *Cell Microbiol.* 9 (2), 397–412. doi: 10.1111/j.1462-5822.2006.00798.x

Balasubramanian, L., Zuzarte-Luis, V., Syed, T., Mullick, D., Deb, S., Ranga-Prasad, H., et al. (2019). Association of Plasmodium Berghei With the Apical Domain of Hepatocytes Is Necessary for the Parasite's Liver Stage Development. *Front. Cell Infect. Microbiol.* 9, 451. doi: 10.3389/fcimb.2019.00451

Beechem, J. M. (2020). High-Plex Spatially Resolved RNA and Protein Detection Using Digital Spatial Profiling: A Technology Designed for Immuno-Oncology Biomarker Discovery and Translational Research. *Methods Mol. Biol.* 2055, 563–583. doi: 10.1007/978-1-4939-9773-2_25

Boonhok, R., Rachaphaew, N., Duangmanee, A., Chobson, P., Pattaradilokrat, S., Utaisincharoen, P., et al. (2016). LAP-Like Process as an Immune Mechanism Downstream of IFN-Gamma in Control of the Human Malaria Plasmodium Vivax Liver Stage. *Proc. Natl. Acad. Sci. U. S. A.* 113 (25), E3519–E3528. doi: 10.1073/pnas.1525606113

Coppi, A., Tewari, R., Bishop, J. R., Bennett, B. L., Lawrence, R., Esko, J. D., et al. (2007). Heparan Sulfate Proteoglycans Provide a Signal to Plasmodium Sporozoites to Stop Migrating and Productively Invade Host Cells. *Cell Host Microbe* 2 (5), 316–327. doi: 10.1016/j.chom.2007.10.002

Dembele, L., Gupta, D. K., Dutta, B., Chua, A. C. Y., Sze, S. K., and Bifani, P. (2019). Quantitative Proteomic Analysis of Simian Primary Hepatocytes Reveals Candidate Molecular Markers for Permissiveness to Relapsing Malaria Plasmodium Cynomolgi. *Proteomics* 19 (19), e1900021. doi: 10.1002/pmic.201900021

Dou, Z., McGovern, O. L., Di Cristina, M., and Carruthers, V. B. (2014). Toxoplasma Gondii Ingests and Digests Host Cytosolic Proteins. *mBio* 5 (4), e01188–e01114. doi: 10.1128/mBio.01188-14

Douglass, A. N., Kain, H. S., Abdullahi, M., Arang, N., Austin, L. S., Mikolajczak, S. A., et al. (2015). Host-Based Prophylaxis Successfully Targets Liver Stage Malaria Parasites. *Mol. Ther.* 23 (5), 857–865. doi: 10.1038/mt.2015.18

Epiphanio, S., Mikolajczak, S. A., Goncalves, L. A., Pamplona, A., Portugal, S., Albuquerque, S., et al. (2008). Heme Oxygenase-1 is an Anti-Inflammatory Host Factor That Promotes Murine Plasmodium Liver Infection. *Cell Host Microbe* 3 (5), 331–338. doi: 10.1016/j.chom.2008.04.003

Frevert, U., Engelmann, S., Zougbede, S., Stange, J., Ng, B., Matuschewski, K., et al. (2005). Intravital Observation of Plasmodium Berghei Sporozoite Infection of the Liver. *PloS Biol.* 3 (6), e192. doi: 10.1371/journal.pbio.0030192

Ge, Z., and Ding, S. (2020). The Crosstalk Between Tumor-Associated Macrophages (TAMs) and Tumor Cells and the Corresponding Targeted Therapy. *Front. Oncol.* 10, 590941. doi: 10.3389/fonc.2020.590941

Glennon, E. K. K., Austin, L. S., Arang, N., Kain, H. S., Mast, F. D., Vijayan, K., et al. (2018). Opportunities for Host-Targeted Therapies for Malaria. *Trends Parasitol.* 34 (10), 843–860. doi: 10.1016/j.pt.2018.07.011

Glennon, E. K. K., Dankwa, S., Smith, J. D., and Kaushansky, A. (2019). Alterations in Phosphorylation of Hepatocyte Ribosomal Protein S6 Control Plasmodium Liver Stage Infection. *Cell Rep.* 26 (12), 3391–3399.e4. doi: 10.1016/j.celrep.2019.02.085

Gola, A., Dorrington, M. G., Speranza, E., Sala, C., Shih, R. M., Radtke, A. J., et al. (2021). Commensal-Driven Immune Zonation of the Liver Promotes Host Defence. *Nature* 589 (7840), 131–136. doi: 10.1038/s41586-020-2977-2

Gomez Perdiguero, E., Schulz, C., Busch, K., Azzoni, E., Crozet, L., et al. (2015). Tissue-Resident Macrophages Originate From Yolk-Sac-Derived Erythro-Myeloid Progenitors. *Nature* 518 (7540), 547–551. doi: 10.1038/nature13989

Guillot, A., and Tacke, F. (2019). Liver Macrophages: Old Dogmas and New Insights. *Hepatol. Commun.* 3 (6), 730–743. doi: 10.1002/hep4.1356

Hanssen, E., Hanssen, E., Knoechel, C., Dearnley, M., Dixon, M. W., Le Gros, M., Larabell, C., et al. (2012). Soft X-Ray Microscopy Analysis of Cell Volume and Hemoglobin Content in Erythrocytes Infected With Asexual and Sexual Stages of Plasmodium Falciparum. *J. Struct. Biol.* 177 (2), 224–232. doi: 10.1016/j.jsb.2011.09.003

He, Y., Sadahiro, T., Noh, S. I., Wang, H., Todo, T., and Chai, N. N. (2009). Flow Cytometric Isolation and Phenotypic Characterization of Two Subsets of ED2 (+) (CD163) Hepatic Macrophages in Rats. *Hepatol. Res.* 39 (12), 1208–1218. doi: 10.1111/j.1872-034X.2009.00528.x

Hornbeck, P. V., Zhang, B., Murray, B., Kornhauser, J. M., Latham, V., and Skrzypek, E. (2015). PhosphoSitePlus, 2014: Mutations, PTMs and Recalibrations. *Nucleic Acids Res.* 43 (Database issue), D512–D520. doi: 10.1093/nar/gku1267

Ishino, T., Chinzei, Y., and Yuda, M. (2005). A Plasmodium Sporozoite Protein With a Membrane Attack Complex Domain is Required for Breaching the Liver Sinusoidal Cell Layer Prior to Hepatocyte Infection. *Cell Microbiol.* 7 (2), 199–208. doi: 10.1111/j.1462-5822.2004.00447.x

Jonscher, E., Flemming, S., Schmitt, M., Sabitzki, R., Reichard, N., Birnbaum, J., et al. (2019). PfVPS45 Is Required for Host Cell Cytosol Uptake by Malaria Blood Stage Parasites. *Cell Host Microbe* 25 (1), 166–173.e5. doi: 10.1016/j.chom.2018.11.010

Kain, H. S., Glennon, E. K. K., Vijayan, K., Arang, N., Douglass, A. N., Fortin, C. L., et al. (2020). Liver Stage Malaria Infection is Controlled by Host Regulators of Lipid Peroxidation. *Cell Death Differ.* 27 (1), 44–54. doi: 10.1038/s41418-019-0338-1

Kang, F. B., Wang, L., Li, D., Zhang, Y. G., and Sun, D. X. (2015). Hepatocellular Carcinomas Promote Tumor-Associated Macrophage M2-Polarization via Increased B7-H3 Expression. *Oncol. Rep.* 33 (1), 274–282. doi: 10.3892/or.2014.3587

Kannan, G., Thaprawat, P., Schultz, T. L., and Carruthers, V. B. (2021). Acquisition of Host Cytosolic Protein by Toxoplasma Gondii Bradyzoites. *mSphere* 6 (1), e00934–20. doi: 10.1128/mSphere.00934-20

Kaushansky, A., Austin, L. S., Mikolajczak, S. A., Lo, F. Y., Miller, J. L., Douglass, A. N., et al. (2013a). Suppression of Host P53 Is Critical for Plasmodium Liver-Stage Infection. *Cell Rep.* 3 (3), 630–637. doi: 10.1016/j.celrep.2013.02.010

Kaushansky, A., Douglass, A. N., Arang, N., Vigdorovich, V., Dambrauskas, N., Kain, H. S., et al. (2013b). Malaria Parasite Liver Stages Render Host Hepatocytes Susceptible to Mitochondria-Initiated Apoptosis. *Cell Death Dis.* 4, e762. doi: 10.1038/cddis.2013.286

Kaushansky, A., Metzger, P. G., Douglass, A. N., Mikolajczak, S. A., Lakshmanan, V., Kain, H. S., et al. (2015a). Malaria Parasites Target the Hepatocyte Receptor EphA2 for Successful Host Infection. *Science* 350 (6264), 1089–1092. doi: 10.1126/science.aad3318

Kaushansky, A., Ye, A. S., Austin, L. S., Mikolajczak, S. A., Vaughan, A. M., Camargo, N., et al. (2015b). Susceptibility to Plasmodium Yoelii Preerythrocytic Infection in BALB/c Substrains is Determined at the Point of Hepatocyte Invasion. *Infect. Immun.* 83 (1), 39–47. doi: 10.1128/IAI.02230-14

Kietzmann, T. (2017). Metabolic Zonation of the Liver: The Oxygen Gradient Revisited. *Redox Biol.* 11, 622–630. doi: 10.1016/j.redox.2017.01.012

Klotz, C., and Frevert, U. (2008). Plasmodium Yoelii Sporozoites Modulate Cytokine Profile and Induce Apoptosis in Murine Kupffer Cells. *Int. J. Parasitol.* 38 (14), 1639–1650. doi: 10.1016/j.ijpara.2008.05.018

Krenkel, O., and Tacke, F. (2017). Liver Macrophages in Tissue Homeostasis and Disease. *Nat. Rev. Immunol.* 17 (5), 306–321. doi: 10.1038/nri.2017.11

LaMonte, G. M., Orjuela-Sanchez, P., Calla, J., Wang, L. T., Li, S., Swann, J., et al. (2019). Dual RNA-Seq Identifies Human Mucosal Immunity Protein Mucin-13 as a Hallmark of Plasmodium Exoerythrocytic Infection. *Nat. Commun.* 10 (1), 488. doi: 10.1038/s41467-019-08349-0

Loubens, M., Vincensini, L., Fernandes, P., Briquet, S., Marinach, C., and Silvie, O. (2021). Plasmodium Sporozoites on the Move: Switching From Cell Traversal to Productive Invasion of Hepatocytes. *Mol. Microbiol.* 115 (5), 870–881. doi: 10.1111/mmi.14645

MacPhee, P. J., Schmidt, E. E., and Groom, A. C. (1992). Evidence for Kupffer Cell Migration Along Liver Sinusoids, From High-Resolution In Vivo Microscopy. *Am. J. Physiol.* 263 (1 Pt 1), G17–G23. doi: 10.1152/ajpgi.1992.263.1.G17

Mao, Y., Chen, L., Wang, F., Zhu, D., Ge, X., Hua, D., et al. (2017). Cancer Cell-Expressed B7-H3 Regulates the Differentiation of Tumor-Associated Macrophages in Human Colorectal Carcinoma. *Oncol. Lett.* 14 (5), 6177–6183. doi: 10.3892/ol.2017.6935

Mikolajczak, S. A., Vaughan, A. M., Kangwanrangsan, N., Roobsoong, W., Fishbaugher, M., Yimamnuaychok, N., et al. (2015). Plasmodium Vivax Liver Stage Development and Hypnozoite Persistence in Human Liver-Chimeric Mice. *Cell Host Microbe* 17 (4), 526–535. doi: 10.1016/j.chom.2015.02.011

Mota, M. M., Pradel, G., Vanderberg, J. P., Hafalla, J. C., Frevert, U., Nussenzweig, R. S., et al. (2001). Migration of Plasmodium Sporozoites Through Cells Before Infection. *Science* 291 (5501), 141–144. doi: 10.1126/science.291.5501.141

Posfai, D., Sylvester, K., Reddy, A., Ganley, J. G., Wirth, J., Cullen, Q. E., et al. (2018). Plasmodium Parasite Exploits Host Aquaporin-3 During Liver Stage Malaria Infection. *PloS Pathog.* 14 (5), e1007057. doi: 10.1371/journal.ppat.1007057

Prudencio, M., Rodrigues, C. D., Hannus, M., Martin, C., Real, E., Goncalves, L. A., et al. (2008). Kinome-Wide RNAi Screen Implicates at Least 5 Host Hepatocyte Kinases in Plasmodium Sporozoite Infection. *PloS Pathog.* 4 (11), e1000201. doi: 10.1371/journal.ppat.1000201

Prudencio, M., Mota, M. M., and Mendes, A. M. (2011). A Toolbox to Study Liver Stage Malaria. *Trends Parasitol.* 27 (12), 565–574. doi: 10.1016/j.pt.2011.09.004

Raphemot, R., Toro-Moreno, M., Lu, K. Y., Posfai, D., Derbyshire, E. R., et al. (2019). Discovery of Druggable Host Factors Critical to Plasmodium Liver-Stage Infection. *Cell Chem. Biol.* 26 (9), 1253–1262.e5. doi: 10.1016/j.chembiol.2019.05.011

Risco-Castillo, V., Topcu, S., Marinach, C., Manzoni, G., Bigorgne, A. E., Briquet, S., et al. (2015). Malaria Sporozoites Traverse Host Cells Within Transient Vacuoles. *Cell Host Microbe* 18 (5), 593–603. doi: 10.1016/j.chom.2015.10.006

Roth, A., Maher, S. P., Conway, A. J., Ubalee, R., Chaumeau, V., Andolina, C., et al. (2018). A Comprehensive Model for Assessment of Liver Stage Therapies Targeting Plasmodium Vivax and Plasmodium Falciparum. *Nat. Commun.* 9 (1), 1837. doi: 10.1038/s41467-018-04221-9

Scott, C. L., Zheng, F., De Baetselier, P., Martens, L., Saeys, Y., De Prijck, S., et al. (2016). Bone Marrow-Derived Monocytes Give Rise to Self-Renewing and Fully Differentiated Kupffer Cells. *Nat. Commun.* 7, 10321. doi: 10.1038/ncomms10321

Sharma, P. K., Kalia, I., Kaushik, V., Brunnert, D., Quadiri, A., Kashif, M., et al. (2021). STK35L1 Regulates Host Cell Cycle-Related Genes and Is Essential for Plasmodium Infection During the Liver Stage of Malaria. *Exp. Cell Res.* 406 (2), 112764. doi: 10.1016/j.yexcr.2021.112764

Steers, N., Schwenk, R., Bacon, D. J., Berenzon, D., Williams, J., and Krzych, U. (2005). The Immune Status of Kupffer Cells Profoundly Influences Their Responses to Infectious Plasmodium Berghei Sporozoites. *Eur. J. Immunol.* 35 (8), 2335–2346. doi: 10.1002/eji.200425680

Stewart, R. L., Matynia, A. P., Factor, R. E., and Varley, K. E. (2020). Spatially-Resolved Quantification of Proteins in Triple Negative Breast Cancers Reveals Differences in the Immune Microenvironment Associated With Prognosis. *Sci. Rep.* 10 (1), 6598. doi: 10.1038/s41598-020-63539-x

Sturm, A., Amino, R., van de Sand, C., Regen, T., Retzlaff, S., Rennenberg, A., et al. (2006). Manipulation of Host Hepatocytes by the Malaria Parasite for Delivery Into Liver Sinusoids. *Science* 313 (5791), 1287–1290. doi: 10.1126/science.1129720

Sun, T. W., Gao, Q., Qiu, S. J., Zhou, J., Wang, X. Y., Yi, Y., et al. (2012). B7-H3 is Expressed in Human Hepatocellular Carcinoma and is Associated With Tumor Aggressiveness and Postoperative Recurrence. *Cancer Immunol. Immunother.* 61 (11), 2171–2182. doi: 10.1007/s00262-012-1278-5

Sun, C., Mezzadra, R., and Schumacher, T. N. (2018). Regulation and Function of the PD-L1 Checkpoint. *Immunity* 48 (3), 434–452. doi: 10.1016/j.immuni.2018.03.014

Tavares, J., Formaglio, P., Thiberge, S., Mordelet, E., Van Rooijen, N., Medvinsky, A., et al. (2013). Role of Host Cell Traversal by the Malaria Sporozoite During Liver Infection. *J. Exp. Med.* 210 (5), 905–915. doi: 10.1084/jem.20121130

Usynin, I., Klotz, C., and Frevert, U. (2007). Malaria Circumsporozoite Protein Inhibits the Respiratory Burst in Kupffer Cells. *Cell Microbiol.* 9 (11), 2610–2628. doi: 10.1111/j.1462-5822.2007.00982.x

Van Gorp, H., Delputte, P. L., and Nauwynck, H. J. (2010). Scavenger Receptor CD163, a Jack-of-All-Trades and Potential Target for Cell-Directed Therapy. *Mol. Immunol.* 47 (7-8), 1650–1660. doi: 10.1016/j.molimm.2010.02.008

Vaughan, A. M., Mikolajczak, S. A., Wilson, E. M., Grompe, M., Kaushansky, A., Camargo, N., et al. (2012). Complete Plasmodium Falciparum Liver-Stage Development in Liver-Chimeric Mice. *J. Clin. Invest.* 122 (10), 3618–3628. doi: 10.1172/JCI62684

Vaughan, A. M., and Kappe, S. H. I. (2017). Genetically Attenuated Malaria Parasites as Vaccines. *Expert Rev. Vaccines* 16 (8), 765–767. doi: 10.1080/14760584.2017.1341835

Vijayan, K., Arang, N., Wei, L., Morrison, R., Geiger, R., Parks, K. R., et al. (2020). A Genome-Wide CRISPR-Cas9 Screen Identifies Host Factors Essential for Optimal Plasmodium Liver Stage Development. *bioRxiv* 2020.08.31.275867. doi: 10.1101/2020.08.31.275867

Vreden, S. G., Sauerwein, R. W., Verhave, J. P., Van Rooijen, N., Meuwissen, J. H., and Van Den Broek, M. F. (1993). Kupffer Cell Elimination Enhances Development of Liver Schizonts of Plasmodium Berghei in Rats. *Infect. Immun.* 61 (5), 1936–1939. doi: 10.1128/iai.61.5.1936-1939.1993

Wake, K., Decker, K., Kirn, A., Knook, D. L., McCuskey, R. S., Bouwens, L., et al. (1989). Cell Biology and Kinetics of Kupffer Cells in the Liver. *Int. Rev. Cytol.* 118, 173–229. doi: 10.1016/S0074-7696(08)60875-X

Wang, N., Li, X., Wang, R., and Ding, Z. (2021). Spatial Transcriptomics and Proteomics Technologies for Deconvoluting the Tumor Microenvironment. *Biotechnol. J.* 16, e2100041. doi: 10.1002/biot.202100041

Winkel, B. M. F., Pelgrom, L. R., van Schuijlenburg, R., Baalbergen, E., Ganesh, M. S., Gerritsma, H., et al. (2020). Plasmodium Sporozoites Induce Regulatory Macrophages. *PloS Pathog.* 16 (9), e1008799. doi: 10.1371/journal.ppat.1008799

Wu, Y., Chen, W., Xu, Z. P., and Gu, W. (2019). PD-L1 Distribution and Perspective for Cancer Immunotherapy-Blockade, Knockdown, or Inhibition. *Front. Immunol.* 10, 2022. doi: 10.3389/fimmu.2019.02022

Yang, A. S. P., O'Neill, M. T., Jennison, C., Lopaticki, S., Allison, C. C., Armistead, J. S., et al. (2017). Cell Traversal Activity Is Important for Plasmodium Falciparum Liver Infection in Humanized Mice. *Cell Rep.* 18 (13), 3105–3116. doi: 10.1016/j.celrep.2017.03.017

Yang, A. S. P., van Waardenburg, Y. M., van de Vegte-Bolmer, M., van Gemert, G. A., Graumans, W., de Wilt, J. H. W., et al. (2021). Zonal Human Hepatocytes are Differentially Permissive to Plasmodium Falciparum Malaria Parasites. *EMBO J.* 40 (6), e106583. doi: 10.15252/embj.2020106583

Conflict of Interest: The authors declare that the research was conducted in the absence of any commercial or financial relationships that could be construed as a potential conflict of interest.

Publisher's Note: All claims expressed in this article are solely those of the authors and do not necessarily represent those of their affiliated organizations, or those of the publisher, the editors and the reviewers. Any product that may be evaluated in this article, or claim that may be made by its manufacturer, is not guaranteed or endorsed by the publisher.

frontiers in Cellular and Infection Microbiology

ORIGINAL RESEARCH
published: 28 January 2022
doi: 10.3389/fcimb.2022.813011

Plasmodium falciparum Parasite Lines Expressing DC8 and Group A PfEMP1 Bind to Brain, Intestinal, and Kidney Endothelial Cells

*Luana S. Ortolan[1], Marion Avril[1], Jun Xue[2], Karl B. Seydel[3,4], Ying Zheng[2] and Joseph D. Smith[1,5]**

[1] Center for Global Infectious Disease Research, Seattle Children's Research Institute, Seattle, WA, United States, [2] Department of Bioengineering, University of Washington, Seattle, WA, United States, [3] Department of Osteopathic Medical Specialties, College of Osteopathic Medicine, Michigan State University, East Lansing, MI, United States, [4] Blantyre Malaria Project, Kamuzu University of Health Sciences, Blantyre, Malawi, [5] Department of Pediatrics, University of Washington, Seattle, WA, United States

OPEN ACCESS

Edited by:
Andrea L. Conroy,
Indiana University, United States

Reviewed by:
Julio Gallego-Delgado,
Lehman College, United States
Gaoqian Feng,
Burnet Institute, Australia

***Correspondence:**
Joseph D. Smith
joe.smith@seattlechildrens.org

Specialty section:
This article was submitted to Parasite and Host, a section of the journal Frontiers in Cellular and Infection Microbiology

Received: 11 November 2021
Accepted: 10 January 2022
Published: 28 January 2022

Citation:
Ortolan LS, Avril M, Xue J, Seydel KB, Zheng Y and Smith JD (2022) Plasmodium falciparum Parasite Lines Expressing DC8 and Group A PfEMP1 Bind to Brain, Intestinal, and Kidney Endothelial Cells. Front. Cell. Infect. Microbiol. 12:813011. doi: 10.3389/fcimb.2022.813011

Cytoadhesion of *Plasmodium falciparum*-infected red blood cells is a virulence determinant associated with microvascular obstruction and organ complications. The gastrointestinal tract is a major site of sequestration in fatal cerebral malaria cases and kidney complications are common in severe malaria, but parasite interactions with these microvascular sites are poorly characterized. To study parasite tropism for different microvascular sites, we investigated binding of parasite lines to primary human microvascular endothelial cells from intestine (HIMEC) and peritubular kidney (HKMEC) sites. Of the three major host receptors for *P. falciparum*, CD36 had low or negligible expression; endothelial protein C receptor (EPCR) had the broadest constitutive expression; and intercellular adhesion molecule 1 (ICAM-1) was weakly expressed on resting cells and was strongly upregulated by TNF-α on primary endothelial cells from the brain, intestine, and peritubular kidney sites. By studying parasite lines expressing *var* genes linked to severe malaria, we provide evidence that both the DC8 and Group A EPCR-binding subsets of the *P. falciparum* erythrocyte membrane protein 1 (PfEMP1) family encodes binding affinity for brain, intestinal, and peritubular kidney endothelial cells, and that DC8 parasite adhesion was partially dependent on EPCR. Collectively, these findings raise the possibility of a brain-gut-kidney binding axis contributing to multi-organ complications in severe malaria.

Keywords: *Plasmodium falciparum*, malaria, cytoadhesion, endothelial protein C receptor, kidney endothelial cell, intestinal endothelial cell

INTRODUCTION

The distinctive virulence of *Plasmodium falciparum* is caused in part through the cytoadhesion of *P. falciparum*-infected erythrocytes (IEs) in the microcirculation of different organs. Extensive sequestration of *P. falciparum*-IEs obstructs blood flow and can promote localized inflammation and organ dysfunction (Miller et al., 2002). The best studied examples are cerebral malaria, associated with high sequestered parasite burdens in the brain microcirculation (Marchiafava and Bignami, 1892; MacPherson et al., 1985; Taylor et al., 2004), and placental malaria, associated with high parasite burdens in the placental intervillous blood circulation (Brabin et al., 2004). However, mature forms of *P. falciparum*-IEs have broad sequestration in diverse microvascular beds, including the brain, gastrointestinal tract, subcutaneous adipose tissue of the skin, heart, lung, spleen and to a lesser extent, the kidney (Spitz, 1946; MacPherson et al., 1985; Milner et al., 2014; Milner et al., 2015), but parasite tropism for most organ sites remains poorly characterized.

Whereas the kidney is not a major site of parasite sequestration (Spitz, 1946; Milner et al., 2014), kidney injury is common in severe malaria. For instance, recent evidence indicates that acute kidney injury (AKI) is a common complication in African children with severe malaria and is associated with increased morbidity and mortality (Conroy et al., 2016; Sypniewska et al., 2017; Conroy et al., 2019; Batte et al., 2021). Moreover, renal impairment occurs in up to 37% of adult severe malaria cases and increased the risk of death by 4-fold (Dondorp et al., 2008b). In a large autopsy series, renal failure was characterized by acute tubular necrosis with accumulation of host monocytes and *P. falciparum*-IEs in the kidneys, especially in the peritubular capillary microcirculation (Nguansangiam et al., 2007). The gastrointestinal tract has been considered a relatively non-pathogenic sequestration site. However, it is a major site of parasite sequestration and there is increasing evidence that gastrointestinal barrier function may be compromised at higher parasite burdens (Wilairatana et al., 1997). For instance, the gastrointestinal tract was the most intense site of parasite sequestration in fatal pediatric CM cases (Seydel et al., 2012; Milner et al., 2014) and blocked capillaries in the rectal mucosa correlate to disease severity and metabolic acidosis in adult SM cases (Dondorp et al., 2008a). Moreover, acidic microbial products contribute to metabolic acidosis in adult severe malaria (Leopold et al., 2019) and children with severe malaria are at risk for invasive bacterial disease (Scott et al., 2011), suggesting compromise of gut integrity. Thus, while kidney and gut pathogenesis are not well understood, autopsy studies have led to the hypothesis that organ injury may result from common pathological processes, precipitated by cytoadherence of *P. falciparum*-IEs.

Cytoadhesion of *P. falciparum*-IEs is mediated by the *P. falciparum* erythrocyte membrane protein-1 (PfEMP1) family, encoded by a repertoire of about 60 *var* genes per parasite genotype (Baruch et al., 1995; Smith et al., 1995; Su et al., 1995). PfEMP1 proteins encode multiple adhesion domains, called Duffy binding-like (DBL) and cysteine-rich interdomain region (CIDR), which confer different binding properties (Smith et al., 2013). For instance, different subsets of PfEMP1 proteins encode binding activity for CD36 (Robinson et al., 2003; Hsieh et al., 2016), endothelial protein C receptor (EPCR) (Turner et al., 2013; Lau et al., 2015), and intercellular adhesion molecule 1 (ICAM-1) (Smith et al., 2000; Lennartz et al., 2019). Whereas the EPCR binders comprise only a small minority of the *var* gene repertoire (~10% of genes) (Rask et al., 2010), this subset is transcriptionally elevated in severe malaria infections and both the DC8 and Group A PfEMP1 variants are linked to severe malaria complications (Lavstsen et al., 2012; Turner et al., 2013; Bernabeu et al., 2016; Kessler et al., 2017; Lennartz et al., 2017; Mkumbaye et al., 2017; Sahu et al., 2021; Wichers et al., 2021). From *in vitro* studies, EPCR-binding variants adhere to human brain endothelial cells (Turner et al., 2013; Avril et al., 2016; Lennartz et al., 2017; Bernabeu et al., 2019; Storm et al., 2019) and to primary human heart and lung microvascular endothelial cells (Avril et al., 2013; Gillrie et al., 2015), suggesting they may have broad affinity for diverse microvascular beds.

Given that kidney injury and gastrointestinal sequestration are common in severe and fatal malaria cases, we investigated if similar parasite binding variants may have affinity for brain, intestinal, and kidney microvascular sites. Our analysis demonstrates that parasites expressing DC8 or Group A PfEMP1 encode broad binding affinity for primary human brain, intestinal, and kidney endothelial cells and are partially dependent on EPCR for adhesion.

MATERIALS AND METHODS

Human Brain, Intestinal, and Peritubular Kidney Microvascular Endothelial Cell Cultures

Primary human brain microvascular endothelial cells (HBMEC) (Cell System, ACBRI 376) were cultured with endothelial cell growth basal medium-2 (EBM-2, Lonza, CC-3156) in accordance with manufacturer specifications with 5% fetal bovine serum (FBS) and supplements provided (Lonza, CC-4147) in tissue culture flasks treated with rat collagen I (Corning, 354236). Primary human intestinal microvascular endothelial cells (HIMEC) (Cell Systems, ACBRI 666) were cultured in complete classic medium with 10% FBS serum and culture boost (Cell Systems 4Z0-500) supplemented with Bac-off (Cell Systems) on an extracellular matrix-coated surface (attachment factor, Cell Systems). HBMEC and HIMEC were certified positive by the manufacturer for expression of Von Willebrand factor, acetylated low-density lipoprotein uptake, and CD31. HBMEC and HIMEC were used in experiments at passages 5 to 10. Primary human kidney peritubular microvascular endothelial cells (HKMEC) were isolated and purified from fetal kidneys as previously reported (Ligresti et al., 2016) and used in experiments at passages 3 to 5. Fetal human kidneys were obtained after informed consent from patients at the University of Washington Medical Center in compliance with Institutional Review Board protocol (IRB 447773EA). Cells were cultured and expanded on matrix-coated surface with 0.2% gelatin (Sigma,

G1890) with EBM2 medium (Lonza, CC-3156) with 10% FBS and supplemented with 5 mg/ml EGCS (Cell Biologics, 1166), 1% antibiotic-antimycotic (Gibco, 15240062), 50 mg/ml of heparin (Sigma, H3149) and 20 ng/ml of vascular endothelial growth factor (VEGF) (R&D Systems, 293-VE-10).

Characterization of Surface Markers on Endothelial Cells by Flow Cytometry

HBMEC, HIMEC and HKMEC monolayers were cultured on matrix-coated tissue culture flasks until confluence. Cells were washed with 1X PBS, lifted with 8 mM EDTA in 1X PBS and then resuspended in 1X PBS (supplemented with 2% FBS). Cell suspensions were stained with monoclonal antibodies (mAb) for CD31-PE (Biolegend, clone WM59), CD36-FITC (Biolegend, clone 5-271), EPCR-APC (Biolegend, clone RCR-401) and CD54/ICAM-1-PE-Cy-7 (Biolegend, clone HA58) at 1:100 dilution and with Live/Dead-V450 (Tonbo Biosciences) for 30 min on ice. For assays with proinflammatory pre-stimulation, confluent cell monolayers were stimulated with 10 ng/ml TNF-α (Sigma, T0157) for 20-24 hours at 37°C. Cells were analyzed in a LSRII (Becton & Dickson) with 100,000 events/sample. Gates were set based on fluorescence minus one (FMO) and IgG isotype controls (Biolegend). Results were expressed relative to IgG isotype controls. Data was analyzed using FlowJo v10 software (TreeStar Inc.).

Immunofluorescence

HBMEC, HIMEC and HKMEC endothelial cells, were cultured in an 8 well pretreated chamber slide until confluence. For assays with proinflammatory pre-stimulation, confluent cell monolayers were stimulated with 10 ng/ml TNF-α (Sigma, T0157) for 24 hours at 5% CO_2 and 37°C. Cells were fixed with 3.7% paraformaldehyde for 30 min. For antibody labeling, cells were pretreated with background blocking agent (Background Buster, Innovex Biosciences, NB306) for 30 min. Cells were then washed with 1x PBS and incubated with primary mouse-anti-human-ICAM-1 (1:200 dilution) in PBS (supplemented with 2% BSA) for 1 hour (Biosource International, ThermoFisher Scientific, clone C14), followed by the secondary antibody goat anti-mouse Alexa Fluor 488 (1:200 dilution) (Invitrogen) for 1 hour. Images taken under 400x magnification (Keyence BZ-X series microscope).

P. falciparum Culture

The *P. falciparum* parasites lines IT4var19 (Avril et al., 2012), HB3var03 (Claessens et al., 2012; Avril et al., 2016), and 3173-S (Bernabeu et al., 2019) were cultured in human red blood cells (O+) and 10% pooled human A^+ serum-rich media (RPMI 1640 medium, GIBCO) and 0.5% Albumax II (Thermo Fischer Scientific) at 5% hematocrit. The IT4var19 and HB3var03 parasite lines were grown in a gas mixture of 5% O_2, 5% CO_2, and 90% N_2 and 3173-S was grown in a gas mixture of 1% O_2, 5% CO_2, and 94% N_2. All parasites were routinely synchronized by treatment with 5% sorbitol and gelatin flotation to ensure that IEs maintained their 'knob-like' adhesion complexes.

Determination of *var* Gene Transcripts

P. falciparum-IEs at ring stage were collected in TRIZOL LS (ThermoFisher Scientific) and RNA was isolated by chloroform and purified with RNeasy Micro Kit (Qiagen), following manufacturer's instructions. Contaminating genomic DNA was eliminated with DNase I treatment. cDNA was synthesized by reverse transcription reaction. For the IT4var19 and HB3var03 parasite lines, *var* transcription was analyzed by real time-PCR with SYBR green (Power SYBR Green PCR Master Mix, Thermo Fisher Scientific) using a set of IT4var primers (Janes et al., 2011) or HB3var primers (Soerli et al., 2009). Transcription unit levels were normalized to the housekeeping control gene coding for STS (*seryl-tRNA synthetase*). To determine the proportion of 3173-S *var1* transcripts expressed by the 3173-S parasite line, DBLα tags were PCR-amplified using the varF_dg2 and brlong2 primers (Lavstsen et al., 2012), cloned into a Zero Blunt TOPO vector, sequenced, and compared to a previous report (Bernabeu et al., 2019).

Binding Assay

For IE binding assays, HBMEC, HIMEC and HKMEC were seeded on collagen coated 8 well slides (BD Biocoat) 3–4 days before the assays and allowed to grow to confluency. Mature forms of *P. falciparum* were purified by magnetic purification with LD columns (Miltenyi Biotec) and checked for purity by Giemsa staining. Binding assays and washes were performed with pre-warmed binding medium (RPMI-1640 medium containing 0.5% BSA, pH 7.2). For binding assays, $5x10^6$ IE/ml were resuspended in 200 µl and added to the wells with endothelial cells. After 1 hour incubation at 37°C, non-bound IE were washed by flipping the slides in a gravity wash for 10 min. For binding quantification, slides were fixed in 1% glutaraldehyde for 30 min at room temperature, then stained with 1× Giemsa for 5 min. Binding was quantified in a blinded fashion, by determining the number of IEs adhering per mm^2 of endothelial cells in six random fields with images taken under 400× magnification (Keyence BZ-X series microscope). For assays with proinflammatory pre-stimulation, confluent cell monolayers were stimulated with 10 ng/ml TNF-α (Sigma, T0157) for 20-24 hours at 37°C prior to the binding assay. For binding inhibition assays, rat anti-human EPCR monoclonal antibody (20 µg/ml, clone RCR-252; Sigma E6280) or rat control IgG (eBiosciences, 20 µg/ml) was added to cells for 30 min of incubation at 37°C prior to the addition of IEs.

Statistical Analysis

Statistical analysis was performed using Prism (version 8, GraphPad Software Inc.). Flow cytometry data were compared using Two-way ANOVA, Sidak's multiple comparison test. Binding assays were compared using Two-tailed Unpaired T test. Flow cytometry assays shows the mean of two technical replicates from three or four different experiments. Binding assays with *P. falciparum*-IEs were performed with two technical replicates and conducted in three to six independent experiments.

RESULTS

Expression of CD36, ICAM-1, and EPCR on Brain, Intestinal, and Kidney Endothelial Cells

To investigate parasite tropism for brain, gut, and kidney microvascular sites, we first characterized the expression of CD36, ICAM-1 and EPCR on CD31$^+$ primary human microvascular endothelial cells. Malaria autopsy studies have indicated that parasite sequestration is higher in the peritubular than the glomerular capillaries (Nguansangiam et al., 2007). Therefore, we compared endothelial cells from brain (HBMEC), intestine (HIMEC) and kidney peritubular (HKMEC) sites by flow cytometry. Cells were compared under resting conditions or following overnight stimulation with TNF-α (see gating strategies in **Supplementary Figure 1**).

Of the three receptors, CD36 had very low expression levels on HBMEC and HIMEC and negligible or absent expression on HKMEC under both resting and TNF-α treatment conditions (**Figure 1**). EPCR had the broadest constitutive expression (100% of HBMEC and HIMEC cells and ~60% of HKMEC cells) and was slightly downregulated on HBMEC and HIMEC following TNF-α treatment (**Figure 1**). By comparison, ICAM-1 had very low constitutive expression levels on a minority of cells (HBMEC, 10%; HIMEC, 1-2%; HKMEC, 10-57%), but its expression was substantially increased by TNF-α treatment reaching nearly 100% surface positive for all three endothelial cell types (**Figure 1** and **Supplementary Figure 2**). Whereas resting EPCR surface levels were higher in HBMEC and HIMEC than HKMEC, constitutive ICAM-1 expression was highest in HKMEC (**Figures 1A, B**). The distinctive expression of the two receptors in HKMEC may be because these cells were cultured in medium supplemented with high concentrations of VEGF to enhance their growth (Ligresti et al., 2016) and VEGF induces ICAM-1 expression on endothelial cells (Kim et al., 2001). Overall, there were similarities in receptor profiles between the three endothelial cell types, especially between the intestinal and brain endothelial cells.

A Parasite Line Expressing a DC8-PfEMP1 Binds to HIMEC and HKMEC and Is Partially Dependent on EPCR

We next evaluated binding of the IT4var19 clonal line to HIMEC and HKMEC cells. The IT4var19 parasite line expresses a DC8-PfEMP1 variant and was originally selected by repeated panning on an immortalized human brain endothelial cell line followed by limited dilution cloning (Avril et al., 2012). From previous work, IT4var19 is partially dependent on EPCR for binding to brain endothelial cells (Turner et al., 2013; Sampath et al., 2015;

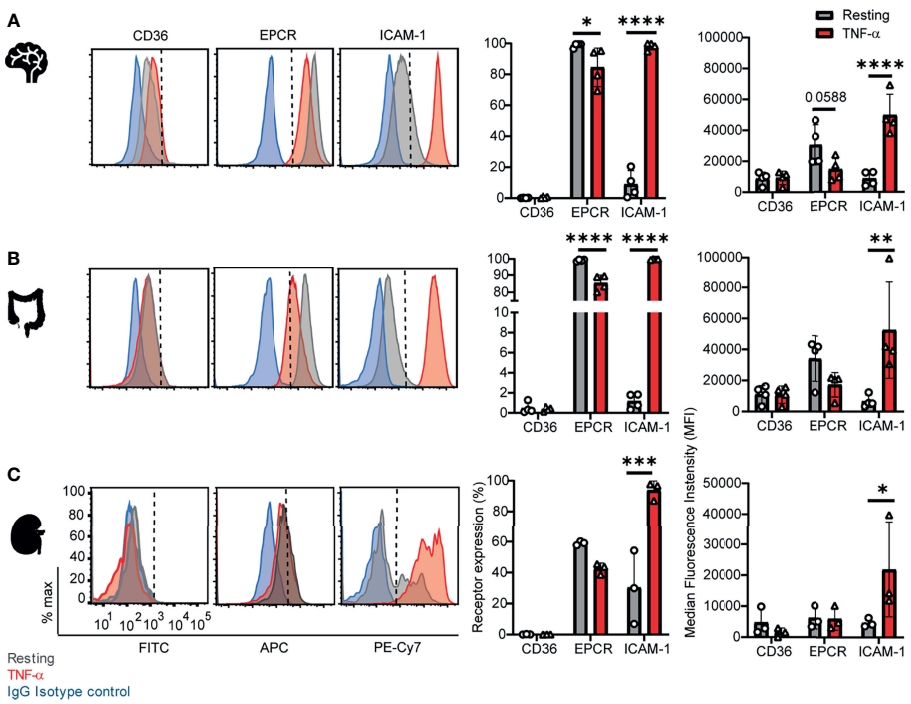

FIGURE 1 | Surface expression of CD36, EPCR, and ICAM-1 on primary human brain, intestinal and kidney endothelial cells. **(A)** Brain, **(B)** Intestinal, or **(C)** Peritubular kidney microvascular endothelial cells were stained for CD36, EPCR and ICAM-1 expression on resting or TNF-α-stimulated cells (20-24 hours treatment). Histograms show expression levels on live/CD31$^+$ cells. The percentage of each receptor expression was determined by subtracting isotype control antibody from the target antibody levels. Positive is defined as being above the vertical dashed line in the histogram. Data in bar graphs are expressed as mean ± SD and were analyzed by 2-way ANOVA, using Sidak's multiple comparisons test. *p<0.05; **p<0.01; ***p<0.001; ****p<0.0001. Additional data is shown in **Supplementary Figures 1, 2**.

Azasi et al., 2018; Bernabeu et al., 2019). The predominant expression of the *var*/PfEMP1 of interest was confirmed by RT-PCR using *var* strain-specific primers for the IT4 parasite genotype (**Supplementary Figure 3**). IT4var19-IEs bound at a slightly higher level to resting than TNF-α-activated HIMEC, albeit it did not reach statistical significance (**Figure 2A**). Binding to both resting and TNF-α-activated cells was substantially inhibited by anti-EPCR monoclonal antibody (median inhibition 80% on resting HIMEC, $p<0.0001$; median inhibition 60% on TNF-α-activated HIMEC, $p = 0.06$) (**Figure 2A**). The lower inhibition of anti-EPCR antibodies on activated cells may be due to the reduced EPCR surface expression levels following TNF-α treatment (**Figure 1**).

Likewise, IT4var19 parasites bound to both resting and TNF-α-stimulated HKMEC cells (**Figure 2B**), but at an approximately 6-fold lower level compared to HIMEC (panels A and B in **Figure 2**). The reduced binding levels to HKMEC may be due in part to their lower EPCR expression levels (**Figure 1**), as the interaction of IT4var19 parasites and HKMEC was substantially inhibited by anti-EPCR monoclonal antibody on both resting (median inhibition 70%) and TNF-α-stimulated cells (median inhibition 60%, $p<0.05$) (**Figure 2B**). Thus, the DC8-PfEMP1 expressing IT4var19 parasite line had binding activity for intestinal and kidney peritubular endothelial cells and is partially dependent on EPCR for adhesion to both cell types, similar to previous findings with primary human brain microvascular endothelial cells (Bernabeu et al., 2019).

A Parasite Line Expressing a Group A-PfEMP1 Binds to HIMEC and HKMEC

We next investigated a parasite line expressing a Group A PfEMP1 variant. The HB3var03 parasite line was originally selected by repeated panning on an immortalized human brain endothelial cell line (Claessens et al., 2012) and encodes dual binding activity for EPCR and ICAM-1 (Avril et al., 2016; Lennartz et al., 2017; Bernabeu et al., 2019). At the time of this study, the HB3var03 parasite line expressed a mixture of four predominant *var* genes, including the *HB3var03* gene of interest (Group A, dual EPCR + ICAM-1 binder), two Group C predicted CD36 binders (*HB3var29* and *HB3var32*) and a chondroitin sulfate A binder (*HB3var2CSA* allele A) (**Supplementary Figure 4**).

The HB3var03 parasite line bound at a slightly higher level to TNF-α-activated HIMEC than resting cells, albeit it did not reach statistical significance (**Figure 3A**). Because the HB3var03 PfEMP1 encodes dual adhesion properties for EPCR and ICAM-1, the higher binding may be due to the substantial increase in ICAM-1 expression and minor reduction in EPCR surface levels on activated cells (**Figure 1**). Consistent with this interpretation, binding to both resting and TNF-α-activated cells was substantially inhibited by combined anti-EPCR and anti-ICAM-1 monoclonal antibody treatment (median inhibition 75% on resting HIMEC, $p<0.001$; median inhibition 45% on TNF-α-activated HIMEC, $p < 0.01$) (**Figure 3A**).

Likewise, HB3var03 parasites bound to both resting and TNF-α-stimulated HKMEC cells (**Figure 3B**). The binding

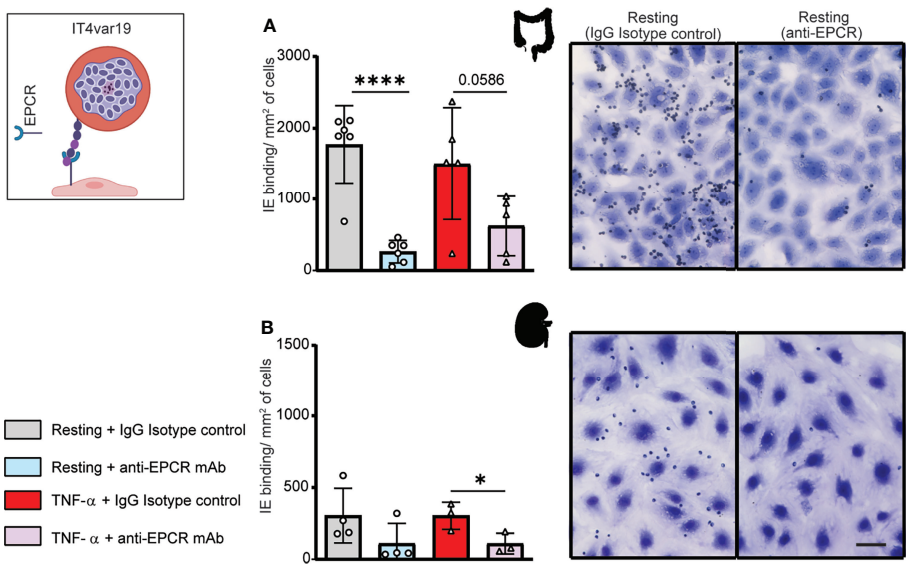

FIGURE 2 | Binding of the IT4var19 clonal parasite line to HIMEC and HKMEC. The IT4var19 parasite was previously selected on brain endothelial cells *in vitro* and expresses a DC8-PfEMP1 protein that interacts with EPCR on endothelial cells (cartoon). **(A)** Binding of IT4var19-IEs to resting and TNF-α-stimulated HIMEC cells in the presence or absence of anti-EPCR antibody. **(B)** Binding of IT4var19-IEs to resting and TNF-α-stimulated HKMEC cells in the presence or absence of anti-EPCR antibody. Data are expressed as mean ± SD and were analyzed by unpaired t test. *$p<0.05$; ****$p<0.0001$. EPCR: endothelial protein C receptor. Scale bar: 50 μm. Additional data is shown in **Supplementary Figure 3**.

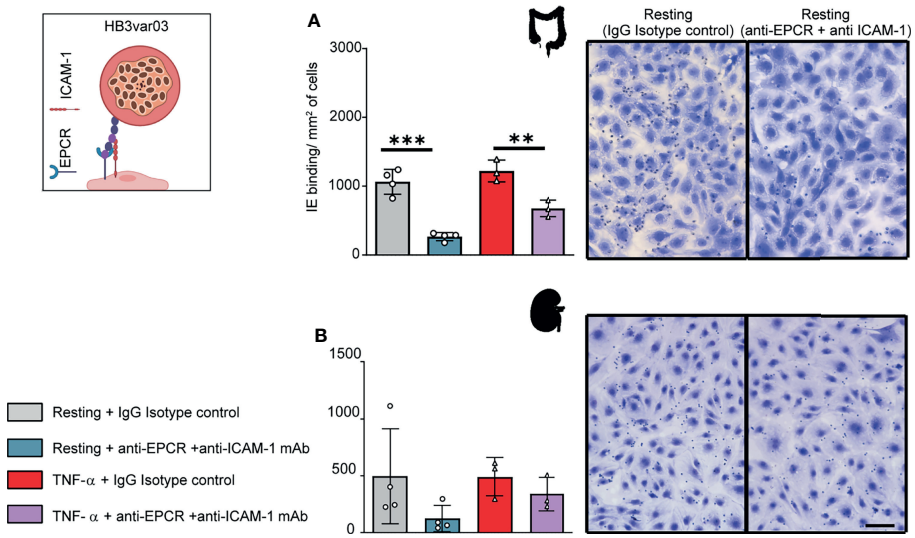

FIGURE 3 | Binding of the HB3var03 parasite line to HIMEC and HKMEC. The HB3var03 parasite was previously selected on brain endothelial cells *in vitro* and expresses a Group A-PfEMP1 protein that interacts with EPCR and ICAM-1 (cartoon). **(A)** Binding of HB3var03-IEs to resting and TNFα-stimulated HIMEC cells in the presence or absence of combined anti-EPCR and anti-ICAM-1 antibodies **(B)** Binding of HB3var03-IEs to resting and TNF-α-stimulated HKMEC cells in the presence or absence of combined anti-EPCR and anti-ICAM-1 antibodies. Data are expressed as mean ± SD and were analyzed by unpaired t test. **p<0.01; ***p<0.001. EPCR: endothelial protein C receptor. Scale bar: 50 μm. Additional data is shown in **Supplementary Figure 4**.

interaction with resting HKMEC was substantially inhibited by combined anti-EPCR and anti-ICAM-1 monoclonal antibody treatment (median inhibition 75%) and less so on TNF-α-stimulated cells (median inhibition 31%) (**Figure 3B**). Like IT4var19, the HB3var03 parasite line had lower binding to HKMEC than HIMEC (panels A and B in **Figure 3**). Taken together, this analysis suggests that Group A PfEMP1 variants with dual EPCR and ICAM-1 binding activity have affinity for intestinal and kidney peritubular endothelial cells.

A DC8-PfEMP1 Expressing Cerebral Malaria Isolate Binds to Brain, Intestinal and Kidney Endothelial Cells

To further investigate parasite-endothelial tropism, we evaluated the 3173-S parasite line that was isolated and cloned by limiting dilution from a retinopathy-positive, pediatric CM patient. 3173-S predominantly expresses a DC8-PfEMP1 variant and was previously characterized for binding to 3D human brain microvessels (Bernabeu et al., 2019). The predominant expression of 3173-S *var1* was confirmed by amplification and sequencing of DBLα tags (**Figure 4A**). The 3173-S parasite line bound to all three endothelial cell types with highest binding levels to HIMEC, followed by HKMEC and HBMEC (**Figures 4B–D**). Binding levels of the 3173-S parasite line were similar on resting and activated cells for all three endothelial cell types. 3173-S binding was partially inhibited by anti-EPCR antibody, not exceeding 40% inhibition in any endothelial cell type (**Figure 4**, $p<0.05$ on resting brain endothelial cells). Taken together, these data suggest that EPCR partially contributes to 3173-S binding to HBMEC, and possibly to HIMEC and HKMEC cells.

DISCUSSION

Cytoadhesion of *Plasmodium falciparum*-infected erythrocytes (IEs) to the endothelial lining of blood vessels protects parasites from splenic destruction, but also leads to inflammation, vessel occlusion, and organ damage (Miller et al., 2002). Whereas previous work has established that EPCR and ICAM-1 are receptors on brain endothelial cells (Turner et al., 2013; Avril et al., 2016; Lennartz et al., 2017; Bernabeu et al., 2019; Storm et al., 2019), little is known about parasite tropism for gut and kidney, even though multiorgan complications affecting the brain and kidney are common in severe malaria (Dondorp et al., 2008b; Batte et al., 2021) and the gastrointestinal tract is a major site of sequestration in high burden parasite infections (Dondorp et al., 2008a; Milner et al., 2014). To address this knowledge gap, we studied whether parasite lines with affinity for primary human brain endothelial cells would bind to primary microvascular endothelial cells from kidney and gut.

Although CD36 binding is the most common of the PfEMP1 adhesion traits and is encoded by up to 80-85% of proteins in each parasite's *var* gene repertoire (Robinson et al., 2003; Rask et al., 2010; Smith et al., 2013), this receptor was expressed at very low or negligible levels on brain, intestinal, and peritubular kidney endothelial cells. From histology, CD36 is strongly expressed on liver, spleen, lung, and muscle blood vessels, but is low or absent on brain and kidney endothelial cells (Turner

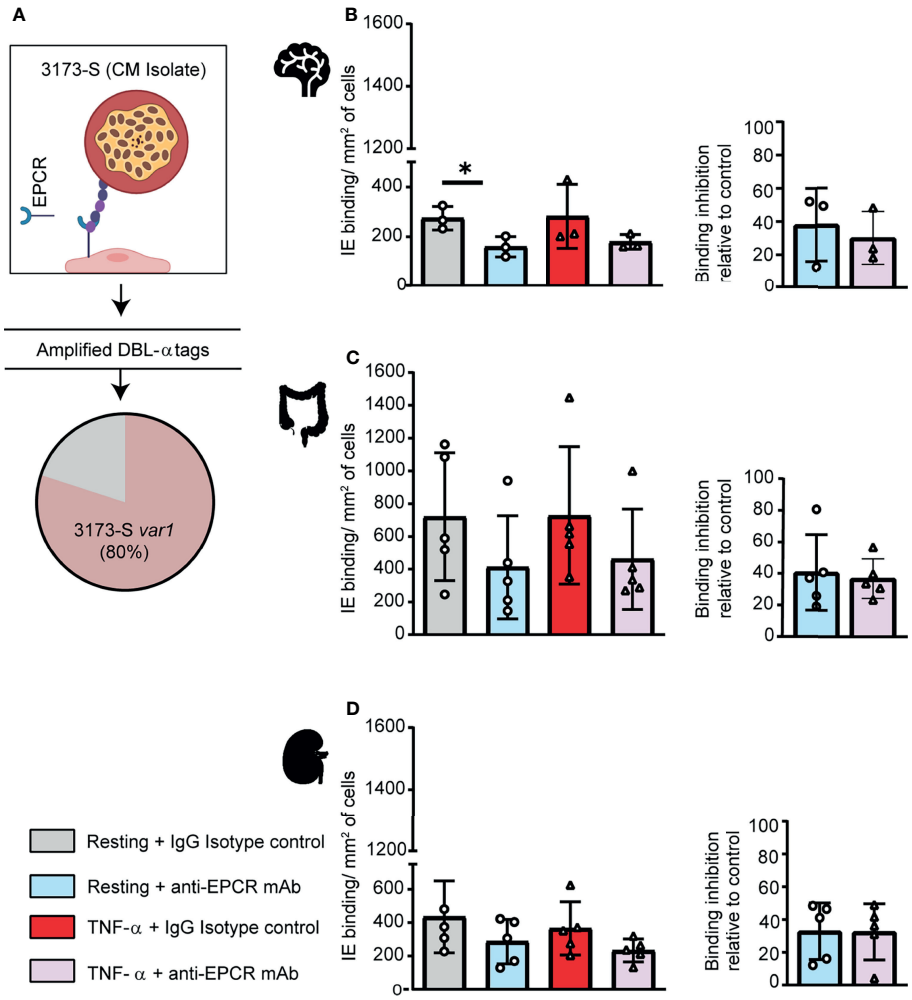

FIGURE 4 | A DC8-PfEMP1 expressing parasite line (3173-S) isolated from a cerebral malaria patient binds to brain, intestinal and kidney endothelial cells**. (A)** The 3173-S parasite line predominantly expresses the *3173-S var1* transcript (DC8-PfEMP1) based on sequencing of DBLα sequence tags. Binding of 3173-S was compared to primary human microvascular endothelial cells from **(B)** brain, **(C)** intestinal, and **(D)** peritubular kidney endothelial cells. Binding levels were compared on resting and TNFα-stimulated cells in the presence and absence of anti-EPCR antibody. Data are expressed as mean ± SD and were analyzed by unpaired t test. *p<0.05. EPCR: endothelial protein C receptor.

et al., 1994). Together, these findings suggest that CD36 is not widely distributed in the microvascular beds of vital organs, such as brain and kidney, impacted by *P. falciparum* sequestration. The pulmonary vasculature is a site of sequestration (Spitz, 1946; Milner et al., 2015), so a role of CD36 in parasite-lung tropism cannot be excluded.

By comparison, EPCR and ICAM-1 binding domains are encoded by a smaller proportion of PfEMP1 variants, but EPCR had the broadest constitutive expression of the three receptors and ICAM-1 had very low basal expression and was essentially expressed by all brain, gut, and peritubular kidney endothelial cells after TNF-α stimulation, leading to striking differences in receptor profiles between resting ($CD36^-$, $EPCR^+$, $ICAM\text{-}1^{-/very\ low}$) and TNF-α stimulated endothelial cells ($CD36^-$, $EPCR^+$, $ICAM\text{-}1^+$). In line with these *in vitro* findings, ICAM-1 is widely upregulated on microvascular endothelial cells during symptomatic malaria infections (Turner et al., 1994). This study is based on primary endothelial cells. Although nothing is known about receptor expression profiles in the intestine, there is good agreement in CD36 and ICAM-1 expression observed here in primary brain and peritubular kidney endothelial cells and *in vivo* findings (Turner et al., 1994). Overall, our analysis suggests very similar receptor profiles for these three major parasite adhesion receptors on primary human brain, intestinal, and peritubular kidney microvascular endothelial cells.

PfEMP1 proteins have diverged in binding activity for CD36 and EPCR (Smith et al., 2013). Whereas previous work has linked EPCR or dual EPCR and ICAM-1 PfEMP1 variants to severe malaria (Lavstsen et al., 2012; Turner et al., 2013; Bernabeu et al., 2016; Kessler et al., 2017; Storm et al., 2019;

Sahu et al., 2021; Wichers et al., 2021), little is known about their endothelial binding specificity. Here, we provide evidence that the DC8 and Group A EPCR-binding PfEMP1 subsets have binding activity for brain, gut, and kidney endothelial cells. Our findings do not preclude that other PfEMP1 variants can sequester in these organs, but they raise the possibility of brain-gut-kidney binding axis contributing to multi-organ complications in severe malaria. A limitation of this study is that binding was studied using cell monolayers and static binding assays. Further work is needed to model parasite binding in organ-specific microvasculature models that better mimic the distinct 3D architecture and microfluidic dynamics of different organs where *P. falciparum*-IEs sequester. Nevertheless, as EPCR-binding variants can inhibit the pro-homeostatic and pro-barrier functions of EPCR by blocking its interaction with the native ligand (Turner et al., 2013; Gillrie et al., 2015; Lau et al., 2015; Petersen et al., 2015; Sampath et al., 2015), multiple organs may be impacted at high parasite burdens.

CONCLUSION

This study provides evidence that DC8 and Group A EPCR-binding PfEMP1 variants have broad affinity for brain, intestinal, and kidney microvascular endothelial cells and raise the possibility that a parasite brain-gut-kidney binding axis may contribute to multi-organ dysfunction in severe malaria.

DATA AVAILABILITY STATEMENT

The original contributions presented in the study are included in the article/**Supplementary Material**. Further inquiries can be directed to the corresponding author.

ETHICS STATEMENT

HKMEC were obtained after voluntary pregnancy interruptions performed at the University of Washington Medical Center in compliance with Institutional Review Board protocol (IRB447773EA).

AUTHOR CONTRIBUTIONS

LO, MA, and JS conceived and designed the study. KS provided the parasite line recovered from a pediatric cerebral malaria patient. JX and YZ provided HKMEC cells and culture conditions. LO and MA performed experiments and data analysis. LO and JS wrote the first draft. All authors contributed to the article and approved the submitted version.

FUNDING

This work was supported by RO1 AI141602 (JS and KS), U19AI089688 (JS), and UG3/UH3 TR002158 (YZ). The content is solely the responsibility of the authors and does not necessarily represent the official views of the National Institutes of Health.

SUPPLEMENTARY MATERIAL

The Supplementary Material for this article can be found online at: https://www.frontiersin.org/articles/10.3389/fcimb.2022.813011/full#supplementary-material

REFERENCES

Avril, M., Bernabeu, M., Benjamin, M., Brazier, A. J., and Smith, J. D. (2016). Interaction Between Endothelial Protein C Receptor and Intercellular Adhesion Molecule 1 to Mediate Binding of Plasmodium Falciparum-Infected Erythrocytes to Endothelial Cells. *MBio* 7 (4), e00615–16. doi: 10.1128/mBio.00615-16

Avril, M., Brazier, A. J., Melcher, M., Sampath, S., and Smith, J. D. (2013). DC8 and DC13 Var Genes Associated With Severe Malaria Bind Avidly to Diverse Endothelial Cells. *PloS Pathog.* 9 (6), e1003430. doi: 10.1371/journal.ppat.1003430

Avril, M., Tripathi, A. K., Brazier, A. J., Andisi, C., Janes, J. H., Soma, V. L., et al. (2012). A Restricted Subset of Var Genes Mediates Adherence of Plasmodium Falciparum-Infected Erythrocytes to Brain Endothelial Cells. *Proc. Natl. Acad. Sci. U.S.A.* 109 (26), E1782–E1790. doi: 10.1073/pnas.1120534109

Azasi, Y., Lindergard, G., Ghumra, A., Mu, J., Miller, L. H., and Rowe, J. A. (2018). Infected Erythrocytes Expressing DC13 PfEMP1 Differ From Recombinant Proteins in EPCR-Binding Function. *Proc. Natl. Acad. Sci. U.S.A.* 115 (5), 1063–1068. doi: 10.1073/pnas.1712879115

Baruch, D. I., Pasloske, B. L., Singh, H. B., Bi, X., Ma, X. C., Feldman, M., et al. (1995). Cloning the P. Falciparum Gene Encoding PfEMP1, a Malarial Variant Antigen and Adherence Receptor on the Surface of Parasitized Human Erythrocytes. *Cell* 82 (1), 77–87. doi: 10.1016/0092-8674(95)90054-3

Batte, A., Berrens, Z., Murphy, K., Mufumba, I., Sarangam, M. L., Hawkes, M. T., et al. (2021). Malaria-Associated Acute Kidney Injury in African Children: Prevalence, Pathophysiology, Impact, and Management Challenges. *Int. J. Nephrol. Renovasc. Dis.* 14, 235–253. doi: 10.2147/IJNRD.S239157

Bernabeu, M., Danziger, S. A., Avril, M., Vaz, M., Babar, P. H., Brazier, A. J., et al. (2016). Severe Adult Malaria is Associated With Specific PfEMP1 Adhesion Types and High Parasite Biomass. *Proc. Natl. Acad. Sci. U.S.A.* 113 (23), E3270–E3279. doi: 10.1073/pnas.1524294113

Bernabeu, M., Gunnarsson, C., Vishnyakova, M., Howard, C. C., Nagao, R. J., Avril, M., et al. (2019). Binding Heterogeneity of Plasmodium Falciparum to Engineered 3d Brain Microvessels Is Mediated by EPCR and ICAM-1. *MBio* 10 (3), e00420-19. doi: 10.1128/mBio.00420-19

Brabin, B. J., Romagosa, C., Abdelgalil, S., Menendez, C., Verhoeff, F. H., McGready, R., et al. (2004). The Sick Placenta-the Role of Malaria. *Placenta* 25 (5), 359–378. doi: 10.1016/j.placenta.2003.10.019

Claessens, A., Adams, Y., Ghumra, A., Lindergard, G., Buchan, C. C., Andisi, C., et al. (2012). A Subset of Group A-Like Var Genes Encodes the Malaria Parasite Ligands for Binding to Human Brain Endothelial Cells. *Proc. Natl. Acad. Sci. U.S.A.* 109 (26), E1772–E1781. doi: 10.1073/pnas.1120461109

Conroy, A. L., Hawkes, M., Elphinstone, R. E., Morgan, C., Hermann, L., Barker, K. R., et al. (2016). Acute Kidney Injury Is Common in Pediatric Severe Malaria and Is Associated With Increased Mortality. *Open Forum Infect. Dis.* 3 (2), ofw046. doi: 10.1093/ofid/ofw046

Conroy, A. L., Opoka, R. O., Bangirana, P., Idro, R., Ssenkusu, J. M., Datta, D., et al. (2019). Acute Kidney Injury is Associated With Impaired Cognition and Chronic Kidney Disease in a Prospective Cohort of Children With Severe Malaria. *BMC Med.* 17 (1), 98. doi: 10.1186/s12916-019-1332-7

Dondorp, A. M., Ince, C., Charunwatthana, P., Hanson, J., van, K. A., Faiz, M. A., et al. (2008a). Direct In Vivo Assessment of Microcirculatory Dysfunction in Severe Falciparum Malaria. *J. Infect. Dis.* 197 (1), 79–84. doi: 10.1086/523762

Dondorp, A. M., Lee, S. J., Faiz, M. A., Mishra, S., Price, R., Tjitra, E., et al. (2008b). The Relationship Between Age and the Manifestations of and Mortality Associated With Severe Malaria. *Clin. Infect. Dis.* 47 (2), 151–157. doi: 10.1086/589287

Gillrie, M. R., Avril, M., Brazier, A. J., Davis, S. P., Stins, M. F., Smith, J. D., et al. (2015). Diverse Functional Outcomes of Plasmodium Falciparum Ligation of EPCR: Potential Implications for Malarial Pathogenesis. *Cell Microbiol.* 17 (12), 1883–1899. doi: 10.1111/cmi.12479

Hsieh, F. L., Turner, L., Bolla, J. R., Robinson, C. V., Lavstsen, T., and Higgins, M. K. (2016). The Structural Basis for CD36 Binding by the Malaria Parasite. *Nat. Commun.* 7, 12837. doi: 10.1038/ncomms12837

Janes, J. H., Wang, C. P., Levin-Edens, E., Vigan-Womas, I., Guillotte, M., Melcher, M., et al. (2011). Investigating the Host Binding Signature on the Plasmodium Falciparum PfEMP1 Protein Family. *PloS Pathog.* 7 (5), e1002032. doi: 10.1371/journal.ppat.1002032

Kessler, A., Dankwa, S., Bernabeu, M., Harawa, V., Danziger, S. A., Duffy, F., et al. (2017). Linking EPCR-Binding PfEMP1 to Brain Swelling in Pediatric Cerebral Malaria. *Cell Host Microbe* 22601-614 (5), e605. doi: 10.1016/j.chom.2017.09.009

Kim, I., Moon, S. O., Kim, S. H., Kim, H. J., Koh, Y. S., and Koh, G. Y. (2001). Vascular Endothelial Growth Factor Expression of Intercellular Adhesion Molecule 1 (ICAM-1), Vascular Cell Adhesion Molecule 1 (VCAM-1), and E-Selectin Through Nuclear Factor-Kappa B Activation in Endothelial Cells. *J. Biol. Chem.* 276 (10), 7614–7620. doi: 10.1074/jbc.M009705200

Lau, C. K., Turner, L., Jespersen, J. S., Lowe, E. D., Petersen, B., Wang, C. W., et al. (2015). Structural Conservation Despite Huge Sequence Diversity Allows EPCR Binding by the PfEMP1 Family Implicated in Severe Childhood Malaria. *Cell Host Microbe* 17 (1), 118–129. doi: 10.1016/j.chom.2014.11.007

Lavstsen, T., Turner, L., Saguti, F., Magistrado, P., Rask, T. S., Jespersen, J. S., et al. (2012). Plasmodium Falciparum Erythrocyte Membrane Protein 1 Domain Cassettes 8 and 13 are Associated With Severe Malaria in Children. *Proc. Natl. Acad. Sci. U.S.A.* 109 (26), E1791–E1800. doi: 10.1073/pnas.1120455109

Lennartz, F., Adams, Y., Bengtsson, A., Olsen, R. W., Turner, L., Ndam, N. T., et al. (2017). Structure-Guided Identification of a Family of Dual Receptor-Binding PfEMP1 That Is Associated With Cerebral Malaria. *Cell Host Microbe* 21 (3), 403–414. doi: 10.1016/j.chom.2017.02.009

Lennartz, F., Smith, C., Craig, A. G., and Higgins, M. K. (2019). Structural Insights Into Diverse Modes of ICAM-1 Binding by Plasmodium Falciparum-Infected Erythrocytes. *Proc. Natl. Acad. Sci. U.S.A.* 116 (40), 20124–20134. doi: 10.1073/pnas.1911900116

Leopold, S. J., Ghose, A., Allman, E. L., Kingston, H. W. F., Hossain, A., Dutta, A. K., et al. (2019). Identifying the Components of Acidosis in Patients With Severe Plasmodium Falciparum Malaria Using Metabolomics. *J. Infect. Dis.* 219 (11), 1766–1776. doi: 10.1093/infdis/jiy727

Ligresti, G., Nagao, R. J., Xue, J., Choi, Y. J., Xu, J., Ren, S., et al. (2016). A Novel Three-Dimensional Human Peritubular Microvascular System. *J. Am. Soc. Nephrol.* 27 (8), 2370–2381. doi: 10.1681/ASN.2015070747

MacPherson, G. G., Warrell, M. J., White, N. J., Looareesuwan, S., and Warrell, D. A. (1985). Human Cerebral Malaria. A Quantitative Ultrastructural Analysis of Parasitized Erythrocyte Sequestration. *Am. J. Pathol.* 119 (3), 385–401.

Marchiafava, E., and Bignami, A. (1892). *Two Monographs on Malaria and the Parasites of Malaria Fevers* (London: The New Sydenham Society).

Miller, L. H., Baruch, D. I., Marsh, K., and Doumbo, O. K. (2002). The Pathogenic Basis of Malaria. *Nature* 415 (6872), 673–679. doi: 10.1038/415673a

Milner, D. A.Jr., Lee, J. J., Frantzreb, C., Whitten, R. O., Kamiza, S., Carr, R. A., et al. (2015). Quantitative Assessment of Multiorgan Sequestration of Parasites in Fatal Pediatric Cerebral Malaria. *J. Infect. Dis.* 212 (8), 1317–1321. doi: 10.1093/infdis/jiv205

Milner, D. A.Jr., Whitten, R. O., Kamiza, S., Carr, R., Liomba, G., Dzamalala, C., et al. (2014). The Systemic Pathology of Cerebral Malaria in African Children. *Front. Cell Infect. Microbiol.* 4. doi: 10.3389/fcimb.2014.00104

Mkumbaye, S. I., Wang, C. W., Lyimo, E., Jespersen, J. S., Manjurano, A., Mosha, J., et al. (2017). The Severity of Plasmodium Falciparum Infection Is Associated With Transcript Levels of Var Genes Encoding Endothelial Protein C Receptor-Binding P. Falciparum Erythrocyte Membrane Protein 1. *Infect. Immun.* 85 (4), e00841–16. doi: 10.1128/IAI.00841-16

Nguansangiam, S., Day, N. P., Hien, T. T., Mai, N. T., Chaisri, U., Riganti, M., et al. (2007). A Quantitative Ultrastructural Study of Renal Pathology in Fatal Plasmodium Falciparum Malaria. *Trop. Med. Int. Health* 12 (9), 1037–1050. doi: 10.1111/j.1365-3156.2007.01881.x

Petersen, J. V., Bouwens, E. M., Tamayo, I., Turner, L., Wang, C. W., Stins, M., et al. (2015). Protein C System Defects Inflicted by the Malaria Parasite Protein PfEMP1 can be Overcome by a Soluble EPCR Variant. *Thromb. Haemost.* 114 (5), 1038–1048. doi: 10.1160/TH15-01-0018

Rask, T. S., Hansen, D. A., Theander, T. G., Gorm, P. A., and Lavstsen, T. (2010). Plasmodium Falciparum Erythrocyte Membrane Protein 1 Diversity in Seven Genomes - Divide and Conquer. *PloS Comput. Biol.* 6 (9), e1000933. doi: 10.1371/journal.pcbi.1000933

Robinson, B. A., Welch, T. L., and Smith, J. D. (2003). Widespread Functional Specialization of Plasmodium Falciparum Erythrocyte Membrane Protein 1 Family Members to Bind CD36 Analysed Across a Parasite Genome. *Mol. Microbiol.* 47 (5), 1265–1278. doi: 10.1046/j.1365-2958.2003.03378.x

Sahu, P. K., Duffy, F. J., Dankwa, S., Vishnyakova, M., Majhi, M., Pirpamer, L., et al. (2021). Determinants of Brain Swelling in Pediatric and Adult Cerebral Malaria. *JCI Insight* 6 (18), e145823. doi: 10.1172/jci.insight.145823

Sampath, S., Brazier, A. J., Avril, M., Bernabeu, M., Vigdorovich, V., Mascarenhas, A., et al. (2015). Plasmodium Falciparum Adhesion Domains Linked to Severe Malaria Differ in Blockade of Endothelial Protein C Receptor. *Cell Microbiol.* 17 (12), 1868–1882. doi: 10.1111/cmi.12478

Scott, J. A., Berkley, J. A., Mwangi, I., Ochola, L., Uyoga, S., Macharia, A., et al. (2011). Relation Between Falciparum Malaria and Bacteraemia in Kenyan Children: A Population-Based, Case-Control Study and a Longitudinal Study. *Lancet* 378 (9799), 1316–1323. doi: 10.1016/S0140-6736(11)60888-X

Seydel, K. B., Fox, L. L., Glover, S. J., Reeves, M. J., Pensulo, P., Muiruri, A., et al. (2012). Plasma Concentrations of Parasite Histidine-Rich Protein 2 Distinguish Between Retinopathy-Positive and Retinopathy-Negative Cerebral Malaria in Malawian Children. *J. Infect. Dis.* 206 (3), 309–318. doi: 10.1093/infdis/jis371

Smith, J. D., Chitnis, C. E., Craig, A. G., Roberts, D. J., Hudson-Taylor, D. E., Peterson, D. S., et al. (1995). Switches in Expression of Plasmodium Falciparum Var Genes Correlate With Changes in Antigenic and Cytoadherent Phenotypes of Infected Erythrocytes. *Cell* 82 (1), 101–110. doi: 10.1016/0092-8674(95)90056-X

Smith, J. D., Craig, A. G., Kriek, N., Hudson-Taylor, D., Kyes, S., Fagen, T., et al. (2000). Identification of a Plasmodium Falciparum Intercellular Adhesion Molecule-1 Binding Domain: A Parasite Adhesion Trait Implicated in Cerebral Malaria. *Proc. Natl. Acad. Sci. U.S.A.* 97 (4), 1766–1771. doi: 10.1073/pnas.040545897

Smith, J. D., Rowe, J. A., Higgins, M. K., and Lavstsen, T. (2013). Malaria's Deadly Grip: Cytoadhesion of Plasmodium Falciparum-Infected Erythrocytes. *Cell Microbiol.* 15 (12), 1976–1983. doi: 10.1111/cmi.12183

Spitz, S. (1946). The Pathology of Acute Falciparum Malaria. *Mil Surg.* 99 (5), 555–572. doi: 10.1093/milmed/99.5.555

Storm, J., Jespersen, J. S., Seydel, K. B., Szestak, T., Mbewe, M., Chisala, N. V., et al. (2019). Cerebral Malaria is Associated With Differential Cytoadherence to Brain Endothelial Cells. *EMBO Mol. Med.* 11 (2), e9164. doi: 10.15252/emmm.201809164

Su, X. Z., Heatwole, V. M., Wertheimer, S. P., Guinet, F., Herrfeldt, J. A., Peterson, D. S., et al. (1995). The Large Diverse Gene Family Var Encodes Proteins Involved in Cytoadherence and Antigenic Variation of Plasmodium Falciparum-Infected Erythrocytes. *Cell* 82 (1), 89–100. doi: 10.1016/0092-8674(95)90055-1

Sypniewska, P., Duda, J. F., Locatelli, I., Althaus, C. R., Althaus, F., and Genton, B. (2017). Clinical and Laboratory Predictors of Death in African Children With Features of Severe Malaria: A Systematic Review and Meta-Analysis. *BMC Med.* 15 (1), 147. doi: 10.1186/s12916-017-0906-5

Taylor, T. E., Fu, W. J., Carr, R. A., Whitten, R. O., Mueller, J. S., Fosiko, N. G., et al. (2004). Differentiating the Pathologies of Cerebral Malaria by Postmortem Parasite Counts. *Nat. Med.* 10 (2), 143–145. doi: 10.1038/nm986

Turner, L., Lavstsen, T., Berger, S. S., Wang, C. W., Petersen, J. E., Avril, M., et al. (2013). Severe Malaria Is Associated With Parasite Binding to Endothelial Protein C Receptor. *Nature* 498 (7455), 502–505. doi: 10.1038/nature12216

Turner, G. D., Morrison, H., Jones, M., Davis, T. M., Looareesuwan, S., Buley, I. D., et al. (1994). An Immunohistochemical Study of the Pathology of Fatal Malaria. Evidence for Widespread Endothelial Activation and a Potential Role for Intercellular Adhesion Molecule-1 in Cerebral Sequestration. *Am. J. Pathol.* 145 (5), 1057–1069.

Wichers, J. S., Tonkin-Hill, G., Thye, T., Krumkamp, R., Kreuels, B., Strauss, J., et al. (2021). Common Virulence Gene Expression in Adult First-Time Infected Malaria Patients and Severe Cases. *Elife* 10, e69040. doi: 10.7554/eLife.69040

Wilairatana, P., Meddings, J. B., Ho, M., Vannaphan, S., and Looareesuwan, S. (1997). Increased Gastrointestinal Permeability in Patients With Plasmodium Falciparum Malaria. *Clin. Infect. Dis.* 24 (3), 430–435. doi: 10.1093/clinids/24.3.430

Conflict of Interest: The authors declare that the research was conducted in the absence of any commercial or financial relationships that could be construed as a potential conflict of interest.

Publisher's Note: All claims expressed in this article are solely those of the authors and do not necessarily represent those of their affiliated organizations, or those of the publisher, the editors and the reviewers. Any product that may be evaluated in this article, or claim that may be made by its manufacturer, is not guaranteed or endorsed by the publisher.

frontiers in Cellular and Infection Microbiology

MINI REVIEW
published: 22 February 2022
doi: 10.3389/fcimb.2022.829413

Malaria Related Neurocognitive Deficits and Behavioral Alterations

Pamela Rosa-Gonçalves[1,2,3]*, *Flávia Lima Ribeiro-Gomes*[1,2] *and Cláudio Tadeu Daniel-Ribeiro*[1,2]

[1] Laboratório de Pesquisa em Malária, Instituto Oswaldo Cruz, Fundação Oswaldo Cruz (Fiocruz), Rio de Janeiro, Brazil, [2] Centro de Pesquisa, Diagnóstico e Treinamento em Malária, Fiocruz and Secretaria de Vigilância em Saúde, Ministério da Saúde, Rio de Janeiro, Brazil, [3] Laboratório de Biologia, campus Duque de Caxias, Colégio Pedro II, Duque de Caxias, Brazil

Typical of tropical and subtropical regions, malaria is caused by protozoa of the genus *Plasmodium* and is, still today, despite all efforts and advances in controlling the disease, a major issue of public health. Its clinical course can present either as the classic episodes of fever, sweating, chills and headache or as nonspecific symptoms of acute febrile syndromes and may evolve to severe forms. Survivors of cerebral malaria, the most severe and lethal complication of the disease, might develop neurological, cognitive and behavioral sequelae. This overview discusses the neurocognitive deficits and behavioral alterations resulting from human naturally acquired infections and murine experimental models of malaria. We highlighted recent reports of cognitive and behavioral sequelae of non-severe malaria, the most prevalent clinical form of the disease worldwide. These sequelae have gained more attention in recent years and therapies for them are required and demand advances in the understanding of neuropathogenesis. Recent studies using experimental murine models point to immunomodulation as a potential approach to prevent or revert neurocognitive sequelae of malaria.

Keywords: severe malaria, non-severe malaria, neurocognitive deficits, behavioral alterations, murine malaria

OPEN ACCESS

Edited by:
Laurent Rénia, Nanyang Technological University, Singapore

Reviewed by:
Celio Geraldo Freire-de-Lima, Federal University of Rio de Janeiro, Brazil
Sara Salinas, Institut National de la Santé et de la Recherche Médicale (INSERM), France

***Correspondence:**
Pamela Rosa-Gonçalves
pamelagoncalves@aluno.fiocruz.br

Specialty section:
This article was submitted to Parasite and Host, a section of the journal Frontiers in Cellular and Infection Microbiology

Received: *05 December 2021*
Accepted: *31 January 2022*
Published: *22 February 2022*

Citation:
Rosa-Gonçalves P, Ribeiro-Gomes FL and Daniel-Ribeiro CT (2022) Malaria Related Neurocognitive Deficits and Behavioral Alterations. Front. Cell. Infect. Microbiol. 12:829413. doi: 10.3389/fcimb.2022.829413

INTRODUCTION

Malaria, an important parasitic infectious disease since antiquity, remains a significant public health problem, being responsible for estimated 229 million cases and 409.000 deaths worldwide annually (World Health Organization, 2020). It is caused by protozoa of the genus *Plasmodium* and is transmitted by the bite of the female *Anopheles* mosquito. There are eight species causing human malaria: *P. falciparum, P. vivax, P. malariae, P. ovale curtisi* and *P. ovale wallikeri* (Sutherland et al., 2010), *P. knowlesi, P. cynomolgi* and *P. simium*, the last three being simian parasites responsible for zoonotic infections (Chin et al., 1965; Singh et al., 2004; Ta et al., 2014; Brasil et al., 2017a), and *P. falciparum*, which accounts for the great majority of cases and severe forms of the disease (Cox, 2010). In the early stages of infection, malaria may present with nonspecific symptoms of febrile syndromes (including nausea and diarrhea) before the emergence of the classic triad (fever, chills, sweating), often associated with headache. The disease may evolve, in case of falciparum malaria, to its severe forms such as cerebral malaria (CM), severe acute respiratory syndrome, severe malarial anemia, among others (Ashley et al., 2018). Although severe anemia is the most common

complication of the disease, CM is the deadliest one, affecting mainly children up to 5 years old, pregnant and non-immune individuals (tourists and military) from non-endemic areas (Porta et al., 1993; Ashley et al., 2018; Ghazanfari et al., 2018).

The neuropathogenesis of CM involves brain intravascular sequestration of *P. falciparum*-parasitized red blood cells occurring through the expression of parasite-encoded *P. falciparum* erythrocyte membrane protein-1 (PfEMP-1) in protuberances of the infected red-cell surface that interacts with host adhesion receptors on endothelium, contributing to the inflammatory process (Lau et al., 2015). These events participate in the generation of blood flow impairment, endothelial dysfunction, intravascular coagulation, vascular occlusion, cerebral hypoxia, microglial activation, astrogliosis, disruption of the blood-brain barrier and neurotoxicity (Medana et al., 2002; Taylor et al., 2004; Dorovini-Zis et al., 2011; Schiess et al., 2020).

Post treatment long-term neurocognitive deficits, including in multiple areas of cognitive function, and behavioral alterations[1] are related to severe malaria, mainly CM (Bangirana et al., 2014; Ssenkusu et al., 2016; Conroy et al., 2019a). Nevertheless, cognitive deficits and behavioral alterations have also been associated to the non-severe presentations of the disease (Vitor-Silva et al., 2009; Fink et al., 2013; Tapajós et al., 2019).

The aim of this mini review is to provide an overview on the state of art and on the available knowledge in the literature on neurocognitive and behavioral damage associated to malaria. There are few articles on the subject and some of them have limitations, due to involving human beings, having been carried out in areas lacking adequate infrastructure, or having critical design or methodological aspects. Although a detailed analysis on the structure of the cited articles is out of this mini review scope, we have tried to indicate points of concern deserving attention whenever appropriate.

NEUROCOGNITIVE AND BEHAVIORAL SEQUELAE OF SEVERE MALARIA

Individuals with CM treated with artesunate, a potent antimalarial treatment that promotes a rapid decline in parasitemia and recovery (Dondorp et al., 2010), still progress to death in about 15-25% of cases (Bruneel, 2019). Unfortunately, approximately 25% of survivors develop neurocognitive and behavioral sequelae (Bruneel, 2019). Several studies have associated the most varied neurological sequelae, cognitive deficits and behavioral alterations, as well as predisposition to mental disorders in children (Carter et al., 2005a; Carter et al., 2005b; Carter et al., 2006; Idro et al., 2006; Boivin et al., 2007; Birbeck et al., 2010; Bangirana et al., 2011; Idro et al., 2016; Ssenkusu et al., 2016; Brim et al., 2017; Langfitt et al., 2019) and adults (Richardson et al., 1997; Varney et al., 1997; Laverse et al., 2013; Peixoto and Kalei, 2013) with CM (**Figure 1**).

Among children up to five years old, a greater risk for the development of impairment in motor skills, receptive and expressive language, visual reception and social interaction has been identified (Brim et al., 2017; Ouma et al., 2021). Multiple seizures, prolonged coma and intracranial hypertension during CM appear to be related to the risk of neurological sequelae including epilepsy (Idro et al., 2004; Idro et al., 2006; Kariuki et al., 2011). CM does also result in deficits in multiple cognitive domains such as attention and associative memory (Bangirana et al., 2014) and increased risk of mental health disorders (Idro et al., 2016).

The dynamics of malaria deficits can be affected by several factors, such as infection at different stages of neurodevelopment, number of previous malaria episodes, methodology used to assess the neurocognitive outcomes, and follow-up time. Although some neurological sequelae of CM in children, such as hypotonia, cortical blindness, tremors and aphasia recover over time (Boivin et al., 2007; John et al., 2008; Dondorp et al., 2010), other such as hemiplegia, paresis, seizures, language deficits and, especially, cognitive impairment in memory, non-verbal function and behavioral alterations may persist (Carter et al., 2006; Birbeck et al., 2010; Oluwayemi et al., 2013; Severe Malaria, 2014) (**Table 1**) for up to nine years after an episode of CM (Carter et al., 2005a).

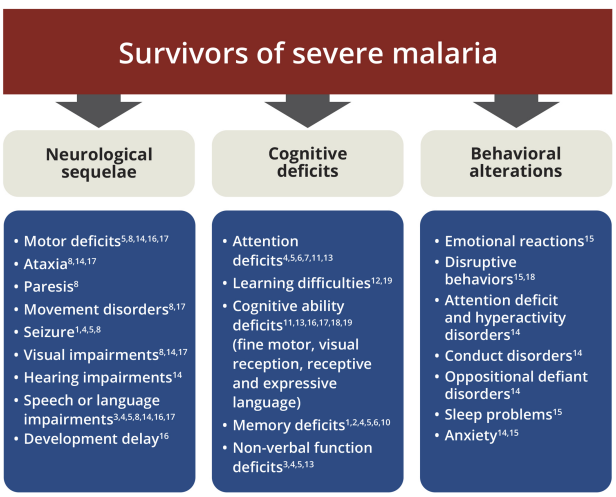

FIGURE 1 | Spectrum of neurologic, cognitive and behavioral sequelae among survivors of severe malaria. List of main impairments after severe malaria. [1] Varney et al. (1997); [2] Richardson et al. (1997); [3] Carter et al. (2005a); [4] Carter et al. (2005b); [5] Idro et al. (2006); [6] Boivin et al. (2007); [7] John et al. (2008); [8] Birbeck et al. (2010); [9] Bangirana et al. (2011); [10] Laverse et al. (2013); [11] Bangirana et al. (2014); [12] Peixoto and Kalei (2013); [13] Bangirana et al. (2016); [14] Idro et al. (2016); [15] Ssenkusu et al. (2016); [16] Brim et al. (2017); [17] Conroy et al. (2019b); [18] Langfitt et al. (2019); [19] Ouma et al. (2021).

[1] Neurologic sequelae: consist of functional loss in motor, speech, vision, and hearing domains, as well as epilepsy; Neurocognitive deficits: a neurological and/or cognitive impairment involving specific brain-located neural phenomena; Cognitive deficits: decrease in skill related to broad sense of consciousness (how one perceives, remembers things, judges oneself); Behavioral alterations: behavior changes, including inattentiveness, hyperactivity, impulsive/ aggressive behaviors and risk of manifestation of mental health disorders.

TABLE 1 | Detection and persistence of neurocognitive and behavioral alterations in children with cerebral malaria.

Outcomes	Impairments at discharge	Months*			n	Reference
		6	12	24		
Neurologic sequelae						
Neurologic deficits	++++++	+	+	+	232	Conroy et al. (2021)
Motor	+++++		+		173	Idro et al. (2016)
	+++++			+	225	Conroy et al. (2019b)
Movement disorders	+			+	225	Conroy et al. (2019b)
Visual	++		-		173	Idro et al. (2016)
	++			-	225	Conroy et al. (2019b)
Hearing	+		-		173	Idro et al. (2016)
Speech and/or language	++		+		131	Oluwayemi et al. (2013)
	++		-		173	Idro et al. (2016)
	+++			+	225	Conroy et al. (2019b)
Paresis	+		+		131	Oluwayemi et al. (2013)
Seizure	+		+		131	Oluwayemi et al. (2013)
Hyporeflexia or Babinski sign	+++			-	225	Conroy et al. (2019b)
Ataxia and/or gait problems	+++		-		173	Idro et al. (2016)
	++++			-	225	Conroy et al. (2019b)
Cognitive deficits						
MSEL	+	+	+		80	Bangirana et al. (2016)
KABC or MDAT	+	+	+		85	Langfitt et al. (2019)
RBMTC				+	152	Carter et al. (2006)
Memory deficits	+		+	+	131	Oluwayemi et al. (2013)
Attention	+	+**		++++	38	John et al. (2008)
Behavioral alterations						
Increased risk of expression of mental disorders	-	-	+++	-	173	Idro et al. (2016)
Behavioral dysfunctions	+	+	+	+	100	Ssenkusu et al. (2016)

**Approximate time of follow up; **not statistically significant; n, number of individuals; +, 0,1-4,99% or detected; ++, 5-9,99%; +++, 10-14,99%; ++++, 15-19,99%; +++++, 20-24,99%; ++++++, >25%; -, not detected; blank spaces, not accessed; MSEL, Mullen Scales of Early Learning; KABC, Kauffman Assessment Battery for Children; MDAT, Malawi Developmental Assessment Tool; RBMTC, Rivermead Behavioural Memory Test for Children; Some studies establish the percentage of damage among individuals who developed any neurocognitive impairment after malaria, or among CM survivors; other displayed the results in z scores that are not interpreted quantitatively as percentage values. Whenever there was a difference in the z score, it was interpreted qualitatively, as a detected or undetected outcome.*

Long-term cognitive ability deficits are also observed in children after severe malarial anemia (Bangirana et al., 2014; Conroy et al., 2019a). Severe anemia might affect the overall cognitive ability related to neurocognitive domains for fine motor scales, visual reception, receptive and expressive languages (Bangirana et al., 2014; Bangirana et al., 2016). Furthermore, acute kidney injury, a complication of severe malaria, is a risk factor for long-term neurocognitive impairment and behavioral problems in children with severe malarial anemia and cerebral malaria in overall cognitive ability (Conroy et al., 2019b), socio-emotional (aggressive behavior) and executive functions (Hickson et al., 2019).

Murine models have made invaluable contributions to malaria research (Lou et al., 2001). Different strains of mice infected by different species of plasmodia reproduce different forms of the disease depending on the combination of parasite and host, exhibiting susceptibility or resistance to severe forms. Neurologic, cognitive and behavioral deficits observed in malaria patients are reproduced in murine model of experimental CM (ECM). Infection of C57BL/6 and Swiss mice with *Plasmodium berghei*, ANKA strain (Grau et al., 1990; Martins et al., 2009; Martins et al., 2016), or Swiss mice with the lethal strain of *P. yoelli* (Li et al., 2001; Reis et al., 2010) are also models of ECM.

C57BL/6 mouse model infected with *P. berghei* ANKA is the classic reference for the study of ECM (Grau et al., 1990). The absence of a protein analogous to PfEMP-1, which binds to ligands overexpressed by influence of inflammatory cytokines on vessel endothelium in *P. berghei*, contributes to a limited sequestration of parasitized erythrocytes in the murine cerebral microvasculature. This model has, nonetheless, many characteristics that resemble human CM (Brian De Souza and Riley, 2002; De Niz and Heussler, 2018; Ghazanfari et al., 2018). Three days after infection (D3), low levels of parasitemia are measured, which gradually increase during the course of the infection. At D4, a slight adhesion of few leukocytes to the cerebral microvasculature may begin, with minimal presence of edema restricted to some punctual areas of the brain (Potter et al., 2006). Clinical neurological signs are identified from D5 on, with the establishment of a clear neurological syndrome at D6, including vascular inflammation, endothelial activation, rupture of the blood-brain barrier, edema and punctiform hemorrhage in parts of the brain, in addition to the set of neurocognitive sequelae and behavioral alterations assessable in behavioral tests in the acute phase and after recovery from ECM (Brian De Souza and Riley, 2002; Hunt et al., 2006; Potter et al., 2006; Desruisseaux et al., 2008; Dai et al., 2010; Reis et al., 2010; Lacerda-Queiroz et al., 2010; Martins et al., 2010; De Miranda et al., 2011; Reverchon et al., 2017; Ghazanfari et al., 2018; Lima et al., 2020). Generally, between days 6 and 9 the animals die (Martins et al., 2010).

During acute ECM, C57BL/6 mice infected with *P. berghei* ANKA exhibit motor impairment. In the course of acute

infection, mice do also present cognitive deficits in object recognition test of working memory (Desruisseaux et al., 2008), anxiety-like behavior in elevated plus maze test (De Miranda et al., 2011) and depressive-like behavior in tail suspension and forced swim tests (Lima et al., 2020). Nonetheless and most important, specific neurological sequelae, including poor performance in balance beam test to evaluate motor coordination, are clearly present as sequelae after treatment of ECM (Dai et al., 2010; Reis et al., 2010). Cognitive deficits in multiple memory impairment (habituation, aversive and recognition memories) and behavioral alterations (depressive-like behavior) are also reported after CM (Reis et al., 2010; Lima et al., 2020).

Some experimental murine models, non-susceptible to the development of experimental CM, are useful to reproduce severe forms of non-cerebral malaria, for instance: *P. berghei* NK65 infected C57BL/6 mice are used as an experimental model to investigate acute respiratory distress syndrome in malaria (Van Den Steen et al., 2010; Scaccabarozzi et al., 2018), while BALB/c mice infected with *P. berghei* ANKA compose a model of severe anemia and severe placental malaria (Neres et al., 2008; De Niz and Heussler, 2018). However, cognitive deficits were not registered in most of these experimental murine models of severe forms other than cerebral malaria (Reis et al., 2010; Freeman et al., 2016). Only a minor occurrence of neurological alterations of locomotor activity and autonomic function was observed in BALB/c mice infected with *P. berghei* ANKA (Reis et al., 2010), as well as cognitive injury in the offspring of infected pregnant BALB/c mice (McDonald et al., 2015).

COGNITIVE AND BEHAVIORAL SEQUELAE OF NON-SEVERE MALARIA

Cognitive and behavioral deficits are also observed after episodes of non-severe malaria in individuals from diverse *P. falciparum* and *P. vivax* endemic areas (Fernando et al., 2003; Vitor-Silva et al., 2009; Thuilliez et al., 2010; Fink et al., 2013; Vorasan et al., 2015; Brasil et al., 2017b; Tapajós et al., 2019). The reported effects have been found in individuals who had uncomplicated febrile episodes of malaria (Vitor-Silva et al., 2009; Vorasan et al., 2015; Brasil et al., 2017b; Tapajós et al., 2019) and even asymptomatic infections (Al Serouri et al., 2000; Nankabirwa et al., 2013; Clarke et al., 2017).

Impairments in the school performance associated with language and logical reasoning in mathematics have been identified in children from Brazil and Sri Lanka after non-severe malaria (Fernando et al., 2003; Vitor-Silva et al., 2009). In addition, children with more than five episodes performed less well than children who had up to three febrile attacks (Fernando et al., 2003). Additional studies with different ranges in the number of past episodes of malaria can confirm and reinforce the observation of a quantitative effect of malaria on the cognitive-behavioral performance of infected children. School performance was evaluated during a nine-month follow-up (Vitor-Silva et al., 2009). Tapajós et al. (2019) clearly demonstrated that an episode of non-severe malaria, caused by *P. vivax*, was a determining factor – independent of the socioeconomic status, family stimulus and child's health status – in triggering cognitive impairment in children aged two to seven years. In Zambia and Uganda, episodes of malaria (with or without anemia) were associated with impaired cognitive ability in children (Fink et al., 2013; Boivin et al., 2016). Fink et al. (2013) point out that children's exposure to malaria was associated with reduced socio-emotional development. It is worth mentioning that the effect size was not shown in this study, which did not evaluate individual infection rates, but rather used national data.

On the other hand, classic murine models of non-severe malaria as C57BL/6 mice infected with *P. chabaudi* and Swiss with *P. yoelii* (non-lethal) were unable to reveal the presence of cognitive impairment (Reis et al., 2010; Guha et al., 2014). Behavioral alterations, such as anxiety-like behavior and social interaction deficits, are observed during the course of non-severe malaria (D9) in C57BL/6 mice infected by *P. chabaudi adami* (Guha et al., 2014). These alterations may be, however, at least partially due to the inflammatory state of animal during the course of the ongoing infection. In this model, infection also predisposes to enhanced post-stress anxiety-like responses when non-severe malaria occurs at a young age (Guha et al., 2020).

More recently, De Sousa et al., (2018) infected C57BL/6 mice with *P. berghei* ANKA (the classic model of experimental CM), treating mice at D4, before any neurological manifestation of CM. This model proved to be useful for detecting cognitive sequelae and late (D92) behavioral alterations following (82 days after parasite clearance) a single episode of non-severe malaria (De Sousa et al., 2021).

THERAPEUTIC APPROACHES TO NEUROCOGNITIVE AND BEHAVIORAL SEQUELAE IN MALARIA

To date, no effective therapy for the cognitive and behavioral sequelae of malaria is available. The lack of an effective therapy is associated with an incomplete understanding of the mechanisms involved in pathogenesis of cognitive and behavioral sequelae, especially in non-severe malaria. This knowledge is important to the development of rational therapies, directed to specific targets.

While several clinical studies to treat CM appeared promising for focusing on specific targets of pathogenesis, as sequestration of parasitized erythrocytes in the microvasculature, inflammation, coagulation, endothelial function and oxidative stress, they have not been successful in reducing neurologic sequelae (Lell et al., 2010; Mwanga-Amumpaire et al., 2015; Schiess et al., 2020). Some approaches have even aggravated these sequelae (Warrell et al., 1982; Van Hensbroek et al., 1996; Akech et al., 2006).

In addition, many studies investigating adjuvant therapies in CM do not assess the effects on neurocognitive sequelae. Although antimalarials may not be considered an approach to treat these sequelae, Conroy et al. (2021) recently showed that

treatment of severe malaria with derivatives of artemisinin in children resulted in a significant reduction in mortality and in neurological deficits, associated with improvement in long-term behavioral alterations compared to quinine treatment. The absence of effect on overall cognition, attention and memory but a specific improvement in the executive function impairment, revealed by the BRIEF (Behaviour Rating Inventory of Executive Function) test observed by the authors, suggest that antimalarials may have distinct impacts on different categories of sequelae. Treatment of cognitive deficits remains a challenge. Some studies showed an expected positive effect of preventive malaria regimens on cognitive function of chronically exposed individuals in endemic areas (Cohee et al., 2020).

Several *in vivo* experimental studies have performed interventions – before infection or associated with antimalarial treatment – in an attempt to improve clinical response, increase survival and reduce neurocognitive and behavioral impairments (Varo et al., 2018; Gul et al., 2021). Serghides et al. (2014) got compelling effects of rosiglitazone, a PPARγ agonist, as an adjuvant treatment of ECM. This treatment ameliorated recognition memory, reduced endothelial activation and oxidative stress, and increased neurotrophic factors (Varo et al., 2018). Currently the neurocognitive impact of this approach on CM is being accessed in a clinical trial. Lima et al. (2020) obtained promising results administrating mesenchymal stem cells (MSC) as adjuvant therapy to chloroquine at day 6 of infection, for ECM. Treatment with a single dose of MSC has protected infected mice against vascular damage and improved depressive-like behavior. Witschkowski et al. (2020) reported that bacillus Calmette-Guérin (BCG) vaccination given 10 or 30 days before infection protected mice from developing clinical symptoms of ECM and improved survival associated with immunosuppressive mechanisms. De Miranda et al. (2017) registered that treatment with MK801, a N-methil-D-aspartate (NMDA) receptor antagonist, before signs of ECM (from D3 to the end of antimalarial chloroquine treatment) prevented long-term memory impairment and depressive-like behavior.

Since diagnosis of CM does occur when the patient's condition is severe, the period required for the introduction of the treatment may not be sufficient for its effectiveness and the adjuvant approaches quoted above may have a very restricted therapeutic window (Idro et al., 2010). In view of these limitations, emphasis should be given to studies approaching the treatment of already established neurocognitive impairments. Neuroinflammation is a hallmark of neurocognitive and behavioral impairments of malaria and may result from peripheral inflammation (Sankowski et al., 2015). Therefore, immunomodulatory approaches hold promise for alleviating or stopping long-term damage.

Cognitive rehabilitation of severe malaria survivors through computerized training has shown an immediate improvement in some neuropsychological and behavioral parameters in children in Africa (Bangirana et al., 2009; Boivin et al., 2019). However, this approach in patients who have survived severe malaria may be limited by the need of specific diagnosis, long-term follow-up and information on how long this effect will last. Another limitation to the use of such approach is that it requires specific computer systems, often unavailable in endemic areas of developing countries (Boivin et al., 2019).

In the last few years, evidence has accumulated pointing to the ability of immune stimuli to modulate neurogenesis, synaptic plasticity, in addition to cognitive and behavioral function (Xia et al., 2014; Li et al., 2015; Li et al., 2016; Yang et al., 2016; Qi et al., 2017; Yang et al., 2020; De Sousa et al., 2021). These findings support the concept of consistent communication and interrelationship between the nervous and immune systems, as plastic and cognitive systems (Jerne and Cocteau, 1984; Pert et al., 1985; Cohen, 1992; Sawada et al., 1993; Josefsson et al., 1996; Amenta et al., 2002; McKenna et al., 2002; Daniel-Ribeiro and Martins, 2017) and the use of immunomodulation as a promising approach in the treatment of neurocognitive and behavioral sequelae of infectious diseases.

In this context, our research group has been investigating the effect of immune stimuli on neurocognition. Active immunization of both healthy and *P. berghei* ANKA infected C57BL/6 mice using different integrated stimuli (elicitors of the Th2 response) improved recognition memory in homeostasis, recovered late deficits in cognitive function and inhibited the manifestation of an anxiety-like phenotype caused by a unique episode of non-severe malaria (De Sousa et al., 2021).

CONCLUSIONS

In summary, accumulating evidence has revealed that malaria might lead to significant global cognitive impairment and behavioral alterations, even after non-severe episodes, that might persist for years. Neurological sequelae, however, seem to be restricted to severe malaria. These neurocognitive and behavioral sequelae of malaria lack specific and effective treatment. Results obtained in a few well conducted recent studies highlight the potential of immunomodulation as a cognitive enhancement strategy to treat cognitive and behavioral sequelae of malaria.

AUTHOR CONTRIBUTIONS

PR-G drafted the manuscript and PR-G, FR-G and CD-R reviewed, edited and prepared its final version. All authors read and approved the submitted version.

FUNDING

FR-G and CD-R are supported by CNPq, Brazil, through a Productivity Research Fellowship, and CD-R is a "*Cientista do Nosso Estado*" by *Faperj*. The *Laboratório de Pesquisa em Malária, Instituto Oswaldo Cruz (IOC), Fiocruz* is an Associated Laboratory of the *Instituto Nacional de Ciência e Tecnologia (INCT)* in Neuroimmunomodulation supported by the CNPq, and of the Rio de Janeiro Neuroinflammation Network financed by Faperj.

ACKNOWLEDGMENTS

PR-G is grateful to the Postgraduate Program in Parasite Biology of the *Instituto Oswaldo Cruz (IOC)*, *Fiocruz*, for the academic support, and to *Conselho Nacional de Desenvolvimento Científico e Tecnológico* (*CNPq*) and *IOC* for MSc and doctoral fellowships. The text of this manuscript originated in a theoretical chapter of the MSc dissertation of PR-G. The authors are thankful to Fernando Vasconcelos for designing the final version of **Figure 1**.

REFERENCES

Akech, S., Gwer, S., Idro, R., Fegan, G., Eziefula, A. C., Newton, C. R. J. C., et al. (2006). Volume Expansion With Albumin Compared to Gelofusine in Children With Severe Malaria: Results of a Controlled Trial. *PloS Clin. Trials* 1, e21. doi: 10.1371/journal.pctr.0010021

Al Serouri, A. W., Grantham-McGregor, S. M., Greenwood, B., and Costello, A. (2000). Impact of Asymptomatic Malaria Parasitaemia on Cognitive Function and School Achievement of Schoolchildren in the Yemen Republic. *Parasitology* 121, 337–345. doi: 10.1017/S0031182099006502

Amenta, F., El-Assouad, D., Mignini, F., Ricci, A., and Tayebati, S. K. (2002). Neurotransmitter Receptor Expression by Peripheral Mononuclear Cells: Possible Marker of Neuronal Damage by Exposure to Radiations. *Cell. Mol. Biol. (Noisy-le-grand).* 48, 415–421.

Ashley, E. A., Pyae Phyo, A., and Woodrow, C. J. (2018). Malaria. *Lancet* 391, 1608–1621. doi: 10.1016/S0140-6736(18)30324-6

Bangirana, P., Giordani, B., John, C. C., Page, C., Opoka, R. O., and Boivin, M. J. (2009). Immediate Neuropsychological and Behavioral Benefits of Computerized Cognitive Rehabilitation in Ugandan Pediatric Cerebral Malaria Survivors. *J. Dev. Behav. Pediatr.* 30, 310–318. doi: 10.1097/DBP.0b013e3181b0f01b

Bangirana, P., Musisi, S., Boivin, M. J., Ehnvall, A., John, C. C., Bergemann, T. L., et al. (2011). Malaria With Neurological Involvement in Ugandan Children: Effect on Cognitive Ability, Academic Achievement and Behaviour. *Malar. J.* 10, 334. doi: 10.1186/1475-2875-10-334

Bangirana, P., Opoka, R. O., Boivin, M. J., Idro, R., Hodges, J. S., and John, C. C. (2016). Neurocognitive Domains Affected by Cerebral Malaria and Severe Malarial Anemia in Children. *Learn. Individ. Differ.* 46, 38–44. doi: 10.1016/j.lindif.2015.01.010

Bangirana, P., Opoka, R. O., Boivin, M. J., Idro, R., Hodges, J. S., Romero, R. A., et al. (2014). Severe Malarial Anemia Is Associated With Longterm Neurocognitive Impairment. *Clin. Infect. Dis.* 59, 336–344. doi: 10.1093/cid/ciu293

Birbeck, G. L., Molyneux, M. E., Kaplan, P. W., Seydel, K. B., Chimalizeni, Y. F., Kawaza, K., et al. (2010). Blantyre Malaria Project Epilepsy Study (BMPES) of Neurological Outcomes in Retinopathy-Positive Paediatric Cerebral Malaria Survivors: A Prospective Cohort Study. *Lancet Neurol.* 9, 1173–1181. doi: 10.1016/S1474-4422(10)70270-2

Boivin, M. J., Bangirana, P., Byarugaba, J., Opoka, R. O., Idro, R., Jurek, A. M., et al. (2007). Cognitive Impairment After Cerebral Malaria in Children: A Prospective Study. *Pediatrics* 119:e360-e366. doi: 10.1542/peds.2006-2027

Boivin, M. J., Nakasujja, N., Sikorskii, A., Ruiseñor-Escudero, H., Familiar-Lopez, I., Walhof, K., et al. (2019). Neuropsychological Benefits of Computerized Cognitive Rehabilitation Training in Ugandan Children Surviving Severe Malaria: A Randomized Controlled Trial. *Brain Res. Bull.* 145, 117–128. doi: 10.1016/j.brainresbull.2018.03.002

Boivin, M. J., Sikorskii, A., Familiar-Lopez, I., Ruiseñor-Escudero, H., Muhindo, M., Kapisi, J., et al. (2016). Malaria Illness Mediated by Anaemia Lessens Cognitive Development in Younger Ugandan Children. *Malar. J.* 15, 210. doi: 10.1186/S12936-016-1266-X

Brasil, P., Zalis, M. G., de Pina-Costa, A., Siqueira, A. M., Júnior, C. B., Silva, S., et al. (2017a). Outbreak of Human Malaria Caused by Plasmodium Simium in the Atlantic Forest in Rio De Janeiro: A Molecular Epidemiological Investigation. *Lancet Glob. Heal.* 5, e1038–e1046. doi: 10.1016/S2214-109X(17)30333-9

Brasil, L. M. B. F., Vieira, J. L. F., Araújo, E. C., Piani, P. P. F., Dias, R. M., Ventura, A. M. R. S., et al. (2017b). Cognitive Performance of Children Living in Endemic Areas for Plasmodium Vivax. *Malar. J.* 16, 370. doi: 10.1186/S12936-017-2026-2

Brian De Souza, J., and Riley, E. M. (2002). Cerebral Malaria: The Contribution of Studies in Animal Models to Our Understanding of Immunopathogenesis. *Microbes Infect.* 4, 291–300. doi: 10.1016/S1286-4579(02)01541-1

Brim, R., Mboma, S., Semrud-Clikeman, M., Kampondeni, S., Magen, J., Taylor, T., et al. (2017). Cognitive Outcomes and Psychiatric Symptoms of Retinopathy-Positive Cerebral Malaria: Cohort Description and Baseline Results. *Am. J. Trop. Med. Hyg.* 97, 225–231. doi: 10.4269/ajtmh.17-0020

Bruneel, F. (2019). Human Cerebral Malaria: 2019 Mini Review. *Rev. Neurol. (Paris).* 175, 445–450. doi: 10.1016/j.neurol.2019.07.008

Carter, J. A., Lees, J. A., Gona, J. K., Murira, G., Rimba, K., Neville, B. G. R., et al. (2006). Severe Falciparum Malaria and Acquired Childhood Language Disorder. *Dev. Med. Child Neurol.* 48, 51–57. doi: 10.1017/S0012162206000107

Carter, J. A., Mung'ala-Odera, V., Neville, B. G. R., Murira, G., Mturi, N., Musumba, C., et al. (2005a). Persistent Neurocognitive Impairments Associated With Severe Falciparum Malaria in Kenyan Children. *J. Neurol. Neurosurg. Psychiatry* 76, 476–481. doi: 10.1136/jnnp.2004.043893

Carter, J. A., Ross, A. J., Neville, B. G. R., Obiero, E., Katana, K., Mung'ala-Odera, V., et al. (2005b). Developmental Impairments Following Severe Falciparum Malaria in Children. *Trop. Med. Int. Heal.* 10, 3–10. doi: 10.1111/j.1365-3156.2004.01345.x

Chin, W., Contacos, P. G., Coatney, G. R., and Kimball, H. R. (1965). A Naturally Acquired Quotidian-Type Malaria in Man Transferable to Monkeys. *Science* 149, 865. doi: 10.1126/science.149.3686.865

Clarke, S. E., Rouhani, S., Diarra, S., Saye, R., Bamadio, M., Jones, R., et al. (2017). Impact of a Malaria Intervention Package in Schools on Plasmodium Infection, Anaemia and Cognitive Function in Schoolchildren in Mali: A Pragmatic Cluster-Randomised Trial. *BMJ Glob. Heal.* 2, e000182. doi: 10.1136/bmjgh-2016-000182

Cohee, L. M., Opondo, C., Clarke, S. E., Halliday, K. E., Cano, J., Shipper, A. G., et al. (2020). Preventive Malaria Treatment Among School-Aged Children in Sub-Saharan Africa: A Systematic Review and Meta-Analyses. *Lancet Glob. Heal.* 8, e1499–e1511. doi: 10.1016/S2214-109X(20)30325-9

Cohen, I. R. (1992). The Cognitive Paradigm and the Immunological Homunculus. *Immunol. Today* 13, 490–494. doi: 10.1016/0167-5699(92)90024-2

Conroy, A. L., Datta, D., and John, C. C. (2019a). Causes Severe Malaria and Its Complications in Children. *BMC Med.* 17, 10–13. doi: 10.1186/s12916-019-1291-z

Conroy, A. L., Opoka, R. O., Bangirana, P., Idro, R., Ssenkusu, J. M., Datta, D., et al. (2019b). Acute Kidney Injury Is Associated With Impaired Cognition and Chronic Kidney Disease in a Prospective Cohort of Children With Severe Malaria. *BMC Med.* 17, 98. doi: 10.1186/S12916-019-1332-7

Conroy, A. L., Opoka, R. O., Bangirana, P., Namazzi, R., Okullo, A. E., Georgieff, M. K., et al. (2021). Parenteral Artemisinins Are Associated With Reduced Mortality and Neurologic Deficits and Improved Long-Term Behavioral Outcomes in Children With Severe Malaria. *BMC Med.* 19, 168. doi: 10.1186/S12916-021-02033-1

Cox, F. E. (2010). History of the Discovery of the Malaria Parasites and Their Vectors. *Parasites Vectors* 3, 5. doi: 10.1186/1756-3305-3-5

Dai, M., Reznik, S. E., Spray, D. C., Weiss, L. M., Tanowitz, H. B., Gulinello, M., et al. (2010). Persistent Cognitive and Motor Deficits After Successful Antimalarial Treatment in Murine Cerebral Malaria. *Microbes Infect.* 12, 1198–1207. doi: 10.1016/j.micinf.2010.08.006

Daniel-Ribeiro, C. T., and Martins, Y. C. (2017). *A Imagem Que Temos Das Coisas: O Uso De Imagens Internas Para o Reconhecimento Neural de Objetos do Mundo Real" in Imagens, Micróbios e Espelhos: Os Sistemas Imune e Nervoso e Nossa Relação Com o Ambiente* (Rio de Janeiro, RJ: Fiocruz), 159–197.

De Miranda, A. S., Brant, F., Vieira, L. B., Rocha, N. P., Vieira, É.L.M., Rezende, G. H. S., et al. (2017). A Neuroprotective Effect of the Glutamate Receptor Antagonist MK801 on Long-Term Cognitive and Behavioral Outcomes Secondary to Experimental Cerebral Malaria. *Mol. Neurobiol.* 54, 7063–7082. doi: 10.1007/s12035-016-0226-3

De Miranda, A. S., Lacerda-Queiroz, N., de Carvalho Vilela, M., Rodrigues, D. H., Rachid, M. A., Quevedo, J., et al. (2011). Anxiety-Like Behavior and

Proinflammatory Cytokine Levels in the Brain of C57BL/6 Mice Infected With Plasmodium Berghei (Strain ANKA). *Neurosci. Lett.* 491, 202–206. doi: 10.1016/j.neulet.2011.01.038

De Niz, M., and Heussler, V. T. (2018). Rodent Malaria Models: Insights Into Human Disease and Parasite Biology. *Curr. Opin. Microbiol.* 46, 93–101. doi: 10.1016/j.mib.2018.09.003

De Sousa, L. P., De Almeida, R. F., Ribeiro-Gomes, F. L., De Moura Carvalho, L. J., E Souza, T. M., De Souza, D. O. G., et al. (2018). Long-Term Effect of Uncomplicated Plasmodium Berghei ANKA Malaria on Memory and Anxiety-Like Behaviour in C57BL/6 Mice. *Parasites Vectors* 11. doi: 10.1186/s13071-018-2778-8

De Sousa, L. P., Ribeiro-Gomes, F. L., de Almeida, R. F., Souza, T. M., Werneck, G. L., Souza, D. O., et al. (2021). Immune System Challenge Improves Recognition Memory and Reverses Malaria-Induced Cognitive Impairment in Mice. *Sci. Rep.* 11, 14857. doi: 10.1038/S41598-021-94167-8

Desruisseaux, M. S., Gulinello, M., Smith, D. N., Lee, S. H. C., Tsuji, M., Weiss, L. M., et al. (2008). Cognitive Dysfunction in Mice Infected With Plasmodium Berghei Strain ANKA. *J. Infect. Dis.* 197, 1621–1627. doi: 10.1086/587908

Dondorp, A. M., Fanello, C. I., Hendriksen, I. C., Gomes, E., Seni, A., Chhaganlal, K. D., et al. (2010). Artesunate Versus Quinine in the Treatment of Severe Falciparum Malaria in African Children (AQUAMAT): An Open-Label, Randomised Trial. *Lancet* 376, 1647–1657. doi: 10.1016/S0140-6736(10)61924-1

Dorovini-Zis, K., Schmidt, K., Huynh, H., Fu, W., Whitten, R. O., Milner, D., et al. (2011). The Neuropathology of Fatal Cerebral Malaria in Malawian Children. *Am. J. Pathol.* 178, 2146–2158. doi: 10.1016/j.ajpath.2011.01.016

Fernando, S. D., Gunawardena, D. M., Bandara, M. R. S. S., De Silva, D., Carter, R., Mendis, K. N., et al. (2003). The Impact of Repeated Malaria Attacks on the School Performance of Children. *Am. J. Trop. Med. Hyg.* 69, 582–588. doi: 10.4269/ajtmh.2003.69.582

Fink, G., Olgiati, A., Hawela, M., Miller, J. M., and Matafwali, B. (2013). Association Between Early Childhood Exposure to Malaria and Children's Pre-School Development: Evidence From the Zambia Early Childhood Development Project. *Malar. J.* 12, 12. doi: 10.1186/1475-2875-12-12

Freeman, B. D., Martins, Y. C., Akide-Ndunge, O. B., Bruno, F. P., Wang, H., Tanowitz, H. B., et al. (2016). Endothelin-1 Mediates Brain Microvascular Dysfunction Leading to Long-Term Cognitive Impairment in a Model of Experimental Cerebral Malaria. *PloS Pathog.* 12, e1005477. doi: 10.1371/JOURNAL.PPAT.1005477

Ghazanfari, N., Mueller, S. N., and Heath, W. R. (2018). Cerebral Malaria in Mouse and Man. *Front. Immunol.* 9, 2016. doi: 10.3389/fimmu.2018.02016

Grau, G. E., Bieler, G., Pointaire, P., De Kossodo, S., Tacchini-Cotier, F., Vassalli, P., et al. (1990). Significance of Cytokine Production and Adhesion Molecules in Malarial Immunopathology. *Immunol. Lett.* 25, 189–194. doi: 10.1016/0165-2478(90)90113-5

Guha, S. K., Sarkar, I., Patgaonkar, M., Banerjee, S., Mukhopadhyay, S., Sharma, S., et al. (2020). A History of Juvenile Mild Malaria Exacerbates Chronic Stress-Evoked Anxiety-Like Behavior, Neuroinflammation, and Decline of Adult Hippocampal Neurogenesis in Mice. *J. Neuroimmunol.* 348, 577363. doi: 10.1016/j.jneuroim.2020.577363

Guha, S. K., Tillu, R., Sood, A., Patgaonkar, M., Nanavaty, I. N., Sengupta, A., et al. (2014). Single Episode of Mild Murine Malaria Induces Neuroinflammation, Alters Microglial Profile, Impairs Adult Neurogenesis, and Causes Deficits in Social and Anxiety-Like Behavior. *Brain. Behav. Immun.* 42, 123–137. doi: 10.1016/j.bbi.2014.06.009

Gul, S., Ribeiro-Gomes, F. L., Moreira, A. S., Sanches, G. S., Conceição, F. G., Daniel-Ribeiro, C. T., et al. (2021). Whole Blood Transfusion Improves Vascular Integrity and Increases Survival in Artemether-Treated Experimental Cerebral Malaria. *Sci. Rep.* 11, 12077. doi: 10.1038/s41598-021-91499-3

Hickson, M. R., Conroy, A. L., Bangirana, P., Opoka, R. O., Idro, R., Ssenkusu, J. M., et al. (2019). Acute Kidney Injury in Ugandan Children With Severe Malaria Is Associated With Long-Term Behavioral Problems. *PloS One* 14, e0226405. doi: 10.1371/JOURNAL.PONE.0226405

Hunt, N. H., Golenser, J., Chan-Ling, T., Parekh, S., Rae, C., Potter, S., et al. (2006). Immunopathogenesis of Cerebral Malaria. *Int. J. Parasitol.* 36, 569–582. doi: 10.1016/j.ijpara.2006.02.016

Idro, R., Carter, J. A., Fegan, G., Neville, B. G. R., and Newton, C. R. J. C. (2006). Risk Factors for Persisting Neurological and Cognitive Impairments Following Cerebral Malaria. *Arch. Dis. Child.* 91, 142–148. doi: 10.1136/adc.2005.077784

Idro, R., Kakooza-Mwesige, A., Asea, B., Ssebyala, K., Bangirana, P., Opoka, R. O., et al. (2016). Cerebral Malaria Is Associated With Long-Term Mental Health Disorders: A Cross Sectional Survey of a Long-Term Cohort. *Malar. J.* 15, 184. doi: 10.1186/s12936-016-1233-6

Idro, R., Karamagi, C., and Tumwine, J. (2004). Immediate Outcome and Prognostic Factors for Cerebral Malaria Among Children Admitted to Mulago Hospital, Uganda. *Ann. Trop. Paediatr.* 24, 17–24. doi: 10.1179/027249304225013240

Idro, R., Marsh, K., John, C. C., and Newton, C. R. J. (2010). Cerebral Malaria: Mechanisms of Brain Injury and Strategies for Improved Neurocognitive Outcome. *Pediatr. Res.* 68, 267–274. doi: 10.1203/PDR.0b013e3181eee738

Jerne, N. K., and Cocteau, J. (1984). Idiotypic Networks and Other Preconceived Ideas. *Immunol. Rev.* 79, 5–24. doi: 10.1111/j.1600-065X.1984.tb00484.x

John, C. C., Bangirana, P., Byarugaba, J., Opoka, R. O., Idro, R., Jurek, A. M., et al. (2008). Cerebral Malaria in Children Is Associated With Long-Term Cognitive Impairment. *Pediatrics* 122, e92–e99. doi: 10.1542/peds.2007-3709

Josefsson, E., Bergquist, J., Ekman, R., and Tarkowski, A. (1996). Catecholamines Are Synthesized by Mouse Lymphocytes and Regulate Function of These Cells by Induction of Apoptosis. *Immunology* 88, 140–146. doi: 10.1046/j.1365-2567.1996.d01-653.x

Kariuki, S. M., Ikumi, M., Ojal, J., Sadarangani, M., Idro, R., Olotu, A., et al. (2011). Acute Seizures Attributable to Falciparum Malaria in an Endemic Area on the Kenyan Coast. *Brain* 134, 1519–1528. doi: 10.1093/BRAIN/AWR051

Lacerda-Queiroz, N., Rodrigues, D. H., Vilela, M. C., de Miranda, A. S., Amaral, D. C. G., da Camargos, E. R. S., et al. (2010). Inflammatory Changes in the Central Nervous System are Associated With Behavioral Impairment in Plasmodium Berghei (Strain ANKA)-Infected Mice. *Exp. Parasitol.* 125, 271–278. doi: 10.1016/j.exppara.2010.02.002

Langfitt, J. T., McDermott, M. P., Brim, R., Mboma, S., Potchen, M. J., Kampondeni, S. D., et al. (2019). Neurodevelopmental Impairments 1 Year After Cerebral Malaria. *Pediatrics* 143, e20181026. doi: 10.1542/peds.2018-1026

Lau, C. K. Y., Turner, L., Jespersen, J. S., Lowe, E. D., Petersen, B., Wang, C. W., et al. (2015). Structural Conservation Despite Huge Sequence Diversity Allows EPCR Binding by the PfEMP1 Family Implicated in Severe Childhood Malaria. *Cell Host Microbe* 17, 118–129. doi: 10.1016/J.CHOM.2014.11.007

Laverse, E., Nashef, L., and Brown, S. (2013). Neurocognitive Sequelae Following Hippocampal and Callosal Lesions Associated With Cerebral Malaria in an Immunenaive Adult. *Postgrad. Med. J.* 89, 671–672. doi: 10.1136/postgradmedj-2013-131758

Lell, B., Köhler, C., Wamola, B., Olola, C. H., Kivaya, E., Kokwaro, G., et al. (2010). Pentoxifylline as an Adjunct Therapy in Children With Cerebral Malaria. *Malar. J.* 9, 368. doi: 10.1186/1475-2875-9-368

Lima, M. N., Oliveira, H. A., Fagundes, P. M., Estato, V., Silva, A. Y. O., Freitas, R. J. R. X., et al. (2020). Mesenchymal Stromal Cells Protect Against Vascular Damage and Depression-Like Behavior in Mice Surviving Cerebral Malaria. *Stem Cell Res. Ther.* 11, 367. doi: 10.1186/s13287-020-01874-6

Li, Q., Qi, F., Yang, J., Zhang, L., Gu, H., Zou, J., et al. (2015). Neonatal Vaccination With Bacillus Calmette-Guérin and Hepatitis B Vaccines Modulates Hippocampal Synaptic Plasticity in Rats. *J. Neuroimmunol.* 288, 1–12. doi: 10.1016/j.jneuroim.2015.08.019

Li, C., Seixas, E., and Langhorne, J. (2001). Rodent Malaria: The Mouse as a Model for Understanding Immune Responses and Pathology Induced by the Erythrocytic Stages of the Parasite. *Med. Microbiol. Immunol.* 189, 115–126. doi: 10.1007/s430-001-8017-8

Li, Q., Zhang, Y., Zou, J., Qi, F., Yang, J., Yuan, Q., et al. (2016). Neonatal Vaccination With Bacille Calmette-Guérin Promotes the Dendritic Development of Hippocampal Neurons. *Hum. Vaccines Immunother.* 12, 140–149. doi: 10.1080/21645515.2015.1056954

Lou, J., Lucas, R., and Grau, G. E. (2001). Pathogenesis of Cerebral Malaria: Recent Experimental Data and Possible Applications for Humans. *Clin. Microbiol. Rev.* 14, 810–820. doi: 10.1128/CMR.14.4.810-820.2001

Martins, Y. C., Freeman, B. D., Akide Ndunge, O. B., Weiss, L. M., Tanowitz, H. B., and Desruisseaux, M. S. (2016). Endothelin-1 Treatment Induces an Experimental Cerebral Malaria–Like Syndrome in C57BL/6 Mice Infected With Plasmodium Berghei NK65. *Am. J. Pathol.* 186, 2957–2969. doi: 10.1016/j.ajpath.2016.07.020

Martins, Y. C., Smith, M. J., Pelajo-Machado, M., Werneck, G. L., Lenzi, H. L., Daniel-Ribeiro, C. T., et al. (2009). Characterization of Cerebral Malaria in the Outbred Swiss Webster Mouse Infected by Plasmodium Berghei ANKA. *Int. J. Exp. Pathol.* 90, 119–130. doi: 10.1111/j.1365-2613.2008.00622.x

Martins, Y. C., Werneck, G. L., Carvalho, L. J., Silva, B. P. T., Andrade, B. G., Souza, T. M., et al. (2010). Algorithms to Predict Cerebral Malaria in Murine Models Using the SHIRPA Protocol. *Malar. J.* 9. doi: 10.1186/1475-2875-9-85

McDonald, C. R., Cahill, L. S., Ho, K. T., Yang, J., Kim, H., Silver, K. L., et al. (2015). Experimental Malaria in Pregnancy Induces Neurocognitive Injury in Uninfected Offspring *via* a C5a-C5a Receptor Dependent Pathway. *PloS Pathog.* 11, e1005140. doi: 10.1371/journal.ppat.1005140

McKenna, F., McLaughlin, P. J., Lewis, B. J., Sibbring, G. C., Cummerson, J. A., Bowen-Jones, D., et al. (2002). Dopamine Receptor Expression on Human T- and B-Lymphocytes, Monocytes, Neutrophils, Eosinophils and NK Cells: A Flow Cytometric Study. *J. Neuroimmunol.* 132, 34–40. doi: 10.1016/S0165-5728(02)00280-1

Medana, I. M., Day, N. P., Hien, T. T., Mai, N. T. H., Bethell, D., Phu, N. H., et al. (2002). Axonal Injury in Cerebral Malaria. *Am. J. Pathol.* 160, 655–666. doi: 10.1016/S0002-9440(10)64885-7

Mwanga-Amumpaire, J., Carroll, R. W., Baudin, E., Kemigisha, E., Nampijja, D., Mworozi, K., et al. (2015). Inhaled Nitric Oxide as an Adjunctive Treatment for Cerebral Malaria in Children: A Phase II Randomized Open-Label Clinical Trial. *Open Forum Infect. Dis.* 2, ofv132. doi: 10.1093/ofid/ofv111

Nankabirwa, J., Wandera, B., Kiwanuka, N., Staedke, S. G., and Kamya, M. R. (2013). And Brooker, sAsymptomatic Plasmodium Infection and Cognition Among Primary Schoolchildren in a High Malaria Transmission Setting in Uganda *Am. J. Trop. Med. Hyg.* 88, 1102–1108. doi: 10.4269/ajtmh.12-0633

Neres, R., Marinho, C. R. F., Gonçalves, L. A., Catarino, M. B., and Penha-Gonçalves, C. (2008). Pregnancy Outcome and Placenta Pathology in Plasmodium Berghei ANKA Infected Mice Reproduce the Pathogenesis of Severe Malaria in Pregnant Women. *PloS One* 3, e1608. doi: 10.1371/journal.pone.0001608

Oluwayemi, I. O., Brown, B. J., Oyedeji, O. A., and Oluwayemi, M. A. (2013). Neurological Sequelae in Survivors of Cerebral Malaria. *Pan Afr. Med. J.* 15, 88. doi: 10.11604/pamj.2013.15.88.1897

Ouma, B. J., Bangirana, P., Ssenkusu, J. M., Datta, D., Opoka, R. O., Idro, R., et al. (2021). Plasma Angiopoietin-2 Is Associated With Age-Related Deficits in Cognitive Sub-Scales in Ugandan Children Following Severe Malaria. *Malar. J.* 20, 17. doi: 10.1186/s12936-020-03545-6

Peixoto, B., and Kalei, I. (2013). To Characterize the Neurocognitive Sequelae of Cerebral Malaria (CM) in an Adult Sample of the City of Benguela, Angola. *Asian Pac. J. Trop. Biomed.* 3, 532–535. doi: 10.1016/S2221-1691(13)60108-2

Pert, C. B., Ruff, M. R., Weber, R. J., and Herkenham, M. (1985). Neuropeptides and Their Receptors: A Psychosomatic Network. *J. Immunol.* 135, 820s–826s.

Porta, J., Carota, A., Pizzolato, G. P., Wildi, E., Widmer, M. C., Margairaz, C., et al. (1993). Immunopathological Changes in Human Cerebral Malaria. *Clin. Neuropathol.* 12 (3), 142–146.

Potter, S., Chan-Ling, T., Ball, H. J., Mansour, H., Mitchell, A., Maluish, L., et al. (2006). Perforin Mediated Apoptosis of Cerebral Microvascular Endothelial Cells During Experimental Cerebral Malaria. *Int. J. Parasitol.* 36, 485–496. doi: 10.1016/j.ijpara.2005.12.005

Qi, F., Zuo, Z., Yang, J., Hu, S., Yang, Y., Yuan, Q., et al. (2017). Combined Effect of BCG Vaccination and Enriched Environment Promote Neurogenesis and Spatial Cognition *via* a Shift in Meningeal Macrophage M2 Polarization. *J. Neuroinflamm.* 14, 32. doi: 10.1186/s12974-017-0808-7

Reis, P. A., Comim, C. M., Hermani, F., Silva, B., Barichello, T., Portella, A. C., et al. (2010). Cognitive Dysfunction Is Sustained After Rescue Therapy in Experimental Cerebral Malaria, and Is Reduced by Additive Antioxidant Therapy. *PloS Pathog.* 6, e1000963. doi: 10.1371/journal.ppat.1000963

Reverchon, F., Mortaud, S., Sivoyon, M., Maillet, I., Laugeray, A., Palomo, J., et al. (2017). IL-33 Receptor ST2 Regulates the Cognitive Impairments Associated With Experimental Cerebral Malaria. *PloS Pathog.* 13, e1006322. doi: 10.1371/journal.ppat.1006322

Richardson, E. D., Varney, N. R., Roberts, R. J., Springer, J. A., and Wood, PS (1997). Long-Term Cognitive Sequelae of Cerebral Malaria in Vietnam Veterans. *Appl. Neuropsychol.* 4, 238–243. doi: 10.1207/s15324826an0404_5

Sankowski, R., Mader, S., and Valdés-Ferrer, S. I. (2015). Systemic Inflammation and the Brain: Novel Roles of Genetic, Molecular, and Environmental Cues as Drivers of Neurodegeneration. *Front. Cell. Neurosci.* 9, 28. doi: 10.3389/FNCEL.2015.00028

Sawada, M., Itoh, Y., Suzumura, A., and Marunouchi, T. (1993). Expression of Cytokine Receptors in Cultured Neuronal and Glial Cells. *Neurosci. Lett.* 160, 131–134. doi: 10.1016/0304-3940(93)90396-3

Scaccabarozzi, D., Deroost, K., Corbett, Y., Lays, N., Corsetto, P., Salè, F. O., et al. (2018). Differential Induction of Malaria Liver Pathology in Mice Infected With Plasmodium Chabaudi AS or Plasmodium Berghei NK65. *Malar. J.* 17, 18. doi: 10.1186/s12936-017-2159-3

Schiess, N., Villabona-Rueda, A., Cottier, K. E., Huether, K., Chipeta, J., and Stins, M. F. (2020). Pathophysiology and Neurologic Sequelae of Cerebral Malaria. *Malar. J.* 19, 266. doi: 10.1186/s12936-020-03336-z

Serghides, L., McDonald, C. R., Lu, Z., Friedel, M., Cui, C., Ho, K. T., et al. (2014). Pparγ Agonists Improve Survival and Neurocognitive Outcomes in Experimental Cerebral Malaria and Induce Neuroprotective Pathways in Human Malaria. *PloS Pathog.* 10, e1003980. doi: 10.1371/JOURNAL.PPAT.1003980

Severe Malaria (2014). *Trop. Med. Int. Health* 19 (Suppl 1), 7–131. doi: 10.1111/TMI.12313_2

Singh, B., Sung, L. K., Matusop, A., Radhakrishnan, A., Shamsul, S. S. G., Cox-Singh, J., et al. (2004). A Large Focus of Naturally Acquired Plasmodium Knowlesi Infections in Human Beings. *Lancet* 363, 1017–1024. doi: 10.1016/S0140-6736(03)14713-7

Ssenkusu, J. M., Hodges, J. S., Opoka, R. O., Idro, R., Shapiro, E., John, C. C., et al. (2016). Long-Term Behavioral Problems in Children With Severe Malaria. *Pediatrics* 138, e20161965. doi: 10.1542/peds.2016-1965

Sutherland, C. J., Tanomsing, N., Nolder, D., Oguike, M., Jennison, C., Pukrittayakamee, S., et al. (2010). Two Nonrecombining Sympatric Forms of the Human Malaria Parasite Plasmodium Ovale Occur Globally. *J. Infect. Dis.* 201, 1544–1550. doi: 10.1086/652240

Ta, T. H., Hisam, S., Lanza, M., Jiram, A. I., Ismail, N., and Rubio, J. M. (2014). First Case of a Naturally Acquired Human Infection With Plasmodium Cynomolgi. *Malar. J.* 13, 1–7. doi: 10.1186/1475-2875-13-68

Tapajós, R., Castro, D., Melo, G., Balogun, S., James, M., Pessoa, R., et al. (2019). Malaria Impact on Cognitive Function of Children in a Peri-Urban Community in the Brazilian Amazon. *Malar. J.* 18, 173. doi: 10.1186/s12936-019-2802-2

Taylor, T. E., Fu, W. J., Carr, R. A., Whitten, R. O., Mueller, J. G., Fosiko, N. G., et al. (2004). Differentiating the Pathologies of Cerebral Malaria by Postmortem Parasite Counts. *Nat. Med.* 10, 143–145. doi: 10.1038/NM986

Thuilliez, J., Sissoko, M. S., Toure, O. B., Kamate, P., Berthélemy, J. C., and Doumbo, O. K. (2010). Malaria and Primary Education in Mali: A Longitudinal Study in the Village of Donéguébougou. *Soc Sci. Med.* 71, 324–334. doi: 10.1016/j.socscimed.2010.02.027

Van Den Steen, P. E., Geurts, N., Deroost, K., Van Aelst, I., Verhenne, S., Heremans, H., et al. (2010). Immunopathology and Dexamethasone Therapy in a New Model for Malaria-Associated Acute Respiratory Distress Syndrome. *Am. J. Respir. Crit. Care Med.* 181, 957–968. doi: 10.1164/rccm.200905-0786OC

Van Hensbroek, M. B., Palmer, A., Onyiorah, E., Schneider, G., Jaffar, S., Dolan, G., et al. (1996). The Effect of a Monoclonal Antibody to Tumor Necrosis Factor on Survival From Childhood Cerebral Malaria. *J. Infect. Dis.* 174, 1091–1097. doi: 10.1093/infdis/174.5.1091

Varney, N. R., Roberts, R. J., Springer, J. A., Connell, S. K., and Wood, P. S. (1997). The Neuropsychiatric Sequelae of Cerebral Malaria in Vietnam Veterans. *J. Nerv. Ment. Dis.* 185, 695–703. doi: 10.1097/00005053-199711000-00008

Varo, R., Crowley, V. M., Sitoe, A., Madrid, L., Serghides, L., Kain, K. C., et al. (2018). Adjunctive Therapy for Severe Malaria: A Review and Critical Appraisal. *Malar. J.* 17, 47. doi: 10.1186/s12936-018-2195-7

Vitor-Silva, S., Reyes-Lecca, R. C., Pinheiro, T. R. A., and Lacerda, M. V. G. (2009). Malaria Is Associated With Poor School Performance in an Endemic Area of the Brazilian Amazon. *Malar. J.* 8, 230. doi: 10.1186/1475-2875-8-230

Vorasan, N., Pan-Ngum, W., Jittamala, P., Maneeboonyang, W., Rukmanee, P., and Lawpoolsri, S. (2015). Long-Term Impact of Childhood Malaria Infection on School Performance Among School Children in a Malaria Endemic Area Along the Thai-Myanmar Border. *Malar. J.* 14, 401. doi: 10.1186/s12936-015-0917-7

Warrell, D. A., Looareesuwan, S., Warrell, M. J., Kasemsarn, P., Intaraprasert, R., Bunnag, D., et al. (1982). Dexamethasone Proves Deleterious in Cerebral Malaria. *N. Engl. J. Med.* 306, 313–319. doi: 10.1056/nejm198202113060601

Witschkowski, J., Behrends, J., Frank, R., Eggers, L., von Borstel, L., Hertz, D., et al. (2020). BCG Provides Short-Term Protection From Experimental Cerebral Malaria in Mice. *Vaccines* 8, 1–15. doi: 10.3390/VACCINES8040745

World Health Organization. (2020). *World Malaria Report 2020: 20 Years of Global Progress and Challenges (Geneva: World Health Organization* Licence: CC BY-NC-SA 3.0 IGO). Available at: https://www.who.int/publications/i/item/9789240015791 [Accessed November 30, 2021]

Xia, Y., Qi, F., Zou, J., Yang, J., and Yao, Z. (2014). Influenza Vaccination During Early Pregnancy Contributes to Neurogenesis and Behavioral Function in Offspring. *Brain. Behav. Immun.* 42, 212–221. doi: 10.1016/j.bbi.2014.06.202

Yang, Y., He, Z., Xing, Z., Zuo, Z., Yuan, L., Wu, Y., et al. (2020). Influenza Vaccination in Early Alzheimer's Disease Rescues Amyloidosis and Ameliorates Cognitive Deficits in APP/PS1 Mice by Inhibiting Regulatory T Cells. *J. Neuroinflamm.* 17, 65. doi: 10.1186/s12974-020-01741-4

Yang, J., Qi, F., Gu, H., Zou, J., Yang, Y., Yuan, Q., et al. (2016). Neonatal BCG Vaccination of Mice Improves Neurogenesis and Behavior in Early Life. *Brain Res. Bull.* 120, 25–33. doi: 10.1016/j.brainresbull.2015.10.012

Conflict of Interest: The authors declare that the research was conducted in the absence of any commercial or financial relationships that could be construed as a potential conflict of interest.

frontiers | Frontiers in Cellular and Infection Microbiology

REVIEW
published: 23 May 2022
doi: 10.3389/fcimb.2022.899581

Experimental Models to Study the Pathogenesis of Malaria-Associated Acute Respiratory Distress Syndrome

Samantha Yee Teng Nguee[1†], *José Wandilson Barboza Duarte Júnior*[2†], *Sabrina Epiphanio*[3], *Laurent Rénia*[1,4,5] *and Carla Claser*[2*]

[1] A*STAR Infectious Diseases Labs (A*STAR ID Labs), Agency for Science, Technology and Research (A*STAR), Singapore, Singapore, [2] Department of Parasitology, Institute of Biomedical Sciences, University of São Paulo, São Paulo, Brazil, [3] Department of Clinical and Toxicological Analyses, Faculty of Pharmaceutical Science, University of São Paulo, São Paulo, Brazil, [4] Lee Kong Chian School of Medicine, Nanyang Technological University, Singapore, Singapore, [5] School of Biological Sciences, Nanyang Technological University, Singapore, Singapore

OPEN ACCESS

Edited by:
Tania F. De Koning-Ward,
Deakin University, Australia

Reviewed by:
Philippe E. Van Den Steen,
KU Leuven, Belgium
Borko Amulic,
University of Bristol, United Kingdom

***Correspondence:**
Carla Claser
carlaclaser@gmail.com

[†]These authors have contributed equally to this work and share first authorship

Specialty section:
This article was submitted to Parasite and Host, a section of the journal Frontiers in Cellular and Infection Microbiology

Received: 18 March 2022
Accepted: 28 April 2022
Published: 23 May 2022

Citation:
Nguee SYT, Júnior JWBD, Epiphanio S, Rénia L and Claser C (2022) Experimental Models to Study the Pathogenesis of Malaria-Associated Acute Respiratory Distress Syndrome. Front. Cell. Infect. Microbiol. 12:899581. doi: 10.3389/fcimb.2022.899581

Malaria-associated acute respiratory distress syndrome (MA-ARDS) is increasingly gaining recognition as a severe malaria complication because of poor prognostic outcomes, high lethality rate, and limited therapeutic interventions. Unfortunately, invasive clinical studies are challenging to conduct and yields insufficient mechanistic insights. These limitations have led to the development of suitable MA-ARDS experimental mouse models. In patients and mice, MA-ARDS is characterized by edematous lung, along with marked infiltration of inflammatory cells and damage of the alveolar-capillary barriers. Although, the pathogenic pathways have yet to be fully understood, the use of different experimental mouse models is fundamental in the identification of mediators of pulmonary vascular damage. In this review, we discuss the current knowledge on endothelial activation, leukocyte recruitment, leukocyte induced-endothelial dysfunction, and other important findings, to better understand the pathogenesis pathways leading to endothelial pulmonary barrier lesions and increased vascular permeability. We also discuss how the advances in imaging techniques can contribute to a better understanding of the lung lesions induced during MA-ARDS, and how it could aid to monitor MA-ARDS severity.

Keywords: *Plasmodium berghei*, mouse, ARDS, pulmonary vascular damage, endothelial dysfunction, vascular permeability

1 INTRODUCTION

Malaria is a fatal parasitic disease that continues to threaten many human populations, especially in the tropical and subtropical regions of the world. Globally, the disease incidences and death rates have been declining slowly since 2000, as a result of numerous global initiatives. Nevertheless, in 2020, there were an estimated 241 million malaria cases with 627 000 people dying from the disease (WHO, 2021). Mortality from severe malaria remains a significant concern where increasing deaths were reported in South Asia, South America, and Eastern Mediterranean regions, apart from the African continent still accounting for most of the global deaths. Among the nine clinically

important *Plasmodium* parasite species responsible for the disease in humans, *P. vivax* and mostly *P. falciparum* are the main causes of severe disease and death (Price et al., 2007; Olliaro, 2008). The other *Plasmodium* species includes *P. ovale*, *P. malariae*, *P. knowlesi*, *P. cynomolgi*, *P. brasilianum*, *P. simium* and *P. inui*, where the last five are zoonotic infections. Despite increased in detection, infection by *P. brasilianum, P. simium and P. inui* are still rare (Singh et al., 2004; Ta et al., 2014; Lalremruata et al., 2015; Brasil et al., 2017; Liew et al., 2021).

The clinical manifestations of malaria and severity are dependent on the host's immune status, infection history, parasite virulence, and genetic variations in both the host and parasite. The first clinical symptoms of malaria are mostly non-specific including flu-like symptoms, fever paroxysm, headache, chills, weakness, myalgias, diarrhea, and nausea (Karunaweera et al., 2003; Bartoloni and Zammarchi, 2012). A large majority of *Plasmodium* infections are uncomplicated and rapidly resolve with early diagnosis and prompt treatment with relevant anti-malarials combinations (van der Pluijm et al., 2021). However, delayed diagnosis or inability to clear the blood forms of the parasite, particularly dire for the virulent *falciparum* malaria, predisposes infected individuals to severe clinical manifestations.

2 MA-ARDS IN HUMANS

Malaria-associated acute respiratory distress syndrome (ARDS) is a complication of severe malaria that is less characterized compared to the most lethal cerebral malaria. MA-ARDS has been described to occur mainly in adults during infection by most clinically important *Plasmodium* species, including *P. knowlesi*, *P. ovale* and *P. malariae* (Lozano et al., 1983; Daneshvar et al., 2009; Haydoura et al., 2011; Taylor et al., 2012). MA-ARDS arising from severe *P. falciparum* and severe *P. vivax* single-infections in adults are more common, with varying prevalence of 5 - 25%, and 1 - 22% respectively (Mohan et al., 2008; Taylor et al., 2012; Val et al., 2017). In recent years, the rising incidence of adult MA-ARDS in Southeast Asia (particularly Malaysia), were largely attributed to severe zoonotic *P. knowlesi* infection, with a prevalence of 6 - 23% (Daneshvar et al., 2009; William et al., 2011; Barber et al., 2013). With the less frequently observed severe *P. ovale* infection, MA-ARDS prevalence was about 22% (Groger et al., 2017). Pregnant women with severe *falciparum* malaria, are predisposed to develop MA-ARDS and have an estimated prevalence of 29% (Taylor et al., 2012). MA-ARDS in adults is a fatal lung complication with a high fatality rate of at least 50% (Van den Steen et al., 2013; Val et al., 2017). On the other hand, MA-ARDS occurrence is rare in infected children. Respiratory distress arising in this population is predominantly caused by lactic acidosis, and to a certain extent by cardiac failure and cerebral complications (Taylor et al., 1993; Krishna et al., 1994; Dzeing-Ella et al., 2005; Taylor et al., 2012). Mortality from MA-ARDS is greatly dependent on several risk factors such as the virulence of *Plasmodium* species, severity of disease upon admission, immune and age status, pre-existing comorbidities, infections or disorders, timing and effectiveness of treatments administered, and availability of respiratory management therapies.

Uncomplicated malaria patients with probable respiratory distress may present early signs of a self-limiting cough with or without expectoration, tachypnea and tachycardia or appear asymptomatic (Maguire et al., 2005; Taylor et al., 2012). Moreover, respiratory distress symptoms may develop suddenly or exacerbate into MA-ARDS after several hours to days of well-tolerated anti-malarial treatment. This is despite diminishing or negative parasitemia (as assessed by microscopy) (Tong et al., 1972; Maguire et al., 2005; Taylor et al., 2012; Elzein et al., 2017), as frequently reported for *vivax* malaria patients receiving standard antimalarial treatments (Anstey et al., 2007; Val et al., 2017). Given that *P. vivax* infection results in a low parasitemia, this suggests that *P. vivax* and its by-products possess greater inflammatory potential that can trigger MA-ARDS post-antimalarial treatment (Karunaweera et al., 1992). Currently, there are no specific treatments for MA-ARDS, only respiratory management interventions following non-malaria ALI/ARDS therapeutic guidelines are implemented.

Patients with MA-ARDS develop clinical edema and diminished lung function (i.e., reduced gas transfer and small airway obstruction) (Anstey et al., 2002; Maguire et al., 2005). The histopathological hallmarks of MA-ARDS observed from human post-mortem lung sections were non-cardiogenic pulmonary edema, inflammation, hemorrhages, and alveolar damage (Taylor et al., 2012). Pulmonary edema is described as the flooding of the alveolar and/or interstitium with proteinaceous fluid. Diffuse alveolar damage is characterized by thickened alveolar septa, that may be plastered by eosinophilic hyaline membranes. Pulmonary inflammation is observed as the congestion of the alveolar capillaries with mono- and polymorphonuclear cells and/or infiltration of these leukocytes into the alveolar or interstitial space. Malaria pigments or hemozoins (Hz), either free or phagocytosed were found to be present as well. Immunostaining of the lung sections revealed that infiltrating nucleated cells were mostly $CD3^+$T lymphocytes, $CD68^+$ monocytes/macrophages, and to a lower extent, neutrophils (Valecha et al., 2009; Lacerda et al., 2012; Milner et al., 2013).

Most pathophysiological characterization of clinical MA-ARDS were drawn from autopsy lung sections, and these are potentially confounded by biasness from snapshot sampling and post-mortem artifacts. Therefore, attempts to study the disease progression in living MA-ARDS patients have been done by assessing the lung function with non-invasive methods. In one study, using a portable pulmonary testing station (TT544; Morgan Transflow System; Morgan Medical) where gas transfer and spirometry (breathing test) were assessed, patients were found to have impaired alveolar capillary membranes, resulting in edema and decreased blood volume in the pulmonary capillaries. The authors have suggested the occlusion of the pulmonary capillaries by immune cells and sequestered infected red blood cells (iRBCs) (Maguire et al., 2005). Findings from this study corroborated with histopathological findings gathered from autopsy series; however, studies beyond these non-invasive tests to gain mechanistic insights of MA-ARDS have proven difficult in living patients.

3 MA-ARDS ANIMAL MODEL

The pathophysiology of MA-ARDS is highly complex and cannot be fully elucidated by clinical observations of infected humans. Undeniably, these clinical studies have revealed the critical hallmarks and correlates of the pathogenesis, yet it deters further understanding of the mechanisms in pathogenesis. Therefore, animal models of MA-ARDS are essential to conduct mechanistic studies, discover potential interventions, and validate the hypotheses drawn from clinical studies. Several combinations of experimental animal host and *Plasmodium* parasites have been used to induce MA-ARDS were summarized. Details about each experimental animal model are listed in **Table 1**, including the parasite species, inoculation, and pathological findings in the lung.

3.1 Rodent Models

The use of rodents as experimental animal hosts makes up most of the experimental models of MA-ARDS developed, due to the practical advantages it offers as a research tool including their small size, various well-established strains, ease of genetic modifications and controlled genetic background.

To date, various strains of mouse inoculated with any of the four rodent *Plasmodium* species, namely, *P. berghei*, *P. yoelii*, *P. chabaudi* and *P. vinckei*, can develop MA-ARDS with varying similarities to the human disease. The C57BL/6 mouse strain develops MA-ARDS when infected with the ANKA strain of *P. berghei* (PbA) (Bafort and Timperman, 1969) and has been used widely for many MA-ARDS studies. Apart from developing MA-ARDS, this is an established model for experimental cerebral malaria (ECM) where at least 60% of infected mice succumb to fulminant cerebral pathology followed by death (Engwerda et al., 2005) before lung pathology can be fully established or studied upon. Nevertheless, it has been demonstrated in this model that MA-ARDS occurs independently of ECM development (Hansen et al., 2005; Lovegrove et al., 2008; Claser et al., 2019). Yet, the lethal onset of cerebral complications in this model restricts the study of MA-ARDS to the early phase of disease development. In view of that, alternative mouse models of MA-ARDS resistant to cerebral complications have been developed to provide a broader window period to study the late phase of lung complication. Epiphanio et al. developed a model inoculating PbA into DBA/2 mouse strain resistant to ECM, where on average, 50% of infected mice develops MA-ARDS (Epiphanio et al., 2010; Sercundes et al., 2016; Dos Santos Ortolan et al., 2019). The infection of C57BL/6 mouse strain with the NK65 strain of *P. berghei* (PbNK65) which were resistant to ECM as well, induces a higher incidence of MA-ARDS (at least 90%) in infected mice (Van den Steen et al., 2010). Infection of C57BL/6 mouse strain with CB strain of *P. chabaudi* is another model of MA-ARDS reported to be resistant to cerebral complications (Lin et al., 2017).

Lung injuries sustained in mouse models of MA-ARDS parallels the clinical pathology. Histological lung sections of infected mice showed flooded alveolar space and interstitium with proteinaceous fluid also containing various inflammatory cells. The integrity of alveolar capillaries was disrupted and mostly leukocytes and iRBCs were often found congested within these capillaries. Lung function test coupled with sophisticated imaging procedures [i.e., X-ray, single-photon emission computed tomography/computed tomography (SPECT/CT) and magnetic resonance imaging (MRI)] conducted on conscious infected mice exhibited pulmonary aeration disturbance, reduced respiration frequency, obstructed airways and increasing timely pulmonary opacities (Ortolan et al., 2014; Claser et al., 2019; Quirino et al., 2020). Ultrastructural analysis using transmission electron microscopy (TEM) in the lung of PbA-infected DBA/2 mice that died of MA-ARDS, provided evidence of eosinophilic hyaline membranes occasionally found to line the alveolar septa (Aitken et al., 2014). However, it was highlighted in previous studies that in some parasite and mouse strain combinations, the lung pathology deviates from the MA-ARDS hallmarks reported in patients. *P. berghei* K173 infection of C57BL/6 mice results in non-proteinaceous edema restricted to the interstitium (Hee et al., 2011; Van den Steen et al., 2013). On the other hand, infection of C57BL/6 mice with the AS strain of *P. chabaudi* induced minimal edema (Van den Steen et al., 2010; Lin et al., 2017). These differences in lung pathology between the mouse models and human beings must be kept in mind before drawing definitive conclusions. Moreover, the details of disease progression, infection method, parasite inoculum dose, parasite line/clone and mouse genetic background should be deeply examined to select suitable mouse models of MA-ARDS and draw valid comparisons between mouse models.

3.2 Non-Human-Primate (NHP) Models

Although rodent models have helped to decipher MA-ARDS pathogenesis and evaluate potential therapeutics, it remains an open question about their full relevance to the human lung pathology. Therefore, NHP models may be more suited since they possess greater genomic, immunogenic, and physiological homologies to humans than rodents.

Some of the earliest reports of MA-ARDS in *Plasmodium*-infected NHP hosts dates as far back as 50 years. Primate malarial species, *P. coatneyi* or *P. knowlesi*, were experimentally inoculated into rhesus macaques (*Macaca mulatta*) and caused multiple organ damages, with gross findings of lung injury involving congested alveolar capillaries with iRBCs (Desowitz et al., 1969; Spangler et al., 1978). In recent years, there has been more detailed documentation of MA-ARDS in NHP hosts such as rhesus or cynomolgus macaques (*Macaca fascicularis*), and black-capped squirrel monkey (*Saimiri boliviensis*) experimentally infected with human-malaria causing *Plasmodia*, like *P. vivax, P. cynomolgi*, or *P. knowlesi*. In these studies, histopathological findings from lung sections of infected NHP parallels those obtained in mouse models and in humans (Joyner et al., 2017; Peterson et al., 2019; Peterson et al., 2021). However, aside from these histological findings, progress into understanding the pathophysiological processes in MA-ARDS with NHP models has remained limited.

However, one major caveat of the studies using NHP was that the animals were splenectomized to induce higher parasitemia and immunogenic responses. Splenectomy in NHP hosts may alter the course of disease progression, parasite clearance and parasite cytoadhesion and sequestration dynamics (David et al.,

TABLE 1 | Animal models of MA-ARDS.

Animal	Strain	Parasite specie	Parasite strain/ clone	Inoculation		First exhibition of lung pathology (days post infection)	Peripheral parasitemia (%)	Lung pathological findings	Other affected organ(s)	Ref
				Route	Dose					
Mouse	C57BL/6 C57BL/6N C57BL/6J	*P. berghei*	ANKA	IP	10^6 iRBCs	6	>0.5%	(↑) Lung edema, Alveolar capillary permeability (Evans blue); Alveolar infiltration with mononuclear and PMN cells	Brain	(Chang et al., 2001)
				IP	10^5 iRBCs	7-10	NR	(↑) Lung weight; Alveolar edema (proteinaceous); Alveolar capillary permeability (Evans blue); Airway reactivity; Alveolar and interstitial infiltration with leukocytes (macrophages, monocytes); Levels of TNF-α, IL-12, IL-1β, IL-6, MCP-1/ CCL2, RANTES/CCL5, KC/ CXCL1 in lung tissue homogenate	Brain	(de Azevedo-Quintanilha et al., 2016)
			ANKA Clone 15cy1	IP	10^6 iRBCs	6	20	Thickened alveolar septa (↑) Alveolar edema; Paracellular fluid hyperpermeability; Alveolar infiltration with leukocytes, ROS production by iRBCs sequestered in the lung microvasculature	NR	(Anidi et al., 2013)
			ANKA (MR4)	IP	5×10^5 iRBCs (Male) 10^6 iRBCs (Female)	6	3-5	(↑) IgM in BALF; Alveolar edema (proteinaceous); Levels of IFN-γ, IL-6, MIP-2/ CXCL2, KC/CXCL1 in lung tissue homogenate; Interstitial inflammation	Brain	(Lovegrove et al., 2008)
			ANKA GFP-*luciferase* Clone 15cy1	IP	10^5-10^6 iRBCs	7	NR	(↑) Parasite sequestration	Brain	(Franke-Fayard et al., 2010)
			ANKA GFP-*luciferase* Clone 231cl1	IP	10^6 iRBCs	6-7	5	(↑) Lung edema (Bronchi opacity by MRI); Lung weight; Alveolar capillary permeability (Vascular leakage); Parasite sequestration; Lung infiltration of activated $CD8^+$ T cells, MODC, MDM (↓) Tight junction protein ZO-1 expression on lung epithelium; Tissue infiltration with cDCs, pDCs, macrophages	Brain	(Claser et al., 2019)
	DBA/2		ANKA	IP	10^6-10^7 iRBCs	7-12	30-50	Thickened alveolar septa (↑) Enhanced respiratory pause (Penh); Alveolar capillary permeability (Evans blue); Alveolar and interstitial infiltration of neutrophils, macrophages; Levels of VEGF, VEGF receptor (sFLT1) in serum and lung	NR	(Epiphanio et al., 2010)

(Continued)

TABLE 1 | Continued

Animal	Strain	Parasite specie	Parasite strain/ clone	Inoculation		First exhibition of lung pathology (days post infection)	Peripheral parasitemia (%)	Lung pathological findings	Other affected organ(s)	Ref
				Route	Dose					
								homogenate (↓) Respiratory frequency		
			ANKA Clone 1.49L	IP	10^6 iRBCs	7	15	Hydrothorax (↑) Penh; Parasite sequestration; Alveolar infiltration of neutrophils, leukocytes; Levels of myeloperoxidase in the BALF and lung homogenate; Levels of KC/CXCL1, MIP-2/CXCL2 in serum	NR	(Sercundes et al., 2016)
								Damaged alveolar septa; Eosinophilic/hyaline membranes adhered to the alveolar ducts and walls	NR	(Ortolan et al., 2014)
								(↑) Lung weight; Pleural effusion; Haemorrhages; Alveolar edema; Alveolar capillary permeability (Evans blue); Alveolar and interstitial infiltration of neutrophils, macrophages, haemorrhages, Pulmonary opacification		
								Ground-glass opacification (↑) Penh; Expiration time; Pulmonary lesions (↓) Respiratory frequency, Tidal volume; Ventilation volume; Aerated tissue	NR	(Quirino et al., 2020)
	129P2Sv/Ev		ANKA Clone BdS	IP	10^6 iRBCs	7-10	NR	(↑) Lung edema; Tissue infiltration with leukocytes (macrophages, neutrophils, T cells); Levels of IFN-γ, TNF-α, MCP-1/CCL2, MIP-1α/ CCL3, RANTES/CCL5, IP-10/CXCL10, CCR2, CCR5, CCR1, CXCR3 in lung tissue homogenate	Brain	(Belnoue et al., 2008)
	129SV/J		ANKA (MR4)	IP	5×10^5 iRBCs (Male) 10^6 iRBCs (Female)	6	9	(↑) IgM in BALF	NR	(Lovegrove et al., 2008)
	BALB/c		ANKA		10^5-10^7 iRBCs	6	6-10	Thickened alveolar septa (↑) IgM in BALF, Lung edema; Alveolar infiltration with leukocytes (macrophages, lymphocytes)	NR	(Hansen et al., 2005; Lovegrove et al., 2008; Epiphanio et al., 2010)
			ANKA Clone 15cy1	IP	10^4 iRBCs; drinking water supplemented with 4-amino benzoic acid	10	10	(↑) Lung weight; IgM in BALF; Alveolar infiltration with leukocytes (macrophages, lymphocytes)	NR	(Vandermosten et al., 2018)

(Continued)

TABLE 1 | Continued

Animal	Strain	Parasite specie	Parasite strain/ clone	Inoculation		First exhibition of lung pathology (days post infection)	Peripheral parasitemia (%)	Lung pathological findings	Other affected organ(s)	Ref
				Route	Dose					
					(0.375 mg/ml PABA)					
	CBA/J		ANKA	IP	10^6 iRBCs	6-10	10	Neutrophils, monocytes-containing Hz, megakaryocytes adhered to the endothelium; Diffuse pulmonary and alveolar edema	Brain, liver	(Carvalho et al., 2000)
	ICR		ANKA	IP	2×10^7 iRBCs	5	50	Congestion of iRBCs in the alveolar space; Hyaline membrane adhered to the alveolar wall; Pulmonary inflammation (↑) Levels of IL27 in serum	Liver	(Fazalul Rahiman et al., 2013)
	Swiss		ANKA	IP	10^7 iRBCs	7	68	(↑) Lung weight; Haemorrhages	Liver, kidney	(Moore et al., 2008)
	C57BL/6 C57BL/6J		NK65	IP	10^4 iRBCs; drinking water supplemented with 4-amino benzoic acid (0.375 mg/ml PABA)	9	5	Thickened alveolar septa (↑) Lung weight; Pleural effusion; Haemorrhages; Alveolar edema; Alveolar capillary permeability (Evans blue); Airway reactivity; Tissue infiltration with $CD8^+$ T cells, MODC; Levels of IFN-γ, TNF-α, MCP-1/CCL2, MIP-1α/CCL3 in the lung tissue homogenate	NR	(Galvao-Filho et al., 2019)
			NK65	IP	10^4 iRBCs; drinking water supplemented with 4-amino benzoic acid (0.375 mg/ml PABA)	8-12	5-20	Eosinophilic/hyaline membranes adhered in the alveolar space (↑) Lung weight; Pleural effusion; Haemorrhages; Alveolar and interstitial edema (Proteinaceous); Alveolar capillary permeability (Evans blue); Alveolar infiltration with leukocytes (macrophages-containing Hz, neutrophils, lymphocytes) and haemorrhages; Levels of IFN-γ, TNF-α, IL-10, IP-10/CXCL10, MIP-2/CXCL2, MCP-1/CCL2, KC/CXCL1, VEGF, PlGF in the lung tissue homogenate	NR	(Van den Steen et al., 2010)
			NK65 Clone 2168cl2	IP	10^4 iRBCs; drinking water supplemented with 4-amino benzoic acid (0.375 mg/ml PABA)	7	6	(↑) Levels of PlGF, VEGF-A in BALF; Levels of PlGF, VEGF-A, TNF-α, IP-10/CXCL10, MIP-2/CXCL2 in the lung tissue homogenate; Tissue infiltration with $CD8^+$ T cells;	NR	(Pham et al., 2017)
			NK65 GFP-*luciferase* E line	IP	10^4 iRBCs; drinking water supplemented with 4-amino	9	20	(↑) Alveolar edema (proteinaceous); IgM in BALF; Alveolar infiltration with leukocytes (macrophages,	NR	(Vandermosten et al., 2018)

(Continued)

TABLE 1 | Continued

Animal	Strain	Parasite specie	Parasite strain/ clone	Inoculation		First exhibition of lung pathology (days post infection)	Peripheral parasitemia (%)	Lung pathological findings	Other affected organ(s)	Ref
				Route	Dose					
			(Clone 2168cl2)		benzoic acid (0.375 mg/ml PABA)			lymphocytes, neutrophils) and hemorrhages		
	C3H/z		KEYBERG Clone 173	IP	3×10^6 iRBCs	8	>6	Severe alveolar and interstitial edema (proteinaceous) (↑) Alveolar infiltration with macrophages	Heart	(Weiss and Kubat, 1983)
	C57BL/6	*P. chabaudi*	CB	IP	10^5 iRBCs	9	50	(↑) IgM in BALF; Alveolar infiltration with leukocytes (myeloids, neutrophils, T cells) and Hz; Cell death of lung tissue; MRP14-associated neutrophil response; Levels of IFN-γ, IL-6, KC/CXCL1, LIX/CXCL5	NR	(Lin et al., 2017)
	BALB/c	*P. yoelii*	17XL	IP	2×10^5 iRBCs	6	90	(↑) Alveolar and interstitial edema (proteinaceous); Alveolar infiltration of mononuclear and PMN cells	Liver, spleen, kidney	(Fu et al., 2012)
	BALB/c	*P. vinckei*	NR	IP	10^5 iRBCs	NR	NR	(↑) Interstitial infiltration of mononuclear cells, neutrophils	Liver, kidney	(Kremsner et al., 1992)
Hamster	NR	*P. berghei*	NYU-2	NR	NR	6	NR	Protein-rich exudate in the alveolar space; Congested capillaries with presence of macrophages; Lymphatic thrombosis	NR	(MacCallum, 1968; MacCallum, 1969)
Non-human primate	*Macaca mulatta* (Rhesus macaque)	*P. knowlesi*	NR	NR	NR	6-7	>70	Mild lung edema; Congested vessels with fibrin deposit, thrombi, mononuclear and PMN cells	Kidney, lymph nodes	(Spangler et al., 1978)
	Macaca fascicularis (kra/ cynomolgus macaques)		Clone Pk1 (A+)	IV	10^5 sporozoites	6-50	<1	Thickened interstitium; Haemorrhage; Fibrosis; Hyperplasia (↑) Parasite sequestration in the lung microvasculature	Liver, kidney, spleen	(Peterson et al., 2021)
	Papio Anubis (Olive baboon)		H strain	IV	10^4-10^6 iRBCs	12-28	5-50	Thickened alveolar septa (↑) Alveolar and interstitial edema; Alveolar infiltration with leukocytes (macrophages-containing Hz, neutrophils), Parasite sequestration	Brain, liver, kidney	(Ozwara et al., 2003)
	Macaca mulatta	*P. cynomolgi*	M/B strain	IV	2×10^3 sporozoites	23	<20	Eosinophilic membranes adhered on the parenchyma; Fibrin deposits on interstitium; Thickened alveolar wall (↑) Alveolar and interstitial edema; Alveolar infiltration with macrophages-containing Hz	Liver, kidney, spleen	(Joyner et al., 2017)
	Saimiri boliviensis (Black-capped	*P. vivax*	Brazil VII strain	IV	10^4 sporozoites	10-25	<1	Thickened alveolar wall (↑) Interstitial edema; Alveolar infiltration with leukocytes (macrophages), Hz,	Liver, kidney	(Peterson et al., 2019)

(Continued)

TABLE 1 | Continued

Animal	Strain	Parasite specie	Parasite strain/ clone	Inoculation		First exhibition of lung pathology (days post infection)	Peripheral parasitemia (%)	Lung pathological findings	Other affected organ(s)	Ref
				Route	Dose					
	squirrel monkey) (splenectomised)							haemorrhages; Parasite sequestration		
Macaca mulatta	(splenectomised)	*P. coatneyi*	NR	IV	NR	NR	NR	(↑) Parasite (schizonts) sequestration in the lung microvasculature	Liver, kidney, heart	(Desowitz et al., 1969)

IP, Intraperitoneal; IV, Intravenous; iRBCs, Infected red blood cells; GFP, Green fluorescent protein; BALF, Bronchoalveolar lavage fluid; TNF, Tumour necrosis factor; IFN, Interferon; IL, Interleukin; CXCL, CXC chemokine ligand; CCR, CC chemokine receptor; KC, Keratinocyte chemoattractant; MCP, Monocyte chemoattractant protein; MIP, Macrophage inflammatory protein; VEGF, Vascular endothelial growth factor; PlGF, Placental growth factor; PMN, Polymorphonuclear; MODCs, Monocyte-derived dendritic cells; MDMs, Monocyte-derived macrophages; Hz, Hemozoin; NR, Not reported; (↓), Decreased; (↑), Increase.

1983). In addition, NHP hosts used in these studies were rarely naïve as they are often re-employed as experimental animal after clearance of previous experimental infections (e.g., malaria or viral infections), or were pre-exposed to malaria, or other pathogens while in breeding colonies. The latter was reported in the study by Spangler et al. where NHP host was potentially infected by *Pneumonyssus simicola* (lung mite) (Spangler et al., 1978). Such pre-exposure to pathogens may have an immune-modulating effect (i.e. cross-reactivity immunity to *Plasmodium* infection) that can affect MA-ARDS pathogenesis.

4 MA-ARDS PATHOGENESIS

4.1 Sequestration of Malaria Parasites

P. falciparum parasites residing within the red blood cells have devised multiple strategies to survive within its host. The parasite alters the iRBCs membrane composition to express cytoadhesive ligands that interact with various adhesion receptors present on the endothelial lining. This cytoadhesive properties allow iRBCs sequestration in the endothelium bed of the organs. This allows the parasite to escape splenic clearance (Henry et al., 2020). Parasite cytoadherence to the endothelium and sequestration in deep tissues are associated to the development of severe malaria (Craig et al., 2012). Cytoadherence and sequestration of iRBCs in the endothelium causes (1) reduced blood flow in the blood capillaries/vessels and (2) activation of endothelial cells leading to inflammation and subsequent disruption of endothelium integrity (Craig et al., 2012).

In the lung sections from deceased *P. falciparum*-infected patients that developed MA-ARDS, iRBCs were found to sequester in the lung microvasculature. These *P. falciparum*-iRBCs sequestered in the vessels were predominantly the matured stages (MacPherson et al., 1985). Sequestration of *falciparum*-iRBCs to the lung microvasculature was proposed as the cause of alveolar capillaries occlusion, resulting in reduced blood volume within these capillaries (MacPherson et al., 1985; Maguire et al., 2005). As for other human *Plasmodia* species, iRBCs cytoadherence properties and sequestration ability alike *falciparum*-iRBCs are emerging. Several histological studies have reported that *P. vivax*-iRBCs were found within congested alveolar capillaries (Valecha et al., 2009; Lacerda et al., 2012). Strikingly in one of these studies, sequestered *P. vivax*-iRBC were observed in the lung sections from a patient whose parasitemia was microscopy negative. Moreover, reduced blood volume was documented in patients with *vivax*-induced MA-ARDS (Anstey et al., 2007). Together, these evidences are in support of recent reports demonstrating that parasite cytoadherence to the endothelium and deep tissue sequestration are not restricted to *falciparum* but extend to other *Plasmodia* infecting humans, such as *P. vivax* (Carvalho et al., 2010; Lopes et al., 2014) and *P. knowlesi* (Miller et al., 1971; Fatih et al., 2012; Lee et al., 2021).

It has been demonstrated that *falciparum*-iRBCs cytoadhere through several families of parasite cytoadherence ligands expressed on its surface, namely PfEMP1, STEVOR and RIFIN (Lee et al., 2019). Of the cytoadhesion interactions between the host receptor and parasite ligand, PfEMP1 with EPCR has been associated with severe malaria, particularly cerebral complications (Moxon et al., 2013; Turner et al., 2013; van der Poll, 2013). In the study by Maknitikul et al., EPCR was expressed on the lung endothelium from post-mortem tissue samples of patients with MA-ARDS, although the levels of EPCR were reported to be negatively correlated to iRBCs accumulation in the lung (Maknitikul et al., 2017). In a separate study, it was further demonstrated that PfEMP1 was able to bind to EPCR expressed on the lung endothelial cells, aside from the brain (Turner et al., 2013). In addition, another receptor that interacts with PfEMP1, namely ICAM-1, its expression was found elevated on the lung endothelium of MA-ARDS patients' organ sections and in *in vitro* studies (Avril et al., 2016; Maknitikul et al., 2017). ICAM-1 was also identified as a receptor that *vivax*-iRBCs cytoadhere to on HLECs under flow conditions *in vitro* (Carvalho et al., 2010). Thus, demonstrating that *vivax*-iRBCs do possess the ability to sequester. This phenomenon was also recently described for *P. knowlesi*-iRBCs that CD36 was a potential binding receptor on HLECs, with enhanced binding when primed with parasite culture supernatant *in vitro* (Lee et al., 2021). Although, at present the parasite cytoadherence ligands of *vivax*-iRBCs and *knowlesi*-iRBCs are yet to be fully defined, sequestration mediated through ligands

such as *vivax*-derived variant interspersed repeats (VIR) proteins and *knowlesi*-derived schizont-infected cell agglutination (SICA) proteins have been suggested (del Portillo et al., 2001; Korir and Galinski, 2006).

As sequestration is crucial for MA-ARDS pathogenesis, there is a clear need for *in vivo* studies to understand its involvement in the process of pathology development with *in vivo* conditions (such as waste clearance, circulatory flow, host immune system). Moreover, experiments with human-malaria causing *Plasmodium* iRBCs isolated from the peripheral circulation of patients with severe malaria, might be biologically different (in terms of cytoadhesive receptor specificity, affinity or avidity, and interactions) to parasite sequestered in the microvasculature. These limitations would eventually cloud the genuine associations of sequestration with the different pathologies.

With the advancement of genetic modification and *in vivo* vascular imaging techniques, infection of mouse strains with transgenic *P. berghei* parasites expressing luciferase can be used to visualize sequestration in relation to its distribution and load in various organs (Claser et al., 2014). Sequestration of luciferase-expressing *P. berghei*-iRBCs was observed in the lung of mice with MA-ARDS (Franke-Fayard et al., 2005; Sercundes et al., 2016; Vandermosten et al., 2018). In a more detailed study, Claser et al. have shown that iRBCs sequester in the perfused lungs (unbound iRBCs were removed) prior to the onset of vascular leakage, once sequestration reaches a saturable level, leakage ensues (Claser et al., 2019). Also, in the same study, the use of intensive anti-malarial treatments to remove circulatory and sequestered iRBCs prior to leakage, were sufficient to protect infected mice from lung hyperpermeability. This clearly demonstrates the importance of parasite sequestration in the lung microvasculature as a pre-requisite for lung pathology development.

Emerging studies have identified several cytoadhesion interactions between the host-derived receptors and *P. berghei*-iRBCs in the mouse lung tissue, which parallels those described with human-malaria causing *Plasmodium* iRBCs. To date, functional homolog of PfEMP1 in *P. berghei*-iRBCs has not been identified. Nonetheless, proteins such as, the Maurer's cleft skeleton binding protein-1 (SBP-1) and histidine-rich protein (MAHRP-1), that mediate the export of parasite cytoadhesion ligands (e.g. PfEMP1) to the surface of the iRBCs, are conserved between human-malaria and rodent-malaria *Plasmodia* (De Niz et al., 2016). With the use of mutant parasites, SBP-1 and MAHRP-1 have been shown to mediate the sequestration of *P. berghei*-iRBCs in the lungs of animals, depleted of circulating erythrocytes by perfusion with a saline solution (De Niz et al., 2016; Possemiers et al., 2021). Apart from reduced parasite load in the lung, the absence of SBP-1 was shown to induce spontaneous resolution and less inflammatory responses in the lung, despite continuous presence of parasite (Possemiers et al., 2021). For *P. vivax*, members of the *vir* multigene family have been suggested to mediate cytoadherence (Carvalho et al., 2010; Bernabeu et al., 2012; Fernandez-Becerra et al., 2020; Schappo et al., 2022), bears close homology to the *P. berghei bir* multigene family (Janssen et al., 2004). In the mouse model, PbA cytoadherence to host-derived receptor, CD36, was identified to be crucial for parasite sequestration (Franke-Fayard et al., 2005; Lovegrove et al., 2008; Fonager et al., 2012; Anidi et al., 2013). This was clearly demonstrated in the study by Anidi et al. that in the absence of CD36, PbA-infected mice were shown to have reduced parasites sequestered to the alveolar capillaries and vessels, with subsequently less induction of alveolar-capillary breakdown and endothelial barrier dysfunction (Anidi et al., 2013). It has been further suggested by Fonager et al., that CD36-dependent cytoadherence to the endothelium by late stage PbA-iRBCs was mediated by the schizont membrane-associated cytoadherence (SMAC) protein, expressed in cytoplasm of the iRBC. However, the study showed that the absence of SMAC had minimal effect on sequestration in the lung during infection with the SMAC mutant PbA parasites, indicating that other parasite molecules are involved in parasite sequestration (Fonager et al., 2012). Indeed, it was suggested that sequestration of *P. berghei*-iRBCs could be mediated by several host-derived receptors such as EPCR, ICAM-1 and VCAM-1, as deficiencies in these receptors led to significant reduction in parasite load in the lung (Favre et al., 1999; Li et al., 2003; Avril et al., 2016; Dos Santos Ortolan et al., 2019). However, El-Assaad et al. have demonstrated that inhibition of ICAM-1 had no effect on the *in vitro* binding of mature stage PbA-iRBCs to lung microvascular endothelial cells (LMVECs) (El-Assaad et al., 2013). Treatment with dexamethasone in DBA/2-infected with PbA, downregulates EPCR expression in the lung and protected the mice from lung hyperpermeability (Dos Santos Ortolan et al., 2019). Nevertheless, it remains to be determined further which of these host-derived receptors are mediating parasite sequestration in the lung and subsequent pathology. Although *Plasmodium*-iRBCs from mice and humans are phenotypically different, identification of similar host-derived receptors may lead to new intervention targets.

4.2 Cytokines

Cytokines and chemokines are small proteins released predominantly by immune cells as part of the host immune system's coordinated defense mechanism against foreign particles or pathogens. They are involved in the recruitment and functional activation of various immune cells. Controlled inflammatory cytokine and chemokine responses are essential for the host to eliminate the parasite growth. However, exaggerated and uncontrolled responses can lead to severe disease. Elevated levels of pro-inflammatory cytokines and chemokines in the serum, TNF-α, IL-1β, IL-6, IL-8, IL-17, IFN-γ, IP-10/CXCL10 (binds to CXCR3) and MCP-1/CCL2 (binds to CCR2) (Day et al., 1999; Armah et al., 2007; Cox-Singh et al., 2011; Kinra and Dutta, 2013; Mandala et al., 2017), and reduced levels of anti-inflammatory cytokines, TGF-β (Esamai et al., 2003; Andrade et al., 2010), have been associated with severe malaria in humans and has been described extensively for cerebral malaria. However, knowledge on these analytes from patients with MA-ARDS or bronchoalveolar lavage fluid (BALF) is limited. Cytokine profiles at the site of pathology are critical as it provide signals that dictate and perpetuate the inflammatory responses locally in

the tissue and may reflect the extent of the injury. To describe cytokines that are associated with MA-ARDS pathogenesis, we will draw on findings obtained from the mouse MA-ARDS models.

Global analysis of lung tissues and BALF of infected mice with MA-ARDS revealed elevated levels of the cytokines and chemokines also reported in the serum of severe malaria in humans mainly, IL-1, IL-6, IL-8, IL-10, TNF-α, IFN-γ, MCP-1/CCL2, MIP-2/CXCL2, IP-10/CXCL10, KC/CXCL1, VEGF, PIGF (Day et al., 1999; Lovegrove et al., 2008; Epiphanio et al., 2010; Van den Steen et al., 2010; Taylor et al., 2012; Deroost et al., 2013; Pham et al., 2017; Galvao-Filho et al., 2019). To understand the role of various cytokines in MA-ARDS development, infections in the specific knockout mouse models were used as, reviewed in **Table 2**.

During the acute phase of blood stage infection, the febrile response is a typical host immune defense triggered by pyrogenic cytokines, IL-6 and TNF-α, produced by circulating innate cells upon recognition by its pattern recognition receptors with pathogen-associated molecular patterns (Netea et al., 2000). Moreover, in the lung, alveolar macrophages that harbor phagocytosed iRBCs and Hz may be an essential source of IL-6 and TNF-α, where the elevated levels were tightly associated with lung inflammation during the acute phase of MA-ARDS establishment (Deroost et al., 2013). In addition, pulmonary endothelial cells were found to produce TNF in DBA/2-infected with PbA (Dos Santos Ortolan et al., 2019). Although the role of IL-6 in MA-ARDS pathogenesis have yet to be reported, studies have suggested that IL-6 plays a pleiotropic role in ARDS (Butt et al., 2016). Furthermore, IL-6 can have a pro-inflammatory effect as part of the host defense mechanism in the acute phase to combat the triggering stimulant. In addition, IL-6 works in synergy with other pro-inflammatory cytokines (significantly associated with TNF-α and IL-1), causing the infiltration of various leukocyte subsets into the lung. When this response becomes excessive, it may have deleterious effects on the lung tissue resulting in injury (Tutkun et al., 2019; West, 2019; Pedersen and Ho, 2020; Ragab et al., 2020). IL-6 can have a pro-fibrotic effect in the later phase of ARDS (Le et al., 2014; Kobayashi et al., 2015). On the other hand, studies have demonstrated that TNF-α does not play a critical role in MA-ARDS pathogenesis (Piguet et al., 2002; Togbe et al., 2008; Galvao-Filho et al., 2019) (**Table 2**). Nonetheless, more studies are needed to understand the role of IL-6 and TNF-α during the establishment of MA-ARDS, and its association with circulatory levels in the serum to evaluate the possibilities as early biomarkers to determine the onset, severity, and outcome of lung injury.

IFN-γ is an essential cytokine induced and has been found to inhibit *Plasmodium* blood stages. IFN-γ is produced by various immune cell subsets from the innate and adaptive immunity arms at different phases of the blood stage infection (Gun et al., 2014). At the early phase of the blood stage infection, NK cells, NKT cells, γδ T cells, and T cells were the main producers, followed by a shift of the role to the T cells ($CD4^+$ and $CD8^+$) at the later phase of infection (King and Lamb, 2015). High levels of IFN-γ at the early phase of the blood stage infection have been largely correlated to protection from severe malaria and control of systemic parasite growth, but may increase the risk of developing severe malaria in the later phase of infection (King and Lamb, 2015). IFN-γ was shown to play a pathogenic role in MA-ARDS development, as the infection of IFN-γ signaling-deficient mouse models were protected from lung injury despite the increased transmigration and infiltration of leukocytes and activated effector T cells in the lung tissue (Belnoue et al., 2008; Villegas-Mendez et al., 2011; Claser et al., 2019; Galvao-Filho et al., 2019) (**Table 2**). Besides, IFN-γ was shown to be required for the maturation of TNF-a/iNOS-producing monocyte-derived dendritic cells that could augment $CD8^+$T cells cytotoxicity to cause lung injury in PbNK65-infected mice (Galvao-Filho et al., 2019). Expression of other pro-inflammatory cytokines were found to be inducible by the canonical IFN-γ cytokine during lung inflammation, such as IP-10/CXCL10 (which binds to its cognate CXCR3 receptor) (Liu et al., 2012), may work in synergy with IFN-γ to promote leukocytes trafficking into the lung to cause the pathology.

4.3 Endothelial Cells

The pulmonary vasculature is formed by a layer of endothelial cells, serving as a semipermeable barrier that separates the pulmonary circulation from the air. It regulates lung homeostasis through intercellular junctions, allowing the paracellular transport of macromolecules and nutrients among the cells (Mehta and Malik, 2006). Disruption of this endothelial barrier causes fluid leakage from the blood vessels into the alveolar lumen, promoting pulmonary edema, recruitment of inflammatory mediators, and accumulation of leukocytes and platelets (Ware, 2006; Millar et al., 2016). During *Plasmodium* infection, the lung vasculature was suggested to be a niche for the parasite to initiate the blood stage in the host. The merosomes originating from the liver schizonts are likely disrupted within the pulmonary capillary, releasing merozoites that will infect the red blood cells. This early interaction may trigger an inflammatory response; however, it would be limited due to the low number of parasites present in the organ (Souza et al., 2013; Aitken et al., 2014).

4.3.1 Endothelial Cells: Adhesion Molecules and Cytokines

Endothelial cells can be activated by vascular endothelial growth factor (VEGF), also known as VEGF-A (Kim et al., 2011), TNF-α, and by mediators produced by the *Plasmodium* parasite during infection (Gillrie et al., 2007). The activated endothelial cells release cytokines that upregulate the expression of adhesion molecules (P-, L- and E-selectin) (Combes et al., 2004; Krishnamurthy et al., 2015). Chemokines such as CCL2, CXCL4, CCL5 (Van den Steen et al., 2010), promote the adhesion of iRBCs, macrophages (Grau et al., 1987), platelets (Wassmer et al., 2004), neutrophils (Souza et al., 2013) and plasma microparticles (Faille et al., 2009) to the endothelium. IFN-γ, TNF-α and IL-1, produced by NK and mononuclear cells (alveolar and interstitial macrophages), are the most prevalent cytokines involved in leukocytes chemotaxis and for ICAM-1/

TABLE 2 | The role of cytokines/chemokines ligand-receptors in experimental MA-ARDS.

Gene knockout ($^{-/-}$)	Parasite used for infection	Effect on MA-ARDS development (vs wild-type). Outcome (left), Histology (Right)		Additional data	Ref
TNFα$^{-/-}$	*P. berghei* ANKA (PbA) GFP-*luciferase*	No difference (=)	=Congested septal capillaries =Haemorrhage =Interstitial edema		(Togbe et al., 2008)
TNFR1$^{-/-}$	PbA	=	=Edema ↓Macrophages in alveolar capillaries	(=) Parasite sequestration	(Piguet et al., 2002)
	PbNK65	=	=Histopathology scores =Edema	(=) Parasite sequestration (↓) MODCs in lung tissue	(Galvao-Filho et al., 2019)
TNFR2$^{-/-}$	PbA	=	=Edema	(=) Parasite sequestration	(Piguet et al., 2002)
IFNγR1$^{-/-}$	PbA Bds	↓	No edema	(↑) CD4$^+$, CD8$^+$ T cells, neutrophils, and macrophages in the lung tissue (↑) MCP-1/CCL2, IP-10/CXCL10 in the lung	(Belnoue et al., 2008)
IFNγ$^{-/-}$	PbA	NR	NR	(=) CD4$^+$ T cells migration markers (CXCR3, CCR5) in the lung tissue (=) CD4$^+$ T cells activation/effector markers (CD62^{low}, Ki67) in the lung tissue (↓) CD4$^+$ T cells activation/effector markers (CD44, CD71, CD11a, CD49D, GrzB) in the lung tissue (=) CD8$^+$ T cells migration markers (CXCR3, CCR5) in the lung tissue (=) CD8$^+$ T cells activation/effector markers (CD62^{low}, CD44, CD71, Ki67, CD49D) in the lung tissue (↑) CD8$^+$ T cells activation/effector markers (CD11a) in the lung tissue (↓) CD8$^+$ T cells activation/effector markers (GrzB) in the lung tissue	(Villegas-Mendez et al., 2011)
	PbA GFP-*luciferase*	↓	NR	(↓) Lung vascular leakage (↓) Parasite sequestration (↑) Total leukocytes, activated CD4$^+$, activated CD8$^+$, Parasite-specific Pb1$^+$ CD8$^+$ T cells in the lung tissue (↓) MHC I expression on lung endothelial cells	(Claser et al., 2019)
IL-12Rβ2$^{-/-}$	PbA GFP-*luciferase*	=	=Thickened alveolar septae =Haemorrhage =Interstitial edema =Congested alveolar capillaries =Leukocytes infiltration in alveoli		(Fauconnier et al., 2012)
IL-12p35$^{-/-}$	PbA GFP-*luciferase*	=	=Thickened alveolar septae =Haemorrhage =Interstitial edema =Congested alveolar capillaries =Leukocytes infiltration in alveoli		(Fauconnier et al., 2012)
IL-12p40$^{-/-}$	PbA GFP-*luciferase*	=	=Thickened alveolar septae =Haemorrhage =Interstitial edema =Congested alveolar capillaries =Leukocytes infiltration in alveoli		(Fauconnier et al., 2012)
CXCL10$^{-/-}$	PbA	↓	↓Alveolar edema ↓Leukocytes infiltration in alveoli	(↑) HO-1 levels in lung tissue, positively associated with free heme	(Liu et al., 2012)

(Continued)

TABLE 2 | Continued

Gene knockout ($^{-/-}$)	Parasite used for infection	Effect on MA-ARDS development (vs wild-type). Outcome (left), Histology (Right)		Additional data	Ref
CCR2$^{-/-}$	PbA	↓	↓Edema	(↓) Monocytes/MDMs in the lung tissue (↑) Hz-containing cells in the lung tissue	(Lagasse et al., 2016)
	PbNK65	=	=Edema =Histopathology scores	(=) Parasite sequestration (↑) Neutrophils in the lung tissue Delayed MODCs infiltration into the lung tissue (↓) Ly6C^{+} Inflammatory monocytes in the lung tissue (=) Alveolar macrophages in the lung tissue (=) CD8^{+} T naïve/effector/central memory cells in the lung tissue (=) CD4^{+} T naïve/effector/central memory cells in the lung tissue	(Galvao-Filho et al., 2019; Pollenus et al., 2020)
CCR4$^{-/-}$	PbNK65	↓	↓Thickened alveolar septae ↓Haemorrhage ↓Edema	(=) Parasite sequestration (↓) MODCs in the lung tissue	(Galvao-Filho et al., 2019)

TNF, Tumour necrosis factor; TNFR, Tumour necrosis factor receptor; IFN, Interferon; IFNR, Interferon receptor; IL, Interleukin; CXCL, CXC chemokine ligand; CCR, CC chemokine receptor; MODCs, Monocyte-derived dendritic cells; MDMs, Monocyte-derived macrophages; Hz, Hemozoin; (=), No difference; NR, Not reported; (↓), Decreased; (↑), Increased.

CD54 and VCAM-1/CD106 expression on the endothelial cells (Smith et al., 2019). IFN-γ activate and enhance the antigen-cross presentation capability of LMVECs, through signaling the upregulation of MHC-I, thus driving the cross-presentation of immunogenic parasite epitope by LECs to cytotoxic CD8^{+} T cells. The consequence of this process is lung endothelium-epithelium hyperpermeability (Claser et al., 2019). Additionally, some studies have demonstrated that IFN-γ and TNF upregulate the expression of adhesion proteins, such as ICAM-1 and VCAM-1, promoting the binding of iRBCs on LMVECs and trafficking of leukocytes into the lung tissue of infected humans oand mice (Ockenhouse et al., 1992; Zielinska et al., 2017).

Activated endothelial cells also release Weibel-Palade bodies (WPBs), which are storage granules containing Von Willebrand factor (VWF) and angiopoietin-2 (Ang-2) (Dole et al., 2005). During endothelial injury, VWF and Ang-2 are released, and have been associated with mortality in patients with MA-ARDS (Yeo et al., 2008; Park et al., 2012; Graham et al., 2016). In one study, *vwf*-deficient mice infected with PbNK65, had reduced alveolar leakage, but surprisingly exacerbated mortality (Kraisin et al., 2019). Endothelium remodeling by Ang-2 was shown to be a physiological condition-dependent mechanism (de Jong et al., 2016). Moreover, Ang-2 and Ang2^{+}-expressing leukocytes were found increased in the alveolar space of lung tissue sections from humans that died of MA-ARDS (Pham et al., 2019).

4.3.2 Vascular Permeability Alterations

Leakage of solutes, cells, both small and larger molecules from the microvasculature into the tissue can occur in normal physiological condition and greatly increased in pathological state. This extravasation can happen by transcellular or paracellular mechanisms, or *via* destabilization of endothelial junctions. In pathological state, increased vascular permeability, a hallmark of ARDS, results in edema (Claesson-Welsh, 2015; Wettschureck et al., 2019).

Many inflammatory factors, such as VEGF, histamine, bradykinin, TNF-α, and IFN-γ, promotes cytoskeleton contraction and alteration on the endothelial junctions by opening the paracellular junctions, which contributes to the inflammatory process (Claesson-Welsh, 2015; Ji et al., 2021). The Rho family of GTPases, whose principal members are Cdc42, Rac, and RhoA, are dynamic regulators of the cytoskeleton, acting as molecular switches that controls cellular processes by hydrolysis of GTP, contributing to different cellular functions (Norbert Voelkel, 2009; Liu et al., 2014). RhoA and RhoB interacts with their effector Rho kinase (ROCK). RhoB regulates endothelial barrier function during inflammation by activating NF-kβ (Vincent et al., 2004). On the other hand, activation of RhoA and its effector ROCK induced by the adhesion of *P. falciparum*-iRBCs to human LMVECs, inhibits myosin phosphatase and increases myosin light chain (MLC) phosphorylation. This phosphorylation induces actomyosin polymerization, contraction, and weakening of inter-endothelial junctions, causing the increase in vascular permeability (McKenzie and Ridley, 2007; Norbert Voelkel, 2009; Beckers et al., 2010; Spindler et al., 2010; Marcos-Ramiro et al., 2014). However, excessive or abnormal activation of RhoA and its effector ROCK, by the factors such as TNF-α, oxidative stress, thrombin, growth factors, and other agents, is associated with decreased endothelial barrier function (Dejana et al., 1999; Zhao et al., 2014; Hartmann et al., 2015). In addition, TNF-α disorganizes the inter-endothelial junctions and causes disarrangement in the cytoskeleton of endothelial cells, thus increasing vascular permeability (Taoufiq et al., 2008; Zang-Edou et al., 2010; Taoufiq et al., 2011; Liu et al., 2014). Moreover, it was demonstrated that human LMVECs stimulated with *P. falciparum* extract (parasite sonicate), had

increased vascular endothelial permeability due to morphological changes in adherent and occlusion junctions (Gillrie et al., 2007).

VEGF is a potent pro-angiogenic cytokine that remodels the endothelium permeability,surface adhesion molecules and mediates the chemotaxis of leukocytes (such as monocytes/macrophages) during inflammation (Heil et al., 2000; Reinders et al., 2003). It was also shown to affect endothelial barrier dysfunction by activating the Rho-GTPase signaling cascade (Gallego-Delgado et al., 2016). Excessive production of VEGF during MA-ARDS was suggested to induce lung capillary hyperpermeability (Ware, 2006; Pham et al., 2017; Pham et al., 2019). In addition, an increase of VEGF-A and PlGF in the lungs, was dependent on effector $CD8^+$T cells to cause alveolar edema (Pham et al., 2017). Using DBA/2- infected with PbA, Epiphanio et al. demonstrated that high levels of circulating VEGF correlated with MA-ARDS. Intravenous infection with sFLT1 (soluble form of the VEGF receptor)-expressing adenovirus, protected the PbA-infected DBA/2 micefrom MA-ARDS and this protection was correlated with decreased levels of VEGF in the circulation (Epiphanio et al., 2010). However, the treatment with a neutralizing monoclonal antibody against VEGF receptor-2 (VEGFR-2), did not prevent MA-ARDS in PbNK65-infected C57BL/6 mice (Pham et al., 2017). Therefore, the role of VEGF in MA-ARDS is still being debated, whether they play an effector role in causing endothelium permeability or released as a result of lung injury.

Primary LMVECs (PLMVECs) from uninfected DBA/2 mice in contact with PbA-iRBCs or its lysate for one hour, induced the production of pro-inflammatory cytokine, TNF-α, cytoskeleton contraction and promoted pulmonary vascular hyperpermeability (Pereira et al., 2016; Dos Santos Ortolan et al., 2019). Furthermore, the adhesion of iRBCs to ICAM-1, leads to alterations in the conformation of actin microfilaments (forming a cup-like structure), which was proposed to be the mechanism associated with the disruption of the blood-brain barrier in the human brain endothelial cell lines (Jambou et al., 2010). On the other hand, it was demonstrated that LMVECs obtained from uninfected DBA/2 mice previously treated with hemin, induces heme oxygenase-1 (HO-1) and an anti-inflammatory effect, which decreases cytoskeleton contraction. This consequently reduced the opening of the inter-endothelial junctions (Pereira et al., 2016).

Studies in murine models and patients have shown the involvement of the epithelial and endothelial cell death in the pathogenesis of ARDS (Bachofen and Weibel, 1977; Fujita et al., 1998). Apoptosis involving the Fas/FasL pathways and activation of caspases have been suggested to mediate pathogenesis in the lung of *P. falciparum*-infected patients with pulmonary edema (Taoufiq et al., 2008; Taoufiq et al., 2011; Punsawad et al., 2015). PLMVECs in contact with PbA-iRBCs for 24 hours showed increased endothelial permeability induced by the activation of caspases mechanism, leading to apoptosis of these cells (Sercundes et al., 2022). The contact between PbA-iRBCs and PLMVECs from DBA/2 mice induce alterations in the conformation of actin microfilaments, with a short network and cross-linked filaments, compared to actin from non-stimulated cells with long, parallel fibers arranged longitudinally (**Figure 1**). The sepsis model demonstrated that cell-free hemoglobin increased lung apoptosis, contributing to endothelial injury and increased vascular permeability (Meegan et al., 2020). Kingston and collaborators showed that cell-free hemoglobin levels were higher in patients with severe malaria than uncomplicated malaria or healthy controls. In addition, cell-free hemoglobin diminishes peripheral perfusion (related to mortality) by NO scavenging (Kingston et al., 2020). Using PbA-infected C57BL/6 mice, Anidi et al. demonstrated that the increase in pulmonary endothelial permeability after cytoadhesion of iRBCs, was mediated by CD36 and Fyn kinase (Anidi et al., 2013).

Treating and preventing ARDS is essential to protect and restore pulmonary endothelial barriers, and to combat

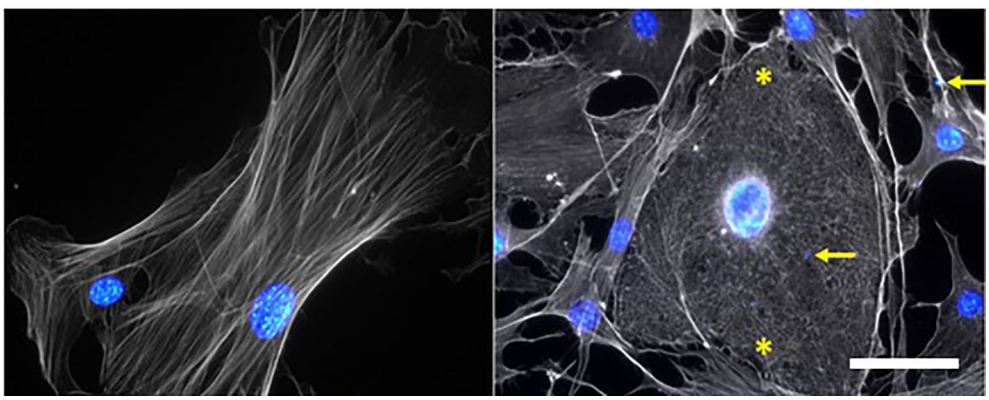

FIGURE 1 | *P. berghei* ANKA-infected red blood cells (PbA-iRBCs) generate morphological alterations in the cytoskeleton of primary pulmonary endothelial cells (PMLECs) of DBA/2 mice. Non-stimulated (NS) cell show elongated actin microfilaments, while adhered PbA-iRBCs cause shortening and entanglement of these filaments, indicated by asterisks. Actin and cell nuclei were stained with Texas Red Phalloidin], Hoechst [1:1000], respectively. Yellow arrows point to PbA-iRBCs nuclei; Scale bar: 50 μm.

endothelial dysfunction. Some molecules such as steroidal anti-inflammatory, RhoA inhibitors, histamine receptor blockades, sphingosine 1-phosphate, angiopoietins, PKC inhibitors, anti-VEGF, and others, have displayed the ability to improve endothelial barrier properties (Ma et al., 2019). Annexin A1, for instance, preserves junction integrity and consequently decreases vascular permeability (Ma et al., 2019; He et al., 2021). Ac2-26, an annexin A2 peptide, was demonstrated to reduce systemic inflammation through decreasing leukocyte migration to the lung, induction of anti-inflammatory IL-10 production (Guido et al., 2013), reducing oxidative stress responses and protecting from ARDS in the LPS model (Ju et al., 2021). According to He and colleagues, this peptide promotes phosphorylation of PI3K and Akt, and inhibits p-NF-κB (p65) expression, reducing pulmonary inflammation and injury (He et al., 2021). Rho-kinase inhibition by fasudil (a potent and selective Rho kinase inhibitor) can be a pertinent approach to reduce the effects of severe malaria, including ARDS patients (Taoufiq et al., 2008). Caspase inhibition by ZVAD-fmvk prevented the increase of pulmonary vascular permeability *in vivo* (PbA-infected DBA/2 mice), and *in vitro* (PbA-iRBCs in PLMVECs for one hour). In addition, PbA-infected DBA/2 mice treated with hemin were protected from MA-ARDS development, especially concerning the alveolar-capillary barrier (Pereira et al., 2016). As much as the endothelium plays a fundamental role in the development of MA-ARDS, drugs that modulate vascular permeability or reduce the inflammatory processes in the lung tissue, are essential targets. However, most of the current studies are done *in vitro* or are still in pre-clinical trials, and there is still a long way before it can be prescribed to malaria patients, especially with lung injuries.

4.4 Leukocytes

Malaria infection incites the inflammation process, triggering intense leukocyte infiltration into the lung parenchyma (Deroost et al., 2013; Aitken et al., 2014). The expression of CAMs on activated endothelial cells and activation of P- and E-selectin, induce the expression of β2-integrins, leading to subsequent leukocyte arrest in the vasculature (Krishnamurthy et al., 2015). The accumulation of these leukocytes in the capillary and alveolar space, and the interaction between leukocyte and endothelium, observed in both humans and animals, were shown to contribute to MA-ARDS pathogenesis (Taylor et al., 2012; Souza et al., 2013). Among the infiltrated leukocytes documented, monocytes, macrophages, lymphocytes, and neutrophils were found in the lung of patients and in the mouse models (reviewed in (Van den Steen et al., 2013).

4.4.1 Monocytes/Macrophages

Upon iRBCs sequestration in the pulmonary vasculature, monocytes/macrophages were found in the lung tissue of *P. falciparum*-infected patients with MA-ARDS (Mohan et al., 2008) and PbA-infected mice. These cells mediate the clearance of iRBCs in a CD36-dependent manner. In addition, $CCR2^{+}CD11b^{+}Ly6C^{hi}$ monocytes from the circulation were found to accumulate in the lungs as monocyte-derived macrophages (MDM) (Lagasse et al., 2016). Furthermore, it was demonstrated that infection of CD36 bone marrow chimeric mice resulted in the phagocytic clearance by monocytes, leading to exaggerated lung pathology (Lagasse et al., 2016). The increase in MDM in the lung on 7 days post-infection (dpi) of PbA-infected C57BL/6 mice was further corroborated by Claser et al. (2019).

Monocytes/macrophages when activated by parasites components, including Hz, secrete pro-inflammatory cytokines that are likely to contribute to MA-ARDS pathogenesis (Mohan et al., 2008). Monocytes and macrophages, with or without ingested Hz, were found sequestered in the lung tissue in both humans (Duarte et al., 1985; Valecha et al., 2009; Lacerda et al., 2012) and mice (Van den Steen et al., 2010; Hee et al., 2011). Hz is shown to be involved in the pathogenesis of MA-ARDS through inflammasome activation in the monocytes/macrophages, thus releasing IL-1β and IL-18 (Dolinay et al., 2012), and causes M1 polarization of activated macrophages that produces pro-inflammatory cytokines (TNF-α, IL-6) (Mills et al., 2000). Hz-containing iRBC were frequently observed in congested small vessels in the lungs of PbA-and PbNK65-infected mice (Deroost et al., 2013). Deroost et al. demonstrated that injection of PfHz into *Plasmodium*-free mice (absence of *Plasmodium* infection), induced pulmonary expression of chemokines (IP-10/CXCL10, MCP-1/CCL2, KC), cytokines (IL-1ß, IL-6, IL-10, TNF, TGF-β), and inflammatory mediators (iNOS, NOX2, Hmox1, ICAM-1), that are associated with alveolar edema (Deroost et al., 2013). During lung injury, recruitment of monocytes/macrophages expressing $CCR2^{+}$ (Hartl et al., 2005), was shown to be MCP-1/CCL2-dependent. In CCR2-deficient mice, PbA infection induces a marginal increase in the lung edema of PbA-infected CCR2-deficient mice (Lagasse et al., 2016), and with PbNK65 infection no improvement in survival was reported (Galvao-Filho et al., 2019), compared to wild-type (WT) mice. Moreover, in this same study done by Lagasse et al., lung pathology still occurred despite hampered MDM recruitment into the lungs, thus excluding MDM as an important mediator of MA-ARDS (Lagasse et al., 2016). Using antimalarial treatment, it was demonstrated that despite monocytes being retained in the bone marrow of CCR2-deficient mice, there was no effect on the development and resolution of MA-ARDS. On the other hand, CCR2 is needed to re-establish the homeostasis of pulmonary leukocytes during recovery (Pollenus et al., 2020).

In the lung, there are two main types of macrophages (1) alveolar macrophages (AMs), located at the air-tissue interface and are the predominant cells present in the alveolus; (2) interstitial macrophages (IMs), located in the space between the alveolar epithelium and vascular endothelium (Schneberger et al., 2011). AMs, also known as tissue-resident macrophages, are the second line of defense against pathogens. Upon infection, these cells undergo a remodelling process, expressing MHC-II on their surface (Guillon et al., 2020). During the earlier stages of MA-ARDS, there are little evidences of AMs activation and proliferation in response to parasite sequestration in the pulmonary vasculature (Lagasse et al., 2016). Recently, Goggi et al. observed that starting on 6 dpi and peaking on 7 dpi, there is an increase in inflammatory macrophages and AMs expressing MHC-II in the lung of PbA-infected C57BL/6 mice. Moreover, using PET imaging, the group

observed that the increase in both populations correlated with the retention of [^{18}F]FEPPA uptake, a PET radioligand developed to target the 18-kDa translocator protein (TSPO) overexpressed in activated macrophages (Goggi et al., 2021). Although several studies have suggested the role of monocytes and macrophages in the pathogenesis of MA-ARDS, more studies are required to uncover whether these immune cells subset could augment the trafficking of other subsets to the lung to induce injury.

4.4.2 Neutrophils

Neutrophils are important for the pathophysiology of various lung injuries (Abraham, 2003). Migration and adhesion to the lung alveoli by neutrophils are strategic to begin the inflammatory process (Reid and Donnelly, 1996). In murine models of ARDS, neutrophils can control endothelial barrier function either by adhering on the endothelial cells or by secretion of their compounds (Ma et al., 2019). Neutrophil adhesion to endothelial cells increases Src phosphorylation of caveolin 1 (through ICAM-1 signaling), forming caveolae's and augmenting transcellular permeability in the lung, thus contributing to edema formation (Hu et al., 2008). Neutrophils discharge (from extracellular vesicles or granular contents) or neutrophils extracellular traps (NETs), can also increase paracellular permeability, promoting gap formation by cytoskeleton contraction, junction disruption, focal adhesion reorganization, and glycocalyx degradation. This secretion-dependent mechanism occurs after the release of ROS, metalloproteinases, elastase, S100A8, S100A9, MPO, cathepsin G, and inflammatory mediators (Ma et al., 2019).

Neutrophils (with or without) phagocytosed Hz are frequently observed in alveolar and interstitial space in the lung with *Plasmodium* infection, associated with iRBCs, monocytes and lymphocytes (MacPherson et al., 1985; Taylor et al., 2012). Although the role of neutrophils in malaria has long been neglected, studies have recently reported both protective and pathogenic functions. Ampawong et al. have identified elastase and neutrophils in the lung of Southeast Asian patients with severe *P. falciparum*, with or without pulmonary edema (Ampawong et al., 2015). On the other hand, neutrophils (identified by the CD15 marker) were detected in lung sections from deceased Brazilian patients infected by *P. vivax* (Lacerda et al., 2012). In murine models, several studies have reported elevated neutrophils in the BALF of PbA-infected DBA/2 mice on 7 dpi (Sercundes et al., 2016), or PbA-infected C57BL/6 mice on 7-8 dpi (Van den Steen et al., 2010), and PbNK65-infected C57BL/6 mice on 10 dpi (Van den Steen et al., 2010). However, findings by Claser et al. reported no significant difference in neutrophil numbers in the lung tissue of PbA-infected C57BL/6 mice on 7dpi (Claser et al., 2019). In PbA-infected DBA/2 mice, neutrophils was shown to be essential to the pathogenesis of ARDS-developing mice releasing ROS, myeloperoxidase (MPO), as well as NETs (Sercundes et al., 2016), an important mechanism to capture and kill parasite outside the cell. In this same study, the authors demonstrated that the increase in mouse survival and decreased MA-ARDS development was possible when neutrophils were depleted with AMD3100 (CXCR4 antagonist), NET formation was blocked with Sivelestat (inhibitor of neutrophil elastase) and NETs were destroyed with Pulmozyme (human recombinant DNase) (Sercundes et al., 2016). Upon neutrophils adhesion to the endothelial cells, ROS and proteases are released, leading to the necrosis of endothelial cells and, thus increasing pulmonary vascular permeability as shown in other experimental system (Ma et al., 2019). In addition, extracellular heme-induced NETs formation, followed by its disintegration (by plasma DNase I), activates the endothelial cells and, consequently enables iRBCs sequestration, contributing to disease severity (Knackstedt et al., 2019).

4.4.3 T Cells

During MA-ARDS, lymphocytes (T cells) are recruited in and around the pulmonary vasculature of patients and mouse models. These cells are also capable of secreting cytokines (TNF-α, IFN-γ, IL-1) that enhance the local inflammatory response leading to endothelial dysfunctions (Chang et al., 2001). Among $CD3^+$ lymphocytes, $CD8^+$T cells were demonstrated to be the main effector cells of MA-ARDS in PbA-infected C57BL/6 mice (Claser et al., 2019). Furthermore, it was shown that during infection, lung endothelial cellsactivated by IFN-γ produced systemically, acquires the capacity to capture, process and cross-present the PbA parasite antigen to parasite-specific $CD8^+$T cells (Claser et al., 2019). Depletion of $CD8^+$T cells with monoclonal antibody significantly reduced pulmonary vascular leakage, alveolar edema, and leukocyte infiltration in infected mice (Chang et al., 2001; Van den Steen et al., 2010; Pham et al., 2017; Claser et al., 2019). Moreover, in the absence of $CD8^+$ T cells, parasite density was shown to be decreased in the lung of PbA-infected C57BL/6 mice on 7 dpi. In addition, tight junction protein *zonula occludens*-1 (ZO-1) expression on the lung epithelium was also significantly maintained (Claser et al., 2019). Vascular permeability factors, such as VEGF-A and placental growth factor (PIGF), were found reduced in the lung of PbNK65-infected C57BL/6 mice depleted of $CD8^+$T cells (Pham et al., 2017). Treatment with dexamethasone decreased $CD8^+$T cells and macrophages in the lung of PbNK65-infected C57BL/6 mice, conferring sufficient protection from MA-ARDS (Van den Steen et al., 2010). Galvão-Filho et al. demonstrated that IFN-γ produced by $CD8^+$T cells was required for inducing the differentiation of TNF-a/iNOS-producing monocyte-derived dendritic cells in the lung, and for the development of MA-ARDS in PbNK65-infected C57BL/6 mice (Galvao-Filho et al., 2019). This finding suggested that infiltrating monocytes and dendritic cells could augment $CD8^+$T cells migration and cytotoxicity leading to lung injury (Yeo et al., 2008).

Besides the conventional T cells that express $CD4^+$ or $CD8^+$, there is a minor population of innate lymphocytes, known as gamma delta T cells (γδ T cells), that are also found in the lung during MA-ARDS (Wei et al., 2021). These cells are known to respond to antigen without presentation (Lawand et al., 2017). Using γδ T cells-deficient mice infected with *P. yoelii*, lung injury still ensued despite the decrease in absolute number of total $CD3^+$ cells including, $CD4^+$ and $CD8^+$T cells. On the other hand, the percentage of IFN-γ-expressing $CD3^+$ and $CD8^+$ cells were higher in infected- γδ T deficient mice compared to WT mice

(Wei et al., 2021). Even though γδ T cells contribute to T cell immune response in the lung of *Plasmodium*-infected mice, further studies are needed to understand their role in MA-ARDS development.

4.5 Platelets

Platelets are anucleated cells traditionally known for their role in thrombosis and hemostasis. In the last few decades, these cells were shown to play a dual role in the pathogenesis of *Plasmodium* infection, by preventing the exponential growth of parasitemia in the early stage, and promoting enhanced immune responses in the later stage (Srivastava, 2014). Platelets were also associated with the pathogenesis and progression of MA-ARDS, because upon its activation, they release various inflammatory mediators (von Willebrand factor, PF4/CXCL4, RANTES/CCL5) that activate neutrophils, monocytes, macrophages, leukocytes, and endothelial cells, leading to pulmonary endothelial damage (Vieira-de-Abreu et al., 2012; Srivastava, 2014; de Azevedo-Quintanilha et al., 2020).

During *Plasmodium* infection, platelets can bind to non-infected and iRBCs and form agglutinates. The interaction between the platelet and iRBCs is mediated through CD31/PECAM-1 and CD36 expressed on platelets with PfEMP-1 expressed on iRBCs (Pain et al., 2001). Platelets also can act as an adhesive bridge between *P. falciparum*-iRBCs and activated endothelial cells (Wassmer et al., 2004). Studies done either *in vitro* using human platelets or in *Plasmodium*-infected mice depleted of platelets demonstrated that platelets are responsible for the killing of iRBCs, a mechanism involving platelet factor 4 (PF4/CXCL4) (McMorran et al., 2009; McMorran et al., 2012). PF4 is a chemokine released from intracellular granules upon platelet activation and has been found highly elevated in malaria patients and mouse models (Srivastava et al., 2008). PF4 was shown to engage the Duffy antigen receptor expressed on iRBCs, inducing the disruption of parasite digestive vacuole without lysing the iRBCs (McMorran et al., 2012), and to bind to $CXCR3^{+}$-expressing cells (monocytes, macrophages, leukocytes), thus being responsible for their activation and attachment to the endothelium (Srivastava, 2014).

Besides iRBCs, platelets can interact with neutrophils and leukocytes. When the receptor P2Y1 is stimulated on platelets, RhoA pathway is activated, resulting in platelet-leukocyte aggregation, followed by migration to the lung and finally binding to the pulmonary endothelium (Amison et al., 2015). The leukocyte-endothelium interaction is further enhanced by microparticles released by the platelets, which stimulates the neutrophils to upregulate their αM integrin expression, allowing its adhesion to LMVECs *via* ICAM-1 (Xie et al., 2015). The interaction between platelets-neutrophils and platelets-leukocytes, results in the activation of leukocytes and neutrophils, contributing to MA-ARDS pathogenesis (Srivastava, 2014). Platelets are also known to have the capacity to activate the classical and alternative pathway of the complement system. As a result of this activation, there is an increase in the inflammatory mediators, such as C3a and C5a, resulting in neutrophil activation thus leading to pulmonary capillary and alveoli damage (Peerschke et al., 2010; Bosmann and Ward, 2012). Using PbA-infected mice, Piguet et al. observed that when the platelet activation was hindered, the leukocyte adhesion to the lung vasculature was decreased (Piguet et al., 2000). Moreover, they also demonstrated that during PbA-infection, the sequestration of platelets in the lung is dependent on urokinase-type plasminogen activator (uPA). In uPA receptor deficient mice infected with PbA, had a prolonged survival with no difference in pulmonary permeability compared to WT mice (Piguet et al., 2000). Recently, another group demonstrated that PbA-infected Nbeal2-deficient mice, which have less platelets, were protected from pulmonary vascular permeability compared to control mice (Darling et al., 2020). Platelet-activating factor (PAF), another mediator of inflammation, is involved in the recruitment and activation of leukocytes, release of cytokines and chemokines, and vascular permeability factor (Chao and Olson, 1993). The role of PAF in the pathogenesis of pulmonary damage was demonstrated in PbA-infected platelet-activating factor receptor (PAFR)-deficient mice. These mice had decreased lung damage characterized by lesser infiltration of neutrophils, macrophages and $CD8^{+}$T cells in the alveolar space (Lacerda-Queiroz et al., 2013).

Platelets are involved in thrombo-inflammation during malaria infection. Thrombocytopenia is a complication observed in infected patients (predominantly with *vivax* or *falciparum* infection) (Lacerda et al., 2011; Bakhubaira, 2013) and mouse models (de Azevedo-Quintanilha et al., 2020), and has been correlated with increase parasite density and disease severity (Gerardin et al., 2002; Ladhani et al., 2002). The mechanism of platelet clearance observed during thrombocytopenia has been widely studied and is still being debated. Some studies have suggested that it is associated with platelet activation (Lacerda et al., 2011; Sharron et al., 2012), followed by platelet adhesion to the endothelium, resulting in endothelial cell activation causing the release of VWF, and hetero-aggregates of platelet and leukocytes (de Azevedo-Quintanilha et al., 2020). When the endothelium is activated, coagulation related proteins are released, such as thrombomodulin and its ligand, thrombin, leading to platelet consumption (Thachil, 2017). On the other hand, Mast et al. demonstrated that thrombocytopenia could happen in the absence of platelet activation or disseminated intravascular coagulation (de Mast et al., 2010). Treatment with heme oxyganese-1 inducer cobalt protoporphyrin IX (CoPPIX) reduced thrombocytopenia and decreased inflammatory infiltrate in the lung parenchyma in PbNK65-infected mice (de Azevedo-Quintanilha et al., 2020). Although a few studies have been conducted to understand the role of platelets in the MA-ARDS pathogenesis, great caution must be taken in platelet-targeted therapeutic treatment. Anti-platelet treatment is highly discouraged in malaria patients with thrombocytopenia. Instead, it was proposed that treatment should target the platelet-leukocytes and platelet-neutrophils interactions (Srivastava, 2014).

5 CONCLUSION

In this review, we draw attention to the importance of using animal models to understand how inflammatory responses and the endothelial activation during MA-ARDS can orchestrate endothelial dysfunction, leading to increase vascular permeability

and disease development. Several mouse MA-ARDS models have been developed and infection of knockout mice have been used to better understand the mechanisms involved in the pathogenesis of MA-ARDS. In the last few years, sophisticated imaging procedures such as SPECT/CT, MRI and PET scans conducted in mice (particularly in the conscious state), have helped to precisely assess early onset of MA-ARDS and track the disease progression. Gaining knowledge is imperative to provide the mechanistic basis and targets to develop adjunct therapies, which are currently unavailable. Although much has been done to uncover the immune responses and mechanisms underlying MA-ARDS pathogenesis, more remains to be done to understand how these responses can be modulated, potentially translating into viable treatments. It is clear that animal models of MA-ARDS are pivotal for the development of methods and tools for early diagnosis to assess and predict the severity of disease and guide the development of therapeutic approaches.

AUTHOR CONTRIBUTIONS

CC conceptualized the review. JD, SN, SE, CC, and LR wrote the draft. All authors contributed to the article and approved the submitted version.

FUNDING

CC was financially supported by 2018/24470-0 grant from the São Paulo Research Foundation (FAPESP). JD was supported by Coordination for the Improvement of higher Education Personnel (Coordenação de Aperfeiçoamento de Pessoal de Nível Superior: CAPES, Brazil) fellowship. SE was supported by 2020/03163-1 from the São Paulo Research Foundation (FAPESP) and 304033/2021-9 from National Council for Scientific and Technological Development (Conselho Nacional de Desenvolvimento Científico e Tecnológico: CNPq, Brazil). LR was supported by Agency for Science, Technology and Research (A*STAR) to a core grant to A*STAR ID labs and a Starting University grant from the Lee Kong Chian School of Medicine, Nanyang Technology University. SN was supported by a postgraduate scholarship from the Yong Loo Lin School of Medicine, National University of Singapore.

ACKNOWLEDGMENTS

The authors would like to thank Daniela Deboni from Laboratory of Malaria Cellular and Molecular Immunopathology for providing the photos used in this review.

REFERENCES

Abraham, E. (2003). Neutrophils and Acute Lung Injury. *Crit. Care Med.* 31 (4 Suppl), S195–S199. doi: 10.1097/01.CCM.0000057843.47705.E8

Aitken, E. H., Negri, E. M., Barboza, R., Lima, M. R., Alvarez, J. M., Marinho, C. R., et al. (2014). Ultrastructure of the Lung in a Murine Model of Malaria-Associated Acute Lung Injury/Acute Respiratory Distress Syndrome. *Malar. J.* 13, 230. doi: 10.1186/1475-2875-13-230

Amison, R. T., Momi, S., Morris, A., Manni, G., Keir, S., Gresele, P., et al. (2015). RhoA Signaling Through Platelet P2Y(1) Receptor Controls Leukocyte Recruitment in Allergic Mice. *J. Allergy Clin. Immunol.* 135 (2), 528–538. doi: 10.1016/j.jaci.2014.09.032

Ampawong, S., Chaisri, U., Viriyavejakul, P., Prapansilp, P., Grau, G. E., Turner, G. D., et al. (2015). A Potential Role for Interleukin-33 and Gamma-Epithelium Sodium Channel in the Pathogenesis of Human Malaria Associated Lung Injury. *Malar. J.* 14, 389. doi: 10.1186/s12936-015-0922-x

Andrade, B. B., Reis-Filho, A., Souza-Neto, S. M., Clarencio, J., Camargo, L. M., Barral, A., et al. (2010). Severe Plasmodium Vivax Malaria Exhibits Marked Inflammatory Imbalance. *Malar. J.* 9, 13. doi: 10.1186/1475-2875-9-13

Anidi, I. U., Servinsky, L. E., Rentsendorj, O., Stephens, R. S., Scott, A. L., and Pearse, D. B. (2013). CD36 and Fyn Kinase Mediate Malaria-Induced Lung Endothelial Barrier Dysfunction in Mice Infected With Plasmodium Berghei. *PloS One* 8 (8), e71010. doi: 10.1371/journal.pone.0071010

Anstey, N. M., Handojo, T., Pain, M. C., Kenangalem, E., Tjitra, E., Price, R. N., et al. (2007). Lung Injury in Vivax Malaria: Pathophysiological Evidence for Pulmonary Vascular Sequestration and Posttreatment Alveolar-Capillary Inflammation. *J. Infect. Dis.* 195 (4), 589–596. doi: 10.1086/510756

Anstey, N. M., Jacups, S. P., Cain, T., Pearson, T., Ziesing, P. J., Fisher, D. A., et al. (2002). Pulmonary Manifestations of Uncomplicated Falciparum and Vivax Malaria: Cough, Small Airways Obstruction, Impaired Gas Transfer, and Increased Pulmonary Phagocytic Activity. *J. Infect. Dis.* 185 (9), 1326–1334. doi: 10.1086/339885

Armah, H. B., Wilson, N. O., Sarfo, B. Y., Powell, M. D., Bond, V. C., Anderson, W., et al. (2007). Cerebrospinal Fluid and Serum Biomarkers of Cerebral Malaria Mortality in Ghanaian Children. *Malar. J.* 6, 147. doi: 10.1186/1475-2875-6-147

Avril, M., Bernabeu, M., Benjamin, M., Brazier, A. J., and Smith, J. D. (2016). Interaction Between Endothelial Protein C Receptor and Intercellular Adhesion Molecule 1 to Mediate Binding of Plasmodium Falciparum-Infected Erythrocytes to Endothelial Cells. *mBio* 7 (4), 1–10. doi: 10.1128/mBio.00615-16

Bachofen, M., and Weibel, E. R. (1977). Alterations of the Gas Exchange Apparatus in Adult Respiratory Insufficiency Associated With Septicemia. *Am. Rev. Respir. Dis.* 116 (4), 589–615. doi: 10.1164/arrd.1977.116.4.589

Bafort, J., and Timperman, G. (1969). Comparative Study of a Generation of Mice Resistant to Plasmodium Berghei. *Z. Tropenmed. Parasitol.* 20 (1), 74–80.

Bakhubaira, S. (2013). Hematological Parameters in Severe Complicated Plasmodium Falciparum Malaria Among Adults in Aden. *Turk J. Haematol.* 30 (4), 394–399. doi: 10.4274/Tjh.2012.0086

Barber, B. E., William, T., Grigg, M. J., Menon, J., Auburn, S., Marfurt, J., et al. (2013). A Prospective Comparative Study of Knowlesi, Falciparum, and Vivax Malaria in Sabah, Malaysia: High Proportion With Severe Disease From Plasmodium Knowlesi and Plasmodium Vivax But No Mortality With Early Referral and Artesunate Therapy. *Clin. Infect. Dis.* 56 (3), 383–397. doi: 10.1093/cid/cis902

Bartoloni, A., and Zammarchi, L. (2012). Clinical Aspects of Uncomplicated and Severe Malaria. *Mediterr. J. Hematol. Infect. Dis.* 4 (1), e2012026. doi: 10.4084/MJHID.2012.026

Beckers, C. M., van Hinsbergh, V. W., and van Nieuw Amerongen, G. P. (2010). Driving Rho GTPase Activity in Endothelial Cells Regulates Barrier Integrity. *Thromb. Haemost.* 103 (1), 40–55. doi: 10.1160/TH09-06-0403

Belnoue, E., Potter, S. M., Rosa, D. S., Mauduit, M., Gruner, A. C., Kayibanda, M., et al. (2008). Control of Pathogenic CD8+ T Cell Migration to the Brain by IFN-Gamma During Experimental Cerebral Malaria. *Parasite Immunol.* 30 (10), 544–553. doi: 10.1111/j.1365-3024.2008.01053.x

Bernabeu, M., Lopez, F. J., Ferrer, M., Martin-Jaular, L., Razaname, A., Corradin, G., et al. (2012). Functional Analysis of Plasmodium Vivax VIR Proteins Reveals Different Subcellular Localizations and Cytoadherence to the ICAM-1 Endothelial Receptor. *Cell Microbiol.* 14 (3), 386–400. doi: 10.1111/j.1462-5822.2011.01726.x

Bosmann, M., and Ward, P. A. (2012). Role of C3, C5 and Anaphylatoxin Receptors in Acute Lung Injury and in Sepsis. *Adv. Exp. Med. Biol.* 946, 147–159. doi: 10.1007/978-1-4614-0106-3_9

Brasil, P., Zalis, M. G., de Pina-Costa, A., Siqueira, A. M., Junior, C. B., Silva, S., et al. (2017). Outbreak of Human Malaria Caused by Plasmodium Simium in the Atlantic Forest in Rio De Janeiro: A Molecular Epidemiological Investigation. *Lancet Glob. Health* 5 (10), e1038–e1046. doi: 10.1016/S2214-109X(17)30333-9

Butt, Y., Kurdowska, A., and Allen, T. C. (2016). Acute Lung Injury: A Clinical and Molecular Review. *Arch. Pathol. Lab. Med.* 140 (4), 345–350. doi: 10.5858/arpa.2015-0519-RA

Carvalho, L. J., Lenzi, H. L., Pelajo-Machado, M., Oliveira, D. N., Daniel-Ribeiro, C. T., Ferreira-da-Cruz, M. F., et al. (2000). Plasmodium berghei: Cerebral Malaria in CBA Mice Is Not Clearly Related to Plasma TNF Levels or Intensity of Histopathological Changes. *Exp. Parasitol.* 95 (1), 1–7. doi: 10.1006/expr.2000.4508

Carvalho, B. O., Lopes, S. C., Nogueira, P. A., Orlandi, P. P., Bargieri, D. Y., Blanco, Y. C., et al. (2010). On the Cytoadhesion of Plasmodium Vivax-Infected Erythrocytes. *J. Infect. Dis.* 202 (4), 638–647. doi: 10.1086/654815

Chang, W. L., Jones, S. P., Lefer, D. J., Welbourne, T., Sun, G., Yin, L., et al. (2001). CD8(+)-T-Cell Depletion Ameliorates Circulatory Shock in Plasmodium Berghei-Infected Mice. *Infect. Immun.* 69 (12), 7341–7348. doi: 10.1128/IAI.69.12.7341-7348.2001

Chao, W., and Olson, M. S. (1993). Platelet-Activating Factor: Receptors and Signal Transduction. *Biochem. J.* 292 (Pt 3), 617–629. doi: 10.1042/bj2920617

Claesson-Welsh, L. (2015). Vascular Permeability–the Essentials. *Ups J. Med. Sci.* 120 (3), 135–143. doi: 10.3109/03009734.2015.1064501

Claser, C., Malleret, B., Peng, K., Bakocevic, N., Gun, S. Y., Russell, B., et al. (2014). Rodent Plasmodium-Infected Red Blood Cells: Imaging Their Fates and Interactions Within Their Hosts. *Parasitol. Int.* 63 (1), 187–194. doi: 10.1016/j.parint.2013.07.012

Claser, C., Nguee, S. Y. T., Balachander, A., Wu Howland, S., Becht, E., Gunasegaran, B., et al. (2019). Lung Endothelial Cell Antigen Cross-Presentation to CD8(+)T Cells Drives Malaria-Associated Lung Injury. *Nat. Commun.* 10 (1), 4241. doi: 10.1038/s41467-019-12017-8

Combes, V., Rosenkranz, A. R., Redard, M., Pizzolato, G., Lepidi, H., Vestweber, D., et al. (2004). Pathogenic Role of P-Selectin in Experimental Cerebral Malaria: Importance of the Endothelial Compartment. *Am. J. Pathol.* 164 (3), 781–786. doi: 10.1016/S0002-9440(10)63166-5

Cox-Singh, J., Singh, B., Daneshvar, C., Planche, T., Parker-Williams, J., and Krishna, S. (2011). Anti-Inflammatory Cytokines Predominate in Acute Human Plasmodium Knowlesi Infections. *PloS One* 6 (6), e20541. doi: 10.1371/journal.pone.0020541

Craig, A. G., Khairul, M. F., and Patil, P. R. (2012). Cytoadherence and Severe Malaria. *Malays J. Med. Sci.* 19 (2), 5–18.

Daneshvar, C., Davis, T. M., Cox-Singh, J., Rafa'ee, M. Z., Zakaria, S. K., Divis, P. C., et al. (2009). Clinical and Laboratory Features of Human Plasmodium Knowlesi Infection. *Clin. Infect. Dis.* 49 (6), 852–860. doi: 10.1086/605439

Darling, T. K., Schenk, M. P., Zhou, C. C., Maloba, F. M., Mimche, P. N., Gibbins, J. M., et al. (2020). Platelet Alpha-Granules Contribute to Organ-Specific Pathologies in a Mouse Model of Severe Malaria. *Blood Adv.* 4 (1), 1–8. doi: 10.1182/bloodadvances.2019000773

David, P. H., Hommel, M., Miller, L. H., Udeinya, I. J., and Oligino, L. D. (1983). Parasite Sequestration in Plasmodium Falciparum Malaria: Spleen and Antibody Modulation of Cytoadherence of Infected Erythrocytes. *Proc. Natl. Acad. Sci. U. S. A.* 80 (16), 5075–5079. doi: 10.1073/pnas.80.16.5075

Day, N. P., Hien, T. T., Schollaardt, T., Loc, P. P., Chuong, L. V., Chau, T. T., et al. (1999). The Prognostic and Pathophysiologic Role of Pro- and Antiinflammatory Cytokines in Severe Malaria. *J. Infect. Dis.* 180 (4), 1288–1297. doi: 10.1086/315016

de Azevedo-Quintanilha, I. G., Medeiros-de-Moraes, I. M., Ferreira, A. C., Reis, P. A., Vieira-de-Abreu, A., Campbell, R. A., et al. (2020). Haem Oxygenase Protects Against Thrombocytopaenia and Malaria-Associated Lung Injury. *Malar. J.* 19 (1), 234. doi: 10.1186/s12936-020-03305-6

de Azevedo-Quintanilha, I. G., Vieira-de-Abreu, A., Ferreira, A. C., Nascimento, D. O., Siqueira, A. M., Campbell, R. A., et al. (2016). Integrin AlphaDbeta2 (CD11d/CD18) Mediates Experimental Malaria-Associated Acute Respiratory Distress Syndrome (MA-ARDS). *Malar. J.* 15 (1), 393. doi: 10.1186/s12936-016-1447-7

Dejana, E., Bazzoni, G., and Lampugnani, M. G. (1999). Vascular Endothelial (VE)-Cadherin: Only an Intercellular Glue? *Exp. Cell Res.* 252 (1), 13–19. doi: 10.1006/excr.1999.4601

de Jong, G. M., Slager, J. J., Verbon, A., van Hellemond, J. J., and van Genderen, P. J. (2016). Systematic Review of the Role of Angiopoietin-1 and Angiopoietin-2 in Plasmodium Species Infections: Biomarkers or Therapeutic Targets? *Malar. J.* 15 (1), 581. doi: 10.1186/s12936-016-1624-8

del Portillo, H. A., Fernandez-Becerra, C., Bowman, S., Oliver, K., Preuss, M., Sanchez, C. P., et al. (2001). A Superfamily of Variant Genes Encoded in the Subtelomeric Region of Plasmodium Vivax. *Nature* 410 (6830), 839–842. doi: 10.1038/35071118

de Mast, Q., de Groot, P. G., van Heerde, W. L., Roestenberg, M., van Velzen, J. F., Verbruggen, B., et al. (2010). Thrombocytopenia in Early Malaria Is Associated With GP1b Shedding in Absence of Systemic Platelet Activation and Consumptive Coagulopathy. *Br. J. Haematol.* 151 (5), 495–503. doi: 10.1111/j.1365-2141.2010.08399.x

De Niz, M., Ullrich, A. K., Heiber, A., Blancke Soares, A., Pick, C., Lyck, R., et al. (2016). The Machinery Underlying Malaria Parasite Virulence Is Conserved Between Rodent and Human Malaria Parasites. *Nat. Commun.* 7, 11659. doi: 10.1038/ncomms11659

Deroost, K., Tyberghein, A., Lays, N., Noppen, S., Schwarzer, E., Vanstreels, E., et al. (2013). Hemozoin Induces Lung Inflammation and Correlates With Malaria-Associated Acute Respiratory Distress Syndrome. *Am. J. Respir. Cell Mol. Biol.* 48 (5), 589–600. doi: 10.1165/rcmb.2012-0450OC

Desowitz, R. S., Miller, L. H., Buchanan, R. D., and Permpanich, B. (1969). The Sites of Deep Vascular Schizogony in Plasmodium Coatneyi Malaria. *Trans. R. Soc. Trop. Med. Hygiene* 63 (2), 198–202. doi: 10.1016/0035-9203(69)90147-3

Dole, V. S., Bergmeier, W., Mitchell, H. A., Eichenberger, S. C., and Wagner, D. D. (2005). Activated Platelets Induce Weibel-Palade-Body Secretion and Leukocyte Rolling *In Vivo*: Role of P-Selectin. *Blood* 106 (7), 2334–2339. doi: 10.1182/blood-2005-04-1530

Dolinay, T., Kim, Y. S., Howrylak, J., Hunninghake, G. M., An, C. H., Fredenburgh, L., et al. (2012). Inflammasome-Regulated Cytokines Are Critical Mediators of Acute Lung Injury. *Am. J. Respir. Crit. Care Med.* 185 (11), 1225–1234. doi: 10.1164/rccm.201201-0003OC

Dos Santos Ortolan, L., Sercundes, M. K., Moura, G. C., de Castro Quirino, T., Debone, D., de Sousa Costa, D., et al. (2019). Endothelial Protein C Receptor Could Contribute to Experimental Malaria-Associated Acute Respiratory Distress Syndrome. *J. Immunol. Res.* 2019, 3105817. doi: 10.1155/2019/3105817

Duarte, M. I., Corbett, C. E., Boulos, M., and Amato Neto, V. (1985). Ultrastructure of the Lung in Falciparum Malaria. *Am. J. Trop. Med. Hyg.* 34 (1), 31–35. doi: 10.4269/ajtmh.1985.34.31

Dzeing-Ella, A., Nze Obiang, P. C., Tchoua, R., Planche, T., Mboza, B., Mbounja, M., et al. (2005). Severe Falciparum Malaria in Gabonese Children: Clinical and Laboratory Features. *Malar. J.* 4, 1. doi: 10.1186/1475-2875-4-1

El-Assaad, F., Wheway, J., Mitchell, A. J., Lou, J., Hunt, N. H., Combes, V., et al. (2013). Cytoadherence of Plasmodium Berghei-Infected Red Blood Cells to Murine Brain and Lung Microvascular Endothelial Cells *In Vitro*. *Infect. Immun.* 81 (11), 3984–3991. doi: 10.1128/IAI.00428-13

Elzein, F., Mohammed, N., Ali, N., Bahloul, A., Albadani, A., and Alsherbeeni, N. (2017). Pulmonary Manifestation of Plasmodium Falciparum Malaria: Case Reports and Review of the Literature. *Respir. Med. Case Rep.* 22, 83–86. doi: 10.1016/j.rmcr.2017.06.014

Engwerda, C., Belnoue, E., Gruner, A. C., and Renia, L. (2005). Experimental Models of Cerebral Malaria. *Curr. Top. Microbiol. Immunol.* 297, 103–143.

Epiphanio, S., Campos, M. G., Pamplona, A., Carapau, D., Pena, A. C., Ataide, R., et al. (2010). VEGF Promotes Malaria-Associated Acute Lung Injury in Mice. *PloS Pathog.* 6 (5), e1000916. doi: 10.1371/journal.ppat.1000916

Esamai, F., Ernerudh, J., Janols, H., Welin, S., Ekerfelt, C., Mining, S., et al. (2003). Cerebral Malaria in Children: Serum and Cerebrospinal Fluid TNF-Alpha and TGF-Beta Levels and Their Relationship to Clinical Outcome. *J. Trop. Pediatr.* 49 (4), 216–223. doi: 10.1093/tropej/49.4.216

Faille, D., Combes, V., Mitchell, A. J., Fontaine, A., Juhan-Vague, I., Alessi, M. C., et al. (2009). Platelet Microparticles: A New Player in Malaria Parasite Cytoadherence to Human Brain Endothelium. *FASEB J.* 23 (10), 3449–3458. doi: 10.1096/fj.09-135822

Fatih, F. A., Siner, A., Ahmed, A., Woon, L. C., Craig, A. G., Singh, B., et al. (2012). Cytoadherence and Virulence - The Case of Plasmodium Knowlesi Malaria. *Malar. J.* 11, 33. doi: 10.1186/1475-2875-11-33

Fauconnier, M., Palomo, J., Bourigault, M. L., Meme, S., Szeremeta, F., Beloeil, J. C., et al. (2012). IL-12Rbeta2 Is Essential for the Development of Experimental Cerebral Malaria. *J. Immunol.* 188 (4), 1905–1914. doi: 10.4049/jimmunol.1101978

Favre, N., Da Laperousaz, C., Ryffel, B., Weiss, N. A., Imhof, B. A., Rudin, W., et al. (1999). Role of ICAM-1 (CD54) in the Development of Murine Cerebral Malaria. *Microbes Infect.* 1 (12), 961–968. doi: 10.1016/s1286-4579(99)80513-9

Fernandez-Becerra, C., Bernabeu, M., Castellanos, A., Correa, B. R., Obadia, T., Ramirez, M., et al. (2020). Plasmodium Vivax Spleen-Dependent Genes Encode Antigens Associated With Cytoadhesion and Clinical Protection. *Proc. Natl. Acad. Sci. U. S. A.* 117 (23), 13056–13065. doi: 10.1073/pnas.1920596117

Fonager, J., Pasini, E. M., Braks, J. A., Klop, O., Ramesar, J., Remarque, E. J., et al. (2012). Reduced CD36-Dependent Tissue Sequestration of Plasmodium-Infected Erythrocytes Is Detrimental to Malaria Parasite Growth *In Vivo*. *J. Exp. Med.* 209 (1), 93–107. doi: 10.1084/jem.20110762

Franke-Fayard, B., Fonager, J., Braks, A., Khan, S. M., and Janse, C. J. (2010). Sequestration and Tissue Accumulation of Human Malaria Parasites: Can We Learn Anything From Rodent Models of Malaria?. *PLoS Pathog.* 6 (9), e1001032. doi: 10.1371/journal.ppat.1001032

Franke-Fayard, B., Janse, C. J., Cunha-Rodrigues, M., Ramesar, J., Buscher, P., Que, I., et al. (2005). Murine Malaria Parasite Sequestration: CD36 Is the Major Receptor, But Cerebral Pathology Is Unlinked to Sequestration. *Proc. Natl. Acad. Sci. U. S. A.* 102 (32), 11468–11473. doi: 10.1073/pnas.0503386102

Fazalul Rahiman, S. S., Basir, R., Talib, H., Tie, T. H., Chuah, Y. K., Jabbarzare, M., et al. (2013). Interleukin-27 Exhibited Anti-Inflammatory Activity During Plasmodium berghei Infection in Mice. *Trop. Biomed.* 30 (4), 663–680

Fu, Y., Ding, Y., Zhou, T. L., Ou, Q. Y., and Xu, W. Y. (2012). Comparative Histopathology of Mice Infected With the 17XL and 17XNL Strains of Plasmodium yoelii. *J. Parasitol.* 98 (2), 310–315. doi: 10.1645/GE-2825.1

Fujita, M., Kuwano, K., Kunitake, R., Hagimoto, N., Miyazaki, H., Kaneko, Y., et al. (1998). Endothelial Cell Apoptosis in Lipopolysaccharide-Induced Lung Injury in Mice. *Int. Arch. Allergy Immunol.* 117 (3), 202–208. doi: 10.1159/000024011

Gallego-Delgado, J., Basu-Roy, U., Ty, M., Alique, M., Fernandez-Arias, C., Movila, A., et al. (2016). Angiotensin Receptors and Beta-Catenin Regulate Brain Endothelial Integrity in Malaria. *J. Clin. Invest.* 126 (10), 4016–4029. doi: 10.1172/JCI87306

Galvao-Filho, B., de Castro, J. T., Figueiredo, M. M., Rosmaninho, C. G., Antonelli, L., and Gazzinelli, R. T. (2019). The Emergence of Pathogenic TNF/iNOS Producing Dendritic Cells (Tip-DCs) in a Malaria Model of Acute Respiratory Distress Syndrome (ARDS) Is Dependent on CCR4. *Mucosal Immunol.* 12 (2), 312–322. doi: 10.1038/s41385-018-0093-5

Gerardin, P., Rogier, C., Ka, A. S., Jouvencel, P., Brousse, V., and Imbert, P. (2002). Prognostic Value of Thrombocytopenia in African Children With Falciparum Malaria. *Am. J. Trop. Med. Hyg.* 66 (6), 686–691. doi: 10.4269/ajtmh.2002.66.686

Gillrie, M. R., Krishnegowda, G., Lee, K., Buret, A. G., Robbins, S. M., Looareesuwan, S., et al. (2007). Src-Family Kinase Dependent Disruption of Endothelial Barrier Function by Plasmodium Falciparum Merozoite Proteins. *Blood* 110 (9), 3426–3435. doi: 10.1182/blood-2007-04-084582

Goggi, J. L., Claser, C., Hartimath, S. V., Hor, P. X., Tan, P. W., Ramasamy, B., et al. (2021). PET Imaging of Translocator Protein as a Marker of Malaria-Associated Lung Inflammation. *Infect. Immun.* 89 (10), e0002421. doi: 10.1128/IAI.00024-21

Graham, S. M., Chen, J., Chung, D. W., Barker, K. R., Conroy, A. L., Hawkes, M. T., et al. (2016). Endothelial Activation, Haemostasis and Thrombosis Biomarkers in Ugandan Children With Severe Malaria Participating in a Clinical Trial. *Malar. J.* 15, 56. doi: 10.1186/s12936-016-1106-z

Grau, G. E., Fajardo, L. F., Piguet, P. F., Allet, B., Lambert, P. H., and Vassalli, P. (1987). Tumor Necrosis Factor (Cachectin) as an Essential Mediator in Murine Cerebral Malaria. *Science* 237 (4819), 1210–1212. doi: 10.1126/science.3306918

Groger, M., Fischer, H. S., Veletzky, L., Lalremruata, A., and Ramharter, M. (2017). A Systematic Review of the Clinical Presentation, Treatment and Relapse Characteristics of Human Plasmodium Ovale Malaria. *Malar. J.* 16 (1), 112. doi: 10.1186/s12936-017-1759-2

Guido, B. C., Zanatelli, M., Tavares-de-Lima, W., Oliani, S. M., and Damazo, A. S. (2013). Annexin-A1 Peptide Down-Regulates the Leukocyte Recruitment and Up-Regulates Interleukin-10 Release Into Lung After Intestinal Ischemia-Reperfusion in Mice. *J. Inflamm. (Lond)* 10 (1), 10. doi: 10.1186/1476-9255-10-10

Guillon, A., Arafa, E. I., Barker, K. A., Belkina, A. C., Martin, I., Shenoy, A. T., et al. (2020). Pneumonia Recovery Reprograms the Alveolar Macrophage Pool. *JCI Insight* 5 (4), 1–20. doi: 10.1172/jci.insight.133042

Gun, S. Y., Claser, C., Tan, K. S., and Renia, L. (2014). Interferons and Interferon Regulatory Factors in Malaria. *Mediators Inflamm.* 2014, 243713. doi: 10.1155/2014/243713

Hansen, D. S., Evans, K. J., D'Ombrain, M. C., Bernard, N. J., Sexton, A. C., Buckingham, L., et al. (2005). The Natural Killer Complex Regulates Severe Malarial Pathogenesis and Influences Acquired Immune Responses to Plasmodium Berghei ANKA. *Infect. Immun.* 73 (4), 2288–2297. doi: 10.1128/IAI.73.4.2288-2297.2005

Hartl, D., Griese, M., Nicolai, T., Zissel, G., Prell, C., Reinhardt, D., et al. (2005). A Role for MCP-1/CCR2 in Interstitial Lung Disease in Children. *Respir. Res.* 6, 93. doi: 10.1186/1465-9921-6-93

Hartmann, S., Ridley, A. J., and Lutz, S. (2015). The Function of Rho-Associated Kinases ROCK1 and ROCK2 in the Pathogenesis of Cardiovascular Disease. *Front. Pharmacol.* 6, 276. doi: 10.3389/fphar.2015.00276

Haydoura, S., Mazboudi, O., Charafeddine, K., Bouakl, I., Baban, T. A., Taher, A. T., et al. (2011). Transfusion-Related Plasmodium Ovale Malaria Complicated by Acute Respiratory Distress Syndrome (ARDS) in a Non-Endemic Country. *Parasitol. Int.* 60 (1), 114–116. doi: 10.1016/j.parint.2010.10.005

Hee, L., Dinudom, A., Mitchell, A. J., Grau, G. E., Cook, D. I., Hunt, N. H., et al. (2011). Reduced Activity of the Epithelial Sodium Channel in Malaria-Induced Pulmonary Oedema in Mice. *Int. J. Parasitol.* 41 (1), 81–88. doi: 10.1016/j.ijpara.2010.07.013

Heil, M., Clauss, M., Suzuki, K., Buschmann, I. R., Willuweit, A., Fischer, S., et al. (2000). Vascular Endothelial Growth Factor (VEGF) Stimulates Monocyte Migration Through Endothelial Monolayers *via* Increased Integrin Expression. *Eur. J. Cell Biol.* 79 (11), 850–857. doi: 10.1078/0171-9335-00113

Henry, B., Roussel, C., Carucci, M., Brousse, V., Ndour, P. A., and Buffet, P. (2020). The Human Spleen in Malaria: Filter or Shelter? *Trends Parasitol.* 36 (5), 435–446. doi: 10.1016/j.pt.2020.03.001

He, Y., Zhang, Y., Wu, H., Luo, J., Cheng, C., and Zhang, H. (2021). The Role of Annexin A1 Peptide in Regulating PI3K/Akt Signaling Pathway to Reduce Lung Injury After Cardiopulmonary Bypass in Rats. *Perfusion* 2676591211052162. doi: 10.1177/02676591211052162

Hu, G., Ye, R. D., Dinauer, M. C., Malik, A. B., and Minshall, R. D. (2008). Neutrophil Caveolin-1 Expression Contributes to Mechanism of Lung Inflammation and Injury. *Am. J. Physiol. Lung Cell Mol. Physiol.* 294 (2), L178–L186. doi: 10.1152/ajplung.00263.2007

Jambou, R., Combes, V., Jambou, M. J., Weksler, B. B., Couraud, P. O., and Grau, G. E. (2010). Plasmodium Falciparum Adhesion on Human Brain Microvascular Endothelial Cells Involves Transmigration-Like Cup Formation and Induces Opening of Intercellular Junctions. *PloS Pathog.* 6 (7), e1001021. doi: 10.1371/journal.ppat.1001021

Janssen, C. S., Phillips, R. S., Turner, C. M., and Barrett, M. P. (2004). Plasmodium Interspersed Repeats: The Major Multigene Superfamily of Malaria Parasites. *Nucleic Acids Res.* 32 (19), 5712–5720. doi: 10.1093/nar/gkh907

Ji, W., Hu, Q., Zhang, M., Zhang, C., Chen, C., Yan, Y., et al. (2021). The Disruption of the Endothelial Barrier Contributes to Acute Lung Injury Induced by Coxsackievirus A2 Infection in Mice. *Int. J. Mol. Sci.* 22 (18), 1–16. doi: 10.3390/ijms22189895

Joyner, J. C.Consortium,T.M, Wood, J. S., Moreno, A., Garcia, A., Galinski, M. R. (2017). Case Report: Severe and Complicated Cynomolgi Malaria in a Rhesus Macaque Resulted in Similar Histopathological Changes as Those Seen in Human Malaria. *Am. J. Trop. Med. Hyg.* 97 (2), 548–555. doi: 10.4269/ajtmh.16-0742

Ju, Y., Qiu, L., Sun, X., Liu, H., and Gao, W. (2021). Ac2-26 Mitigated Acute Respiratory Distress Syndrome Rats *via* Formyl Peptide Receptor Pathway. *Ann. Med.* 53 (1), 653–661. doi: 10.1080/07853890.2021.1925149

Karunaweera, N. D., Grau, G. E., Gamage, P., Carter, R., and Mendis, K. N. (1992). Dynamics of Fever and Serum Levels of Tumor Necrosis Factor Are Closely

Associated During Clinical Paroxysms in Plasmodium Vivax Malaria. *Proc. Natl. Acad. Sci. U. S. A.* 89 (8), 3200–3203. doi: 10.1073/pnas.89.8.3200

Karunaweera, N. D., Wijesekera, S. K., Wanasekera, D., Mendis, K. N., and Carter, R. (2003). The Paroxysm of Plasmodium Vivax Malaria. *Trends Parasitol.* 19 (4), 188–193. doi: 10.1016/s1471-4922(03)00036-9

Kim, H., Higgins, S., Liles, W. C., and Kain, K. C. (2011). Endothelial Activation and Dysregulation in Malaria: A Potential Target for Novel Therapeutics. *Curr. Opin. Hematol.* 18 (3), 177–185. doi: 10.1097/MOH.0b013e328345a4cf

King, T., and Lamb, T. (2015). Interferon-Gamma: The Jekyll and Hyde of Malaria. *PloS Pathog.* 11 (10), e1005118. doi: 10.1371/journal.ppat.1005118

Kingston, H. W. F., Ghose, A., Rungpradubvong, V., Satitthummanid, S., Herdman, M. T., Plewes, K., et al. (2020). Cell-Free Hemoglobin Is Associated With Increased Vascular Resistance and Reduced Peripheral Perfusion in Severe Malaria. *J. Infect. Dis.* 221 (1), 127–137. doi: 10.1093/infdis/jiz359

Kinra, P., and Dutta, V. (2013). Serum TNF Alpha Levels: A Prognostic Marker for Assessment of Severity of Malaria. *Trop. BioMed.* 30 (4), 645–653.

Knackstedt, S. L., Georgiadou, A., Apel, F., Abu-Abed, U., Moxon, C. A., Cunnington, A. J., et al. (2019). Neutrophil Extracellular Traps Drive Inflammatory Pathogenesis in Malaria. *Sci. Immunol.* 4 (40), 1–17. doi: 10.1126/sciimmunol.aaw0336

Kobayashi, T., Tanaka, K., Fujita, T., Umezawa, H., Amano, H., Yoshioka, K., et al. (2015). Bidirectional Role of IL-6 Signal in Pathogenesis of Lung Fibrosis. *Respir. Res.* 16, 99. doi: 10.1186/s12931-015-0261-z

Korir, C. C., and Galinski, M. R. (2006). Proteomic Studies of Plasmodium Knowlesi SICA Variant Antigens Demonstrate Their Relationship With P. Falciparum EMP1. *Infect. Genet. Evol.* 6 (1), 75–79. doi: 10.1016/j.meegid.2005.01.003

Kraisin, S., Verhenne, S., Pham, T. T., Martinod, K., Tersteeg, C., Vandeputte, N., et al. (2019). Von Willebrand Factor in Experimental Malaria-Associated Acute Respiratory Distress Syndrome. *J. Thromb. Haemost.* 17 (8), 1372–1383. doi: 10.1111/jth.14485

Kremsner, P. G., Neifer, S., Chaves, M. F., Rudolph, R., and Bienzle, U. (1992). Interferon-Gamma Induced Lethality in the Late Phase of Plasmodium vinckei Malaria Despite Effective Parasite Clearance by Chloroquine. *Eur. J. Immunol.* 22 (11), 2873–2878. doi: 10.1002/eji.1830221118

Krishnamurthy, V. R., Sardar, M. Y., Ying, Y., Song, X., Haller, C., Dai, E., et al. (2015). Glycopeptide Analogues of PSGL-1 Inhibit P-Selectin *In Vitro* and *In Vivo*. *Nat. Commun.* 6, 6387. doi: 10.1038/ncomms7387

Krishna, S., Waller, D. W., ter Kuile, F., Kwiatkowski, D., Crawley, J., Craddock, C. F., et al. (1994). Lactic Acidosis and Hypoglycaemia in Children With Severe Malaria: Pathophysiological and Prognostic Significance. *Trans. R. Soc. Trop. Med. Hyg.* 88 (1), 67–73. doi: 10.1016/0035-9203(94)90504-5

Lacerda, M. V., Fragoso, S. C., Alecrim, M. G., Alexandre, M. A., Magalhaes, B. M., Siqueira, A. M., et al. (2012). Postmortem Characterization of Patients With Clinical Diagnosis of Plasmodium Vivax Malaria: To What Extent Does This Parasite Kill? *Clin. Infect. Dis.* 55 (8), e67–e74. doi: 10.1093/cid/cis615

Lacerda, M. V., Mourao, M. P., Coelho, H. C., and Santos, J. B. (2011). Thrombocytopenia in Malaria: Who Cares? *Mem. Inst. Oswaldo Cruz* 106 Suppl 1, 52–63. doi: 10.1590/s0074-02762011000900007

Lacerda-Queiroz, N., Rachid, M. A., Teixeira, M. M., and Teixeira, A. L. (2013). The Role of Platelet-Activating Factor Receptor (PAFR) in Lung Pathology During Experimental Malaria. *Int. J. Parasitol.* 43 (1), 11–15. doi: 10.1016/j.ijpara.2012.11.008

Ladhani, S., Lowe, B., Cole, A. O., Kowuondo, K., and Newton, C. R. (2002). Changes in White Blood Cells and Platelets in Children With Falciparum Malaria: Relationship to Disease Outcome. *Br. J. Haematol.* 119 (3), 839–847. doi: 10.1046/j.1365-2141.2002.03904.x

Lagasse, H. A., Anidi, I. U., Craig, J. M., Limjunyawong, N., Poupore, A. K., Mitzner, W., et al. (2016). Recruited Monocytes Modulate Malaria-Induced Lung Injury Through CD36-Mediated Clearance of Sequestered Infected Erythrocytes. *J. Leukoc. Biol.* 99 (5), 659–671. doi: 10.1189/jlb.4HI0315-130RRR

Lalremruata, A., Magris, M., Vivas-Martinez, S., Koehler, M., Esen, M., Kempaiah, P., et al. (2015). Natural Infection of Plasmodium Brasilianum in Humans: Man and Monkey Share Quartan Malaria Parasites in the Venezuelan Amazon. *EBioMedicine* 2 (9), 1186–1192. doi: 10.1016/j.ebiom.2015.07.033

Lawand, M., Dechanet-Merville, J., and Dieu-Nosjean, M. C. (2017). Key Features of Gamma-Delta T-Cell Subsets in Human Diseases and Their Immunotherapeutic Implications. *Front. Immunol.* 8, 761. doi: 10.3389/fimmu.2017.00761

Lee, W. C., Russell, B., and Renia, L. (2019). Sticking for a Cause: The Falciparum Malaria Parasites Cytoadherence Paradigm. *Front. Immunol.* 10, 1444. doi: 10.3389/fimmu.2019.01444

Lee, W. C., Shahari, S., Nguee, S. Y. T., Lau, Y. L., and Renia, L. (2021). Cytoadherence Properties of Plasmodium Knowlesi-Infected Erythrocytes. *Front. Microbiol.* 12, 4417. doi: 10.3389/fmicb.2021.804417

Le, T. T., Karmouty-Quintana, H., Melicoff, E., Le, T. T., Weng, T., Chen, N. Y., et al. (2014). Blockade of IL-6 Trans Signaling Attenuates Pulmonary Fibrosis. *J. Immunol.* 193 (7), 3755–3768. doi: 10.4049/jimmunol.1302470

Li, J., Chang, W. L., Sun, G., Chen, H. L., Specian, R. D., Berney, S. M., et al. (2003). Intercellular Adhesion Molecule 1 Is Important for the Development of Severe Experimental Malaria But Is Not Required for Leukocyte Adhesion in the Brain. *J. Investig. Med.* 51 (3), 128–140. doi: 10.1136/jim-51-03-15

Liew, J. W. K., Bukhari, F. D. M., Jeyaprakasam, N. K., Phang, W. K., Vythilingam, I., and Lau, Y. L. (2021). Natural Plasmodium Inui Infections in Humans and Anopheles Cracens Mosquito, Malaysia. *Emerg. Infect. Dis.* 27 (10), 2700–2703. doi: 10.3201/eid2710.210412

Lin, J. W., Sodenkamp, J., Cunningham, D., Deroost, K., Tshitenge, T. C., McLaughlin, S., et al. (2017). Signatures of Malaria-Associated Pathology Revealed by High-Resolution Whole-Blood Transcriptomics in a Rodent Model of Malaria. *Sci. Rep.* 7, 41722. doi: 10.1038/srep41722

Liu, M., Amodu, A. S., Pitts, S., Patrickson, J., Hibbert, J. M., Battle, M., et al. (2012). Heme Mediated STAT3 Activation in Severe Malaria. *PloS One* 7 (3), e34280. doi: 10.1371/journal.pone.0034280

Liu, M., Gu, C., and Wang, Y. (2014). Upregulation of the Tight Junction Protein Occludin: Effects on Ventilation-Induced Lung Injury and Mechanisms of Action. *BMC Pulm. Med.* 14, 94. doi: 10.1186/1471-2466-14-94

Lopes, S. C., Albrecht, L., Carvalho, B. O., Siqueira, A. M., Thomson-Luque, R., Nogueira, P. A., et al. (2014). Paucity of Plasmodium Vivax Mature Schizonts in Peripheral Blood Is Associated With Their Increased Cytoadhesive Potential. *J. Infect. Dis.* 209 (9), 1403–1407. doi: 10.1093/infdis/jiu018

Lovegrove, F. E., Gharib, S. A., Pena-Castillo, L., Patel, S. N., Ruzinski, J. T., Hughes, T. R., et al. (2008). Parasite Burden and CD36-Mediated Sequestration Are Determinants of Acute Lung Injury in an Experimental Malaria Model. *PloS Pathog.* 4 (5), e1000068. doi: 10.1371/journal.ppat.1000068

Lozano, F., Leal, M., Lissen, E., Munoz, J., Bautista, A., and Regordan, C. (1983). [P. Falciparum and P. Malariae Malaria Complicated by Pulmonary Edema With Disseminated Intravascular Coagulation]. *Presse Med.* 12 (47), 3004–3005.

MacCallum, D. K. (1968). Pulmonary Changes Resulting From Experimental Malaria Infection in Hamsters. *Arch. Pathol.* 86 (6), 681–688.

MacCallum, D. K. (1969). A Study of Macrophage–Pulmonary Vascular Bed Interactions in Malaria-Infected Hamsters. *J. Reticuloendothel. Soc.* 6 (3), 253–270.

MacPherson, G. G., Warrell, M. J., White, N. J., Looareesuwan, S., and Warrell, D. A. (1985). Human Cerebral Malaria. A Quantitative Ultrastructural Analysis of Parasitized Erythrocyte Sequestration. *Am. J. Pathol.* 119 (3), 385–401.

Maguire, G. P., Handojo, T., Pain, M. C., Kenangalem, E., Price, R. N., Tjitra, E., et al. (2005). Lung Injury in Uncomplicated and Severe Falciparum Malaria: A Longitudinal Study in Papua, Indonesia. *J. Infect. Dis.* 192 (11), 1966–1974. doi: 10.1086/497697

Maknitikul, S., Luplertlop, N., Grau, G. E. R., and Ampawong, S. (2017). Dysregulation of Pulmonary Endothelial Protein C Receptor and Thrombomodulin in Severe Falciparum Malaria-Associated ARDS Relevant to Hemozoin. *PloS One* 12 (7), e0181674. doi: 10.1371/journal.pone.0181674

Mandala, W. L., Msefula, C. L., Gondwe, E. N., Drayson, M. T., Molyneux, M. E., and MacLennan, C. A. (2017). Cytokine Profiles in Malawian Children Presenting With Uncomplicated Malaria, Severe Malarial Anemia, and Cerebral Malaria. *Clin. Vaccine Immunol.* 24 (4), 1–11. doi: 10.1128/CVI.00533-16

Marcos-Ramiro, B., Garcia-Weber, D., and Millan, J. (2014). TNF-Induced Endothelial Barrier Disruption: Beyond Actin and Rho. *Thromb. Haemost.* 112 (6), 1088–1102. doi: 10.1160/TH14-04-0299

Ma, Y., Yang, X., Chatterjee, V., Meegan, J. E., Beard, R. S.Jr., and Yuan, S. Y. (2019). Role of Neutrophil Extracellular Traps and Vesicles in Regulating Vascular Endothelial Permeability. *Front. Immunol.* 10, 1037. doi: 10.3389/fimmu.2019.01037

McKenzie, J. A., and Ridley, A. J. (2007). Roles of Rho/ROCK and MLCK in TNF-Alpha-Induced Changes in Endothelial Morphology and Permeability. *J. Cell Physiol.* 213 (1), 221–228. doi: 10.1002/jcp.21114

McMorran, B. J., Marshall, V. M., de Graaf, C., Drysdale, K. E., Shabbar, M., Smyth, G. K., et al. (2009). Platelets Kill Intraerythrocytic Malarial Parasites and Mediate Survival to Infection. *Science* 323 (5915), 797–800. doi: 10.1126/science.1166296

McMorran, B. J., Wieczorski, L., Drysdale, K. E., Chan, J. A., Huang, H. M., Smith, C., et al. (2012). Platelet Factor 4 and Duffy Antigen Required for Platelet Killing of Plasmodium Falciparum. *Science* 338 (6112), 1348–1351. doi: 10.1126/science.1228892

Meegan, J. E., Shaver, C. M., Putz, N. D., Jesse, J. J., Landstreet, S. R., Lee, H. N. R., et al. (2020). Cell-Free Hemoglobin Increases Inflammation, Lung Apoptosis, and Microvascular Permeability in Murine Polymicrobial Sepsis. *PloS One* 15 (2), e0228727. doi: 10.1371/journal.pone.0228727

Mehta, D., and Malik, A. B. (2006). Signaling Mechanisms Regulating Endothelial Permeability. *Physiol. Rev.* 86 (1), 279–367. doi: 10.1152/physrev.00012.2005

Millar, F. R., Summers, C., Griffiths, M. J., Toshner, M. R., and Proudfoot, A. G. (2016). The Pulmonary Endothelium in Acute Respiratory Distress Syndrome: Insights and Therapeutic Opportunities. *Thorax* 71 (5), 462–473. doi: 10.1136/thoraxjnl-2015-207461

Miller, L. H., Fremount, H. N., and Luse, S. A. (1971). Deep Vascular Schizogony of Plasmodium Knowlesi in Macaca Mulatta. Distribution in Organs and Ultrastructure of Parasitized Red Cells. *Am. J. Trop. Med. Hyg.* 20 (6), 816–824. doi: 10.4269/ajtmh.1971.20.816

Mills, C. D., Kincaid, K., Alt, J. M., Heilman, M. J., and Hill, A. M. (2000). M-1/M-2 Macrophages and the Th1/Th2 Paradigm. *J. Immunol.* 164 (12), 6166–6173. doi: 10.4049/jimmunol.164.12.6166

Milner, D. Jr., Factor, R., Whitten, R., Carr, R. A., Kamiza, S., Pinkus, G., et al. (2013). Pulmonary Pathology in Pediatric Cerebral Malaria. *Hum. Pathol.* 44 (12), 2719–2726. doi: 10.1016/j.humpath.2013.07.018

Mohan, A., Sharma, S. K., and Bollineni, S. (2008). Acute Lung Injury and Acute Respiratory Distress Syndrome in Malaria. *J. Vector Borne Dis.* 45 (3), 179–193.

Moore, B. R., Jago, J. D., and Batty, K. T. (2008). Plasmodium berghei: Parasite Clearance After Treatment With Dihydroartemisinin in an asplenic Murine Malaria Model. *Exp. Parasitol.* 118 (4), 458–467. doi: 10.1016/j.exppara.2007.10.011

Moxon, C. A., Wassmer, S. C., Milner, D. A.Jr., Chisala, N. V., Taylor, T. E., Seydel, K. B., et al. (2013). Loss of Endothelial Protein C Receptors Links Coagulation and Inflammation to Parasite Sequestration in Cerebral Malaria in African Children. *Blood* 122 (5), 842–851. doi: 10.1182/blood-2013-03-490219

Netea, M. G., Kullberg, B. J., and van der Meer, J. W. (2000). Circulating Cytokines as Mediators of Fever. *Clin. Infect. Dis.* 31 Suppl 5, S178–S184. doi: 10.1086/317513

Norbert Voelkel, S. R. (2009). *The Pulmonary Endothelium: Function in Health and Disease* (Wiley-Blackwell).

Ockenhouse, C. F., Tegoshi, T., Maeno, Y., Benjamin, C., Ho, M., Kan, K. E., et al. (1992). Human Vascular Endothelial Cell Adhesion Receptors for Plasmodium Falciparum-Infected Erythrocytes: Roles for Endothelial Leukocyte Adhesion Molecule 1 and Vascular Cell Adhesion Molecule 1. *J. Exp. Med.* 176 (4), 1183–1189. doi: 10.1084/jem.176.4.1183

Olliaro, P. (2008). Editorial Commentary: Mortality Associated With Severe Plasmodium Falciparum Malaria Increases With Age. *Clin. Infect. Dis.* 47 (2), 158–160. doi: 10.1086/589288

Ortolan, L. S., Sercundes, M. K., Barboza, R., Debone, D., Murillo, O., Hagen, S. C., et al. (2014). Predictive Criteria to Study the Pathogenesis of Malaria-Associated ALI/ARDS in Mice. *Mediators Inflamm.* 2014, 872464. doi: 10.1155/2014/872464

Ozwara, H., Langermans, J. A., Maamun, J., Farah, I. O., Yole, D. S., Mwenda, J. M., et al. (2003). Experimental Infection of the Olive Baboon (Paplio anubis) With Plasmodium knowlesi: Severe Disease Accompanied by Cerebral Involvement. *Am. J. Trop. Med. Hyg.* 69 (2), 188–194.

Pain, A., Ferguson, D. J., Kai, O., Urban, B. C., Lowe, B., Marsh, K., et al. (2001). Platelet-Mediated Clumping of Plasmodium Falciparum-Infected Erythrocytes Is a Common Adhesive Phenotype and Is Associated With Severe Malaria. *Proc. Natl. Acad. Sci. U. S. A.* 98 (4), 1805–1810. doi: 10.1073/pnas.98.4.1805

Park, G. S., Ireland, K. F., Opoka, R. O., and John, C. C. (2012). Evidence of Endothelial Activation in Asymptomatic Plasmodium Falciparum Parasitemia and Effect of Blood Group on Levels of Von Willebrand Factor in Malaria. *J. Pediatr. Infect. Dis. Soc.* 1 (1), 16–25. doi: 10.1093/jpids/pis010

Pedersen, S. F., and Ho, Y. C. (2020). SARS-CoV-2: A Storm Is Raging. *J. Clin. Invest.* 130 (5), 2202–2205. doi: 10.1172/JCI137647

Peerschke, E. I., Yin, W., and Ghebrehiwet, B. (2010). Complement Activation on Platelets: Implications for Vascular Inflammation and Thrombosis. *Mol. Immunol.* 47 (13), 2170–2175. doi: 10.1016/j.molimm.2010.05.009

Pereira, M. L., Ortolan, L. S., Sercundes, M. K., Debone, D., Murillo, O., Lima, F. A., et al. (2016). Association of Heme Oxygenase 1 With Lung Protection in Malaria-Associated ALI/ARDS. *Mediators Inflamm.* 2016, 4158698. doi: 10.1155/2016/4158698

Peterson, M. S., Joyner, C. J., Brady, J. A., Wood, J. S., Cabrera-Mora, M., Saney, C. L., et al. (2021). Clinical Recovery of Macaca Fascicularis Infected With Plasmodium Knowlesi. *Malar. J.* 20 (1), 486. doi: 10.1186/s12936-021-03925-6

Peterson, M. S., Joyner, C. J., Cordy, R. J., Salinas, J. L., Machiah, D., Lapp, S. A., et al. (2019). Plasmodium Vivax Parasite Load Is Associated With Histopathology in Saimiri Boliviensis With Findings Comparable to P Vivax Pathogenesis in Humans. *Open Forum Infect. Dis.* 6 (3), ofz021. doi: 10.1093/ofid/ofz021

Pham, T. T., Punsawad, C., Glaharn, S., De Meyer, S. F., Viriyavejakul, P., and Van den Steen, P. E. (2019). Release of Endothelial Activation Markers in Lungs of Patients With Malaria-Associated Acute Respiratory Distress Syndrome. *Malar. J.* 18 (1), 395. doi: 10.1186/s12936-019-3040-3

Pham, T. T., Verheijen, M., Vandermosten, L., Deroost, K., Knoops, S., Van den Eynde, K., et al. (2017). Pathogenic CD8(+) T Cells Cause Increased Levels of VEGF-A in Experimental Malaria-Associated Acute Respiratory Distress Syndrome, But Therapeutic VEGFR Inhibition Is Not Effective. *Front. Cell Infect. Microbiol.* 7, 416. doi: 10.3389/fcimb.2017.00416

Piguet, P. F., Da Laperrousaz, C., Vesin, C., Tacchini-Cottier, F., Senaldi, G., and Grau, G. E. (2000). Delayed Mortality and Attenuated Thrombocytopenia Associated With Severe Malaria in Urokinase- and Urokinase Receptor-Deficient Mice. *Infect. Immun.* 68 (7), 3822–3829. doi: 10.1128/IAI.68.7.3822-3829.2000

Piguet, P. F., Kan, C. D., and Vesin, C. (2002). Role of the Tumor Necrosis Factor Receptor 2 (TNFR2) in Cerebral Malaria in Mice. *Lab. Invest.* 82 (9), 1155–1166. doi: 10.1097/01.lab.0000028822.94883.8a

Pollenus, E., Pham, T. T., Vandermosten, L., Possemiers, H., Knoops, S., Opdenakker, G., et al. (2020). CCR2 Is Dispensable for Disease Resolution But Required for the Restoration of Leukocyte Homeostasis Upon Experimental Malaria-Associated Acute Respiratory Distress Syndrome. *Front. Immunol.* 11, 628643. doi: 10.3389/fimmu.2020.628643

Possemiers, H., Pham, T. T., Coens, M., Pollenus, E., Knoops, S., Noppen, S., et al. (2021). Skeleton Binding Protein-1-Mediated Parasite Sequestration Inhibits Spontaneous Resolution of Malaria-Associated Acute Respiratory Distress Syndrome. *PloS Pathog.* 17 (11), e1010114. doi: 10.1371/journal.ppat.1010114

Price, R. N., Tjitra, E., Guerra, C. A., Yeung, S., White, N. J., and Anstey, N. M. (2007). Vivax Malaria: Neglected and Not Benign. *Am. J. Trop. Med. Hyg.* 77 (6 Suppl), 79–87. doi: 10.4269/ajtmh.2007.77.79

Punsawad, C., Viriyavejakul, P., Setthapramote, C., and Palipoch, S. (2015). Enhanced Expression of Fas and FasL Modulates Apoptosis in the Lungs of Severe P. Falciparum Malaria Patients With Pulmonary Edema. *Int. J. Clin. Exp. Pathol.* 8 (9), 10002–10013.

Quirino, T. C., Ortolan, L. D. S., Sercundes, M. K., Marinho, C. R. F., Turato, W. M., and Epiphanio, S. (2020). Lung Aeration in Experimental Malaria-Associated Acute Respiratory Distress Syndrome by SPECT/CT Analysis. *PloS One* 15 (5), e0233864. doi: 10.1371/journal.pone.0233864

Ragab, D., Salah Eldin, H., Taeimah, M., Khattab, R., and Salem, R. (2020). The COVID-19 Cytokine Storm; What We Know So Far. *Front. Immunol.* 11, 1446. doi: 10.3389/fimmu.2020.01446

Reid, P. T., and Donnelly, S. C. (1996). Predicting Acute Respiratory Distress Syndrome and Intrapulmonary Inflammation. *Br. J. Hosp. Med.* 55 (8), 499–502.

Reinders, M. E., Sho, M., Izawa, A., Wang, P., Mukhopadhyay, D., Koss, K. E., et al. (2003). Proinflammatory Functions of Vascular Endothelial Growth Factor in Alloimmunity. *J. Clin. Invest.* 112 (11), 1655–1665. doi: 10.1172/JCI17712

Schappo, A. P., Bittencourt, N. C., Bertolla, L. P., Forcellini, S., da Silva, A., Dos Santos, H. G., et al. (2022). Antigenicity and Adhesiveness of a Plasmodium Vivax VIR-E Protein From Brazilian Isolates. *Mem. Inst. Oswaldo Cruz* 116, e210227. doi: 10.1590/0074-02760210227

Schneberger, D., Aharonson-Raz, K., and Singh, B. (2011). Monocyte and Macrophage Heterogeneity and Toll-Like Receptors in the Lung. *Cell Tissue Res.* 343 (1), 97–106. doi: 10.1007/s00441-010-1032-2

Sercundes, M. K., Ortolan, L. S., da Silva Julio, V., Bella, L. M., de Castro Quirino, T., Debone, D., et al. (2022). Blockade of Caspase Cascade Overcomes Malaria-Associated Acute Respiratory Distress Syndrome in Mice. *Cell Death Dis.* 13 (2), 144. doi: 10.1038/s41419-022-04582-6

Sercundes, M. K., Ortolan, L. S., Debone, D., Soeiro-Pereira, P. V., Gomes, E., Aitken, E. H., et al. (2016). Targeting Neutrophils to Prevent Malaria-Associated Acute Lung Injury/Acute Respiratory Distress Syndrome in Mice. *PloS Pathog.* 12 (12), e1006054. doi: 10.1371/journal.ppat.1006054

Sharron, M., Hoptay, C. E., Wiles, A. A., Garvin, L. M., Geha, M., Benton, A. S., et al. (2012). Platelets Induce Apoptosis During Sepsis in a Contact-Dependent Manner That Is Inhibited by GPIIb/IIIa Blockade. *PloS One* 7 (7), e41549. doi: 10.1371/journal.pone.0041549

Singh, B., Kim Sung, L., Matusop, A., Radhakrishnan, A., Shamsul, S. S., Cox-Singh, J., et al. (2004). A Large Focus of Naturally Acquired Plasmodium Knowlesi Infections in Human Beings. *Lancet* 363 (9414), 1017–1024. doi: 10.1016/S0140-6736(04)15836-4

Smith, K. G., Kamdar, A. A., and Stark, J. M. (2019). "Lung Defenses: Intrinsic, Innate, and Adaptive" in *Kendig's Disorders of the Respiratory Tract in Children* (Elsevier), 120–133.e122. doi: 10.1016/B978-0-323-44887-1.00008-0

Souza, M. C., Silva, J. D., Padua, T. A., Capelozzi, V. L., Rocco, P. R., and Henriques, M. (2013). Early and Late Acute Lung Injury and Their Association With Distal Organ Damage in Murine Malaria. *Respir. Physiol. Neurobiol.* 186 (1), 65–72. doi: 10.1016/j.resp.2012.12.008

Spangler, W. L., Gribble, D., Abildgaard, C., and Harrison, J. (1978). Plasmodium Knowlesi Malaria in the Rhesus Monkey. *Vet. Pathol.* 15 (1), 83–91. doi: 10.1177/030098587801500110

Spindler, V., Schlegel, N., and Waschke, J. (2010). Role of GTPases in Control of Microvascular Permeability. *Cardiovasc. Res.* 87 (2), 243–253. doi: 10.1093/cvr/cvq086

Srivastava, K. (2014). The Role of Platelets in Malarial Acute Lung Injury and Acute Respiratory Distress Syndrome: A World of Possibilities. *Acta Medica Int.* 1 (2), 117–123. doi: 10.5530/ami.2014.2.16

Srivastava, K., Cockburn, I. A., Swaim, A., Thompson, L. E., Tripathi, A., Fletcher, C. A., et al. (2008). Platelet Factor 4 Mediates Inflammation in Experimental Cerebral Malaria. *Cell Host Microbe* 4 (2), 179–187. doi: 10.1016/j.chom.2008.07.003

Ta, T. H., Hisam, S., Lanza, M., Jiram, A. I., Ismail, N., and Rubio, J. M. (2014). First Case of a Naturally Acquired Human Infection With Plasmodium Cynomolgi. *Malar. J.* 13, 68. doi: 10.1186/1475-2875-13-68

Taoufiq, Z., Gay, F., Balvanyos, J., Ciceron, L., Tefit, M., Lechat, P., et al. (2008). Rho Kinase Inhibition in Severe Malaria: Thwarting Parasite-Induced Collateral Damage to Endothelia. *J. Infect. Dis.* 197 (7), 1062–1073. doi: 10.1086/528988

Taoufiq, Z., Pino, P., N'Dilimabaka, N., Arrouss, I., Assi, S., Soubrier, F., et al. (2011). Atorvastatin Prevents Plasmodium Falciparum Cytoadherence and Endothelial Damage. *Malar. J.* 10, 52. doi: 10.1186/1475-2875-10-52

Taylor, T. E., Borgstein, A., and Molyneux, M. E. (1993). Acid-Base Status in Paediatric Plasmodium Falciparum Malaria. *Q. J. Med.* 86 (2), 99–109.

Taylor, W. R. J., Hanson, J., Turner, G. D. H., White, N. J., and Dondorp, A. M. (2012). Respiratory Manifestations of Malaria. *Chest* 142 (2), 492–505. doi: 10.1378/chest.11-2655

Thachil, J. (2017). Platelets and Infections in the Resource-Limited Countries With a Focus on Malaria and Viral Haemorrhagic Fevers. *Br. J. Haematol.* 177 (6), 960–970. doi: 10.1111/bjh.14582

Togbe, D., de Sousa, P. L., Fauconnier, M., Boissay, V., Fick, L., Scheu, S., et al. (2008). Both Functional LTbeta Receptor and TNF Receptor 2 Are Required for the Development of Experimental Cerebral Malaria. *PloS One* 3 (7), e2608. doi: 10.1371/journal.pone.0002608

Tong, M. J., Ballantine, T. V., and Youel, D. B. (1972). Pulmonary Function Studies in Plasmodium Falciparum Malaria. *Am. Rev. Respir. Dis.* 106 (1), 23–29. doi: 10.1164/arrd.1972.106.1.23

Turner, L., Lavstsen, T., Berger, S. S., Wang, C. W., Petersen, J. E., Avril, M., et al. (2013). Severe Malaria Is Associated With Parasite Binding to Endothelial Protein C Receptor. *Nature* 498 (7455), 502–505. doi: 10.1038/nature12216

Tutkun, L., Iritas, S. B., Deniz, S., Oztan, O., Abusoglu, S., Unlu, A., et al. (2019). TNF-Alpha and IL-6 as Biomarkers of Impaired Lung Functions in Dimethylacetamide Exposure. *J. Med. Biochem.* 38 (3), 276–283. doi: 10.2478/jomb-2018-0040

Valecha, N., Pinto, R. G., Turner, G. D., Kumar, A., Rodrigues, S., Dubhashi, N. G., et al. (2009). Histopathology of Fatal Respiratory Distress Caused by Plasmodium Vivax Malaria. *Am. J. Trop. Med. Hyg.* 81 (5), 758–762. doi: 10.4269/ajtmh.2009.09-0348

Val, F., Machado, K., Barbosa, L., Salinas, J. L., Siqueira, A. M., Costa Alecrim, M. G., et al. (2017). Respiratory Complications of Plasmodium Vivax Malaria: Systematic Review and Meta-Analysis. *Am. J. Trop. Med. Hyg.* 97 (3), 733–743. doi: 10.4269/ajtmh.17-0131

Van den Steen, P. E., Deroost, K., Deckers, J., Van Herck, E., Struyf, S., and Opdenakker, G. (2013). Pathogenesis of Malaria-Associated Acute Respiratory Distress Syndrome. *Trends Parasitol.* 29 (7), 346–358. doi: 10.1016/j.pt.2013.04.006

Van den Steen, P. E., Geurts, N., Deroost, K., Van Aelst, I., Verhenne, S., Heremans, H., et al. (2010). Immunopathology and Dexamethasone Therapy in a New Model for Malaria-Associated Acute Respiratory Distress Syndrome. *Am. J. Respir. Crit. Care Med.* 181 (9), 957–968. doi: 10.1164/rccm.200905-0786OC

Vandermosten, L., Pham, T. T., Possemiers, H., Knoops, S., Van Herck, E., Deckers, J., et al. (2018). Experimental Malaria-Associated Acute Respiratory Distress Syndrome Is Dependent on the Parasite-Host Combination and Coincides With Normocyte Invasion. *Malar. J.* 17 (1), 102. doi: 10.1186/s12936-018-2251-3

van der Pluijm, R. W., Amaratunga, C., Dhorda, M., and Dondorp, A. M. (2021). Triple Artemisinin-Based Combination Therapies for Malaria - A New Paradigm? *Trends Parasitol.* 37 (1), 15–24. doi: 10.1016/j.pt.2020.09.011

van der Poll, T. (2013). The Endothelial Protein C Receptor and Malaria. *Blood* 122 (5), 624–625. doi: 10.1182/blood-2013-06-508531

Vieira-de-Abreu, A., Campbell, R. A., Weyrich, A. S., and Zimmerman, G. A. (2012). Platelets: Versatile Effector Cells in Hemostasis, Inflammation, and the Immune Continuum. *Semin. Immunopathol.* 34 (1), 5–30. doi: 10.1007/s00281-011-0286-4

Villegas-Mendez, A., de Souza, J. B., Murungi, L., Hafalla, J. C., Shaw, T. N., Greig, R., et al. (2011). Heterogeneous and Tissue-Specific Regulation of Effector T Cell Responses by IFN-Gamma During Plasmodium Berghei ANKA Infection. *J. Immunol.* 187 (6), 2885–2897. doi: 10.4049/jimmunol.1100241

Vincent, P. A., Xiao, K., Buckley, K. M., and Kowalczyk, A. P. (2004). VE-Cadherin: Adhesion at Arm's Length. *Am. J. Physiol. Cell Physiol.* 286 (5), C987–C997. doi: 10.1152/ajpcell.00522.2003

Ware, L. B. (2006). Pathophysiology of Acute Lung Injury and the Acute Respiratory Distress Syndrome. *Semin. Respir. Crit. Care Med.* 27 (4), 337–349. doi: 10.1055/s-2006-948288

Wassmer, S. C., Lepolard, C., Traore, B., Pouvelle, B., Gysin, J., and Grau, G. E. (2004). Platelets Reorient Plasmodium Falciparum-Infected Erythrocyte Cytoadhesion to Activated Endothelial Cells. *J. Infect. Dis.* 189 (2), 180–189. doi: 10.1086/380761

Wei, H., Jin, C., Peng, A., Xie, H., Xie, S., Feng, Y., et al. (2021). Characterization of gammadeltaT Cells in Lung of Plasmodium Yoelii-Infected C57BL/6 Mice. *Malar. J.* 20 (1), 89. doi: 10.1186/s12936-021-03619-z

Weiss, M. L., and Kubat, K. (1983). Plasmodium berghei: A Mouse Model for the "Sudden Death" and "Malarial Lung" Syndromes. *Exp. Parasitol.* 56 (1), 143–151. doi: 10.1016/0014-4894(83)90105-4

West, N. R. (2019). Coordination of Immune-Stroma Crosstalk by IL-6 Family Cytokines. *Front. Immunol.* 10, 1093. doi: 10.3389/fimmu.2019.01093

Wettschureck, N., Strilic, B., and Offermanns, S. (2019). Passing the Vascular Barrier: Endothelial Signaling Processes Controlling Extravasation. *Physiol. Rev.* 99 (3), 1467–1525. doi: 10.1152/physrev.00037.2018

WHO. (2021). *World Malaria Report 2021* (Geneva: World Health Organization).

William, T., Menon, J., Rajahram, G., Chan, L., Ma, G., Donaldson, S., et al. (2011). Severe Plasmodium Knowlesi Malaria in a Tertiary Care Hospital, Sabah, Malaysia. *Emerg. Infect. Dis.* 17 (7), 1248–1255. doi: 10.3201/eid1707.101017

Xie, R. F., Hu, P., Wang, Z. C., Yang, J., Yang, Y. M., Gao, L., et al. (2015). Platelet-Derived Microparticles Induce Polymorphonuclear Leukocyte-Mediated Damage of Human Pulmonary Microvascular Endothelial Cells. *Transfusion* 55 (5), 1051–1057. doi: 10.1111/trf.12952

Yeo, T. W., Lampah, D. A., Gitawati, R., Tjitra, E., Kenangalem, E., Piera, K., et al. (2008). Angiopoietin-2 Is Associated With Decreased Endothelial Nitric Oxide and Poor Clinical Outcome in Severe Falciparum Malaria. *Proc. Natl. Acad. Sci. U. S. A.* 105 (44), 17097–17102. doi: 10.1073/pnas.0805782105

Zang-Edou, E. S., Bisvigou, U., Taoufiq, Z., Lekoulou, F., Lekana-Douki, J. B., Traore, Y., et al. (2010). Inhibition of Plasmodium Falciparum Field Isolates-Mediated

Endothelial Cell Apoptosis by Fasudil: Therapeutic Implications for Severe Malaria. *PloS One* 5 (10), e13221. doi: 10.1371/journal.pone.0013221

Zhao, T., Liu, M., Gu, C., Wang, X., and Wang, Y. (2014). Activation of C-Src Tyrosine Kinase Mediated the Degradation of Occludin in Ventilator-Induced Lung Injury. *Respir. Res.* 15, 158. doi: 10.1186/s12931-014-0158-2

Zielinska, K. A., de Cauwer, L., Knoops, S., van der Molen, K., Sneyers, A., Thommis, J., et al. (2017). Plasmodium Berghei NK65 in Combination With IFN-Gamma Induces Endothelial Glucocorticoid Resistance *via* Sustained Activation of P38 and JNK. *Front. Immunol.* 8, 1199. doi: 10.3389/fimmu.2017.01199

Conflict of Interest: The authors declare that the research was conducted in the absence of any commercial or financial relationships that could be construed as a potential conflict of interest.

Publisher's Note: All claims expressed in this article are solely those of the authors and do not necessarily represent those of their affiliated organizations, or those of the publisher, the editors and the reviewers. Any product that may be evaluated in this article, or claim that may be made by its manufacturer, is not guaranteed or endorsed by the publisher.

frontiers | Frontiers in Cellular and Infection Microbiology

MINI REVIEW
published: 02 June 2022
doi: 10.3389/fcimb.2022.917267

Uncovering a Cryptic Site of Malaria Pathogenesis: Models to Study Interactions Between *Plasmodium* and the Bone Marrow

Tamar P. Feldman[1,2] *and Elizabeth S. Egan*[1,2]*

[1] Department of Pediatrics, Stanford University School of Medicine, Stanford, CA, United States, [2] Department of Microbiology and Immunology, Stanford University School of Medicine, Stanford, CA, United States

The bone marrow is a critical site of host-pathogen interactions in malaria infection. The discovery of *Plasmodium* asexual and transmission stages in the bone marrow has renewed interest in the tissue as a niche for cellular development of both host and parasite. Despite its importance, bone marrow in malaria infection remains largely unexplored due to the challenge of modeling the complex hematopoietic environment *in vitro*. Advancements in modeling human erythropoiesis *ex-vivo* from primary human hematopoietic stem and progenitor cells provide a foothold to study the host-parasite interactions occurring in this understudied site of malaria pathogenesis. This review focuses on current *in vitro* methods to recapitulate and assess bone marrow erythropoiesis and their potential applications in the malaria field. We summarize recent studies that leveraged *ex-vivo* erythropoiesis to shed light on gametocyte development in nucleated erythroid stem cells and begin to characterize host cell responses to *Plasmodium* infection in the hematopoietic niche. Such models hold potential to elucidate mechanisms of disordered erythropoiesis, an underlying contributor to malaria anemia, as well as understand the biological determinants of parasite sexual conversion. This review compares the advantages and limitations of the *ex-vivo* erythropoiesis approach with those of *in vivo* human and animal studies of the hematopoietic niche in malaria infection. We highlight the need for studies that apply single cell analyses to this complex system and incorporate physical and cellular components of the bone marrow that may influence erythropoiesis and parasite development.

Keywords: *Plasmodium*, bone marrow, hematopoietic stem cells, erythropoiesis, malaria anemia, *ex-vivo* erythropoiesis model

OPEN ACCESS

Edited by:
Andrea L. Conroy, Indiana University, United States

Reviewed by:
Catherine Lavazec, INSERM U1016 Institut Cochin, France

***Correspondence:**
Elizabeth S. Egan
eegan@stanford.edu

Specialty section:
This article was submitted to Parasite and Host, a section of the journal Frontiers in Cellular and Infection Microbiology

Received: *11 April 2022*
Accepted: *03 May 2022*
Published: *02 June 2022*

Citation:
Feldman TP and Egan ES (2022) Uncovering a Cryptic Site of Malaria Pathogenesis: Models to Study Interactions Between Plasmodium and the Bone Marrow. Front. Cell. Infect. Microbiol. 12:917267. doi: 10.3389/fcimb.2022.917267

INTRODUCTION

Malaria caused by *Plasmodium* spp. parasites remains a major global public health problem, responsible for an estimated 241 million cases and ~627,000 deaths per year (WHO, 2021). Of the five species that infect humans, *Plasmodium vivax* has the widest geographic spread whereas *Plasmodium falciparum* is the predominant cause of mortality. More than 90% of global malaria

deaths are concentrated in endemic regions of western and sub-Saharan Africa. Although increased investments in effective anti-malarial treatment and disease prevention have led to marked improvements in malaria control over the past decade, the emergence of drug-resistant parasites and mosquitoes present continuing challenges.

Plasmodia are obligate, intracellular eukaryotic parasites transmitted by anopheline mosquitos and are characterized by a complex lifecycle in the mosquito and vertebrate host. Upon injection from the mosquito, parasites traffic to the liver where they undergo a massive, but clinically silent replication before entering the bloodstream. Symptoms of malaria occur exclusively during the blood stage of infection, when parasites invade and replicate exponentially in human erythrocytes. A small proportion of parasites commit to sexual reproduction, becoming male or female gametocytes. Circulating gametocytes can be transmitted to the mosquito vector as it takes a blood meal. Outside of circulation, *P. falciparum* and *P. vivax* can also be found in deep tissues, including the spleen and bone marrow.

The bone marrow is an important site of cellular development for both the parasite and its host. Post-natal hematopoiesis in humans occurs in the bone marrow where multipotent progenitors give rise to blood cell lineages, including red blood cells (RBCs) by a process termed erythropoiesis. Numerous case reports have demonstrated the presence of *Plasmodium* parasites, hemozoin, and abnormal erythroblast morphology in bone marrow biopsies of malaria patients (Abdalla et al., 1980; Dormer et al., 1983; Wickramasinghe et al., 1987). More recently, two quantitative studies using patient samples revealed that the bone marrow is a site of enrichment for sexual-stage gametocytes (Aguilar et al., 2014a; Joice et al., 2014), one of which also noted an association between severe anemia, dyserythropoiesis, and gametocyte load (Aguilar et al., 2014a). Together, these observations point to the bone marrow as an under-recognized site of malarial pathogenesis.

Although the observation of *Plasmodium* in human bone marrow dates back over 130 years (Marchiafava and Bigmani, 1894), our understanding of the impact of parasite infection on the hematopoietic niche is limited. The invasive procedure to obtain bone marrow aspirates, which is generally not clinically indicated for disease management, limits direct investigation in patient samples. Therefore, innovation in cell culture and animal models of erythropoiesis is crucial for understanding, and eventually disrupting, host-parasite interactions in the bone marrow that contribute to malaria pathogenesis. Here, we summarize available models for the study of host-parasite interactions in the hematopoietic niche, highlighting recent work that has leveraged advancements in *ex vivo* erythropoiesis of primary hematopoietic stem and progenitor cells (HSPCs) to generate and test hypotheses about the host response to parasite infection and parasite development in the bone marrow. Finally, we discuss avenues to improve existing models and the value of applying novel, single-cell technologies to the study of a complex tissue. Obtaining both cell-intrinsic and population-level views of how malaria parasites exploit and modulate the human bone marrow and specifically the erythroid lineage will lay the foundation for novel therapies for malaria.

OVERVIEW OF HUMAN ERYTHROPOIESIS

In adult humans, erythropoiesis occurs in the extravascular compartment of the bone marrow and proceeds in two stages (Zivot et al., 2018) (**Figure 1**). First, multipotent hematopoietic stem and progenitor cells (HSPCs) lose their capacity to self-renew and become increasingly restricted in their lineage potential. The first erythroid committed progenitors, the burst forming unit-erythroid (BFU-E), give rise to colony forming unit-erythroid (CFU-E) (Hattangadi et al., 2011). The proliferation and survival of BFU-E, CFU-E, and proerythroblasts are promoted by stem cell factor (SCF), which binds to the c-KIT receptor (Sui et al., 2000). Erythropoietin (EPO), a hormone produced in the kidney, is an important regulator of erythropoiesis that balances the survival, proliferation, and differentiation of CFU-E. Binding of EPO to its receptor, EPOR, activates JAK2, which subsequently induces the activation of several cellular pathways including STAT5, RAS/MAP kinase and PI3K/AKT, thus promoting an erythroid lineage-restricted transcriptional program (Hattangadi et al., 2011; Caulier and Sankaran, 2022).

Terminal differentiation of erythroid cells proceeds through a limited number of cell divisions during which there are dramatic changes to cellular morphology, membrane properties, and gene expression (Zivot et al., 2018). As erythroblasts mature, cell size decreases, the nucleus condenses, and gene expression is gradually turned off, except for globin genes and other erythroid-specific factors. Finally, the orthochromatic erythroblast expels its nucleus and other organelles to become an enucleated reticulocyte. The reticulocyte undergoes further maturation and is released from the bone marrow into circulation, where it quickly matures into an erythrocyte (red blood cell; RBC).

EX-VIVO MODELS OF HUMAN ERYTHROPOIESIS

The concept of generating human erythrocytes from hematopoietic stem cells by *ex-vivo* culture has long been a focus of the transfusion medicine field, with the goal of achieving a stable supply of mature red blood cells to meet worldwide clinical need (Anstee et al., 2012). To meaningfully recapitulate erythropoiesis, such an *in vitro* culture system needs to satisfy three criteria: large-scale proliferation of stem/progenitor cells, stable transition from multi-potent progenitors to commitment to the erythroid lineage, and successful terminal differentiation down the erythroid lineage to functional enucleated RBCs (Gregory and Eaves, 1978; Metcalf, 1993; Giarratana et al., 2005). As dyserythropoiesis is implicated in the pathogenesis of severe malaria, such *ex-vivo* models of erythropoiesis also hold

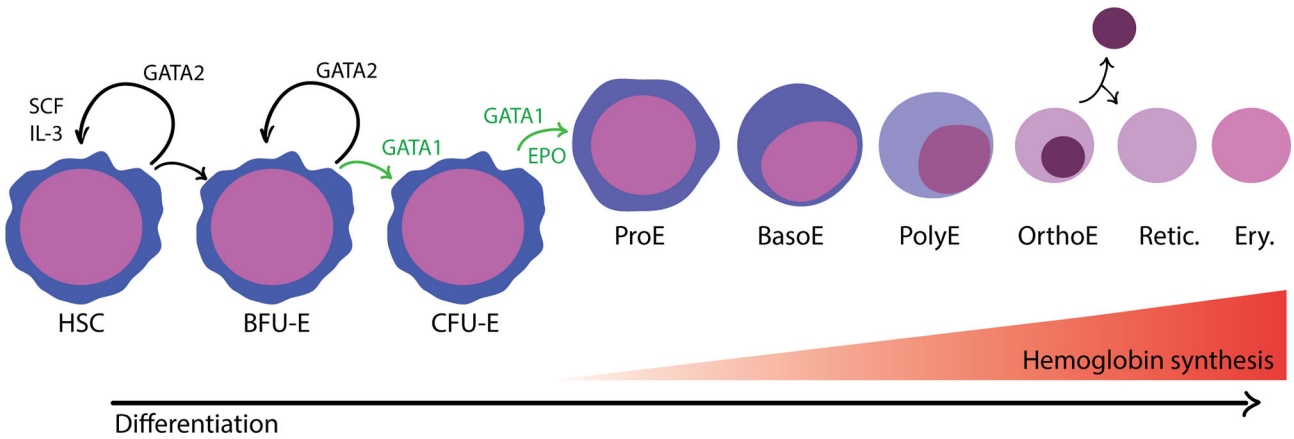

FIGURE 1 | Overview of adult, definitive erythropoiesis in the bone marrow. The bone marrow is populated with hematopoietic stem cells with the capacity for long-term self-renewal and the potential to differentiate down any of the blood cell lineages. The balance between self-renewal and lineage commitment is informed by physical and chemical signals present in the surrounding microenvironment and coordinated by master transcription factors. Erythroid commitment is largely controlled by the activity of GATA1, which promotes differentiation and inhibits opposing factors for self-renewal, such as GATA2. In the first phase of development, progenitor cells become gradually more erythroid committed in response to environmental cues that promote proliferation and differentiation. Burst forming unit-erythroid (BFU-E) are considered the first irreversibly committed erythroid cells. In the subsequent stage, colony forming unit-erythroid (CFU-E) cells are highly proliferative and begin to activate erythroid transcriptional programs regulated by GATA1, in response to erythropoietin (EPO). In the terminal differentiation phase, erythroblasts develop in a specialized compartments called erythroblastic islands. Erythroblasts are found in close association with a central macrophage that provides signals to support proliferation and differentiation as well as the iron needed for hemoglobin synthesis. As erythroblasts differentiate, they decrease in size, undergo nuclear condensation, and turn off gene expression with the exception of a subset of erythroid-specific genes, most notably hemoglobin. Distinct morphological stages are visible by hematological staining: proerythroblast (ProE), basophilic erythroblast (BasE), polychromatic erythroblast (PolyE), and orthochromatic erythroblast (OrthoE). In the final stage of development, the nucleus and organelles are extruded. The enucleated reticulocyte (Retic.) undergoes further development as it enters circulation, eventually becoming a mature erythrocyte (Ery.).

potential for advancing our understanding of host-pathogen interactions unique to the hematopoietic niche.

EX-VIVO ERYTHROPOIESIS OF PRIMARY CELLS

Early *ex-vivo* liquid culture systems using primary $CD34^+$ cells demonstrated a high proliferative capacity in culture in the presence of cytokines, but efficient terminal differentiation and enucleation proved challenging (Fibach et al., 1989; Wada et al., 1990; Sui et al., 1996; Panzenbock et al., 1998; Freyssinier et al., 1999; von Lindern et al., 1999). A significant advance came with the development of an approach enabling the large-scale production and detailed characterization of RBCs generated from primary human $CD34^+$ HSPCs using a three-phase protocol (Giarratana et al., 2005). This involved mimicking the microenvironment of the hematopoietic niche through addition of cytokines such as SCF and EPO, and co-culture on a murine stromal layer to promote enucleation. Importantly, the cultured progenitors were observed to differentiate normally down the erythroid lineage as measured by morphology and cell surface markers, and the terminally differentiated, cultured RBCs (cRBCs) had similar enzyme content and functional hemoglobin as natural adult RBCs.

In subsequent work, a modified approach that enhanced the feasibility of large-scale production of RBCs by removing the need for co-culture on a stromal layer was reported (Giarratana et al., 2011). This advance was achieved using human plasma, which was hypothesized to provide some of the necessary extracellular signals to promote survival, terminal differentiation and enucleation. While the resulting RBCs were more similar to reticulocytes than mature erythrocytes based on cell volume, membrane deformability, and surface protein expression, they matured to erythrocytes when transferred back to NOD/SCID mice or a human donor. This study provided strong experimental evidence for the quality and functionality of this *ex-vivo* approach for erythroid differentiation. Further validation of this *ex-vivo* erythropoiesis model has come from its application to the study of *P. falciparum*, in which genetic manipulation of erythroid progenitors followed by terminal differentiation enabled discovery and interrogation of novel host factors in enucleated cRBCs (Egan et al., 2015; Shakya et al., 2021).

Other potential sources of primary cells to model human erythropoiesis include human cord blood, embryonic stem cells (hESC), and induced pluripotent stem cells (iPSCs), but none have the demonstrated utility of primary adult $CD34^+$ HSPCs. Human cord blood is a readily available source of $CD34^+$ HSPCs, but these are fetal cells that predominantly generate HbF rather than adult hemoglobin (Anstee et al., 2012). hESC have high proliferative potential, but limited ability to enucleate and express adult hemoglobin. iPSC approaches are hampered by limited proliferative capacity, inefficient terminal differentiation,

and presence of fetal or embryonic rather than adult hemoglobin (Dias et al., 2011; Trakarnsanga et al., 2014). More recent research suggests that combining insights from human genetic variation with advances in genome editing can help optimize proliferation and erythroid differentiation of hESC and iPSC (Giani et al., 2016).

ERYTHROID CELL LINES

Initial *in vitro* models of erythropoiesis made use of erythroleukemic cancer cell lines (Friend et al., 1971; Tsiftsoglou et al., 2009). While valuable for their reproducible growth and ease of genetic manipulation, many cancerous cell lines do not recapitulate important aspects of healthy, adult erythropoiesis, in terms of responsiveness to EPO-signaling, hemoglobin expression, and efficiency of terminal differentiation and enucleation (Tsiftsoglou et al., 2009). One promising cell line is the JK-1 erythroleukemia cell line, which can be induced to differentiate using bromodomain inhibitors (Kanjee et al., 2017). JK-1-derived erythroblasts have been shown by morphological analyses to resemble established erythroid progenitor populations, and quantitative plasma membrane proteomics of JK-1 cells predominantly at the polychromatic erythroblast stage revealed that their proteome resembled that of polychromatic erythroblasts derived from primary human HSPCs, with ~68% of proteins within a 2-fold equivalent range of relative abundance. While JK-1 cells do not enucleate, they can support invasion by *P. falciparum*, and have some demonstrated utility for the genetic analysis of erythrocyte receptors for malaria (Kanjee et al., 2017).

MODELS OF HUMAN ERYTHROPOIESIS FROM IMMORTALIZED CELL LINES

Immortalized erythroid progenitor cell lines derived from $CD34^+$ HSPCs offer alternative models of healthy erythropoiesis that may assuage some of the technical challenges and expense associated with primary cells (**Table 1**). Cell lines can be cloned, genetically manipulated, and grown to high numbers in culture, ideally yielding an unlimited source of reproducible material for erythropoiesis-focused applications and molecular investigations. In recent years, several immortalized erythroid cell lines have been reported, with continued improvements toward their ability to recapitulate healthy erythropoiesis, yet limitations to their applicability still persist.

The HUDEP-2 erythroid progenitor cell line was generated from human umbilical cord blood CD34+ HSPCs (Kurita et al., 2013). These cells were immortalized using the doxycycline-inducible HPV16-E6/E7 construct after initial growth in a non-erythroid specific medium. Incubation in defined media including SCF, EPO, dexamethasone, and doxycycline enabled continued proliferation, and transitioning to differentiation media with EPO alone induced differentiation down the erythroid lineage. This cell line has been characterized to some degree in terms of transcription factor and cell surface protein expression, and expresses functional ß-globin. Though HUDEP-2 have the potential to enucleate, the rate of enucleation is low (5-20% depending on the media used) and significant cell loss is seen as cells reach the orthochromatic erythroblast stage, suggesting terminal differentiation is not fully functional in these cells (Kurita et al., 2013; Daniels et al., 2020).

In 2017, the first erythroid cell line immortalized from adult bone marrow $CD34^+$ HSPCs was reported, termed BEL-A (Trakarnsanga et al., 2017). BEL-A were initially maintained in an optimized erythroid culture medium, and then immortalized using the same doxycycline-inducible HPV16-E6/E7 construct as was used for HUDEP-2. The BEL-A cells have been shown to proliferate at similar rates as HUDEP-2, but they differentiate more quickly and have a higher enucleation rate, up to 40% (Daniels et al., 2020). However this enucleation rate is still modest relative to primary cell cultures, and BEL-A suffers a viability loss similar to HUDEP-2 after ~ 8 days of differentiation, suggesting a defect in the transition from orthochromatic erythroblasts to reticulocytes. Functionally, BEL-A have been used to study erythrocyte proteins required for *P. falciparum* invasion, and were used to further validate basigin as an essential receptor for malaria (Satchwell et al., 2019).

Recently, Daniels et al. showed that the immortalization approach used to make BEL-A could be adapted to erythroblasts from various sources, including human bone marrow, peripheral blood, and cord blood (Daniels et al., 2020). Through characterization of the proteome of immortalized cells derived from different sources compared to primary cells, a molecular signature for immortalization began to emerge, involving cell cycle regulation. Importantly, the progenitors immortalized using this approach were shown to recapitulate primary cells in terms of differentiation potential and adult hemoglobin expression levels (Daniels et al., 2020).

APPLICATION OF *IN VITRO* MODELS TO STUDY MALARIA IN THE HEMATOPOIETIC NICHE

Ex vivo erythropoiesis of primary cells presents an opportunity to study host responses and parasite development within in the hematopoietic niche. Much remains to be understood about the host response to exposure with *P. falciparum*, and how it might lead to disordered erythropoiesis. Recent work in the field has begun to elucidate the effects of *P. falciparum* and the heme degradation product hemozoin (Hz) on gross, phenotypic measurements of erythroid development, including proliferation, cell cycle staging, and expression of key erythroid-related genes.

Hz is found in large quantities in malaria-infected bone marrow, both in the extracellular environment and within phagocytic monocytes (Casals-Pascual et al., 2006; Aguilar et al., 2014b; Joice et al., 2014). Several studies have used *ex vivo* culture of erythroid precursors to study the effect of Hz on

TABLE 1 | Summary of models for *ex-vivo* erythropoiesis.

Model		Strengths	Limitations	Prior use in *Plasmodium*	References
Erythro-leukemic cell line	JK-1	Unlimited proliferation Ease of genetic engineering Heterogeneity can be reduced epigenetically	Poor enucleation Differentiation only to polychromatic erythroblast stage	Used as model for peripheral blood RBCs to study host determinants of invasion	(Okuno et al., 1990; Kanjee et al., 2017)
Primary HSPC	CD34+ from bone marrow or peripheral blood	Efficient *ex-vivo* erythropoiesis in liquid culture mirrors *in vivo* development All erythroblast stages can be generated Efficient enucleation	Limited proliferative capacity (~10,000-fold) Optimal terminal differentiation requires co-culture on stromal layer High heterogeneity Genetic engineering is technically challenging	Used as model for peripheral blood RBCs to study host determinants of invasion Used to define erythroblast populations susceptible to *Pf* infection Bulk transcriptomic analysis of *Pf*-infected erythroblast cultures Supports gametocyte formation	(Tamez et al., 2009; Bei et al., 2010; Giarratana et al., 2011; Tamez et al., 2011; Joice et al., 2014; Egan et al., 2015; Neveu et al., 2020; Shakya et al., 2021)
	CB	Readily available Efficient *ex-vivo* erythropoiesis in liquid culture All erythroblast stages can be generated Efficient enucleation	Limited proliferation Optimal terminal differentiation requires co-culture on stromal layer Expresses fetal hemoglobin High heterogeneity Genetic engineering is technically challenging	Culture of *P. vivax* Effects of co-culture with *P. falciparum* on expression of globin genes Effects of Hz on erythropoiesis	(Casals-Pascual et al., 2006; Panichakul et al., 2007; Anstee et al., 2012; Pathak et al., 2018)
	hESC, iPSC	High proliferative capacity HbF expression may be useful therapeutically (e.g. sickle cell) Feasible for targeted genomic modification	Poor enucleation Optimal terminal differentiation requires co-culture on stromal layer Expresses predominantly fetal hemoglobin (HbF), although switching to adult Hb observed *in vivo* in NOD/SCID mice	N/A	(Hanna et al., 2007; Dias et al., 2011; Trakarnsanga et al., 2014; Giani et al., 2016)
Immortalized cell line	HUDEP-2	High proliferative capacity Low heterogeneity Ease of genetic engineering Adult hemoglobin	Poor enucleation and loss of viability at the orthochromatic erythroblast stage	N/A	(Kurita et al., 2013)
	BEL-A	High proliferative capacity Low heterogeneity Ease of genetic engineering	Modest enucleation and loss of viability at the orthochromatic erythroblast stage	Used as model for peripheral blood RBCs to study host determinants of invasion	(Trakarnsanga et al., 2017; Satchwell et al., 2019; Daniels et al., 2020)

erythropoiesis. The addition of Hz, or conditioned media from monocytes fed with Hz, to primary cell cultures of BFU-E/CFU-E reduced colony formation (Giribaldi et al., 2004; Skorokhod et al., 2010). Similarly, periodic addition of Hz to primary CD34+ cells during differentiation down the erythroid lineage reduced cell growth (Casals-Pascual et al., 2006; Skorokhod et al., 2010). Co-cultivation with Hz also resulted in cell cycle defects in primary cells and changes to protein expression of cell cycle markers p53, p21, and Cyclin A in K562 cells (Skorokhod et al., 2010). This result provides one possible explanation for the observation of cell cycle defects in bone marrow aspirates from malaria patients. In a study using microarray-generated gene expression profiles, incubation of primary erythroblasts with Hz was shown to increase expression of some stress response genes, including those that mediate apoptosis (Lamikanra et al., 2015). Together, the current evidence supports a role for Hz in disordered erythropoiesis in the bone marrow.

Ex vivo erythropoiesis has also been used to investigate direct interactions between *P. falciparum* and developing erythroblasts. A study on the use of *in vitro*-produced reticulocytes for culture of *P. vivax* observed ring-stage parasites and gametocytes inside nucleated erythroid precursors by Giemsa staining (Panichakul et al., 2007). This observation was also confirmed for *P. falciparum* asexual (Tamez et al., 2009) and sexual stage parasites (Joice et al., 2014; Neveu et al., 2020). These studies further demonstrated that invasion and development of the parasite were dependent on erythroblast stage. Neveu *et al.* leveraged a GFP-expressing parasite line and host markers for erythroid development to show by flow cytometry that erythroid cells as early as the basophilic erythroblast are susceptible to

parasite invasion. The authors discovered two indicators of dyserythropoiesis that are specific to infected cells, reduced enucleation rate and generation of reactive oxygen species. Intriguingly, this study also demonstrated the presence of infected, nucleated erythroid precursors in bone marrow aspirates of malaria patients by immunofluorescence.

Little is known about the gene expression response to *P. falciparum* in infected erythroblasts. Through microarray profiling, Tamez et al. provided some evidence that 24-hr co-culture with *P. falciparum* was associated with transcriptional upregulation of a number of host genes in late-stage erythroblasts. This includes changes to genes encoding transcription factors related to erythroid development (JUN, MYC, SOX6) and mediators of the cellular stress response (HMOX1, DNAJB1, HSPA1A, HSP90AB1, STIP1) (Tamez et al., 2011). However, the conclusions from this study were limited, in part because the methodology did not distinguish between infected versus bystander cells, and the erythroblasts were heterogeneous in terms of developmental stage.

COMPLEMENTARY APPROACHES *IN VIVO*

Although there are advantages to the reductionist approach of cell culture models, erythroid cells in the bone marrow respond to complex combinations of local and systemic signals that cannot be easily or fully reconstituted *in vitro*. Studies on anemia of inflammation show that erythropoiesis is modulated by activity of the immune system, including by production of cytokines that act on erythroid precursors and immune-regulated changes in iron availability (Hom et al., 2015). While chemical signals can be added exogenously in *ex-vivo* cultures, reproducing inter-organ signaling is not straightforward. For example, IL-6, a proinflammatory cytokine that is elevated in malaria infection, regulates expression of hepcidin in the liver, which controls the flow of iron to developing RBCs in the bone marrow (Nemeth et al., 2004). Primary HSPC cultures are also limited in their utility for modeling spatiotemporal aspects of infection and may have issues of cost and reproducibility due to dependence on donors, and inherent donor-to-donor variability.

Animal models, especially small rodents, have long been an invaluable tool for studies of the hematopoietic niche that are not easily pursued in humans or with cell culture experiments (Doulatov et al., 2012). *In vivo* models preserve the spatial organization, signaling, and physical properties of the diverse cell types that define the bone marrow niche. No single murine model recapitulates all aspects of human malaria; however, the numerous combinations of host and parasite strains enable interrogation of a wide range of mechanistic questions about malarial pathogenesis. Excellent reviews on leveraging rodent malaria as an experimental system are available elsewhere (Lamikanra et al., 2007; De Niz and Heussler, 2018).

Murine models have extended insights from post-mortem studies and *in vitro* models of host-parasite interactions in the hematopoietic niche. One major avenue of investigation is in how, when, and at what stage parasites arrive in the bone marrow and exit into circulation. Intravital imaging during murine infection with a gametocyte-forming, fluorescent strain of *Plasmodium berghei* found gametocytes specifically accumulated in the extravascular space, arriving early in infection (De Niz et al., 2018). The same work demonstrated that gametocytes were enriched in RBC precursors in the bone marrow after 24 hours of infection and that mature gametocytes could translocate across the endothelial barrier from the bone marrow into circulation (De Niz et al., 2018). Infection with *P. berghei* has also revealed that parasites invade nucleated erythroblasts *in vivo* as well as enucleated, early reticulocytes (Lee et al., 2018). Single cell RNA-seq (scRNA-seq) of bone marrow HSPCs from *P. berghei*-infected mice revealed a shift in lineage commitment toward the myeloid and basophil lineages at the expense of erythroid and megakaryocyte production, revealing a potential mechanism of impaired red cell production during infection (Haltalli et al., 2020). In another study of *P. berghei* infection in the hematopoietic niche, infected cells from the spleen, bone marrow, and liver were analyzed by CITE-seq (Cellular Indexing of Transcriptomes and Epitopes by Sequencing) using antibodies against markers of erythroid maturation (Hentzschel et al., 2022). The authors found differences in parasite metabolism and likelihood of gametocyte commitment based on the maturation state of the host cell. Animal models are also key for investigating early infection events in the exoerythrocytic stage, which have received less attention in recent studies on the bone marrow. The finding that the hematopoietic niche responds to natural infection in the liver stage of *P. berghei* infection, including by increasing proliferation of HSC and loss of myeloid-committed progenitors, warrants further investigation of hematopoietic changes during the liver stage (Vainieri et al., 2016).

Mouse malaria has also provided insight into interactions between developing erythroid cells and the immune system. Infection with GFP-expressing *Plasmodium yoelii* yielded parasitized, nucleated erythroblasts in the bone marrow, again suggesting that infection of erythroid precursors is a generalized aspect of pathogenesis across *Plasmodium* species. Isolation of parasitized erythroblasts from infected mice showed that infected erythroid precursors express MHC class I at the cell surface and are capable of activating $CD8^+$ T cells. Several studies investigated dyserythropoiesis in the context of severe malaria anemia (SMA) using rodent malaria; however, the results are difficult to interpret due to differences in erythropoiesis and the manifestation of severe malaria in mice and humans (Lamikanra et al., 2007). Increased use of non-human primates to model malaria is a promising solution (Craig et al., 2012). New World monkeys belonging to the genus *Aotus* and *Saimiri* are infectable with *P. vivax* and histological studies of post-mortem tissue show parasites accumulated in the bone marrow (Obaldia et al., 2018). Vaccinated, semi-immune *Aotus* has also been suggested as model of SMA with features that are analogous to infection in children living in malaria-endemic areas (Egan et al., 2002). In contrast to mice, infection at low parasitemia produced severe malaria symptoms including bone marrow suppression (Egan et al., 2002).

FUTURE PERSPECTIVES

Existing models for *ex vivo* erythropoiesis, in combination with novel transcriptomic and proteomic strategies, have potential to provide a detailed picture of the host response to *P. falciparum* in erythroid progenitor cells. To date, host transcriptional responses in co-culture of *P. falciparum* and erythroblasts have only been studied in bulk. Improved resolution is needed to remove confounding factors from bulk readouts in an environment that contains a mix of cell types as well as uninfected and infected cells. Advances in surface phenotyping of developing erythroblasts by flow cytometry could be used to sort cell populations before sequencing (Hu et al., 2013; Li et al., 2014; Yan et al., 2018; Yan et al., 2021). Single cell RNA-seq (scRNA-seq) enables transcriptomic analysis of heterogeneous cell populations on the level of individual cells, and has yet to be applied to *Plasmodium*-infected erythroblasts in a human system. Single cell techniques at the protein-level could also be used to overcome artifacts from bulk analysis. Mass cytometry is an increasingly utilized way of monitoring expression of proteins that reflect complex cellular phenotypes and functions. Mass cytometry, also called Cytometry by Time of Flight (CyTOF), is a variation of flow cytometry in which elemental (heavy metal) isotopes are conjugated to antibodies in the place of fluorophores to allow dozens of markers to be analyzed simultaneously (Hartmann and Bendall, 2020). CyTOF has been successfully applied in many studies of hematopoiesis and to a limited extent, erythropoiesis (Thomson-Luque et al., 2018; Palii et al., 2019). This technology could be applied to study dyserythropoiesis in malaria infection, especially with the addition of a parasite marker to distinguish infected cells. The application of single cell technology to existing models would add to our understanding of host responses to parasite infection at different stages of erythropoiesis and generate testable hypotheses about mechanisms of dyserythropoiesis related to direct and indirect interactions between host and parasite.

The bone marrow is a challenging tissue to model *in vitro* because of its complex architecture, heterogeneous microenvironments, and diverse cell types. Current *in vitro* studies of *Plasmodium* in the hematopoietic niche are primarily limited to interactions with a single lineage, usually in 2D culture. To improve *in vitro* models of complex tissues and reduce reliance on animal research, there is growing interest in microfluidic organ-on-a-chip (OOAC) devices that are capable of mimicking physical cues, such as shear flow and mechanical stress, that regulate cell growth and differentiation (Wu et al., 2020; Li et al., 2021). In the study of malaria pathogenesis, OOACs have primarily been used to study how physical parameters of infected RBCs influence adhesion and accumulation in the microvasculature (Baddal and Marrazzo, 2021). Unlike capillary models, bone marrow-on-a-chip (BMoC) requires maintaining multiple cell types and a delicate balance of cytokines to coordinate self-renewal, proliferation, and lineage commitment of HSCs.

Recent methods for engineering BMoC have made promising advances for *in vitro* modeling of the hematopoietic niche. The first successful BMoC involved *in vivo* implantation of a device in murine bone marrow where new bone and blood-filled marrow would form that could then be removed and transferred to a microfluidic device for culture (Torisawa et al., 2014). The authors showed that the engineered bone marrow in culture contained differentiated blood cell lineages in similar proportions to *in vivo* bone marrow over 7 days of culture and that HSCs retained their self-renewal and lineage potential *in vitro* (Torisawa et al., 2014). Such a system would be useful for visualizing cell-cell interactions in co-culture with *Plasmodium* parasites enables the study of immune cell activity in the bone marrow in response to parasite infection. There has also been success with a human BMoC perfused device containing one chamber for 3D co-culture of $CD34^+$ cells and bone marrow stromal cells and a second chamber for culture of endothelial cells (Chou et al., 2020). The authors report proliferation of hematopoietic cells over 28 days of culture and differentiation down the erythroid and myeloid lineages. Interestingly, mature neutrophils and cells of the myeloid lineage intravasated into the chamber containing endothelial cells, mimicking exit of cells into the peripheral blood (Chou et al., 2020). This model would be especially useful for the study of factors involved in entry and exit of gametocytes in the bone marrow.

Although advancements in *ex vivo* culture of primary HSPCs hold promise, it is still important to consider host-parasite interactions in the context of human infection. An ideal animal model would allow study of human malaria species, particularly *P. falciparum* for investigation of chronic anemia of malaria. So-called "humanized" mice are a potential solution to the non-analogous aspects of murine erythropoiesis and malaria infection. Humanized mice have been successfully used to study accumulation of *P. falciparum* in deep tissue and test chemotherapy against sequestered gametocytes (Duffier et al., 2016). Such models have yet to be used in the study of dyserythropoiesis during malaria infection. The application of humanized mice would answer questions about the *in vivo* relevance of infection of erythroid progenitors and pave the way for studies of host responses related to the erythroid lineage.

CONCLUSIONS

A variety of approaches have been developed to model human erythropoiesis, enabling the study of *Plasmodium* host-parasite interactions in the hematopoietic niche. *Ex vivo* erythropoiesis of human primary HSPCs has provided important insights into gametocyte commitment and characterization of *Plasmodium* infection of a non-canonical host cell type, and holds potential as a powerful tool for dissecting host responses and mechanisms of impaired erythropoiesis during malaria infection. In combination with *in vivo* models, *ex vivo* erythropoiesis can be leveraged to provide insight into key aspects of malaria pathogenesis and transmission. As host-parasite interactions in the hematopoietic niche come into focus, so will opportunities for therapeutic interventions for dyserythropoiesis and strategies to eliminate transmission of malaria.

AUTHOR CONTRIBUTIONS

TF and EE designed and conceptualized the manuscript, carried out the literature search, generated the first draft of the manuscript, and reviewed and approved the final manuscript.

FUNDING

This work was supported by the National Institutes of Health under Award Numbers T32GM007276 (TF) and 1DP2HL13718601 (EE), and by a Burroughs Wellcome Fund PATH Award, under Award Number 1021370 (EE).

ACKNOWLEDGMENTS

We thank members of the Egan Lab for helpful discussions. Elizabeth S. Egan, M.D., Ph.D. holds an Investigators in the Pathogenesis of Infectious Disease Award from the Burroughs Wellcome Fund, and is a Tashia and John Morgridge Endowed Faculty Scholar in Pediatric Translational Medicine through the Stanford Maternal Child Health Research Institute.

REFERENCES

Abdalla, S., Weatherall, D. J., Wickramasinghe, S. N., and Hughes, M. (1980). The Anaemia of P. Falciparum Malaria. *Br. J. Haematol.* 46 (2), 171–183. doi: 10.1111/j.1365-2141.1980.tb05956.x

Aguilar, R., Magallon-Tejada, A., Achtman, A. H., Moraleda, C., Joice, R., Cistero, P., et al. (2014a). Molecular Evidence for the Localization of Plasmodium Falciparum Immature Gametocytes in Bone Marrow. *Blood* 123 (7), 959–966. doi: 10.1182/blood-2013-08-520767

Aguilar, R., Moraleda, C., Achtman, A. H., Mayor, A., Quinto, L., Cistero, P., et al. (2014b). Severity of Anaemia is Associated With Bone Marrow Haemozoin in Children Exposed to Plasmodium Falciparum. *Br. J. Haematol.* 164 (6), 877–887. doi: 10.1111/bjh.12716

Anstee, D. J., Gampel, A., and Toye, A. M. (2012). *Ex-Vivo* Generation of Human Red Cells for Transfusion. *Curr. Opin. Hematol.* 19 (3), 163–169. doi: 10.1097/MOH.0b013e328352240a

Baddal, B., and Marrazzo, P. (2021). Refining Host-Pathogen Interactions: Organ-On-Chip Side of the Coin. *Pathogens* 10 (2). doi: 10.3390/pathogens10020203

Bei, A. K., Brugnara, C., and Duraisingh, M. T. (2010). *In Vitro* Genetic Analysis of an Erythrocyte Determinant of Malaria Infection. *J. Infect. Dis.* 202 (11), 1722–1727. doi: 10.1086/657157

Casals-Pascual, C., Kai, O., Cheung, J. O., Williams, S., Lowe, B., Nyanoti, M., et al. (2006). Suppression of Erythropoiesis in Malarial Anemia is Associated With Hemozoin *In Vitro* and *In Vivo*. *Blood* 108 (8), 2569–2577. doi: 10.1182/blood-2006-05-018697

Caulier, A. L., and Sankaran, V. G. (2022). Molecular and Cellular Mechanisms That Regulate Human Erythropoiesis. *Blood* 139, 2450–2459. doi: 10.1182/blood.2021011044

Chou, D. B., Frismantas, V., Milton, Y., David, R., Pop-Damkov, P., Ferguson, D., et al. (2020). On-Chip Recapitulation of Clinical Bone Marrow Toxicities and Patient-Specific Pathophysiology. *Nat. BioMed. Eng.* 4 (4), 394–406. doi: 10.1038/s41551-019-0495-z

Craig, A. G., Grau, G. E., Janse, C., Kazura, J. W., Milner, D., Barnwell, J. W., et al. (2012). The Role of Animal Models for Research on Severe Malaria. *PloS Pathog.* 8 (2), e1002401. doi: 10.1371/journal.ppat.1002401

Daniels, D. E., Downes, D. J., Ferrer-Vicens, I., Ferguson, D. C. J., Singleton, B. K., Wilson, M. C., et al. (2020). Comparing the Two Leading Erythroid Lines BEL-A and HUDEP-2. *Haematologica* 105 (8), e389–e394. doi: 10.3324/haematol.2019.229211

De Niz, M., and Heussler, V. T. (2018). Rodent Malaria Models: Insights Into Human Disease and Parasite Biology. *Curr. Opin. Microbiol.* 46, 93–101. doi: 10.1016/j.mib.2018.09.003

De Niz, M., Meibalan, E., Mejia, P., Ma, S., Brancucci, N. M. B., Agop-Nersesian, C., et al. (2018). Plasmodium Gametocytes Display Homing and Vascular Transmigration in the Host Bone Marrow. *Sci. Adv.* 4 (5), eaat3775. doi: 10.1126/sciadv.aat3775

Dias, J., Gumenyuk, M., Kang, H., Vodyanik, M., Yu, J., Thomson, J. A., et al. (2011). Generation of Red Blood Cells From Human Induced Pluripotent Stem Cells. *Stem Cells Dev.* 20 (9), 1639–1647. doi: 10.1089/scd.2011.0078

Dormer, P., Dietrich, M., Kern, P., and Horstmann, R. D. (1983). Ineffective Erythropoiesis in Acute Human P. Falciparum Malaria. *Blut* 46 (5), 279–288.

Doulatov, S., Notta, F., Laurenti, E., and Dick, J. E. (2012). Hematopoiesis: A Human Perspective. *Cell Stem Cell* 10 (2), 120–136. doi: 10.1016/j.stem.2012.01.006

Duffier, Y., Lorthiois, A., Cistero, P., Dupuy, F., Jouvion, G., Fiette, L., et al. (2016). A Humanized Mouse Model for Sequestration of Plasmodium Falciparum Sexual Stages and *In Vivo* Evaluation of Gametocytidal Drugs. *Sci. Rep.* 6, 35025. doi: 10.1038/srep35025

Egan, A. F., Fabucci, M. E., Saul, A., Kaslow, D. C., and Miller, L. H. (2002). Aotus New World Monkeys: Model for Studying Malaria-Induced Anemia. *Blood* 99 (10), 3863–3866. doi: 10.1182/blood.v99.10.3863

Egan, E. S., Jiang, R. H., Moechtar, M. A., Barteneva, N. S., Weekes, M. P., Nobre, L. V., et al. (2015). Malaria. A Forward Genetic Screen Identifies Erythrocyte CD55 as Essential for Plasmodium Falciparum Invasion. *Science* 348 (6235), 711–714. doi: 10.1126/science.aaa3526

Fibach, E., Manor, D., Oppenheim, A., and Rachmilewitz, E. A. (1989). Proliferation and Maturation of Human Erythroid Progenitors in Liquid Culture. *Blood* 73 (1), 100–103.

Freyssinier, J. M., Lecoq-Lafon, C., Amsellem, S., Picard, F., Ducrocq, R., Mayeux, P., et al. (1999). Purification, Amplification and Characterization of a Population of Human Erythroid Progenitors. *Br. J. Haematol.* 106 (4), 912–922. doi: 10.1046/j.1365-2141.1999.01639.x

Friend, C., Scher, W., Holland, J. G., and Sato, T. (1971). Hemoglobin Synthesis in Murine Virus-Induced Leukemic Cells *In Vitro*: Stimulation of Erythroid Differentiation by Dimethyl Sulfoxide. *Proc. Natl. Acad. Sci. U.S.A.* 68 (2), 378–382. doi: 10.1073/pnas.68.2.378

Giani, F. C., Fiorini, C., Wakabayashi, A., Ludwig, L. S., Salem, R. M., Jobaliya, C. D., et al. (2016). Targeted Application of Human Genetic Variation Can Improve Red Blood Cell Production From Stem Cells. *Cell Stem Cell* 18 (1), 73–78. doi: 10.1016/j.stem.2015.09.015

Giarratana, M. C., Kobari, L., Lapillonne, H., Chalmers, D., Kiger, L., Cynober, T., et al. (2005). *Ex-Vivo* Generation of Fully Mature Human Red Blood Cells From Hematopoietic Stem Cells. *Nat. Biotechnol.* 23 (1), 69–74. doi: 10.1038/nbt1047

Giarratana, M. C., Rouard, H., Dumont, A., Kiger, L., Safeukui, I., Le Pennec, P. Y., et al. (2011). Proof of Principle for Transfusion of *In Vitro*-Generated Red Blood Cells. *Blood* 118 (19), 5071–5079. doi: 10.1182/blood-2011-06-362038

Giribaldi, G., Ulliers, D., Schwarzer, E., Roberts, I., Piacibello, W., and Arese, P. (2004). Hemozoin- and 4-Hydroxynonenal-Mediated Inhibition of Erythropoiesis. Possible Role in Malarial Dyserythropoiesis and Anemia. *Haematologica* 89 (4), 492–493.

Gregory, C. J., and Eaves, A. C. (1978). Three Stages of Erythropoietic Progenitor Cell Differentiation Distinguished by a Number of Physical and Biologic Properties. *Blood* 51 (3), 527–537.

Haltalli, M. L. R., Watcham, S., Wilson, N. K., Eilers, K., Lipien, A., Ang, H., et al. (2020). Manipulating Niche Composition Limits Damage to Haematopoietic Stem Cells During Plasmodium Infection. *Nat. Cell Biol.* 22 (12), 1399–1410. doi: 10.1038/s41556-020-00601-w

Hanna, J., Wernig, M., Markoulaki, S., Sun, C. W., Meissner, A., Cassady, J. P., et al. (2007). Treatment of Sickle Cell Anemia Mouse Model With iPS Cells Generated From Autologous Skin. *Science* 318 (5858), 1920–1923. doi: 10.1126/science.1152092

Hartmann, F. J., and Bendall, S. C. (2020). Immune Monitoring Using Mass Cytometry and Related High-Dimensional Imaging Approaches. *Nat. Rev. Rheumatol.* 16 (2), 87–99. doi: 10.1038/s41584-019-0338-z

Hattangadi, S. M., Wong, P., Zhang, L., Flygare, J., and Lodish, H. F. (2011). From Stem Cell to Red Cell: Regulation of Erythropoiesis at Multiple Levels by Multiple Proteins, RNAs, and Chromatin Modifications. *Blood* 118 (24), 6258–6268. doi: 10.1182/blood-2011-07-356006

Hentzschel, F., Gibbins, M. P., Attipa, C., Beraldi, D., Moxon, C., Otto, T. D., et al. (2022). Host Cell Maturation Modulates Parasite Invasion and Sexual Differentiation in *Plasmodium berghei*. *Sci. Adv.* 8, eabm7348. doi: 10.1126/sciadv.abm7348

Hom, J., Dulmovits, B. M., Mohandas, N., and Blanc, L. (2015). The Erythroblastic Island as an Emerging Paradigm in the Anemia of Inflammation. *Immunol. Res.* 63 (1-3), 75–89. doi: 10.1007/s12026-015-8697-2

Hu, J., Liu, J., Xue, F., Halverson, G., Reid, M., Guo, A., et al. (2013). Isolation and Functional Characterization of Human Erythroblasts at Distinct Stages: Implications for Understanding of Normal and Disordered Erythropoiesis *In Vivo*. *Blood* 121 (16), 3246–3253. doi: 10.1182/blood-2013-01-476390

Joice, R., Nilsson, S. K., Montgomery, J., Dankwa, S., Egan, E., Morahan, B., et al. (2014). Plasmodium Falciparum Transmission Stages Accumulate in the Human Bone Marrow. *Sci. Transl. Med.* 6 (244), 244re245. doi: 10.1126/scitranslmed.3008882

Kanjee, U., Gruring, C., Chaand, M., Lin, K. M., Egan, E., Manzo, J., et al. (2017). CRISPR/Cas9 Knockouts Reveal Genetic Interaction Between Strain-Transcendent Erythrocyte Determinants of Plasmodium Falciparum Invasion. *Proc. Natl. Acad. Sci. U.S.A.* 114 (44), E9356–E9365. doi: 10.1073/pnas.1711310114

Kurita, R., Suda, N., Sudo, K., Miharada, K., Hiroyama, T., Miyoshi, H., et al. (2013). Establishment of Immortalized Human Erythroid Progenitor Cell Lines Able to Produce Enucleated Red Blood Cells. *PloS One* 8 (3), e59890. doi: 10.1371/journal.pone.0059890

Lamikanra, A. A., Brown, D., Potocnik, A., Casals-Pascual, C., Langhorne, J., and Roberts, D. J. (2007). Malarial Anemia: Of Mice and Men. *Blood* 110 (1), 18–28. doi: 10.1182/blood-2006-09-018069

Lamikanra, A. A., Merryweather-Clarke, A. T., Tipping, A. J., and Roberts, D. J. (2015). Distinct Mechanisms of Inadequate Erythropoiesis Induced by Tumor Necrosis Factor Alpha or Malarial Pigment. *PloS One* 10 (3), e0119836. doi: 10.1371/journal.pone.0119836

Lee, R. S., Waters, A. P., and Brewer, J. M. (2018). A Cryptic Cycle in Haematopoietic Niches Promotes Initiation of Malaria Transmission and Evasion of Chemotherapy. *Nat. Commun.* 9 (1), 1689. doi: 10.1038/s41467-018-04108-9

Li, J., Hale, J., Bhagia, P., Xue, F., Chen, L., Jaffray, J., et al. (2014). Isolation and Transcriptome Analyses of Human Erythroid Progenitors. *Blood* 124 (24), 3636–3645. doi: 10.1182/blood-2014-07-588806

Li, H., Luo, Q., Shan, W., Cai, S., Tie, R., Xu, Y., et al. (2021). Biomechanical Cues as Master Regulators of Hematopoietic Stem Cell Fate. *Cell Mol. Life Sci.* 78 (16), 5881–5902. doi: 10.1007/s00018-021-03882-y

Marchiafava, E., and Bigmani, A. (1894). "On Summer-Autumn Malarial Fevers," in *Two Monographs on Malaira and the Parasites of Malairal Fevers*. Ed. E. Marchiafava (London: New Syndenham Society), 1–232.

Metcalf, D. (1993). The Molecular Control of Proliferation and Differentiation in Hemopoietic Cells. *C R Acad. Sci. III* 316 (9), 860–870.

Nemeth, E., Rivera, S., Gabayan, V., Keller, C., Taudorf, S., Pedersen, B. K., et al. (2004). IL-6 Mediates Hypoferremia of Inflammation by Inducing the Synthesis of the Iron Regulatory Hormone Hepcidin. *J. Clin. Invest.* 113 (9), 1271–1276. doi: 10.1172/JCI20945

Neveu, G., Richard, C., Dupuy, F., Behera, P., Volpe, F., Subramani, P. A., et al. (2020). Plasmodium Falciparum Sexual Parasites Develop in Human Erythroblasts and Affect Erythropoiesis. *Blood* 136 (12), 1381–1393. doi: 10.1182/blood.2019004746

Obaldia, N., Meibalan, E., Sa, J. M., Ma, S., Clark, M. A., Mejia, P., et al. (2018). Bone Marrow Is a Major Parasite Reservoir in Plasmodium Vivax Infection. *mBio* 9 (3). doi: 10.1128/mBio.00625-18

Okuno, Y., Suzuki, A., Ichiba, S., Takahashi, T., Nakamura, K., Hitomi, K., et al. (1990). Establishment of an Erythroid Cell Line (JK-1) That Spontaneously Differentiates to Red Cells. *Cancer* 66 (7), 1544–1551. doi: 10.1002/1097-0142(19901001)66:7<1544::AID-CNCR2820660719>3.0.CO;2-9

Palii, C. G., Cheng, Q., Gillespie, M. A., Shannon, P., Mazurczyk, M., Napolitani, G., et al. (2019). Single-Cell Proteomics Reveal That Quantitative Changes in Co-Expressed Lineage-Specific Transcription Factors Determine Cell Fate. *Cell Stem Cell* 24 (5), 812–820, e815. doi: 10.1016/j.stem.2019.02.006

Panichakul, T., Sattabongkot, J., Chotivanich, K., Sirichaisinthop, J., Cui, L., and Udomsangpetch, R. (2007). Production of Erythropoietic Cells *In Vitro* for Continuous Culture of Plasmodium Vivax. *Int. J. Parasitol.* 37 (14), 1551–1557. doi: 10.1016/j.ijpara.2007.05.009

Panzenbock, B., Bartunek, P., Mapara, M. Y., and Zenke, M. (1998). Growth and Differentiation of Human Stem Cell Factor/Erythropoietin-Dependent Erythroid Progenitor Cells *In Vitro*. *Blood* 92 (10), 3658–3668.

Pathak, V., Colah, R., and Ghosh, K. (2018). Plasmodium Falciparum Malaria Skews Globin Gene Expression Balance in *in-Vitro* Haematopoietic Stem Cell Culture System: Its Implications in Malaria Associated Anemia. *Exp. Parasitol.* 185, 29–38. doi: 10.1016/j.exppara.2018.01.003

Satchwell, T. J., Wright, K. E., Haydn-Smith, K. L., Sanchez-Roman Teran, F., Moura, P. L., Hawksworth, J., et al. (2019). Genetic Manipulation of Cell Line Derived Reticulocytes Enables Dissection of Host Malaria Invasion Requirements. *Nat. Commun.* 10 (1), 3806. doi: 10.1038/s41467-019-11790-w

Shakya, B., Patel, S. D., Tani, Y., and Egan, E. S. (2021). Erythrocyte CD55 Mediates the Internalization of Plasmodium Falciparum Parasites. *Elife* 10. doi: 10.7554/eLife.61516

Skorokhod, O. A., Caione, L., Marrocco, T., Migliardi, G., Barrera, V., Arese, P., et al. (2010). Inhibition of Erythropoiesis in Malaria Anemia: Role of Hemozoin and Hemozoin-Generated 4-Hydroxynonenal. *Blood* 116 (20), 4328–4337. doi: 10.1182/blood-2010-03-272781

Sui, X., Krantz, S. B., and Zhao, Z. J. (2000). Stem Cell Factor and Erythropoietin Inhibit Apoptosis of Human Erythroid Progenitor Cells Through Different Signalling Pathways. *Br. J. Haematol.* 110 (1), 63–70. doi: 10.1046/j.1365-2141.2000.02145.x

Sui, X., Tsuji, K., Tajima, S., Tanaka, R., Muraoka, K., Ebihara, Y., et al. (1996). Erythropoietin-Independent Erythrocyte Production: Signals Through Gp130 and C-Kit Dramatically Promote Erythropoiesis From Human CD34+ Cells. *J. Exp. Med.* 183 (3), 837–845. doi: 10.1084/jem.183.3.837

Tamez, P. A., Liu, H., Fernandez-Pol, S., Haldar, K., and Wickrema, A. (2009). Stage-Specific Susceptibility of Human Erythroblasts to Plasmodium Falciparum Malaria Infection. *Blood* 114 (17), 3652–3655. doi: 10.1182/blood-2009-07-231894

Tamez, P. A., Liu, H., Wickrema, A., and Haldar, K. (2011). P. Falciparum Modulates Erythroblast Cell Gene Expression in Signaling and Erythrocyte Production Pathways. *PloS One* 6 (5), e19307. doi: 10.1371/journal.pone.0019307

Thomson-Luque, R., Wang, C., Ntumngia, F. B., Xu, S., Szekeres, K., Conway, A., et al. (2018). In-Depth Phenotypic Characterization of Reticulocyte Maturation Using Mass Cytometry. *Blood Cells Mol. Dis.* 72, 22–33. doi: 10.1016/j.bcmd.2018.06.004

Torisawa, Y. S., Spina, C. S., Mammoto, T., Mammoto, A., Weaver, J. C., Tat, T., et al. (2014). Bone Marrow-on-a-Chip Replicates Hematopoietic Niche Physiology *In Vitro*. *Nat. Methods* 11 (6), 663–669. doi: 10.1038/nmeth.2938

Trakarnsanga, K., Griffiths, R. E., Wilson, M. C., Blair, A., Satchwell, T. J., Meinders, M., et al. (2017). An Immortalized Adult Human Erythroid Line Facilitates Sustainable and Scalable Generation of Functional Red Cells. *Nat. Commun.* 8, 14750. doi: 10.1038/ncomms14750

Trakarnsanga, K., Wilson, M. C., Griffiths, R. E., Toye, A. M., Carpenter, L., Heesom, K. J., et al. (2014). Qualitative and Quantitative Comparison of the Proteome of Erythroid Cells Differentiated From Human iPSCs and Adult Erythroid Cells by Multiplex TMT Labelling and nanoLC-Ms/MS. *PloS One* 9 (7), e100874. doi: 10.1371/journal.pone.0100874

Tsiftsoglou, A. S., Vizirianakis, I. S., and Strouboulis, J. (2009). Erythropoiesis: Model Systems, Molecular Regulators, and Developmental Programs. *IUBMB Life* 61 (8), 800–830. doi: 10.1002/iub.226

Vainieri, M. L., Blagborough, A. M., MacLean, A. L., Haltalli, M. L., Ruivo, N., Fletcher, H. A., et al. (2016). Systematic Tracking of Altered Haematopoiesis During Sporozoite-Mediated Malaria Development Reveals Multiple Response Points. *Open Biol.* 6 (6). doi: 10.1098/rsob.160038

von Lindern, M., Zauner, W., Mellitzer, G., Steinlein, P., Fritsch, G., Huber, K., et al. (1999). The Glucocorticoid Receptor Cooperates With the Erythropoietin Receptor and C-Kit to Enhance and Sustain Proliferation of Erythroid Progenitors *In Vitro*. *Blood* 94 (2), 550–559.

Wada, H., Suda, T., Miura, Y., Kajii, E., Ikemoto, S., and Yawata, Y. (1990). Expression of Major Blood Group Antigens on Human Erythroid Cells in a Two Phase Liquid Culture System. *Blood* 75 (2), 505–511.

WHO (2021). *"World Malaria Report 2021"* (Geneva: World Health Organization).

Wickramasinghe, S. N., Phillips, R. E., Looareesuwan, S., Warrell, D. A., and Hughes, M. (1987). The Bone Marrow in Human Cerebral Malaria: Parasite Sequestration Within Sinusoids. *Br. J. Haematol.* 66 (3), 295–306. doi: 10.1111/j.1365-2141.1987.tb06913.x

Wu, Q., Liu, J., Wang, X., Feng, L., Wu, J., Zhu, X., et al. (2020). Organ-On-a-Chip: Recent Breakthroughs and Future Prospects. *BioMed. Eng. Online* 19 (1), 9. doi: 10.1186/s12938-020-0752-0

Yan, H., Ali, A., Blanc, L., Narla, A., Lane, J. M., Gao, E., et al. (2021). Comprehensive Phenotyping of Erythropoiesis in Human Bone Marrow: Evaluation of Normal and Ineffective Erythropoiesis. *Am. J. Hematol.* 96 (9), 1064–1076. doi: 10.1002/ajh.26247

Yan, H., Hale, J., Jaffray, J., Li, J., Wang, Y., Huang, Y., et al. (2018). Developmental Differences Between Neonatal and Adult Human Erythropoiesis. *Am. J. Hematol.* 93 (4), 494–503. doi: 10.1002/ajh.25015

Zivot, A., Lipton, J. M., Narla, A., and Blanc, L. (2018). Erythropoiesis: Insights Into Pathophysiology and Treatments in 2017. *Mol. Med.* 24 (1), 11. doi: 10.1186/s10020-018-0011-z

Conflict of Interest: The authors declare that the research was conducted in the absence of any commercial or financial relationships that could be construed as a potential conflict of interest.

frontiers | Frontiers in Cellular and Infection Microbiology

ORIGINAL RESEARCH
published: 16 June 2022
doi: 10.3389/fcimb.2022.877253

Differential Trafficking and Expression of PIR Proteins in Acute and Chronic *Plasmodium* Infections

*Maria Giorgalli[1], Deirdre A. Cunningham[1], Malgorzata Broncel[2], Aaron Sait[3], Thomas E. Harrison[4], Caroline Hosking[1], Audrey Vandomme[1], Sarah I. Amis[1], Ana Antonello[1], Lauren Sullivan[1], Faith Uwadiae[1], Laura Torella[1], Matthew K. Higgins[4] and Jean Langhorne[1]**

[1] Malaria Immunology Laboratory, The Francis Crick Institute, London, United Kingdom, [2] Proteomics Science Technology Platform, The Francis Crick Institute, London, United Kingdom, [3] Electron Microscopy Science Technology Platform, The Francis Crick Institute, London, United Kingdom, [4] Laboratory of Molecular Parasitology, Department of Biochemistry, University of Oxford, Oxford, United Kingdom

OPEN ACCESS

Edited by:
Alister Craig, Liverpool School of Tropical Medicine, United Kingdom

Reviewed by:
Andrew Oleinikov, Florida Atlantic University, United States
Eri Saki H. Hayakawa, Jichi Medical University, Japan

***Correspondence:**
Jean Langhorne
Jean.Langhorne@crick.ac.uk

Specialty section:
This article was submitted to Parasite and Host, a section of the journal Frontiers in Cellular and Infection Microbiology

Received: *16 February 2022*
Accepted: *12 May 2022*
Published: *16 June 2022*

Citation:
Giorgalli M, Cunningham DA, Broncel M, Sait A, Harrison TE, Hosking C, Vandomme A, Amis SI, Antonello A, Sullivan L, Uwadiae F, Torella L, Higgins MK and Langhorne J (2022) Differential Trafficking and Expression of PIR Proteins in Acute and Chronic Plasmodium Infections. Front. Cell. Infect. Microbiol. 12:877253. doi: 10.3389/fcimb.2022.877253

Plasmodium multigene families are thought to play important roles in the pathogenesis of malaria. *Plasmodium interspersed repeat (pir)* genes comprise the largest multigene family in many *Plasmodium* species. However, their expression pattern and localisation remain to be elucidated. Understanding protein subcellular localisation is fundamental to reveal the functional importance and cell-cell interactions of the PIR proteins. Here, we use the rodent malaria parasite, *Plasmodium chabaudi chabaudi*, as a model to investigate the localisation pattern of this gene family. We found that most PIR proteins are co-expressed in clusters during acute and chronic infection; members of the S7 clade are predominantly expressed during the acute-phase, whereas members of the L1 clade dominate the chronic-phase of infection. Using peptide antisera specific for S7 or L1 PIRS, we show that these PIRs have different localisations within the infected red blood cells. S7 PIRs are exported into the infected red blood cell cytoplasm where they are co-localised with parasite-induced host cell modifications termed Maurer's clefts, whereas L1 PIRs are localised on or close to the parasitophorous vacuolar membrane. This localisation pattern changes following mosquito transmission and during progression from acute- to chronic-phase of infection. The presence of PIRs in Maurer's clefts, as seen for *Plasmodium falciparum* RIFIN and STEVOR proteins, might suggest trafficking of the PIRs on the surface of the infected erythrocytes. However, neither S7 nor L1 PIR proteins detected by the peptide antisera are localised on the surface of infected red blood cells, suggesting that they are unlikely to be targets of surface variant-specific antibodies or to be directly involved in adhesion of infected red blood cells to host cells, as described for *Plasmodium falciparum* VAR proteins. The differences in subcellular localisation of the two major clades of *Plasmodium chabaudi* PIRs across the blood cycle, and the apparent lack of expression on the red cell surface strongly suggest that the function(s) of this gene family may differ from those of other multigene families of *Plasmodium*, such as the *var* genes of *Plasmodium falciparum*.

Keywords: malaria, *Plasmodium*, multigene families, *pir* genes, acute infection, chronic infection

1 INTRODUCTION

Plasmodium multigene families are thought to play important roles in malaria pathogenesis and immune evasion. The largest multigene family is the *Plasmodium interspersed repeat* (*pir*) gene family. This gene family is present in the genomes of many *Plasmodium* species including those infecting rodents and human, with the exception of the Laverania subgenus such as *Plasmodium falciparum* (Janssen et al., 2002; Yam et al., 2016). The number of *pir* genes varies considerably between the species, from 134 members in *Plasmodium berghei*, up to 1949 members in *Plasmodium ovale curtisi* (Aurrecoechea et al., 2009; Rutledge et al., 2017). Unlike the most highly studied multigene family, the *var* gene family of *Plasmodium falciparum*, the members of which are thought to be involved in antigenic variation, immune evasion and sequestration to host tissues (Buffet et al., 2011; Scherf et al., 1998; Scherf et al., 2008), the function of *pirs* remains unknown. In contrast to the *var* genes (Scherf et al., 1998), multiple *pir* genes are expressed simultaneously in the same blood-stage parasite (Cunningham et al., 2009; Howick et al., 2019; Otto et al., 2014; Reid et al., 2018; Sa et al., 2020) suggesting that antigenic variation of proteins on the surface of infected red blood cells (iRBC) may not be one of the roles of PIRs.

To elucidate the function of PIRs, it is necessary to be able to study them in a tractable experimental model. *Plasmodium chabaudi* is a well-studied, robust model to investigate mechanisms of immune evasion and antigenic variation, in particular with regards to the *pir* genes (Lamb et al., 2006; Langhorne et al., 2008). There are approximately 200 *pir* genes in *Plasmodium chabaudi chabaudi*. In the AS strain, the most commonly established laboratory strain, parasites isolated from the acute-phase of a mosquito-transmitted (MT) blood-stage infection have a different transcriptional profile of *pir* genes and show different virulence behaviour compared to those isolated at the chronic-phase of infection (Brugat et al., 2017; Spence et al., 2013). *Pir* genes of the S7 clade within particular loci called acute-associated loci (AAPLs) are more highly expressed in the acute-phase of infection and are associated with avirulent infection, whereas a more restricted number of *pirs* from the L1 clade that are associated with the chronic-associated loci (ChAPLs) are highly transcribed during the chronic-phase of infection and are associated with a more virulent course of infection (Brugat et al., 2017). This change from predominantly S7 to L1-expressing parasites and this association has suggested a role of *pirs* in virulence of the blood-stage infections (Brugat et al., 2017).

Earlier immunofluorescence studies using *P. chabaudi pir* genes expressed in *Plasmodium yoelii*, or transgenic *P. berghei* parasites expressing a known *pir*/*bir* gene and *P. falciparum* expressing a *Plasmodium vivax pir*, have shown PIR proteins to be present in all compartments of an iRBC during asexual development: exported to the host-cell cytosol, on the parasitophorous vacuolar membrane (PVM) or within the parasitophorous vacuole (PV) and parasite cytosol (Cunningham et al., 2005; Del Portillo et al., 2001; Fougere et al., 2016; Pasini et al., 2013; Yam et al., 2016) and are also associated with lipid rafts (or detergent-resistant membranes) in these species (Di Girolamo et al., 2008). Some studies indicate that, in fixed preparations of *Plasmodium*-infected RBCs, PIR proteins may also be present on, or close to the infected erythrocyte surface (Cunningham et al., 2005; Del Portillo et al., 2001; Pasini et al., 2013; Yam et al., 2016). A number of other *P. falciparum* multigene families, known to be associated with the parasites' ability to sequester and evade the host immunity, are also destined for the surface of iRBC, through the Maurer's clefts, the parasites' trafficking platforms for export of proteins to the erythrocyte surface (Sam-Yellowe 2009). The foremost exported protein *via* the Maurer's clefts is *Pf*EMP1, also a virulence factor that mediates cytoadherence and sequestration of late-stage–infected erythrocytes in deep tissues (Baruch et al., 1996; Kyes et al., 2001; Leech et al., 1984; Su et al., 1995). Other virulence proteins transiently associated with Maurer's clefts on their way to the erythrocyte plasma membrane are the *P. falciparum* RIFINs, STEVOR, *Pf*MC-2TMm, FIKK kinase and probably members of the CLAG family (Ekland et al., 2011; Kaviratne et al., 2002; Nunes et al., 2007; Przyborski et al., 2005; Tsarukyanova et al., 2009).

Here, we show that neither S7 nor L1 PIR proteins could be detected on the surface of live unfixed iRBC, suggesting that they are unlikely to be targets of surface variant-specific antibodies or be involved directly in adhesion of iRBC to host cells. The differences in subcellular localisation of the two major clades of *P. chabaudi* PIRs across the blood cycle and the apparent lack of expression on the red cell surface, strongly suggest that this gene family possibly has diverse functions that could further differ from those known functions of the *var* genes in *Plasmodium falciparum.* Using the *P. chabaudi* model for PIRs, we report here a detailed study of PIR expression of the two major clades of *P. chabaudi* PIR proteins, S7 and L1, in blood-stage parasites following mosquito transmission, in order to obtain a clearer definition of their location in RBC infected with wild-type (WT) *P. chabaudi* parasites. Elucidation of their localisation and proteomic profile following natural transmission may give us clues to the potential functions of PIR proteins and cell-cell interactions during malaria infection.

2 MATERIALS AND METHODS

2.1 Mouse and Parasite Lines Used

All experiments were performed in accordance with the UK Animals (Scientific Procedures) Act 1986 (PPL 70/8326 and PADD88D48) and were approved by The Francis Crick Institute Ethical Committee. V(D)J recombination activation gene RAG1 knockout (RAG1$^{-/-}$) (Mombaerts et al., 1992) on a C57BL/6 background and C57BL/6 WT mice were obtained from the specific-pathogen-free (SPF) unit and subsequently conventionally housed with autoclaved cages, bedding and food at the Biological Research Facility (BRF) of the Francis Crick Institute. Experiments were performed with six- to eight-week-old female mice under reverse light conditions (light 19:00pm-07:00am and dark 07:00am-19:00pm), at 20-22°C.

Cloned lines of *P. chabaudi chabaudi AS* parasites were used (originally obtained from David Walliker, University of Edinburgh, UK). To initiate infection, mice were injected intraperitoneally (i.p.) with 1 x 10^5 infected erythrocytes or submitted to the bites of 25 infected mosquitoes, as previously described (Spence et al., 2012). Parasitaemia was monitored by the counting of blood stage parasites in air dried, methanol fixed, and Giemsa (Sigma)-stained thin tail-blood smears.

2.2 Production of *P. chabaudi* Anti-Peptide Antisera

Protein sequences from all members of the S7 and L1 PIR clades were collated and analysed *via* the MEME suite of bioinformatics software to identify the top ten most conserved peptide motifs within those clades. From these motifs, those located within the C-terminal hydrophobic domain of the proteins were excluded from further analysis. The remaining motif sequences were aligned to their target and off-target PIR clades, to choose those that match as many proteins as possible within the target clade and *vice versa*. The original sequences, taken directly from the candidate PIR proteins, were taken forward. L1 motif 1: CKTNYERINALGAYLY; L1 motif 2: ACTLLREVDAYFNNE; S7 motif 1: CEKCSKDAKEFVNKYNELN; S7 motif 2: CHSYDEMISSAVLFF. Both L1 motifs match the N-terminal of the L1 clade PIRs (39% and 76% conserved among all L1-clade members, respectively), whereas one of the S7 motifs aligns at the N-terminal (58% conserved among all S7-clade members) and the other at the C-terminal (45% conserved among all S7-clade members) of the S7 clade PIRs (**Figure 1A**). The proportion of L1 and S7 clade PIRs targeted by each peptide are summarised in **Supplementary Table S1**. BlastP hits and scores are listed in **Supplementary Table S2**.

The peptides were commercially generated and chemically coupled to a KLH carried protein in order to stabilize the peptide and elicit a stronger and more persistent immunological response. The conjugated to KLH peptides were then used to immunise rabbits and generate the anti-S7 and anti-L1 specific antisera (Cambridge Research Biochemicals, Billingham, UK). Their immunoreactivity to the peptides was verified using standard Enzyme-Linked Immunosorbent Assay (ELISA) procedures. To maximise the proportion of PIRs belonging to the same clade that are recognised by the individual peptide antisera (named anti-S7 motif 1 peptide antiserum, anti-S7 motif 2 peptide antiserum etc), we pooled together the two antisera generated against the two individual motifs that belong to each clade (named anti-S7 and anti-L1 peptide antisera). The individual peptide antisera were mixed proportionally to guarantee similar levels of reactivity with the PIR proteins.

2.3 *P. chabaudi* PIR Proteins Expression and Purification

Synthetic genes encoding a panel of *P. chabaudi* PIR proteins (PCHAS_1200500, PCHAS_1100300, PCHAS_0600600, PCHAS_0400300 and PCHAS_1300101) were cloned into the AscI (NEB) and NotI (NEB) restriction sites of the pTT3 vector (Crosnier et al., 2013) that carries a C-terminal His6 tag. Putative C-terminal hydrophobic domains were removed, and putative *N*-linked glycosylation sites were removed through mutation of the S or T residue of the NxS/T motif to alanine.

Protein expression and purification were carried out as previously described (Harrison et al., 2020). Briefly, all plasmids were transfected into HEK293F cells (Thermo Fisher Scientific) using polyethylenimine, and after five days (density of about 2.5x10^6 cells/mL) harvested by centrifugation at 5,000 × *g*. The supernatant was buffer-exchanged into 20 mM HEPES pH 7.5, 150 mM NaCl, and 20 mM imidazole by tangential flow filtration, and the protein was purified by immobilised metal affinity chromatography using Ni^{2+}-NTA resin, followed by size exclusion chromatography using a Superdex 75 10/300 column (GE Healthcare Life Sciences).

2.4 ELISA

PCHAS_1200500, PCHAS_1100300, PCHAS_0600600, PCHAS_0400300 and PCHAS_1300101 were purified as described above and re-solubilised in 1 x PBS. For the preparation of parasite protein lysates, whole blood was depleted of leukocytes by filtration (Plasmodipur, EuroProxima) and red cell debris by saponin lysis (Sigma) and centrifugation. Purified parasites were then lysed in RIPA buffer (Sigma) supplemented with 1% SDS (ThermoFisher) and 10 µg/mL (1X) Protease Inhibitors (PI) (cOmplete EDTA free, Roche). Approximately 5 µg/mL in 1 x Phosphate Buffered Saline (PBS) (pH 7.4) of each recombinant protein and 50 µg/mL in 1 x PBS of parasite protein lysate were propped with the titrated (two-fold serial dilutions) rabbit anti-peptide antisera, using standard ELISA assay procedures (Spence et al., 2013). Starting concentrations of the antisera were anti-S7 motif 1 peptide antiserum (1:500), anti-S7 motif 2 peptide antiserum (1:500), anti-L1 motif 1 peptide antiserum (1:500), anti-L1 motif 2 peptide antiserum (1:500), anti-S7 peptide antiserum (pooled motif 1 and 2) (1:1000), anti-L1 peptide antiserum (pooled motif 1 and 2) (1:1000), anti-S7 pre-immune serum (1:1000) and anti-L1 pre-immune serum (1:1000) in 1% (w/v) BSA, 0.3% (v/v) in 1x PBS, incubated at 37°C for 1.5 h. Following three washes with 0.25% (v/v) Tween-20 (Sigma) in 1 x PBS, wells were incubated with goat anti-rabbit IgG (H+L) alkaline phosphatase conjugated secondary antibody (Southern Biotech) for 1 h at 37°C. Samples were developed with 1 mg/mL 4-Nitrophenyl phosphate disodium salt hexahydrate (PNPP; Sigma) and OD was measured at 405 nm on a Tecan Infinite M1000 plate reader (LifeSciences). Data were analysed with Magenta software (LifeSciences).

2.5 Membrane Fractionation of Parasitised Erythrocytes, Protein Sample Preparation and Western Blotting

For the preparation of *P. chabaudi* membrane fractionated samples, magnetically enriched infected erythrocytes at the trophozoite-stage were pelleted in aliquots of 2.5 x 10^6 iRBC and then resuspended into approximately 20 µL (10 volumes of the pellet volume) in 1 x PBS containing 4 haemolytic units of activated Streptolysin-O (SLO) (Sigma), as previously described (Jackson et al., 2007; Ruecker et al., 2012). Following incubation for 15 min at 37°C, the parasite-containing fractions were separated by centrifugation at 12,400 × g

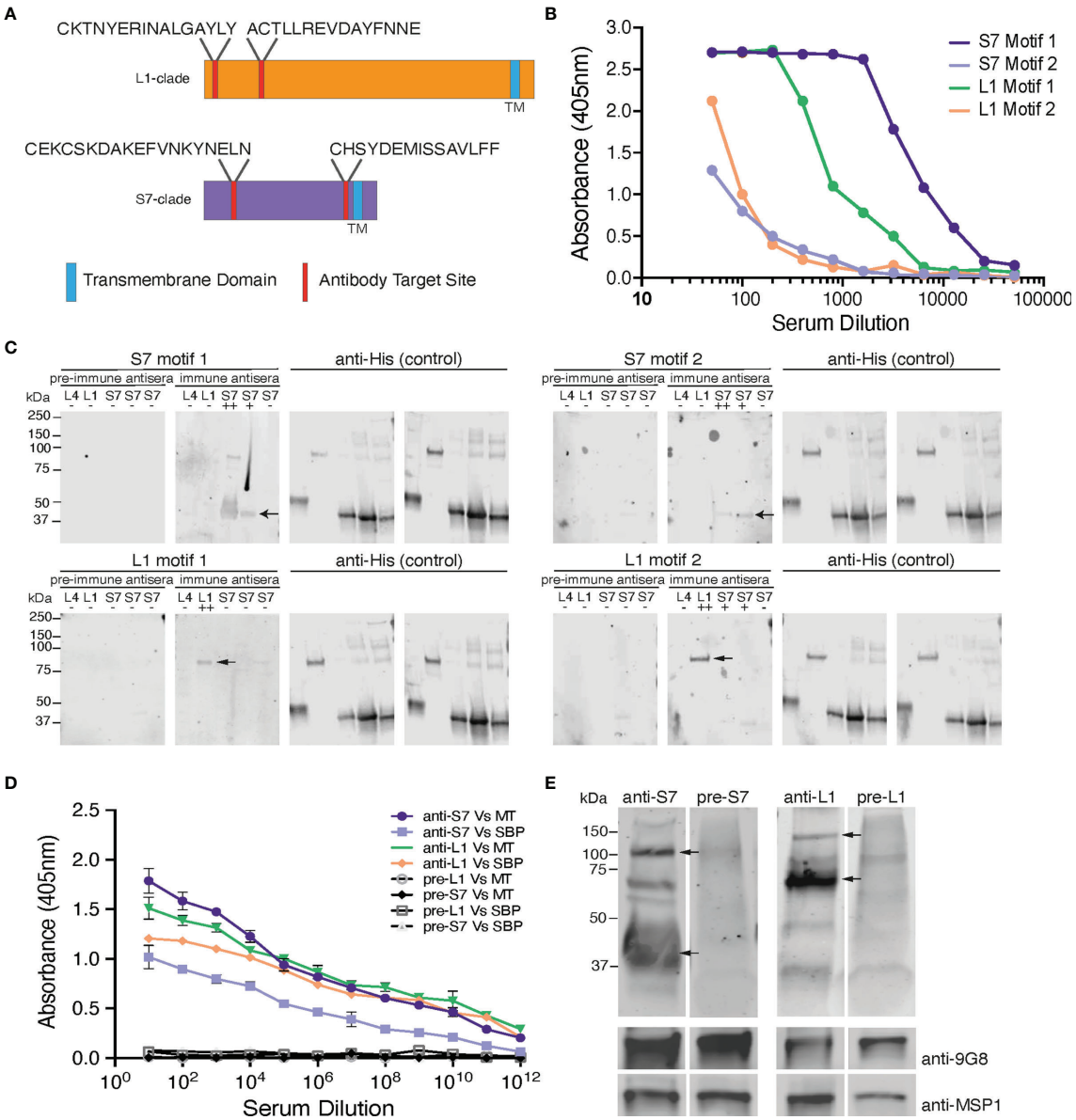

FIGURE 1 | Design and validation of the anti-S7 and anti-L1 peptide antisera. **(A)** Schematic model of S7- and L1-clade proteins showing position of the designed target peptide motifs. One of the S7 target motifs is located towards the N-terminus of the S7 protein clade, while the other is located further towards the C-terminus. Both the target motifs identified in the L1 PIRs are located towards the N-terminus of the protein sequence. TM, Transmembrane Domain. **(B)** ELISA reactivity of the individual anti-S7 and anti-L1 peptide sera (anti-S7 motif 1 peptide antiserum, anti-S7 motif 2 peptide antiserum, anti-L1 motif 1 peptide antiserum, anti-L1 motif 2 peptide antiserum) against the target *P. chabaudi* PIR peptides that were used to immunise rabbits. ELISAs performed by Cambridge Research Biomedicals, and figure adapted from those supplied by Cambridge Research Biochemicals. **(C)** Western blot analysis of S7, L1 and L4 his-tagged recombinant proteins probed with the individual anti-S7 and anti-L1 peptide antisera. Migration of S7 proteins was between 33-37 kDa markers and of L1 proteins between the 75-150 kDa markers (arrows indicate monomers). Probing against the his-tag served as loading control. Pre-immune sera served as negative controls, where they were found to be unreactive and did not recognise any of the recombinant proteins, confirming the lack of pre-existing reactivity to PIRs in the rabbit serum. ++ denotes a protein that highly matches the sequence of the peptide motif that the sera were raised against; + denotes a protein that contains a similar peptide motif (50-60% alignment) to that used for raising the immune sera; - denotes a protein that it does not contain any of the anti-sera target motifs. The specific recombinant proteins loaded are the PCHAS_0600600 (L4), PCHAS_1100300 (L1), PCHAS_0400300 (S7), PCHAS_1200500 (S7) and PCHAS_1300101 (S7). **(D)** ELISA reactivity of the pooled anti-S7 and anti-L1 peptide sera (pooled motif 1 and 2 for each antiserum) against WT parasite lysates extracted from MT and SBP acute-stage parasites. Pre-immune serum served as negative control. OD 405 ± standard deviation of three replicate assays is shown. MT, Mosquito Transmitted; SBP, Serially Blood Passaged. **(E)** Western blot analysis of whole parasite lysates (reducing conditions) prepared from *P. chabaudi* MT WT parasites at the trophozoite-stage, using the anti-S7 and anti-L1 pooled peptide immune sera. Arrows indicate the estimated average size of the monomers or dimers of each PIR clade (S7 33-50 and 100 kDa; L1 75-150 kDa). Probing with the pre-immune sera served as negative control. Probing against the *Plasmodium* EXP2 was used as stage-specific and loading control. The molecular weights on the right indicate the positions to which size markers had migrated.

for 10 min at 4°C. Parasite fractions were then washed twice in ice cold 1 x PBS containing 10 µg/mL (1X) PI and resuspended in 10 volumes of 0.15% (w/v) saponin (Sigma) in 1 x PBS for 10 min at 4°C. Following centrifugation, pellets were washed twice in ice cold 1 x PBS/PI and resuspended in 50 mM Tris HCl-PBS-PI (pH 7.4) buffer, mechanically homogenised for 1 min and stored at -80°C until frozen. Immediately upon thawing, the samples were centrifuged and washed twice in ice cold 1 x PBS/PI. The remaining membrane soluble fractions were extracted in RIPA whole cell lysis buffer supplemented with 1% SDS and PI for 20 min at 4°C. Following centrifugation, Laemmli buffer (BioRad) was added to all samples used for western blot analysis, or directly stored at -80°C until further proteomic analysis. Whole protein lysates were prepared as described above. After the last centrifugation, the supernatant was mixed with Laemmli buffer until further western blot analysis. Approximately 70 ng of purified recombinant proteins were mixed with Laemmli buffer until further western blot analysis. For reducing conditions, +3-5% (v/v) 2-mercapthoethanol was added to the sample buffer.

Proteins from all samples were separated on a 4–20% gradient polyacrylamide gel electrophoresis (Mini-PROTEAN TGX™ Precast Protein Gels, BioRad) in Tris-Glycine buffer (BioRad), followed by transfer to nitrocellulose membranes (iBlot Transfer Stack, Invitrogen). The blots were then blocked in 3% (w/v) BSA in 1 x PBS (blocking buffer) and probed with the following antibodies: rabbit anti-S7 motif 1 peptide antiserum (1:1000), rabbit anti-S7 motif 2 peptide antiserum (1:1000), rabbit anti-L1 motif 1 peptide antiserum (1:1000), rabbit anti-L1 motif 2 peptide antiserum (1:1000), rabbit anti-S7 peptide antiserum (pooled motif 1 and 2) (1:1000), rabbit anti-L1 peptide antiserum (pooled motif 1 and 2) (1:1000), rabbit anti-S7 pre-immune serum (1:1000), rabbit anti-L1 pre-immune serum (1:1000), mouse anti-his (1:1000; Novagen), mouse anti-9G8 (1:5000), mouse anti-MSP1 (1:2000), rat anti-Ter119 (1:5000), rabbit anti-*Py*EXP2 (a kind gift of James Burns, Drexel University College of Medicine, Philadelphia, United States; Meibalan et al., 2015) (1:500) overnight at 4°C. After three washes with 0.05% (v/v) Tween-20 in 1 x PBS, anti-rabbit IgG 680LT IRDye, anti-mouse 800CW IRDye and anti-rat 800CW IRDye secondary antibody (Li-Cor), diluted 1:10000 in blocking buffer, was applied for 1 h at room temperature. Odyssey Imaging system (Li-Cor) was used for detection and image analysis.

2.6 Immunofluorescence Assays and Live Cell Imaging

P. chabaudi has a synchronous erythrocytic life cycle and therefore blood could be collected at several time points in the 24-hour cycle in order to study the different asexual stages. Thin smears at the ring-, early trophozoite-, mature trophozoite- and late trophozoite/schizont-stages were prepared at 01 h, 16 h, 19 h and 23 h, respectively. For IFAs on *in vitro* maturated schizonts, infected mouse blood was cultured for five hours as previously described (Spence et al., 2011) and cells were then centrifuged, prior to preparing thin smears. Thin smears were fixed in cold acetone:methanol (9:1) for 10 min at -20°C and air-dried. Fixed cells were then re-hydrated in 1 × PBS, washed once in 1 × PBS, blocked in 3% BSA (w/v) in 1 x PBS for 1 h at room temperature and subsequently incubated with primary antibodies for 1 h at room temperature or overnight at 4°C. Rabbit anti-S7 peptide antiserum, rabbit anti-L1 peptide antiserum, mouse anti-9G8 (Hartz et al., 1993), mouse anti-MSP1 (NIMP23; Boyle et al., 1982), rabbit anti-SBP1-C (a kind gift of Tobias Spielmann, Bernhard Nocht Institute for Tropical Medicine, Hamburg, Germany; De Niz et al., 2016) and rat anti-Ter119 antibodies were used at 1:1000, 1:1000, 1:1000, 1:500, 1:100 and 1:1000 dilution in blocking buffer, respectively. After three washes with 1 x PBS, slides were incubated for 1 h at room temperature with secondary antibodies in blocking solution. Secondary antibodies used were goat anti-rabbit Alexa Fluor 568, goat anti-mouse Alexa Fluor 488 and donkey anti-rat Alexa Fluor 647 (Life Technologies) at 1:1000 dilution in blocking solution. Following three washes with 1 x PBS, nuclei were stained with 1 µg/mL−1 4′,6′-diamidine-2′-phenylindole dihydrochloride (DAPI) (Roche) in 1 x PBS for 5 min at room temperature. Slides were mounted with ProLong antifade mounting medium (ThermoFisher Scientific) and viewed under a Leica SP5 MP confocal laser-scanning microscope. Images were processed by deconvolution using the Huygens software and visualised using the ImageJ x 38 (NIH) software. In these experiments, Ter119 antibodies were used to define the red cell membrane and not direct light microscopic images.

For live cell imaging, parasites were incubated with the primary antibodies for 30 min at room temperature, washed three times in 1 x PBS, and incubated with the secondary antibodies for 20 min at room temperature. The cells were then viewed immediately under a Leica SP5 MP confocal laser-scanning microscope between slide and coverslip, as described above. After acquisition, contrast and brightness levels were optimised using the Image J x 38 software.

2.7 Electron Microscopy

Magnetically enriched infected erythrocytes at the trophozoite-stage were pelleted and fixed with 4% (v/v) paraformaldehyde/ 0.01% (v/v) glutaraldehyde in 1 x PBS for 30 mins at room temperature, followed by a second fixation step using 4% formaldehyde (v/v)/2.5% (v/v) glutaraldehyde in 0.1 M Sorenson's phosphate buffer (0.1 M Na_2HPO_4/ddH2O, pH 7.4) for 60 min at room temperature.

The cell pellet was then processed using a modified version of the NCMIR protocol (Deerinck et al., 2010). Briefly, the cells were washed in 0.1 M phosphate buffer and post-fixed with 1% reduced osmium (1% w/v OsO4/1.5% w/v $K_3Fe(CN)_6$) for 60 min at 4°C, and then washed in double distilled water (ddH2O). The cells were incubated in 1% thiocarbohydrazide (TCH) for 20 min at room temperature, rinsed in ddH2O and further fixed with 2% (w/v) osmium tetroxide for 30 min at room temperature. The cells were then stained with 1% (w/v) uranyl acetate at 4°C overnight, washed in ddH2O and stained with Walton's lead aspartate for 30 min at 60°C. The cells were then washed in ddH2O and dehydrated stepwise using serial dilutions of ethanol: 30% (v/v) at room temperature for 5 min, then 50% (v/v), 70% (v/v), 90% (v/v) and twice with 100% for 10 min each. The cells were incubated in propylene oxide (PO) for 10 min.

The cells were subsequently infiltrated with 3:1 mixture of PO : Durcupan resin (Sigma) for 45 min at room temperature, followed by 1:1 and 1:3 mixtures for 45 min each at room temperature, then with 100% Durcupan resin for 48 h. The cell pellet was then polymerised in fresh Durcupan resin at 60°C for 48 h. The sample was cut into 70 nm ultrathin sections using an ultramicrotome (UC7, Leica Biosystems UK) and picked up onto copper mesh grids (Agar Scientific). Images were obtained on a 120 kV transmission electron microscope (TEM) (JEM-1400Flash, JEOL) using a sCMOS camera (Matataki Flash, JEOL).

2.8 Flow Cytometric Investigation of S7 and L1 PIRs Localisation

Investigation of iRBC surface antigens was performed using a flow cytometry-based assay modified protocol from Elsworth et al., 2014. Two microliters of whole blood from C57Bl/6 RAG1$^{-/-}$ ^{P}. *chabaudi* AS infected mice (parasitaemia 15-20%) at the trophozoite-stage, were collected in 20 µL of saline-heparin (25 U/mL, Wockhardt) in U-shaped 96-well plates. After two washes with 1 x PBS supplemented with 2% (v/v) foetal bovine serum (FBS) and 3 mM EDTA (ThermoFisher), cells were either stored at 4°C to be stained later or fixed in 500 µL of 1:1 acetone:methanol for 10 mins at -20°C. Fixed cells were then washed twice in 1 x PBS/FBS/EDTA. Both live and fixed cells were then incubated with the anti-S7 and anti-L1 rabbit peptide antisera diluted in 1 x PBS/FBS/EDTA for 45 min at 4°C. Equal amounts of the anti-S7 motifs 1 and 2 and anti-L1 motifs 1 and 2 were mixed together prior to cell staining, and diluted 1:500 in 1 x PBS/FBC/EDTA. Following three washes in 1 x PBS/FBS/EDTA, cells were stained simultaneously with anti-Ter119 PE conjugated antibody (BioLegend) and goat anti-rabbit Alexa Fluor 568 (Life Technologies) for 20 mins at 4°C in the dark. Both the rat anti-Ter119 PE and the goat anti-rabbit Alexa Fluor 568 antibodies were diluted 1/1,000 in 1 x PBS/FBS/EDTA. Cells were then washed twice and stained immediately in 200 µL Hoechst 33342 (10 µg/mL in 1 x PBS/FBS/EDTA) for 15 mins at 37°C to stain for DNA. After washing twice in 1 x PBS/FBS/EDTA, cells were resuspended in 250 µL 1 x PBS/FBS/EDTA and acquired by flow cytometry on an Amnis® CellStream® benchtop flow cytometer (Luminex).

A total of 500,000 single RBC (selected based on their FCS/SSC and FSC/AspectRatio FSC) were analysed for each sample. The gating strategy established for the analysis of the results is described in (**Supplementary Figure S1**). FlowJo (Tree Star) was used for all flow cytometry analyses. Fixation in acetone:methanol also permeabilises the cells, therefore fixed cells were used as a control to validate antibody integrity. "Fluorescence minus one" (FMO) and single staining controls were included as controls, as well as a negative control sample from a non-infected mouse to define the threshold of positivity for the antibody signal.

2.9 Mass-Spectrometric (MS) Analyses

2.9.1 MS SDS-PAGE

Approximately 50 µg of the SLO fraction, and 15-20 µg of the SAP, Tris and RIPA fractions were added to 8 µL of Laemmli buffer containing 3% (v/v) 1,4-dithiothreitol (DTT; Roche). The mixture was heated for 10 min at 95°C and ran on a 16.5% Tris-Tricine gel electrophoresis (Mini-Protean Tris-Tricine Precast Protein Gels, BioRad) in Tris-Tricine buffer (BioRad). Gel was allowed to run at constant voltage (120 V) until track lengths (top to tracking dye) averaged 5 cm. Following gel incubation with colloidal Coomassie (abcam) and de-staining in HPLC grade water, protein bands below 17 kDa were excised and discarded to ensure mouse haemoglobin depletion (Mouse haemoglobin size: 14.4 kDa).

2.9.2 In-Gel Digestion and Fractionation

Gel lanes corresponding to each sample were cut into pieces and spread out into 8 wells of a 96-well U-shaped-bottom polystyrene plate (Costar). Gel pieces were de-stained overnight in 50% (v/v) Acetonitrile/100 mM Ammonium Bicarbonate, de-hydrated in 100% Acetonitrile (5 min) and aired-dried for 10 min at room temperature. Following reduction with 10 mM Dithiothreitol (60 min, room temperature) and alkylation with 55 mM Iodoacetamide (30 min, room temperature, in the dark), gel pieces were washed once with 50% (v/v) Acetonitrile/100 mM Ammonium Bicarbonate with shaking (10 min), de-hydrated with 100% Acetonitrile (5 min) and air-dried for 10 min at room temperature.

MS-grade Trypsin (Pierce) in 50 mM Ammonium Bicarbonate was added to each well (200 ng) in sufficient volume to allow for complete gel saturation. Samples were then digested overnight at 37°C with shaking. Peptides were extracted by incubation with 50% (v/v) Acetonitrile/100 mM Ammonium Bicarbonate (20 min) followed by 100% Acetonitrile (10 min). Peptide solutions corresponding to each sample were then pooled and partially dried in a vacuum centrifuge. Quantitative Colorimetric Peptide Assay (Pierce) was used to assess peptide content in each sample. 5 µg aliquots were then removed, acidified with neat Trifluoroacetic acid (TFA) and fractionated on a stage tip using high pH reverse phase (bRP). Briefly, each stage tip was packed with two C18 Empore discs (3M), conditioned with 100 µL of 100% Acetonitrile, followed by 200 µL of 0.1% (v/v) TFA. The samples were loaded in 1% (v/v) TFA, washed once with 200 µL water and fractionated by elution with increasing amounts of Acetonitrile (10% v/v, 17.5% v/v, 25% v/v and 50% v/v) in 0.1% (v/v) Triethylamine. Resulting fractions (25 µL each) were pooled non-consecutively, i.e. fraction 1 with 3 and fraction 2 with 4. The two final bRP fractions were vacuum dried.

2.9.3 LC-MS/MS

Samples were resuspended in 2% (v/v) Acetonitrile/0.1% (v/v) TFA supplemented with iRT standards (Biognosys) and loaded on a 50 cm Easy Spray PepMap column (75 µm inner diameter, 2 µm particle size, Thermo Fisher Scientific) equipped with an integrated electrospray emitter. Reverse phase chromatography was performed using the RSLC nano U3000 (Thermo Fisher Scientific) with a binary buffer system (solvent A: 0.1% v/v Formic acid, 5% v/v DMSO; solvent B: 80% v/v Acetonitrile, 0.1% v/v Formic acid, 5% v/

v DMSO) at a flow rate of 275 nL/min. The samples were run on a linear gradient of 2-8% B in 5.5 min, 8-25%B in 54.5 min, 25-40% B in 31 min, and 40-50% B in 7 min with a total run time of 120 min including column conditioning. The nanoLC was coupled to an Orbitrap Eclipse mass spectrometer using an EasySpray nano source (Thermo Fisher Scientific). The Orbitrap Eclipse was operated in data-independent mode (DIA) with following settings: MS1 data acquired in the Orbitrap with a resolution of 120,000, max injection time of 20 ms, AGC target of 1e6, in positive ion mode and profile mode, over the mass range 375-1,500 m/z. DIA segments over this mass range (variable size windows, 34 in total) were acquired in the Orbitrap following fragmentation in the HCD cell (30%), with 30,000 resolution over the mass range 200-2000 m/z and with a max injection time of 70 ms and AGC target of 1e6.

2.9.4 Data Analysis

Acquired raw data were analysed with Spectronaut v15.4.210913 (Biognosys AG) using directDIA analysis option. Data were searched against *P. c. chabaudi* (PlasmoDB), *Mus musculus* (UniProt) and contaminants (Spectronaut) FASTA files using Pulsar search engine. Cysteine carbamidomethylation was selected as a fixed modification, whereas oxidation (M), acetylation (Protein N-term) and deamidation (NQ) were selected as variable modifications. The enzyme specificity was set to trypsin with a maximum of 2 missed cleavages. The datasets were filtered on posterior error probability (PEP) to achieve a 1% false discovery rate on protein, peptide and PSM level. MS1 and MS2 tolerances were set to dynamic and retention time calibration was based on iRT regression generated in Spectronaut. Interference correction was activated, keeping a minimum of 2 precursor ions and 3 fragment ions. Quant 2.0 was selected as protein LFQ method and Quantity MS-level was set to MS2 with Q value ≤ 0.01 used for data filtering. No intensity normalisation was performed.

Data were further processed with Microsoft Office Excel 2016 (**Supplementary Table S3**). Protein group data were filtered to remove common contaminant entries as well as for the presence of 1 valid value. Quantity values were then log2 transformed and no further data transformations were performed. The mass spectrometry proteomics data have been deposited on the ProteomeXchange Consortium *via* the PRIDE (Perez-Riverol et al., 2019) partner repository with the dataset identifier PXD031586.

2.10 Statistical Analysis

Statistical analysis was determined by using Graphpad Prism5 software. The one-way analysis of variance (ANOVA) test was used. *P*-value of <0.05 was considered as statistically significant.

3 RESULTS

3.1 Generation and Validation of Rabbit Antisera

The two largest clades of *P. chabaudi* PIRs, the S7s and the L1s, together account for 68% of the PIRs in *P. chabaudi*. There are 70 S7s and 82 L1s PIRs in the *P. chabaudi* genome. PIR members of each clade share conserved regions (Brugat et al., 2017) and in order to examine their expression and localisation more holistically, we generated peptide antisera that targeted as many members of each PIR clade as possible.

The localisation of PIR proteins within *P. chabaudi*-parasitised erythrocytes during the acute- and chronic-phases of infection was investigated, using rabbit polyclonal antisera that were generated against 20-conserved residue sequences of the S7 (acute-associated) and of L1 (chronic-associated) PIR clades, respectively (Freitas-Junior et al., 2000; Otto et al., 2014), the two major *pir* clades expressed in *P. chabaudi* blood-stage parasites (Brugat et al., 2017; Little et al., 2021). Two peptide motifs were chosen for each clade (**Figure 1A**), whose sequence had the highest number of BlastP hits within the same clade they were designed for and the lowest off-target activity. In summary, the peptides recognised by the anti-S7 peptide antisera designed against motif 1 and motif 2 are present in 37/70 and 12/70 S7 PIRs, respectively. Similarly, the peptide motif 1 and motif 2 identified for the L1 clade can be found in 49/82 and 29/82 of the L1 PIRs, respectively. Some off-target proteins (i.e. PIRs of a different clade) could not be avoided. Peptide sequences are described in **Supplementary Table S1**, and materials and methods. The BlastP hits for each motif designed against each clade are summarised in **Supplementary Table S2**.

Antisera to the selected peptides, generated in rabbits (Cambridge Research Biochemicals, Billingham, UK) were tested by ELISA against their respective target peptides (**Figure 1B**). Peptide antisera that were generated against S7 motif 1 and L1 motif 1 recognise their target peptide at high titres, whereas peptide antisera against the S7 motif 2 and L1 motif 2 antigens indicated lower titres. Western blot analysis against the his-tagged recombinant PIR proteins PCHAS_0600600 (L4), PCHAS_1100300 (L1), PCHAS_0400300 (S7), PCHAS_1200500 (S7) and PCHAS_1300101 (S7) confirmed specificity of each antiserum to their target clades (S7 at approximately 33-37 kDa, L1 at approximately 75-151 kDa, and L4 at approximately 40 kDa). Pre-immune rabbit antisera did not recognise any of the recombinant proteins (**Figure 1C**).

To maximise the proportion of PIRs belonging to the same clade that are picked up by the individual peptide antisera, we pooled together the two antisera generated against the individual motifs from each clade. The pooled antisera were then checked for reactivity against the PIR proteins in *P. chabaudi* WT parasites by ELISA and western blot analysis. ELISA assays using a lysate of *P. chabaudi* blood-stage parasites showed that both rabbit anti-S7 and anti-L1 sera contained antibodies that recognised proteins from lysates of both MT and serially passaged blood-stage (SBP) parasites (**Figure 1D**), with the overall reactivity being higher for both antisera with the parasite lysate derived from MT blood-stage parasites. The increased reactivity of the antisera with MT blood-stage parasites agrees with the increased RNA expression in MT parasites compared with SBP parasites, previously observed (Spence et al., 2013; Brugat et al., 2017). Western blot analysis

of the pooled rabbit anti-S7 and anti-L1 sera against whole protein lysates of *P. chabaudi WT* MT parasites demonstrated that both antisera are able to recognise naturally produced PIR proteins. The two antisera display differing patterns of bands across the lysates, with S7 and L1 antisera having predominant bands of 33-50 kDa, and 75-151 kDa, respectively, reflecting the expected size of *PIR* proteins of the S7 and L1 clades (**Figure 1E**). The S7 antisera also interact with a protein of approximately 100 kDa, which may be due to formation of multimers, as purified recombinant protein exhibits a similar migration and interaction (**Figure 1C**). Arrows indicate the major interacting proteins.

3.2 Localisation of S7 and L1 PIRs in Mature *P. chabaudi* Trophozoites in Acute- and Chronic-Phases of Infection

The proportion of acetone:methanol fixed/permeabilised *P. chabaudi* iRBC that stained positively for S7 and L1 PIRs is similar between acute and chronic blood-stage infection and between MT and SBP parasites (**Figure 2A**). However, the proportion of L1-positive iRBC (mean value: 95.33 ± 0.53% SEM) is significantly higher (p=0.0286) in all cases, compared to the percentage of positive cells enumerated for the anti-S7 serum (mean value: 78.95 ± 0.60% SEM). Individual *P. chabaudi* parasites are thought to co-express multiple *pir* genes, as well as expressing many *pir* genes at a population level (Bozdech et al., 2008; Cunningham et al., 2009; Yam et al., 2016). Our data suggest that at each stage, individual parasites also express multiple PIR proteins across different clades.

Subcellular localisation of S7 and L1 PIRs was investigated in fixed/permeabilised RBC from *P. chabaudi* infections, at both acute- and chronic-phases of the infection (at day 10 and day 35 post infection, respectively) (Brugat et al., 2017) in immunofluorescence assays using the anti-S7 and anti-L1 peptide antisera described above. Trophozoite-stage parasites from MT blood-stage *P. chabaudi* were initially assessed, as it has been previously demonstrated that *pir* transcripts are increased in blood-stage parasites following mosquito transmission (Spence et al., 2013; Yam et al., 2016; Brugat et al., 2017). In iRBC taken from an acute-stage MT infection, S7 PIRs are mainly exported into the host's iRBC cytoplasm where they can be seen as multiple discrete foci. They are also seen, less abundantly, close to the PVM. This pattern changes in iRBC collected at the chronic phase of infection, where in approximately 98% of iRBC, PIRs were localised closed to the iRBC surface and to a lesser extent exported into its cytoplasm (**Figure 2B**; top panel, **Supplementary Figure S2**). L1 PIRs in acute-phase MT blood-stage parasites are localised on or close to the PVM, but with progression to the chronic-phase of infection, they also translocate to the iRBC cytoplasm. Specifically, in approximately 80% of the iRBC, L1 PIRs persist in close proximity to the PVM while also being secreted within the iRBC cytoplasm where they accumulate in granular structures that further co-localise with clone 6 following labelling with 9G8, a monoclonal antibody that recognises a tryptophan-rich protein (PCHAS_0624800) known to be found in the cytoplasm of *P. chabaudi* iRBC (Hartz et al., 1993) (**Figure 2B**; bottom panel, **Supplementary Figure S2**).

Transcription of *pir* genes in MT *P. chabaudi* iRBC differs from that observed in the more commonly used SBP parasites, in both amount and diversity of *pir* genes expressed (Spence et al., 2013; Brugat et al., 2017). This seems to also apply at the expression level where PIR proteins are more highly abundant in MT parasites compared to SBP, as described above (**Figure 1D**). We therefore asked whether PIRs in *P. chabaudi* SBP infected erythrocytes also have a different localisation pattern compared to the MT parasitised erythrocytes. Immunofluorescence staining of *P. chabaudi* SBP iRBC at the acute- and chronic-phases of infection with the anti-S7 and anti-L1 peptide antisera, have shown that S7 PIRs are exported into the iRBC cytoplasm during both the acute- and chronic-phases of a SBP infection (**Figure 2C**; top panel), whereas L1 PIRs are localised in close proximity to the PVM in both acute- and chronic-phases parasites (**Figure 2C**; bottom panel).

Neither S7 nor L1 PIR proteins could be detected at the surface membrane of RBC infected with either MT or SBP blood-stage parasites (**Figures 2B, C**). However, as there are predicted transmembrane domains in PIR proteins (Harrison et al., 2020), S7s may be located on vesicle-like structures within the iRBC cytoplasm and L1s on the PVM. In agreement with this, S7 showed co-localisation with 9G8 monoclonal antibodies, and L1 was found to be localised closely to MSP1, known to be concentrated at the parasite periphery which is consistent with PV localisation (Holder et al., 1992). Some co-localisation of the S7 PIRs with MSP1 was observed in acute-phase MT blood-stage parasites, whereas L1 PIRs seem to translocate on a similar vesicle-like pattern as 9G8 when progressing into the chronic-phase of MT blood-stage parasites. For clarification, the localisation data are summarised in a schematic (**Figure 2D**).

3.3 Localisation of S7 and L1 PIRs Throughout the Asexual Developmental Cycle

PIR expression in iRBC during acute and chronic *P. chabaudi* infection described above was determined using only the trophozoite-stage of the parasite. We next examined whether the subcellular localisation of the S7 and L1 PIRs changed during the 24-hour developmental cycle in iRBC taken from acute- and chronic-stages of an MT infection using the S7 and L1 peptide-specific antisera. PIR localisation was examined at rings (01 h), early trophozoites (16 h), mature trophozoites (19 h) and late trophozoites/schizonts (23 h) on blood films directly *ex vivo* (**Figure 3A; Supplementary Figure S3**). However, as *P. chabaudi* schizonts are normally not present or only at very low levels in peripheral blood because of sequestration in organs and tissues (Gilks et al., 1990; Mota et al., 2000; Brugat et al., 2014), PIR expression was also determined in schizont-iRBC that had been matured *in vitro* (**Figure 3B**).

S7 PIRs were exported to the iRBC cytosol and appeared as dense granules, in both trophozoite- and ring-stages of both acute- and chronic-phase parasites. In agreement with our observations for trophozoites described in **Figure 2**, S7 PIRs

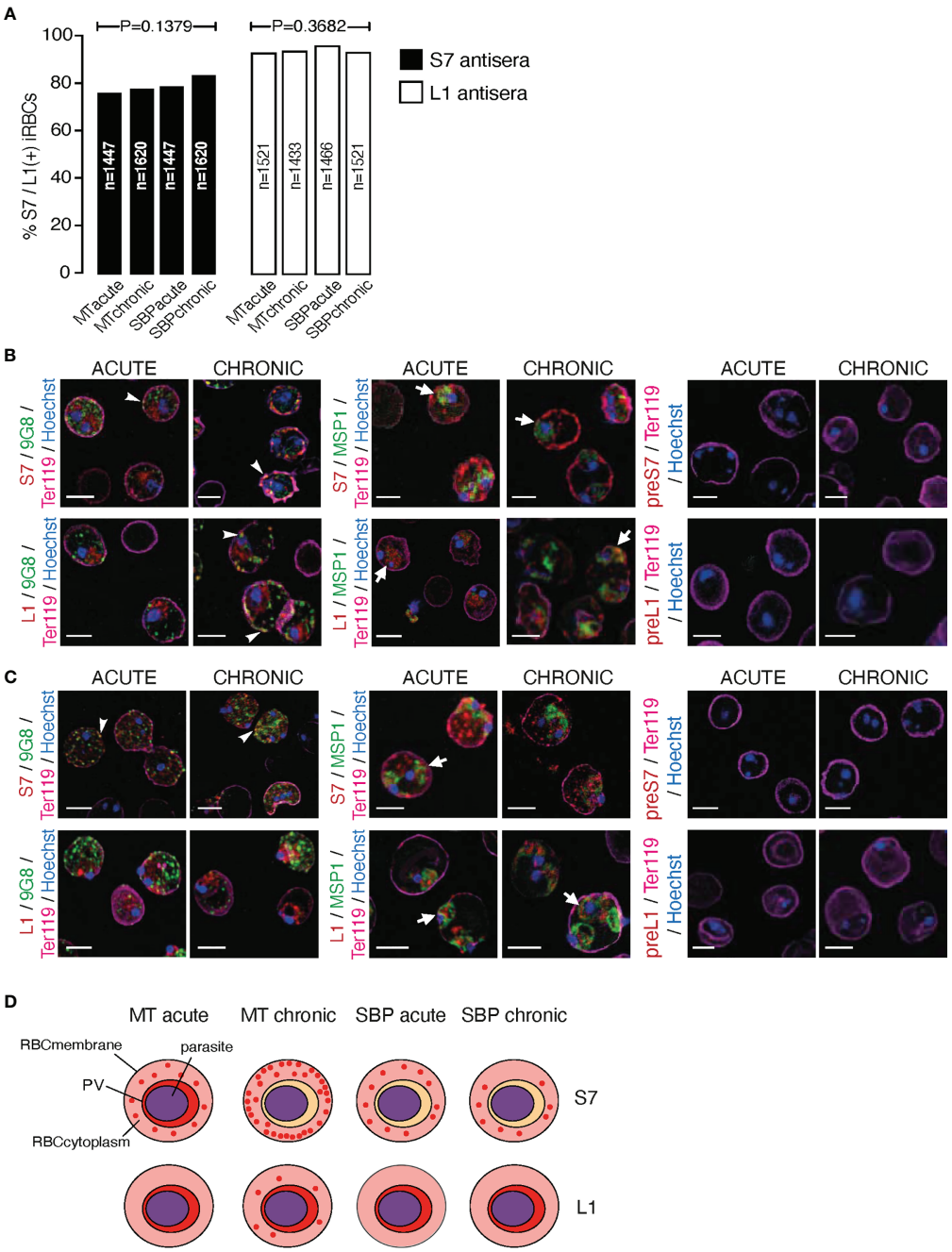

FIGURE 2 | Subcellular localisation of S7 and L1 PIRs in the late trophozoite-stage of MT and SBP *P. c. chabaudi AS* parasites, during the acute- and chronic-phases of infection. **(A)** Percentage of MT and SBP S7-positive (dark grey) and L1-positive (light grey) parasitised erythrocytes, at the late trophozoite-stage. N represents the total number of iRBC analysed in three biological replicates. Data are presented as mean with SEM. Statistical significance was calculated using one-way Analysis Of Variance (ANOVA) tests ($P < 0.05$). **(B, C)** Immunofluorescence assays of MT **(B)** and SBP **(C)** WT *P. chabaudi* parasites at the late trophozoite-stage. Blood was isolated from C57Bl/6 RAG1$^{-/-}$ mice. Parasites were primarily stained with the anti-S7 or anti-L1 peptide sera (red), and later with the anti-clone 6 (9G8) or anti-MSP1 monoclonal antibodies (green). The white arrowheads indicate co-localisation of the S7s or L1s with 9G8, whereas the white arrows indicate co-localisation of the S7s and L1s with MSP1. Erythrocyte membrane was stained with the rat anti-Ter119 monoclonal antibody (magenta), and parasite nuclei were stained with Hoechst (blue). Staining with pre-immune sera was used as negative control (right panel). Images were taken from confocal sections of acetone: methanol fixed parasites at X630 magnification. Scale bar length corresponds to 5 μm. **(D)** Schematic representation summarising the results obtained following confocal imaging of MT and SBP *P. chabaudi* parasites. The localisation pattern of S7s and L1s across the acute- and chronic-phases of infection in MT and SBP parasites is indicated in red. RBCmembrane, Red Blood Cell Membrane; PV, Parasitophorous Vacuole.

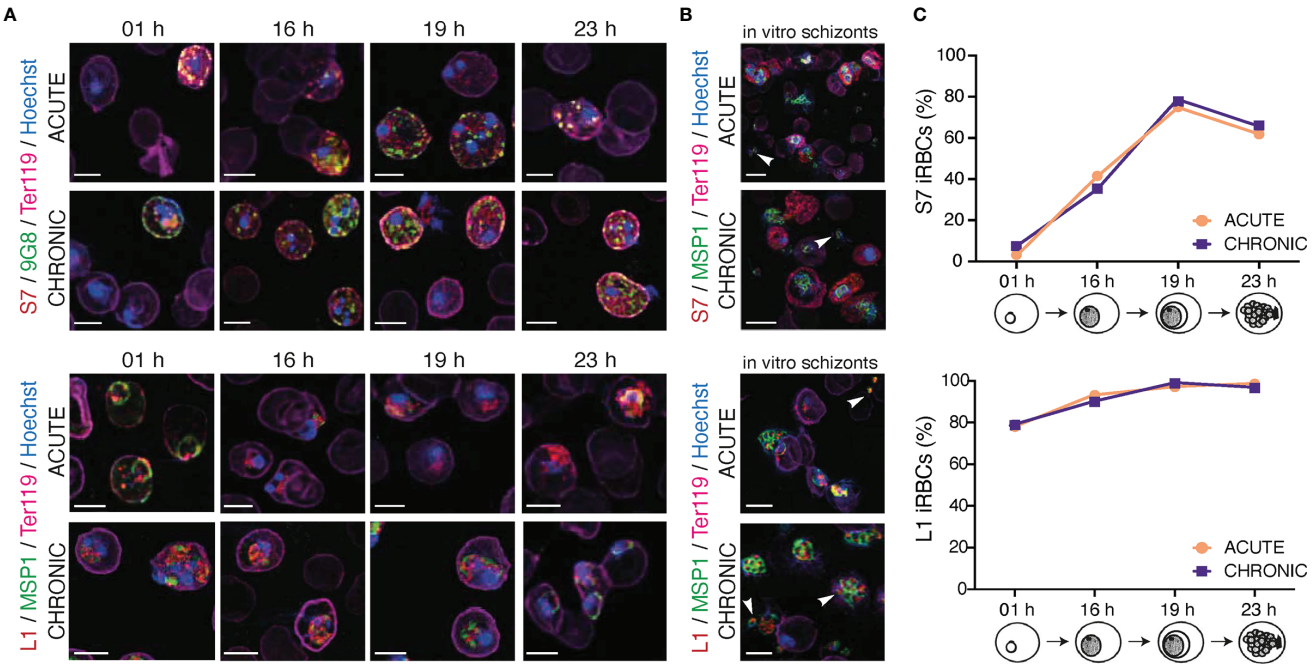

FIGURE 3 | Localisation pattern of S7 and L1 PIRs across the 24-hour asexual blood cycle of MT *P. c. chabaudi AS* parasites, during the acute- and chronic-phases of infection. **(A, B)** Immunofluorescence assays of MT WT *P. chabaudi* parasites at different developmental stages of their asexual blood cycle. WT mice were directly exposed to infected mosquitoes and following infection establishment, acute- (at day-7 post infection) or chronic-phase (at day-45 post infection) parasites were passaged into C57Bl/6 RAG1$^{-/-}$ mice. Upon infection establishment, blood tail smears were prepared for immunofluorescent staining at the ring (1 h), early trophozoite (16 h), mature trophozoite (19 h) **(A)**, and late trophozoite/schizont (23 h) **(B)** developmental stages. Blood smears from *in vitro* schizont cultures, following five hours of culture, were also prepared. Parasites were primarily stained with the anti-S7 (top panels) or anti-L1 peptide sera (bottom panels) (red). S7-incubated slides were then probed with the anti-clone 6 (9G8) (green) antibody, whereas L1-incubated slides were probed with the anti-MSP1 monoclonal antibody (green). The RBC surface membrane was stained with an anti-Ter119 antibody (magenta), and parasite nuclei were stained with Hoechst (blue). Images were taken from confocal sections of acetone:methanol fixed parasites at X630 magnification. Asterisks indicate free merozoites. Scale bar length correspond to 5 µm. **(C)** Percentage of S7-positive (top panel) and L1-positive (bottom panel) iRBC throughout the 24-hour life cycle, in MT parasites during acute- and chronic-phases of infection. About 950-1,000 red blood cells were analysed across two individual biological replicates, where data are presented as mean.

appeared to be more closely associated with the iRBC membrane in the chronic-phase of infection throughout the 24-hour cycle. Furthermore, co-localisation of the S7 PIRs with the tryptophan-rich protein recognised by the 9G8 antibody indicates vesicle-like distribution of the S7s across the iRBC cytoplasm (**Figure 3A**; top panel). L1 PIRs were found to be associated with the PVM during the ring- and trophozoite-stages; further supported by their co-localisation with the merozoite surface protein MSP1. With progression to the chronic-phase of infection and during ring-to-trophozoite developmental transition, traces of L1 PIRs were seen in the host cell cytoplasm (**Figure 3A**; bottom panel), validating our previous observations.

In *in vitro*-matured schizonts, S7 PIRs were found to be exclusively exported beyond the parasite plasma membrane and PVM, and distributed evenly throughout the iRBC cytosol. However, in the few cases where free merozoites were detected, upon schizont rupture, S7 PIRs were found to be highly associated with their cytoplasm as a single vesicle-like structure; about 80% of the released merozoites were found to be positive for S7 expression. Progression from acute- to chronic-phases of infection did not alter S7 PIR localisation (**Figure 3B**; top panel). L1 PIRs in *in vitro* schizonts from both acute- and chronic-phase were found to be localised within the individual merozoites' cytoplasm as discrete dots. Upon schizont rupture, L1 expression could still be observed in approximately 95% of the released merozoites possibly suggesting a potential function of the L1s in merozoite egress or invasion. Co-localisation of the L1s with MSP1 was not observed, further suggesting that L1 PIRs are not localised on the merozoites surface (**Figure 3B**; bottom panel). Similar distribution pattern of the S7 and L1 PIRs has been also observed in SBP acute-stage *in vitro* maturated schizonts (**Supplementary Figure S4**).

These results show that localisation of both S7 and L1 clades does not change across *P. chabaudi* 24-hour developmental cycle in the blood. The only difference observed between expression in the different developmental stages was the proportion of iRBC that stained positively with the peptide antisera (**Figure 3C**). The proportion of detectable S7-expressing cells peaked at 19 h (mature trophozoites), after which they rapidly declined with minimum expression levels at 01 h (ring-stage). The proportion of L1-expressing cells did not significantly change between early (16 h) and late trophozoites (19 h), at 97-98% abundance. After the trophozoite-stage, the proportion of L1-positive iRBC decreased to about 77-78% abundance in the ring-stage.

Importantly, the proportion of S7+/L1+ iRBC in acute and chronic *P. chabaudi* parasites did not change indicating the lack of further regulation between acute- and chronic-phase.

3.4 Maurer's Clefts in the Cytosol of *P. chabaudi* Infected Erythrocytes Show Similar Localisation Pattern to S7 PIRs

Previous staining of MT acute and chronic *P. chabaudi* blood-stage parasites with the anti-S7 peptide antisera displayed a similar punctuate localisation pattern to that of clone 6 following immunostaining with the 9G8 monoclonal antibody (**Figure 2B**). This vesicle-like pattern of both S7 PIRs and clone 6 is typical of Maurer's clefts. Maurer's clefts are sack-like structures spread across the iRBC cytosol of most malaria species (Langreth et al., 1978; Atkinson and Aikawa, 1990; Henrich et al., 2009) and they have been shown to be involved in sorting parasite proteins on the surface of iRBC (Mundwiler-Pachlatko and Beck, 2013). The presence of Maurer's clefts has not yet been examined in *P. chabaudi*. By conducting electron microscopy (**Figure 4A**) and fluorescence (**Figure 4B**) imaging analysis of *P. chabaudi* iRBC at the trophozoite-stage, we investigated whether Maurer's clefts exist in the cytoplasm of *P. chabaudi* parasitised erythrocytes, in similar vesicle-like structures as in other malaria species.

Transmission electron microscopy (TEM) analysis revealed membrane structures with sizes ranging from 30 to 150 nm, scattered between the PVM and the erythrocyte membrane (**Figure 4A**). They appear as narrow flattened clefts with either a dense or slightly expanded lucent lumen, suggesting that these vesicles are likely to be Maurer's clefts. However, to confirm that these vesicle-like structures are Maurer's clefts, we performed fluorescence microscopy-based imaging of MT blood-stage parasites at the acute- and chronic-phases of the infection following staining with the *P. berghei* anti-SBP1 antiserum (a gift of Tobias Spielmann; De Niz et al., 2016). *Pb*SBP1 is essential for parasite sequestration (De Niz et al., 2016) and it has been shown to co-localise with IBIS1, a marker protein of previously identified Maurer's clefts-like structures in *P. berghei* (Ingmundson et al.,

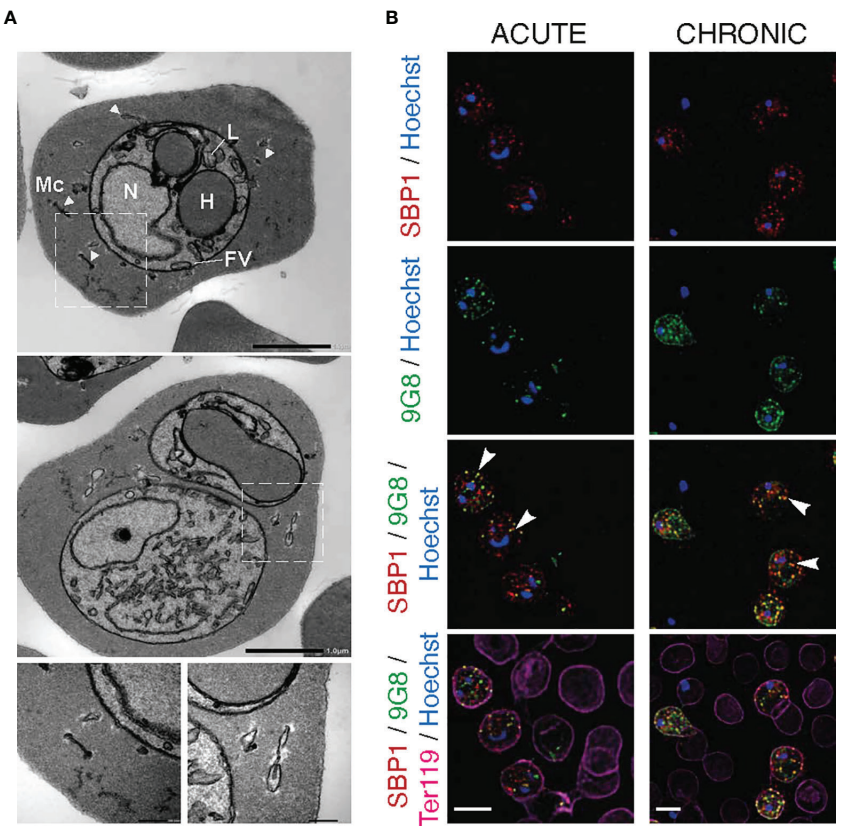

FIGURE 4 | Maurer's clefts-like structures in *P. c. chabaudi AS* infected erythrocytes. **(A)** Transmission electron micrographs of a *P. chabaudi* MT acute phase trophozoite, inside a mouse erythrocyte. The white arrowheads indicate Maurer's clefts within the iRBC cytosol. Insets show sections of the areas highlighted. Scale bar length corresponds to 1 μm and 0.2 μm in insets. FV, Food Vacuole; H, Haemoglobin Filled Compartment; L, Lipid Droplets; Mc, Maurer's clefts; N, Nucleus. **(B)** Immunofluorescence assays of MT acute- (left panels) and chronic- (right panels) phase WT *P. chabaudi* parasites at the late trophozoite-stage. Blood was isolated from C57Bl/6 RAG1$^{-/-}$ mice. Parasites were primarily stained with the anti-PbSBP1 antibody (De Niz et al., 2016) (red) and then with the anti-clone 6 (9G8) monoclonal antibody (green). The RBC surface membrane was stained with the anti-Ter119 monoclonal antibody (magenta), and parasite nuclei were stained with Hoechst (blue). The white arrowheads indicate co-localisation of SBP1 with 9G8. Images were taken from confocal sections of acetone:methanol fixed parasites at X630 magnification. Scale bar length corresponds to 5 μm.

2012). Since there are very few available antibodies for *P. chabaudi* and *P. berghei* SBP1 (*Pb*SBP1) shares 64% similarity with its *P. chabaudi* orthologue, anti-*Pb*SBP1 was used as a marker for identifying Maurer's clefts in *P. chabaudi*. Moreover, since staining with the 9G8 monoclonal antibody displays the same localisation pattern as that of the S7 PIRs, both the anti-*Pb*SBP1 antiserum and 9G8 monoclonal antibody were used to co-stain *P. chabaudi* iRBC. Direct co-localisation experiment using the *P. berghei* anti-SBP1 and the *P. chabaudi* anti-S7 peptide antisera simultaneously was not conducted, as both were produced in rabbits. Immunofluorescence assays showed that SBP1 and clone 6 are exported into the cytosol of *P. chabaudi* acute-stage infected erythrocytes where they were found to be co-localised in multiple discrete foci (83% co-staining of clone 6 and SBP1) (**Figure 4B**), resembling the typical labelling of proteins located in *P. falciparum* Maurer's clefts. Both clone 6 and SBP1 were found to have similar localisation patterns in chronic-stage infected erythrocytes, where about 76% of the discrete foci detected were positive for both proteins. Some localisation of clone 6 was also observed close to the periphery of the iRBC in 91% of the examined discreet dots (**Figure 4B**), however our flow cytometry data on unfixed iRBC (**Figures 5B, D**) suggest that 9G8 is not externally located on the iRBC membrane at this stage of the infection. We have previously shown that S7 PIRs, at the chronic phase of infection, are found to be localised as granular structures across the iRBC cytosol and near the iRBC membrane (**Figures 2B**, **3A**). However, the use of anti-*Pb*SBP1 to identify *P. chabaudi* Maurer's clefts indicates that their localisation does not change in iRBC at the acute and chronic infection (**Figure 4B**). These data suggest that S7 PIRs do not co-localise with the Maurer's clefts in chronic-phase iRBC and are possibly released as infection progresses to the chronic-phase.

With progression to the chronic-phase of infection and during ring-to-trophozoite developmental transition, traces of L1 PIRs were seen in the host cell cytoplasm to co-localise with clone 6 following 9G8 labelling (**Figure 3A; bottom panel).** This suggests that Maurer's clefts might also be involved in the trafficking of L1 PIRs but to a lesser extent compared to the S7 PIRs.

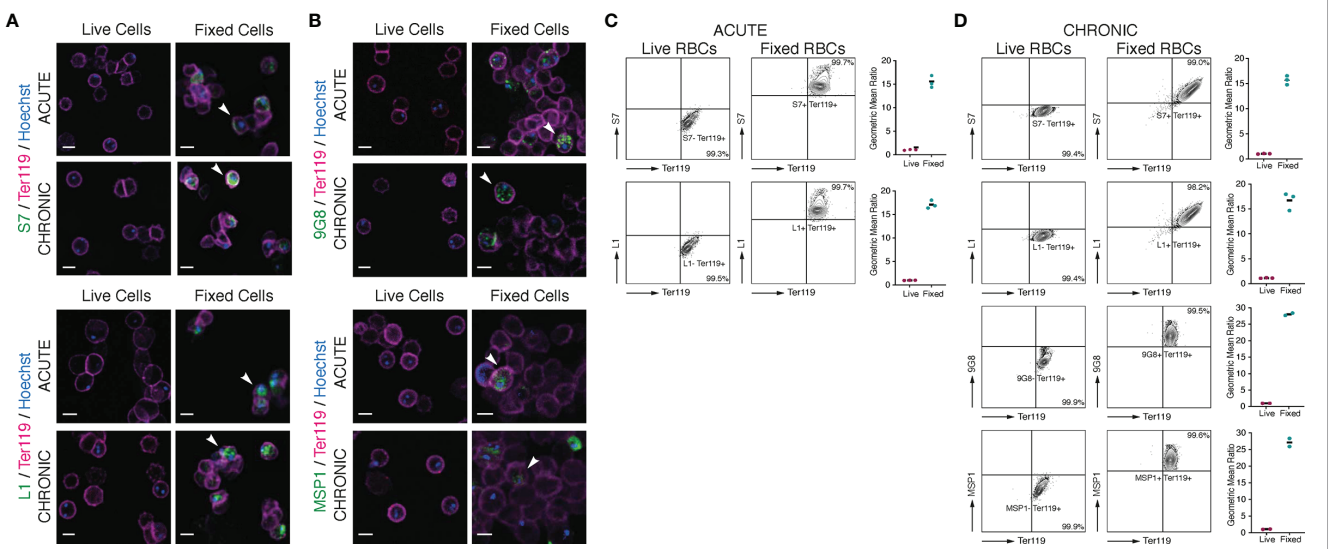

FIGURE 5 | Localisation of S7 and L1 PIRs in live acute and chronic MT *P. c. chabaudi AS* parasitised erythrocytes. **(A, B)** Immunofluorescence staining of live (left panels) and acetone:methanol-fixed iRBC (right panels) of MT *P. chabaudi* parasites at the late trophozoite-stage, isolated from blood of C57Bl/6 RAG1$^{-/-}$ mouse during acute (at day-7 post infection) (upper panels) and chronic (at day-45 post infection) (lower panels) infection. **(A)** *P. chabaudi* parasites were stained with either anti-S7 or anti-L1 peptide antisera (green). **(B)** 9G8 (upper panels) or anti-MSP1 (lower panels) monoclonal antibodies, which recognise parasite antigens internal to the iRBC or parasite, were used as negative controls for live imaging and positive controls for imaging the acetone:methanol fixed iRBC. The RBC surface membrane was stained with anti-Ter119 antibody (magenta), and parasite nuclei were stained with Hoechst (blue). Staining with pre-immune rabbit serum was used as a negative control in the case of peptide antisera (data not shown). The white arrowheads in the panels with fixed iRBC indicate L1, S7, 9G8 or MSP1 positive cells. Images were taken from confocal sections of live and acetone:methanol fixed parasites at X630 magnification and are representative of a total of 500-600 iRBC imaged across two individual replicates. Scale bar length corresponds to 5 µm. **(C, D)** Live *P. chabaudi* iRBC at the acute- **(C)** and chronic- **(D)** phases of infection in C57Bl/6 WT mice were labelled with the anti-S7 or anti-L1 peptide antisera, and anti-Ter119 monoclonal antibody, and analysed using the Amnis® CellStream® Cytometer. Representative contour plots (of 2-3 mice) show the percentage of the iRBC population (Hoechst+/Ter119+) that is either positive or negative for anti-S7 or anti-L1 peptide antisera binding. The quadrant gate was set based on the anti-S7 or anti-L1 background signal detected in the Hoechst- RBC for each condition. Acetone:methanol fixed cells, which are also permeabilised, were used as a control to confirm antibody reactivity with *P. chabaudi* parasites. 9G8 or anti-MSP1 monoclonal antibodies were used as negative controls for live cells, and as a positive control for staining internal parasite proteins in fixed/permeabilised cells. The side plots show the ratio of the geometric mean fluorescence intensity (MFI) detected following binding of the anti-S7 or anti-L1 antibodies on Hoechst+ and Hoechst-, live and fixed (control) RBC. Higher ratios indicate presence and higher abundance of the investigated proteins in Hoechst+ compared to the Hoechst- cells. Ratio of around 1 indicates no difference in the fluorescence intensity of antibody binding (and therefore protein abundance) between the Hoechst+ and Hoechst- RBC. Three biological replicates (i.e., infected mice) were performed for antibody labelling of the S7 or L1 PIRs, whereas two replicates were conducted for antibody labelling with the 9G8 and anti-MSP1 monoclonal antibodies. Data for each individual mouse are presented in (**Supplementary Figure S5**).

3.5 S7 and L1 PIRs Are Not Detected on the Surface of *P. chabaudi*-Infected Erythrocytes

It has been suggested that PIR proteins, similar to proteins of other *Plasmodium* multigene families (Niang et al., 2009; Niang et al., 2014; Saito et al., 2017; Kyes et al., 1999; Blythe et al., 2008), are present on or close to the surface of iRBC (Del Portillo et al., 2001; Cunningham et al., 2005; Pasini et al., 2013; Yam et al., 2016; Harrison et al., 2020). The distribution of flexible, sequence-variable loops across their structures is also characteristic of a protein family undergoing diversification to avoid immunoglobulin-mediated clearance (Harrison et al., 2020). As shown above (**Figures 2B**, **3A**), immunofluorescence studies of acetone:methanol fixed *P. chabaudi* RBC using the anti-S7 and anti-L1 peptide antisera showed that S7 appeared to be associated with vesicle-like structures in the iRBC cytoplasm and L1 PIRs with the PV, in both acute- and chronic-stage parasites. However, in *P. chabaudi* iRBC obtained from chronic infection, S7 PIRs were observed to localise in close proximity to the iRBC membrane suggesting they might be localised on the surface. Fixation can adversely destroy the integrity of the cell membrane and thus it is not possible to conclude that PIR proteins are expressed on the outer surface of the iRBC. Therefore, live imaging and flow cytometry analysis of *P. chabaudi* iRBC following labelling with the same peptide antisera were performed to investigate whether S7 and L1 PIRs are externally localised on the iRBC membrane (**Figure 5**).

Live-cell immunofluorescent imaging of approximately 500-600 iRBC, across two individual biological replicates, obtained from acute and chronic *P. chabaudi* infections, showed complete absence of S7 and L1 PIRs on the iRBC surface, following staining with the anti-S7 or anti-L1 peptide antisera (**Figure 5A**; top panels), confirming that the S7s and L1s recognised by these antisera are not associated with the outer iRBC plasma membrane at the trophozoite-stage. They seem rather to remain within the iRBC, as shown in fixed sample preparations (81.18 ± 0.10% SEM S7+ iRBC and 98.03 ± 0.21% SEM L1+ iRBC). Labelling with the 9G8 and anti-MSP1 monoclonal antibodies, known to specifically target proteins located within the iRBC (Holder et al., 1992; Hartz et al., 1993) (**Figure 4A**; bottom panels), revealed positive staining only of acetone:methanol fixed/permeabilised iRBC.

To increase detection sensitivity of PIRs, we also conducted flow cytometric analysis of *P. chabaudi* iRBC at the acute- and chronic-phases of infection. Live (unfixed) iRBC were stained with anti-S7 and anti-L1 peptide antisera and compared with the same antibody staining on acetone:methanol fixed/permeabilised iRBC (**Figures 5C, D; Supplementary Figure S5**). The gating strategy used for the flow cytometry analysis is described in **Supplementary Figure S1**. The contour plots clearly demonstrate that live iRBC (Hoechst+) are not stained positively for the anti-S7 or anti-L1 antisera (mean 99.3 ± 0.3% SEM S7 and 99.5 ± 0.2% SEM L1 acute-phase parasitised RBC; mean 99.4 ± 0.4% SEM S7 and 99.4 ± 0.4% SEM L1 chronic-phase parasitised iRBC), whereas almost the entire population of the fixed/permeabilised iRBC (Hoechst+) was stained positive for either the anti-S7 or anti-L1 peptide antisera (mean 99.7 ± 0.1% SEM S7 and 99.7 ± 0.2% SEM L1 acute-phase parasitised RBC; mean 99.0 ± 0.5% SEM S7 and 98.2 ± 1.5% SEM L1 chronic-phase parasitised RBC). As with IFAs, positive staining with the 9G8 and anti-MSP1 monoclonal antibodies was observed only on fixed/permeabilised iRBC (**Figure 5B**; bottom panels).

Therefore, no significant staining of live iRBC on IFA or by flow cytometry could be seen with either the anti-S7 or anti-L1 peptide antisera. By contrast, fixed/permeabilised iRBC demonstrated clear labelling of the internal S7 and L1 PIR proteins with anti-S7 and anti-L1 peptide antisera. These data confirm that the S7 and L1 PIRs as recognised by these antisera, are not exposed on the surface of live iRBC but rather localised within them.

3.6 Fractionation of *P. chabaudi* iRBC to Investigate PIRs Localisation

To further investigate PIRs subcellular localisation, membrane fractionations were carried out using samples of iRBC at the trophozoite-stage to separate proteins translocated to the periphery and the host-cell cytoplasm from those localised in the PV/PVM or those remaining in the internal of the parasite. **Figure 6A** illustrates schematically the strategy and workflow of the fractionation procedures employed to separate proteins associated with each subcellular compartment. Briefly, to isolate proteins localised on the iRBC membrane and host-cell cytoplasm, *P. chabaudi* MT acute- and chronic-stage erythrocytic parasites at the trophozoite-stage were magnetically enriched and treated with Streptolysin-O (SLO fraction). The main function of SLO is to cause haemolysis, and therefore to permeabilise the iRBC plasma membrane without affecting the PVM (Jackson et al., 2007; Ruecker et al., 2012). SLO-treated cells were then treated with saponin (SAP fraction), which disrupts the PVM without affecting the plasma membrane of the parasite. This allows extraction of proteins that are localised either on the PVM or within the PV. Subsequently, the membrane soluble fraction was extracted in a buffer containing Tris.HCl (Tris fraction), which causes osmotic lysis. Following this step, all proteins localised in the parasite cytoplasm are released. Lastly, hydrophobic proteins associated with the parasite plasma membrane and proteins that interact with other parasite plasma membrane proteins were extracted in a RIPA lysis buffer supplemented with additional SDS and Triton (RIPA fraction) (**Figure 6A**).

Samples collected as previously described were subjected to western blot analysis using the rabbit anti-S7 and anti-L1 peptide antisera (**Figure 6B**). The results showed that the antisera-specific S7 PIRs are present in the SLO-fraction, represented by bands that migrate at about 40 kDa and 100 kDa, meaning they are localised either on the host-cell membrane or cytoplasm. No differences in the localisation were observed between SBP acute and MT acute- or chronic-phase parasites. The weak signal observed in the SAP fraction of MT parasites might be related to carry over proteins from the SLO fraction, since a Ter119 faint band can be also observed in the SAP fraction. The size of S7

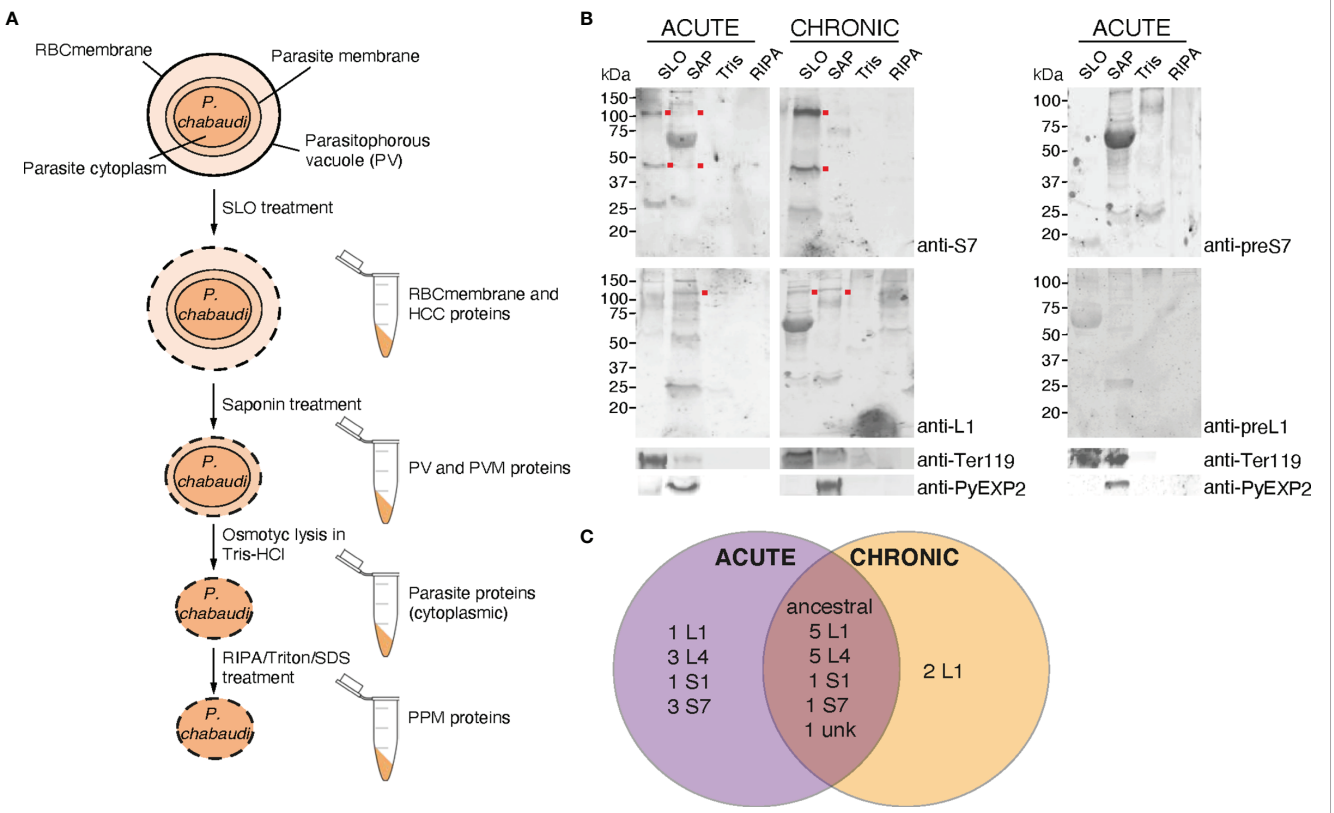

FIGURE 6 | Subcellular fractionation of *P. c. chabaudi AS* iRBC and localisation pattern of the PIR proteins. **(A)** Schematic representation of the fractionation workflow used to map the subcellular localisation of *P. chabaudi* PIR proteins. Briefly, *P. chabaudi* iRBC at the trophozoite-stage were magnetically enriched and treated with SLO, prior to being centrifuged to obtain a supernatant and a pellet fraction. Proteins localised on the iRBC membrane and cytoplasm are expected to be found in the supernatant. The pellet was then treated with saponin to release all proteins localised on the PV and PVM. Following centrifugation, the resulting pellet was incubated with Tris-HCl hypotonic lysis buffer and frozen. Following osmotic shock of the cells, proteins localised within the parasite cytoplasm are expected to be released. The remaining parasite membrane-associated proteins were extracted by treating the resulting pellet with RIPA lysis buffer enriched with SDS and Triton. The lysed membrane following each treatment is represented by a dotted line. The composition of each pellet sample obtained is also indicated. RBCmembrane: Red Blood Cell membrane, PV; Parasitophorous Vacuole, PPM; Parasite Plasma Membrane, PVM; Parasitophorous Vacuole Membrane, HCC; Host-Cell Cytoplasm. **(B)** Western blot analysis of *P. chabaudi* trophozoite fractionated protein samples, under reducing conditions. Fractionated samples were prepared from infected blood of C57Bl/6 RAG1$^{-/-}$ mice during acute- and chronic-phases of infection. Red dots indicate the estimated average size of the monomers or dimers of each PIR clade (S7 33-37 kDa and L1 75-151 kDa). Probing with pre-immune sera served as negative control. Antibodies against the mouse erythroid-specific marker Ter119 and *Plasmodium* EXP2 were used as stage-specific controls as well as to assess the samples purity. The molecular weights on the right indicate the positions to which size markers had migrated. SLO, Streptolysin-O fraction; SAP, Saponin fraction; Tris, Tris-HCl lysis. **(C)** Venn diagram depicting the overlap between the PIR proteins identified by mass spectrometry in all fractionated samples prepared from acute- and chronic-stage *P. chabaudi* infected erythrocytes. All PIR proteins identified in each set of samples are listed in **Tables 1** and **2**.

PIRs is predicted to be between 33-37 kDa, therefore the specific band observed at about 100 kDa suggests polymerisation. L1 PIRs have an expected size range between 75-151 kDa. Following western blot analysis of membrane fractionated samples of MT acute- or chronic- and SBP acute-phase parasites (**Supplementary Figure S6**), L1 antisera-specific PIRs were found to migrate at around 100 kDa and are predominantly present in the SAP fraction, where proteins associated with the PV and PVM are expected to be localised. In the MT chronic-phase parasites, a clear band was also observed in the SLO fraction. This agrees with the fluorescence microscopy data above (**Figures 2B**, **3A**), further suggesting secretion of L1 PIRs in the iRBC cytoplasm at this stage. The purity of the different samples was assessed by western blot probed with antibodies against the RBC membrane protein Ter119 and the PVM protein EXP2 (a gift of James Burns; Meibalan et al., 2015). The anti-EXP2 antibody revealed a ~30 kDa polypeptide, exclusively in the SAP fraction. Ter119 can be predominantly found in the SLO fraction, however some cross-contamination can be also observed in the SAP fraction. This is possibly associated with the high abundance of this protein on the RBC membrane, which is maintained in the sample after multiple washes, rather than RBC membrane debris contamination.

The anti-S7 and anti-L1 peptide antisera do not target all members of the PIR clades (**Supplementary Table S2**), therefore we performed mass spectrometry-based proteome analysis of the same fractionated samples (described above) as a more holistic approach to investigate the localisation of PIRs. Protein samples

from three individual experiments were in-gel digested and analysed by LC-MS/MS using data independent acquisition. Acquired MS/MS spectra were then searched against databases of tryptic peptides predicted from all *P. chabaudi* as well as all host proteins. The results indicated that purity of the samples is likely to be of high quality since proteins whose location is known e.g. MSP1 (Holder et al., 1992), EXP2 (Meibalan et al., 2015), PCHAS_0624800 (Hartz et al., 1993), were identified in the corresponding fraction. Nevertheless, localisation of some of the recovered proteins indicated low-level contamination between serially prepared fractions. We compared the proteome of the acute-stage parasites with the proteome of the chronic-stage parasites to identify (1) PIR proteins that are highly expressed during the acute- and/or chronic-phases of blood-stage infection, and (2) their localisation on the iRBC (iRBC membrane/Host-Cell Cytoplasm (HCC), PV/PVM, Parasite Cytoplasm (PCyt) or Parasite Plasma Membrane (PPM)). PIR proteins identified in the fractionated samples are shown in **Table 1**, **2**. The full list of *P. chabaudi* and *Mus musculus* proteins identified is given in **Supplementary Table S3**.

Proteomic analysis of four fractionated samples prepared from acute- or chronic-stage parasitised erythrocytes recovered on average 2,311 *P. chabaudi* and 3,634 *Mus musculus* proteins, across three individual biological replicates (**Supplementary Table S3**). Altogether, 23 individual PIRs were identified across all fractions of acute- and chronic-stage parasite preparations and all replicates conducted. Among them, 22 acute-stage associated PIRs and 16 chronic-stage associated PIRs were identified (**Table 1**, **2**, respectively). Among the PIRs recovered samples prepared from acute-stage parasites, 6 (27%) belong to the L1 clade, 8 (36%) to the L4 clade and 4 (18%) to the S7 clade. Additionally, 9 (41%) PIRs are located within the AAPL loci and 5 (23%) within the ChAPL loci. In total, 7 PIRs are located on chromosome 3 and 8 PIRs on chromosome 6. With regard to their subcellular localisation, 13 PIRs were picked up in at least 3 fractions suggesting that acute-associated PIRs are not limited to one subcellular compartment. Only 5 (23%) PIRs were exclusively found in one fractionated sample/subcellular compartment (1 in PV/PVM, 1 in PCyt and 3 in PPM). No association between clade or AAPL/ChAPL loci and subcellular compartment was found, however 14 PIRs were found to be localised in the iRBC membrane/HCC fraction, suggesting that they are exported proteins and further confirming our previous IFA findings (**Figure 2B**). Among the PIRs detected in samples prepared from parasites at the chronic phase of infection, only 1 (6%) of them belong to the S7 clade, 5 (31%) to the L4 clade and 7 (44%) to the L1 clade. Among the recovered PIRs, 3 (19%) are associated with the AAPL loci and 5 (31%) with the ChAPL loci. The majority of PIRs detected (9 PIRs; 56%) are located on chromosome 6, previously shown to be largely composed of ChAPL-associated clusters of *pir* genes (Brugat et al., 2017). Additionally, 7 PIRs (44%) were identified in all four subcellular compartments, 1 (6%) PIR in three subcellular compartments, and 8 PIRs (50%) were recovered exclusively within the parasite (either in PCyt or PPM). All identified PIRs, except PCHAS_0200031, were always being detected in the PPM fraction suggesting parasite membrane localisation within the iRBC. Comparing the PIRs identified at each phase of infection, a larger variation (e.g. AAPL/ChAPL loci association,

TABLE 1 | Localisation pattern of PIR proteins identified in proteome analyses of fractionated samples prepared from *P. chabaudi* infected erythrocytes at the acute phase of infection. .

Gene ID	Localization	Clade	AAPL/ChAPL Loci[1]	Chromosome
PCHAS_0101200	RBCmembrane/HCC, PV/PVM, PCyt, PPM	Ancestral		1
PCHAS_0200011	RBCmembrane/HCC, PV/PVM, PCyt, PPM	L4	AAPL	2
PCHAS_0200021	RBCmembrane/HCC, PV/PVM, PCyt, PPM	S1	AAPL	2
PCHAS_0200031	RBCmembrane/HCC, PV/PVM, PCyt, PPM	L4	AAPL	2
PCHAS_0300400	PV/PVM, PCyt	S7		3
PCHAS_0301400	RBCmembrane/HCC, PCyt, PPM	L1	ChAPL	3
PCHAS_0300900	PV/PVM, PPM	L1	ChAPL	3
PCHAS_0319600	RBCmembrane/HCC, PV/PVM, PPM	L4	AAPL	3
PCHAS_0319900	RBCmembrane/HCC, PV/PVM, PCyt, PPM	S7	AAPL	3
PCHAS_0320200	RBCmembrane/HCC, PV/PVM, PPM	S1	AAPL	3
PCHAS_0320000	PV/PVM, PCyt	S7	AAPL	3
PCHAS_0400500	PCyt	L4	AAPL	4
PCHAS_0524800	PPM	Unk		5
PCHAS_0600200	RBCmembrane/HCC, PCyt, PPM	S7		6
PCHAS_0600300	RBCmembrane/HCC, PV/PVM, PCyt, PPM	L4		6
PCHAS_0600500	RBCmembrane/HCC, PPM	L4		6
PCHAS_0600600	RBCmembrane/HCC, PV/PVM, PCyt, PPM	L4		6
PCHAS_0600700	PPM	L1		6
PCHAS_0600800	RBCmembrane/HCC, PV/PVM, PCyt, PPM	L1	ChAPL	6
PCHAS_0601100	RBCmembrane/HCC, PV/PVM, PCyt, PPM	L1	ChAPL	6
PCHAS_0626300	PV/PVM	L1	ChAPL	6
PCHAS_1200300	PPM	L4	AAPL	12

[1]*AAPL/ChAPL classification was first referenced in Thibaut et al., 2017.*

The localisation was defined based on which fractionated sample each PIR protein was recovered. RBC membrane, Red Blood Cell Membrane; HCC, Host-Cell Cytoplasm; PV, Parasitophorous Vacuole; PVM, Parasitophorous Vacuole Membrane; PCyt, Parasite Cytoplasm; PPM, Parasite Plasma Membrane.

TABLE 2 | Localisation pattern of PIR proteins identified in proteome analyses of fractionated samples prepared from *P. chabaudi* infected erythrocytes at the chronic phase of infection.

Gene ID	Localization	Clade	AAPL/ChAPL Loci[1]	Chromosome
PCHAS_0101200	RBCmembrane/HCC, PV/PVM, PCyt, PPM	Ancestral		1
PCHAS_0200011	PPM	L4	AAPL	2
PCHAS_0200021	PPM	S1	AAPL	2
PCHAS_0200031	PCyt	L4	AAPL	2
PCHAS_0301400	PV/PVM, PCyt, PPM	L1	ChAPL	3
PCHAS_0524800	PPM	Unk		5
PCHAS_0600200	PPM	S7		6
PCHAS_0600300	RBCmembrane/HCC, PV/PVM, PCyt, PPM	L4		6
PCHAS_0600500	PPM	L4		6
PCHAS_0600600	RBCmembrane/HCC, PV/PVM, PCyt, PPM	L4		6
PCHAS_0600700	PCyt, PPM	L1		6
PCHAS_0600800	RBCmembrane/HCC, PV/PVM, PCyt, PPM	L1	ChAPL	6
PCHAS_0601000	PCyt, PPM	L1	ChAPL	6
PCHAS_0601100	RBCmembrane/HCC, PV/PVM, PCyt, PPM	L1	ChAPL	6
PCHAS_0626300	RBCmembrane/HCC, PV/PVM, PCyt, PPM	L1	ChAPL	6
PCHAS_0731300	RBCmembrane/HCC, PV/PVM, PCyt, PPM	L1		7

[1]*AAPL/ChAPL classification was first referenced in Brugat et al., 2017.*

The localisation was defined based on which fractionated sample each PIR protein was recovered. RBC membrane, Red Blood Cell Membrane; HCC, Host-Cell Cytoplasm; PV, Parasitophorous Vacuole; PVM, Parasitophorous Vacuole Membrane; PCyt, Parasite Cytoplasm; PPM, Parasite Plasma Membrane.

chromosomal location, localisation pattern) and number of PIRs was recovered in acute-phase compared to chronic-phase parasite preparations (**Figure 6C**) possibly reflecting the complexity at this phase of infection.

Some of the PIRs detected in protein preparations of acute-phase parasites showed a wide distribution across all subcellular compartments, but as infection progresses to the chronic-phase, they appear to concentrate exclusively in one subcellular compartment e.g. PCHAS_0200011, PCHAS_0200021 and PCHAS_0200031 were recovered in all subcellular compartments of acute-phase parasites, but were not found to be secreted at the chronic-phase of infection.

The ancestral PIR, PCHAS_0101200 (Little et al., 2021), was consistently recovered in all samples prepared from both acute- and chronic-phase parasites and across all replicates conducted. Its high abundance in all subcellular compartments of the iRBC suggests that it is likely to be essential during parasite blood development.

In conclusion, there does not seem to be an exclusive subcellular compartment where PIR proteins are localised during both the acute- and chronic-phases of infection. This observation further supports the diverse nature of this family of proteins and consequently, the diversity in their function during *Plasmodium* blood development.

4 DISCUSSION

The *pir* multigene family, present in the genomes of most species of the malaria parasite, *Plasmodium*, with the exception of members of the *Laverania* subgenus, has so far no known functions. Transcription of the genes is upregulated in the late liver-stages of the parasite in mice, and remains high in the asexual blood cycle (Spence et al., 2013; Brugat et al., 2017; Little et al., 2021) further suggesting they are important at these stages of the life cycle. As a prerequisite to understanding the role of *pirs* in the erythrocytic-stages of *Plasmodium* infection, we have carried out a detailed investigation of the location of *P. chabaudi* PIR proteins within iRBC of this rodent-infecting parasite using a variety of approaches: IFA, Electron microscopy, subcellular fractionation, western blot and mass spectrometry. *Pir* genes of *P. chabaudi* have been the most widely characterised (Lawton et al., 2012; Otto et al., 2014), which offers the possibility of studying their expression and role in acute and chronic infections (Brugat et al., 2017), and in genetically diverse strains of the parasites (Lin et al., 2017). Thus *P. chabaudi* can serve as a model for exploring their potential roles in human malarias caused by *P. vivax*, *P.* ovale, *P. malariae* and *P. knowlesi*.

We generated antisera specific for a large fraction of PIRs within each of the S7 and L1 clades, the two clades of the *pir* gene family predominantly transcribed in *P. chabaudi* (Otto et al., 2014; Brugat et al., 2017). In agreement with previous transcriptional data (Spence et al., 2013) MT blood-stages parasites seem to express more PIR proteins than SBP parasites (**Figure 2C**). By immunofluorescence assay and western blot analysis with mass spectrometry, both S7 and L1 PIR proteins are detected in iRBC; S7s are located as discrete foci in the cytoplasm of iRBC at the acute-phase of infection. L1 PIRs are localised close to the PV/PVM, with some expression in the iRBC cytoplasm at the chronic-phase of infection. For both S7 and L1 localisation does not change over the 24-hour life cycle in the iRBC; however, as infection progresses to the chronic-phase S7 PIRs are detected close to the periphery of iRBC suggesting they may be exported to the surface of the iRBC. *P. chabaudi* schizonts are sequestered during the infection in mice (Gilks et al., 1990; Brugat et al., 2014), and can only be obtained after a period of *in vitro* culture, which may affect the detection of PIR at that stage and improving the culture of *P. chabaudi* would clarify PIR expression at this stage of parasite development. The differential PIR protein expression shown here is similar to that described for PIR/CIR by Yam et al. (2016), by immunofluorescent assay, using antisera specific for either A

or B PIRs, classified according to an earlier phylogenetic analysis of the encoded PIR proteins (Lawton et al., 2012), or GFP-tagged PIRs in transfected *P. chabaudi* parasites, where at trophozoite-stage most of the fluorescent signal was observed in the red cell cytosol, while at schizont-stage the signal was predominantly associated with individual merozoites. Another study using transgenic fluorescently tagged lines described PIR localisation as either patchy or punctate cytoplasmic, depending on the PIR, whereas in the liver most PIRs localised to the parasitophorous vacuole (Fougere et al., 2016). In agreement with our data, an earlier proteomic study also demonstrated an association of some PIRs with lipid rafts and trafficking beyond the PVM (Di Girolamo et al., 2008). Together these data suggest that PIR proteins of the different *pir* clades may have different functions.

Previously, we have shown that *P. chabaudi* parasites transmitted to mice *via* the mosquito vector are transcriptionally modified in asexual blood-stage parasite (Spence et al., 2013), and S7 *pir* genes are transcriptionally upregulated during the acute-phase of infection, whereas the chronic-phase is mostly dominated by the L1 *pirs* (Brugat et al., 2017). These S7 and L1 *pirs* were further categorised into virulence-associated clusters, called AAPL and ChAPL, respectively, as they occupy adjacent and distinct chromosomal loci, with L1 *pir* genes being particularly associated with chromosome 6 (Brugat et al., 2017). Here using mass spectrometry, we identify multiple PIR proteins of both S7 and L1 clades. While there is not a distinct expression profile of S7 or L1 and AAPL or ChAPL proteins at the acute-phase of *P. chabaudi* infections, as infection progresses to the chronic-phase, L1 PIRs seem to be predominantly expressed, with some of them belonging to the ChAPL loci, in agreement with the previous transcription data.

The observation of discrete foci of S7 staining at the acute- and chronic-phases of infection and L1 staining at the chronic-phase of infection in the iRBC cytoplasm, raises the possibility that S7s and L1s might be temporally associated with Maurer's clefts. Maurer's clefts are thought to function as sorting centres, through which *Plasmodium* proteins are trafficked on their way to the iRBC surface (Kriek et al., 2003; Tilley et al., 2008). The most important of these are surface parasite proteins involved in binding of iRBC to the host blood vessels, such as PfEMP1 encoded by the *var* multigene family, repetitive interspersed family proteins (RIFINs), and sub-telomeric variant open reading frame proteins (STEVORs), all of which localise to the Maurer's clefts on their way to the iRBC surface (Kaviratne et al., 2002; Kriek et al., 2003; Haeggstrom et al., 2004; McRobert et al., 2004; Blythe et al., 2008). A number of other parasite proteins involved in modifying the host cell also localise to the Maurer's clefts such as PfMC-2TMs (Tsarukyanova et al., 2009), several FIKK serine/threonine kinases (Nunes et al., 2007), as well as some members of the *Plasmodium* helical interspersed subtelomeric (PHIST) family of parasite proteins, with roles in host cell remodelling (reviewed by Warncke et al., 2016) and rigidity of the infected cell (Davies et al., 2020). Although the PEXEL/VTS protein export motif, a characteristic of many of the secreted proteins of *Plasmodium*, is absent from PIR proteins, they have transmembrane helices (Del Portillo et al., 2001; Janssen et al., 2004). Other Maurer's cleft-associated proteins such as SBP1 and MAHRP1, which are localised on *P. falciparum* and *P. berghei* Maurer's clefts, lack the PEXEL motif and are classified as PEXEL-negative exported proteins (PNEPs) (Blisnick et al., 2000; Spycher et al., 2003). SBP1 and MAHRP1 are part of the Maurer's clefts trafficking machinery previously shown to be essential for the transport of PfEMP1 and other surface antigens to the iRBC surface. In *P. berghei* blood-stage parasites the PIRs analysed were found in the cytoplasm while in liver-stage parasites they remained associated with the parasitophorous vacuole (Fougere et al., 2016).

It is possible that the differential co-localisation of SBP1 and 9G8 may be due to different proteins being assembled prior to export, as described for proteins within J-dots, structures within the iRBC containing proteins for further export (Külzer et al., 2010; Kulzer et al., 2012) (i.e. some dots are double positive for SBP1 and 9G8, where others are single positive for either SBP1 or 9G8). Maurer's clefts have previously been described in *P. chabaudi* iRBC (Lanners et al., 1999) and here electron microscopy revealed Maurer's cleft-like structures in the cytoplasm of iRBC. As both the SBP1 and S7/L1 are rabbit antibodies, co-localisation studies could not be performed. However, the antigen recognised by 9G98 monoclonal antibodies, co-localises with both the Maurer's cleft protein SBP1 and with S7 PIRs, strongly suggesting that S7s are present in Maurer's cleft at least during the acute-stage of infection in the mouse. In chronic-phase parasites S7s move closer to the inner periphery of the iRBC membrane and are no longer co-localised with the Maurer's clefts (based on the SBP1 localisation). Direct visualisation of S7 proteins within Maurer's cleft clefts is ongoing.

The association of S7 PIRs with Maurer's clefts and their later location close to the iRBC membrane would suggest that PIRs, like the RIFINs, STEVORs and PfEMP1 of *P. falciparum*, are being relocated to the iRBC membrane (Kaviratne et al., 2002; Kriek et al., 2003; Haeggstrom et al., 2004; McRobert et al., 2004; Blythe et al., 2008). These antigenically variant *P. falciparum* proteins have been shown to be at the surface of the iRBC, and are thought to be involved in immune evasion as well as adhering to host cells such as endothelium and red blood cells (reviewed by Kyes et al., 2001). However, despite an association with Maurer's clefts, PIRs cannot readily be ascribed to these roles. Unlike PfEMP1, where a single iRBC expresses a single variant which would be required for successfully evading the host antibody response by antigenic variation, our IFA and previous studies by Yam et al. (2016) suggest that iRBC can simultaneously express both S7 and L1 (or A and B) PIRs. This is in agreement with the observations of the Franke-Fayard laboratory (Fougere et al., 2016) where fluorescent signal was observed from both tagged PIRs in a double PIR transgenic line, and also single cell transcriptional data using *P. berghei* (Howick et al., 2019) showing expression of more than one *pir*/PIR in an individual iRBC. Furthermore, although S7 PIRs were observed close the iRBC membrane, we were unable to detect either S7 or L1 PIRs on live iRBC suggesting that they are not on the outer iRBC membrane. As

our antisera do not detect all members of each clade, it is possible that those PIRs that were not picked up by our antisera are exposed on the iRBC surface. Alternatively, PIRs may be exposed transiently at only a particular time point in the 24-hour cycle, which we may have missed. It is also possible that peptide antisera do not recognise the S7 and L1 PIRs in their natural form in live iRBCs, since the linear peptides, used for immunisation to generate the peptide antisera, might be exposed in denatured but not in the native protein structures.

As mentioned above, *P. chabaudi* schizonts sequester in tissues and organs (Gilks et al., 1990; Brugat et al., 2014) and thus are difficult to obtain *ex vivo*, and *in vitro* culture of *P. chabaudi* is so far not very successful. *In situ* tagging of individual *pirs* and development of culture conditions to yield good viable schizonts may provide unequivocal evidence of location on the surface of the iRBC.

If PIRs are not located on the outer surface of iRBC, then where and why are they being transported by Maurer's clefts? This may be explained by the fact that they are components of the *Plasmodium* translocon of exported proteins (PTEX) (De Koning-Ward et al., 2009) and thus, they may act as adaptors or chaperones for the transport of other proteins to the iRBC surface, as it has been described for HSP101 in *P. falciparum* (Beck et al., 2014; Elsworth et al., 2014). They may also be part of the parasite machinery involved in cytoskeleton remodelling as it has been described for the FIKKs of *P. falciparum*, which are also transported in Maurer's clefts, as mentioned above (Davies et al., 2020). If these are possibilities, one is left with the question of why there are so many PIRs and why are they so diverse?

The P. chabaudi model for investigating this family of genes that exist in many *Plasmodium* species will allow us to address these questions and their roles in acute and chronic infection. The elucidation of proteins which interact with proteins of this multigene family, particularly those PIRs identified by mass spectrometry, may shed some light on their function.

DATA AVAILABILITY STATEMENT

The datasets presented in this study can be found in online repositories. The names of the repository/repositories and accession number(s) can be found in the article/**Supplementary Material**.

ETHICS STATEMENT

The animal study was reviewed and approved by The Francis Crick Institute Ethical Committee.

AUTHOR CONTRIBUTIONS

MG, DC, and JL designed the project, analysed the data, and wrote the manuscript. MG performed research with experimental help from DC, CH, AV, SA, AA, LS, FU, and LT. MB performed the mass-spectrometric analysis. AS carried out the electron microscopy imaging and analysis. TH and MH carried out recombinant protein expression and purification. JL and MH provided reagents/materials/analysis tools. All authors read, critically revised, and approved the final manuscript.

FUNDING

This work was supported by the Francis Crick Institute which receives its core funding from the UK Medical Research Council (FC001101), Cancer Research UK (FC001101) and the Wellcome Trust (FC001101); JL is a Wellcome Trust Senior Investigator (grant reference WT101777MA). MH is a Wellcome Investigator (220797/Z/20/Z) and this work was funded by the Medical Research Council (MR/T000368/1).

ACKNOWLEDGMENTS

We thank the Biological Research Facility, Advanced Light Microscopy Science Technology Platform, Proteomics Science Technology Platform and, Lucy Collinson and the Electron Microscopy Science Technology Platform at the Francis Crick Institute for their support; Joe Brock from the Research and Illustration team for his help with the figures, and Prisca Hill and Sarah Manni for their technical assistance. We would also like to thank Tobias Spielmann (Bernhard Nocht Institute for Tropical Medicine, Hamburg, Germany) and James Burns (Drexel University College of Medicine, Philadelphia, United States) for kindly providing us with the anti-*Pb*SBP1 and anti-*Py*EXP2 antibodies, respectively.

SUPPLEMENTARY MATERIAL

The Supplementary Material for this article can be found online at: https://www.frontiersin.org/articles/10.3389/fcimb.2022.877253/full#supplementary-material

Supplementary Figure S1 | Representative flow cytometry plots describing the gating strategy followed to investigate the surface localisation of S7 or L1 PIRS in P. c. chabaudi AS iRBC.

Supplementary Figure S2 | Subcellular localisation of S7 and L1 PIRs in the late trophozoite stage of MT and SBP P. c. chabaudi AS parasites, during the acute- and chronic-phases of infection.

Supplementary Figure S3 | Localisation pattern of S7 and L1 PIRs across the 24-hour asexualblood cycle of MT P. c. chabaudi AS parasites, during acute- and chronic-phases of infection.

Supplementary Figure S4 | Localisation pattern of S7 and L1 PIRs in in vitro SBP acute-stage P. c. chabaudi AS schizonts.

Supplementary Figure S5 | Contour plots of each individual replicate of the flow cytometric analysis performed on live and acetone:methanol fixed (control) P. c. chabaudi AS iRBC, following labelling with the anti-S7 or anti-L1 peptide antisera.

Supplementary Figure S6 | Western blot analysis of fractionated protein samples of P. c. chabaudi SBP acute-phase parasites at the trophozoite-stage.

Supplementary Table 1 | P. chabaudi PIR clade peptide motifs and BlastP results against clade members.

Supplementary Table 2 | P. chabaudi PIR proteins identified as reciprocal best hits of each motif designed against the S7 and L1 clades.

Supplementary Table 3 | Mass spectrometry-based analysis of PIR expression and subcellular localization during acute and chronic phases of infection.

REFERENCES

Atkinson, C. T., and Aikawa, M. (1990). Ultrastructure of Malaria-Infected Erythrocytes. *Blood Cells* 16 (2-3), 351–368.

Aurrecoechea, C., Brestelli, J., Brunk, B. P., Dommer, J., Fischer, S., Gajria, B., et al. (2009). PlasmoDB: A Functional Genomic Database for Malaria Parasites. *Nucleic Acids Res.* 37, D539–D543. doi: 10.1093/nar/gkn814

Baruch, D. I., Gormely, J. A., Ma, C., Howard, R. J., and Pasloske, B. L. (1996). *Plasmodium Falciparum* Erythrocyte Membrane Protein 1 is a Parasitised Erythrocyte Receptor for Adherence to CD36, Thrombospondin, and Intercellular Adhesion Molecule 1. *Proc. Natl. Acad. Sci. U.S.A.* 93 (8), 3497–3502. doi: 10.1073/pnas.93.8.3497

Beck, J. R., Muralidharan, V., Oksman, A., and Goldberg, D. E. (2014). PTEX Component HSP101 Mediates Export of Diverse Malaria Effectors Into Host Erythrocytes. *Nature* 511 (7511), 592–595. doi: 10.1038/nature13574

Blisnick, T., Morales-Betoulle, M. E., Barale, J. C., Uzureau, P., Berry, L., Desroses, S., et al. (2000). Pfsbp1, a Maurer's Cleft *Plasmodium Falciparum* Protein, is Associated With the Erythrocyte Skeleton. *Mol. Biochem. Parasitol.* 111 (1), 107–121. doi: 10.1016/s0166-6851(00)00301-7

Blythe, J. E., Yam, X. Y., Kuss, C., Bozdech, Z., Holder, A. A., Marsh, K., et al. (2008). *Plasmodium Falciparum* STEVOR Proteins are Highly Expressed in Patient Isolates and Located in the Surface Membranes of Infected Red Blood Cells and the Apical Tips of Merozoites. *Infect. Immun.* 76 (7), 3329–3336. doi: 10.1128/IAI.01460-07

Boyle, D. B., Newbold, C. I., Smith, C. C., and Brown, K. N. (1982). Monoclonal Antibodies That Protect *In Vivo* Against *Plasmodium Chabaudi* Recognise a 250,000-Dalton Parasite Polypeptide. *Infect. Immun.* 38 (1), 94–102. doi: 10.1128/iai.38.1.94-102.1982

Bozdech, Z., Mok, S., Hu, G., Imwong, M., Jaidee, A., Russell, B., et al. (2008). The Transcriptome of *Plasmodium Vivax* Reveals Divergence and Diversity of Transcriptional Regulation in Malaria Parasites. *Proc. Natl. Acad. Sci. U.S.A.* 105 (42), 16290–16295. doi: 10.1073/pnas.0807404105

Brugat, T., Cunningham, D. A., Sodenkamp, J., Coomes, S., Wilson, M., Spence, P. J., et al. (2014). Sequestration and Histopathology in *Plasmodium Chabaudi* Malaria are Influenced by the Immune Response in an Organ-Specific Manner. *Cell Microbiol.* 16 (5), 687–700. doi: 10.1111/cmi.12212

Brugat, T., Reid, A. J., Lin, J. W., Cunningham, D. A., Tumwine, I., Kushinga, G., et al. (2017). Antibody-Independent Mechanisms Regulate the Establishment of Chronic *Plasmodium* Infection. *Nat. Microbiol.* 2, 16276. doi: 10.1038/nmicrobiol.2016.276

Buffet, P. A., Safeukui, I., Deplaine, G., Brousse, V., Prendki, V., Thellier, M., et al. (2011). The Pathogenesis of *Plasmodium Falciparum* Malaria in Humans: Insights From Splenic Physiology. *Blood* 117, 381–392. doi: 10.1182/blood-2010-04-202911

Crosnier, C., Wanaguru, M., McDade, B., Osier, F. H., Marsh, K., Rayner, J. C., et al. (2013). A Library of Functional Recombinant Cell-Surface and Secreted *P. Falciparum* Merozoite Proteins. *Mol. Cell Prot.* 12 (12), 3976–3986. doi: 10.1074/mcp.O113.028357

Cunningham, D. A., Fonager, J., Jarra, W., Carret, C., Preiser, P., and Langhorne, J. (2009). Rapid Changes in Transcription Profiles of the *Plasmodium Yoelii Yir* Multigene Family in Clonal Populations: Lack of Epigenetic Memory? *PloS One* 4, e4285. doi: 10.1371/journal.pone.0004285

Cunningham, D. A., Jarra, W., Koernig, S., Fonager, J., Fernandez-Reyes, D., Blythe, J. E., et al. (2005). Host Immunity Modulates Transcriptional Changes in a Multigene Family (*Yir*) of Rodent Malaria. *Mol. Microbiol.* 58, 636–647. doi: 10.1111/j.1365-2958.2005.04840.x

Davies, H., Belda, H., Broncel, M., Ye, X., Bisson, C., Introini, V., et al. (2020). An Exported Kinase Family Mediates Species-Specific Erythrocyte Remodelling and Virulence in Human Malaria. *Nat. Microbiol.* 5 (6), 848–863. doi: 10.1038/s41564-020-0702-4

Deerinck, T. J., Bushong, E. A., Thor, A., and Ellisman, M. H. (2010). NCMIR Methods for 3D EM: A New Protocol for Preparation of Biological Specimens for Serial Block Face Scanning Electron Microscopy. *Microscopy*, 6–8. https://ncmir.ucsd.edu

De Koning-Ward, T. F., Gilson, P. R., Boddey, J. A., Rug, M., Smith, B. J., Papenfuss, A. T., et al. (2009). A Newly Discovered Protein Export Machine in Malaria Parasites. *Nature* 459 (7249), 945–949. doi: 10.1038/nature08104

Del Portillo, H. A., Fernandez-Becerra, C., Bowman, S., Oliver, K., Preuss, M., Sanchez, C. P., et al. (2001). A Superfamily of Variant Genes Encoded in the Subtelomeric Region of *Plasmodium Vivax*. *Nature* 410, 839–842. doi: 10.1038/35071118

De Niz, M., Ullrich, A. K., Heiber, A., Blancke-Soares, A., Pick, C., Lyck, R., et al. (2016). The Machinery Underlying Malaria Parasite Virulence is Conserved Between Rodent and Human Malaria Parasites. *Nat. Comms.* 7, 11659. doi: 10.1038/ncomms11659

Di Girolamo, F., Raggi, C., Birago, C., Pizzi, E., Lalle, M., Picci, L., et al. (2008). Plasmodium Lipid Rafts Contain Proteins Implicated in Vesicular Trafficking and Signalling as Well as Members of the PIR Superfamily, Potentially Implicated in Host Immune System Interactions. *Proteomics* 8 (12), 2500–2513. doi: 10.1002/pmic.200700763

Ekland, E. H., Akabas, M. H., and Fidock, D. A. (2011). Taking Charge: Feeding Malaria *via* Anion Channels. *Cell* 145 (5), 645–647. doi: 10.1016/j.cell.2011.05.012

Elsworth, B., Matthews, K., Nie, C. Q., Kalanon, M., Charnaud, S. C., Sanders, P. R., et al. (2014). PTEX is an Essential Nexus for Protein Export in Malaria Parasites. *Nature* 31, 511(7511):587–91. doi: 10.1038/nature13555

Fougere, A., Jackson, A. P., Bechtsi, D. P., Braks, J. A., Annoura, T., Fonager, J., et al. (2016). Variant Exported Blood-Stage Proteins Encoded by *Plasmodium* Multigene Families are Expressed in Liver Stages Where They are Exported Into the Parasitophorous Vacuole. *PloS Pathog.* 12, e1005917. doi: 10.1371/journal.ppat.1005917

Freitas-Junior, L. H., Bottius, E., Pirrit, L. A., Deitsch, K. W., Scheidig, C., Guinet, F., et al. (2000). Frequent Ectopic Recombination of Virulence Factor Genes in Telomeric Chromosome Clusters of *P. Falciparum*. *Nature* 26, 407 (6807):1018–22. doi: 10.1038/35039531

Gilks, C. F., Walliker, D., and Newbold, C. I. (1990). Relationships Between Sequestration, Antigenic Variation and Chronic Parasitism in *Plasmodium Chabaudi Chabaudi*-a Rodent Malaria Model. *Parasit. Immunol.* 12 (1), 45–64. doi: 10.1111/j.1365-3024.1990.tb00935.x

Haeggstrom, M., Kironde, F., Berzins, K., Chen, Q., Wahlgren, M., and Fernandez, V. (2004). Common Trafficking Pathway for Variant Antigens Destined for the Surface of the *Plasmodium Falciparum*-Infected Erythrocyte. *Mol. Biochem. Parasitol.* 133 (1), 1–14. doi: 10.1016/j.molbiopara.2003.07.006

Harrison, T. E., Reid, A. J., Cunningham, D. A., Langhorne, J., and Higgins, M. K. (2020). Structure of the *Plasmodium*-Interspersed Repeat Proteins of the Malaria Parasite. *Proc. Natl. Acad. Sci. U.S.A.* 117, 32098–32104. doi: 10.1073/pnas.2016775117

Hartz, D., Ayane, M., Chluba-De Tapia, J., Wirbelauer, C., Langhorne, J., and Gillard-Blass, S. (1993). Cloning and Sequencing of a cDNA Fragment From *Plasmodium Chabaudi Chabaudi* That Contains Repetitive Sequences Coding for a Potentially Lysine-Rich Aspartic Acid-Rich Protein. *Parasitol. Res.* 79 (2), 133–139. doi: 10.1007/BF00932259

Henrich, P., Kilian, N., Lanzer, M., and Cyrklaff, M. (2009). 3-D Analysis of the *Plasmodium Falciparum* Maurer's Clefts Using Different Electron Tomographic Approaches. *Biotechnol. J.* 4 (6), 888–894. doi: 10.1002/biot.200900058

Holder, A. A., Blackman, M. J., Burghaus, P. A., Chappel, J. A., Ling, I. T., McCallum-Deighton, N., et al. (1992). A Malaria Merozoite Surface Protein (MSP1)-Structure, Processing and Function. *Mem. Inst. Oswaldo Cruz* 87 (3), 37–42. doi: 10.1590/s0074-02761992000700004

Howick, V. M., Russell, A. J. C., Andrews, T., Heaton, H., Reid, A. J., Natarajan, K., et al. (2019). The Malaria Cell Atlas: Single Parasite Transcriptomes Across the Complete *Plasmodium* Life Cycle. *Science* 365, eaaw2619. doi: 10.1126/science.aaw2619

Ingmundson, A., Nahar, C., Brinkmann, V., Lehmann, M. J., and Matuschewski, K. (2012). The Exported *Plasmodium Berghei* Protein IBIS1 Delineates Membranous Structures in Infected Red Blood Cells. *Mol. Microbiol.* 83 (6), 1229–1243. doi: 10.1111/j.1365-2958.2012.08004.x

Jackson, K. E., Spielmann, T., Adisa, A., Separovic, F., Dixon, M. W., Trenholme, P. L., et al. (2007). Selective Permeabilisation of the Host Cell Membrane of *Plasmodium Falciparum*-Infected Red Blood Cells With Streptolysin O and Equinatoxin II. *Biochem. J.* 403 (1), 167–175. doi: 10.1042/BJ20061725

Janssen, C. S., Barrett, M. P., Turner, C. M., and Phillips, R. S. (2002). A Large Gene Family for Putative Variant Antigens Shared by Human and Rodent Malaria Parasites. *Proc. R Soc. Lond. B Biol. Sc.*, 269 (1489), 431–436. doi: 10.1098/rspb.2001.1903

Janssen, C. S., Phillips, R. S., Turner, C. M., and Barrett, M. P. (2004). *Plasmodium* Interspersed Repeats: The Major Multigene Superfamily of Malaria Parasites. *Nucleic Acids Res.* 32 (19), 5712–5720. doi: 10.1093/nar/gkh907

Kaviratne, M., Khan, S. M., Jarra, W., and Preiser, P. R. (2002). Small Variant STEVOR Antigen is Uniquely Located Within Maurer's Clefts in *Plasmodium Falciparum*-Infected Red Blood Cells. *Eukaryot. Cell.* 1, 926–935. doi: 10.1128/EC.1.6.926-935.2002

Kriek, N., Tilley, L., Horrocks, P., Pinches, R., Elford, B. C., Ferguson, D. J., et al. (2003). Characterisation of the Pathway for Transport of the Cytoadherence-Mediating Protein, PfEMP1, to the Host Cell Surface in Malaria Parasite-Infected Erythrocytes. *Mol. Microbiol.* 50 (4), 1215–1227. doi: 10.1046/j.1365-2958.2003.03784.x

Külzer, S., Rug, M., Brinkmann, K., Cannon, P., Cowman, A., Lingelbach, K., et al. (2010). Parasite-Encoded Hsp40 Proteins Define Novel Mobile Structures in the Cytosol of the *P. Falciparum*-Infected Erythrocyte. *Cell Microbiol.* 12 (10), 1398–1420. doi: 10.1111/j.1462-5822.2010.01477.x

Kyes, S., Horrocks, P., and Newbold, C. (2001). Antigenic Variation at the Infected Red Cell Surface in Malaria. *Annu. Rev. Microbiol.* 55, 673–707. doi: 10.1146/annurev.micro.55.1.673

Kyes, S. A., Rowe, J. A., Kriek, N., and Newbold, C. I. (1999). RIFINS: A Second Family of Clonally Variant Proteins Expressed on the Surface of Red Cells Infected With *Plasmodium Falciparum*. *Proc. Natl. Acad. Sci. U.S.A.* 96 (16), 9333–9338. doi: 10.1073/pnas.96.16.9333

Lamb, T. J., Brown, D. E., Potocnik, A. J., and Langhorne, J. (2006). Insights Into the Immunopathogenesis of Malaria Using Mouse Models. *Expert Rev. Mol. Med.* 8 (6), 1–22. doi: 10.1017/S1462399406010581

Langhorne, J., Ndungu, F. M., Sponaas, A. M., and Marsh, K. (2008). Immunity to Malaria: More Questions Than Answers. *Nat. Immunol.* 9 (7), 725–732. doi: 10.1038/ni.f.205

Langreth, S. G., Jensen, J. B., Reese, R. T., and Trager, W. (1978). Fine Structure of Human Malaria *In Vitro*. *J. Protozool.* 25 (4), 443–452. doi: 10.1111/j.1550-7408.1978.tb04167.x

Lanners, H. N., Bafford, R. A., and Wiser, M. F. (1999). Characterization of the Parasitophorous Vacuole Membrane From *Plasmodium Chabaudi* and Implications About its Role in the Export of Parasite Proteins. *Parasitol. Res.* 85 (5), 349–355. doi: 10.1007/s004360050561

Lawton, J., Brugat, T., Yan, Y. X., Reid, A. J., Böhme, U., Otto, T. D., et al. (2012). Characterisation and Gene Expression Analysis of the Cir Multi-Gene Family of *Plasmodium Chabaudi Chabaudi* (as). *BMC Genomics* 13, 125. doi: 10.1186/1471-2164-13-125

Leech, J. H., Barnwell, J. W., Miller, L. H., and Howard, R. J. (1984). Identification of a Strain-Specific Malarial Antigen Exposed on the Surface of *Plasmodium Falciparum*-Infected Erythrocytes. *J. Exp. Med.* 159, 1567–1575. doi: 10.1084/jem.159.6.1567

Lin, J. W., Sodenkamp, J., Cunningham, D., Deroost, K., Tshitenge, T. C., McLaughlin, S., et al. (2017). Signatures of Malaria-Associated Pathology Revealed by High-resolution Whole-Blood Transcriptomics in a Rodent Model of Malaria. *Sci. Rep* 7, 41722. doi: 10.1038/srep41722

Little, T. S., Cunningham, D. A., Lopez, C. T., Amis, S. I., Alder, C., Addy, J. W. G., et al. (2021). Analysis of Pir Gene Expression Across the *Plasmodium* Life Cycle. *Malar J.* 445–59. doi: 10.1186/s12936-021-03979-6

McRobert, L., Preiser, P., Sharp, S., Jarra, W., Kaviratne, M., Taylor, M. C., et al. (2004). Distinct Trafficking and Localisation of STEVOR Proteins in Three Stages of the *Plasmodium Falciparum* Life Cycle. *Infect. Immun.* 72 (11), 6597–6602. doi: 10.1128/IAI.72.11.6597-6602.2004

Meibalan, E., Comunale, M. A., Lopez, A. M., Bergman, L. W., Mehta, A., Vaidya, A. ,. B., et al. (2015). Host Erythrocyte Environment Influences the Localisation of Exported Protein 2, an Essential Component of the *Plasmodium* Translocon. *Eukaryot. Cell.* 14 (4), 371–384. doi: 10.1128/EC.00228-14

Mombaerts, P., Iacomini, J., Johnson, R. S., Herrup, K., Tonegawa, S., and Papaioannou, V. E. (1992). RAG-1-Deficient Mice Have No Mature B and T Lymphocytes. *Cell* 68, 869–877. doi: 10.1016/0092-8674(92)90030-g

Mota, M. M., Jarra, W., Hirst, E., Patnaik, P. K., and Holder, A. A. (2000). *Plasmodium Chabaudi*-Infected Erythrocytes Adhere to CD36 and Bind to Microvascular Endothelial Cells in an Organ-Specific Way. *Infect. Immun.* 68 (7), 4135–4144. doi: 10.1128/IAI.68.7.4135-4144.2000

Mundwiler-Pachlatko, E., and Beck, H. P. (2013). Maurer's Clefts, the Enigma of *Plasmodium Falciparum*. *Proc. Natl. Acad. Sci. U.S.A.* 110 (50), 19987–19994. doi: 10.1073/pnas.1309247110

Niang, M., Yan Yam, X., and Preiser, P. R. (2009). The *Plasmodium falciparum* STEVOR Multigene Family Mediates Antigenic Variation of the Infected Erythrocyte. *PLoS Pathog.* 5 (2), e1000307. doi: 10.1371/journal.ppat.1000307

Niang, M., Bei, A. K., Madnani, K. G., Pelly, S., Dankwa, S., Kanjee, U., et al. (2014). STEVOR is a *Plasmodium Falciparum* Erythrocyte Binding Protein That Mediates Merozoite Invasion and Rosetting. *Cell Host Microbe* 16 (1), 81–93. doi: 10.1016/j.chom.2014.06.004

Nunes, M. C., Goldring, J. P., Doerig, C., and Scherf, A. (2007). A Novel Protein Kinase Family in *Plasmodium Falciparum* is Differentially Transcribed and Secreted to Various Cellular Compartments of the Host Cell. *Mol. Microbiol.* 63 (2), 391–403. doi: 10.1111/j.1365-2958.2006.05521.x

Otto, T. D., Bohme, U., Jackson, A. P., Hunt, M., Franke-Fayard, B., Hoeijmakers, W. A., et al. (2014). A Comprehensive Evaluation of Rodent Malaria Parasite Genomes and Gene Expression. *BMC Biol.* 12, 86. doi: 10.1186/s12915-014-0086-0

Pasini, E. M., Braks, J. A., Fonager, J., Klop, O., Aime, E., Spaccapelo, R., et al. (2013). Proteomic and Genetic Analyses Demonstrate That *Plasmodium Berghei* Blood Stages Export a Large and Diverse Repertoire of Proteins. *Mol. Cell Proteomics* 12, 426–448. doi: 10.1074/mcp.M112.021238

Perez-Riverol, Y., Csordas, A., Bai, J., Bernal-Llinares, M., Hewapathirana, S., Kundu, D. J., et al. (2019). The PRIDE Database and Related Tools and Resources in 2019: Improving Support for Quantification Data. *Nucleic Acids Res.* 47 (D1), D442–D450. doi: 10.1093/nar/gky1106

Przyborski, J. M., Miller, S. K., Pfahler, J. M., Henrich, P. P., Rohrbach, P., Crabb, B. S., et al. (2005). Trafficking of STEVOR to the Maurer's Clefts in *Plasmodium Falciparum*-Infected Erythrocytes. *EMBO J.* 24 (13), 2306–2317. doi: 10.1038/sj.emboj.76007202005

Reid, A. J., Talman, A. M., Bennett, H. M., Gomes, A. R., Sanders, M. J., Illingworth, C. J. R., et al. (2018). Single-Cell RNA-Seq Reveals Hidden Transcriptional Variation in Malaria Parasites. *Elife* 7, e33105. doi: 10.7554/eLife.33105

Ruecker, A., Shea, M., Hackett, F., Suarez, C., Hirst, E. M., Milutinovic, K., et al. (2012). Proteolytic Activation of the Essential Parasitophorous Vacuole Cysteine Protease SERA6 Accompanies Malaria Parasite Egress From its Host Erythrocyte. *J. Biol. Chem.* 287 (45), 37949–37963. doi: 10.1074/jbc.M112.400820

Rutledge, G. G., Bohme, U., Sanders, M., Reid, A. J., Cotton, J. A., Maiga-Ascofare, O., et al. (2017). *Plasmodium malariae* and *P. ovale* Genomes Provide Insights Into Malaria Parasite Evolution. *Nature* 542 (7639), 101–104 doi: 10.1038/nature21038

Sa, J. M., Cannon, M. V., Caleon, R. L., Wellems, T. E., and Serre, D. (2020). Single-Cell Transcription Analysis of *Plasmodium Vivax* Blood-Stage Parasites Identifies Stage- and Species-Specific Profiles of Expression. *PloS Biol.* 18, e3000711. doi: 10.1371/journal.pbio.3000711

Saito, F., Hirayasu, K., Satoh, T., Wang, C. W., Lusingu, J., Arimori, T., et al. (2017). Immune Evasion of *Plasmodium Falciparum* by RIFIN *via* Inhibitory Receptors. *Nature* 552 (7683), 101–105. doi: 10.1038/nature24994

Sam-Yellowe, T. Y. (2009). The Role of the Maurer's Clefts in Protein Transport in *Plasmodium Falciparum*. *Trends Parasitol.* 25 (6), 277–284. doi: 10.1016/j.pt.2009.03.009

Scherf, A., Hernandez-Rivas, R., Buffet, P., Bottius, E., Benatar, C., Pouvelle, B., et al. (1998). Antigenic Variation in Malaria: In *Situ* Switching, Relaxed and Mutually Exclusive Transcription of Var Genes During Intra-Erythrocytic Development in *Plasmodium Falciparum*. *EMBO J.* 17, 5418–5426. doi: 10.1093/emboj/17.18.5418

Scherf, A., Lopez-Rubio, L. L., and Riviere, L. (2008). Antigenic Variation in *Plasmodium Falciparum*. *Annu. Rev. Microbiol.* 62, 445–470. doi: 10.1146/annurev.micro.61.080706.093134

Spence, P. J., Cunningham, D. A., Jarra, W., Lawton, J., Langhorne, J., and Thompson, J. (2011). Transformation of the Rodent Malaria Parasite *Plasmodium Chabaudi*. *Nat. Protoc.* 6 (4), 553–561. doi: 10.1038/nprot.2011.313

Spence, P. J., Jarra, W., Levy, P., Nahrendorf, W., and Langhorne, J. (2012). Mosquito Transmission of the Rodent Malaria Parasite *Plasmodium Chabaudi*. *Malar J.* 11, 407. doi: 10.1186/1475-2875-11-407

Spence, P. J., Jarra, W., Levy, P., Reid, A. J., Chappell, L., Brugat, T., et al. (2013). Vector Transmission Regulates Immune Control of *Plasmodium* Virulence. *Nature* 498, 228–231. doi: 10.1038/nature12231

Spycher, C., Klonis, N., Spielmann, T., Kump, E., Steiger, S., Tilley, L., et al. (2003). MAHRP-1, a Novel *Plasmodium Falciparum* Histidine-Rich Protein, Binds Ferriprotoporphyrin IX and Localises to the Maurer's Clefts. *J. Biol. Chem.* 278 (37), 35373–35383. doi: 10.1074/jbc.M305851200

Su, X. Z., Heatwole, V. M., Wertheimer, S. P., Guinet, F., Herrfeldt, J. A., Peterson, D. S., et al. (1995). The Large Diverse Gene Family Var Encodes Proteins Involved in Cytoadherence and Antigenic Variation of *Plasmodium Falciparum*-Infected Erythrocytes. *Cell* 82, 89–100. doi: 10.1016/0092-8674(95)90055-1

Tilley, L., Sougrat, R., Lithgow, T., and Hanssen, E. (2008). The Twists and Turns of Maurer's Cleft Trafficking in *P. Falciparum*-Infected Erythrocytes. *Traffic* 9 (2), 187–197. doi: 10.1111/j.1600-0854.2007.00684.x

Tsarukyanova, I., Drazba, J. A., Fujioka, H., Yadav, S. P., and Sam-Yellowe, T. Y. (2009). Proteins of the *Plasmodium Falciparum* Two Transmembrane Maurer's Cleft Protein Family, PfMC-2TM, and the 130 kDa Maurer's Cleft Protein Define Different Domains of the Infected Erythrocyte Intramembranous Network. *Parasitol. Res.* 104 (4), 875–891. doi: 10.1007/s00436-008-1270-3

Warncke, J. D., Vakonakis, I., and Beck, H. P. (2016). *Plasmodium* Helical Interspersed Subtelomeric (PHIST) Proteins, at the Center of Host Cell Remodeling. *Microbiol. Mol. Biol. Rev.* 80 (4), 905–927. doi: 10.1128/MMBR.00014-16

Yam, X. Y., Brugat, T., Siau, A., Lawton, J., Wong, D. S., Farah, A., et al. (2016). Characterisation of the *Plasmodium* Interspersed Repeats (PIR) Proteins of *Plasmodium Chabaudi* Indicates Functional Diversity. *Sci. Rep.* 6, 23449. doi: 10.1038/srep23449

Conflict of Interest: The authors declare that the research was conducted in the absence of any commercial or financial relationships that could be construed as a potential conflict of interest.

frontiers | Frontiers in Cellular and Infection Microbiology

ORIGINAL RESEARCH
published: 23 June 2022
doi: 10.3389/fcimb.2022.888496

Plasmodium knowlesi Cytoadhesion Involves SICA Variant Proteins

*Mariko S. Peterson[1,2†], Chester J. Joyner[1,2,3†], Stacey A. Lapp[1,2], Jessica A. Brady[4†], Jennifer S. Wood[5], Monica Cabrera-Mora[1,2†], Celia L. Saney[1,2†], Luis L. Fonseca[6†], Wayne T. Cheng[3], Jianlin Jiang[1,2], Stephanie R. Soderberg[1,2†], Mustafa V. Nural[7], Allison Hankus[1,2†], Deepa Machiah[8], Ebru Karpuzoglu[1,2†], Jeremy D. DeBarry[7†], MaHPIC-Consortium[1,2], Rabindra Tirouvanziam[9], Jessica C. Kissinger[3,7,10], Alberto Moreno[1,2,11], Sanjeev Gumber[8,12†], Eberhard O. Voit[6], Juan B. Gutierrez[13†], Regina Joice Cordy[1,2†] and Mary R. Galinski[1,2,11]**

[1] Emory National Primate Research Center, Emory University, Atlanta, GA, United States, [2] Emory Vaccine Center, Emory University, Atlanta, GA, United States, [3] Center for Tropical and Emerging Global Diseases, University of Georgia, Athens, GA, United States, [4] School of Chemical, Materials and Biomedical Engineering, University of Georgia, Athens, GA, United States, [5] Division of Animal Resources, Yerkes National Primate Research Center, Emory University, Atlanta, GA, United States, [6] The Wallace H. Coulter Department of Biomedical Engineering, Georgia Institute of Technology and Emory University, Atlanta, GA, United States, [7] Institute of Bioinformatics, University of Georgia, Athens, GA, United States, [8] Division of Pathology, Yerkes National Primate Research Center, Atlanta, GA, United States, [9] Department of Pediatrics, Emory University School of Medicine, Atlanta, GA, United States, [10] Department of Genetics, University of Georgia, Athens, GA, United States, [11] Division of Infectious Diseases, Department of Medicine, Emory University School of Medicine, Atlanta, GA, United States, [12] Department of Pathology and Laboratory Medicine, Emory School of Medicine, Atlanta, GA, United States, [13] Department of Mathematics, University of Georgia, Athens, GA, United States

OPEN ACCESS

Edited by:
Laurent Rénia, Nanyang Technological University, Singapore

Reviewed by:
Wenn-Chyau Lee, University of Malaya, Malaysia
Casper Hempel, Technical University of Denmark, Denmark
Sebastien Dechavanne, IRD UMR216 Mère et enfant face aux infections tropicales (MERIT), France

***Correspondence:**
Mary R. Galinski
Mary.Galinski@emory.edu

Specialty section:
This article was submitted to Parasite and Host, a section of the journal Frontiers in Cellular and Infection Microbiology

Received: *02 March 2022*
Accepted: *22 April 2022*
Published: *23 June 2022*

Citation:
Peterson MS, Joyner CJ, Lapp SA, Brady JA, Wood JS, Cabrera-Mora M, Saney CL, Fonseca LL, Cheng WT, Jiang J, Soderberg SR, Nural MV, Hankus A, Machiah D, Karpuzoglu E, DeBarry JD, MaHPIC-Consortium, Tirouvanziam R, Kissinger JC, Moreno A, Gumber S, Voit EO, Gutierrez JB, Cordy RJ and Galinski MR (2022) Plasmodium knowlesi Cytoadhesion Involves SICA Variant Proteins. Front. Cell. Infect. Microbiol. 12:888496. doi: 10.3389/fcimb.2022.888496

Plasmodium knowlesi poses a health threat throughout Southeast Asian communities and currently causes most cases of malaria in Malaysia. This zoonotic parasite species has been studied in *Macaca mulatta* (rhesus monkeys) as a model for severe malarial infections, chronicity, and antigenic variation. The phenomenon of *Plasmodium* antigenic variation was first recognized during rhesus monkey infections. *Plasmodium*-encoded variant proteins were first discovered in this species and found to be expressed at the surface of infected erythrocytes, and then named the Schizont-Infected Cell Agglutination (SICA) antigens. SICA expression was shown to be spleen dependent, as SICA expression is lost after *P. knowlesi* is passaged in splenectomized rhesus. Here we present data from longitudinal *P. knowlesi* infections in rhesus with the most comprehensive analysis to date of clinical parameters and infected red blood cell sequestration in the vasculature of tissues from 22 organs. Based on the histopathological analysis of 22 tissue types from 11 rhesus monkeys, we show a comparative distribution of parasitized erythrocytes and the degree of margination of the infected erythrocytes with the endothelium. Interestingly, there was a significantly higher burden of parasites in the gastrointestinal tissues, and extensive margination of the parasites along the endothelium, which may help explain gastrointestinal symptoms frequently reported by patients with *P. knowlesi* malarial infections. Moreover, this margination was not observed in splenectomized rhesus that were infected with parasites not expressing the SICA proteins. This work provides data that directly supports the view that a subpopulation of *P. knowlesi* parasites cytoadheres and sequesters, likely *via* SICA variant antigens acting as ligands. This process is akin to the

cytoadhesive function of the related variant antigen proteins, namely Erythrocyte Membrane Protein-1, expressed by *Plasmodium falciparum*.

Keywords: malaria, antigenic variation, rhesus monkey (*Macaca mulatta*), gastritis, anemia, infected erythrocytes, *Plasmodium falciparum*, histopathology (HPE)

INTRODUCTION

Malaria is a blood-borne disease of major global importance that is caused by infection with parasitic protozoa from the genus *Plasmodium* and afflicts hundreds of millions of people annually (World Health Organization, 2021). Malarial illness presents with a wide array of clinical signs and symptoms that range from minimal to severe and life-threatening (reviewed in Miller et al., 2013; Milner, 2018). Parasite species and genotype, variant antigen expression, infected red blood cell (iRBC) cytoadhesion and sequestration in the microvasculature, iRBC concealment, and divergent host genetics and host immune responses contribute to the range of disease severity observed during *Plasmodium* infections (Miller et al., 2002; Baird, 2013; Miller et al., 2013; Wassmer et al., 2015; Fonseca et al., 2017). Given the complexities of malaria, the continued rise in drug resistance, and the general need for new parasite and possible host-directed antimalarial treatments, new insights into host-parasite interactions and mechanisms that govern malarial disease progression and resilience are of great importance (Miller et al., 2013; Ashley et al., 2014; Amato et al., 2018).

Plasmodium knowlesi is a zoonotic simian malaria parasite that causes a spectrum of malarial disease manifestations in humans in Southeast Asia (Singh et al., 2004; Cox-Singh et al., 2008; Cox-Singh and Singh, 2008; Daneshvar et al., 2009; William et al., 2011; Barber et al., 2017; Barber et al., 2018; Rajahram et al., 2019). This parasite naturally infects kra monkeys (*Macaca fascicularis*) and other macaque species that are native to Southeast Asia, and these animals control their parasitemia without treatment, leading to chronic infections (Knowles and Gupta, 1932; Garnham, 1966; Collins et al., 1992). In contrast, if left untreated with antimalarial drugs, *P. knowlesi* causes severe, lethal disease nearly universally in Indian rhesus macaques (*Macaca mulatta*) (Knowles and Gupta, 1932; Garnham, 1966; Coatney et al., 1971; Spangler et al., 1978; Coatney et al., 2003). Relevantly, key differences between the transcriptomic responses of *M. fascicularis* and *M. mulatta* to *P. knowlesi* infection were recently documented by Gupta and colleagues, bringing emphasis to the utility of cross-species comparisons (Gupta et al., 2021; Gupta et al., 2022).

Severe *P. knowlesi* infections in humans have been specifically associated with gastrointestinal (GI) pathology (Cox-Singh et al., 2008; Barber et al., 2013). Autopsy studies from fatal *P. knowlesi* human cases to better understand this phenomenon and other disease factors are scarce due to cultural considerations (Cox-Singh et al., 2010). Autopsy reports from *P. falciparum* cases are more common (Menezes et al., 2012), and *P. falciparum* trophozoite and schizont (T/S)-iRBCs have been documented in the microvasculature of the GI tract, with some studies demonstrating associated histopathology and GI symptoms (Romero et al., 1993; Seydel et al., 2006). Studies with rhesus macaques have reported *P. knowlesi* iRBCs in the microvasculature of the GI tract and other tissues, suggestive of cytoadhesion and sequestration, despite – unlike *P. falciparum* – the peripheral circulation of all asexual blood-stage developmental forms from the life cycle of this species (Miller et al., 1971b; Spangler et al., 1978). However, potential associations between the *P. knowlesi* parasite burden in the microvasculature of various tissues, adhesive interactions, and tissue damage have yet to be explored.

While all *P. knowlesi* blood-stage forms circulate, a subpopulation of *P. knowlesi* iRBCs may cytoadhere and sequester in tissues due to receptor-ligand interactions mediated by schizont-infected cell agglutination (SICA) proteins, which are variant antigens expressed by *P. knowlesi* that are related to and share features with *P. falciparum* erythrocyte membrane protein 1 (*Pf*EMP1) and the genes that encode them (Korir and Galinski, 2006; Bunnik et al., 2019). SICA and *Pf*EMP1 are large multi-domain proteins (~200-300 kDa) (Howard et al., 1983; Leech et al., 1984) that are encoded by large, diverse multigene families termed *SICAvar* and *var*, respectively (Baruch et al., 1995; Smith et al., 1995; Su et al., 1995; Al-Khedery et al., 1999). The expressed SICA proteins become inserted in the iRBC membrane with variant domains exposed at the surface of SICA positive (SICA[+]) iRBCs (Howard et al., 1983), and their expression in rhesus monkeys has been associated with virulence (Barnwell et al., 1983b). *SICAvar* gene and protein expression are dependent upon the presence of the spleen, with SICA[+] parasites taking on a SICA negative (SICA[-]) phenotype after passage in splenectomized rhesus (Barnwell et al., 1982; Barnwell et al., 1983a). The SICA[-] phenotype is characterized by downregulated *SICAvar* and SICA protein expression, notably to an 'off state' (Lapp et al., 2013). Infection of spleen-intact rhesus monkeys with SICA[-] parasites may result in milder disease, or return of SICA expression along with severe outcomes and fatality (Barnwell et al., 1983a). Similarly in *in vitro* cultures, *SICAvar* gene family expression was shown to be downregulated (Lapp et al., 2015). *Plasmodium falciparum* variant antigen expression has also been shown to be spleen-dependent *in vivo* in nonhuman primate (NHP) models and human infections (David et al., 1983; Hommel et al., 1983; Bachmann et al., 2009). SICA protein expression may mediate cytoadhesion and sequestration of a subpopulation of *P. knowlesi* iRBCs in the microvasculature of tissues, akin to *P. falciparum* T/S-iRBCs populations that express *Pf*EMP-1 (Aley et al., 1984; Leech et al., 1984; Biggs et al., 1991; Biggs et al., 1992), enabling widespread host-parasite receptor-ligand interactions and sequestration of *P. falciparum* iRBCs in the tissues (reviewed

in Smith, 2014). Whether and to what degree *P. knowlesi* parasite sequestration concomitant with local and systemic inflammation may associate with enhanced symptomology and histopathology, which is evident with *Pf*EMP-1 expression, cytoadhesion, and sequestration (reviewed in Craig et al., 2012; Smith et al., 2013; Wahlgren et al., 2017; Lee et al., 2019), are questions of prime interest.

The experimental *P. knowlesi*-rhesus macaque infection model has provided significant insights into malarial immunity, notably, the major discovery of malarial antigenic variation during the course of longitudinal infections, which entails changes in the antigenic phenotype of iRBCs in concert with the development of antigen-specific immunity (Brown and Brown, 1965). This model then enabled the first identification and characterization of *Plasmodium*-encoded iRBC surface-exposed immunodominant variant proteins, namely the *P. knowlesi* SICA proteins (Barnwell et al., 1983a; Howard et al., 1983; Howard and Barnwell, 1984a; Howard and Barnwell, 1984b; Howard and Barnwell, 1985), which preceded the identification of *Pf*EMP1 based on similar extraction and characterization procedures (Howard et al., 1984; Leech et al., 1984; Howard et al., 1988).

The longitudinal *P. knowlesi* sporozoite-induced infections in malaria-naïve rhesus monkeys presented here delve into histopathology questions pertinent to understanding *P. knowlesi* infections in humans. These experiments were generated by the Malaria Host-Parasite Interaction Center (MaHPIC) systems biology research consortium, which previously reported the utilization and integration of multi-omic technologies to investigate and compare host-pathogen interactions during acute, chronic, and relapse phases of malarial infections caused by *Plasmodium cynomolgi* or *Plasmodium coatneyi* (Joyner et al., 2016; Joyner et al., 2017; Tang et al., 2017; Cordy et al., 2019; Joyner et al., 2019; Tang et al., 2019; Debarry et al., 2020), and *P. knowlesi* in kra and rhesus monkeys (Gupta et al., 2021; Peterson et al., 2021; Gupta et al., 2022). Within the rhesus monkey cohorts presented here, longitudinal clinical data and pathological relationships were documented and modest relationships were identified between organ pathology and parasite tissue load assessed in 22 tissue types. Of note, extensive margination of SICA[+] iRBCs was observed along the vascular endothelium of the GI tract. Strikingly, SICA[+] iRBC margination was observed with abundant juxtaposition of iRBCs with the endothelium, but this was not observed in the tissues of splenectomized rhesus infected with SICA[-] parasites. In summary, the rhesus macaque animal model was utilized to systematically characterize clinical features of malarial disease, *P. knowlesi* sequestration and tissue pathology, and the results point to SICA proteins functioning at the interface of iRBCs and the GI tract.

MATERIALS AND METHODS

Animal Use

All NHP experiments were performed at the Yerkes National Primate Research Center (YNPRC), an AAALAC Internationally accredited facility. All experimental, surgical, and necropsy procedures were approved by Emory's Institutional Animal Care and Use Committee (approval number: PROTO201700484-YER-2003344-ENTRPR-A) and the Animal Care and Use Review Office of the US Department of Defense and followed accordingly. All animal procedures used are consistent with the ARRIVE guidelines (Percie Du Sert et al., 2020).

Sixteen rhesus monkeys were assigned within six cohorts (**Supplemental Table 1**; Experiments 30, 06, 33, 34, 35 and Spx; splenectomy experiment). Eleven animals within four of these cohorts were designated for sequential iterative longitudinal *P. knowlesi* sporozoite-induced infection experiments (**Supplemental Figures 1–4**), aiming to understand the virulence of *P. knowlesi* blood-stage infections in rhesus monkeys. Three animals were designated as control animals and two for a final SICA[-] blood-stage infection experiment requiring splenectomy. The study involved only male monkeys to avoid confounding blood loss and anemia due to menstruation. All rhesus were of Indian origin and all but two were born and raised at the YNPRC; the animals with codes 13_116 and 13_136 were acquired from a domestic breeding facility and quarantined per YNPRC standard operating procedures before being involved in this study. All animals were healthy and housed socially, with 12 h light-dark cycles, and received environmental enrichment with food, foraging activities, and other physical manipulanda, compliant with the Animal Welfare Act and the Guide for the Care and Use of Laboratory Animals. The animals received training prior to the initiation of the experiments to familiarize them with daily or twice-daily ear stick collections of small blood volumes as described previously with kra monkey infections (Peterson et al., 2021). End points for each cohort were pre-determined to understand the pathophysiology of infection longitudinally. All animals were necropsied at the pre-determined end points by anesthetizing them using ketamine and then euthanizing *via* intravenous administrations of barbiturates, an acceptable method of euthanasia for NHP per recommendations of the "AVMA Guidelines for the Euthanasia of Animals".

Parasite Isolates and Inoculations

Eleven malaria naïve rhesus (cohorts E30, E06, E33 and E35) were infected intravenously with cryopreserved *P. knowlesi* clone Pk1(A+) sporozoites derived from the Malayan Strain of *P. knowlesi* (Barnwell et al., 1983a; Lapp et al. 2018) (kindly provided by John W. Barnwell, Centers for Disease Control and Prevention, Atlanta, GA). In addition, two previously infected and then splenectomized adult male rhesus were infected intravenously with cryopreserved *P. knowlesi* clone Pk1(A-)1- iRBCs, a cloned parasite line that is phenotypically negative for expression of the *SICAvar* family and encoded SICA proteins, derived from the passage of Pk1(A+) cloned parasites through a splenectomized monkey (Barnwell et al., 1983a).

Subcurative Drug Treatments

To prevent hyperparasitemia and mortality of rhesus monkeys that were not sacrificed while parasitemia was escalating, subcurative antimalarial treatments were administered when the peripheral parasitemia reached approximately 1% of infected RBCs and the parasite replication rate was not decreasing. Subcurative treatments consisted of artemether at 1 mg/kg (for cohorts E30 and E35) or

chloroquine at 5 mg/kg (for cohort E33), administered intramuscularly. Further descriptions and experimental details by cohort are discussed in **Supplemental Table 1**.

Sample Collections

Standard ear-stick procedures were performed to obtain capillary blood samples in EDTA for complete blood counts (CBCs) and monitoring of parasitemias. Larger volume blood collections were performed from the saphenous or femoral vein into EDTA under ketamine anesthesia.

Telemetry

The animals in cohorts E30 and E06 had telemetry devices surgically implanted prior to infection for real-time monitoring of temperature and other vital signs. Raw temperature data processing, definition of normal temperature range, and determination of febrile threshold and time-to-temperature responses were conducted as described previously (Gatton and Cheng, 2002; Peterson et al., 2021 and Brady et al, manuscript in preparation).

Calculation of Reticulocyte Production Index

RPI calculation was performed to correct for raw reticulocyte count in the setting of anemia, and determine appropriateness of bone marrow response, as described previously (Peterson et al., 2021).

Quantification of Serum Erythropoietin

Serum erythropoietin for samples collected at baseline and days 8-10 post-inoculation was measured using the Human Erythropoietin Quantikine IVD ELISA kit (R&D Systems) on undiluted serum as described previously (Peterson et al., 2021).

Multiplex Cytokine Array

Plasma samples collected at baseline and between days 8-10 post-inoculation with sporozoites were used to quantify the concentration of 29 cytokines using the Cytokine 29-Plex Monkey Panel (Thermofisher, Inc) according to the manufacturer's suggested protocol (serum sample dilution of 1:2). Per the manufacturer, this kit was developed and validated for rhesus monkeys. Data were analyzed using the Luminex software suite. A floor of the minimum detected value for each analyte was then substituted for undetectable values, and then the data were $\log_{10}$ transformed before statistical analyses. Analytes included in this kit were EGF, Eotaxin, FGF, G-CSF, CM-CSF, HGF, IFNγ, IL-10, IL-12, IL 15, IL 17, IL-1b, IL-1RA, IL-2, IL-4, IL-5, IL-6, IL-8, IP-10, I-TAC, MCP-1, MDC, MIF, MIG, MIP-1α, MIP-1β, Rantes, TNFα, and VEGF. Only cytokines with statistically significant changes from baseline are discussed.

Parasite Enumeration

Blood smears were monitored for the presence of parasites once daily between 1 PM and 3 PM until the infections became patent, after which, parasitemia was monitored twice daily (8 AM, schizonts; and 1-3 PM ring stages). Smear preparation, examination, and enumeration were performed as described previously (Peterson et al., 2021). Cumulative parasitemia was calculated for each animal by adding together the daily parasitemia (parasites/μl) from the day of inoculation to the day of necropsy.

Quantification of Parasite Replication Rate

The replication rate of parasites was calculated as described previously (Fonseca et al., 2017; Peterson et al., 2021). Only the first peak was considered because it had the most robust sample size.

Tissue Collection, Preservation, and Pathology Analysis

Twenty-two tissue sample types were collected at necropsy from all infection experiments (**Figure 5**), except cohort E33 which was limited to the tissues of most interest, namely liver, lung, kidney, spleen, adrenal gland, bone marrow (BM), stomach, duodenum, jejunum, and colon. The tissues were fixed processed, sectioned, and stained with hematoxylin and eosin (H&E) as described previously (Peterson et al., 2021). The slides were examined using regular bright field light microscopy and also under polarized light to highlight hemozoin crystals, which are birefringent, distinguishing them from hemosiderin (Lawrence and Olson, 1986). Sections for transmission electron microscopy (TEM) (in 2.5% glutaraldehyde) were also collected, stored, and analyzed using appropriate equipment and technologies (Sheehan and Hrapchak, 1980). All tissue slides were blinded and randomized for diagnosis and characterization of histopathology. Tissue scoring was performed as previously described (Peterson et al., 2019; Peterson et al., 2021).

Infected RBC Quantification Within Tissues

iRBC densities in the tissues were determined by counting the number of iRBCs in ten high power fields (HPFs) (1000x) under oil immersion on a standard light microscope (Milner et al., 2013; Joice et al., 2014; Milner et al., 2015; Peterson et al., 2019). All sections were randomized and blinded. Standardized tissue densities, indicating relative differences between acute and chronic infection, taking into account parasitemia, were determined by dividing the parasite tissue density of each monkey in each tissue by the sum of all the parasite tissue densities in each group (acute and chronic infection). The resultant proportions were combined in a vector and binned to create a color scale. The color scale for a parasite distribution heat map was created using the bin_data command in the mltools package in R, with a bin value of seven, and a quantile bin type. The colors in the heat map are from the Blues Brewer Color Palette from the RColorBrewer package in R (Holtz, 2018), imported into Adobe Illustrator as.ase files.

Infected RBC Margination

For quantification of marginated iRBCs, 20 parasitized blood vessels were quantified, or 350 total vessels, whichever was observed first. Fields were examined at 1000x under oil emersion, on a standard light microscope. Infected RBCs

appearing to touch the endothelium were scored as marginated, others in the lumen were classified as non-marginated. The proportion of marginating parasites in each organ was calculated as the number of marginated iRBCs divided by the total number of iRBCs. Analysis was performed on tissues from infected rhesus and splenectomized rhesus.

Transmission Electron Microscopy

TEM was performed on infected duodenum tissue from selected monkeys. Tissue grids were prepared by primary fixation in 2.5% glutaraldehyde, followed by washing, secondary fixation in 1% osmium tetroxide, dehydration in graded ethanol solutions and staining with uranyl acetate, treatment with 100% propylene oxide, infiltration of resin, and resin embedding (Sheehan and Hrapchak, 1980). Semi-thin tissue sections were stained with toluidine blue and examined by light microscopy prior to grid preparation to aid in the proper orientation of samples. Ultrathin grid sections were prepared at 10-20 nm thickness and examined by electron microscopy (JEOL model 1011), and image acquisition (Gatan model 785).

Computation of the Removal of Uninfected RBCs

The degree of removal of uninfected RBCs was computed with a recursive mathematical model of RBC dynamics as previously performed for macaques infected with *P. cynomolgi* (Fonseca et al., 2017).

Statistical Analyses

Data were generally divided into two categories for these analyses. Samples and data acquired during the timeframe in which the monkeys required subcurative treatment were considered "pre-control," and those thereafter were considered "controlled." (**Figure 1** and **Supplemental Figures 1–4**). Statistics and figures were produced in R Studio, under R version 3.4.3 (R-Core-Team, 2021) GUI version 1.70. Pairwise comparisons were performed using Welch's *t*-test and paired t-tests, and adjusted using the false discovery rate method, where appropriate. Multiple comparisons were performed using ANOVA analysis, including repeated measures ANOVA, and the Tukey's HSD post-hoc comparison tests. Repeated measures ANOVA and associated post-hoc comparisons were performed using the psycho package v. 0.4.9 in R (Makowski, 2019). Associations were tested using the Pearson's correlation test, and hierarchical multiple linear regression analyses. Multicollinearity was assessed using the olsrr package v. 0.5.2. in R (Aravind, 2018). Graphs were prepared using the ggplot2 package v. 3.1.1 (Wickham et al., 2019) and the Brewer Color Palette in RStudio (Holtz, 2018). Comparisons were considered significant with raw or adjusted *p*-values below 0.05.

RESULTS

The experimental cohorts from this study (E06, E33, E34, and E35), including the number of animals, sporozoite inoculations, monitoring, treatments, etc., are detailed in **Supplemental Table 1**. Schematics with parasitemias and sampling points for each animal by cohort are included in **Supplemental Figures 1–4**.

Rhesus Monkeys Control Acute Blood-Stage Infections With Sub-Curative Therapeutic Intervention

Rhesus monkeys (n=11) inoculated with *P. knowlesi* sporozoites became patent 6-8 dpi and showed escalating parasitemia 7-10 dpi (**Figure 1A** and **Supplemental Figures 1–4**). The parasite replication rate in the rhesus monkeys was 23.36-fold ± 2.91 (mean ± SEM), and showed no signs of deceleration, supporting the notion that these animals were not controlling their infections (**Figure 1A**) (Fonseca et al., 2017). As expected from earlier studies (Brown and Brown, 1965), subcurative drug treatments led to the establishment of chronic infections (**Figure 1A**, bottom 3 panels). Per the study design used here, a subcurative dose of artemether (**Supplemental Figures 1, 4**) or chloroquine (**Supplemental Figure 3**) was administered intramuscularly when the parasitemia reached greater than or equal to 1% with no evidence of control (**Figure 1A**). This pharmacological regimen differs from the originally reported use of quinine (Brown and Brown, 1965). The drug dampened the parasitemias to sub-patent levels, which then recrudesced, with incremental reduction of parasitemia spikes to below the 1% parasitemia treatment threshold until the rhesus no longer required subcurative treatment and the infection became chronic (**Figures 1A, B**). The recrudescent and cumulative parasitemias were calculated and compared longitudinally (**Figures 1B, C**). Paired t-test analysis of the final recrudescent peak prior to necropsy to the primary peak was statistically significantly lower (p-value = 0.04), consistent with the establishment of a controlled infection without antimalarial treatment (**Figure 1B**). The cumulative parasitemia prior to and after control was not statistically significant (**Figure 1C**). Altogether, these experiments reliably produced *P. knowlesi* parasitemia kinetics in rhesus monkeys, as expected from previous studies (Knowles and Gupta, 1932; Garnham, 1966; Coatney et al., 1971; Collins et al., 1992; Coatney et al., 2003).

Rhesus monkey host responses were examined during the acute phase of infection, when they were unable to naturally control their infections, and compared after administration of sub-curative antimalarial therapy. Hematological parameters were evaluated to study the temporal development and degree of severity of anemia and thrombocytopenia. By 10-11 dpi, all rhesus had high escalating parasitemias requiring subcurative treatment (**Figures 1A**, **2A**). White blood cells and their subset populations rose corresponding with troughs in parasitemia (**Figure 2B**). While one animal experienced a hemoglobin nadir as low as 7 g/dL, the hemoglobin levels subsequently stabilized post-treatment at nadirs of 10.11 g/dL ± 0.45, an average of 75.45% ± 2.59% relative to baseline (**Figure 2C**). 5-day averages were calculated to compare hematological parameters longitudinally, and the hemoglobin nadirs, which occurred 11-15 dpi were statistically significantly lower than

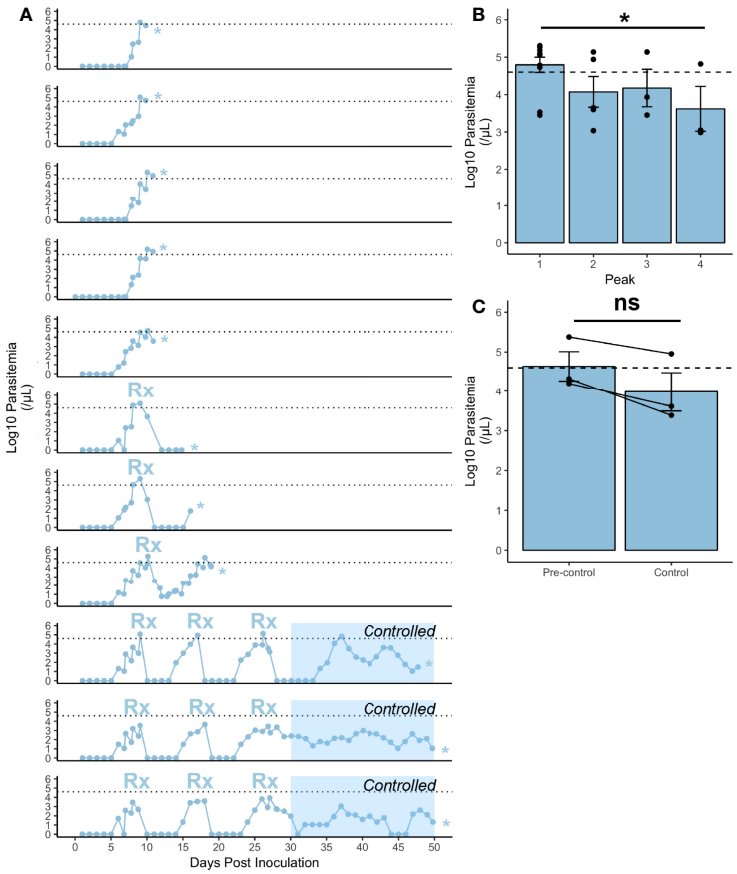

FIGURE 1 | Infection characteristics of rhesus monkeys infected with *P. knowlesi*. **(A)** Log_{10}-transformed parasitemia curves for 11 monkeys infected with *P. knowlesi* sporozoites. Treatment threshold (1% parasitemia = 40,000 parasites/µL) is indicated by the dotted line, and necropsy day is marked with an asterisk. Time points of subcurative treatment with either artemether or chloroquine are indicated by the "Rx" symbol. The interval in which the monkeys controlled parasitemia without the need for subcurative treatment is indicated by blue shading labeled "Controlled". **(B)** Average log_{10}-transformed parasitemias for the primary and recrudescent peaks showing gradual reduction in magnitude. The primary parasitemic peak was compared to the final recrudescence and found to be statistically significantly different *via* paired t-test comparison (*p-value < 0.05). **(C)** Cumulative parasitemia prior to, and after parasitemic control (30 dpi) shows similar parasitemia burdens between earlier and later times in infection *via* paired t-test comparison. ns (not significant) =p–value > 0.05. Error bars represent standard error of the mean.

baseline (p-value = $1.14x10^{-4}$) (**Figure 2D**). Interestingly, the animals did not experience dramatic platelet nadirs, the lowest being 75,000 platelets/uL (mean 163,909 ± 19,636.91) (**Figure 2E**). Platelet levels at 11-15 dpi were not different from baseline (**Figure 2F**). Platelet nadirs corresponded with rises in parasitemia (**Figures 2A, E**).

Insufficient RBC production to match RBC removal contributes to and exacerbates the development of anemia in rhesus monkeys infected with either *P. cynomolgi* or *P. coatneyi* (Moreno et al., 2013; Joyner et al., 2016; Tang et al., 2017; Cordy et al., 2019; Joyner et al., 2019). Here it was hypothesized that insufficient erythropoiesis could similarly contribute to the development of anemia during the acute stage of infections with *P. knowlesi*, prior to administering subcurative treatment regimens. As such, several metrics for BM function were examined. Indeed, prior to the administration of subcurative treatment, the Reticulocyte Production Index (RPI) remained below 2, the threshold that indicates an appropriate BM response to a drop in hemoglobin. However, it increased after the administration of subcurative treatment in pulses corresponding to parasitemia (**Figures 2A, G**). The peak output of reticulocytes, as measured by peripheral reticulocyte count occurred at 31-35 dpi, which was significantly higher than baseline counts (p-value = 0.03) and occurred around the same time as parasitemic control (**Figures 2A, H**). Histologically, BM "at rest" normally contains adipose tissue as a proportion of age, along with platelet and red and white blood cell progenitors. Microscopic examination of BM samples revealed that BM expansion was stunted in the rhesus monkeys prior to treatment as is evidenced by a similar proportion of fat droplets seen between baseline prior to infection and a representative sample taken at 10 dpi (**Figure 2I**). With activation, myeloid and erythroid precursors expand and crowd out fat droplets, as can be shown in a representative section taken at 48 dpi, suggesting eventual BM recovery later during the infection (**Figure 2I**). Serum erythropoietin was measured in a subset of monkeys prior to treatment and found to not be significantly

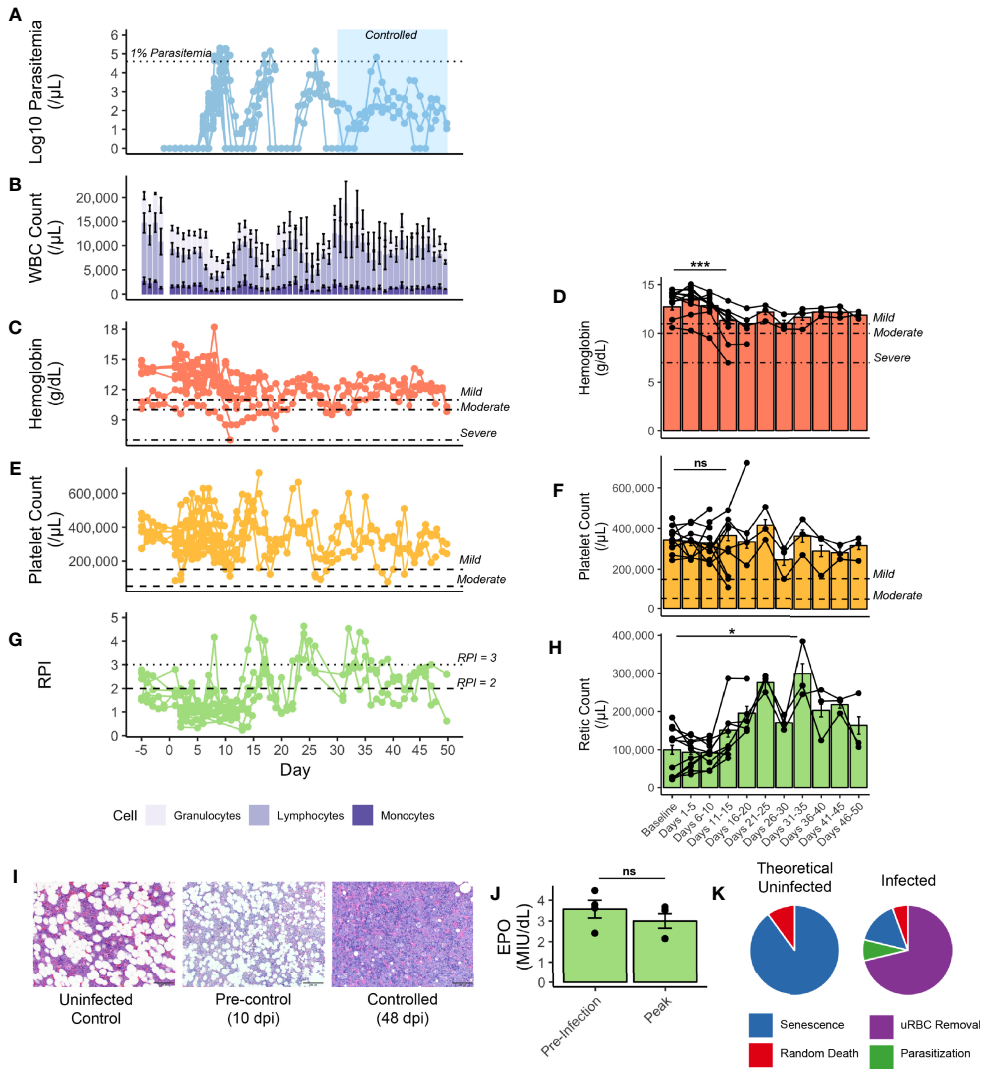

FIGURE 2 | Hematological parameters of rhesus monkeys infected with *P. knowlesi*. **(A)** Longitudinal faceted plots showing parasitemia, with treatment threshold and control interval indicated, compared with **(B)** white blood cell count with population fractions indicated, **(C)** hemoglobin with mild, moderate, and severe anemia thresholds labeled (at 11 g/dL, 10 g/dL, and 7 g/dL, respectively), with **(D)** five day hemoglobin average, **(E)** platelet count with mild and moderate thrombocytopenia labeled (at 150,000 platelets/mL and 75,000 platelets/µL, respectively), with **(F)** five day platelet average, **(G)** reticulocyte production index (with RPI of 2 and of 3 labeled), and **(H)** five-day average of reticulocyte counts. **(I)** 600x H&E-stained tissue sections of bone marrow from an uninfected control monkey, a monkey prior to controlling parasitemia, and a monkey after controlling parasitemia. **(J)** Erythopoietin levels from select monkeys demonstrating no difference between baseline and 10 dpi, prior to antimalarial treatment. **(K)** Mathematical modeling predicting the relative proportions of infected and uninfected red blood cell removal. Statistical comparisons were performed using paired t-tests. ***p-value < 0.0005, *p-value < 0.05, and ns (not significant) = p-value > 0.05. Error bars represent standard error of the mean.

different from baseline, consistent with a delayed BM response to infection-induced anemia (**Figure 2J**).

Since the drop in hemoglobin, though relatively mild, could not be explained by parasite-mediated destruction alone, the magnitude of destruction of uninfected RBCs was predicted using a mathematical model (Fonseca et al., 2016; Fonseca et al., 2017; Peterson et al., 2021). Analysis of a rhesus monkey from cohort E35 (**Supplemental Table 1**), demonstrated that destruction of uninfected RBCs accounted for 71% of all RBCs removed during the experiment, while only 8% were lost due to parasitization (**Supplemental Figure 5** and **Figure 2K**), and a compensatory release of reticulocytes with each subcurative treatment (**Figures 2A, G**).

Core body temperature was studied as a proxy for inflammation. Telemetry devices were surgically implanted before experimental infection into two cohorts of monkeys (E06 and E30) to collect densely sampled and real-time temperature data (6 rhesus; **Figure 3A**, and **Supplemental Table 1**). The parasitemia at which the monkeys waged a temperature response (pyrogenic threshold) was determined by

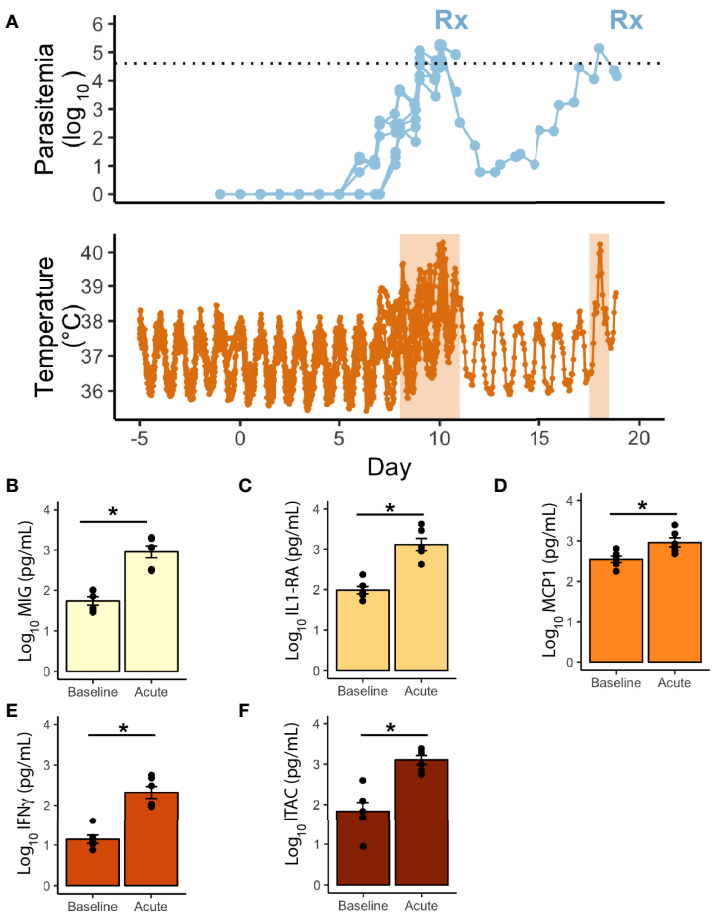

FIGURE 3 | Telemetric temperature response to *P. knowlesi* parasitemia. **(A)** Top: Longitudinal parasitemia curve of the 6 monkeys with implanted telemetry devices, with treatment threshold indicated by dotted line. Bottom: Temperature data obtained from implanted telemetry devices indicating rises in temperature above each individual's baseline corresponding to rises in parasitemia. Febrile periods are marked with orange shading. Statistically significant cytokine results from a 29-cytokine array including **(B)** MIG, **(C)** IL1-RA, **(D)** MCP1, **(E)** IFNγ, **(F)** ITAC. Statistical comparisons were performed using paired t-tests, with FDR correction. *Corrected p-value<0.05. Error bars represent standard error of the mean.

comparing each monkey's baseline to the nearest parasitemia corresponding to when the temperature rose above the individual's baseline. The rhesus monkeys responded on average to a parasite density of 364/μl during the acute infection period and took approximately 8 days post-infection to do so, including one animal that waged a fever at early recrudescent peaks, and at a higher threshold than its primary peak (390/μl vs 29,070/μl). A 29-cytokine array was also performed to compare inflammatory cytokines at baseline with peak parasitemia, occurring in the febrile period. Of these, five were statistically significantly elevated, including IL1RA and IFNγ, monocyte associated markers MIG and MCP1, and T-cell associated factor, ITAC (**Figures 3B–F**).

Major Histopathological Findings in the Liver, Lungs, Kidney, and Stomach

Although uncontrolled parasitemia is a primary contributor to severe disease in rhesus monkeys, prior studies with rhesus have not reported comparative evaluations of histopathological changes that occur during *P. knowlesi* infections, particularly when overwhelming parasitemia is being limited by antimalarial treatments (Knowles and Gupta, 1932; Knisely et al., 1964; Garnham, 1966). Therefore, this study design included an extensive analysis of H&E-stained tissue sections from 22 different organs from infected monkeys at the time of sacrifice.

Ten of the eleven infected rhesus monkeys exhibited pulmonary hyperplasia, interstitial thickening, and fibrotic changes in the lung (**Figures 4A, B** and **Supplemental Table 2**). Abundant hemozoin was noted in both iRBCs and phagocytes in the interstitial areas and vasculature of infected parenchymal lung tissue (**Figure 4A**). Fibrotic changes in the lungs are highlighted in bright blue with Masson trichrome staining (**Figure 4B**). A less common but severe histological finding included mild to moderate pulmonary hemorrhage (**Figure 4A**). The liver showed periportal mononuclear infiltrate, Kupffer cell hyperplasia, and congestion in the hepatic sinuses (**Figure 4C**). Hemozoin was abundantly distributed in the vasculature as well in phagocytes in the sinuses. Neither hepatocellular necrosis nor cholestasis were

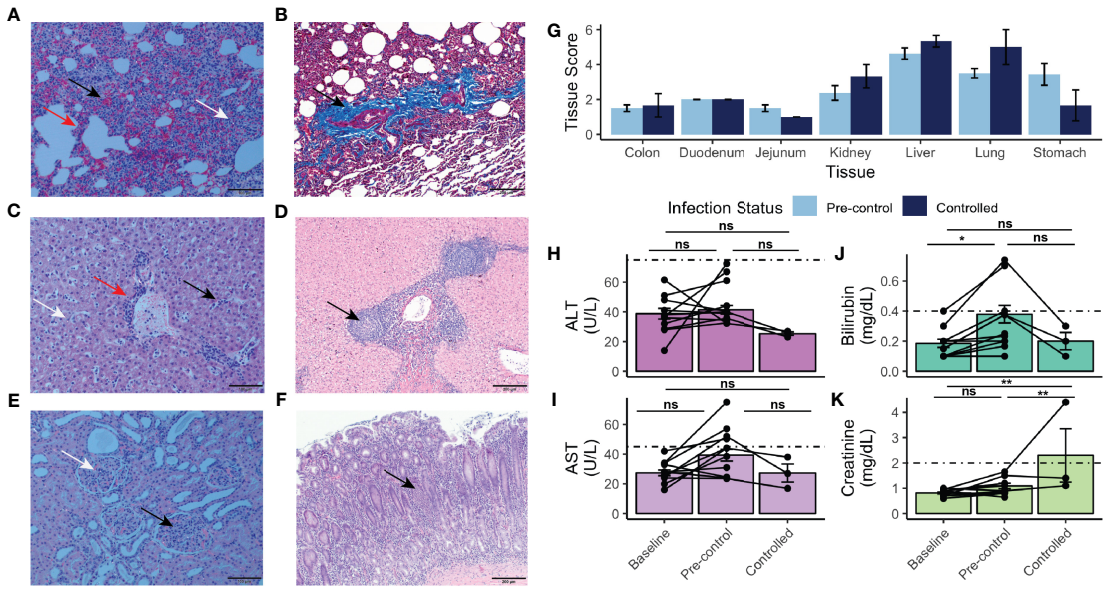

FIGURE 4 | Histopathology, tissue damage, and results of chemistry analysis of rhesus monkeys infected with *P. knowlesi*. **(A)** H&E-stained section of rhesus lung under polarized light microscopy (scale bar = 100 μm). Hemorrhage (black arrow), interstitial thickening and infiltration (red arrow), and diffuse hemozoin (white arrow) are indicated. **(B)** Masson's trichrome-stained section (scale bar = 200 μm) of rhesus lung highlighting fibrotic changes with infection (black arrow, and bright blue color of fibrin). **(C)** H&E-stained section (scale bar = 100 μm) of rhesus liver showing periportal inflammation (red arrow), sinusoidal congestion (black arrow), and parenchymal hemozoin deposition (white arrow). **(D)** H&E-stained section (scale bar = 200 μm) of liver from a monkey infected for 48 days showing unique lobular mononuclear infiltration in the periportal area (black arrow). **(E)** H&E-stained section (scale bar = 100 μm) of kidney under polarized light showing hypercellular glomeruli (black arrow) and abundant hemozoin (white arrow). **(F)** H&E stained section (scale bar = 200 μm) of stomach demonstrating mononuclear infiltration of the mucosa (black arrow), and submucosal edema, consistent with gastritis. **(G)** Semi-quantitative tissue scores of infected monkeys necropsied prior to and after parasitemic control. No statistically significant differences were noted using Tukey's HSD post-hoc analysis. **(H)** ALT and **(I)** AST measurements taken at baseline, pre-control, and after control indicating no statistically significant difference relative to baseline. **(J)** Bilirubin and **(K)** creatinine measurements taken at baseline, pre-control, and after control indicating elevation of bilirubin pre-control relative to baseline and creatinine post-control relative to pre-control and baseline. Values compared with repeat-measures ANOVA with ns, not significant, *p-value <0.05, and **p-value <0.005. Error bars represent standard error of the mean.

observed (**Figure 4C**). Chronically infected monkeys exhibited similar pathological findings as that of acute infections, with the exception of one animal that had unique nodular infiltrates and material consistent with fibrous tissue deposition in the periportal areas of the liver (**Figure 4D**). The kidneys of all animals had glomerular hypercellularity. No glomerulonephritis was observed. Six animals displayed tubular degeneration, and five had interstitial inflammation (**Figure 4E** and **Supplemental Table 2**).

Remarkably, nine rhesus monkeys had moderate to severe stomach inflammation (**Figure 4F** and **Supplemental Table 2**). The duodenum, jejunum, and colon showed mild to moderate mucosal mononuclear infiltration, and mild edema was present in the colon (**Supplemental Table 2**). The tissues were assessed to provide semi-quantitative scores for statistical comparison (**Supplemental Table 2**), as performed in recent studies with *Saimiri boliviensis* and *M. fascicularis* infections with *P. vivax* and *P. knowlesi*, respectively (Peterson et al., 2019; Peterson et al., 2021). Though none of the tissues either prior to or after the rhesus monkeys controlled their infections exhibited any statistically significant changes, stomach (pre-control mean score = 3.44 ± 1.76; post-control mean score = 1.67 ± 1.52), liver (pre-control mean score = 4.62 ± 0.92; post-control mean score = 5.33 ± 0.58), and lung (pre-control mean score = 3.50 ± 0.76; post-control mean score = 5.00 ± 1.73) tended to exhibit the highest scores (**Figure 4G**). Consistent with the observation that chronically infected rhesus monkeys suffered similar organ pathology to rhesus monkeys with shorter courses of infection, pairwise comparisons revealed no statistically significant difference of organ pathology between those necropsied prior to parasitemic control and those necropsied afterwards (**Figure 4G**). Mixed-effects modeling revealed that neither necropsy day nor parasitemia affected the score (**Supplemental Table 3**); however, the tissue itself did (p-value = 7.78 x 10^{-12}).

Differences in systemic measurements of liver function [i.e., alanine transaminase (ALT), aspartate aminotransferase (AST), and total bilirubin], were also assessed by comparing values obtained from baseline time points prior to infection (days -49 to -3), those taken in the pre-control period (determined to be prior to days 31-35 post infection), and in the controlled period (**Figures 4H–K**). Neither ALT nor AST values were significantly elevated from baseline levels (**Figures 4H, I**). Bilirubin was significantly elevated from baseline in the pre-control period (p-value = 0.04) (**Figure 4J**). Systemic kidney function was also assessed. Creatinine was significantly elevated post-parasitemic control relative to baseline (p-value = 1.90 x 10^{-3}) (**Figure 4K**).

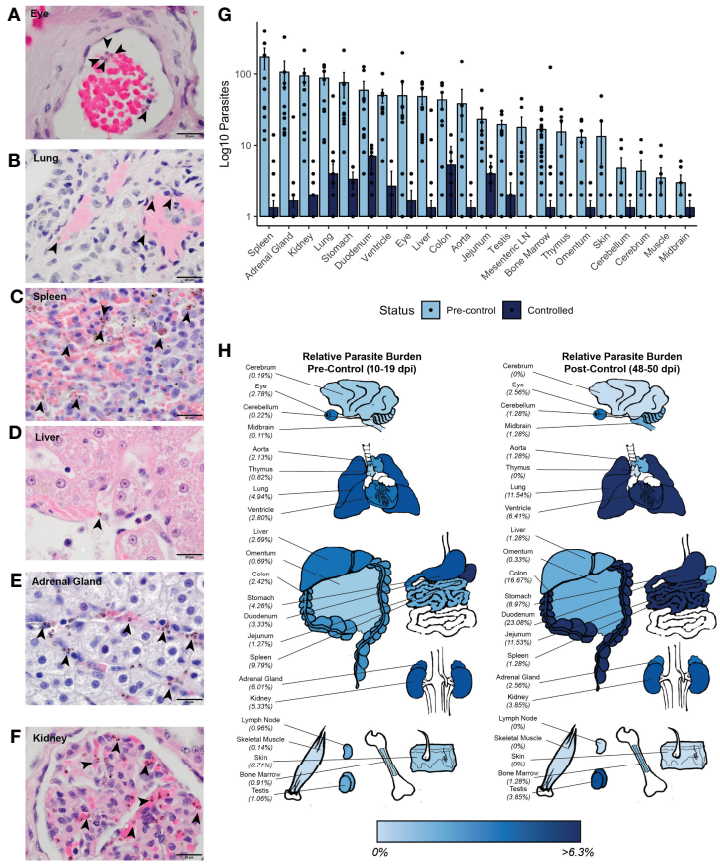

FIGURE 5 | Parasite tissue burden in *P. knowlesi*-infected rhesus monkeys. Examples of iRBCs at 1000x (oil immersion) in H&E-stained tissue sections of **(A)** eye, **(B)** lung, **(C)** spleen, **(D)** liver, **(E)** adrenal gland, and **(F)** kidney. Parasitized RBCs are indicated with black arrowheads. **(G)** Mean $\log_{10}$-transformed parasite counts in 10 high-powered fields for 22 different tissues in pre-control and post-control monkeys. Error bars represent standard error of the mean. **(H)** Heat map of relative parasite densities indicating parasite burden in pre-control and controlled infections.

Parasite Accumulation in Rhesus Monkey Tissue Vasculature During Acute *P. knowlesi* Infection Parallels Histopathology

Parasite accumulation in the tissue vasculature prior to and after control of parasitemia in each of the infected rhesus was evaluated to assess possible associations with organ histopathology. The number of iRBCs in 10 high-power fields (HPFs) was enumerated in 22 tissues to provide approximate iRBC densities within each tissue (**Supplemental Table 4**). Representative images of parasites identified in selected tissues are shown in **Figures 5A–F**. Consistent with the lower, on average, circulating parasitemias after the monkeys were able to control their parasitemias (**Figure 1**), there was less accumulation of iRBCs at these time points relative to earlier time points (**Figure 5G** and **Supplemental Table 4**). Hierarchical multivariate analysis revealed that counts were significantly associated with the circulating parasitemia and tissue (**Supplemental Table 5**).

To determine if there may be a preference for iRBC accumulation in specific tissues, the distributions of the iRBCs in the tissues was compared against a uniform distribution using a χ^2 test. This analysis indicated that the distribution of the iRBCs in the tissues was not evenly distributed prior to control of parasitemia, consistent with a preference for iRBC accumulation in specific tissues (**Figure 5G** and **Supplemental Table 4**). To assess if there were differences in iRBC accumulation in the tissues irrespective of their different parasitemias, relative parasite densities were 1) determined by normalizing the iRBC load, and 2) displayed in a heat map (**Figure 5H**). Tissues with the highest parasite accumulation included the spleen, colon, stomach, lung, liver, heart, and kidney prior to parasitemia control. Post-control, the spleen is less evident as a reservoir, but the GI tract, lungs, and heart remain predominant sites for parasite accumulation (**Figure 5H**).

Multiple analyses were used to assess if the accumulation of parasites in the tissues was associated with tissue damage, as quantified by histopathology scores (**Supplemental Table 2**). First, univariate analysis using Spearman's correlation was performed between tissue score and iRBC density. Parasite iRBC burden positively correlated with tissue score ($\rho = 0.308$,

p-value = $4.66x10^{-5}$), with a stronger correlation prior to monkey control of parasitemia ($\rho = 0.432$, p-value = $2.32x10^{-5}$). Next, a hierarchical multiple linear regression analysis was performed to determine which factors affected tissue scores the most (**Supplemental Table 5**). A model considering only iRBC tissue burden did not result in a linear relationship (adjusted $R^2 = 0.060$, p-value = 0.0008), however, when combined with the tissue type, the relationship was essentially linear (adjusted $R^2 = 0.856$, p-value < 2.20×10^{-16}). The contribution of the iRBC tissue burden to the model remained significant after the addition of tissue type (p-value = 5.20×10^{-15}). A model including an interaction term between the tissue iRBC burden and tissue histopathology score did not improve the fit of the model ($R^2 = 0.856$, p-value = 2.20×10^{-16}), and the interaction term was not a significant contributor. No multicollinearity was noted. Parasitemia at necropsy and cumulative parasitemia were not significant contributors. Thus, although there is a relationship between parasite accumulation and overall histopathology within tissues during acute infection, parasite accumulation alone does not determine the degree to which tissues are damaged.

P. knowlesi Accumulation in the Rhesus Monkey Tissue Vasculature May be Due to the Expression of SICA Variant Antigens

Small mucosal and submucosal blood vessels throughout the GI tract were observed to be packed with iRBCs in five of six pre-control monkeys at the acute phase of infection (**Figure 6A**, top row). Most dramatically, the iRBCs appeared to stud the endothelium of larger vessels, suggesting cytoadhesion of the iRBCs at the vascular interface (**Figure 6A**, top row). These 'marginating' iRBCs, visualized directly adjacent to endothelial cells, were evaluated by examining duodenal tissue samples by TEM (**Figure 6B**, left panel). Indeed, this analysis suggested direct interactions of parasitized RBCs with the endothelium.

Despite the presence of trophozoites and schizonts on blood smears, the parasite kinetics showed an undulating saw-tooth pattern consistent with cytoadhesion and sequestration of the maturing T/S-iRBC forms (**Supplemental Figures 1-4**; blood smears were performed twice daily during the acute period of the infections, when the parasitemias were rising (Taliaferro and Taliaferro, 1949)). This pattern reflects fewer parasites present as schizonts in the peripheral blood at the 8 AM time point than would be the case if all the developing ring-stage parasites seen in the afternoon the day before were still present in the circulation. These results are consistent with the cytoadhesion and sequestration of some but not all *P. knowlesi* iRBCs that constitute the blood-stage infections.

Since *P. falciparum* iRBC cytoadhesion is mediated by *Pf*EMP1surface-expressed variant antigens (reviewed in Lee et al., 2019), an experiment was performed to test the hypothesis that the related SICA proteins may likewise mediate the *P. knowlesi* iRBC margination phenotype. Two splenectomized rhesus monkeys were infected with SICA[-] parasites, and the GI tissues were collected and examined in the same manner as the SICA[+] infected animals. The percentage of iRBCs marginated within 350 vessels was calculated from the stomach, duodenum, jejunum, and colon and compared between splenectomized rhesus infected with SICA[-] parasites and the spleen-intact rhesus infected with SICA[+] parasites. In stark contrast to the iRBC margination observed in the tissues of the spleen-intact rhesus infected with SICA[+] parasites, there was no comparable margination of the SICA[-] iRBCs observed by light microscopy in the GI tissues from the splenectomized rhesus (**Figure 6A**, bottom row), and no endothelial cell contact was observed by TEM (**Figure 6B**, right panel). In agreement with the microscopy data, the percentage of iRBCs appearing to be marginated in the digestive tract (stomach, duodenum, jejunum, and colon) was significantly reduced in the rhesus infected with SICA[-] compared to SICA[+] parasites (**Figure 6C**). This was the case despite much higher parasitemias in the SICA[-] compared to SICA[+] infected animals. These analyses support the premise that, comparable to *Pf*EMP-1-endothelial cell interactions, a subpopulation of *P. knowlesi* iRBCs cytoadheres and sequesters, in part, due to the expression of SICA proteins on the surface of *P. knowlesi*-iRBCs.

DISCUSSION

This study determined clinical features of infection and host-parasite interactions that underpin disease severity in *P. knowlesi* infections in rhesus macaques, providing insights into mechanisms of severe illness in human *Plasmodium* infections. In the absence of treatment, overwhelming parasitemia is the main cause of death for rhesus macaques infected with *P. knowlesi* (reviewed in Howard, 1984). Importantly, rhesus monkeys in this study became febrile by day 8 post-inoculation of sporozoites, one day on average later than kra monkeys (Peterson et al., 2021), which, as expected, showed natural resilience to experimental *P. knowlesi* infections without treatment (Knowles and Gupta, 1932; Garnham, 1966; Collins et al., 1992). This 'one-day' difference in fever response was apparent even though both macaque species developed blood-stage parasitemias within a typical time frame of 6-7 days from the time of sporozoite inoculation. The later febrile episodes in the rhesus monkeys suggest that they were less able or unable to detect and mount appropriate, timely systemic inhibitory responses to control the blood-stage parasites. Since *P. knowlesi*-iRBCs multiply approximately 10-fold every 24 hours, this seemingly unremarkable 'one-day delay' in rhesus monkey responsiveness is significant. The delayed containment of parasitemia resulted in apparent prolonged inflammation in the rhesus compared to recovery processes in the kra monkeys (Gupta et al., 2021; Gupta et al., 2022).

Bilirubinemia has been associated with severe *P. knowlesi* malaria in humans (Barber et al., 2013), and it was mildly elevated in the rhesus monkeys in this study prior to them controlling their parasitemia. Fractionated bilirubin measurements were unavailable, however, and given that there was no histological evidence for cholestasis or other hepatic injury, the elevation in total bilirubin may reflect increased

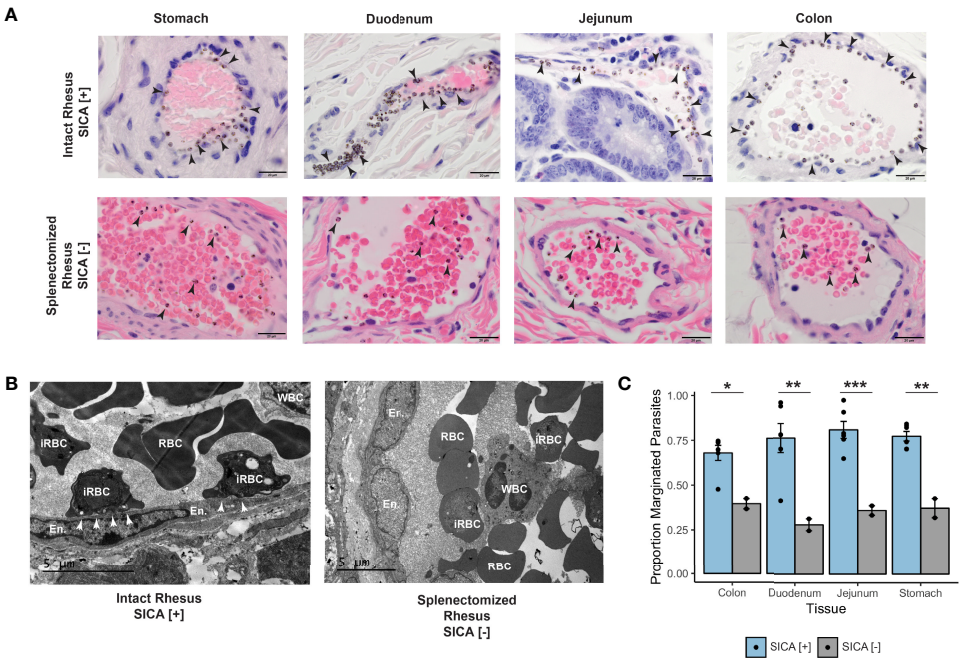

FIGURE 6 | Margination, SICA protein expression, and binding of *P. knowlesi*-infected RBCs. **(A)** Top: infected iRBCs were noted to form a very clear margination pattern in rhesus monkeys infected with SICA-expressing parasites in the tissues of the gastrointestinal tract (1000x). Bottom: The margination phenotype is lost when monkeys are infected with SICA protein phenotypic negative parasites. Infected RBCs are indicated with black arrowheads (1000x). **(B)** Top: TEM of representative rhesus monkey duodenum samples shows contact between SICA[+] iRBCs and the endothelium (white arrowheads). Bottom: No contact was observed between SICA[-] iRBCs. **(C)** Quantification of the percentage of iRBCs located on the periphery of vessels in H&E-stained sections revealed significant differences between SICA[+]-infected and SICA[-]-infected splenectomized monkeys. Statistical comparison analysis was conducted with FDR-corrected Student's t-tests comparing SICA [-] and SICA [+] infected tissues, by tissue (*p-value <0.05, **p-value<0.005, ***p-value<0.0005). Error bars represent standard error of the mean.

hemolysis. The anemia in the rhesus monkeys was mostly mild and may correspond to the relatively modest increase in serum bilirubin observed. Neither AST nor ALT was significantly different from baseline, however an increase in AST was observed. ALT and AST are both measures of cell integrity, with ALT being more specific to the liver. An elevation of AST without a concurrent elevation of ALT in concert with the absence of hepatocyte necrosis is consistent with a picture of nonspecific tissue stress caused by an infection (Giannini et al., 2005). Despite notable histopathology in the kidneys, both prior to and after parasitemic control, no significant elevation in creatine was observed until after control of the infection.

After subcurative antimalarial medication was administered to the acutely infected rhesus, to ensure their survival and to establish chronic infections, the observed infection-based decreased hemoglobin and platelet levels rebounded rapidly in the animals. The relatively mild anemia and thrombocytopenia occurring in the animals are consistent with expectations based on human cases after antimalarial treatment (Daneshvar et al., 2009). Insufficient erythropoiesis has been reported in rhesus macaques infected with *P. cynomolgi* and *P. coatneyi*, as well in rodents and humans infected with *Plasmodium* parasites (Chang et al., 2004; Chang and Stevenson, 2004; Perkins et al., 2011; Moreno et al., 2013; Thawani et al., 2014; Joyner et al., 2016; Tang et al., 2017; Cordy et al., 2019). Likewise, here, the BM response was blunted in the face of *P. knowlesi* infection, until treatment was provided. Interestingly, in stark contrast, the BM response was timely in kra monkeys infected with *P. knowlesi*, with the kra monkey BM responding naturally to the infection without treatment (Peterson et al., 2021). This is consistent with their faster overall recovery from infection compared to the rhesus, as indicated by transcriptomics (Gupta et al., 2021; Peterson et al., 2021; Gupta et al., 2022). Future determinations of the mechanism(s) by which hemoglobin levels in rhesus monkeys stabilize after subcurative treatment may lead to a better understanding of malarial anemia in relation to patient care.

Much remains to be learned about the specific systemic host-parasite interactions and biological, immunological, and metabolic cascades that influence the ultimate pathology and disease course of malaria in both humans and NHPs. Tissue data obtained from autopsy and necropsy procedures, respectively, to better understand malaria pathology in the context of clinical data and the clinical spectrum of the disease, can be powerful, providing a holistic assessment far beyond what can be achieved with either cross-sectional samples or multiple time points during infections. Previous studies have reported the presence of *P. knowlesi* iRBCs in various tissues from infected rhesus monkeys (Miller et al., 1971b; Anderios et al., 2010). The data presented here expand upon that knowledge by quantitatively

determining that *P. knowlesi* iRBCs are preferentially found in specific organs like the spleen, adrenal gland, lung, kidney, and the organs of the GI tract. Similar to prior studies with *P. vivax* infections of *S. boliviensis* monkeys (Peterson et al., 2019), a modest relationship was identified here between the rhesus histopathology scores and *P. knowlesi* iRBC accumulation in these tissues. While *P. knowlesi* iRBC accumulation in the tissues may directly or indirectly cause histopathology, our data suggest that it is neither necessary nor sufficient. Instead, host responses are likely the main contributors to the observed tissue damage. This hypothesis, which warrants further exploration, is in fact consistent with tissue-damage studies that have directly shown that *P. falciparum*-iRBC accumulation in the brain is not necessarily the main driver of cerebral malaria (Seydel et al., 2006; Milner et al., 2014; Milner et al., 2015; Coban et al., 2018).

Acute *Plasmodium* infections from multiple species – whether in NHPs or humans – are known to cause damage to tissues and vital organs, which can contribute to clinical complications and death (Spitz, 1946; Spangler et al., 1978; Cox-Singh et al., 2010; Lacerda et al., 2012; Milner et al., 2014). Therefore, it was anticipated in this study that escalating parasitemias in rhesus would cause tissue damage that, at least in part, would contribute to the inability of this species to survive infection without treatment (Spangler et al., 1978). Surprisingly, the histopathology observations during the acute phase of the rhesus infections proved to be comparable to those reported previously for *P. knowlesi*-infected kra monkey tissues (Peterson et al., 2021) and dramatic pathological findings in vital organs (*e.g.*, lung, liver, kidney) were not identified. However, gastritis was specifically noted in the rhesus stomach tissue samples acquired from necropsy performed at the time of the acute infections. This finding is noteworthy from a clinical perspective because gastritis and other GI complications and clinical manifestations occur frequently in humans with *P. knowlesi* malaria (Cox-Singh et al., 2008; Barber et al., 2013).

Striking observations presented here include microscopic evidence for sequestration of *P. knowlesi* SICA[+] iRBCs with presumptive cytoadhesion that was pronounced in the spleen-intact rhesus. Frank margination of the iRBCs was observed in the mucosal and submucosal vessels of the stomach, duodenum, jejunum, and colon tissues from these animals, and this phenotype was dramatic even with relatively low parasitemias (1-3%) at the time of necropsy. Rheological changes and 'sludging,' as reported previously in rhesus infection studies, in part explain capillary congestion with the *P. knowlesi*-iRBCs (Knisely et al., 1945; Knisely et al., 1964; Miller et al., 1971a; Barber et al., 2018). Yet, the clear predilection shown here for iRBCs at the margins of venules over the lumen implicates iRBC endothelial interaction(s) and cytoadhesion as an apparent mechanism.

A few studies have examined cytoadhesion of *P. knowlesi* T/S-iRBCs using *ex vivo* (Fatih et al., 2012) and *in vitro* (Lee et al., 2022) cultivated parasites, leaving questions as to the parasite ligand(s) involved and the number and types of possible host receptor specificities. Critically, *in vitro* cultivated *P. knowlesi* iRBCs have been shown to lose expression of the *SICAvar* gene family, and these were classified in the 'off state' with regards to *SICAvar* expression (Lapp et al., 2015). Expression of the *SICAvar* gene family and the encoded SICA proteins were shown to be downregulated to the 'off state' in iRBCs from splenectomized hosts, bringing emphasis to the importance of the *in vivo* splenic environment for regulating SICA expression (Lapp et al., 2013) and ultimately virulence of *P. knowlesi* infections (Barnwell et al., 1983b). In turn, experimental systems to test for receptor-ligand interactions may require *ex vivo* parasites obtained from spleen-intact animals. Our preliminary findings in this area (unpublished data), as others (Fatih et al., 2012; Lee et al., 2022), suggest levels of complexity on par with *P. falciparum*. Therefore, sorting out the precise receptors, ligands, and interactions that support *P. knowlesi* cytoadhesion and sequestration will not be an easy task.

SICA proteins have been considered prime candidates mediating possible adhesive interaction(s), due to their commonalities with *Pf*EMP1, including iRBC surface localization and multiple diverse externalized cysteine-rich domains (Al-Khedery et al., 1999; Korir and Galinski, 2006); these features are hallmarks of *Pf*EMP1 that account for *P. falciparum*'s selective T/S-iRBC cytoadhesion characteristics and sequestration (reviewed in Howard, 1984; Smith, 2014). Here, tissues from splenectomized rhesus monkeys infected with SICA[-] parasites lacked the frank margination phenotype observed in the tissues from spleen-intact monkeys infected with SICA[+] parasites. This observation strongly supports the premise that SICA proteins mediate the adhesion of the iRBCs to the endothelium and provides further impetus for studying the SICA[+] and SICA[-] parasites in parallel infections to better understand the pathological mechanisms and biological implications of iRBC adherence to the endothelium. SICA protein expression at the surface of *P. knowlesi*-iRBCs is associated with virulence in rhesus and *SICAvar* gene family expression is somehow regulated by the spleen (Barnwell et al., 1983a; Lapp et al., 2013), as is *Pf*EMP1 variant antigen gene and protein expression in *Saimiri* monkeys and humans (David et al., 1983; Hommel et al., 1983; Bachmann et al., 2009).

Nonetheless, as for *Pf*EMP1, it is worth noting that the biological function of SICA in the context of the iRBC membrane remains unknown (reviewed in Howard, 1984; Galinski et al., 2018). In this context, it is important to recognize that cytoadhesion – as proposed to avoid circulation through the spleen – is not necessarily (nor likely) the sole function of either of these proteins (reviewed in Howard, 1984). It would be a breakthrough if an essential iRBC function were to be discovered for the *Pf*EMP-1 and SICA proteins, commensurate with these parasite species' evolved strategies to maintain numerous *var/SICAvar* family members to ensure survival. Clearly, as is known for *P. knowlesi* and most species of *Plasmodium* where all blood-stage forms circulate, avoidance of the spleen does not fit as the main function of potentially adhesive surface-exposed proteins. In fact, all other *Plasmodium* species known to infect humans do not have comparable *var/SICAvar* genes (*P. vivax*, *P. malariae*, *P. ovale*, *P. cynomolgi*) (Tachibana et al., 2012; Rutledge et al., 2017; Imwong et al., 2018) and all their iRBC developmental life cycle stages circulate, seemingly unaffected by passage through the spleen (or

potentially even benefiting from intra-splenic interactions (reviewed in Kho et al., 2021; Fernandez-Becerra et al., 2022). All iRBC developmental forms of these species circulate despite *P. malariae* and *P. ovale* sharing knobby iRBC surface phenotypes (Matsumoto et al., 1986; Li et al., 2010) that are morphologically similar to those in *P. falciparum* infections (Gruenberg et al., 1983; Aikawa et al., 1996). The iRBCs of each of these species differ from *P. knowlesi*, which has occasional indentations in the form of caveolae peppering the iRBC and no knobby protrusions (Liu et al., 2019). In fact, *P. knowlesi* is the simplest of them all, having neither knobs nor caveolae vesicle complexes, which are especially abundant at the iRBC surface of *P. vivax*- and *P. cynomolgi*-iRBCs (Aikawa et al., 1975; Akinyi et al., 2012). The simplicity, by comparison, of the *P. knowlesi* iRBC membrane, even compared to the phylogenetically related 'knobby, variant and sequestering' simian malaria parasites *P. fragile* and *P. coatneyi* (Garnham, 1966; Fremount and Miller, 1975; Handunnetti et al., 1987; Nakano et al., 1996; Collins et al., 2006; Chien et al., 2016), makes it an attractive parasite model for understanding the essential features of *Plasmodium*-iRBC parasitism and their evolution.

In sum, this study reports a systematic study of *P. knowlesi* sporozoite-infected rhesus monkeys that expands our understanding of pathogenic features of severe disease and makes comparisons with comparable data from kra monkeys that support resilience to *P. knowlesi* malaria (Peterson et al., 2021). Multiple physiological and immunological responses were found to be associated with pathology or resilience. Additionally, an association of SICA variant proteins with cytoadhesion and sequestration came to light in comparisons of SICA[+] and SICA [-] parasites in tissues obtained from spleen-intact and splenectomized rhesus, respectively. Studies using multiple NHP models in biomedical research have been beneficial for several decades towards understanding HIV pathogenesis, specifically with the comparison of SIV-infected rhesus macaques and sooty mangabeys in relation to the development of AIDS (Bosinger et al., 2009; Palesch et al., 2018). Correspondingly, a two-host animal model system that includes rhesus and kra monkeys and longitudinal infections is now poised for significant advances towards understanding host-parasite interactions, cascades and networks. Host mechanistic differences in physiology, immune responses, and pathogenesis, can be unravelled to better understand malaria severity and resilience against *P. knowlesi* and potentially other species of *Plasmodium* that can infect these species.

CONSORTIUM MEMBERSHIP

MaHPIC members participating in discussions at the time of the planning, implementation, or analysis of this project include: Dave C. Anderson, Ferhat Ay, Cristiana F. A. Brito, John W. Barnwell, Megan DeBarry, Steven E. Bosinger, Jung-Ting Chien, Jinho Choi, Anuj Gupta, Jay C. Humphrey, Chris Ibegbu, Xuntian Jiang, Dean P. Jones, Nicolas Lackman, Tracey J. Lamb, Frances E.-H. Lee, Karine Gaelle Le Roche, Shuzhao Li, Esmeralda V.S. Meyer, Diego M. Moncada-Giraldo, Dan Ory, Jan Pohl, Saeid Safaei, Ignacio Sanz, Maren Smith, Gregory Tharp, ViLinh Tran, Elizabeth D. Trippe, Karan Uppal, Susanne Warrenfeltz, Tyrone Williams, Zerotti L. Woods.

DATA AVAILABILITY STATEMENT

The clinical datasets generated and analyzed for this study can be found in the NIAID Bioinformatics Resource Center Database, PlasmoDB.org, https://plasmodb.org/plasmo/app/static-content/PlasmoDB/mahpic.html (Aurrecoechea et al., 2009; Amos et al., 2022).

ETHICS STATEMENT

The animal study was reviewed and approved by Emory University's Institutional Animal Care and Use Committee (IACUC) and the Animal Care and Use Review Office (ACURO) of the US Department of Defense.

AUTHOR CONTRIBUTIONS

Conceived and designed the experiments: MP, CJ, JB, JW, LF, RT, JK, AM, SG, EV, JG, RC, MG, and members of the MaHPIC-Consortium. Performed the experiments: MP, CJ, JB, JW, MC-M, CS, LF, WC, JJ, SL, SS, AH, DM, EK. Performed data analysis: MP, CJ, JB, LF, SG, JG. Interpreted the data analysis: MP, CJ, RC, MG and members of the MaHPIC-Consortium. Managed and led validation and quality control of datasets for clinical and telemetry results and deposited the data and metadata: MN, JD, JK. Generated the figures: MP, CJ, LF, SG. Wrote the paper: MP, MG. Provided manuscript editorial contributions: CJ, SL, LF, JD, RT, JK, AM, SG, EV, JG, RC. All authors reviewed the manuscript. All authors read and approved the final manuscript.

FUNDING

This project was funded in part by the National Institute of Allergy and Infectious Diseases; National Institutes of Health, Department of Health and Human Services, which established the MaHPIC [Contract No. HHSN272201200031C; MG], the NIH Office of Research Infrastructure Programs/OD P51OD011132, the Defense Advanced Research Program Agency and the US Army Research Office *via* a cooperative agreement [Contract No. W911NF16C0008; MG], which funded the Technologies for Host Resilience-Host Acute Models of Malaria to study Experimental Resilience (THoR's HAMMER) consortium.

ACKNOWLEDGMENTS

The authors thank John W. Barnwell for discussions, bringing knowledge of *P. knowlesi* infections and malaria to this project and the provision of cryopreserved sporozoites. Elizabeth Strobert is thanked for consultations and advice on animal protocols.

E-van Dessasau is thanked for technical assistance in preparing and staining histopathological slides. The YNPRC staff are acknowledged for assistance with procedures involving NHPs. The authors also acknowledge that the YNPRC has recently been re-named as the Emory National Primate Research Center.

SUPPLEMENTARY MATERIAL

The Supplementary Material for this article can be found online at: https://www.frontiersin.org/articles/10.3389/fcimb.2022.888496/full#supplementary-material

REFERENCES

Aikawa, M., Kamanura, K., Shiraishi, S., Matsumoto, Y., Arwati, H., Torii, M., et al. (1996). Membrane Knobs of Unfixed *Plasmodium Falciparum* Infected Erythrocytes: New Findings as Revealed by Atomic Force Microscopy and Surface Potential Spectroscopy. *Exp. Parasitol.* 84, 339–343. doi: 10.1006/expr.1996.0122

Aikawa, M., Miller, L. H., and Rabbege, J. (1975). Caveola–vesicle Complexes in the Plasmalemma of Erythrocytes Infected by *Plasmodium Vivax* and *P. Cynomolgi*. Unique Structures Related to Schuffner's Dots. *Am. J. Pathol.* 79, 285–300.

Akinyi, S., Hanssen, E., Meyer, E. V., Jiang, J., Korir, C. C., Singh, B., et al. (2012). A 95 kDa Protein of *Plasmodium Vivax* and P. Cynomolgi Visualized by Three-Dimensional Tomography in the Caveola-Vesicle Complexes (Schuffner's Dots) of Infected Erythrocytes is a Member of the PHIST Family. *Mol. Microbiol.* 84, 816–831. doi: 10.1111/j.1365-2958.2012.08060.x

Aley, S. B., Sherwood, J. A., and Howard, R. J. (1984). Knob-Positive and Knob-Negative *Plasmodium Falciparum* Differ in Expression of a Strain-Specific Malarial Antigen on the Surface of Infected Erythrocytes. *J. Exp. Med.* 160, 1585–1590. doi: 10.1084/jem.160.5.1585

Al-Khedery, B., Barnwell, J. W., and Galinski, M. R. (1999). Antigenic Variation in Malaria: A 3' Genomic Alteration Associated With the Expression of a *P. Knowlesi* Variant Antigen. *Mol. Cell* 3, 131–141. doi: 10.1016/s1097-2765(00)80304-4

Amato, R., Pearson, R. D., Almagro-Garcia, J., Amaratunga, C., Lim, P., Suon, S., et al. (2018). Origins of the Current Outbreak of Multidrug-Resistant Malaria in Southeast Asia: A Retrospective Genetic Study. *Lancet Infect. Dis.* 18, 337–345. doi: 10.1016/S1473-3099(18)30068-9

Amos, B., Aurrecoechea, C., Barba, M., Barreto, A., Basenko, E. Y., Bazant, W., et al. (2022). VEuPathDB: The Eukaryotic Pathogen, Vector and Host Bioinformatics Resource Center. *Nucleic Acids Res.* 50, D898–D911. doi: 10.1093/nar/gkab929

Anderios, F., Noorrain, A., and Vythilingam, I. (2010). In Vivo Study of Human *Plasmodium Knowlesi* in Macaca Fascicularis. *Exp. Parasitol.* 124, 181–189. doi: 10.1016/j.exppara.2009.09.009

Aravind, H. (2018) *"Olsrr. R Package "*. Available at: https://cloud.r-project.org/package=olsrr (Accessed March 2, 2022).

Ashley, E. A., Dhorda, M., Fairhurst, R. M., Amaratunga, C., Lim, P., Suon, S., et al. (2014). Spread of Artemisinin Resistance in Plasmodium Falciparum Malaria. *N Engl. J. Med.* 371, 411–423. doi: 10.1056/NEJMoa1314981

Aurrecoechea, C., Brestelli, J., Brunk, B. P., Dommer, J., Fischer, S., Gajria, B., et al. (2009). PlasmoDB: A Functional Genomic Database for Malaria Parasites. *Nucleic Acids Res.* 37, D539–D543. doi: 10.1093/nar/gkn814

Bachmann, A., Esser, C., Petter, M., Predehl, S., Von Kalckreuth, V., Schmiedel, S., et al. (2009). Absence of Erythrocyte Sequestration and Lack of Multicopy Gene Family Expression in *Plasmodium Falciparum* From a Splenectomized Malaria Patient. *PLoS One* 4, e7459. doi: 10.1371/journal.pone.0007459

Baird, J. K. (2013). Evidence and Implications of Mortality Associated With Acute *Plasmodium Vivax* Malaria. *Clin. Microbiol. Rev.* 26, 36–57. doi: 10.1128/CMR.00074-12

Barber, B. E., Rajahram, G. S., Grigg, M. J., William, T., and Anstey, N. M. (2017). World Malaria Report: Time to Acknowledge *Plasmodium Knowlesi* Malaria. *Malar J.* 16, 135. doi: 10.1186/s12936-017-1787-y

Barber, B. E., Russell, B., Grigg, M. J., Zhang, R., William, T., Amir, A., et al. (2018). Reduced Red Blood Cell Deformability in *Plasmodium Knowlesi* Malaria. *Blood Adv.* 2, 433–443. doi: 10.1182/bloodadvances.2017013730

Barber, B. E., William, T., Grigg, M. J., Menon, J., Auburn, S., Marfurt, J., et al. (2013). A Prospective Comparative Study of Knowlesi, Falciparum, and Vivax Malaria in Sabah, Malaysia: High Proportion With Severe Disease From *Plasmodium Knowlesi* and *Plasmodium Vivax* But No Mortality With Early Referral and Artesunate Therapy. *Clin. Infect. Dis.* 56, 383–397. doi: 10.1093/cid/cis902

Barnwell, J. W., Howard, R. J., Coon, H. G., and Miller, L. H. (1983a). Splenic Requirement for Antigenic Variation and Expression of the Variant Antigen on the Erythrocyte Membrane in Cloned *Plasmodium Knowlesi* Malaria. *Infect. Immun.* 40, 985–994. doi: 10.1128/iai.40.3.985-994.1983

Barnwell, J. W., Howard, R. J., and Miller, L. H. (1982). Altered Expression of *Plasmodium Knowlesi* Variant Antigen on the Erythrocyte Membrane in Splenectomized Rhesus Monkeys. *J. Immunol.* 128, 224–226.

Barnwell, J. W., Howard, R. J., and Miller, L. H. (1983b). Influence of the Spleen on the Expression of Surface Antigens on Parasitized Erythrocytes. *Ciba Found Symp.* 94, 117–136. doi: 10.1002/9780470715444.ch8

Baruch, D. I., Pasloske, B. L., Singh, H. B., Bi, X., Ma, X. C., Feldman, M., et al. (1995). Cloning the P. Falciparum Gene Encoding PfEMP1, a Malarial Variant Antigen and Adherence Receptor on the Surface of Parasitized Human Erythrocytes. *Cell* 82, 77–87. doi: 10.1016/0092-8674(95)90054-3

Biggs, B. A., Anders, R. F., Dillon, H. E., Davern, K. M., Martin, M., Petersen, C., et al. (1992). Adherence of Infected Erythrocytes to Venular Endothelium Selects for Antigenic Variants of *Plasmodium Falciparum*. *J. Immunol.* 149, 2047–2054.

Biggs, B. A., Gooze, L., Wycherley, K., Wollish, W., Southwell, B., Leech, J. H., et al. (1991). Antigenic Variation in *Plasmodium Falciparum*. *Proc. Natl. Acad. Sci. U.S.A.* 88, 9171–9174. doi: 10.1073/pnas.88.20.9171

Bosinger, S. E., Li, Q., Gordon, S. N., Klatt, N. R., Duan, L., Xu, L., et al. (2009). Global Genomic Analysis Reveals Rapid Control of a Robust Innate Response in SIV-Infected Sooty Mangabeys. *J. Clin. Invest.* 119, 3556–3572. doi: 10.1172/JCI40115

Brown, K. N., and Brown, I. N. (1965). Immunity to Malaria: Antigenic Variation in Chronic Infections of *Plasmodium Knowlesi*. *Nature* 208, 1286–1288. doi: 10.1038/2081286a0

Bunnik, E. M., Venkat, A., Shao, J., Mcgovern, K. E., Batugedara, G., Worth, D., et al. (2019). Comparative 3D Genome Organization in Apicomplexan Parasites. *Proc. Nat. Acad. Sci.* 116, 3183–3192. doi: 10.1073/pnas.1810815116

Chang, K. H., and Stevenson, M. M. (2004). Malarial Anaemia: Mechanisms and Implications of Insufficient Erythropoiesis During Blood-Stage Malaria. *Int. J. Parasitol.* 34, 1501–1516. doi: 10.1016/j.ijpara.2004.10.008

Chang, K. H., Tam, M., and Stevenson, M. M. (2004). Inappropriately Low Reticulocytosis in Severe Malarial Anemia Correlates With Suppression in the Development of Late Erythroid Precursors. *Blood* 103, 3727–3735. doi: 10.1182/blood-2003-08-2887

Chien, J. T., Pakala, S. B., Geraldo, J. A., Lapp, S. A., Humphrey, J. C., Barnwell, J. W., et al. (2016). High-Quality Genome Assembly and Annotation for *Plasmodium Coatneyi*, Generated Using Single-Molecule Real-Time PacBio Technology. *Genome Announc.* 4, 1–2. doi: 10.1128/genomeA.00883-16

Coatney, G. R., Collins, W. E., Warren, M., and Contacos, P. G. (1971). *The Primate Malarias* (Washington, DC: U.S Department of Health, Education and Welfare).

Coatney, G. R., Collins, W. E., Warren, M., and Contacos, P. G. (2003) *The Primate Malarias, E-Book* (Atlanta, GA, USA: Division of Parasitic Diseases, CDC). Available at: http://www.mcdinternational.org/trainings/malaria/english/DPDx5/HTML/PDF_Files/PrimateMalariasChapters/primate_24.pdf (Accessed March 2. 2022).

Coban, C., Lee, M. S. J., and Ishii, K. J. (2018). Tissue-Specific Immunopathology During Malaria Infection. *Nat. Rev. Immunol.* 18, 266–278. doi: 10.1038/nri.2017.138

Collins, W. E., Skinner, J. C., Broderson, J. R., Filipski, V. K., Morris, C. M., Stanfill, P. S., et al. (1992). Susceptibility of *Macaca Fascicularis* Monkeys From Mauritius to Different Species of *Plasmodium*. *J. Parasitol.* 78, 505–511. doi: 10.2307/3283652

Collins, W. E., Warren, M., Sullivan, J. S., Galland, G. G., Strobert, E., Nace, D., et al. (2006). Studies on Sporozoite-Induced and Chronic Infections With *Plasmodium Fragile* in *Macaca Mulatta* and New World Monkeys. *J. Parasitol.* 92, 1019–1026. doi: 10.1645/GE-848R.1

Cordy, R. J., Patrapuvich, R., Lili, L. N., Cabrera-Mora, M., Chien, J.-T., Tharp, G. K., et al. (2019). Distinct Amino Acid and Lipid Perturbations Characterize Acute Versus Chronic Malaria. *JCI Insight* 4, 1–21. doi: 10.1172/jci.insight.125156

Cox-Singh, J., Davis, T. M., Lee, K. S., Shamsul, S. S., Matusop, A., Ratnam, S., et al. (2008). *Plasmodium Knowlesi* Malaria in Humans is Widely Distributed and Potentially Life Threatening. *Clin. Infect. Dis.* 46, 165–171. doi: 10.1086/524888

Cox-Singh, J., Hiu, J., Lucas, S. B., Divis, P. C., Zulkarnaen, M., Chandran, P., et al. (2010). Severe Malaria - a Case of Fatal *Plasmodium Knowlesi* Infection With Post-Mortem Findings: A Case Report. *Malar J.* 9, 10. doi: 10.1186/1475-2875-9-10

Cox-Singh, J., and Singh, B. (2008). Knowlesi Malaria: Newly Emergent and of Public Health Importance? *Trends Parasitol.* 24, 406–410. doi: 10.1016/j.pt.2008.06.001

Craig, A. G., Khairul, M. F., and Patil, P. R. (2012). Cytoadherence and Severe Malaria. *Malays J. Med. Sci.* 19, 5–18.

Daneshvar, C., Davis, T. M., Cox-Singh, J., Rafa'ee, M. Z., Zakaria, S. K., Divis, P. C., et al. (2009). Clinical and Laboratory Features of Human *Plasmodium Knowlesi* Infection. *Clin. Infect. Dis.* 49, 852–860. doi: 10.1086/605439

David, P. H., Hommel, M., Miller, L. H., Udeinya, I. J., and Oligino, L. D. (1983). Parasite Sequestration in *Plasmodium Falciparum* Malaria: Spleen and Antibody Modulation of Cytoadherence of Infected Erythrocytes. *Proc. Natl. Acad. Sci. U.S.A.* 80, 5075–5079. doi: 10.1073/pnas.80.16.5075

Debarry, J. D., Kissinger, J. C., Nural, M. V., Pakala, S. B., Humphrey, J. C., Meyer, E. V. S., et al. (2020). Practical Recommendations for Supporting a Systems Biology Cyberinfrastructure. *Data Sci. J.* 19, 1–12. doi: 10.5334/dsj-2020-024

Fatih, F. A., Siner, A., Ahmed, A., Woon, L. C., Craig, A. G., Singh, B., et al. (2012). Cytoadherence and Virulence - the Case of *Plasmodium Knowlesi* Malaria. *Malar J.* 11, 33. doi: 10.1186/1475-2875-11-33

Fernandez-Becerra, C., Aparici-Herraiz, I., and Del Portillo, H. A. (2022). Cryptic Erythrocytic Infections in *Plasmodium Vivax*, Another Challenge to its Elimination. *Parasitol. Int.* 87, 102527. doi: 10.1016/j.parint.2021.102527

Fonseca, L. L., Alezi, H. S., Moreno, A., Barnwell, J. W., Galinski, M. R., and Voit, E. O. (2016). Quantifying the Removal of Red Blood Cells in *Macaca Mulatta* During a *Plasmodium Coatneyi* Infection. *Malar J.* 15, 410. doi: 10.1186/s12936-016-1465-5

Fonseca, L. L., Joyner, C. J.MaHPIC-Consortium, , Galinski, M. R., Voit, E. O. (2017). A Model of *Plasmodium Vivax* Concealment Based on *Plasmodium Cynomolgi* Infections in *Macaca Mulatta*. *Malar J.* 16, 1–16. doi: 10.1186/s12936-017-2008-4

Fremount, H. N., and Miller, L. H. (1975). Deep Vascular Schizogony in *Plasmodium Fragile*: Organ Distribution and Ultrastructure of Erythrocytes Adherent to Vascular Endothelium. *Am. J. Trop. Med. Hyg* 24, 1–8. doi: 10.4269/ajtmh.1975.24.1.TM0240010001

Galinski, M. R., Lapp, S. A., Peterson, M. S., Ay, F., Joyner, C. J., LeRoch, K., et al. (2018). *Plasmodium Knowlesi*: A Superb *In Vivo* Nonhuman Primate Model of Antigenic Variation in Malaria. *Parasitology* 145, 85–100. doi: 10.1017/S0031182017001135

Garnham, P. C. C. (1966). "Plasmodium Knowlesi and Subspecies, Plasmodium Coatneyi and Plasmodium Fragile," in *Malaria Parasites and Other Haemosporidia*, vol. 1966. (Oxford: Blackwell Scientific Publications), 323–356.

Gatton, M. L., and Cheng, Q. (2002). Evaluation of the Pyrogenic Threshold for *Plasmodium Falciparum* Malaria in Naive Individuals. *Am. J. Trop. Med. Hyg* 66, 467–473. doi: 10.4269/ajtmh.2002.66.467

Giannini, E. G., Testa, R., and Savarino, V. (2005). Liver Enzyme Alteration: A Guide for Clinicians. *CMAJ* 172, 367–379. doi: 10.1503/cmaj.1040752

Gruenberg, J., Allred, D. R., and Sherman, I. W. (1983). Scanning Electron Microscope-Analysis of the Protrusions (Knobs) Present on the Surface of *Plasmodium Falciparum*-Infected Erythrocytes. *J. Cell Biol.* 97, 795–802. doi: 10.1083/jcb.97.3.795

Gupta, A., Galinski, M. R., and Voit, E. O. (2022). Dynamic Control Balancing Cell Proliferation and Inflammation is Crucial for an Effective Immune Response to Malaria. *Front. Mol. Biosci.* 8. doi: 10.3389/fmolb.2021.800721

Gupta, A., Styczynski, M. P., Galinski, M. R., Voit, E. O., and Fonseca, L. L. (2021). Dramatic Transcriptomic Differences in *Macaca Mulatta* and *Macaca Fascicularis* With *Plasmodium Knowlesi* Infections. *Sci. Rep.* 11, 19519. doi: 10.1038/s41598-021-98024-6

Handunnetti, S. M., Mendis, K. N., and David, P. H. (1987). Antigenic Variation of Cloned *Plasmodium Fragile* in its Natural Host *Macaca Sinica*. Sequential Appearance of Successive Variant Antigenic Types. *J. Exp. Med.* 165, 1269–1283. doi: 10.1084/jem.165.5.1269

Holtz, Y. (2018) *"RColorBrewer"*. Available at: https://www.r-graph-gallery.com/38-rcolorbrewers-palettes (Accessed March 2, 2022).

Hommel, M., David, P. H., and Oligino, L. D. (1983). Surface Alterations of Erythrocytes in *Plasmodium Falciparum* Malaria. Antigenic Variation, Antigenic Diversity, and the Role of the Spleen. *J. Exp. Med.* 157, 1137–1148. doi: 10.1084/jem.157.4.1137

Howard, R. J. (1984). Antigenic Variation of Bloodstage Malaria Parasites. *Philos. Trans. R Soc. Lond B Biol. Sci.* 307, 141–158. doi: 10.1098/rstb.1984.0115

Howard, R. J., and Barnwell, J. W. (1984a). The Detergent Solubility Properties of a Malarial (*Plasmodium Knowlesi*) Variant Antigen Expressed on the Surface of Infected Erythrocytes. *J. Cell Biochem.* 24, 297–306. doi: 10.1002/jcb.240240310

Howard, R. J., and Barnwell, J. W. (1984b). Solubilization and Immunoprecipitation of ^{125}I-Labelled Antigens From *Plasmodium Knowlesi* Schizont-Infected Erythrocytes Using non-Ionic, Anionic and Zwitterionic Detergents. *Parasitology* 88 (Pt 1), 27–36. doi: 10.1017/S0031182000054317

Howard, R. J., and Barnwell, J. W. (1985). Immunochemical Analysis of Surface Membrane Antigens on Erythrocytes Infected With non-Cloned SICA[+] or Cloned SICA[-] *Plasmodium Knowlesi*. *Parasitology* 91 (Pt 2), 245–261. doi: 10.1017/S0031182000057346

Howard, R. J., Barnwell, J. W., and Kao, V. (1983). Antigenic Variation of *Plasmodium Knowlesi* Malaria: Identification of the Variant Antigen on Infected Erythrocytes. *Proc. Natl. Acad. Sci. U.S.A.* 80, 4129–4133. doi: 10.1073/pnas.80.13.4129

Howard, R. J., Barnwell, J. W., Rock, E. P., Neequaye, J., Ofori-Adjei, D., Maloy, W. L., et al. (1988). Two Approximately 300 Kilodalton *Plasmodium Falciparum* Proteins at the Surface Membrane of Infected Erythrocytes. *Mol. Biochem. Parasitol.* 27, 207–223. doi: 10.1016/0166-6851(88)90040-0

Howard, R. J., Lyon, J. A., Diggs, C. L., Haynes, J. D., Leech, J. H., Barnwell, J. W., et al. (1984). Localization of the Major *Plasmodium Falciparum* Glycoprotein on the Surface of Mature Intraerythrocytic Trophozoites and Schizonts. *Mol. Biochem. Parasitol.* 11, 349–362. doi: 10.1016/0166-6851(84)90078-1

Imwong, M., Madmanee, W., Suwannasin, K., Kunasol, C., Peto, T. J., Tripura, R., et al. (2018). Asymptomatic Natural Human Infections With the Simian Malaria Parasites *Plasmodium Cynomolgi* and *Plasmodium Knowlesi*. *J. Infect. Dis.* 219, 695–702. doi: 10.1093/infdis/jiy519

Joice, R., Nilsson, S. K., Montgomery, J., Dankwa, S., Egan, E., Morahan, B., et al. (2014). *Plasmodium Falciparum* Transmission Stages Accumulate in the Human Bone Marrow. *Sci. Transl. Med.* 6, 244re245. doi: 10.1126/scitranslmed.3008882

Joyner, C. J., Brito, C. F. A., Saney, C. L., Cordy, R. J., Smith, M. L., Lapp, S. A., et al. (2019). Humoral Immunity Prevents Clinical Malaria During Plasmodium Relapses Without Eliminating Gametocytes. *PLoS Pathog.* 15, e1007974. doi: 10.1371/journal.ppat.1007974

Joyner, C. J.MaHPIC-Consortium, , Wood, J. S., Moreno, A., Garcia, A., Galinski, M. R. (2017). Case Report: Severe and Complicated Cynomolgi Malaria in a Rhesus Macaque Resulted in Similar Histopathological Changes as Those Seen in Human Malaria. *Am. J. Trop. Med. Hyg.* 97, 548–555. doi: 10.4269/ajtmh.16-0742

Joyner, C. J., Moreno, A., Meyer, E. V. S., Cabrera-Mora, M.MaHPIC-Consortium, , Kissinger, J. C., et al. (2016). *Plasmodium Cynomolgi* Infections in Rhesus Macaques Display Clinical and Parasitological Features Pertinent to Modelling Vivax Malaria Pathology and Relapse Infections. *Malar J.* 15, 1–18. doi: 10.1186/s12936-016-1480-6

Kho, S., Qotrunnada, L., Leonardo, L., Andries, B., Wardani, P. A. I., Fricot, A., et al. (2021). Hidden Biomass of Intact Malaria Parasites in the Human Spleen. *N Engl. J. Med.* 384, 2067–2069. doi: 10.1056/NEJMc2023884

Knisely, M. H., Stratman-Thomas, W. K., Eliot, T. S., and Bloch, E. H. (1945). Knowlesi Malaria in Monkeys; Microscopic Pathological Circulatory Physiology of Rhesus Monkeys During Acute *Plasmodium Knowlesi* Malaria. *J. Natl. Malar Soc.* 4, 285–300.

Knisely, M. H., Stratman-Thomas, W. K., Eliot, T. S., and Bloch, E. H. (1964). Knowlesi Malaria in Monkeys Ii: A First Step in the Separation of the

Mechanical Pathologic Circulatory Factors of One Sludge Disease From Possible Specific Toxic Factors of That Disease. *Angiology* 15, 411–416. doi: 10.1177/000331976401500905

Knowles, R., and Gupta, B. M. D. (1932). A Study of Monkey-Malaria, and Its Experimental Transmission to Man. *Ind. Med. Gaz.* 67, 301–320.

Korir, C. C., and Galinski, M. R. (2006). Proteomic Studies of *Plasmodium Knowlesi* SICA Variant Antigens Demonstrate Their Relationship With *P. Falciparum* EMP1. *Infect. Genet. Evol.* 6, 75–79. doi: 10.1016/j.meegid.2005.01.003

Lacerda, M. V., Fragoso, S. C., Alecrim, M. G., Alexandre, M. A., Magalhaes, B. M., Siqueira, A. M., et al. (2012). Postmortem Characterization of Patients With Clinical Diagnosis of *Plasmodium Vivax* Malaria: To What Extent Does This Parasite Kill? *Clin. Infect. Dis.* 55, e67–e74. doi: 10.1093/cid/cis615

Lapp, S. A., Korir-Morrison, C., Jiang, J., Bai, Y., Corredor, V., and Galinski, M. R. (2013). Spleen-Dependent Regulation of Antigenic Variation in Malaria Parasites: *Plasmodium Knowlesi SICAvar* Expression Profiles in Splenic and Asplenic Hosts. *PLoS One* 8, e78014. doi: 10.1371/journal.pone.0078014

Lapp, S. A., Mok, S., Zhu, L., Wu, H., Preiser, P. R., Bozdech, Z., et al. (2015). *Plasmodium Knowlesi* Gene Expression Differs in *Ex Vivo* Compared to *In Vitro* Blood-Stage Cultures. *Malar J.* 14, 1–16. doi: 10.1186/s12936-015-0612-8

Lapp, S. A., Geraldo, J. A., Chien, J. T., Ay, F., Pakala, S. B., Batugedara, G., et al. (2018). PacBio assembly of a *Plasmodium knowlesi* genome sequence with Hi-C correction and manual annotation of the SICAvar gene family. *Parasitology* 145:71–84. doi: 10.1017/S0031182017001329

Lawrence, C., and Olson, J. A. (1986). Birefringent Hemozoin Identifies Malaria. *Am. J. Clin. Pathol.* 86, 360–363. doi: 10.1093/ajcp/86.3.360

Leech, J. H., Barnwell, J. W., Miller, L. H., and Howard, R. J. (1984). Identification of a Strain-Specific Malarial Antigen Exposed on the Surface of *Plasmodium Falciparum*-Infected Erythrocytes. *J. Exp. Med.* 159, 1567–1575. doi: 10.1084/jem.159.6.1567

Lee, W. C., Russell, B., and Renia, L. (2019). Sticking for a Cause: The Falciparum Malaria Parasites Cytoadherence Paradigm. *Front. Immunol.* 10, 1444. doi: 10.3389/fimmu.2019.01444

Lee, W. C., Shahari, S., Nguee, S. Y. T., Lau, Y. L., and Renia, L. (2022). Cytoadherence Properties of *Plasmodium Knowlesi*-Infected Erythrocytes. *Front. Microbiol.* 12, 804417. doi: 10.3389/fmicb.2021.804417

Li, A., Russell, B., Renia, L., Lek-Uthai, U., Nosten, F., and Lim, C. T. (2010). High Density of 'Spiky' Excrescences Covering the Surface of an Erythrocyte Infected With *Plasmodium Malariae*. *Br. J. Haematol.* 151, 1. doi: 10.1111/j.1365-2141.2010.08261.x

Liu, B., Blanch, A. J., Namvar, A., Carmo, O., Tiash, S., Andrew, D., et al. (2019). Multi-Modal Analysis of *Plasmodium Knowlesi*-Infected Erythrocytes Reveals Large Invaginations, Swelling of the Host Cell and Rheological Defects. *Cell Microbiol.* 19, e13005. doi: 10.1111/cmi.13005

Makowski, D. (2019) *"Psycho. R Package"*. Available at: https://github.com/neuropsychology/psycho.R (Accessed March 2, 2022).

Matsumoto, Y., Matsuda, S., and Yoshida, Y. (1986). Ultrastructure of Human Erythrocytes Infected With *Plasmodium Ovale*. *Am. J. Trop. Med. Hyg.* 35, 697–703. doi: 10.4269/ajtmh.1986.35.697

Menezes, R. G., Pant, S., Kharoshah, M. A., Senthilkumaran, S., Arun, M., Nagesh, K. R., et al. (2012). Autopsy Discoveries of Death From Malaria. *Leg Med. (Tokyo)* 14, 111–115. doi: 10.1016/j.legalmed.2012.01.007

Miller, L. H., Ackerman, H. C., Su, X. Z., and Wellems, T. E. (2013). Malaria Biology and Disease Pathogenesis: Insights for New Treatments. *Nat. Med.* 19, 156–167. doi: 10.1038/nm.3073

Miller, L. H., Baruch, D. I., Marsh, K., and Doumbo, O. K. (2002). The Pathogenic Basis of Malaria. *Nature* 415, 673–679. doi: 10.1038/415673a

Miller, L. H., Fremount, H. N., and Luse, S. A. (1971a). Deep Vascular Schizogony of *Plasmodium Knowlesi* in *Macaca Mulatta*. Distribution in Organs and Ultrastructure of Parasitized Red Cells. *Am. J. Trop. Med. Hyg.* 20, 816–824. doi: 10.4269/ajtmh.1971.20.816

Miller, L. H., Usami, S., and Chien, S. (1971b). Alteration in the Rheologic Properties of *Plasmodium Knowlesi*-Infected Red Cells. A Possible Mechanism for Capillary Obstruction. *J. Clin. Invest.* 50, 1451–1455. doi: 10.1172/JCI106629

Milner, D. A. Jr. (2018). Malaria Pathogenesis. *Cold Spring Harb. Perspect. Med.* 8, 1–11. doi: 10.1101/cshperspect.a025569

Milner, D. A. Jr., Lee, J. J., Frantzreb, C., Whitten, R. O., Kamiza, S., Carr, R. A., et al. (2015). Quantitative Assessment of Multiorgan Sequestration of Parasites in Fatal Pediatric Cerebral Malaria. *J. Infect. Dis.* 212, 1317–1321. doi: 10.1093/infdis/jiv205

Milner, D. A. Jr., Valim, C., Carr, R. A., Chandak, P. B., Fosiko, N. G., Whitten, R., et al. (2013). A Histological Method for Quantifying *Plasmodium Falciparum* in the Brain in Fatal Paediatric Cerebral Malaria. *Malar J.* 12, 191. doi: 10.1186/1475-2875-12-191

Milner, D. A. Jr., Whitten, R. O., Kamiza, S., Carr, R., Liomba, G., Dzamalala, C., et al. (2014). The Systemic Pathology of Cerebral Malaria in African Children. *Front. Cell Infect. Microbiol.* 4, 104. doi: 10.3389/fcimb.2014.00104

Moreno, A., Cabrera-Mora, M., Garcia, A., Orkin, J., Strobert, E., Barnwell, J. W., et al. (2013). *Plasmodium Coatneyi* in Rhesus Macaques Replicates the Multisystemic Dysfunction of Severe Malaria in Humans. *Infect. Imm* 81, 1889–1904. doi: 10.1128/IAI.00027-13

Nakano, Y., Fujioka, H., Luc, K. D., Rabbege, J. R., Todd, G. D., Collins, W. E., et al. (1996). A Correlation of the Sequestration Rate of *Plasmodium Coatneyi*-Infected Erythrocytes in Cerebral and Subcutaneous Tissues of a Rhesus Monkey. *Am. J. Trop. Med. Hyg* 55, 311–314. doi: 10.4269/ajtmh.1996.55.311

Palesch, D., Bosinger, S. E., Tharp, G. K., Vanderford, T. H., Paiardini, M., Chahroudi, A., et al. (2018). Sooty Mangabey Genome Sequence Provides Insight Into AIDS Resistance in a Natural SIV Host. *Nature* 553, 77–81. doi: 10.1038/nature25140

Percie Du Sert, N., Hurst, V., Ahluwalia, A., Alam, S., Avey, M. T., Baker, M., et al. (2020). The ARRIVE Guidelines 2.0: Updated Guidelines for Reporting Animal Research. *PLoS Biol.* 18, e3000410. doi: 10.1111/bph.15193

Perkins, D. J., Were, T., Davenport, G. C., Kempaiah, P., Hittner, J. B., and Ong'echa, J. M. (2011). Severe Malarial Anemia: Innate Immunity and Pathogenesis. *Int. J. Biol. Sci.* 7, 1427–1442. doi: 10.7150/ijbs.7.1427

Peterson, M. S., Joyner, C. J., Brady, J. A., Wood, J. S., Cabrera-Mora, M., Saney, C. L., et al. (2021). Clinical Recovery of *Macaca Fascicularis* Infected With *Plasmodium Knowlesi*. *Malar J.* 20, 486. doi: 10.1186/s12936-021-03925-6

Peterson, M. S., Joyner, C. J., Cordy, R. J., Salinas, J. L., Machiah, D., Lapp, S. A., et al. (2019). *Plasmodium Vivax* Parasite Load is Associated With Histopathology in *Saimiri Boliviensis* With Findings Comparable to P. Vivax Pathogenesis in Humans. *Open Forum Infect. Dis.* 6, 1–9. doi: 10.1093/ofid/ofz021

Rajahram, G. S., Cooper, D. J., William, T., Grigg, M. J., Anstey, N. M., and Barber, B. E. (2019). Deaths From *Plasmodium Knowlesi* Malaria: Case Series and Systematic Review. *Clin. Infect. Dis.* 69, 1703–1711. doi: 10.1093/cid/ciz011

R-Core-Team (2021) *R: A Language and Environment for Statistical Computing* (Vienna, Austria). Available at: https://www.R-project.org/ (Accessed March 2, 2022).

Romero, A., Matos, C., Gonzalez, M. M., Nunez, N., Bermudez, L., and De Castro, G. (1993). [Changes in Gastric Mucosa in Acute Malaria]. *G E N* 47, 123–128.

Rutledge, G. G., Bohme, U., Sanders, M., Reid, A. J., Cotton, J. A., Maiga-Ascofare, O., et al. (2017). *Plasmodium Malariae* and *P. Ovale* Genomes Provide Insights Into Malaria Parasite Evolution. *Nature* 542, 101–104. doi: 10.1038/nature21038

Seydel, K. B., Milner, D. A. Jr., Kamiza, S. B., Molyneux, M. E., and Taylor, T. E. (2006). The Distribution and Intensity of Parasite Sequestration in Comatose Malawian Children. *J. Infect. Dis.* 194, 205–208. doi: 10.1086/505078

Sheehan, D. C., and Hrapchak, B. B. (1980). *Theory and Practice of Histotechnology* (St Louis, MO: CV Mosby).

Singh, B., Kim Sung, L., Matusop, A., Radhakrishnan, A., Shamsul, S. S., Cox-Singh, J., et al. (2004). A Large Focus of Naturally Acquired *Plasmodium Knowlesi* Infections in Human Beings. *Lancet* 363, 1017–1024. doi: 10.1016/S0140-6736(04)15836-4

Smith, J. D. (2014). The Role of PfEMP1 Adhesion Domain Classification in *Plasmodium Falciparum* Pathogenesis Research. *Mol. Biochem. Parasitol.* 195, 82–87. doi: 10.1016/j.molbiopara.2014.07.006

Smith, J. D., Chitnis, C. E., Craig, A. G., Roberts, D. J., Hudson-Taylor, D. E., Peterson, D. S., et al. (1995). Switches in Expression of *Plasmodium Falciparum Var* Genes Correlate With Changes in Antigenic and Cytoadherent Phenotypes of Infected Erythrocytes. *Cell* 82, 101–110. doi: 10.1016/0092-8674(95)90056-X

Smith, J. D., Rowe, J. A., Higgins, M. K., and Lavstsen, T. (2013). Malaria's Deadly Grip: Cytoadhesion of *Plasmodium Falciparum*-Infected Erythrocytes. *Cell Microbiol.* 15, 1976–1983. doi: 10.1111/cmi.12183

Spangler, W. L., Gribble, D., Abildgaard, C., and Harrison, J. (1978). *Plasmodium Knowlesi* Malaria in the Rhesus Monkey. *Vet. Pathol.* 15, 83–91. doi: 10.1177/030098587801500110

Spitz, S. (1946). The Pathology of Acute Falciparum Malaria. *Mil Surg.* 99, 555–572. doi: 10.1093/milmed/99.5.555

Su, X. Z., Heatwole, V. M., Wertheimer, S. P., Guinet, F., Herrfeldt, J. A., Peterson, D. S., et al. (1995). The Large Diverse Gene Family *Var* Encodes Proteins Involved in Cytoadherence and Antigenic Variation of *Plasmodium Falciparum*-Infected Erythrocytes. *Cell* 82, 89–100. doi: 10.1016/0092-8674(95)90055-1

Tachibana, S., Sullivan, S. A., Kawai, S., Nakamura, S., Kim, H. R., Goto, N., et al. (2012). *Plasmodium Cynomolgi* Genome Sequences Provide Insight Into *Plasmodium Vivax* and the Monkey Malaria Clade. *Nat. Genet.* 44, 1051–1055. doi: 10.1038/ng.2375

Taliaferro, W. H., and Taliaferro, L. G. (1949). Asexual Reproduction of *Plasmodium Knowlesi* in Rhesus Monkeys. *J. Infect. Dis.* 85, 107–125. doi: 10.1093/infdis/85.2.107

Tang, Y., Joyner, C. J., Cabrera-Mora, M., Lapp, S. A., Nural, M. V., Pakala, S. B., et al. (2017). Integrative Analysis Associates Monocytes With Insufficient Erythropoiesis During Acute *Plasmodium Cynomolgi* Malaria in Rhesus Macaques. *Malar J.* 16, 1–16. doi: 10.1186/s12936-017-2029-z

Tang, Y., Joyner, C. J., Cordy, R. J.MaHPIC-Consortium, , Galinski, M. R., Lamb, T. J., et al. (2019). "Multi-Omics Integrative Analysis of Acute and Relapsing Malaria in a non-Human Primate Model of P. Vivax Infection," in *BioRxiv* (New York: Cold Spring Harbor Laboratory, Laurel Hollow). doi: 10.1101/564195v1

Thawani, N., Tam, M., Bellemare, M. J., Bohle, D. S., Olivier, M., De Souza, J. B., et al. (2014). Plasmodium Products Contribute to Severe Malarial Anemia by Inhibiting Erythropoietin-Induced Proliferation of Erythroid Precursors. *J. Infect. Dis.* 209, 140–149. doi: 10.1093/infdis/jit417

Wahlgren, M., Goel, S., and Akhouri, R. R. (2017). Variant Surface Antigens of *Plasmodium Falciparum* and Their Roles in Severe Malaria. *Nat. Rev. Microbiol.* 15, 479–491. doi: 10.1038/nrmicro.2017.47

Wassmer, S. C., Taylor, T. E., Rathod, P. K., Mishra, S. K., Mohanty, S., Arevalo-Herrera, M., et al. (2015). Investigating the Pathogenesis of Severe Malaria: A Multidisciplinary and Cross-Geographical Approach. *Am. J. Trop. Med. Hyg* 93, 42–56. doi: 10.4269/ajtmh.14-0841

Wickham, H., Chang, W., Henry, L., Pederson, T. L., Takahashi, K., Wilke, C., et al. (2019) *"Ggplot2. R Package "*. Available at: https://github.com/tidyverse/ggplot2http://ggplot2.tidyverse.org.

William, T., Menon, J., Rajahram, G., Chan, L., Ma, G., Donaldson, S., et al. (2011). Severe *Plasmodium Knowlesi* Malaria in a Tertiary Care Hospital, Sabah, Malaysia. *Emerg. Infect. Dis.* 17, 1248–1255. doi: 10.3201/eid1707.101017

World Health Organization (2021) *World Malaria Report 2021*. Available at: https://www.who.int/teams/global-malaria-programme/reports/world-malaria-report-2021 (Accessed March 2, 2022).

Conflict of Interest: The authors declare that the research was conducted in the absence of any commercial or financial relationships that could be construed as a potential conflict of interest.

Publisher's Note: All claims expressed in this article are solely those of the authors and do not necessarily represent those of their affiliated organizations, or those of the publisher, the editors and the reviewers. Any product that may be evaluated in this article, or claim that may be made by its manufacturer, is not guaranteed or endorsed by the publisher.

†*Present addresses: Mariko S. Peterson, Emory University School of Medicine, Atlanta, GA, United States; Chester J. Joyner, Center for Vaccines and Immunology, Department of Infectious Diseases, College of Veterinary Medicine, University of Georgia, Athens GA, United States; Jessica A. Brady, Eli Lilly and Company, Indianapolis, IN, United States; Monica Cabrera-Mora, Emory University School of Medicine, Atlanta, GA, United States; Celia L. Saney, Center for Vaccines and Immunology, Department of Infectious Diseases, College of Veterinary Medicine, University of Georgia, Athens, GA, United States; Luis L. Fonseca, Department of Medicine, University of Florida, Gainesville, Florida, United States; Stephanie R. Soderberg, Thermo Fisher Scientific, South San Francisco, CA, United States; Allison Hankus, The Mitre Corporation, Atlanta, GA, United States; Ebru Karpuzoglu, Department of Endocrinology, Atlanta VA Medical Center, Decatur, GA, United States; Jeremy D. DeBarry, Center for Topical and Emerging Global Diseases, University of Georgia, Athens, GA, United States; Sanjeev Gumber, Boehringer Ingelheim Animal Health USA Inc., Athens, GA, United States; Juan B. Gutierrez, Department of Mathematics, University of Texas at San Antonio, San Antonio, TX, United States; Regina Joice Cordy, Department of Biology, Wake Forest University, Winston-Salem, NC, United States*

frontiers | Frontiers in Cellular and Infection Microbiology

REVIEW
published: 08 July 2022
doi: 10.3389/fcimb.2022.945924

Plasmodium 6-Cysteine Proteins: Functional Diversity, Transmission-Blocking Antibodies and Structural Scaffolds

Frankie M. T. Lyons[1,2], *Mikha Gabriela*[1,2], *Wai-Hong Tham*[1,2] *and Melanie H. Dietrich*[1,2]*

[1] The Walter and Eliza Hall Institute of Medical Research, Infectious Diseases and Immune Defence Division, Parkville, VIC, Australia, [2] Department of Medical Biology, The University of Melbourne, Melbourne, VIC, Australia

The 6-cysteine protein family is one of the most abundant surface antigens that are expressed throughout the *Plasmodium falciparum* life cycle. Many members of the 6-cysteine family have critical roles in parasite development across the life cycle in parasite transmission, evasion of the host immune response and host cell invasion. The common feature of the family is the 6-cysteine domain, also referred to as s48/45 domain, which is conserved across Aconoidasida. This review summarizes the current approaches for recombinant expression for 6-cysteine proteins, monoclonal antibodies against 6-cysteine proteins that block transmission and the growing collection of crystal structures that provide insights into the functional domains of this protein family.

Keywords: monoclonal antibodies, 6-cysteine proteins, plasmodium, recombinant protein, structural biology, transmission-blocking, malaria

OPEN ACCESS

Edited by:
Alister Craig,
Liverpool School of Tropical Medicine, United Kingdom

Reviewed by:
Evelien M. Bunnik,
The University of Texas Health Science Center at San Antonio, United States
Michael Theisen,
Statens Serum Institut (SSI), Denmark

***Correspondence:**
Melanie H. Dietrich
dietrich.m@wehi.edu.au

Specialty section:
This article was submitted to Parasite and Host, a section of the journal Frontiers in Cellular and Infection Microbiology

Received: *17 May 2022*
Accepted: *22 June 2022*
Published: *08 July 2022*

Citation:
Lyons FMT, Gabriela M, Tham W-H and Dietrich MH (2022) Plasmodium *6-Cysteine Proteins: Functional Diversity, Transmission-Blocking Antibodies and Structural Scaffolds. Front. Cell. Infect. Microbiol. 12:945924. doi: 10.3389/fcimb.2022.945924*

INTRODUCTION

Malaria and Disease Burden

Malaria is a parasitic disease caused by the *Plasmodium* genus. Six species of malaria parasite are responsible for human disease, namely *P. falciparum*, *P. vivax*, *P. ovale curtisi, P. ovale wallikeri*, *P. malariae* and *P. knowlesi*, with *P. falciparum* responsible for most deaths. The global burden of malaria is significant, with over half of the world's population at risk of infection. In 2020, there was an estimated 241 million cases and 627,000 deaths, with over three quarters of deaths occurring in children under five (WHO, 2021).

Having steadily declined over the last 20 years, malaria deaths increased between 2019 and 2020, reflecting the impact of the COVID-19 pandemic on services in endemic regions (WHO, 2021). In addition, resistance to anti-malarial drugs is a growing issue, with recent reports of resistance to first-line drugs in Africa (Uwimana et al., 2020; Balikagala et al., 2021; Uwimana et al., 2021), the region that accounts for approximately 95% of cases and 96% of deaths (WHO, 2021). In 2021, the WHO recommended the RTS,S/AS01 vaccine for children at risk of malaria. While this has potential for positive public health impacts, the vaccine shows a moderate efficacy of <40% (RTS S Clinical Trials Partnership, 2015). These challenges to effective malaria treatment and prevention highlight the urgency of developing effective vaccines and novel drugs to progress on-going malaria elimination programs.

There has been considerable interest in 6-cysteine proteins, a family of surface-exposed and conserved *Plasmodium* proteins which are expressed throughout the parasite life cycle (**Figure 1A**) as new vaccine candidates or targets for antibody therapies that stop malaria transmission and infection.

The 6-Cysteine Family

The first member of the 6-cysteine family to be characterized was Pfs230, a protein originally thought to be 230 kDa in size and notable for its ability to elicit antibodies that block transmission of malaria to mosquitoes (Quakyi et al., 1987). Sequencing of Pfs230 led to the identification of a cysteine-rich motif shared by Pf12 (Williamson et al., 1993) and with the increasing availability of *P. falciparum* genome sequences, this motif was subsequently identified in 14 P. *falciparum* proteins, namely Pf36, Pf52, PfLISP2, PfB9, Pf12, Pf12p, Pf41, Pf38, Pf92, Pfs48/45, Pfs230, Pfs230p, Pfs47 and PfPSOP12 (**Figure 1A**) (Templeton and Kaslow, 1999; Kappe et al., 2001; Thompson et al., 2001; Gardner et al., 2002; Gerloff et al., 2005; Arredondo et al., 2012; Orito et al., 2013; Annoura et al., 2014). These proteins are highly conserved and most have orthologues across *Plasmodium* species (Arredondo and Kappe, 2017).

The common feature of the family is the 6-cysteine domain, also referred to as the s48/45 domain (Arredondo et al., 2012; Annoura et al., 2014), which is conserved across Aconoidasida. For the purpose of this review, we will refer to this domain as the 6-cysteine domain. It is related to the SAG1-related sequence (SRS) domain that characterizes the SRS superfamily of *Toxoplasma* proteins (Arredondo et al., 2012), and both domains are likely derived from an ephrin-like host protein acquired by a common ancestor. The 6-cysteine domain folds into a β-sandwich and has up to six cysteines involved in stabilization through disulfide bonding (Templeton and Kaslow, 1999; Gerloff et al., 2005; Arredondo et al., 2012). All 6-cysteine family members have a signal sequence and between one and 14 6-cysteine domains (**Figure 1B**). In addition, some members have putative or confirmed GPI-anchors, repetitive regions, or an N-terminal β-propeller domain (**Figure 1B**).

The 6-Cysteine Proteins in *P. falciparum*

Members of the 6-cysteine family are present across the parasite life cycle (**Figure 1A**), fulfilling many critical roles in parasite development. The life cycle of *P. falciparum* begins when an infected female *Anopheles* mosquito takes a blood meal from a human. Sporozoites are injected from the mosquito's salivary glands into the skin and travel through the bloodstream to the liver. Within the liver, sporozoites mature into liver schizonts, which in turn rupture and release merozoites into the bloodstream. Merozoites invade red blood cells to initiate the blood stage cycle. Within 48 hours, the malaria parasite replicates into 16-36 new merozoites that proceed to invade more red blood cells. Within the bloodstream a subset of parasites differentiates to form male and female gametocytes. When a female *Anopheles* mosquito takes a blood meal, gametocytes are taken up into the mosquito midgut, where male microgametes and female macrogametes egress from red blood cells. Fertilization occurs between microgametes and macrogametes, forming zygotes. Zygotes elongate to form ookinetes, which then develop into oocysts on the mosquito midgut. Oocysts rupture and release sporozoites, which travel to the mosquito's salivary glands, ready to infect another human during the next blood meal.

We will provide an overview of the 6-cysteine protein family on their functional diversity, respective recombinant protein expression, transmission blocking capability and structural scaffold. Their cellular localization and orthologues have been reviewed in detail previously (Arredondo and Kappe, 2017).

Pre-Erythrocytic Stages

Pf36, Pf52, PfLISP2 and PfB9 are expressed during the liver stages. Pf36 and Pf52 have two 6-cysteine domains, but only Pf52 contains a predicted GPI anchor. These two proteins are localized to the micronemes of salivary sporozoites and are important for parasitophorous vacuole membrane formation within hepatocytes (Arredondo et al., 2018). Pf36 is attached to the parasite membrane where it binds host receptors EphA2 (Kaushansky et al., 2015), CD81 and SR-B1 (Manzoni et al., 2017) to facilitate sporozoite invasion, although the exact mechanisms by which it is anchored to the membrane or facilitates invasion have not yet been elucidated. In *P. yoelii*, P36 forms a complex with GPI-anchored P52 and both proteins are likely involved in the formation of the liver stage parasitophorous vacuole (Arredondo et al., 2018). A genetically attenuated parasite (GAP) vaccine with deletions of Pf36, Pf52 and another liver stage antigen SAP1 has undergone a Phase I clinical trial (NCT03168854), and was able to elicit antibodies that inhibited sporozoite invasion and traversal (Kublin et al., 2017).

PfLISP2, also known as Sequestrin, has two 6-cysteine domains (Annoura et al., 2014). It is expressed in the mid to late liver stages and can be used as a marker of liver stage development (Gupta et al., 2019). PfLISP2 is exported into the host hepatocyte (Orito et al., 2013). The precise function of PfLISP2 is not clear but it may have a dual role in schizogony and egress from the liver as well as immune evasion. A GAP vaccine including a PfLISP2 deletion has been shown to protect mice from malaria infection (Vaughan et al., 2018).

PfB9 has three 6-cysteine domains and a predicted GPI anchor (**Figure 1B**). It is predicted to localize to the plasma membrane of liver stage parasites (Annoura et al., 2014) and the micronemes of sporozoites in *P. berghei* (Fernandes et al., 2021). The function of PfB9 has not been precisely defined, but knockout parasites display growth arrest in the liver and a lack of parasitophorous vacuole markers, indicating a critical role for PfB9 in liver-stage development and parasitophorous vacuole integrity (Annoura et al., 2014). A Phase I/2a trial (NCT03163121) of a GAP vaccine including a PfB9 deletion showed the vaccine to be safe and immunogenic, although the strength of protective efficacy is yet to be established (Roestenberg et al., 2020).

Erythrocytic Stages

Pf12, Pf12p, Pf41, Pf92 and Pf38 are expressed during the blood stage cycle. Pf12 is the structural archetype of the 6-cysteine family as well

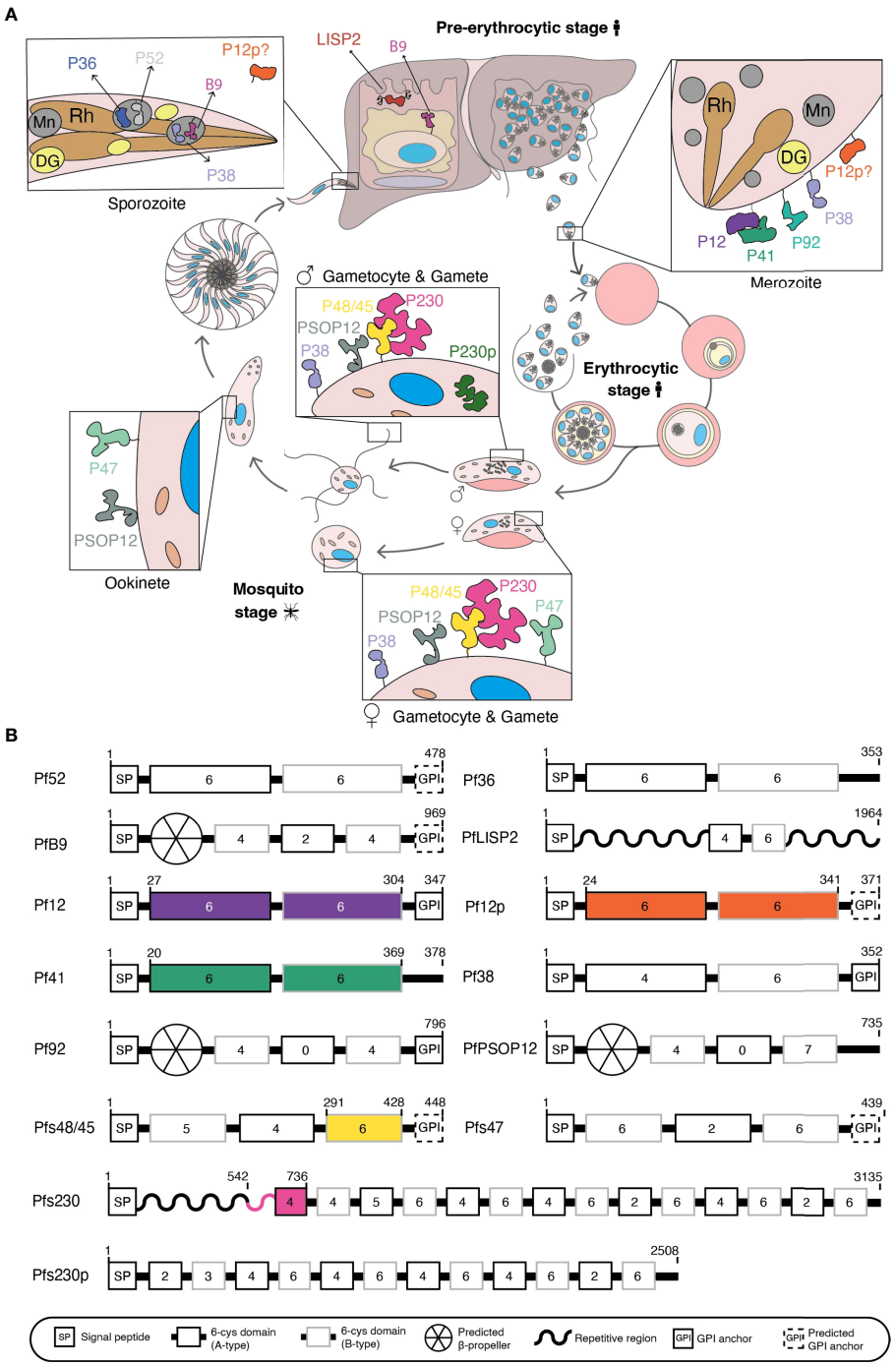

FIGURE 1 | **(A)** Schematic of *Plasmodium falciparum* life cycle. 6-cysteine proteins are expressed in the pre-erythrocytic and erythrocytic stages (merozoite) of the human host and the mosquito stages (gametocyte, gametes, zygote, ookinete, and sporozoite). Mn, microneme; Rh, rhoptry; DG, dense granule. **(B)** Domain architecture of the 14 P. *falciparum* 6-cysteine proteins. The illustration shows the signal peptide (SP), the number of cysteines within each domain (number in the boxes), A-type (black box), B-type (grey box) 6-cysteine domains, validated or putative GPI-anchors, and other specific features (i.e. repetitive/non-structured region or putative β-propeller domain). Colored regions represent the part(s) of the protein for which crystal structures are available.

as being its smallest member (Gerloff et al., 2005). It is comprised of two 6-cysteine domains and a GPI anchor (Tonkin et al., 2013). Pf12 is expressed on the surface of schizonts and merozoites (Taechalertpaisarn et al., 2012; Tonkin et al., 2013). Pf12 forms a heterodimer with Pf41 (Taechalertpaisarn et al., 2012; Crosnier et al., 2013; Tonkin et al., 2013; Parker et al., 2015; Dietrich et al., 2022), another blood stage 6-cysteine protein with similar localization patterns (Sanders et al., 2005). Pf41 has two 6-cysteine domains and no GPI anchor, likely being tethered to the membrane *via* its interaction with Pf12. Deletions of these genes in *P. falciparum* produced no observable phenotype in blood stage parasites (Taechalertpaisarn et al., 2012) and thus the functions of these proteins remain unknown. Seroprevalence for anti-Pf12 and -Pf41 antibodies is high in malaria-exposed individuals, although this does not always correlate strongly with protection against clinical disease (Richards et al., 2013; Osier et al., 2014; Kana et al., 2018; Kana et al., 2019).

Pf12p, a paralog of Pf12, has two 6-cysteine domains and a GPI anchor. The recently solved crystal structure of Pf12p revealed its structural similarity to Pf12, despite which it does not interact with Pf41 (Dietrich et al., 2021). Transcription of P12p has been reported in the blood stages (Bozdech et al., 2003; Lopez-Barragan et al., 2011; Toenhake et al., 2018; Tang et al., 2020) and expression has been detected in sporozoites (Lasonder et al., 2008; Lindner et al., 2013) but its localization, function and precise expression patterns are unknown.

Pf92 has three 6-cysteine domains and a confirmed GPI anchor (**Figure 1B**). It is expressed in blood stage schizonts and merozoites, where it is localized to the parasite surface (Sanders et al., 2005; Gilson et al., 2006). Pf92 recruits Factor H, a host complement regulator, to the surface of merozoites as an immune evasion strategy to prevent complement-mediated lysis (Kennedy et al., 2016). Pf92 is the only member of the 6-cysteine proteins without a known orthologue in rodent *Plasmodium* species.

Pf38 has two 6-cysteine domains and a confirmed GPI anchor (Sanders et al., 2005; Gilson et al., 2006). In *P. falciparum* it has been detected on the surface (Feller et al., 2013) and apical end (Sanders et al., 2005) of the asexual blood stages, as well as on gametocytes, gametes and zygotes (Feller et al., 2013; Arredondo and Kappe, 2017). In *P. yoelii* P38 has also been localized to the micronemes of sporozoites (Harupa, 2015). The function of this protein has yet to be fully elucidated. In *P. berghei* and *P. yoelii*, P38 gene deletions have no obvious effect on asexual or sexual parasite development (van Dijk et al., 2010). However, in *P. falciparum*, Pf38-derived peptides have an inhibitory effect on red blood cell invasion (Garcia et al., 2009) and polyclonal anti-Pf38 antibodies are capable of inhibiting blood-stage growth and zygote formation (Feller et al., 2013).

Mosquito Stages

Pfs48/45, Pfs230, Pfs47, Pfs230p and PfPSOP12 are expressed during the sexual stages. Pfs48/45 has three 6-cysteine domains and a putative GPI-anchor and is localized to the surface of gametocytes and gametes (Vermeulen et al., 1986; Kocken et al., 1993). Knockout studies in *P. falciparum* and *P. berghei* implicate a role in male fertility, with P48/45-deficient males unable to attach to female gametes, leading to reduced ookinete production (van Dijk et al., 2001; van Dijk et al., 2010; Ramiro et al., 2015). It remains unclear, however, whether this effect is due to the loss of Pfs48/45 itself or due to an absence of Pfs230 from the parasite surface, which is anchored to the membrane by its interaction with Pfs48/45 (Eksi et al., 2006). Recognition of Pfs48/45 by human sera correlates with the ability of sera to block parasite transmission (Graves et al., 1998; Mulder et al., 1999; van der Kolk et al., 2006; Bousema et al., 2010; Ouédraogo et al., 2011; Stone et al., 2018) and antibodies against Pfs48/45 have transmission-blocking activity (Targett, 1988; Targett et al., 1990; Roeffen et al., 2001; Outchkourov et al., 2008; Lennartz et al., 2018; Stone et al., 2018). Pfs48/45-based transmission-blocking vaccines are under development against both *P. falciparum* (Theisen et al., 2017; Mistarz et al., 2017; Singh et al., 2017a; Singh et al., 2017b; Mamedov et al., 2019; Lee et al., 2020; Singh et al., 2021a) and *P. vivax* (Arevalo-Herrera et al., 2015; Tachibana et al., 2015; Cao et al., 2016; Arevalo-Herrera et al., 2021; Arevalo-Herrera et al., 2022).

Pfs230 is the largest member of the 6-cysteine family at >300 kDa and with 14 6-cysteine domains. It is expressed from stage II gametocytes until the end of fertilization and is localized to the surface of gametocytes and gametes (Rener et al., 1983; Vermeulen et al., 1985; van Dijk et al., 2010), likely *via* its interaction with GPI-anchored Pfs48/45 (Kumar, 1987; Williamson et al., 1996). In addition to this interaction, it is suggested that Pfs230 forms a multimeric protein complex involving other sexual stage antigens, Pfs25 and PfCCp family proteins (Simon et al., 2016). Pfs230 undergoes two independent N-terminal cleavage events during gametogenesis, resulting in 300 and 307 kDa versions of the protein (Williamson et al., 1996; Brooks and Williamson, 2000). Knockout studies show that Pfs230 is critical for male fertility, with Pfs230-deficient males unable to bind to red blood cells and establish exflagellation centers in *P. falciparum* (Eksi et al., 2006). In *P. berghei*, Pbs230-deficient males fail to recognize female gametes (van Dijk et al., 2010). Pfs230 has long been considered as a potential transmission-blocking malaria vaccine candidate (Quakyi et al., 1987) and seropositivity of human sera against Pfs230 is a predictor for transmission-blocking immunity (Premawansa et al., 1994; Graves et al., 1998; Mulder et al., 1999; van der Kolk et al., 2006; Bousema et al., 2010; Ouédraogo et al., 2011; Stone et al., 2018). As such, a number of recombinant N-terminal fragments of Pfs230 are under investigation as vaccine candidates (Farrance et al., 2011; Tachibana et al., 2011; MacDonald et al., 2016; Lee et al., 2017; Chan et al., 2019; Wetzel et al., 2019; Miura et al., 2019; Lee et al., 2019a; Lee et al., 2019b; Coelho et al., 2019; Huang et al., 2020; Healy et al., 2021; Coelho et al., 2021) in addition to a Pfs230-Pfs48/45 chimera (Singh et al., 2019; Singh et al., 2020; Singh et al., 2021b).

Pfs47, the paralog of Pfs48/45, is comprised of three 6-cysteine domains and a predicted GPI anchor. It is localized to the surface of female gametes and gametocytes (van Schaijk et al., 2006) and ookinetes (Molina-Cruz et al., 2013). Pfs47 binds to a mosquito receptor protein, termed P47Rec, through which it is thought to mediate evasion of the mosquito complement-like system (Molina-Cruz et al., 2013; Ramphul et al., 2015; Molina-

Cruz et al., 2020). In *P. berghei*, Pbs47 serves a dual function in gamete fertility and evasion of the mosquito complement-like response (van Dijk et al., 2010; Ukegbu et al., 2017). A number of Pfs47-based vaccine candidates have been developed and shown to elicit transmission-blocking antibodies against *P. falciparum* (Canepa et al., 2018; Yenkoidiok-Douti et al., 2019; Yenkoidiok-Douti et al., 2021) and *P. berghei* (Yenkoidiok-Douti et al., 2020).

Pfs230p, the paralog of Pfs230, contains 12 6-cysteine domains. Pfs230p is expressed only in male gametocytes (stages IV-V) and is the only 6-cysteine protein known to be localized to the cytoplasm in *P. falciparum* (Eksi and Williamson, 2002; van Dijk et al., 2010; Schneider et al., 2015). A critical role for P230p in ookinete formation has been described in *P. falciparum*, although this function is not observed in rodent malaria parasites (van Dijk et al., 2010; Marin-Mogollon et al., 2018).

PfPSOP12 has three predicted 6-cysteine domains (**Figure 1B**). It is expressed in gametocytes, ookinetes and oocyts and is localized to the surface of the parasite (Sala et al., 2015), although this protein has no predicted GPI anchor (**Figure 1B**). Knockout studies in *P. berghei* have demonstrated a mild effect on oocyst production and anti-PbPSOP12 antibodies have transmission-blocking activity (Ecker et al., 2008; Sala et al., 2015), both suggesting a potential role in fertility. In contrast, the function of *P. falciparum* PfPSOP12 has yet to be characterized.

The 6-cysteine proteins act throughout the malaria life and some have critical roles in parasite development. However, the precise function, structure and transmission-blocking potential of many members have not been fully elucidated. Below we describe methods that have been used to produce and characterize this protein family thus far and discuss methods that could be used to further understand the interactions of the 6-cysteine proteins and target them effectively.

EXPRESSION OF RECOMBINANT 6-CYSTEINE PROTEINS

Recombinant protein expression of properly folded 6-cysteine proteins is important for the structural and biochemical characterization of this protein family and the generation of specific antibodies. However, there are significant challenges for expressing sufficient yields of correctly folded protein. In prokaryotic expression systems, additional components such as conjugation to a fusion partner or co-expression of folding catalysts are often required for proper disulfide bonding of the 6-cysteine domain. In eukaryotic systems, glycans on *Plasmodium* proteins are truncated compared to those of other eukaryotes (Bushkin et al., 2010; Swearingen et al., 2016) and incorrect glycosylation can affect the conformation of proteins expressed in these systems. Enzymatic deglycosylation or mutation of glycosylation sites can be employed to prevent erroneous glycosylation, although glycosylation patterns may still differ to the native protein. Due to the AT richness of the *Plasmodium* genome, codon optimization is often required for optimum yields between the different recombinant expression systems. Below and in **Supplementary Table 1** we summarize the various protein expression systems used to produce recombinant 6-cysteine proteins and the strategies employed to induce correct conformation.

Prokaryotic Systems for the Expression of 6-Cysteine Proteins

Escherichia coli Expression

Initial attempts to express recombinant 6-cysteine proteins were carried out in *E. coli* (Kocken et al., 1993; Williamson et al., 1993; Riley et al., 1995; Williamson et al., 1995). However, correct disulfide bond formation can be difficult to achieve in this system as protein production occurs largely in the cytoplasm, while disulfide bond formation is carried out by oxidoreductases in the periplasm. For this reason, early attempts to produce full length Pfs48/45 resulted in incorrectly folded protein unable to elicit transmission-blocking antibodies in mice or rabbits (Milek et al., 1998).

Solubility tags such as glutathione-*S*-transferase (GST) or maltose binding protein (MBP) fused to the recombinant protein can assist folding. MBP was used for the early expression of Pfs230 fragments (Williamson et al., 1993; Riley et al., 1995; Williamson et al., 1995; Milek et al., 1998; Bustamante et al., 2000) and GST for Pfs48/45 fragments (Kocken et al., 1993; Milek et al., 1998; Outchkourov et al., 2007). Co-expression of an MBP-tagged Pfs48/45 fragment (10C, aa 159-428) with periplasmic folding catalysts produced a properly folded protein with an increased yield relative to the GST fusion of the same fragment (Outchkourov et al., 2007; Outchkourov et al., 2008). The full ectodomain and single domain constructs of Pfs47 have been expressed as a fusion to *E. coli* protein thioredoxin. These proteins were used to identify domain 2 (D2) as the region of Pfs47 targeted by transmission-blocking antibodies (Canepa et al., 2018) and to elucidate the essential function of Pbs47 (Ukegbu et al., 2017). A fusion of the Pvs48/45 ectodomain to thioredoxin was recognized by sera from naturally infected individuals and elicited transmission-blocking antibodies (Arevalo-Herrera et al., 2015). A fusion of Pfs48/45 10C with the granule lattice protein of *Tetrahymena thermophila* similarly yielded a correctly folded protein that elicited transmission-blocking antibodies (Agrawal et al., 2019).

Other strategies to encourage correct folding without reliance on a fusion partner include the use of *E. coli* strains that enhance disulfide bond formation in the cytoplasm, which was used to investigate the immunogenicity and immunoreactivity of Pvs48/45 (Arevalo-Herrera et al., 2015; Arevalo-Herrera et al., 2021; Arevalo-Herrera et al., 2022). Correctly folded full-length Pfs48/45 has also been reported without a fusion partner through codon harmonization (Chowdhury et al., 2009).

Despite the challenges, *E. coli* remains a popular expression system and has recently been used for pre-clinical evaluation of vaccine candidates Pfs47 (Yenkoidiok-Douti et al., 2019; Yenkoidiok-Douti et al., 2021), Pbs47 (Yenkoidiok-Douti et al., 2020) and Pfs48/45 (Pritsch et al., 2016) in animal immunization studies. The system has been used to produce

Pf12 D2 for structural characterization (Arredondo et al., 2012) and the full ectodomains of Pfs48/45 and Pvs48/45 to demonstrate the cross-reactivity of immune responses to these antigens (Cao et al., 2016).

Lactococcus lactis Expression

The *L. lactis* system has been used to express Pf12, Pf38 and Pf41 (Singh et al., 2018; Kana et al., 2018) in addition to Pfs48/45- and Pfs230-based vaccine candidates. This system can be optimized to produce correctly folded protein with yields of 25 mg/L, which is sufficient for use in clinical studies (Singhet al., 2017a; Singh et al., 2021).

Vaccine candidates based on a fusion of a P48/45 fragment with the R0 region of glutamate-rich protein (GLURP) have been expressed in *L. lactis*. Fusion of the Pfs48/45 10C fragment to R0 yielded a correctly folded protein that elicited transmission-blocking antibodies (Theisen et al., 2014; Roeffen et al., 2015) and it is hypothesized that fusion to R0 stabilizes Pfs48/45 and enhances expression. A vaccine candidate comprised of R0 and the Pfs48/45 6C fragment (aa 291-428) is also capable of eliciting transmission-blocking antibodies (Singh et al., 2015; Singh et al., 2017a), and protocols have been developed for expression of this construct as a virus-like particle (VLP) (S.K. Singh et al., 2017b) and under cGMP settings (Singh et al., 2021a). A fusion of Pfs48/45 6C to R0 and a region of merozoite surface protein 3 (GMZ2.6C) elicited parasite-specific antibodies (Baldwin et al., 2016) and a 10C version of this vaccine candidate (GMZ2'.10C) elicited transmission-blocking antibodies (Mistarz et al., 2017). A fusion protein comprising Pfs48/45 6C and the pro-domain of Pfs230 (aa 443-590) is under investigation as a vaccine candidate, with the glutamate-rich pro-domain assisting the proper folding of Pfs48/45 in a similar manner to the R0 region of GLURP (Singh et al., 2019; Singh et al., 2021b).

Successful expression of Pfs48/45 6C and a region of Pfs230 (aa 443-590) in *L. lactis* without fusion partners has also been reported, enabling investigation of the immune response against these 6-cysteine proteins without needing to account for the immune response generated by the fusion partner (Acquah et al., 2017).

Eukaryotic Systems for the Expression of 6-Cysteine Proteins

Baculovirus/Insect Cell Expression

The baculovirus/insect cell system was used to express Pfs48/45 in the first reported expression of a 6-cysteine protein (Kocken et al., 1993) and has since been employed for investigation of 6-cysteine protein structure, interactions and immunogenicity.

Expression of recombinant Pf12 (Tonkin et al., 2013), Pf12p (Dietrich et al., 2021) and Pf41 (Parker et al., 2015) *via* this system has yielded high resolution crystal structures of these proteins, as well as the Pf12-Pf41 complex (Dietrich et al., 2022). Recombinant Pfs47 expressed using the baculovirus system was used to identify its binding partner, the mosquito receptor protein P47Rec, and elucidate the involvement of this interaction in evading the mosquito immune system (Molina-Cruz et al., 2020).

The baculovirus system also produced full-length Pfs48/45 and Pfs48/45 6C vaccine candidates, though only the latter elicited transmission-reducing antibodies (Lee et al., 2020). A PbPSOP12 vaccine candidate produced in this system showed modest transmission-reducing activity (Sala et al., 2015). Pfs230C1 (aa 443-731) produced in this system was able to elicit antibodies that hinder parasite development (Lee et al., 2017; Miura et al., 2019; Huang et al., 2020). Optimization of the production of Pfs230C1 resulted in a final yield of 10 mg/L with the potential to produce over 1g of protein (Lee et al., 2019a). Expression of a shorter Pfs230 fragment, Pfs230D1+ (aa 552-731), also elicited antibodies with transmission-blocking activity and yields were two-fold higher than obtained for Pfs230C1 at 23 mg/L (Lee et al., 2019b).

Mammalian Cell Expression

Recombinant proteins expressed in HEK293 cells were used to elucidate the interactions of Pf12 and Pf41 (Taechalertpaisarn et al., 2012) and of *P. yoelii* P36, which in complex with P52 engages host receptor EphA2 (Kaushansky et al., 2015). Pfs48/45 6C was expressed in this system for crystallization in complex with transmission-blocking mAb 85RF45.1 (Kundu et al., 2018). The Chinese Hamster Ovary (CHO) cell line was used to express full-length Pvs48/45, which demonstrated higher immunogenicity than when expressed in *E. coli* (Arevalo-Herrera et al., 2021; Arevalo-Herrera et al., 2022).

The scalability of mammalian cell expression was utilized to produce a library of recombinant proteins including P12, P38, P41 and P92 from *P. falciparum*, *P. vivax, P. malariae, P. ovale and P. knowlesi*. The library was used to investigate cross-reactivity of sera across *Plasmodium* as a serological assay for diagnosing exposure to *P. ovale, P. malariae* or *P. knowlesi* (Muller-Sienerth et al., 2020). In *P. falciparum*, a library of secreted and surface merozoite proteins including Pf12, Pf12p, Pf38, Pf92 and Pf41 was produced. The library was used to confirm the interaction of Pf12 with Pf41 and demonstrate that these 6-cysteine proteins, with the exception of Pf12p, are immunoreactive with immune sera (Crosnier et al., 2013). Similarly, a recombinant protein library of *P. vivax* antigens confirmed the interaction of Pv12 with Pv41 and identified additional potential interaction partners for Pv12 (Hostetler et al., 2015).

Plant-Based Expression

The Australasian tobacco plant *Nicotiana benthamiana* has been used for the expression of recombinant 6-cysteine proteins including Pf38, which was recognized by sera of semi-immune donors and elicited antibodies with transmission-reducing activity upon immunization of mice, although only a low yield of 4 mg/kg of fresh leaf biomass was obtained (Feller et al., 2013). In contrast, expression of a Pfs230 region referred to as 230CMB (aa 444-730) in *N. benthamiana* resulted in yields of 800 mg/kg of fresh whole leaf tissue (Farrance et al., 2011). Antibodies generated against this recombinant protein in rabbits were able to bind native parasite and demonstrated transmission-blocking

activity with a reduction of >99% in oocyst counts (Farrance et al., 2011).

In this system, *in vivo* deglycosylation of 6-cysteine proteins has been explored through co-expressing 6-cysteine proteins with enzymes PNGase F or Endo H. Co-expression of a region of Pfs48/45 (aa 28-401) referred to as Pfs48F1, which contains seven putative N-glycosylation sites, and PNGase F to remove all N-linked glycans resulted in a yield of 50 mg/kg of fresh leaf biomass. Anti-Pfs48/45 monoclonal antibodies (mAbs) showed higher affinity to the *in vivo* deglycosylated protein compared to the glycosylated protein and slightly higher affinity to the protein deglycosylated *in vivo* compared to *in vitro* (Mamedov et al., 2012). Developments to this protocol have included expressing Pfs48F1 and PNGase F from a single vector (Prokhnevsky et al., 2015) and co-expressing full length Pfs48/45 (aa 28-428) or Pfs48/45 10C with Endo H, which removes only certain types of N-linked carbohydrates. This resulted in a higher yield of protein than co-expression with PNGase F (52 mg/kg *vs* 27 mg/kg, respectively) that was more stable and elicited antibodies with stronger transmission-reducing activity (Mamedov et al., 2017; Mamedov et al., 2019).

Yeast-Based Expression

Expression of Pfs48/45 in *Saccharomyces cerevisiae* was initially attempted but did not produce sufficient levels of protein for detection. In contrast, recombinant Pfs48/45 could be detected in *P. pastoris*, but with an expression efficiency of only 1% (Milek et al., 2000). More recently, efficient expression of Pfs230D1M (aa 542-736) was achieved in *P. pastoris* for use in a vaccine currently undergoing Phase I and II clinical trials (MacDonald et al., 2016; Coelho et al., 2019; Healy et al., 2021). This system has produced recombinant Pfs230D1 for crystallization with transmission-blocking antibodies LMIV230–01 (Coelho et al., 2021) and 4F12 (Singh et al., 2020). *H. polymorpha* has been employed to express Pfs230 constructs in a VLP alongside sexual stage antigen Pfs25, which elicited antibodies with transmission-reducing activity (Chan et al., 2019; Wetzel et al., 2019).

Other Eukaryotic Expression Systems

The stable Drosophila Schneider-2 cell line was employed to express full-length Pfs48/45 due to its ability to produce large quantities of correctly folded protein without the need for a fusion partner or carrier protein. The recombinant protein was recognized by known anti-P48/45 mAbs and induced antibodies with transmission-blocking activity in mice, suggesting it had adopted the correct conformation (Lennartz et al., 2018). A Pfs48/45 6C fragment produced by the same method was crystallized in complex with transmission-blocking antibody 85RF45.1, representing one of the first crystal structures of a Pfs48/45 fragment (Lennartz et al., 2018).

Chlamydomonas reinhardtii, a species of green algae, has been investigated as a low-cost option for production of vaccine candidate Pfs48/45. A region comprising aa 178-448 was successfully expressed and could be recognized by the mAb IIC5-10, known to recognize Pfs48/45, indicating the protein folded in the correct conformation (Jones et al., 2013).

Cell Free Systems

Cell free systems such as the wheat germ cell-free (WGCF) system offer the potential for rapid, high-throughput protein expression of *Plasmodium* proteins (Tsuboi et al., 2008). For this reason, cell free systems have been used to express multiple antigens for high-throughput screening of patient sera against an array of antigens. Such studies have shown that antibodies against Pf38 have an intermediate association with protection against symptomatic malaria (Richards et al., 2013) and antibody levels against Pfs230C may be associated with age (Muthui et al., 2021). Unfortunately, not all antigens appear to be amenable to expression *via* this system, with production of recombinant Pfs48/45, Pfs47 and PfPSOP12 proving unsuccessful (Muthui et al., 2021). This system has also been used to produce multiple vaccine candidates for functional comparison, supporting the further development of Pfs230C as a vaccine candidate (Miura et al., 2013).

The WGCF system was used to express multiple fragments of Pfs230, which due to its size is difficult to express as a full-length protein. Expression of fragments spanning the Pfs230C region (aa 443-1132) demonstrated that truncated fragments were capable of eliciting transmission-blocking antibodies (Tachibana et al., 2011). This contrasts observations for *E. coli* where only the full Pfs230C fragment was capable of eliciting transmission-blocking antibodies (Bustamante et al., 2000), suggesting the native topology of the proteins was better retained by the WGCF-produced fragments. Expression of protein fragments that together span the entirety of Pfs230 was used to further pinpoint the functional transmission-blocking epitopes of Pfs230 (Tachibana et al., 2019; Miura et al., 2022).

Cell free systems have been used to express *P. vivax* orthologues Pv12 (Li et al., 2012) and Pv41 (Cheng et al., 2013), demonstrating the immunoreactivity of naturally acquired sera with these antigens. The recombinant proteins were also used to generate anti-Pv12 and anti-Pv41 antibodies used to reveal the subcellular localization of these proteins. High-throughput screening of immune sera against *P. vivax* proteins identified 18 highly immunoreactive proteins, with Pv12 and Pv41 being among them (Chen et al., 2010). A panel of 20 P. *vivax* proteins including Pv12 were expressed by nucleic acid programmable protein array/*in vitro* transcription/translation, confirming the interaction of Pv12 with Pv41 as well as identifying additional putative interaction partners (Arevalo-Pinzon et al., 2018).

Recombinant protein expression is a bottleneck for the structural and biochemical characterization of 6-cysteine proteins. Differences between the cellular machinery of *Plasmodium* and the expression system often requires additional measures such as codon harmonisation, conjugation to a fusion partner and deglycosylation to produce properly folded protein. The choice of an appropriate expression system will depend on the protein and domain being expressed, considering its size, the numbers of disulphide bonds and glycosylation sites it contains and its intended downstream applications.

MONOCLONAL ANTIBODIES FOR THE CHARACTERIZATION OF 6-CYSTEINE PROTEINS

Monoclonal antibodies generated against the 6-cysteine proteins have been used to elucidate protein structure and functional domains, and some are capable of inhibiting parasite development and transmission. In this review, we will focus on the description of these inhibitory mAbs against the three transmission-blocking vaccine candidates, Pfs230, Pfs48/45, and Pfs47 (**Supplementary Table 2**).

Pfs230

The mature form of Pfs230 contains an additional non-structured pro-domain region of ~100 amino acids upstream of the first 6-cysteine domain (D1) (Carter et al., 1995; Brooks and Williamson, 2000; Gerloff et al., 2005). Epitope mapping of anti-Pfs230 antibodies suggests that part of the pro-domain and D1 of Pfs230 can elicit transmission-blocking antibodies (Tachibana et al., 2019; Miura et al., 2022) (**Supplementary Table 2**).

To date, 20 inhibitory mAbs specific for *P. falciparum* Pfs230 have been reported (**Supplementary Table 2**), which reduce the formation of oocysts on the mosquito midgut to varying degrees (42.2%-100%) when assayed using the standard membrane feeding assay (SMFA) (**Supplementary Table 2**). Of these antibodies, 16 (63F2A2.2a & 2b, 2B4, 1B3, 11E3, 12F10, 1H2, 3G9, 7A6, 8C11, 17E9, 4C10, 11C12F7, 21C1, 12A1A5, and 1A3-B8) were generated *via* direct animal immunization with the sexual stage parasites (either intact cells or whole cell lysate) (Rener et al., 1983; Quakyi et al., 1987; Read et al., 1994; Roeffen et al., 1995a; Roeffen et al., 1995; Williamson et al., 1995). Two mAbs, 4F12 and 5H1, were obtained *via* animal immunization with recombinant protein (MacDonald et al., 2016; Singh et al., 2020), and two mAbs, LMIV230-01 and LMIV230-02, were directly isolated from memory B cells of vaccinated Malian adults (Coelho et al., 2019). In these studies, recombinant Pfs230 proteins containing parts of the pro-domain region and D1 of Pfs230 were used as antigens (MacDonald et al., 2016; Coelho et al., 2019; Singh et al., 2020). Using structural biology approaches, the 4F12 and LMIV230-01 binding epitopes were identified to be within conserved regions of Pfs230 D1 (Coelho et al., 2019; Singh et al., 2020). Three additional transmission-blocking mAbs (1A3-B8, 11C5-B10, and 29F432) are reactive against both Pfs230 and Pfs48/45 (Rener et al., 1983; Quakyi et al., 1987; Read et al., 1994; Roeffen et al., 1995a; Roeffenet al., 1995b; Williamson et al., 1995).

The inhibitory mechanism of anti-Pfs230 antibodies has been thought to be predominantly complement-dependent (Healer et al., 1997), which could explain the higher transmission reducing activity observed for Pfs230 in a Phase I clinical trial compared to benchmark transmission-blocking vaccine candidate Pfs25 (Healy et al., 2021). Indeed, many Pfs230 mAbs lose their transmission-blocking ability in the absence of human serum (**Supplementary Table 2**). The chimeric rh4F12 mAb, containing the original mouse fragment antigen binding (Fab) region fused with human IgG1 crystallizable fragment (Fc), showed increased potency relative to the original mouse antibody, possibly due the presence of human IgG1 Fc, which is thought to enhance complement fixing activity (Singh et al., 2020). However, 4F12, LMIV230-01 and 1A3-B8 can inhibit transmission in the absence of complement activity (Rener et al., 1983; MacDonald et al., 2016; Singh et al., 2020; Coelho et al., 2021) (**Supplementary Table 2**), suggesting that complement-independent inhibitory mechanisms exist for anti-Pfs230 antibodies.

Pfs48/45

Anti-Pfs48/45 antibodies with transmission-blocking activity target at least four epitope groups (epitopes I, IIb, III, and V) that span all three 6-cysteine domains of Pfs48/45 (N. Targett, 1988; Targett et al., 1990; Roeffen et al., 2001b; Outchkourov et al., 2007; Outchkourov et al., 2008; Lennartz et al., 2018) (**Supplementary Table 2**). The disulfide bonds within the central and C-terminal 6-cysteine domains are critical for the presentation of the transmission-blocking epitopes, but dispensable for epitope presentation on the N-terminal domain of Pfs48/45 (Outchkourov et al., 2007).

There are 15 reported transmission-blocking anti-Pfs48/45 mAbs, with relatively well characterized epitopes. When assessed by SMFA, all 15 mAbs were able to reduce oocyst formation by 55.5%-100% under the conditions tested (**Supplementary Table 2**). Six mAbs, 85RF45.1 and its humanized version TB31F, 85RF45.5, 32F3, 32F5, and 3E12, were generated by animal immunization with intact sexual stage parasites (Vermeulen et al., 1985; Targett, 1988; Carter et al., 1990; Targett et al., 1990; Roeffen et al., 2001a). All these antibodies recognize the C-terminal domain of Pfs48/45 except for 85RF45.5, which recognizes the N-terminal domain. The remaining eight antibodies were generated *via* animal immunization with full-length Pfs48/45 protein obtained either through affinity purification from *P. falciparum* cell lysate (82C4-A9, 81D3-D2, 42A6-F3, 84A2-A4, and 82D6-A10) (Targett, 1988), or recombinant protein expression (1F10, 3G3, 6A10, 10D8) (Lennartz et al., 2018). These eight antibodies, including two unique IgM antibodies 82C4-A9 and 81D3-D2, recognize either the N-terminal or central domains of Pfs48/45 (Targett, 1988; Lennartz et al., 2018).

The most potent anti-Pfs48/45 mAb is the humanized version of mAb 85RF45.1 (TB31F), which reduces oocyst formation in mosquitos by 80% at a concentration of 1-2 μg/mL (Roeffen et al., 2001a; Kundu et al., 2018), approximately 15x more potent than the anti-Pfs25 mAb 4B7 (IC_{80} of 30.7 μg/mL) (de Jong et al., 2021). The crystal structures of mAb 85RF45.1 and its humanized version TB31F in complex with recombinant C-terminal domain of Pfs48/45 (Pfs48/45-6C) suggest that the antibody binds to a relatively conserved conformational epitope (Kundu et al., 2018; Lennartz et al., 2018) and existing field polymorphisms do not alter antibody binding and transmission-reducing efficacy substantially (Kundu et al., 2018; Lennartz et al., 2018; Stone et al., 2018; de Jong et al., 2021) (**Supplementary Table 2**). In contrast to Pfs230, the inhibitory mechanism of anti-Pfs48/45 antibodies are complement-independent (Patel and Tolia, 2021).

Pfs47

Recent studies show that immunization with D2 of Pfs47 and Pbs47 elicited antibodies with transmission-blocking activity (Canepa et al., 2018; Yenkoidiok-Douti et al., 2020), whereas antibodies that preferentially bind D1 and D3 did not exhibit transmission-blocking activity (Canepa et al., 2018; Yenkoidiok-Douti et al., 2020). Pfs47 D2-specific inhibitory mAbs, IB2 and BM2, have been shown to bind to the linear epitope on the central region of D2 and reduce transmission by >85% at 200 µg/mL. In contrast, JH11, which binds the N-terminal region of D2, increases transmission (Canepa et al., 2018). The transmission-blocking activity of the Pfs47 mAbs is complement-independent like mAbs to its paralogue Pfs48/45 (Canepa et al., 2018; Yenkoidiok-Douti et al., 2020; Patel and Tolia, 2021) (**Supplementary Table 2**).

STRUCTURAL CHARACTERIZATION OF 6-CYSTEINE PROTEINS

The 6-Cysteine Domain

The common structural feature of the family is the 6-cysteine domain. The 6-cysteine domain folds into a β-sandwich of parallel and antiparallel β-strands and contains up to six cysteines that form disulfide bonds, where cysteines C1–C2, C3–C6, C4–C5 are connected (**Figure 2A**) (Gerloff et al., 2005; Arredondo et al., 2012). 'Degenerate' domains containing less than six cysteines have been identified (Templeton and Kaslow, 1999). The β-sandwich is formed by two β-sheets and is usually stabilized by two disulfide bonds. A third disulfide bond connects a loop region to the core structure. Typically, a small β-sheet of two antiparallel β-strands runs perpendicular along the side of the β-sandwich. (**Figure 2A**) (Arredondo et al., 2012; Tonkin et al., 2013; Parker et al., 2015; Dietrich et al., 2021). 6-cysteine domains are present in each member, with the number of domains ranging from 2-14, and are often found in tandem pairs of A- and B-type 6-cysteine domains (**Figure 1B** and **Figure 2A**) (Carter et al., 1995; Gerloff et al., 2005). In comparison to A-type domains, the first β-strand in B-type domains is split into two parallel β-strands (β1 and β1' in **Figure 2A**). Compared with SAG1, the prototypic member of the SRS-superfamily the 6-cysteine domains share a structural scaffold. However, differences in β-strand topology and disulfide bond connectivity exist between 6-cysteine and SRS domains (Gerloff et al., 2005; Arredondo et al., 2012) (**Figure 2A**). Tandem domains of SRS-proteins characterized to date adopt a

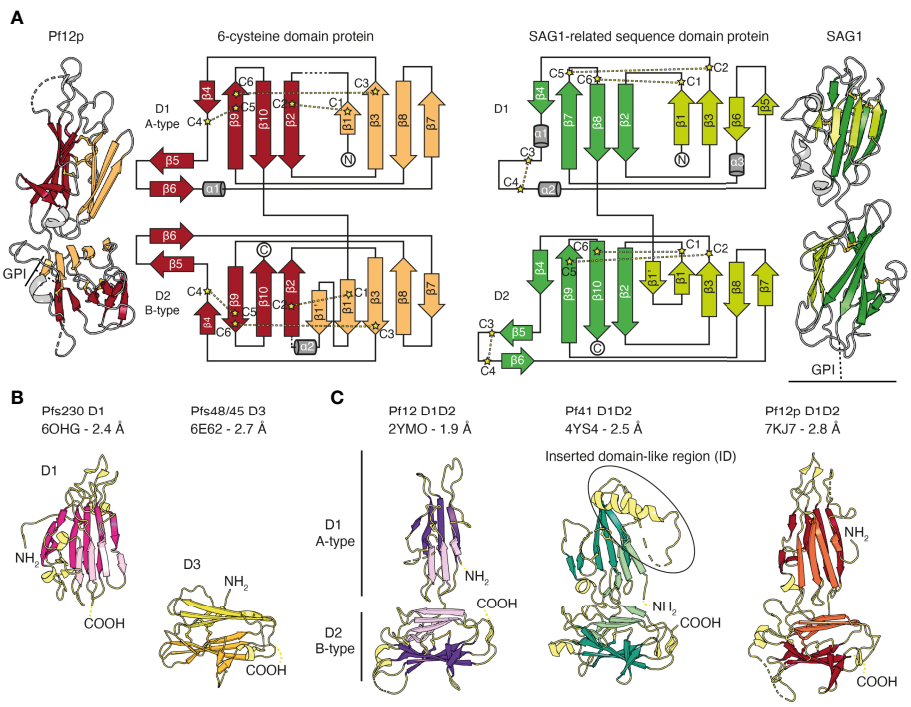

FIGURE 2 | The structural scaffold of 6-cysteine domains. **(A)** Schematic representation of 6-cysteine protein Pf12p with its N-terminal A-type 6-cysteine domain (D1) and C-terminal B-type 6-cysteine domain (D2). The β-strands of the top β-sheet of the β-sandwich are colored orange and the bottom β-sheet are colored red. Cysteines forming disulfide bonds are shown in ball-and-stick representation in yellow (PDB ID 7KJ7). Dotted lines indicate unmodeled regions. Topology diagram of Pf12p colored similarly to the schematic representation. Disulfide bond connectivity is indicated by yellow lines. Topology diagram and schematic representation of SAG1 from *Toxoplasma gondii*, the prototypic member of the SRS-superfamily (right, PDB ID 1KZQ). The β-strands of the top β-sheet of the β-sandwich are colored light green and the bottom β-sheet are colored green. **(B)** Crystal structure of single 6-cysteine domains of Pfs230 D1 (left) and Pfs48/45 D3 (right). **(C)** Crystal structures of 6-cysteine proteins containing a tandem pair of A- and B-type 6-cysteine domains. PDB IDs with corresponding resolution, N-terminal domain 1 (D1), C-terminal domain 2 (D2) as well as N- and C-termini are indicated (NH2 and COOH, respectively).

linear head-to-tail orientation with limited D1-D2 interdomain contacts, which suggests potential mobility between SRS-domains (**Figure 2A**) (He et al., 2002; Crawford et al., 2009; Crawford et al., 2010). In contrast, tandem domains of 6-cysteine domains have a non-linear organization, potentially with restricted mobility (Tonkin et al., 2013; Parker et al., 2015; Dietrich et al., 2021).

Of the 14 members of the 6-cysteine protein family, structural information is available for five *P. falciparum* proteins, namely Pf12, Pf12p, Pf41, Pfs48/45 and Pfs230 (**Figures 2B, C** and **Figure 3**). The 6-cysteine domain was first described in 2012 by the nuclear magnetic resonance (NMR) structure of the C-terminal Pf12 D2 domain, which confirmed the structural similarities with the *Toxoplasma* SRS domain (Arredondo et al., 2012). Crystal structures with single 6-cysteine domains are available for Pfs48/45 and Pfs230, which have been characterized in the presence of antibody fragments (**Figure 2B** and **Figure 3C**) (Kundu et al., 2018; Lennartz et al., 2018; Singh et al., 2020; Coelho et al., 2021). The Pf12 D2 and the Pfs48/45 D3 domains are B-type 6-cysteine domains containing three disulfide bonds. Pfs230 D1 is a degenerate 6-cysteine domain in which two disulfide bonds pin the β-sandwich together. In comparison to other 6-cysteine domains, Pfs230 D1 contains an N-terminal extension (residues 557-579) that packs against the 6-cysteine domain core (Coelho et al., 2021).

Crystal structures of the tandem domains of Pf12, Pf12p and Pf41 have been determined (**Figure 2C**) (Tonkin et al., 2013; Parker et al., 2015; Dietrich et al., 2021). Their overall structural architecture is similar in that the two 6-cysteine domains are connected by a short linker and tilted against each other. The domain-domain organization appears rather rigid as networks of interdomain contacts bury extended surface areas between 461-911 Å^2 in these crystal structures. The domain-domain contacts are predominantly formed between residues of β-strands connecting loops of D1 and residues of the top β-sheet of D2. Two nanobodies, Nb B9 and Nb D9, were successfully crystallized in complex with recombinant Pf12p and both bind specifically to the Pf12p interdomain (D1-D2 junction) area (**Figure 3B**) (Dietrich et al., 2021). These Pf12p nanobodies were highly specific, showing very little cross-reactivity against Pf12 or Pf41, despite these proteins adopting the same two 6-cysteine domain arrangement (Dietrich et al., 2021). While the overall fold and the spatial position of the disulfide bonds are similar in Pf12, Pf41 and Pf12p, their amino acid sequence identity is low (18-27%), and loops connecting β-strands vary especially in length and conformation. In the case of Pf41, a ~110 amino acid insertion, termed the inserted domain-like region (ID), connects the last two β-strands of the D1 domain and is critical for the interaction with Pf12 (Parker et al., 2015; Dietrich et al., 2022).

Several members of the 6-cysteine protein family form hetero-complexes, such as Pfs230 and Pfs48/45, Pf12 and Pf41, and Pf36 and Pf52 (Kumar, 1987; Kumar and Wizel, 1992; Taechalertpaisarn et al., 2012; Parker et al., 2015; Arredondo et al., 2018). Recently, the first crystal structure of a 6-cysteine hetero-complex of Pf12 and Pf41 was determined (**Figure 3A**) (Dietrich et al., 2022). This Pf12-

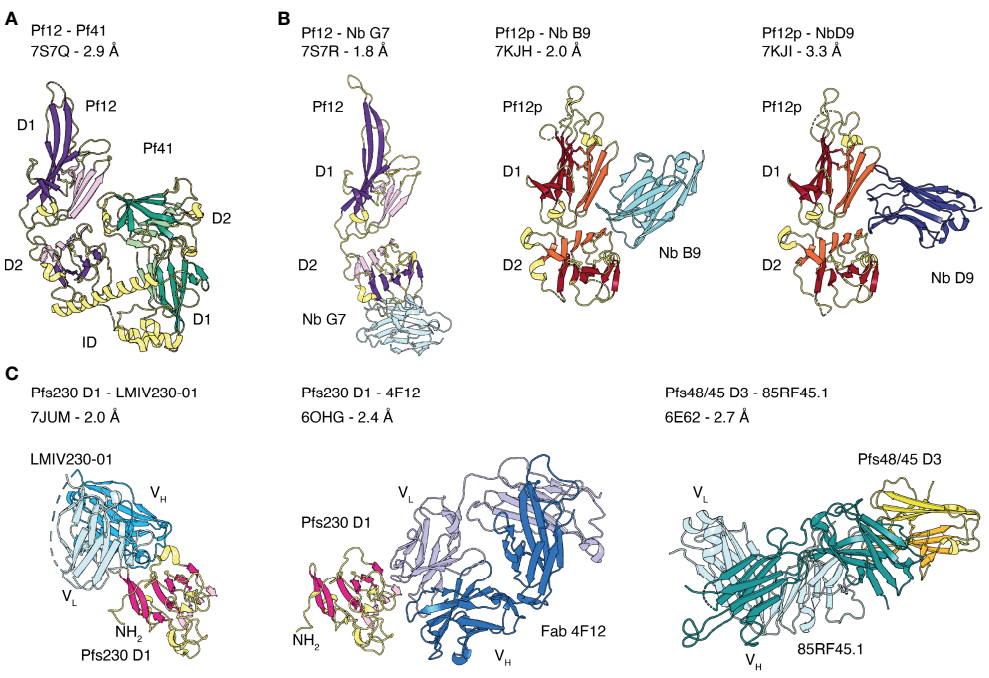

FIGURE 3 | Crystal structures of the 6-cysteine proteins of *P. falciparum* in complex with another 6-cysteine protein or antibody fragments. **(A)** Crystal structure of the hetero-dimeric complex of Pf12 and Pf41 with indicated D1 and D2 domains and the inserted domain-like region **(ID)** of Pf41. **(B)** 6-cysteine proteins bound to nanobodies. Pf12 bound to Nb G7 (left), Pf12p bound to Nb B9 (middle) and Nb D9 (right). **(C)** 6-cysteine protein domains bound to Fab and single-chain fragment variable (scFv) regions. Pfs230 D1 in complex with scFv of LMIV230-01 (left) and Fab of 4F12 (middle). Pfs48/45 D3 bound to Fab of 85RF45.1 (right).

Pf41 structure identified two distinct binding sites and showed that the ID of Pf41 forms a 25 amino acid-long α-helix that binds to a concave surface of the Pf12 D2 domain. The second interaction site involves extended loops on one side of the Pf41 D2 domain that recognize residues at the Pf12 D1-D2 domain junction. Critical residues for complex formation have been identified on both proteins, suggesting that both binding sites are important for the interaction of Pf12 and Pf41. In addition, Pf12 specific nanobodies were able to inhibit complex formation between Pf12 and Pf41 (Dietrich et al., 2022). The crystal structure of one of these nanobodies, Nb G7, in complex with recombinant Pf12 showed that Nb G7 bound to a hydrophobic groove on Pf12 that overlaps with the Pf41 ID binding site (**Figure 3B**). However, Nb G7 was not inhibitory to merozoite invasion or egress (Dietrich et al., 2022), which is consistent with the genetic knockout of these proteins being dispensable for blood stage growth (Taechalertpaisarn et al., 2012).

Structures are available for Pf12 (PDB IDs 2YMO, 7S7R and 7S7Q), Pf41 (PDB IDs 4YS4 and 7S7Q) and Pfs48/45 (PDB IDs 6E62 and 6H5N) that were solved using different protein constructs that vary in sequence, amino acid range, or recombinant protein expression system (**Supplementary Table 1**). These structures agree with each other, and all described 6-cysteine domains show their predicted number of disulfide bonds.

6-Cysteine Protein Family Members in Complex With Inhibitory Antibody Fragments

The Fab fragment of 4F12 and the single chain fragment variable (scFv) of LMIV230-01 were crystallized in complex with Pfs230 D1 (Singh et al., 2020; Coelho et al., 2021). Both antibody fragments recognize distinct conformational epitopes on different sides of the 6-cysteine domain (**Figure 3C**). 4F12 contacts Pfs230 D1 along one edge of the β-sandwich, interacting with residues of both β-sheets and several residues of the β-strand connecting loop formed by F595-K607. The light chain of 4F12 forms more contacts with Pfs230 D1 than the heavy chain. Both, light and heavy chain together bury an average surface area of about 1500 $Å^2$ on Pfs230 D1 (Singh et al., 2020). Binding of LMIV230-01 involves all six CDRs and buries a surface area of 1047 $Å^2$ on Pfs230 D1 with heavy and light chains contributing to 750 $Å^2$ and 297 $Å^2$, respectively (Coelho et al., 2021). LMIV230-01 contacts residues of five β-strands all located on one side of the β-sandwich, a β-strand connecting loop and residues of the long N-terminal extension of Pfs230 D1. The interaction of LMIV230-01 and Pfs230 D1 is mostly stabilized by hydrophobic contacts, and five residues of Pfs230 are involved in hydrogen bonds or salt bridges with LMIV230-01. The epitope is conserved as all major polymorphisms identified from 2512 analyzed sequences from Africa and Asia are outside the binding site of LMIV230-01.

MAb 85RF45.1 is a potent transmission-reducing antibody targeting the C-terminal D3 domain of Pfs48/45 (Roeffen et al., 2001b; Kundu et al., 2018; Lennartz et al., 2018). There are two crystal structures of the Fab fragment of 85RF45.1 in complex with the D3 domain of Pfs48/45 at 2.7 Å (Kundu et al., 2018) and 3.2 Å (Lennartz et al., 2018) resolution. These two crystal structures, Protein Data Bank (PDB) entry 6E62 and 6H5N, align well with root mean square deviations (r.m.s.d.) of ~0.977 Å. The r.m.s.d. of two superimposed protein structures describes the average distance between corresponding atom positions. The smaller the r.m.s.d. value the more similar the two structures are, where a value of zero means a perfect fit. Here, we will describe the interactions between the Fab of 85RF45.1 and Pfs48/45 using the higher resolution structure (Kundu et al., 2018). Binding of 85RF45.1 to Pfs48/45 involved all six CDRs and led to a total buried surface area of 1039 $Å^2$ on Pfs48/45 with the heavy chain contributing with 650 $Å^2$ and the light chain with 389 $Å^2$ (Kundu et al., 2018). 85RF45.1 binds at an edge of the β-sandwich of Pfs48/45 D3, by engaging many residues of the β-strand connecting loops and forming several hydrogen bonds and salt bridges (**Figure 3C**). Sequence analysis showed that three low frequency polymorphisms (I/V349, Q/L355, K/E414) are located within the epitope but 85RF45.1 can recognize single-point mutant proteins representing these polymorphisms with nanomolar affinity (Kundu et al., 2018).

TB31F, a humanized version of the potent transmission-blocking antibody 85RF45.1 has been generated for potential usage as a biologic for malaria interventions (Kundu et al., 2018). The crystal structure of TB31F bound to Pfs48/45 revealed a conserved mode of antigen recognition compared to the parental antibody (Kundu et al., 2018). TB31F retained a similar low nanomolar affinity for antigen binding (~3 nM affinity) and potent transmission-reducing activity in SMFA while showing an improved pH tolerance and thermostability with a ~10°C higher melting temperature.

DISCUSSION

Structural Characterization of the 6-Cysteine Proteins

Structural characterization is important for understanding the interactions of the 6-cysteine proteins and how they can be inhibited. Most 6-cysteine protein structures have yet to be solved, including structures of the complete ectodomain of the major vaccine candidates Pfs230, Pfs48/45 and Pfs47. Confirmation of their structures would enable functional epitopes to be further defined, with implications for rational vaccine design. Below we discuss some key advances in structural techniques that could help to structurally characterize the 6-cysteine proteins.

AlphaFold for Structure Prediction of 6-Cysteine Proteins

AlphaFold enables prediction of protein structures with atomic accuracy, even in cases where no similar structures have been solved before (Senior et al., 2020; Jumper et al., 2021). It has already been employed to predict structures of *Plasmodium* proteins that are difficult to express (Kaur et al., 2022) and to study the interactions of *Plasmodium* proteins with inhibitors (Chagot et al., 2022). AlphaFold appears capable of predicting *Plasmodium* protein structures with high accuracy (Chagot et al., 2022).

For the 6-cysteine proteins of *P. falciparum*, AlphaFold could be utilized for construct and novel antigen design. For this purpose, AlphaFold predictions could assist in defining domain boundaries to obtain well-folded, soluble protein. In addition, it could simplify the process of structural determination. Due to the low amino acid sequence identity between the 14 different family members (17-36%) and the few available crystal structures, phasing *via* molecular replacement has been challenging for 6-cysteine proteins. Experimental phasing was used to determine the structure of Pf41 (Parker et al., 2015), or in the case of 6-cysteine-antibody complexes initial phases were obtained by molecular replacement using antibody fragments as search models only (Kundu et al., 2018; Lennartz et al., 2018; Singh et al., 2020; Coelho et al., 2021). The 6-cysteine part of these structures were built from scratch by iterative cycles of model building and refinement. Instead, AlphaFold predictions could be valuable search models for molecular replacement to solve the phase problem of structurally uncharacterized 6-cysteine proteins.

AlphaFold-Multimer is an AlphaFold model trained on multimeric inputs for the prediction of oligomers and multi-chain protein complexes of known stoichiometry. It could be utilized for *P. falciparum* to provide insights into ligand recognition by 6-cysteine proteins (Evans et al., 2022). This is exemplified by the high accuracy that AlphaFold-Multimer predicts the Pf12-Pf41 hetero-dimer even when excluding the PDB entry of the hetero-complex in the template search of the pre-processing step (**Figure 4A**). The AlphaFold model and the crystal structure of the Pf12-Pf41 hetero-complex overlay with a low r.m.s.d. value of 0.902 Å across 1778 atoms (**Figure 4B**). The core structures of both proteins are predicted with high confidence, as well as most parts of the Pf41 ID. The fold of the Pf41 ID has not been fully characterized by X-ray crystallography, likely due to its flexible nature. In the crystal structure of Pf41 alone the Pf41 ID was likely proteolyzed and therefore mostly absent (PDB 4YS4) (Parker, Peng, and Boulanger 2015). In the crystal structure of the hetero-complex parts of this region were not visible in the electron density and are not connected to the core structure of the 6-cysteine domain (PDB 7S7Q) (Dietrich et al., 2022). Low and very low confidence regions of the AlphaFold model comprise mostly the N-terminal signal sequence of the two proteins and the C-terminal region of Pf12. The arrangement of Pf12 and Pf41 in relation to each other resembles the crystal structure of the complex (Dietrich et al., 2022) and important interactions as shown by mutagenesis studies are predicted within 4 Å. Hence, AlphaFold predicted the overall hetero-complex with high accuracy compared with an experimentally determined structure, and may have shed insights into the fold of a previously uncharacterized region of Pf41. The prediction of hetero-complexes of other 6-cysteine proteins such as P36-P52 or P48/45-P230, or the prediction of 6-cysteine proteins in complex with specific antibodies or nanobodies might be informative but validation with experimental methods remains important.

To date only single and tandem 6-cysteine domains have been structurally characterized by NMR and X-ray crystallography. AlphaFold predictions of larger members of the 6-cysteine protein family will be useful to better understand the arrangement and three-dimensional organization of multiple 6-cysteine domains. For 6-cysteine proteins that contain three 6-cysteine domains, namely P47, P48/45, B9, PSOP12 and P92 (**Figure 1B**), AlphaFold predictions have high and very high per residue confidence scores (pLDDT, predicted local distance difference test) for the core structure of the 6-cysteine domains as well as for most β-strand connecting loops (https://alphafold.ebi.ac.uk/). The models show that all three 6-cysteine domains are highly engaged with each other with many inter-domain contacts between them. The predicted aligned error plot of the AlphaFold models allows assessment of the inter-domain accuracy. Except for Pf92, the expected position error has low values across the whole predicted inter-domain regions of the 6-cysteine domains indicating a high inter-domain accuracy for the 6-cysteine domain arrangement in Pf47, Pfs48/45, PfB9 and PfPSOP12. The proteins Pf92, PfPSOP12 and PfB9 contain in addition to their 6-cysteine domains a predicted N-terminal β-propellor domain which structures are predicted with confidence and have mostly high and very high pLDDT values. The relative position of the β-propellor domains towards the 6-cysteine domains are predicted with confidence for the Pf92 and the PfPSOP12 models. The β-propellor domains were first suggested by structure prediction using HHpred which is now further supported by the AlphaFold predictions.

For Pfs230, the largest member of the family, an AlphaFold prediction shows 14 6-cysteine domains and indicates a mostly unstructured N-terminal pro-domain, where residues 1-575 have very low per-residue confidence scores (**Figure 4C**). Several pro-domain residues form contacts with the first 6-cysteine domain similar to the crystal structures of Pfs230 D1 in complex with antibody fragments (Singh et al., 2020; Coelho et al., 2021). The core structure of the 14 6-cysteine domains and inter-domain regions of A-type and B-type tandem pairs are predicted with high and very high confidence scores. In contrast, several extended loops of the 6-cysteine domains and linker regions between following tandem pairs have low or very low pLDDT values. Some inter-domain contacts are suggested between domains that are not directly adjacent. However, due to the low pLDDT values which could indicate flexibility between tandem domains the model may not allow an accurate description of the inter-domain organization of Pfs230. The predicted model describes one static representation of a possible arrangement of the 14 domains. It remains possible that the packing of the multiple domains is different or requires other interaction partners for its native organization. Similarly, it is possible that the tandem pairs could be mobile relative to each other with no fixed packing, at least in absence of other interaction partners. While the inter-domain arrangement of the Pfs230 model may differ from the native structure, the model provides details about individual tandem pairs of 6-cysteine domains with high confidence and could be valuable for antigen design and as fit and search models for cryo-electron microscopy (cryo-EM) and X-ray crystallography, respectively.

Taken together, structure prediction using AlphaFold will benefit research of 6-cysteine proteins by assisting in construct design, contributing to a better understanding of their fold and interactions with binding partners although validation of the models and their interactions will still require experimental validation.

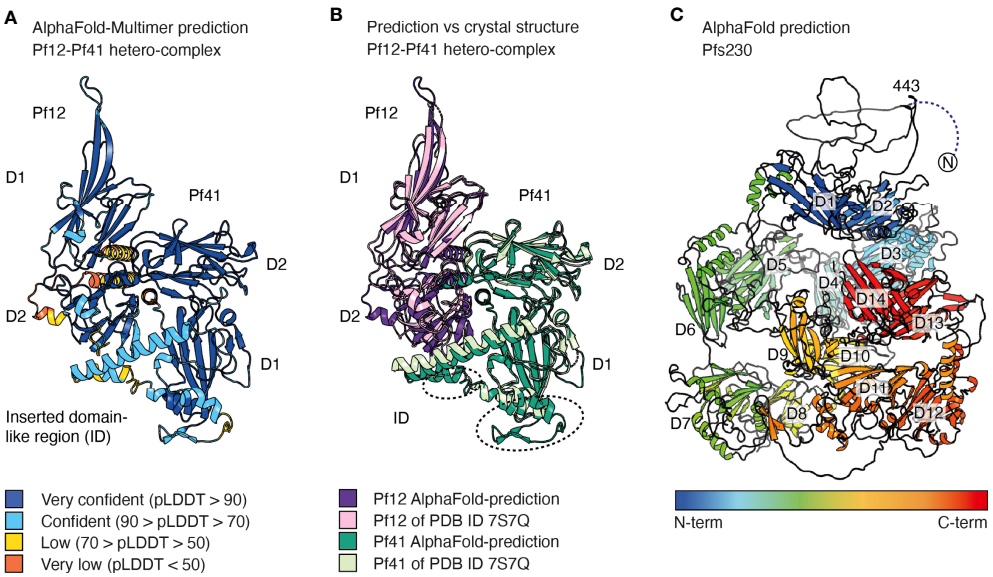

FIGURE 4 | AlphaFold predictions of selected 6-cysteine proteins. **(A)** AlphaFold-Multimer prediction of the hetero-dimeric complex of Pf12 and Pf41. Amino acids are colored based on their per-residue confidence score (pLDDT), which values can be between 0 and 100. Low values indicate low confidence and high numbers indicate very confident predictions. Amino acids are either colored orange (pDLLT <50), yellow (70> pDLLT >50), light blue (50< pDLLT >70), or dark blue (pDLLT >90). Regions with pLDDT <50 may be unstructured in isolation. **(B)** Alignment of the AlphaFold prediction (dark purple and dark green) of the Pf12-Pf41 hetero-dimeric complex with the Pf12-Pf41 crystal structure (light purple and light green, PDB ID 7S7Q). Regions of the Pf41 ID which are not defined in the crystal structure are indicated by dotted circles. **(C)** AlphaFold prediction of Pfs230 colored from blue to red from N- to C-terminus. The N-terminal residues 1-575 have low pDLLT values of <50. Residues 1-442 are not shown for clarity of the image. The 14 6-cysteine domains are indicated from D1-D14. AlphaFold models were generated at WEHI (Australia) using the AlphaFold algorithm.

Cryo-EM for Structural Characterization of 6-Cysteine Proteins *In Situ*

Cryo-EM is increasingly used for structural characterization and has been used to solve the structures of key *Plasmodium* proteins at resolutions higher than 4 Å (Kim et al., 2019; Dijkman et al., 2021; Schureck et al., 2021; Lyu et al., 2021). Recent advances have enabled resolutions of under 1.5 Å, allowing direct visualization of atom positions (Nakane et al., 2020; Yip et al., 2020).

Cryo-EM requires less sample than X-ray crystallography and could therefore be particularly valuable for the structural characterization of 6-cysteine proteins that are difficult to express recombinantly. Techniques such as microcrystal electron diffraction (MicroED) allow for structural determination of proteins from as little as a single nanocrystal of protein (Yonekura et al., 2015; Assaiya et al., 2021).

Experimental confirmation of the structure of Pfs230 is important for vaccine design; however, its size complicates expression and crystallization of the full-length protein. The amount of sample required for cryo-EM is sufficiently low to enable structure determination from endogenous *Plasmodium* proteins (Ho et al., 2018; Ho et al., 2021; Anton et al., 2022), which will be useful for proteins such as Pfs230 that cannot be easily expressed recombinantly. Further, with advances in cryo-electron tomography (cryoET) workflows and image processing techniques it is possible to solve the structure of proteins *in situ* at a resolution of 3.5 Å (Wagner et al., 2020; Tegunov et al., 2021). These techniques could be employed to determine the structure of Pfs230 *in situ*, allowing the 14 domains of this protein to be studied in their native conformation.

Structural Characterization of Inhibitory Antibodies

Supplementary Table 2 highlights the paucity of reported inhibitory antibodies for several proteins in the 6-cysteine family. Despite the essentiality of at least nine out of 14 P. *falciparum* 6-cysteine proteins, inhibitory mAbs have only been identified for three proteins, namely Pfs230, Pfs48/45 and Pfs47. Generation and characterization of inhibitory antibodies for the remaining proteins could produce valuable research tools and identify additional vaccine candidates. Moreover, there is a lack of structural information for transmission-blocking antibodies in complex with proteins. Structural data for inhibitory mAbs in complex with Pfs48/45 6C and Pfs230 D1 indicate that the mAbs bind to conserved regions of the proteins (Kundu et al., 2018; Lennartz et al., 2018; Singh et al., 2020; Coelho et al., 2021). Structural characterization of additional mAbs interacting with 6-cysteine proteins would aid discovery of conserved binding epitopes and non-competing antibodies that have the potential to act synergistically.

Synergistic Antibodies for Investigating and Targeting 6-Cysteine Proteins

Much of the work on 6-cysteine proteins to date has focused on characterizing individual mAbs and there has been little investigation into the potential synergistic effects of antibody combinations. Antibody synergy occurs when the activity of an antibody is enhanced by the presence of other antibodies and can be achieved by combining synergistic mAbs in a cocktail or by including multiple epitopes or antigens in an immunogen to elicit synergistic polyclonal antibodies.

Combining mAbs against different antigens has the potential to increase transmission-blocking activity, as does combining mAbs against different epitopes of the same antigen, which can increase activity through heterotypic interactions (Ragotte et al., 2022). Combining mAbs against different epitopes of Pfs230 D1 or Pfs230 D1 and Pfs48/45 significantly increased transmission-blocking activity (Singh et al., 2020), warranting further investigation of different mAb combinations. Combinations of antibodies with and without transmission-blocking activity may also act synergistically, as was observed for antibodies against PfRh5, where a non-neutralizing antibody was found to enhance the activity of neutralizing antibodies by increasing the time available for them to bind (Alanine et al., 2019). This warrants further characterization of mAbs against 6-cysteine proteins without transmission-blocking or neutralizing activity. The design of bispecific antibodies combining synergistic antibodies targeting multiple epitopes or antigens may enhance activity (Alanine et al., 2019). Synergistic mAbs have therapeutic potential; an antimalarial mAb administered to patients in a Phase I trial demonstrated prophylactic effects (Gaudinski et al., 2021) and treatment with a cocktail of synergistic mAbs could enhance protection.

There are also implications for vaccine design. Targeting multiple epitopes or antigens can induce a synergistic polyclonal response, increasing immune response and reducing the likelihood of escape mutations. A number of 6-cysteine multi-antigen vaccine candidates are under investigation, including Pfs48/45-GLURP (Theisen et al., 2014; Roeffen et al., 2015; Singh et al., 2015; Singh et al., 2017a; Singh et al., 2017b; Singh et al., 2021a), Pfs48/45-GLURP-MSP3 (Baldwin et al., 2016; Mistarz et al., 2017), Pfs230-Pfs48/45 (Singh et al., 2019; Singh et al., 2020; Singh et al., 2021b) and Pfs230-Pfs25 (Menon et al., 2017; Healy et al., 2021). A recent study found a higher prevalence of naturally infected individuals with antibodies against a Pfs48/45-GLURP-MSP3-based vaccine than against the individual proteins, suggesting the combination of antigens has an additive effect on immune response (Baptista et al., 2022). Moreover, animal immunization with the Pfs230-Pfs48/45 chimera elicited transmission-blocking antibody responses three-fold higher than the single antigens alone (Singh et al., 2019), suggesting further investigation of 6-cysteine antigen combinations is warranted.

The epitopes displayed by immunogens should be carefully considered; displaying multiple antigens can elicit antibodies that work synergistically but eliciting a wide polyclonal response can elicit antagonistic antibodies that reduce transmission-blocking activity (Alanine et al., 2019; Ragotte et al., 2022). In addition, synergistic effects appear to be dependent on antigen combination; vaccination with both Pfs230 and Pfs25 was found to elicit antibody responses no higher than those elicited by each antigen individually (Menon et al., 2017; Healy et al., 2021) and combinations of anti-Pfs230 and -Pfs25 mAbs did not show increased transmission-blocking activity (Singh et al., 2020). Identifying antibodies that work synergistically and carefully targeting key epitopes is important for effective malaria control strategies.

CONCLUSIONS

The 6-cysteine proteins are a family of highly conserved, surface exposed proteins expressed throughout the *Plasmodium* life cycle. Structural and functional insights have been derived from mAbs and crystal structures generated using recombinantly expressed 6-cysteine proteins. The structural and functional characterization of Pfs230, Pfs48/45 and Pfs47 as key candidates for transmission-blocking vaccines is a key priority. However, there is still a paucity of structural information for these proteins and their inhibitory antibodies and further characterization, exploiting advances in techniques such as AlphaFold and cryo-EM, would further elucidate the interactions of these proteins and specify functional epitopes for effective targeting of the 6-cysteine proteins.

AUTHOR CONTRIBUTIONS

FL, MG, W-HT, and MD wrote the manuscript. All authors contributed to the article and approved the submitted version.

FUNDING

W-HT is a Howard Hughes Medical Institute-Wellcome Trust International Research Scholar (208693/Z/17/Z) and supported by National Health and Medical Research Council of Australia (GNT2001385, GNT1154937).

ACKNOWLEDGMENTS

We thank Julie Iskander for implementing the AlphaFold algorithm into the WEHI high performance computing system. We are grateful to Julie and Richard Birkinshaw for help with the AlphaFold prediction of Pfs230. We thank Gabrielle M. Watson for constructive feedback and helpful suggestions on figures and manuscript.

SUPPLEMENTARY MATERIAL

The Supplementary Material for this article can be found online at: https://www.frontiersin.org/articles/10.3389/fcimb.2022.945924/full#supplementary-material

REFERENCES

Acquah, F. K., Obboh, E. K., Asare, K., Boampong, J. N., Nuvor, S. V., Singh, S. K., et al. (2017). Antibody Responses to Two New Lactococcus Lactis-Produced Recombinant Pfs48/45 and Pfs230 Proteins Increase With Age in Malaria Patients Living in the Central Region of Ghana. *Malar J.* 16 (1), 306. doi: 10.1186/s12936-017-1955-0

Agrawal, A., Bisharyan, Y., Papoyan, A., Bednenko, J., Cardarelli, J., Yao, M., et al. (2019). Fusion to Tetrahymena Thermophila Granule Lattice Protein 1 Confers Solubility to Sexual Stage Malaria Antigens in Escherichia Coli. *Protein Expr Purif* 153, 7–17. doi: 10.1016/j.pep.2018.08.001

Alanine, D. G. W., Quinkert, D., Kumarasingha, R., Mehmood, S., Donnellan, F. R., Minkah, N. K., et al. (2019). Human Antibodies That Slow Erythrocyte Invasion Potentiate Malaria-Neutralizing Antibodies. *Cell* 178 (1), 216–228.e21. doi: 10.1016/j.cell.2019.05.025

Annoura, T., van Schaijk, B. C., Ploemen, I. H., Sajid, M., Lin, J. W., Vos, M. W., et al. (2014). Two Plasmodium 6-Cys Family-Related Proteins Have Distinct and Critical Roles in Liver-Stage Development. *FASEB J.* 28 (5), 2158–2170. doi: 10.1096/fj.13-241570

Anton, L., Cobb, D. W., and Ho, C. M. (2022). Structural Parasitology of the Malaria Parasite Plasmodium Falciparum. *Trends Biochem. Sci.* 47 (2), 149–159. doi: 10.1016/j.tibs.2021.10.006

Arevalo-Herrera, M., Miura, K., Cespedes, N., Echeverry, C., Solano, E., Castellanos, A., et al. (2021). Immunoreactivity of Sera From Low to Moderate Malaria-Endemic Areas Against Plasmodium Vivax Rpvs48/45 Proteins Produced in Escherichia Coli and Chinese Hamster Ovary Systems. *Front. Immunol.* 12. doi: 10.3389/fimmu.2021.634738

Arevalo-Herrera, M., Miura, K., Solano, E., Sebastian Ramirez, J., Long, C. A., Corradin, G., et al. (2022). Immunogenicity of Full-Length P. Vivax Rpvs48/45 Protein Formulations in BALB/c Mice. *Vaccine* 40 (1), 133–140. doi: 10.1016/j.vaccine.2021.11.036

Arevalo-Herrera, M., Vallejo, A. F., Rubiano, K., Solarte, Y., Marin, C., Castellanos, A., et al. (2015). Recombinant Pvs48/45 Antigen Expressed in E. Coli Generates Antibodies That Block Malaria Transmission in Anopheles Albimanus Mosquitoes. *PLoS One* 10 (3), e0119335. doi: 10.1371/journal.pone.0119335

Arevalo-Pinzon, G., Gonzalez-Gonzalez, M., Suarez, C. F., Curtidor, H., Carabias-Sanchez, J., Muro, A., et al. (2018). Self-Assembling Functional Programmable Protein Array for Studying Protein-Protein Interactions in Malaria Parasites. *Malar J.* 17 (1), 270. doi: 10.1186/s12936-018-2414-2

Arredondo, S. A., Cai, M., Takayama, Y., MacDonald, N. J., Anderson, D. E., Aravind, L., et al. (2012). Structure of the Plasmodium 6-Cysteine S48/45 Domain. *Proc. Natl. Acad. Sci. U.S.A.* 109 (17), 6692–6697. doi: 10.1073/pnas.1204363109

Arredondo, S. A., and Kappe, S. H. I. (2017). The S48/45 Six-Cysteine Proteins: Mediators of Interaction Throughout the Plasmodium Life Cycle. *Int. J. Parasitol.* 47 (7), 409–423. doi: 10.1016/j.ijpara.2016.10.002

Arredondo, S. A., Swearingen, K. E., Martinson, T., Steel, R., Dankwa, D. A., Harupa, A., et al. (2018). The Micronemal Plasmodium Proteins P36 and P52 Act in Concert to Establish the Replication-Permissive Compartment Within Infected Hepatocytes. *Front. Cell Infect. Microbiol.* 8. doi: 10.3389/fcimb.2018.00413

Assaiya, A., Burada, A. P., Dhingra, S., and Kumar, J. (2021). An Overview of the Recent Advances in Cryo-Electron Microscopy for Life Sciences. *Emerg. Top. Life Sci.* 5 (1), 151–168. doi: 10.1042/ETLS20200295

Baldwin, S. L., Roeffen, W., Singh, S. K., Tiendrebeogo, R. W., Christiansen, M., Beebe, E., et al. (2016). Synthetic TLR4 Agonists Enhance Functional Antibodies and CD4+ T-Cell Responses Against the Plasmodium Falciparum GMZ2.6C Multi-Stage Vaccine Antigen. *Vaccine* 34 (19), 2207–2215. doi: 10.1016/j.vaccine.2016.03.016

Balikagala, B., Fukuda, N., Ikeda, M., Katuro, O. T., Tachibana, S. I., Yamauchi, M., et al. (2021). Evidence of Artemisinin-Resistant Malaria in Africa. *N Engl. J. Med.* 385 (13), 1163–1171. doi: 10.1056/NEJMoa2101746

Baptista, B. O., de Souza, A. B. L., Riccio, E. K. P., Bianco-Junior, C., Totino, P. R. R., Martins da Silva, J. H., et al. (2022). Naturally Acquired Antibody Response to a Plasmodium Falciparum Chimeric Vaccine Candidate GMZ2.6c and its Components (MSP-3, GLURP, and Pfs48/45) in Individuals Living in Brazilian Malaria-Endemic Areas. *Malar J.* 21 (1), 6. doi: 10.1186/s12936-021-04020-6

Bousema, T., Roeffen, W., Meijerink, H., Mwerinde, H., Mwakalinga, S., van Gemert, G. J., et al. (2010). The Dynamics of Naturally Acquired Immune Responses to Plasmodium Falciparum Sexual Stage Antigens Pfs230 & Pfs48/45 in a Low Endemic Area in Tanzania. *PLoS One* 5 (11), e141145. doi: 10.1371/journal.pone.0014114

Bozdech, Z., Llinas, M., Pulliam, B. L., Wong, E. D., Zhu, J., and DeRisi, J. L. (2003). The Transcriptome of the Intraerythrocytic Developmental Cycle of Plasmodium Falciparum.". *PLoS Biol.* 1 (1), E5. doi: 10.1371/journal.pbio.0000005

Brooks, S. R., and Williamson, K. C. (2000). Proteolysis of *Plasmodium Falciparum* Surface Antigen, Pfs230, During Gametogenesis. *Mol. Biochem. Parasitol.* 106, 77–82. doi: 10.1016/S0166-6851(99)00201-7

Bushkin, G. G., Ratner, D. M., Cui, J., Banerjee, S., Duraisingh, M. T., Jennings, C. V., et al. (2010). Suggestive Evidence for Darwinian Selection Against Asparagine-Linked Glycans of Plasmodium Falciparum and Toxoplasma Gondii. *Eukaryot Cell* 9 (2), 228–241. doi: 10.1128/EC.00197-09

Bustamante, P. J., Woodruff, D. C., Oh, J., Keister, D. B., Muratova, O., and Williamson, K. C. (2000). Differential Ability of Specific Regions of Plasmodium Falciparum Sexual-Stage Antigen, Pfs230, to Induce Malaria Transmission-Blocking Immunity. *Parasite Immunol.* 22, 373–380. doi: 10.1046/j.1365-3024.2000.00315.x

Canepa, G. E., Molina-Cruz, A., Yenkoidiok-Douti, L., Calvo, E., Williams, A. E., Burkhardt, M., et al. (2018). Antibody Targeting of a Specific Region of Pfs47 Blocks Plasmodium Falciparum Malaria Transmission. *NPJ Vaccines* 3, 26. doi: 10.1038/s41541-018-0065-5

Cao, Y., Bansal, G. P., Merino, K., and Kumar, N. (2016). Immunological Cross-Reactivity Between Malaria Vaccine Target Antigen P48/45 in Plasmodium Vivax and P. Falciparum and Cross-Boosting of Immune Responses. *PLoS One* 11 (7), e0158212. doi: 10.1371/journal.pone.0158212

Carter, R., Coulson, A., Bhatti, S., Taylor, B. J., and Elliott, J. F. (1995). Predicted Disulfide-Bonded Structures for Three Uniquely Related Proteins of *Plasmodium Falciparum*, Pfs230, Pfs48/45 and Pf12. *Mol. Biochem. Parasitol.* 71, 203–210. doi: 10.1016/0166-6851(94)00054-q

Carter, R., Graves, P. M., Keister, D. B., and Quakyi, I. A. (1990). Properties of Epitopes of Pfs 48/45, a Target of Transmission Blocking Monoclonal Antibodies, on Gametes of Different Isolates of *Plasmodium Falciparum*. *Parasite Immunol.* 12, 587–603. doi: 10.1111/j.1365-3024.1990.tb00990.x

Chagot, M. E., Boutilliat, A., Kriznik, A., and Quinternet, M. (2022). Structural Analysis of the Plasmodial Proteins ZNHIT3 and NUFIP1 Provides Insights Into the Selectivity of a Conserved Interaction. *Biochemistry* 61 (7), 479–93. doi: 10.1021/acs.biochem.1c00792

Chan, J. A., Wetzel, D., Reiling, L., Miura, K., Drew, D. R., Gilson, P. R., et al. (2019). Malaria Vaccine Candidates Displayed on Novel Virus-Like Particles are Immunogenic and Induce Transmission-Blocking Activity. *PLoS One* 14 (9), e0221733. doi: 10.1371/journal.pone.0221733

Cheng, Y., Lu, F., Tsuboi, T., and Han, E. T. (2013). Characterization of a Novel Merozoite Surface Protein of Plasmodium Vivax, Pv41. *Acta Trop.* 126 (3), 222–228. doi: 10.1016/j.actatropica.2013.03.002

Chen, J. H., Jung, J. W., Wang, Y., Ha, K. S., Lu, F., Lim, C. S., et al. (2010). Immunoproteomics Profiling of Blood Stage Plasmodium Vivax Infection by High-Throughput Screening Assays. *J. Proteome Res.* 9, 6479–6489. doi: 10.1021/pr100705g

Chowdhury, D. R., Angov, E., Kariuki, T., and Kumar, N. (2009). A Potent Malaria Transmission Blocking Vaccine Based on Codon Harmonized Full Length Pfs48/45 Expressed in Escherichia Coli. *PLoS One* 4 (7), e6352. doi: 10.1371/journal.pone.0006352

Coelho, C. H., Gazzinelli-Guimaraes, P. H., Howard, J., Barnafo, E., Alani, N. A. H., Muratova, O., et al. (2019). Chronic Helminth Infection Does Not Impair Immune Response to Malaria Transmission Blocking Vaccine Pfs230D1-EPA/Alhydrogel(R) in Mice. *Vaccine* 37 (8), 1038–1045. doi: 10.1016/j.vaccine.2019.01.027

Coelho, C. H., Tang, W. K., Burkhardt, M., Galson, J. D., Muratova, O., Salinas, N. D., et al. (2021). A Human Monoclonal Antibody Blocks Malaria Transmission and Defines a Highly Conserved Neutralizing Epitope on Gametes. *Nat. Commun.* 12 (1), 17505. doi: 10.1038/s41467-021-21955-1

Crawford, J., Grujic, O., Bruic, E., Czjzek, M., Grigg, M. E., and Boulanger, M. J. (2009). Structural Characterization of the Bradyzoite Surface Antigen (BSR4)

From Toxoplasma Gondii, a Unique Addition to the Surface Antigen Glycoprotein 1-Related Superfamily. *J. Biol. Chem.* 284 (14), 9192–9198. doi: 10.1074/jbc.M808714200

Crawford, J., Lamb, E., Wasmuth, J., Grujic, O., Grigg, M. E., and Boulanger, M. J. (2010). Structural and Functional Characterization of SporoSAG: A SAG2-Related Surface Antigen From Toxoplasma Gondii. *J. Biol. Chem.* 285 (16), 12063–12070. doi: 10.1074/jbc.M109.054866

Crosnier, C., Wanaguru, M., McDade, B., Osier, F. H., Marsh, K., Rayner, J. C., et al. (2013). A Library of Functional Recombinant Cell-Surface and Secreted P. Falciparum Merozoite Proteins. *Mol. Cell Proteomics* 12 (12), 3976–3986. doi: 10.1074/mcp.O113.028357

de Jong, R. M., Meerstein-Kessel, L., Da, D. F., Nsango, S., Challenger, J. D., van de Vegte-Bolmer, M., et al. (2021). Monoclonal Antibodies Block Transmission of Genetically Diverse Plasmodium Falciparum Strains to Mosquitoes. *NPJ Vaccines* 6 (1), 1015. doi: 10.1038/s41541-021-00366-9

Dietrich, M. H., Chan, L. J., Adair, A., Boulet, C., O'Neill, M. T., Tan, L. L., et al. (2022). Structure of the Pf12 and Pf41 Heterodimeric Complex of Plasmodium Falciparum 6-Cysteine Proteins. *FEMS Microbes* 3, xtac005. doi: 10.1093/femsmc/xtac005

Dietrich, M. H., Chan, L. J., Adair, A., Keremane, S., Pymm, P., Lo, A. W., et al. (2021). Nanobody Generation and Structural Characterization of Plasmodium Falciparum 6-Cysteine Protein Pf12p. *Biochem. J.* 478 (3), 579–595. doi: 10.1042/BCJ20200415

Dijkman, P. M., Marzluf, T., Zhang, Y., Chang, S.-Y. S., Helm, D., Lanzer, M., et al. (2021). Structure Ofthe Merozoite Surface Protein 1 From Plasmodium Falciparum. *Sci. Adv.* 7 (23), eabg0465. doi: 10.1126/sciadv.abg0465

Ecker, A., Bushell, E. S., Tewari, R., and Sinden, R. E. (2008). Reverse Genetics Screen Identifies Six Proteins Important for Malaria Development in the Mosquito. *Mol. Microbiol.* 70 (1), 209–220. doi: 10.1111/j.1365-2958.2008.06407.x

Eksi, S., Czesny, B., van Gemert, G. J., Sauerwein, R. W., Eling, W., and Williamson, K. C. (2006). Malaria Transmission-Blocking Antigen, Pfs230, Mediates Human Red Blood Cell Binding to Exflagellating Male Parasites and Oocyst Production. *Mol. Microbiol.* 61 (4), 991–998. doi: 10.1111/j.1365-2958.2006.05284.x

Eksi, S., and Williamson, K. C. (2002). Male-Specific Expression of the Paralog of Malaria Transmission Blocking Target Antigen Pfs230, PfB0400w. *Mol. Biochem. Parasitol.* 122 (2), 127–130. doi: 10.1016/S0166-6851(02)00091-9

Evans, R., O'Neill, M., Pritzel, A., Antropova, N., Senior, A., Green, T., et al. (2022). Protein Complex Prediction With AlphaFold-Multimer. *bioRxiv* https. doi: 10.1101/2021.10.04.463034

Farrance, C. E., Rhee, A., Jones, R. M., Musiychuk, K., Shamloul, M., Sharma, S., et al. (2011). A Plant-Produced Pfs230 Vaccine Candidate Blocks Transmission of Plasmodium Falciparum. *Clin. Vaccine Immunol.* 18 (8), 1351–1375. doi: 10.1128/CVI.05105-11

Feller, T., Thom, P., Koch, N., Spiegel, H., Addai-Mensah, O., Fischer, R., et al. (2013). Plant-Based Production of Recombinant Plasmodium Surface Protein Pf38 and Evaluation of its Potential as a Vaccine Candidate. *PLoS One* 8 (11), e79920. doi: 10.1371/journal.pone.0079920

Fernandes, P., Loubens, M., Marinach, C., Coppée, R., Grand, M., Andre, T.-P., et al. (2021). *Plasmodium* Sporozoites Require the Protein B9 to Invade Hepatocytes. *bioRxiv* https. doi: 10.1101/2021.10.25.465731

Garcia, J., Curtidor, H., Pinzon, C. G., Vanegas, M., Moreno, A., and Patarroyo, M. E. (2009). Identification of Conserved Erythrocyte Binding Regions in Members of the Plasmodium Falciparum Cys6 Lipid Raft-Associated Protein Family. *Vaccine* 27 (30), 3953–3962. doi: 10.1016/j.vaccine.2009.04.039

Gardner, M. J., Hall, N., Fung, E., White, O., Berriman, M., Hyman, R. W., et al. (2002). Genome Sequence of the Human Malaria Parasite *Plasmodium Falciparum*. *Nature* 419 (6906), 498–511. doi: 10.1038/nature01097

Gaudinski, M. R., Berkowitz, N. M., Idris, A. H., Coates, E. E., Holman, L. A., Mendoza, F., et al. (2021). A Monoclonal Antibody for Malaria Prevention. *N Engl. J. Med.* 385 (9), 803–814. doi: 10.1056/NEJMoa2034031

Gerloff, D. L., Creasey, A., Maslau, S., and Carter, R. (2005). Structural Models for the Protein Family Characterized by Gamete Surface Protein Pfs230 of Plasmodium Falciparum. *Proc. Natl. Acad. Sci. U.S.A.* 102 (38), 13598–13603. doi: 10.1073/pnas.0502378102

Gilson, P. R., Nebl, T., Vukcevic, D., Moritz, R. L., Sargeant, T., Speed, T. P., et al. (2006). Identification and Stoichiometry of Glycosylphosphatidylinositol-Anchored Membrane Proteins of the Human Malaria Parasite Plasmodium Falciparum. *Mol. Cell Proteomics* 5 (7), 1286–1299. doi: 10.1074/mcp.M600035-MCP200

Graves, P. M., Carter, R., Burkot, T. R., Quakyi, I. A., and Kumar, N. (1998). Antibodies to *Plasmodium Falciparum* Gamete Surface Antigens in Papua New Guinea Sera. *Parasite Immunol.* 10, 209–218. doi: 10.1111/j.1365-3024.1988.tb00215.x

Gupta, D. K., Dembele, L., Voorberg-van der Wel, A., Roma, G., Yip, A., Chuenchob, V., et al. (2019). The Plasmodium Liver-Specific Protein 2 (LISP2) is an Early Marker of Liver Stage Development. *Elife* 8, e43362. doi: 10.7554/eLife.43362

Harupa, A. (2015). *Identification and Functional Analysis of Novel Sporozoite Surface Proteins in the Rodent Malaria Parasite Plasmodium Yoelii* (Berlin: Doctor rerum naturalium (Dr. rer. nat.), Department of Biology, Chemistry and Pharmacy, Freie Universität Berlin). doi: 10.17169/refubium-4904

Healer, J., McGuinness, D., Hopcroft, P., Haley, S., Carter, R., and Riley, E. (1997). Complement-Mediated Lysis of *Plasmodium Falciparum* Gametes by Malaria-Immune Human Sera Is Associated With Antibodies to the Gamete Surface Antigen Pfs230. *Infect. Immun.* 65 (8), 3017–3023. doi: 10.1128/iai.65.8.3017-3023.1997

Healy, S. A., Anderson, C., Swihart, B. J., Mwakingwe, A., Gabriel, E. E., Decederfelt, H., et al. (2021). Pfs230 Yields Higher Malaria Transmission-Blocking Vaccine Activity Than Pfs25 in Humans But Not Mice. *J. Clin. Invest.* 131 (7), e146221. doi: 10.1172/JCI146221

He, X. L., Grigg, M. E., Boothroyd, J. C., and Garcia, K. C. (2002). Structure of the Immunodominant Surface Antigen From the Toxoplasma Gondii SRS Superfamily. *Nat. Struct. Biol.* 9 (8), 606–611. doi: 10.1038/nsb819

Ho, C. M., Beck, J. R., Lai, M., Cui, Y., Goldberg, D. E., Egea, P. F., et al. (2018). Malaria Parasite Translocon Structure and Mechanism of Effector Export. *Nature* 561 (7721), 70–75. doi: 10.1038/s41586-018-0469-4

Ho, C. M., Jih, J., Lai, M., Li, X., Goldberg, D. E., Beck, J. R., et al. (2021). Native Structure of the RhopH Complex, a Key Determinant of Malaria Parasite Nutrient Acquisition. *Proc. Natl. Acad. Sci. U.S.A.* 118 (35), e2100514118. doi: 10.1073/pnas.2100514118

Hostetler, J. B., Sharma, S., Bartholdson, S. J., Wright, G. J., Fairhurst, R. M., and Rayner, J. C. (2015). A Library of Plasmodium Vivax Recombinant Merozoite Proteins Reveals New Vaccine Candidates and Protein-Protein Interactions. *PLoS Negl. Trop. Dis.* 9 (12), e0004264. doi: 10.1371/journal.pntd.0004264

Huang, W. C., Deng, B., Seffouh, A., Ortega, J., Long, C. A., Suresh, R. V., et al. (2020). Antibody Response of a Particle-Inducing, Liposome Vaccine Adjuvant Admixed With a Pfs230 Fragment. *NPJ Vaccines* 5 (1), 23. doi: 10.1038/s41541-020-0173-x

Jones, C. S., Luong, T., Hannon, M., Tran, M., Gregory, J. A., Shen, Z., et al. (2013). Heterologous Expression of the C-Terminal Antigenic Domain of the Malaria Vaccine Candidate Pfs48/45 in the Green Algae Chlamydomonas Reinhardtii. *Appl. Microbiol. Biotechnol.* 97 (5), 1987–1995. doi: 10.1007/s00253-012-4071-7

Jumper, J., Evans, R., Pritzel, A., Green, T., Figurnov, M., Ronneberger, O., et al. (2021). "Highly Accurate Protein Structure Prediction With AlphaFold. *Nature* 596 (7873), 583–589. doi: 10.1038/s41586-021-03819-2

Kana, I. H., Garcia-Senosiain, A., Singh, S. K., Tiendrebeogo, R. W., Chourasia, B. K., Malhotra, P., et al. (2018). Cytophilic Antibodies Against Key Plasmodium Falciparum Blood Stage Antigens Contribute to Protection Against Clinical Malaria in a High Transmission Region of Eastern India. *J. Infect. Dis.* 218 (6), 956–965. doi: 10.1093/infdis/jiy258

Kana, I. H., Singh, S. K., Garcia-Senosiain, A., Dodoo, D., Singh, S., Adu, B., et al. (2019). Breadth of Functional Antibodies Is Associated With Plasmodium Falciparum Merozoite Phagocytosis and Protection Against Febrile Malaria. *J. Infect. Dis.* 220 (2), 275–284. doi: 10.1093/infdis/jiz088

Kappe, S. H., Gardner, M. J., Brown, S. M., Ross, J., Matuschewski, K., Ribeiro, J. M., et al. (2001). Exploring the Transcriptome of the Malaria Sporozoite Stage. *Proc. Natl. Acad. Sci. U.S.A.* 98 (17), 9895–9900. doi: 10.1073/pnas.171185198

Kaur, H., Pacheco, M. A., Garber, L., Escalante, A. A., and Vinetz, J. M. (2022). Evolutionary Insights Into the Microneme-Secreted, Chitinase Containing High-Molecular-Weight Protein Complexes Involved in *Plasmodium* Invasion of the Mosquito Midgut. *Infect. Immun.* 90 (1), e00314–21. doi: 10.1128/IAI.00314-21

Kaushansky, A., Douglass, A. N., Arang, N., Vigdorovich, V., Dambrauskas, N., Kain, H. S., et al. (2015). Malaria Parasites Target the Hepatocyte Receptor

EphA2 for Successful Host Infection. *Science* 350 (6264), 1089–1092. doi: 10.1126/science.aad3318

Kennedy, A. T., Schmidt, C. Q., Thompson, J. K., Weiss, G. E., Taechalertpaisarn, T., Gilson, P. R., et al. (2016). Recruitment of Factor H as a Novel Complement Evasion Strategy for Blood-Stage Plasmodium Falciparum Infection. *J. Immunol.* 196 (3), 1239–1248. doi: 10.4049/jimmunol.1501581

Kim, J., Tan, Y. Z, Wicht, K. J., Erramilli, S. K., Dhingra, S. K., Okombo, J., et al. (2019). Structure and Drug Resistance of the Plasmodium Falciparum Transporter PfCRT. *Nature* 576 (7786), 315–320. doi: 10.1038/s41586-019-1795-x

Kocken, C. H. M., Jansen, J., Kaan, A. M., Beckers, P. J. A., Ponnudurai, T., Kaslow, D. C., et al. (1993). Cloning and Expression of the Gene Coding for the Transmission Blocking Target Antigen Pfs48/45 of *Plasmodium Falciparum*. *Mol. Biochem. Parasitol.* 61, 59–68. doi: 10.1016/0166-6851(93)90158-t

Kublin, J. G., Mikolajczak, S. A., Sack, B. K., Fishbaugher, M. E., Seilie, A., Shelton, L., et al. (2017). Complete Attenuation of Genetically Engineered *Plasmodium Falciparum* Sporozoites in Human Subjects. *Sci. Trans. Med.* 9, 371. doi: 10.1126/scitranslmed.aad9099

Kumar, N. (1987). Target Antigens of Malaria Transmission Blocking Immunity Exist as a Stable Membrane Bound Complex. *Parasite Immunol.* 9, 321–335. doi: 10.1111/j.1365-3024.1987.tb00511.x

Kumar, N., and Wizel, B. (1992). Further Characterization of Interactions Between Gamete Surface Antigens of *Plasmodium Falciparum*. *Mol. Biochem. Parasitol.* 53, 113–120. doi: 10.1016/0166-6851(92)90013-a

Kundu, P., Semesi, A., Jore, M. M., Morin, M. J., Price, V. L., Liang, A., et al. (2018). Structural Delineation of Potent Transmission-Blocking Epitope I on Malaria Antigen Pfs48/45. *Nat. Commun.* 9 (1) 4458. doi: 10.1038/s41467-018-06742-9

Lasonder, E., Janse, C. J., van Gemert, G. J., Mair, G. R., Vermunt, A. M., Douradinha, B. G., et al. (2008). Proteomic Profiling of Plasmodium Sporozoite Maturation Identifies New Proteins Essential for Parasite Development and Infectivity. *PLoS Pathog.* 4 (10), e1000195. doi: 10.1371/journal.ppat.1000195

Lee, S. M., Hickey, J. M., Miura, K., Joshi, S. B., Volkin, D. B., King, C. R., et al. (2020). A C-Terminal Pfs48/45 Malaria Transmission-Blocking Vaccine Candidate Produced in the Baculovirus Expression System. *Sci. Rep.* 10 (1), 395. doi: 10.1038/s41598-019-57384-w

Lee, S. M., Plieskatt, J., Krishnan, S., Raina, M., Harishchandra, R., and King, C. R. (2019a). Expression and Purification Optimization of an N-Terminal Pfs230 Transmission-Blocking Vaccine Candidate. *Protein Expr Purif* 160, 56–65. doi: 10.1016/j.pep.2019.04.001

Lee, S. M., Wu, Y., Hickey, J. M., Miura, K., Whitaker, N., Joshi, S. B., et al. (2019b). The Pfs230 N-Terminal Fragment, Pfs230D1+: Expression and Characterization of a Potential Malaria Transmission-Blocking Vaccine Candidate. *Malar J.* 18 (1), 356. doi: 10.1186/s12936-019-2989-2

Lee, S. M., Wu, C. K., Plieskatt, J. L., Miura, K., Hickey, J. M., and King, C. R. (2017). N-Terminal Pfs230 Domain Produced in Baculovirus as a Biological Active Transmission-Blocking Vaccine Candidate. *Clin. Vaccine Immunol.* 24 (10), e00140–17. doi: 10.1128/CVI.00140-17

Lennartz, F., Brod, F., Dabbs, R., Miura, K., Mekhaiel, D., Marini, A., et al. (2018). Structural Basis for Recognition of the Malaria Vaccine Candidate Pfs48/45 by a Transmission Blocking Antibody. *Nat. Commun.* 9 (1), 3822. doi: 10.1038/s41467-018-06340-9

Li, J., Ito, D., Chen, J. H., Lu, F., Cheng, Y., Wang, B., et al. (2012). Pv12, a 6-Cys Antigen of Plasmodium Vivax, is Localized to the Merozoite Rhoptry. *Parasitol. Int.* 61 (3), 443–449. doi: 10.1016/j.parint.2012.02.008

Lindner, S. E., Swearingen, K. E., Harupa, A., Vaughan, A. M., Sinnis, P., Moritz, R. L., et al. (2013). Total and Putative Surface Proteomics of Malaria Parasite Salivary Gland Sporozoites. *Mol. Cell Proteomics* 12 (5), 1127–1143. doi: 10.1074/mcp.M112.024505

Lopez-Barragan, M. J., Lemieux, J., Quinones, M., Williamson, K. C., Molina-Cruz, A., Cui, K., et al. (2011). Directional Gene Expression and Antisense Transcripts in Sexual and Asexual Stages of Plasmodium Falciparum. *BMC Genomics* 12, 587. doi: 10.1186/1471-2164-12-587

Lyu, M., Su, C. C., Kazura, J. W., and Yu, E. W. (2021). Structural Basis of Transport and Inhibition of the Plasmodium Falciparum Transporter PfFNT. *EMBO Rep.* 22 (3), e51628. doi: 10.15252/embr.202051628

MacDonald, N. J., Nguyen, V., Shimp, R., Reiter, K., Herrera, R., Burkhardt, M., et al. (2016). Structural and Immunological Characterization of Recombinant 6-Cysteine Domains of the Plasmodium Falciparum Sexual Stage Protein Pfs230. *J. Biol. Chem.* 291 (38), 19913–19922. doi: 10.1074/jbc.M116.732305

Mamedov, T., Cicek, K., Gulec, B., Ungor, R., and Hasanova, G. (2017). *In Vivo* Production of non-Glycosylated Recombinant Proteins in Nicotiana Benthamiana Plants by Co-Expression With Endo-Beta-N-Acetylglucosaminidase H (Endo H) of Streptomyces Plicatus. *PLoS One* 12 (8), e0183589. doi: 10.1371/journal.pone.0183589

Mamedov, T., Cicek, K., Miura, K., Gulec, B., Akinci, E., Mammadova, G., et al. (2019). A Plant-Produced *In Vivo* Deglycosylated Full-Length Pfs48/45 as a Transmission-Blocking Vaccine Candidate Against Malaria. *Sci. Rep.* 9 (1) 9868. doi: 10.1038/s41598-019-46375-6

Mamedov, T., Ghosh, A., Jones, R. M., Mett, V., Farrance, C. E., Musiychuk, K., et al. (2012). Production of non-Glycosylated Recombinant Proteins in Nicotiana Benthamiana Plants by Co-Expressing Bacterial PNGase F. *Plant Biotechnol. J.* 10 (7), 773–782. doi: 10.1111/j.1467-7652.2012.00694.x

Manzoni, G., Marinach, C., Topcu, S., Briquet, S., Grand, M., Tolle, M., et al. (2017). Plasmodium P36 Determines Host Cell Receptor Usage During Sporozoite Invasion. *Elife* 6, e25903. doi: 10.7554/eLife.25903

Marin-Mogollon, C., van de Vegte-Bolmer, M., van Gemert, G. J., van Pul, F. J. A., Ramesar, J., Othman, A. S., et al. (2018). The Plasmodium Falciparum Male Gametocyte Protein P230p, a Paralog of P230, is Vital for Ookinete Formation and Mosquito Transmission. *Sci. Rep.* 8 (1), 149025. doi: 10.1038/s41598-018-33236-x

Menon, V., Kapulu, M. C., Taylor, I., Jewell, K., Li, Y., Hill, F., et al. (2017). Assessment of Antibodies Induced by Multivalent Transmission-Blocking Malaria Vaccines. *Front. Immunol.* 8. doi: 10.3389/fimmu.2017.01998

Milek, R. L. B., Roeffen, W. F. G., Kocken, C. H. M., Jansen, J., Kaan, A. M., Eling, W. M. C., et al. (1998). Immunological Properties of Recombinant Proteins of the Transmission Blocking Vaccine Candidate, Pfs48/45, of the Human Malaria Parasite *Plasmodium Falciparum* Produced in *Escherichia Coli*. *Parasite Immunol.* 20, 377–385. doi: 10.1046/j.1365-3024.1998.00171.x

Milek, R. L. B., Stunnenberg, H. G., and Konings, R. N. H. (2000). Assembly and Expression of a Synthetic Gene Encoding the Antigen Pfs48/45 of the Human Malaria Parasite *Plasmodium Falciparum* in Yeast. *Vaccine* 18, 1402–1411. doi: 10.1016/s0264-410x(99)00392-8

Mistarz, U. H., Singh, S. K., Tttn Nguyen, W., Yang, F., Lissau, C., Madsen, S. M., et al. (2017). Expression, Purification and Characterization of GMZ2'.10C, a Complex Disulphide-Bonded Fusion Protein Vaccine Candidate Against the Asexual and Sexual Life-Stages of the Malaria-Causing Plasmodium Falciparum Parasite. *Pharm. Res.* 34 (9), 1970–19835. doi: 10.1007/s11095-017-2208-1

Miura, K., Deng, B., Wu, Y., Zhou, L., Pham, T. P., Diouf, A., et al. (2019). ELISA Units, IgG Subclass Ratio and Avidity Determined Functional Activity of Mouse Anti-Pfs230 Antibodies Judged by a Standard Membrane-Feeding Assay With Plasmodium Falciparum. *Vaccine* 37 (15), 2073–2078. doi: 10.1016/j.vaccine.2019.02.071

Miura, K., Takashima, E., Deng, B., Tullo, G., Diouf, A., Moretz, S. E., et al. (2013). Functional Comparison of Plasmodium Falciparum Transmission-Blocking Vaccine Candidates by the Standard Membrane-Feeding Assay. *Infect. Immun.* 81 (12), 4377–4382. doi: 10.1128/iai.01056-13

Miura, K., Takashima, E., Pham, T. P., Deng, B., Zhou, L., Huang, W. C., et al. (2022). Elucidating Functional Epitopes Within the N-Terminal Region of Malaria Transmission Blocking Vaccine Antigen Pfs230. *NPJ Vaccines* 7 (1), 4. doi: 10.1038/s41541-021-00423-3

Molina-Cruz, A., Canepa, G. E., E. Silva, T. L., Williams, A. E., Nagyal, S., Yenkoidiok-Douti, L., et al. (2020). Plasmodium Falciparum Evades Immunity of Anopheline Mosquitoes by Interacting With a Pfs47 Midgut Receptor. *Proc. Natl. Acad. Sci. U.S.A.* 117 (5), 2597–26055. doi: 10.1073/pnas.1917042117

Molina-Cruz, A., Garver, L. S., Alabaster, A., Bangiolo, L., Haile, A., Winikor, J., et al. (2013). The Human Malaria Parasite Pfs47 Gene Mediates Evasion of the Mosquito Immune System. *Science* 340 (6135), 984–987. doi: 10.1126/science.1235264

Mulder, B., Lensen, T., Tchuinkam, T., Roeffen, W., Verhave, J. P., Boudin, C., et al. (1999). *Plasmodium Falciparum*: Membrane Feeding Assays and Competition ELISAs for the Measurement of Transmission Reduction in Sera From Cameroon. *Exp. Parasitol.* 92, 81–86. doi: 10.1006/expr.1999.4398

Muller-Sienerth, N., Shilts, J., Kadir, K. A., Yman, V., Homann, M. V., Asghar, M., et al. (2020). A Panel of Recombinant Proteins From Human-Infective Plasmodium Species for Serological Surveillance. *Malar J.* 19 (1), 31. doi: 10.1186/s12936-020-3111-5

Muthui, M. K., Takashima, E., Omondi, B. R., Kinya, C., Muasya, W. I., Nagaoka, H., et al. (2021). Characterization of Naturally Acquired Immunity to a Panel of Antigens Expressed in Mature P. Falciparum Gametocytes. *Front. Cell Infect. Microbiol.* 11. doi: 10.3389/fcimb.2021.774537

Nakane, T., Kotecha, A., Sente, A., McMullan, G., Masiulis, S., Pmge Brown, I. T., et al. (2020). Single-Particle Cryo-EM at Atomic Resolution. *Nature* 587 (7832), 152–156. doi: 10.1038/s41586-020-2829-0

Orito, Y., Ishino, T., Iwanaga, S., Kaneko, I., Kato, T., Menard, R., et al. (2013). Liver-Specific Protein 2: A Plasmodium Protein Exported to the Hepatocyte Cytoplasm and Required for Merozoite Formation. *Mol. Microbiol.* 87 (1), 66–79. doi: 10.1111/mmi.12083

Osier, F. H., Mackinnon, M. J., Crosnier, C., Fegan, G., Kamuyu, G., Wanaguru, M., et al. (2014). New Antigens for a Multicomponent Blood-Stage Malaria Vaccine. *Sci. Transl. Med.* 6 (247), 247ra102. doi: 10.1126/scitranslmed.3008705

Ouédraogo, AndréL., Roeffen, W., Luty, A. J.F., de Vlas, S. J., Nebie, I., Ilboudo-Sanogo, E., et al. (2011). Naturally Acquired Immune Responses to Plasmodium Falciparum Sexual Stage Antigens Pfs48/45 and Pfs230 in an Area of Seasonal Transmission. *Infect Immun.* 79 (12), 4957–49645. doi: 10.1128/iai.05288-11

Outchkourov, N. S., Roeffen, W., Kaan, A., Jansen, J., Luty, A., Schuiffel, D., et al. (2008). Correctly Folded Pfs48/45 Protein of Plasmodium Falciparum Elicits Malaria Transmission-Blocking Immunity in Mice. *Proc. Natl. Acad. Sci. U.S.A.* 105 (11), 4301–4355. doi: 10.1073/pnas.0800459105

Outchkourov, N., Vermunt, A., Jansen, J., Kaan, A., Roeffen, W., Teelen, K., et al. (2007). Epitope Analysis of the Malaria Surface Antigen Pfs48/45 Identifies a Subdomain That Elicits Transmission Blocking Antibodies. *J. Biol. Chem.* 282 (23), 17148–17565. doi: 10.1074/jbc.M700948200

Parker, M. L., Peng, F., and Boulanger, M. J. (2015). The Structure of Plasmodium Falciparum Blood-Stage 6-Cys Protein Pf41 Reveals an Unexpected Intra-Domain Insertion Required for Pf12 Coordination. *PLoS One* 10 (9), e0139407. doi: 10.1371/journal.pone.0139407

Patel, P. N., and Tolia, N. (2021). Structural Vaccinology of Malaria Transmission-Blocking Vaccines. *Expert Rev. Vaccines* 20 (2), 199–214. doi: 10.1080/14760584.2021.1873135

Premawansa, S., Gamage-Mendis, A., Perera, L., Begarnie, S., Mendis, K., and Carter, R. (1994). *Plasmodium Falciparum* Malaria Transmission-Blocking Immunity Under Conditions of Low Endemicity as in Sri Lanka. *Parasite Immunol.* 16, 35–42. doi: 10.1111/j.1365-3024.1994.tb00302.x

Pritsch, M., Ben-Khaled, N., Chaloupka, M., Kobold, S., Berens-Riha, N., Peter, A., et al. (2016). Comparison of Intranasal Outer Membrane Vesicles With Cholera Toxin and Injected MF59C.1 as Adjuvants for Malaria Transmission Blocking Antigens AnAPN1 and Pfs48/45. *J. Immunol. Res.* 2016, 3576028. doi: 10.1155/2016/3576028

Prokhnevsky, A., Mamedov, T., Leffet, B., Rahimova, R., Ghosh, A., Mett, V., et al. (2015). Development of a Single-Replicon miniBYV Vector for Co-Expression of Heterologous Proteins. *Mol. Biotechnol.* 57 (2), 101–110. doi: 10.1007/s12033-014-9806-5

Quakyi, A., Carter, R., Rener, J., Kumar, N., Good, M. F., and Miller, L. H. (1987). The 230-kDa Gamete Surface Protein of Plasmodium Falciparum is Also a Target for Transmission-Blocking Antibodies. *J. Immunol.* 139 (12), 4213–4217.

Ragotte, R. J., Pulido, D., Lias, A. M., Quinkert, D., Alanine, D. G. W., Jamwal, A., et al. (2022). Heterotypic Interactions Drive Antibody Synergy Against a Malaria Vaccine Candidate. *Nat. Commun.* 13 (1), 933. doi: 10.1038/s41467-022-28601-4

Ramiro, R. S., Khan, S. M., Franke-Fayard, B., Janse, C. J., Obbard, D. J., and Reece, S. E. (2015). Hybridization and Pre-Zygotic Reproductive Barriers in Plasmodium. *Proc. Biol. Sci.* 282 (1806), 20143027. doi: 10.1098/rspb.2014.3027

Ramphul, U. N., Garver, L. S., Molina-Cruz, A., Canepa, G. E., and Barillas-Mury, C. (2015). Plasmodium Falciparum Evades Mosquito Immunity by Disrupting JNK-Mediated Apoptosis of Invaded Midgut Cells. *Proc. Natl. Acad. Sci. U.S.A.* 112 (5), 1273–1280. doi: 10.1073/pnas.1423586112

Read, D., Lensen, A. H. W., Begarnie, S., Haley, S., Raza, A., and Carter, R. (1994). Transmission-Blocking Antibodies Against Multiple, non-Variant Target Epitopes of the *Plasmodium Falciparum* Gamete Surface Antigen Pfs230 are All Complement-Fixing. *Parasite Immunol.* 16 (10), 511–519. doi: 10.1111/j.1365-3024.1994.tb00305.x

Rener, J., Graves, P. M., Carter, R., Williams, J. L., and Burkot, T. R. (1983). Target Antigens of Transmission-Blocking Immunity on Gametes of Plasmodium Falciparum. *J. Exp. Med.* 158, 976–981. doi: 10.1084/jem.158.3.976

Richards, J. S., Arumugam, T. U., Reiling, L., Healer, J., Hodder, A. N., Fowkes, F. J., et al. (2013). Identification and Prioritization of Merozoite Antigens as Targets of Protective Human Immunity to Plasmodium Falciparum Malaria for Vaccine and Biomarker Development. *J. Immunol.* 191 (2), 795–809. doi: 10.4049/jimmunol.1300778

Riley, E. M., Williamson, K. C., Greenwood, B. M., and Kaslow, D. C. (1995). Human Immune Recognition of Recombinant Proteins Representing Discrete Domains of the *Plasmodium Falciparum* Gamete Surface Protein, Pfs230. *Parasite Immunol.* 17 (1), 11–19. doi: 10.1111/j.1365-3024.1995.tb00961.x

Roeffen, W., Beckers, P. J. A., Lensen, T. K., Sauerwein, R. W., Meuwissen, J. H. E. T., and Eling, W. (1995a). *Plasmodium Falciparum*: A Comparison of the Activity of Pfs230-Specific Antibodies in an Assay of Transmission-Blocking Immunity and Specific Competition ELISAs. *Exp. Parasitol.* 80 (1), 15–26. doi: 10.1006/expr.1995.1003

Roeffen, W., Geeraedts, F., Eling, W., Beckers, P., Wizel, B., Kumar, N., et al. (1995b). Transmission Blockade of *Plasmodium Falciparum* Malaria by Anti-Pfs230-Specific Antibodies is Isotype Dependent. *Infect. Immun.* 63 (2), 467–471. doi: 10.1128/iai.63.2.467-471.1995

Roeffen, W. F., Raats, J. M., Teelen, K., Hoet, R. M., Eling, W. M., van Venrooij, W. J., et al. (2001a). Recombinant Human Antibodies Specific for the Pfs48/45 Protein of the Malaria Parasite Plasmodium Falciparum. *J. Biol. Chem.* 276 (23), 19807–19811. doi: 10.1074/jbc.M100562200

Roeffen, W., Teelen, K., van As, J., vd Vegte-Bolmer, M., Eling, W., and Sauerwein, R. (2001b). Plasmodium Falciparum: Production and Characterization of Rat Monoclonal Antibodies Specific for the Sexual-Stage Pfs48/45 Antigen. *Exp. Parasitol.* 97 (1), 45–49. doi: 10.1006/expr.2000.4586

Roeffen, W., Theisen, M., van de Vegte-Bolmer, M., van Gemert, G., Arens, T., Andersen, G., et al. (2015). Transmission-Blocking Activity of Antibodies to Plasmodium Falciparum GLURP.10C Chimeric Protein Formulated in Different Adjuvants. *Malar J.* 14, 443. doi: 10.1186/s12936-015-0972-0

Roestenberg, M., Walk, J., van der Boor, S. C., Langenberg, M. C. C., Hoogerwerf, M.-A., Janse, J. J., et al. (2020). A Double-Blind, Placebo-Controlled Phase 1/2a Trial of the Genetically Attenuated Malaria Vaccine PfSPZ-Ga1. *Sci. Trans. Med.* 12, 544. doi: 10.1126/scitranslmed.aaz5629

RTS, S Clinical Trials Partnership (2015). Efficacy and Safety of RTS,S/AS01 Malaria Vaccine With or Without a Booster Dose in Infants and Children in Africa: Final Results of a Phase 3, Individually Randomised, Controlled Trial. *Lancet* 386 (9988), 31–45. doi: 10.1016/s0140-6736(15)60721-8

Sala, K. A., Nishiura, H., Upton, L. M., Zakutansky, S. E., Delves, M. J., Iyori, M., et al. (2015). The Plasmodium Berghei Sexual Stage Antigen PSOP12 Induces Anti-Malarial Transmission Blocking Immunity Both *In Vivo* and *In Vitro*. *Vaccine* 33 (3), 437–445. doi: 10.1016/j.vaccine.2014.11.038

Sanders, P. R., Gilson, P. R., Cantin, G. T., Greenbaum, D. C., Nebl, T., Carucci, D. J., et al. (2005). Distinct Protein Classes Including Novel Merozoite Surface Antigens in Raft-Like Membranes of Plasmodium Falciparum. *J. Biol. Chem.* 280 (48), 40169–40765. doi: 10.1074/jbc.M509631200

Schneider, P., Reece, S. E., van Schaijk, B. C., Bousema, T., Lanke, K. H., Meaden, C. S., et al. (2015). Quantification of Female and Male Plasmodium Falciparum Gametocytes by Reverse Transcriptase Quantitative PCR. *Mol. Biochem. Parasitol.* 199 (1-2), 29–33. doi: 10.1016/j.molbiopara.2015.03.006

Schureck, M. A., Darling, J. E., Merk, A., Shao, J., Daggupati, G., Srinivasan, P., et al. (2021). Malaria Parasites Use a Soluble RhopH Complex for Erythrocyte Invasion and an Integral Form for Nutrient Uptake. *Elife* 10, e65282. doi: 10.7554/eLife.65282

Senior, A. W., Evans, R., Jumper, J., Kirkpatrick, J., Sifre, L., Green, T., et al. (2020). Improved Protein Structure Prediction Using Potentials From Deep Learning. *Nature* 577 (7792), 706–710. doi: 10.1038/s41586-019-1923-7

Simon, N., Kuehn, A., Williamson, K. C., and Pradel, G. (2016). Adhesion Protein Complexes of Malaria Gametocytes Assemble Following Parasite Transmission to the Mosquito. *Parasitol. Int.* 65 (1), 27–30. doi: 10.1016/j.parint.2015.09.007

Singh, K., Burkhardt, M., Nakuchima, S., Herrera, R., Muratova, O., Gittis, A. G., et al. (2020). Structure and Function of a Malaria Transmission Blocking Vaccine Targeting Pfs230 and Pfs230-Pfs48/45 Proteins. *Commun. Biol.* 3 (1), 395. doi: 10.1038/s42003-020-01123-9

Singh, S. K., Plieskatt, J., Chourasia, B. K., Fabra-Garcia, A., Garcia-Senosiain, A., Singh, V., et al. (2021a). A Reproducible and Scalable Process for Manufacturing a Pfs48/45 Based Plasmodium Falciparum Transmission-Blocking Vaccine. *Front. Immunol.* 11. doi: 10.3389/fimmu.2020.606266

Singh, S. K., Plieskatt, J., Chourasia, B. K., Singh, V., Bengtsson, K. L., Reimer, J. M., et al. (2021b). Preclinical Development of a Pfs230-Pfs48/45 Chimeric Malaria Transmission-Blocking Vaccine. *NPJ Vaccines* 6 (1), 1205. doi: 10.1038/s41541-021-00383-8

Singh, S. K., Roeffen, W., Andersen, G., Bousema, T., Christiansen, M., Sauerwein, R., et al. (2015). A Plasmodium Falciparum 48/45 Single Epitope R0.6C Subunit Protein Elicits High Levels of Transmission Blocking Antibodies. *Vaccine* 33 (16), 1981–1986. doi: 10.1016/j.vaccine.2015.02.040

Singh, S. K., Roeffen, W., Mistarz, U. H., Chourasia, B. K., Yang, F., Rand, K. D., et al. (2017a). Construct Design, Production, and Characterization of Plasmodium Falciparum 48/45 R0.6C Subunit Protein Produced in Lactococcus Lactis as Candidate Vaccine. *Microb. Cell Fact* 16 (1), 97. doi: 10.1186/s12934-017-0710-0

Singh, S. K., Thrane, S., Chourasia, B. K., Teelen, K., Graumans, W., Stoter, R., et al. (2019). Pfs230 and Pfs48/45 Fusion Proteins Elicit Strong Transmission-Blocking Antibody Responses Against Plasmodium Falciparum. *Front. Immunol.* 10. doi: 10.3389/fimmu.2019.01256

Singh, S. K., Thrane, S., Janitzek, C. M., Nielsen, M. A., Theander, T. G., Theisen, M., et al. (2017b). Improving the Malaria Transmission-Blocking Activity of a Plasmodium Falciparum 48/45 Based Vaccine Antigen by SpyTag/SpyCatcher Mediated Virus-Like Display. *Vaccine* 35 (30), 3726–3732. doi: 10.1016/j.vaccine.2017.05.054

Singh, S. K., Tiendrebeogo, R. W., Chourasia, B. K., Kana, I. H., Singh, S., and Theisen, M. (2018). Lactococcus Lactis Provides an Efficient Platform for Production of Disulfide-Rich Recombinant Proteins From Plasmodium Falciparum. *Microb. Cell Fact* 17 (1), 55. doi: 10.1186/s12934-018-0902-2

Stone, W. J. R., Campo, J. J., Ouedraogo, A. L., Meerstein-Kessel, L., Morlais, I., Da, D., et al. (2018). Unravelling the Immune Signature of Plasmodium Falciparum Transmission-Reducing Immunity. *Nat. Commun.* 9 (1), 5585. doi: 10.1038/s41467-017-02646-2

Swearingen, K. E., Lindner, S. E., Shi, L., Shears, M. J., Harupa, A., Hopp, C. S., et al. (2016). Interrogating the Plasmodium Sporozoite Surface: Identification of Surface-Exposed Proteins and Demonstration of Glycosylation on CSP and TRAP by Mass Spectrometry-Based Proteomics. *PLoS Pathog.* 12 (4), e1005606. doi: 10.1371/journal.ppat.1005606

Tachibana, M., Miura, K., Takashima, E., Morita, M., Nagaoka, H., Zhou, L., et al. (2019). Identification of Domains Within Pfs230 That Elicit Transmission Blocking Antibody Responses. *Vaccine* 37 (13), 1799–1806. doi: 10.1016/j.vaccine.2019.02.021

Tachibana, M., Suwanabun, N., Kaneko, O., Iriko, H., Otsuki, H., Sattabongkot, J., et al. (2015). Plasmodium Vivax Gametocyte Proteins, Pvs48/45 and Pvs47, Induce Transmission-Reducing Antibodies by DNA Immunization. *Vaccine* 33 (16), 1901–1908. doi: 10.1016/j.vaccine.2015.03.008

Tachibana, M., Wu, Y., Iriko, H., Muratova, O., MacDonald, N. J., Sattabongkot, J., et al. (2011). N-Terminal Prodomain of Pfs230 Synthesized Using a Cell-Free System is Sufficient to Induce Complement-Dependent Malaria Transmission-Blocking Activity. *Clin. Vaccine Immunol.* 18 (8), 1343–1350. doi: 10.1128/CVI.05104-11

Taechalertpaisarn, T., Crosnier, C., Bartholdson, S. J., Hodder, A. N., Thompson, J., Bustamante, L. Y., et al. (2012). Biochemical and Functional Analysis of Two Plasmodium Falciparum Blood-Stage 6-Cys Proteins: P12 and P41. *PLoS One* 7 (7), e41937. doi: 10.1371/journal.pone.0041937

Tang, J., Chisholm, S. A., Yeoh, L. M., Gilson, P. R., Papenfuss, A. T., Day, K. P., et al. (2020). Histone Modifications Associated With Gene Expression and Genome Accessibility are Dynamically Enriched at Plasmodium Falciparum Regulatory Sequences. *Epigenet. Chromatin* 13 (1), 50. doi: 10.1186/s13072-020-00365-5

Targett, G. (1988). *Plasmodium Falciparum*: Natural and Experimental Transmission Blocking Immunity. *Immunol. Lett.* 19, 235–240. doi: 10.1016/0165-2478(88)90148-4

Targett, G. A. T., Harte, P. G., Eida, S., Rogers, N. C., and Ong, C. S. L. (1990). *Plasmodium Falciparum* Sexual Stage Antigens: Immunogenicity and Cell-Mediated Responses. *Immunol. Lett.* 25, 77–82. doi: 10.1016/0165-2478(90)90095-8

Tegunov, D., Xue, L., Dienemann, C., Cramer, P., and Mahamid, J. (2021). Multi-Particle Cryo-EM Refinement With M Visualizes Ribosome-Antibiotic Complex at 3.5 A in Cells. *Nat. Methods* 18 (2), 186–193. doi: 10.1038/s41592-020-01054-7

Templeton, T. J., and Kaslow, D. C. (1999). Identification of Additional Members Define a *Plasmodium Falciparum* Gene Superfamily Which Includes Pfs48/45 and Pfs230. *Mol. Biochem. Parasitol.* 101, 223–227. doi: 10.1016/S0166-6851(99)00066-3

Theisen, M., Jore, M. M., and Sauerwein, R. (2017). Towards Clinical Development of a Pfs48/45-Based Transmission Blocking Malaria Vaccine. *Expert Rev. Vaccines* 16 (4), 329–336. doi: 10.1080/14760584.2017.1276833

Theisen, M., Roeffen, W., Singh, S. K., Andersen, G., Amoah, L., van de Vegte-Bolmer, M., et al. (2014). A Multi-Stage Malaria Vaccine Candidate Targeting Both Transmission and Asexual Parasite Life-Cycle Stages. *Vaccine* 32 (22), 2623–2305. doi: 10.1016/j.vaccine.2014.03.020

Thompson, J., Janse, C. J., and Waters, A. P. (2001). Comparative Genomics in *Plasmodium*: A Tool for the Identification of Genes and Functional Analysis. *Mol. Biochem. Parasitol.* 118, 147–154. doi: 10.1016/S0166-6851(01)00377-2

Toenhake, C. G., Fraschka, S. A., Vijayabaskar, M. S., Westhead, D. R., van Heeringen, S. J., and Bartfai, R. (2018). Chromatin Accessibility-Based Characterization of the Gene Regulatory Network Underlying Plasmodium Falciparum Blood-Stage Development. *Cell Host Microbe* 23 (4), 557–569.e9. doi: 10.1016/j.chom.2018.03.007

Tonkin, M. L., Arredondo, S. A., Loveless, B. C., Serpa, J. J., Makepeace, K. A., Sundar, N., et al. (2013). Structural and Biochemical Characterization of Plasmodium Falciparum 12 (Pf12) Reveals a Unique Interdomain Organization and the Potential for an Antiparallel Arrangement With Pf41. *J. Biol. Chem.* 288 (18), 12805–12817. doi: 10.1074/jbc.M113.455667

Tsuboi, T., Takeo, S., Iriko, H., Jin, L., Tsuchimochi, M., Matsuda, S., et al. (2008). Wheat Germ Cell-Free System-Based Production of Malaria Proteins for Discovery of Novel Vaccine Candidates. *Infect. Immun.* 76 (4), 1702–1708. doi: 10.1128/IAI.01539-07

Ukegbu, C. V., Giorgalli, M., Yassine, H., Ramirez, J. L., Taxiarchi, C., Barillas-Mury, C., et al. (2017). Plasmodium Berghei P47 is Essential for Ookinete Protection From the Anopheles Gambiae Complement-Like Response. *Sci. Rep.* 7 (1) 6026. doi: 10.1038/s41598-017-05917-6

Uwimana, A., Legrand, E., Stokes, B. H., Ndikumana, J. M., Warsame, M., Umulisa, N., et al. (2020). Emergence and Clonal Expansion of *In Vitro* Artemisinin-Resistant Plasmodium Falciparum Kelch13 R561H Mutant Parasites in Rwanda. *Nat. Med.* 26 (10), 1602–1608. doi: 10.1038/s41591-020-1005-2

Uwimana, A., Umulisa, N., Venkatesan, M., Svigel, S. S., Zhou, Z., Munyaneza, T., et al. (2021). Association of Plasmodium Falciparum Kelch13 R561H Genotypes With Delayed Parasite Clearance in Rwanda: An Open-Label, Single-Arm, Multicentre, Therapeutic Efficacy Study. *Lancet Infect. Dis.* 21 (8), 1120–11285. doi: 10.1016/s1473-3099(21)00142-0

van der Kolk, M., de Vlas, S. J., and Sauerwein, R. W. (2006). Reduction and Enhancement of Plasmodium Falciparum Transmission by Endemic Human Sera. *Int. J. Parasitol.* 36 (10-11), 1091–1095. doi: 10.1016/j.ijpara.2006.05.004

van Dijk, M. R., Janse, C. J., Thompson, J., Waters, A. P., Braks, J. A. M., Dodemont, H. J., et al. (2001). A Central Role for P48/45 in Malaria Parasite Male Gamete Fertility. *Cell* 104, 153–164. doi: 10.1016/s0092-8674(01)00199-4

van Dijk, M. R., van Schaijk, B. C., Khan, S. M., van Dooren, M. W., Ramesar, J., Kaczanowski, S., et al. (2010). Three Members of the 6-Cys Protein Family of Plasmodium Play a Role in Gamete Fertility. *PLoS Pathog.* 6 (4), e1000853. doi: 10.1371/journal.ppat.1000853

van Schaijk, B. C., van Dijk, M. R., van Gemert, G. J., van Dooren, M. W., Eksi, S., Roeffen, W. F., et al. (2006). Pfs47, Paralog of the Male Fertility Factor Pfs48/45, is a Female Specific Surface Protein in Plasmodium Falciparum.". *Mol. Biochem. Parasitol.* 149 (2), 216–225. doi: 10.1016/j.molbiopara.2006.05.015

Vaughan, A. M., Sack, B. K., Dankwa, D., Minkah, N., Nguyen, T., Cardamone, H., et al. (2018). A Plasmodium Parasite With Complete Late Liver Stage Arrest Protects Against Preerythrocytic and Erythrocytic Stage Infection in Mice. *Infect. Immun.* 86 (5), e00088–18. doi: 10.1128/IAI.00088-18

Vermeulen, A. N., Ponnudurai, T., Beckers, P. J. A., Verhave, J. P., Smits, M. A., and Meuwissen, J. H. E. T. (1985). Sequential Expression of Antigens on Sexual Stages of Plasmodium Falciparum Accessible to Transmission-Blocking Antibodies in the Mosquito. *J. Exp. Med.* 162, 1460–1476. doi: 10.1084/jem.162.5.1460

Vermeulen, A. N., van Deursen, J., Brakenhoff, R. H., Lensen, T. H. W., Ponnudurai, T., and Meuwissen, J. H. E. T. (1986). Characterization of *Plasmodium Falciparum* Sexual Stage Antigens and Their Biosynthesis in Synchronised Gametocyte Cultures. *Mol. Biochem. Parasitol.* 20, 155–163. doi: 10.1016/0166-6851(86)90027-7

Wagner, F. R., Watanabe, R., Schampers, R., Singh, D., Persoon, H., Schaffer, M., et al. (2020). Preparing Samples From Whole Cells Using Focused-Ion-Beam Milling for Cryo-Electron Tomography. *Nat. Protoc.* 15 (6), 2041–2070. doi: 10.1038/s41596-020-0320-x

Wetzel, D., Chan, J. A., Suckow, M., Barbian, A., Weniger, M., Jenzelewski, V., et al. (2019). Display of Malaria Transmission-Blocking Antigens on Chimeric Duck Hepatitis B Virus-Derived Virus-Like Particles Produced in Hansenula Polymorpha. *PLoS One* 14 (9), e0221394. doi: 10.1371/journal.pone.0221394

WHO (2021). *World Malaria Report 2021* (Geneva: World Health Organization). Available at: https://www.who.int/publications/i/item/9789240040496.

Williamson, K. C., Criscio, M. D., and Kaslow, D. C. (1993). Cloning and Expression of the Gene for *Plasmodium Falciparum* Transmission-Blocking Target Antigen, Pfs230. *Mol. Biochem. Parasitol.* 58, 355–358. doi: 10.1016/0166-6851(93)90058-6

Williamson, K. C., Fujioka, H., Aikawa, M., and Kaslow, D. C. (1996). Stage-Specific Processing of Pfs230, a Plasmodium Falciparum Transmission-Blocking Vaccine Candidate. *Mol. Biochem. Parasitol.* 78 (1-2), 161–169. doi: 10.1016/s0166-6851(96)02621-7

Williamson, K. C., Keister, D. B., Muratova, O., and Kaslow, D. C. (1995). Recombinant Pfs230, a *Plasmodium Falciparum* Gametocyte Protein, Induces Antisera That Reduce the Infectivity of *Plasmodium Falciparum* to Mosquitoes. *Mol. Biochem. Parasitol.* 75, 33–42.

Yenkoidiok-Douti, L., Barillas-Mury, C., and Jewell, C. M. (2021). Design of Dissolvable Microneedles for Delivery of a Pfs47-Based Malaria Transmission-Blocking Vaccine. *ACS Biomater Sci. Eng.* 7 (5), 1854–1862. doi: 10.1021/acsbiomaterials.0c01363

Yenkoidiok-Douti, L., Canepa, G. E., Barletta, A. B. F., and Barillas-Mury, C. (2020). *In Vivo* Characterization of Plasmodium Berghei P47 (Pbs47) as a Malaria Transmission-Blocking Vaccine Target. *Front. Microbiol.* 11. doi: 10.3389/fmicb.2020.01496

Yenkoidiok-Douti, L., Williams, A. E., Canepa, G. E., Molina-Cruz, A., and Barillas-Mury, C. (2019). Engineering a Virus-Like Particle as an Antigenic Platform for a Pfs47-Targeted Malaria Transmission-Blocking Vaccine. *Sci. Rep.* 9 (1), 16833. doi: 10.1038/s41598-019-53208-z

Yip, K. M., Fischer, N., Paknia, E., Chari, A., and Stark, H. (2020). Atomic-Resolution Protein Structure Determination by Cryo-EM. *Nature* 587 (7832), 157–161. doi: 10.1038/s41586-020-2833-4

Yonekura, K., Kato, K., Ogasawara, M., Tomita, M., and Toyoshima, C. (2015). Electron Crystallography of Ultrathin 3D Protein Crystals: Atomic Model With Charges. *Proc. Natl. Acad. Sci. U.S.A.* 112 (11), 3368–3373. doi: 10.1073/pnas.1500724112

Conflict of Interest: The authors declare that the research was conducted in the absence of any commercial or financial relationships that could be construed as a potential conflict of interest.

Publisher's Note: All claims expressed in this article are solely those of the authors and do not necessarily represent those of their affiliated organizations, or those of the publisher, the editors and the reviewers. Any product that may be evaluated in this article, or claim that may be made by its manufacturer, is not guaranteed or endorsed by the publisher.

frontiers | Frontiers in Cellular and Infection Microbiology

TYPE Original Research
PUBLISHED 08 August 2022
DOI 10.3389/fcimb.2022.915792

OPEN ACCESS

EDITED BY
Andrea L. Conroy,
Indiana University, United States

REVIEWED BY
Julio Gallego-Delgado,
Lehman College, United States
Paula Mello De Luca,
Oswaldo Cruz Foundation (Fiocruz), Brazil
Tarun Keswani,
Massachusetts General Hospital and Harvard Medical School, United States
Carla Claser,
University of São Paulo, Brazil

*CORRESPONDENCE
Philippe E. Van den Steen
philippe.vandensteen@kuleuven.be

SPECIALTY SECTION
This article was submitted to Parasite and Host, a section of the journal Frontiers in Cellular and Infection Microbiology

RECEIVED 08 April 2022
ACCEPTED 18 July 2022
PUBLISHED 08 August 2022

CITATION
Possemiers H, Pollenus E, Prenen F, Knoops S, Koshy P and Van den Steen PE (2022) Experimental malaria-associated acute kidney injury is independent of parasite sequestration and resolves upon antimalarial treatment.
Front. Cell. Infect. Microbiol. 12:915792.
doi: 10.3389/fcimb.2022.915792

Experimental malaria-associated acute kidney injury is independent of parasite sequestration and resolves upon antimalarial treatment

Hendrik Possemiers[1], Emilie Pollenus[1], Fran Prenen[1], Sofie Knoops[1], Priyanka Koshy[2] and Philippe E. Van den Steen[1]*

[1]Laboratory of Immunoparasitology, Department of Microbiology, Immunology and Transplantation, Rega Institute for Medical Research, KU Leuven, KU, Leuven, Belgium, [2]Department of Pathology, University Hospitals Leuven, Leuven, Belgium

Malaria remains a important global disease with more than 200 million cases and 600 000 deaths each year. Malaria-associated acute kidney injury (MAKI) may occur in up to 40% of patients with severe malaria and is associated with increased mortality. Histopathological characteristics of AKI in malaria are acute tubular injury, interstitial nephritis, focal segmental glomerulosclerosis, collapsing glomerulopathy and glomerulonephritis. We observed that C57BL/6 mice infected with *Plasmodium berghei* NK65 (*Pb*NK65) develop MAKI in parallel with malaria-associated acute respiratory distress syndrome (MA-ARDS). MAKI pathology was associated with proteinuria, acute tubular injury and collapse of glomerular capillary tufts, which resolved rapidly after treatment with antimalarial drugs. Importantly, parasite sequestration was not detected in the kidneys in this model. Furthermore, with the use of skeleton binding protein-1 (SBP-1) KO *Pb*NK65 parasites, we found that parasite sequestration in other organs and its subsequent high parasite load are not required for the development of experimental MAKI. Similar proteinuria, histopathological features, and increases in kidney expression of interferon-γ, TNF-α, kidney injury molecule-1 (KIM-1) and heme oxygenase-1 (HO-1) was observed in both infected groups despite a significant difference in parasite load. Taken together, we introduce a model of experimental AKI in malaria with important similarities to AKI in malaria patients. Therefore, this mouse model might be important to further study the pathogenesis of AKI in malaria.

KEYWORDS

malaria, kidney, sequestration, resolution, inflammation

Introduction

Malaria remains a important global disease with more than 200 million clinical cases and 600 000 deaths each year (World Health Organization, 2021). Five different *Plasmodium* species are known to infect humans, with *Plasmodium falciparum* and *Plasmodium vivax* causing most of the infections. Malaria-associated acute kidney injury (MAKI) is a common complication in severe malaria, affecting up to 40% of the adults patients (Koopmans et al., 2015; Conroy et al., 2016). Recent studies also showed the presence of MAKI in 45 to 60% of children with severe malaria (Conroy et al., 2016; Oshomah-Bello et al., 2020). MAKI is associated with increased mortality, which led to case fatality rates up to 75% without appropriate renal replacement therapy (Trang et al., 1992; Conroy et al., 2016). The most important histopathological characteristics of AKI in malaria are acute tubular injury, interstitial nephritis, focal segmental glomerulosclerosis, collapsing glomerulopathy and glomerulonephritis (Nguansangiam et al., 2007; Mishra and Das, 2008; Amoura et al., 2020).

To investigate the pathogenesis of AKI in malaria, several malaria mouse models of AKI have been used in the past. AKI has been described in C57BL/6 mice infected with *Plasmodium berghei* ANKA (*Pb*ANKA) in various studies in parallel with experimental cerebral malaria (ECM) (Abreu et al., 2014; Souza et al., 2015; Silva et al., 2018). AKI pathology in this model was characterized by an increase in plasma concentrations of blood urea nitrogen (BUN) and creatinine, proteinuria, glomerular hypercellularity and increased expression of pro-inflammatory cytokines in the kidney. Similar MAKI pathology was described in BALB/c mice infected with *Pb*ANKA (Elias et al., 2012). In addition, Yashima et al. observed MAKI in NC mice infected with *P. chabaudi* AS (Yashima et al., 2017). This was characterized by mesangial proliferative glomerulonephritis with endothelial damage, proteinuria and the deposition of immunoglobulin G and complement component 3 in mesangium and glomerular capillaries.

Parasite sequestration, which is the binding of infected red blood cells (iRBCs) to endothelial cells (ECs), has been proposed as a potential contributor to AKI pathogenesis in malaria (Katsoulis et al., 2021). Post-mortem studies observed parasite sequestration of *P. falciparum* in glomerular and peritubular capillaries in adults and children with MAKI (Nguansangiam et al., 2007; Milner et al., 2014). Sequestration is mediated by specific parasite adhesins, which are expressed on the surface of the iRBCs. The export of the parasite adhesins to the surface of the iRBCs is mediated by several parasite proteins, including skeleton binding protein-1 (SBP-1) in the Maurer's cleft. SBP-1 is both expressed in human and rodent malaria parasites (De Niz et al., 2016). The export system for the adhesins is relatively conserved but the adhesins mediating sequestration of *P. falciparum* and *P. berghei* are not conserved. The *Plasmodium falciparum* erythrocyte membrane protein-1 (*Pf*EMP-1) adhesins encoded by the *var* genes mediate sequestration of *P. falciparum* parasites (Scherf et al., 2008). These *var* genes are absent in the genome of *P. berghei* and the adhesins mediating sequestration of *P. berghei* are currently not known (Possemiers et al., 2021). De Niz et al. showed that knock-out (KO) of SBP-1 in *Pb*ANKA led to reduced sequestration, the absence of the development of ECM and also a lower parasitemia, consistent with the notion that sequestering parasites avoid splenic clearance (De Niz et al., 2016). Moreover, we showed that SBP-1 KO-mediated parasite sequestration had no influence on the development of experimental MA-ARDS but inhibited the spontaneous resolution of MA-ARDS (Possemiers et al., 2021).

A recent study by Amoura et al. found collapsing focal segmental glomerulosclerosis (FSGS) in 91% of kidney biopsies from malaria patients after successful treatment of malaria (Amoura et al., 2020). In addition, various *P. falciparum* cases with collapsing FSGS were reported (Niang et al., 2008; Kute et al., 2013; Sehar et al., 2015). This shows that malaria may be a new causal factor for secondary FSGS. FSGS is the most common primary glomerular histologic lesion associated with proteinuria and with end-stage renal disease (Bose and Cattran, 2014). The primary form of FSGS is idiopathic and the secondary form includes genetic, virus-associated and drug-induced etiologies (D'Agati et al., 2004; Rosenberg and Kopp, 2017).

In this study, we observed that C57BL/6 mice infected with *Pb*NK65 Edinburgh strain (*Pb*NK65-E) parasites develop AKI in parallel with malaria-associated acute respiratory distress syndrome (MA-ARDS). AKI pathology was associated with increased proteinuria, acute tubular injury and collapse of glomerular capillary tufts, which resolved rapidly after treatment with antimalarial drugs. Furthermore, we investigated the role of sequestration in experimental AKI by using SBP-1 KO *Pb*NK65 parasites, which have a decreased capacity to sequester, in compared to the wildtype (WT) *Pb*NK65 parasites. We did not observe direct parasite sequestration in the kidneys but parasite load was significantly reduced in SBP-1 KO infected mice compared to WT infected mice. However, both infected groups had similar renal histopathological features, similar increased renal expression of interferon-γ (IFN-γ), TNF-α, kidney injury molecule-1 (KIM-1) and heme oxygenase-1 (HO-1) and similar increased proteinuria. These data suggest that parasite sequestration and subsequent high parasite load are not required for the development of experimental AKI.

Materials and methods

Ethical statement

All experiments at the KU Leuven were performed according to the regulations of the European Union (directive 2010/63/EU)

and the Belgian Royal Decree of 29 May 2013, and were approved by the Animal Ethics Committee of the KU Leuven (License LA1210251, project P196/2015 and license LA1210186, project P052/2020, Belgium).

Parasites and mice

Equal numbers of male and female C57BL/6 mice were obtained from Janvier (7–8 weeks old, Le Genest-Saint-Isle, France). All mice were housed in individually ventilated cages in a 12 h light and 12 h dark cycle in SPF animal facility. Drinking water was supplemented with 4-amino benzoic acid (0.422 mg/ml PABA, Sigma-Aldrich, Bornem, Belgium).

For ART + CQ treatment experiments, C57BL/6 mice were infected with *P. berghei* NK65 Edinburgh strain (*Pb*NK65-E) parasites by intraperitoneal (i.p.) injection of 10^4 iRBCs as described previously (Van den Steen et al., 2010). For WT vs. SBP-1 KO experiments, C57BL/6 mice were infected with *P. berghei* NK65 2168cl2 (WT) (Pham et al., 2017) or SBP-1 KO *P. berghei* NK65 2559cl2 (SBP-1 KO) (Possemiers et al., 2021) parasites by i.p. injection of 10^4 iRBCs.

Scoring of disease progression and parasitemia determination

Parasitemia, body weight and clinical score were evaluated daily starting from day 5 post infection (p.i.) in the WT vs. SBP-1 KO experiments and from day 6 p.i. in ART + CQ treatment experiments. Blood smears of tail blood were stained with 10% Giemsa (VWR, Heverlee, Belgium) and parasitemia was calculated by microscopic analysis. The clinical score was calculated by evaluating different clinical parameters including social activity (SA), limb grasping (LG), body tone (BT), trunk curl (TC), pilo-erection (PE), shivering (Sh), abnormal breathing (AB), dehydration (D), incontinence (I) and paralysis (P). A score of 0 (absent) or 1 (present) was given for TC, PE, Sh and AB and 0 (normal), 1 (intermediate) or 2 (most serious) for the other parameters. The total clinical score was calculated using the following formula: SA + LG + BT + TC + PE + 3 * (Sh + AB + D + I + P). In WT vs. SBP-1 KO experiments and ART + CQ treatment experiments mice were euthanized when the body weight decrease was >20% and >25% respectively compared to day 0 p.i. or when clinical score reached 10 or more.

Antimalarial treatment

Where indicated, mice were treated with antimalarial drugs from day 8 p.i. to day 12 p.i. with a combination of artesunate (ART, 10 mg/kg in 0.9% NaCl with 0.1% $NaHCO_3$; Sigma-Aldrich) and chloroquine diphosphate salt (CQ, 30 mg/kg in 0.9% NaCl; Sigma-Aldrich) *via* a daily i.p. injection of 100 µl as described by Pollenus et al. (Pollenus et al., 2021).

Retro-orbital puncture and dissection

In part of the WT vs. SBP-1 KO experiments, mice were anesthetized with 3% isoflurane (Iso-Vet, Dechra, Nortwhich, United Kingdom) before retro-orbital puncture was performed with a heparinized (LEO Pharma, Lier, Belgium) glass capillary tube (Hirschmann-Laborgeräte, Eberstadt, Germany). The collected blood was injected in a cartridge in the Epoc Blood Analysis System (Siemens, Munich, Germany) for biochemical analysis. After the blood collection, mice were euthanized by performing heart puncture under anaesthesia with 3% isoflurane. After a transcardial perfusion with 20 ml PBS the left kidney was removed, laterally cut into two equal pieces and fixed in 4% formaldehyde (Klinipath, Duiven, The Netherlands) for 48 h at 4°C.

In the ART + CQ treatment experiments and part of the WT vs. SBP-1 KO experiments, mice were euthanized with Dolethal (Vétoquinol, Aartselaar, Belgium; 200 mg/mL, i.p. injection of 100 µL) followed by heart puncture at indicated time points. After a transcardial perfusion with 20 ml PBS the left kidney was removed and laterally cut into two equal pieces and fixed in 4% formaldehyde for 48 h at 4°C. In the plasma samples obtained from heart puncture, BUN levels were measured with the Urea Nitrogen (BUN) Colorimetric Detection Kit (Thermo Fisher Scientific Inc., Waltham, MA, USA) for the WT vs. SBP-1 KO experiments.

Analysis of urine samples

Urine samples were collected in a 1.5 mL Eppendorf tube at the indicated time points in the morning. The albumin/creatinine ratio in the urine was determined to assess proteinuria and kidney function as described in Vandermosten et al. (Vandermosten et al., 2018).

Kidney histology

After fixation, kidney tissues were dehydrated by applying gradually increasing ethanol concentrations in the Excelsior MS tissue processor (Thermo Fisher Scientific, Waltham, USA). Next, the tissues were embedded in paraffin with the HistoStar Workstation (Thermo Fisher Scientific) and 5 µm thick tissue sections were made using with Microm HM 355S microtome (Thermo Fisher Scientific). Tissue sections were stained with the Periodic Acid Schiff's (PAS) staining kit (Carl

Roth GmbH, Karlsruhe, Germany). Histological assessment was performed with a Leica DM 2000 microscope. The percentage of collapsed glomeruli and renal blood vessels with intravascular accumulation of one or more leukocytes was calculated on whole sections.

Quantitative reverse transcription-polymerase chain reaction (qRT-PCR)

RNeasy Mini Kit (Qiagen, Hilden, Germany) was used to extract RNA from the kidney after mechanical homogenisation in RLT buffer. After extraction, RNA was quantified and cDNA was synthesized using the High Capacity cDNA Reverse Transcription Kit (Applied Biosystems, Waltham, USA). ABI Prism 7500 Sequence Detection System (Applied Biosystems) was used to perform qRT-PCR reaction on cDNA with specific primers (IDT, Leuven, Belgium, Table 1) in the TaqMan® Fast Universal PCR master mix (Applied Biosystems). The relative mRNA expression was determined as $2^{-\Delta\Delta CT}$, normalized to the mean 2^{-CT} value of the uninfected control mice and to the 2^{-CT} value of the 18S housekeeping gene.

Statistical analysis

Statistical analysis was done using the GraphPad Prism software (GraphPad software, San Diego, USA, version 8.3.1). The non-parametric Mann–Whitney U test was used to determine the statistical significance between two groups. P-values smaller than 0.05 were considered statistically significant. P-values were defined as follows: *p < 0.05, **p < 0.01, ***p < 0.001, ****p < 0.0001. To correct for multiple testing, the Holm-Bonferroni method was applied when 4 or more comparisons were made. Unless otherwise specified, each dot represents the result from an individual mouse. Horizontal lines represent group medians. Asterisks without horizontal lines represent significant differences compared to the control group. Horizontal lines with asterisk on top indicate significant differences between groups.

Results

Malaria-associated acute kidney injury occurs in C57BL/6 mice infected with *Pb*NK65-E parasites and resolves upon antimalarial treatment

We observed that C57BL/6 mice infected with *Pb*NK65-E, a model for experimental MA-ARDS, develop MAKI in parallel with lung pathology. At day 8 post infection (p.i.), proteinuria was observed with a significant increase in albumin/creatinine ratio in the *Pb*NK65-E infected mice compared to the control mice (Figures 1A–C). Furthermore, we studied the effect of antimalarial treatment on MAKI. *Pb*NK65-E infected mice were treated with artesunate and chloroquine (ART + CQ) from day 8 until day 12 p.i. as described by Pollenus et al. (Pollenus et al., 2021). In this model, resolution of MA-ARDS occurs from day 8 p.i. to day 15 p.i., with alveolar edema and clinical score resolving to control level by day 15 p.i (Pollenus et al., 2021). A significant decrease in proteinuria was observed in the treated mice from day 9 p.i. to day 12 p.i. (Figures 1A–C and Supplementary Figure 1). This decrease occurred in parallel with a decrease in clinical score and parasitemia (Figures 1D, E).

We performed Periodic Acid Schiff (PAS) staining on kidney sections of control and *Pb*NK65-E infected mice with and without antimalarial treatment to study the histopathology of experimental MAKI. At day 8 p.i., acute tubular injury was observed with vacuolization and occasional loss of brush border of proximal tubular epithelial cells, which was more pronounced in the cortex of the kidney (Figure 2A). Sclerosis of the glomeruli was also detected, with the collapse of glomerular capillary tufts in <10% of glomeruli (Figures 2A, B and Supplementary Figure 2).

The kidneys of the ART + CQ treated mice showed resolution of the tubular damage in the cortical region with almost no vacuolization and normal brush border of the proximal tubular epithelial cells at day 12 and 19 p.i. (Figure 2A). Moreover, a significant decrease in percentage of collapsed glomerular capillary tufts in the kidneys of the ART + CQ treated mice was observed from day 8 p.i. to day 19 p.i. (Figure 2B). Moreover, increased intravascular accumulation of

TABLE 1 List of primers used for RT-qPCR.

Predesigned qPCR assays (IDT)

Name	Ref Seq	Exon location	Assay ID
18S	NR_003286(1)	Exon 1-1	Hs.PT.39a.22214856.g
HO-1	NM_010442(1)	Exon 3-4	Mm.PT.51.8600055
IFN-γ	NM_008337(1)	Exon 1-2	Mm.PT.58.41769240
KIM-1	NM_001166631(3)	Exon 3-4	Mm.PT.58.43283412
TNF-α	NM_013693(1)	Exon 2-4	Mm.PT.58.12575861

10.3389/fcimb.2022.915792

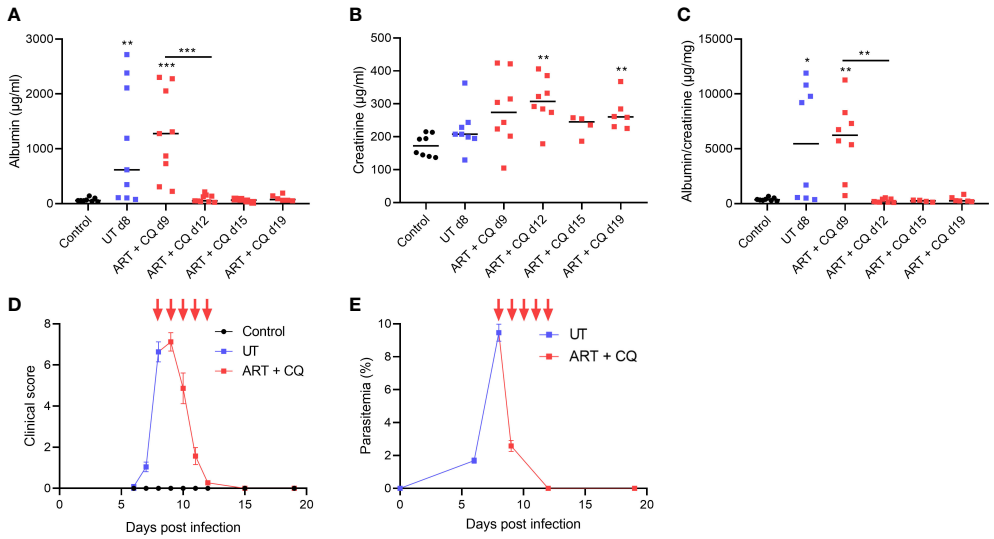

FIGURE 1
Antimalarial treatment decreased proteinuria in *Pb*NK65-E infected mice. C57BL/6 mice were infected with *Pb*NK65-E and were treated daily from day 8 until day 12 p.i. with 10 mg/kg ART + 30 mg/kg CQ (ART+CQ). **(A–C)** Albumin, creatinine and albumin/creatinine ratios in the urine were determined. **(D)** The clinical score was monitored daily from day 6 p.i. onwards, daily ART + CQ treatment indicated with red arrows. **(E)** Peripheral parasitemia was determined on blood smears, daily ART + CQ treatment indicated with red arrows. Asterisks above data points indicate significant differences compared to control mice, asterisks above a horizontal line show significant differences between different time points, *p < 0.05, **p < 0.01, ***p < 0.001. **(A–C)** Data of two experiments, Control: n = 8, untreated *Pb*NK65-E infected mice (UT) d8: n = 8-9, ART+CQ d9-d19: n = 4-9. **(D, E)** Data of two experiments, Control: n = 6, UT/ART+CQ: n = 6-22. Mann-Whitney U test with Holm-Bonferroni correction for multiple testing (number of tests = 6) was performed.

leukocytes was detected in kidneys of *Pb*NK65-E infected mice at day 8 p.i. compared to control mice or ART + CQ treated mice (Figures 3A, B).

Overall, these data suggest that infection of C57BL/6 mice with *Pb*NK65 leads to mild but significant MAKI and that the MAKI pathology is resolved by antimalarial treatment.

SBP-1-mediated sequestration and subsequent high parasite load is dispensable for the development of MAKI

To study the role of whole-body parasite sequestration and subsequent high parasite load on the pathogenesis of experimental AKI, C57BL/6 mice were infected with transgenic WT and SBP-1 KO *Pb*NK65 parasites and the AKI pathology was compared. We previously showed with bioluminescence imaging and RT-qPCR that the SBP-1 KO *Pb*NK65 has a significantly reduced sequestration capacity compared to WT parasites with subsequent reduced parasite load and parasitemia (Possemiers et al., 2021).

The WT clone, which is used in the WT versus SBP-1 KO experiments, was generated from the *Pb*NK65-E line and is characterized by a slightly faster growth than the original *Pb*NK65-E line (Pham et al., 2017). Therefore, parasitemia and pathological symptoms occur 1 day earlier than with the original *Pb*NK65-E line in the above-described experiments. Otherwise, the pathology and disease course are similar. The SBP-1 KO parasites were generated from the WT clone and the effects on disease course and lung pathology were described previously (Possemiers et al., 2021).

Proteinuria was similarly increased in both WT and SBP-1 KO infected mice at day 7 and 8 p.i., when disease symptoms are at their peak. (Figures 4A–C). Parasitemia in the SBP-1 KO infected mice was significantly lower compared to the WT infected mice at day 7 and 8 p.i. (Figure 4E). This suggests that SBP-1 mediated sequestration and parasite load has no influence on proteinuria, as measured by the urinary albumin/creatinine ratio. BUN values were significantly increased in the WT infected mice at day 7 and day 8 p.i. compared to the control mice (Figure 4D). Despite similar proteinuria, a significant difference was observed in the BUN values between WT and SBP-1 KO infected mice at 8 days p.i., which might be related to extrarenal causes (Figure 4D).

AKI pathogenesis is associated with immune cell infiltration and increased cytokine secretion in the renal tissue (Zuk and Bonventre, 2016). Therefore, we measured the expression of inflammatory cytokines in the kidney at mRNA level. The mRNA expression of the inflammatory cytokines IFN-γ and TNF-α was significantly increased in the kidneys of both WT

10.3389/fcimb.2022.915792

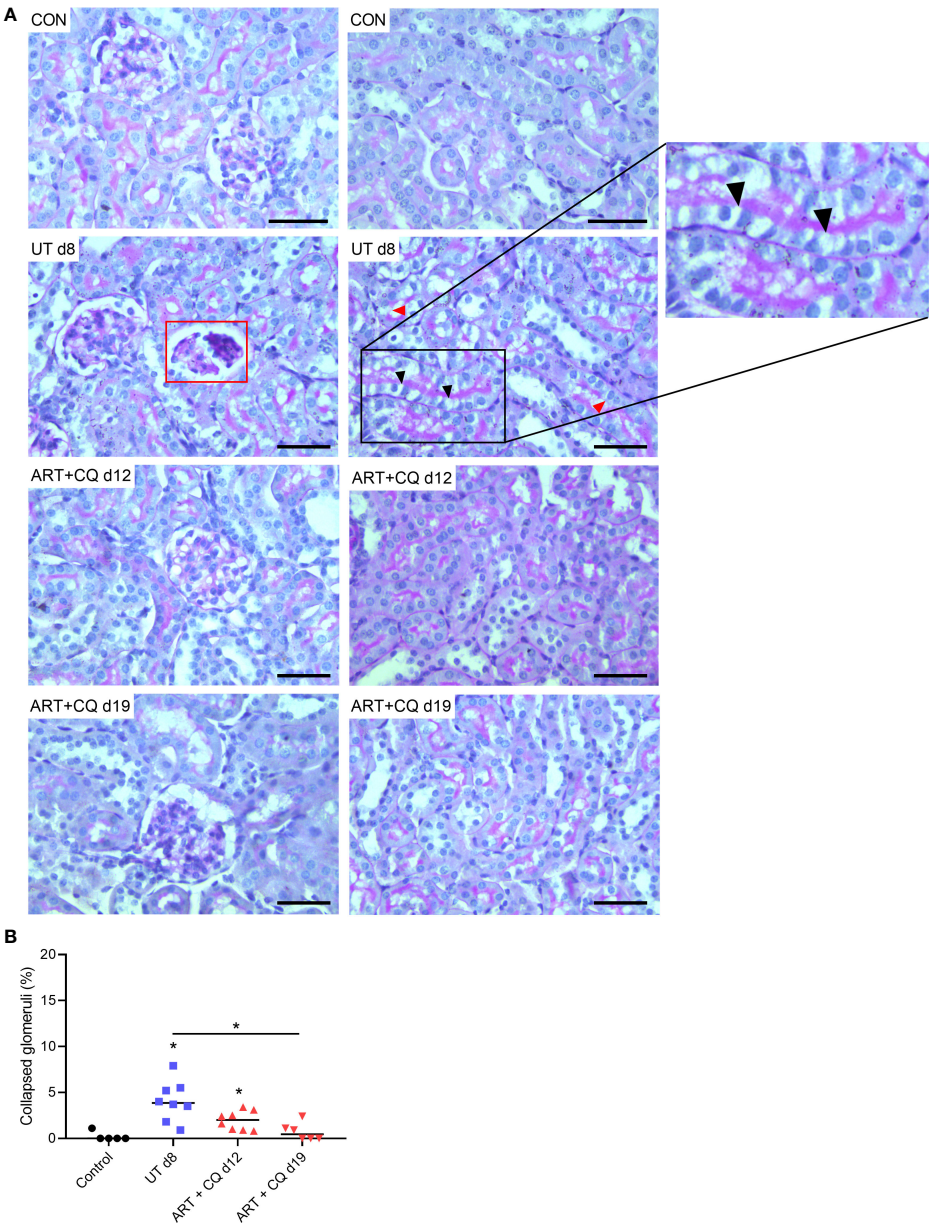

FIGURE 2
Antimalarial treatment decreased tubular injury and collapse of glomerular capillary tuft in kidneys of *Pb*NK65-E infected mice. C57BL/6 mice were infected with *Pb*NK65-E parasites and kidneys were dissected at the indicated times. From day 8 until day 12 p.i., mice were treated daily with antimalarial drugs (ART + CQ). **(A)** Sections were stained with PAS. Representative images are shown (original magnification x40, bar = 50 µm). Red frames indicate collapse of glomerular tufts. Black arrowheads indicate vacuolization of proximal tubular epithelial cells, red arrowheads indicate loss of brush border of proximal tubular epithelial cells. **(B)** Percentage of glomeruli with collapsed glomerular tufts counted on PAS stained kidney sections Asterisks above data points indicate significant differences compared to control mice, asterisks above a horizontal line show significant differences between different time points, *p < 0.05. Data of two experiments, Control: n = 6, untreated *Pb*NK65-E infected mice (UT) d8: n = 8, ART+CQ d12: n = 8, ART+CQ d19: n = 6. Mann-Whitney U test with Holm-Bonferroni correction for multiple testing (number of tests = 6) was performed in panel **(B)**.

and SBP-1 KO infected mice at day 7 and 8 p.i. compared to the control group (Figures 5A, B).

The mRNA expression of KIM-1, a marker of early AKI, was also significantly increased at day 7 and day 8 p.i. in the WT infected mice and at day 7 p.i. in the SBP-1 KO infected mice (Figure 5C). The increase in renal KIM-1 expression was similar in WT and SBP-1 KO infected mice, further suggesting a similar AKI pathology in both infected groups.

The renal mRNA expression of HO-1 was measured, which has anti-inflammatory effects and is protective against kidney

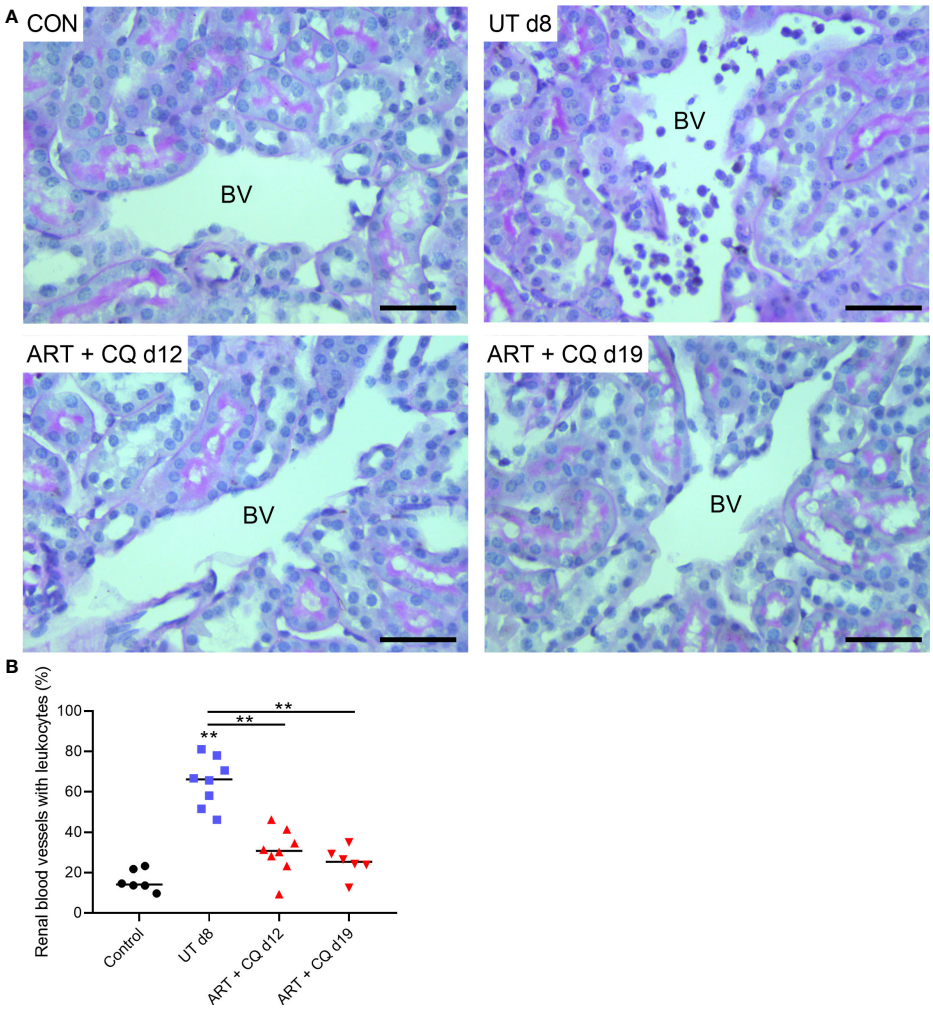

FIGURE 3
Antimalarial treatment decreased intravascular accumulation of leukocytes in kidneys of *Pb*NK65-E infected mice. C57BL/6 mice were infected with *Pb*NK65-E parasites and at day 8 p.i. kidneys were dissected. C57BL/6 mice infected with *Pb*NK65-E were treated from day 8 to day 12 p.i. with antimalarial drugs (ART + CQ) and at day 12 and 19 p.i. mice were dissected. Kidney sections were stained with PAS. **(A)** Representative images are shown (original magnification x40, bar = 50 µm). BV indicates blood vessel on renal section. **(B)** Percentage of renal blood vessels with intravascular accumulation of leukocytes Asterisks above data points indicate significant differences compared to control mice, asterisks above a horizontal line show significant differences between different time points, **p < 0.01. Data of two experiments, Control: n = 6, untreated *Pb*NK65-E infected mice (UT) d8: n = 8, ART+CQ d12: n = 8, ART+CQ d19: n = 6.

injury (Courtney and Maxwell, 2008; Srivastava et al., 2020). We observed in both WT and SBP-1 KO infected mice a significant increase in the renal expression of HO-1 compared to the control group (Figure 5D).

Tubular injury and collapse of glomerular capillary tuft in kidneys of C57BL/6 mice infected with WT and SBP-1 KO *Pb*NK65

We performed PAS staining on kidney sections of control, WT and SBP-1 KO infected mice to study whether parasite sequestration and parasite load had an influence on the histopathology of the experimental MAKI. Acute tubular injury with vacuolization of tubular epithelial cells and loss of the brush border in proximal tubular epithelial cells was present in both WT and SBP-1 KO infected mice (Figure 6A). These observations were more pronounced in the cortex of the kidney. Similar to the *Pb*NK65-E infected mice, glomerulosclerosis was detected with the collapse of some glomerular capillary tufts, in the kidneys of both WT and SBP-1 KO infected mice at day 7 and day 8 p.i. (Figure 6A and Supplementary Figure 3). Between 1 to 15% of the glomeruli were affected in both infected groups, with no significant difference in the percentage of affected glomeruli between WT and SBP-1 KO infected mice (Figure 6B). Parasite sequestration was not detected in

10.3389/fcimb.2022.915792

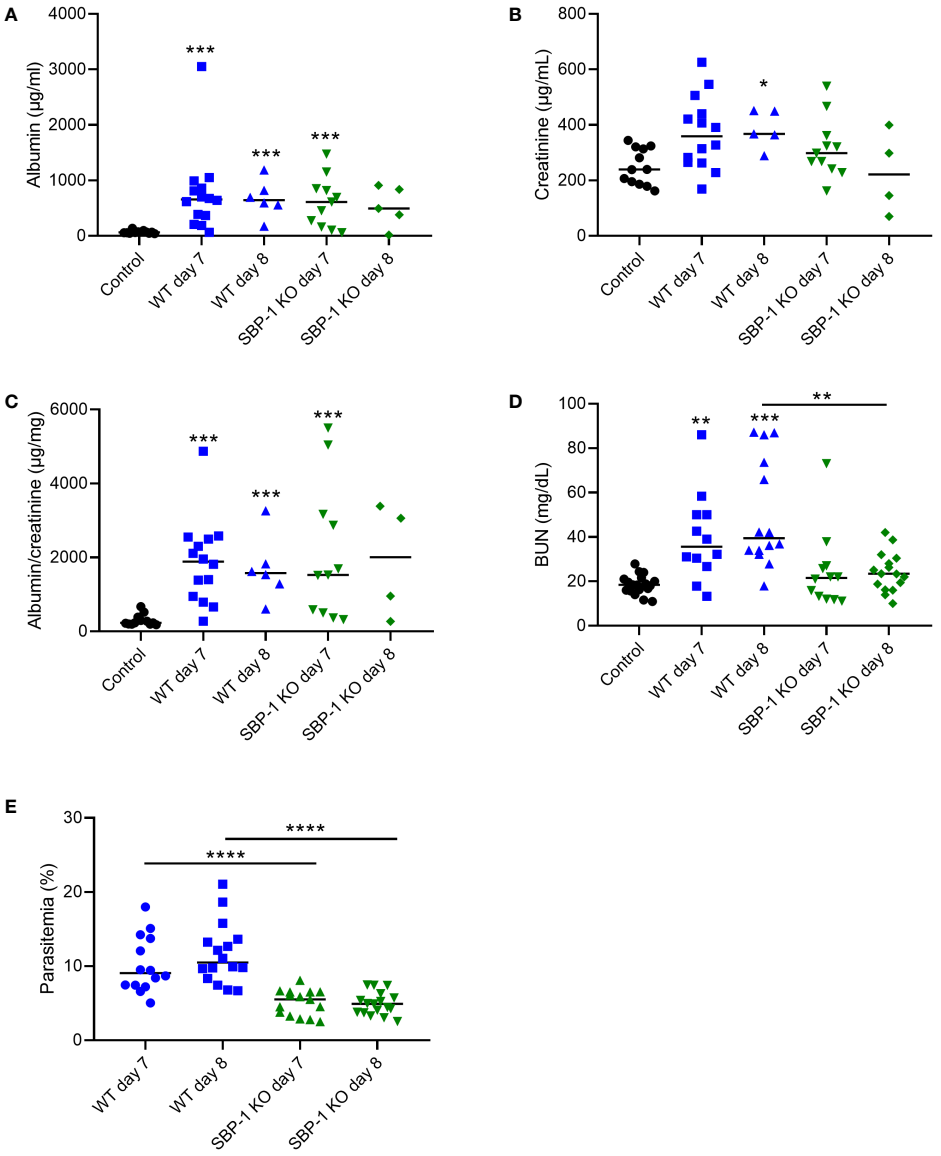

FIGURE 4
Similar proteinuria in WT and SBP-1 KO infected mice. C57BL/6 mice were infected with WT and SBP-1 KO *Pb*NK65 parasites. **(A–C)** Albumin, creatinine and albumin/creatinine ratios were determined in urine samples. **(D)** BUN values were determined in blood collected *via* retro-orbital puncture or in plasma collected *via* heart puncture. **(E)** Peripheral parasitemia was determined on blood smears. Asterisks above data points indicate significant differences compared to control mice, asterisks above a horizontal line show significant differences between infected groups, *p < 0.05, **p < 0.01, ***p < 0.001, ****p < 0.0001. **(A–C)** Data of 4 experiments, Control: n = 12, WT d7-d8: n = 5-14, SBP-1 KO d7-d8: n = 4-11, **(D, E)** data of 8 experiments, Control: n = 18, WT d7-d8: n = 12-16, SBP-1 KO d7-d8: n = 12-17. Mann-Whitney U test with Holm-Bonferroni correction for multiple testing (number of tests = 6) was performed.

glomeruli or tubular blood vessels. We observed intravascular accumulation of leukocytes in the kidneys of WT and SBP-1 KO infected mice (Figures 7A, B). Infiltration of leukocytes in the renal interstitium was not detected.

Overall, these data indicate that SBP-1 mediated sequestration and subsequent high parasite load have no major effect in our experimental model of MAKI. Lower BUN values were detected in SBP-1 KO versus WT-infected mice, suggesting pre-renal effects of sequestration-induced high parasite load.

Discussion

In this study, we describe that MAKI occurs in *Pb*NK65-infected C57BL/6 mice, in parallel with MA-ARDS

10.3389/fcimb.2022.915792

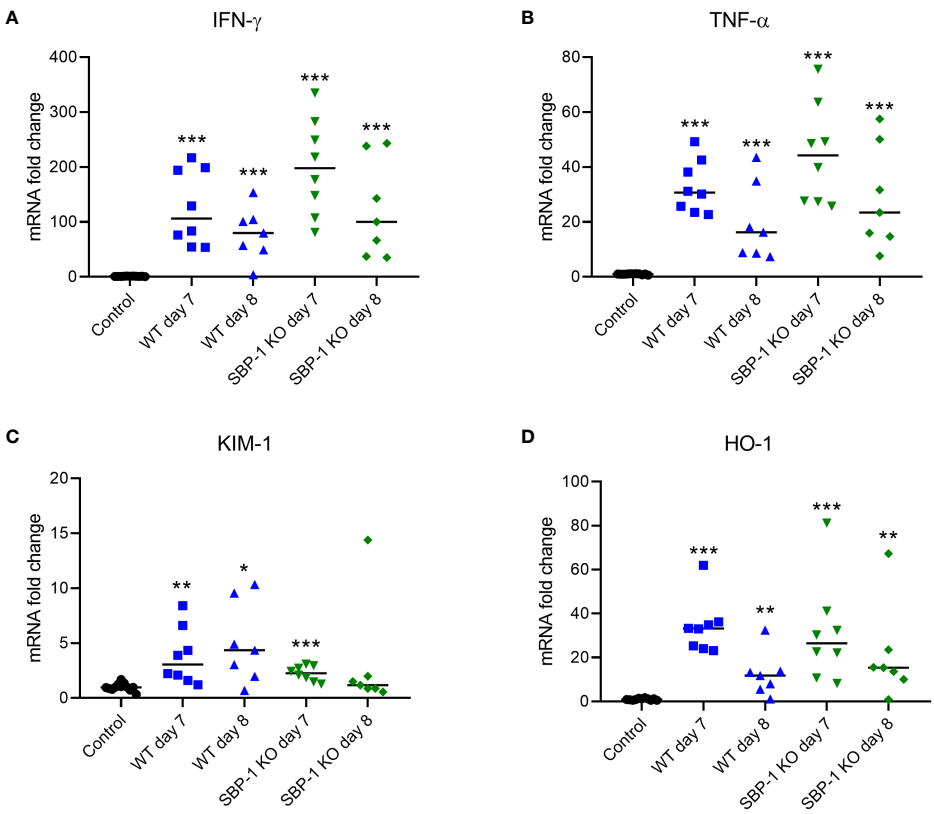

FIGURE 5
Increased expression of inflammatory cytokines, kidney injury molecule-1 and heme oxygenase 1 in kidneys of WT and SBP-1 KO infected mice. C57BL/6 mice were infected with WT and SBP-1 KO *Pb*NK65 parasites and at day 7 and 8 p.i. kidneys were dissected. Kidneys mRNA levels of **(A)** IFN-γ, **(B)** TNF-α, **(C)** KIM-1 and **(D)** HO-1 were measured by qRT-PCR. Asterisks above data points indicate significant differences compared to control mice, asterisks above a horizontal line show significant differences between infected groups ,*p < 0.05, **p < 0.01, ***p < 0.001. Data of 3 experiments, Control: n = 12, WT d7-d8: n = 7-8, SBP-1 KO d7-d8: n = 7-8. Mann-Whitney U test with Holm-Bonferroni correction for multiple testing (number of tests = 6) was performed.

(Van den Steen et al., 2010). These two complications are most likely independent of each other, as MAKI may also occur in mice without MA-ARDS (Elias et al., 2012). MAKI pathology was characterized by vacuolization in the proximal tubular epithelial cells and collapse of glomerular capillary tufts. The collapse of glomerular capillary tufts in our mouse model has similarities with the collapsing focal segmental glomerulosclerosis (FSGS) described in patients infected with *P. falciparum* (Niang et al., 2008; Kute et al., 2013; Sehar et al., 2015; Amoura et al., 2020). However, such collapse was observed in less than 15% of the glomeruli and the tubular epithelial damage was relatively mild, indicating a less severe and/or earlier form of AKI than collapsing FSGS. The glomerular filtration barrier is composed of fenestrated endothelial cells, the glomerular basement membrane and podocytes (Greka and Mundel, 2012; Wen et al., 2018). FSGS is characterized by damage to podocytes, which damages the glomerular filter barrier and leads to proteinuria. This is in accordance with the occurrence of high proteinuria (>1000 μg/mg of albumin/creatinine) in malaria infected mice with AKI, which is suggestive of glomerular pathology.

The ART + CQ treated mice showed rapid decrease in proteinuria and decrease in histopathological features with a significant decrease in the number of collapsed glomerular tufts. These data indicate the resolution of the glomerular damage or glomerulosclerosis and regeneration of glomerular tissue. Similar to these findings, Remuzzi et al. found in an experimental rat model for progressive kidney disease that after 10 weeks of ACE inhibition more than 20% of glomeruli were completely free of sclerosis, whereas before treatment all glomeruli had some degree of sclerosis (Remuzzi et al., 2006). In contrast, Amoura et al. still observed collapsing FSGS in 91% of kidney biopsies after successful treatment of malaria in patients (Amoura et al., 2020). The difference in resolution between our model and the malaria patients might be due to a difference in severity of glomerulosclerosis. Amoura et al. showed that 64% of the glomeruli from the kidney biopsies displayed segmental and sclerotic lesions, a much higher percentage than what we

10.3389/fcimb.2022.915792

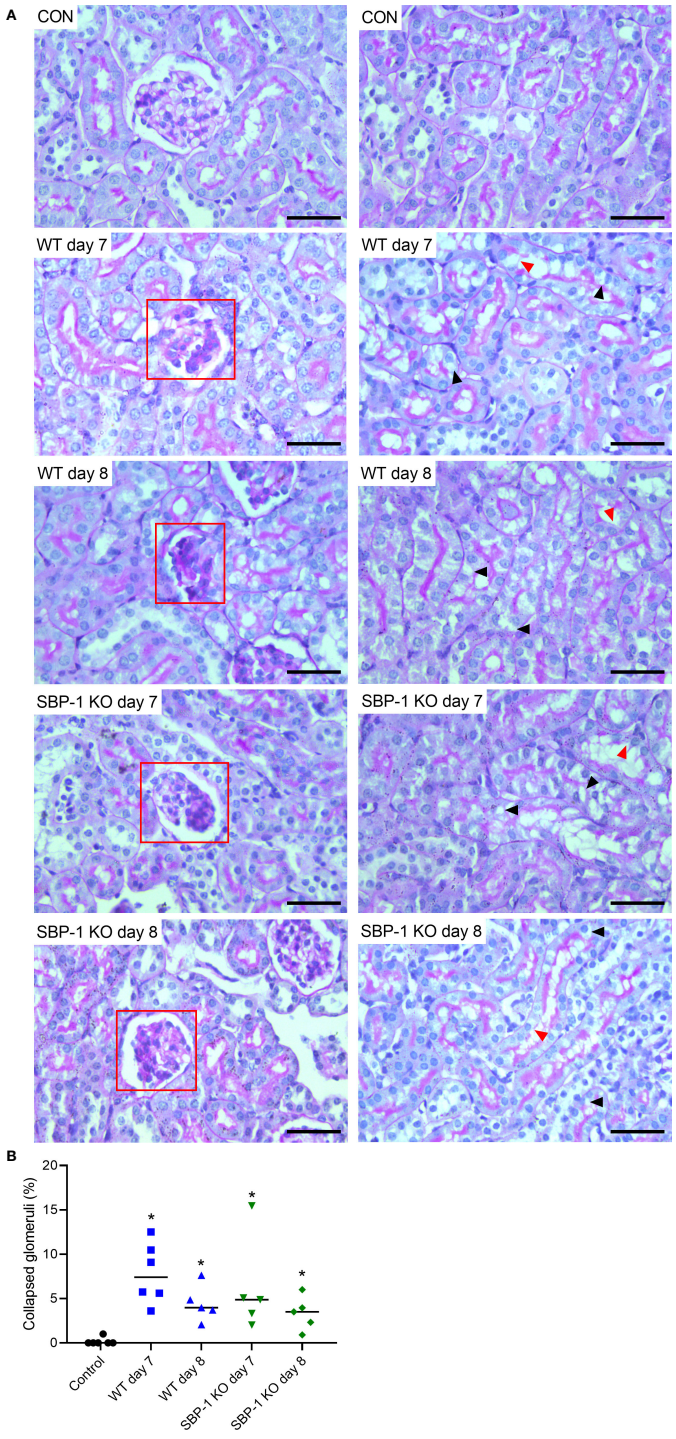

FIGURE 6
Similar tubular injury and collapse of glomerular capillary tuft in kidneys of WT and SBP-1 KO infected mice. C57BL/6 mice were infected with WT and SBP-1 KO *Pb*NK65 parasites and at day 7 and 8 p.i. kidneys were dissected. **(A)** Sections were stained with PAS. Representative images are shown (original magnification x40, bar = 50 µm). Red frames indicate collapse of glomerular tufts. Black arrowheads indicate vacuolization of proximal tubular epithelial cells, red arrowheads indicate loss of brush border of proximal tubular epithelial cells. **(B)** Percentage of glomeruli with collapsed glomerular tufts counted on PAS stained kidney sections Asterisks above data points indicate significant differences compared to control mice, *p < 0.05. Data of two experiments, Control: n = 6, WT d7-d8: n = 5-6, SBP-1 KO d7-d8: n = 5. Mann-Whitney U test with Holm-Bonferroni correction for multiple testing (number of tests = 6) was performed in panel B.

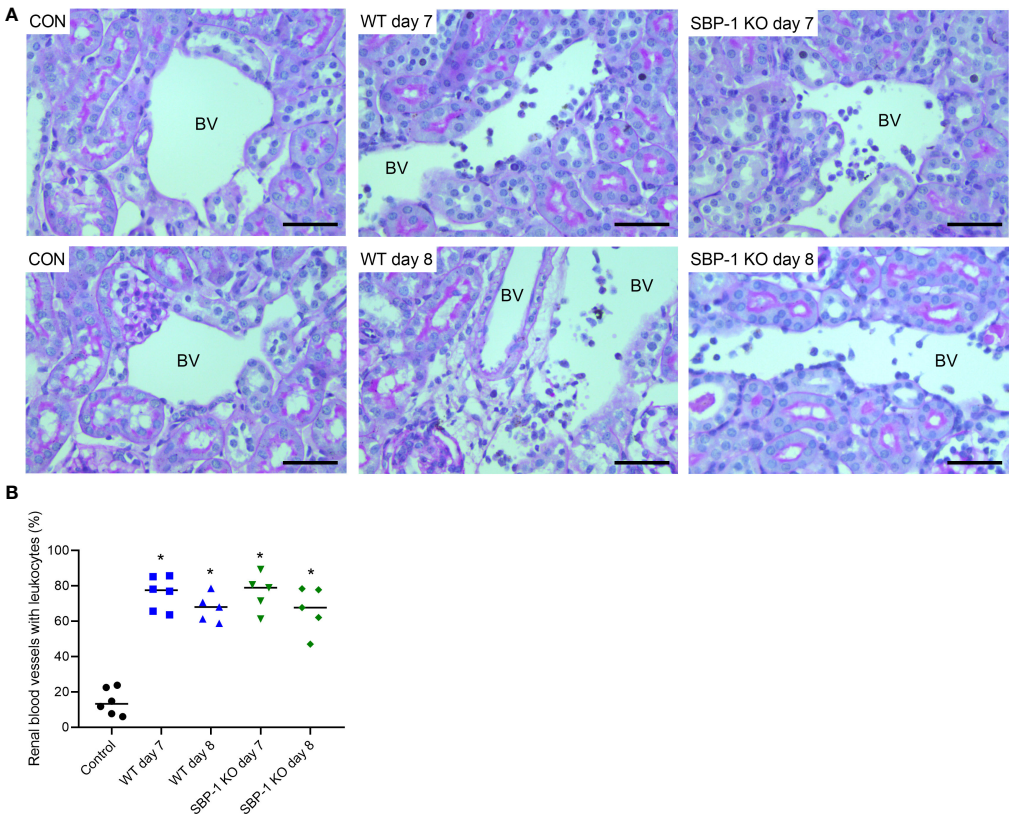

FIGURE 7
Similar intravascular accumulation of leukocytes in the kidneys of WT and SBP-1 KO infected mice. C57BL/6 mice were infected with WT and SBP-1 KO *Pb*NK65 parasites and at day 7 and 8 p.i. kidneys were dissected. Kidney sections were stained with PAS. **(A)** Representative images are shown (original magnification x40, bar = 50 µm). BV indicates blood vessel on renal section. **(B)** Percentage of renal blood vessels with intravascular accumulation of leukocytes Asterisks above data points indicate significant differences compared to control mice, *p < 0.05. Data of two experiments, Control: n = 6, WT d7-d8: n = 5-6, SBP-1 KO d7-d8: n = 5. Mann-Whitney U test with Holm-Bonferroni correction for multiple testing (number of tests = 6) was performed in panel B.

observed in our model (<15%), which suggests more severe glomerulosclerosis in the studied malaria patients. Furthermore, Wharram et al. shows in genetically engineered rats that a threshold of 20% podocyte loss determines whether repair could occur or whether progressive sclerosis develops (Wharram et al., 2005). Therefore, the percentage of affected podocytes may be lower in our MAKI model compared with the malaria patients in the study of Amoura et al. (Amoura et al., 2020).

Tubular vacuolization has been observed in many renal diseases (Christensen and Maunsbach, 1979; Isik et al., 2006; Kambham et al., 2007; Ding et al., 2020). Vacuolization in the cytoplasm may result from accumulation of a variety of substances, such as lipid droplets, water, glycogen and plasma (Morishita et al., 2005; Dickenmann et al., 2008; Declèves et al., 2014). The precise composition and origin of these vacuoles is not yet clear. However, with the PAS staining, which detects carbohydrates, we noticed that these vacuoles did not contain glycogen. Furthermore, proteinuria may lead to damage to tubular epithelial cells, as documented by Wang et al. (Wang et al., 2018). The AKI pathology in our malaria mouse model is also characterized by significant proteinuria. Therefore, the leaking proteins due to the damaged glomerular filter barrier might lead to damage and vacuolization in the tubular epithelial cells in our MAKI model.

Previously, it has been proposed that parasite sequestration in the kidney may play a role in the pathogenesis of AKI in malaria (Katsoulis et al., 2021). In post-mortem studies, sequestration of *P. falciparum* parasites was higher in glomerular and peritubular capillaries of patients with AKI compared to malaria patients without AKI (Nguansangiam et al., 2007). We did not observe renal sequestration in the WT *Pb*NK65 infected mice. This is in accordance with the results of Franke-Fayard et al., who did not detect major parasite accumulation in perfused kidneys of C57BL/6 mice infected with *Pb*ANKA (Franke-Fayard et al., 2005). This suggests that the kidneys are not a major site of sequestration of *P. berghei* parasites. However, sequestration does occur in

other sites, mainly the lungs and umbilical fat tissue and mediate a high parasite load (Franke-Fayard et al., 2005; De Niz et al., 2016; Possemiers et al., 2021). Our data show that the sequestration-mediated high parasite load is dispensable for the occurrence of MAKI.

An important characteristic of AKI pathogenesis is the upregulation of cytokine expression and increased immune cell accumulation and infiltration (Zuk and Bonventre, 2016). In our model, we found a significant increase in the expression of renal IFN-γ and TNF-α. Despite a significant difference in parasite load between WT and SBP-1 KO infected mice, no difference in renal inflammation was observed. We previously observed that parasite sequestration and load had no effect on the induction of lung inflammation in experimental MA-ARDS (Possemiers et al., 2021). In contrast, Plewes et al. observed a significant correlation between parasite load, immune activation and MAKI severity in adult patients with severe falciparum malaria (Plewes et al., 2014).

Surprisingly, BUN levels were significantly different between WT and SBP-1 KO infected mice at day 8 p.i., although proteinuria, renal inflammation and kidney histology were similar in both infected groups. BUN levels are inversely correlated with the decline of kidney function (Seki et al., 2019). However, BUN levels may also be affected by extrarenal factors (Seki et al., 2019). Decreased renal perfusion related to higher parasite load and peripheral sequestration in the WT infected mice may lead to reduction in glomerular filtration rate and increased BUN levels. Moreover, malaria parasites produce high levels of ammonia, which is converted by the liver to urea through the urea cycle (Zeuthen et al., 2006). Therefore, the higher parasite load in the WT infected mice could lead to higher ammonia production by the parasites and may result in increased BUN levels.

The significant transcriptional upregulation of renal HO-1 that we observed in both WT and SBP-1 KO infected mice is important to protect the kidneys from more damage *via* its anti-inflammatory effects. Ramos et al. also found HO-1 mRNA and protein induction in the kidneys of *P. chabaudi* infected C57BL/6 mice and showed that heme catabolism by HO-1 is essential to establish disease tolerance to malaria (Ramos et al., 2019). In contrast, Elias et al. observed a decreased HO-1 expression in kidneys of *Pb*ANKA infected BALB/c mice with AKI (Elias et al., 2012).

Furthermore, we observed that renal KIM-1 mRNA expression was significantly increased in WT and SBP-1 KO infected mice. KIM-1, a transmembrane protein that is expressed in damaged tubular epithelial cells, is widely recognized as an early biomarker of AKI (Bonventre and Yang, 2010; Tian et al., 2017). In accordance with our data, Punsawad et al. detected with immunohistochemical staining a significant increase in KIM-1 expression in proximal tubular cells in all kidney tissues from severe *P. falciparum* malaria patients with AKI (Punsawad and Viriyavejakul, 2017). Various other mouse models of AKI were associated with increased renal KIM-1 expression (Yang et al., 2018; Huang et al., 2020). The renal KIM-1 expression in our malaria mouse model was lower than in cisplatin and LPS induced AKI models. This suggests that the AKI pathology that we observe is less severe and/or at an early stage. This early stage AKI was characterized by intravascular leukocyte accumulation but no leukocyte infiltration in the renal interstitium. Similarly, the majority of patients infected with *P. falciparum* with MAKI showed mainly intravascular localization of leukocytes, only a minority of the patients had a significant mononuclear cell infiltration in the renal interstitium (Nguansangiam et al., 2007). In contrast, Elias *et al.* showed mild mononuclear cell infiltration at day 7 p.i. and pro-inflammatory hypercellularity at day 15 p.i. in the renal interstitium in *Pb*ANKA infected BALB/c mice (Elias et al., 2012).

In conclusion, we describe in this study a model of experimental AKI in malaria with important similarities to AKI in malaria patients. Antimalarial treatment induced the resolution of AKI pathology with significantly decreased proteinuria, tubular injury and collapsing glomerular tufts. Moreover, parasite sequestration and subsequent high parasite load did not affect the AKI pathology.

Data availability statement

The original contributions presented in the study are included in the article/Supplementary Material. Further inquiries can be directed to the corresponding authors.

Ethics statement

The animal study was reviewed and approved by Animal Ethics Committee KU Leuven.

Author contributions

HP, EP, FP, and SK performed the experiments. HP analysed the data. PV and HP conceived the study. PK analysed the histological sections. HP and PV wrote the first drafts of the manuscript. All authors critically read and edited the manuscript. All authors read and approved the final manuscript.

Funding

This work has been supported by the Research Foundation Flanders (F.W.O. Vlaanderen, URL: https://www.fwo.be/)

(Grant No G0C9720N to PV) and the Research Fund (C1 project C16/17/010 to PV) of the KU Leuven (URL: https://www.kuleuven.be/kuleuven/). HP holds an aspirant PhD fellowship of the F.W.O. Vlaanderen. EP is a recipient of the L'Oréal-Unesco Women for Sciences FWO PhD fellowship.

Acknowledgments

The authors thank Prof. B. Sprangers for interesting discussions.

Conflict of interest

The authors declare that the research was conducted in the absence of any commercial or financial relationships that could be construed as a potential conflict of interest.

Publisher's note

All claims expressed in this article are solely those of the authors and do not necessarily represent those of their affiliated organizations, or those of the publisher, the editors and the reviewers. Any product that may be evaluated in this article, or claim that may be made by its manufacturer, is not guaranteed or endorsed by the publisher.

Supplementary material

The Supplementary Material for this article can be found online at: https://www.frontiersin.org/articles/10.3389/fcimb.2022.915792/full#supplementary-material

SUPPLEMENTARY FIGURE 1
Antimalarial treatment decreased proteinuria in PbNK65-E infected mice. C57BL/6 mice were infected with PbNK65-E and were treated daily from day 8 until day 12 p.i. with 10 mg/kg ART + 30 mg/kg CQ (ART+CQ). **(A–C)** Albumin, creatinine and albumin/creatinine ratios in the urine were determined. Asterisks above data points indicate significant differences compared to control mice, asterisks above a horizontal line show significant differences between different time points. Data of two experiments, Control: n = 8, untreated *Pb*NK65-E infected mice (UT) d8: n = 8-9, ART+CQ d9-d19: n = 4-9. Mann-Whitney U test with Holm-Bonferroni correction for multiple testing (number of tests = 6) was performed.

SUPPLEMENTARY FIGURE 2
Antimalarial treatment decreased collapse of glomerular capillary tuft in kidneys of PbNK65-E infected mice. C57BL/6 mice were infected with PbNK65-E parasites and kidneys were dissected at the indicated times. From day 8 p.i., mice were treated daily with antimalarial drugs (ART + CQ). Sections were stained with PAS. Representative images are shown (original magnification x20, bar = 100 µm). Red frames indicate collapse of glomerular tufts. Data of two experiments, Control: n = 6, untreated PbNK65-E infected mice (UT) d8: n = 8, ART+CQ d12: n = 8, ART+CQ d19: n = 6.

SUPPLEMENTARY FIGURE 3
Similar collapse of glomerular capillary tuft in kidneys of WT and SBP-1 KO infected mice. C57BL/6 mice were infected with WT and SBP-1 KO *Pb*NK65 parasites and at day 7 and 8 p.i. kidneys were dissected. Sections were stained with PAS. Representative images are shown (original magnification x20, bar = 100 µm). Red frames indicate collapse of glomerular tufts. Data of two experiments, Control: n = 6, WT d7-d8: n = 5-6, SBP-1 KO d7-d8: n = 5.

References

Abreu, T. P., Silva, L. S., Takiya, C. M., Souza, M. C., Henriques, M. G., Pinheiro, A. A. S., et al. (2014). Mice rescued from severe malaria are protected against renal injury during a second kidney insult. *PLoS One* 9 (4), e93634. doi: 10.1371/journal.pone.0093634

Amoura, A., Moktefi, A., Halfon, M., Karras, A., Rafat, C., Gibier, J. B., et al. (2020). Malaria, collapsing glomerulopathy, and focal and segmental glomerulosclerosis. *Clin. J. Am. Soc. Nephrol.* 15 (7), 964–972. doi: 10.2215/CJN.00590120

Bonventre, J. V., and Yang, L. (2010). Kidney injury molecule-1. *Curr. Opin. Crit. Care* 16 (6), 556–561. doi: 10.1097/MCC.0b013e32834008d3

Bose, B., and Cattran, D. (2014). Glomerular diseases: FSGS. *Clin. J. Am. Soc. Nephrol.* 9 (3), 626–632. doi: 10.2215/CJN.05810513

Christensen, E. I., and Maunsbach, A. B. (1979). Effects of dextran on lysosomal ultrastructure and protein digestion in renal proximal tubule. *Kidney Int.* 16 (3), 301–311. doi: 10.1038/ki.1979.132

Conroy, A. L., Hawkes, M., Elphinstone, R. E., Morgan, C., Hermann, L., Barker, K. R., et al. (2016). Acute kidney injury is common in pediatric severe malaria and is associated with increased mortality. *Open Forum Infect. Dis.* 3 (2), 1–9. doi: 10.1093/ofid/ofw046

Courtney, A. E., and Maxwell, A. P. (2008). Heme oxygenase 1: Does it have a role in renal cytoprotection? *Am. J. Kidney Dis.* 51 (4), 678–690. doi: 10.1053/j.ajkd.2007.11.033

D'Agati, V. D., Fogo, A. B., Bruijn, J. A., and Jennette, J. C. (2004). Pathologic classification of focal segmental glomerulosclerosis: A working proposal. *Am. J. Kidney Dis.* 43 (2), 368–382. doi: 10.1053/j.ajkd.2003.10.024

Declèves, A. E., Zolkipli, Z., Satriano, J., Wang, L., Nakayama, T., Rogac, M., et al. (2014). Regulation of lipid accumulation by AMK-activated kinase in high fat diet-induced kidney injury. *Kidney Int.* 85 (3), 611–623. doi: 10.1038/ki.2013.462

De Niz, M., Ullrich, A., Heiber, A., Soares, A. B., Pick, C., Lyck, R., et al. (2016). The machinery underlying malaria parasite virulence is conserved between rodent and human malaria parasites. *Nat. Commun.* 7, 1–12. doi: 10.1038/ncomms11659

Dickenmann, M., Oettl, T., and Mihatsch, M. J. (2008). Osmotic nephrosis: Acute kidney injury with accumulation of proximal tubular lysosomes due to administration of exogenous solutes. *Am. J. Kidney Dis.* 51 (3), 491–503. doi: 10.1053/j.ajkd.2007.10.044

Ding, L., Li, L., Liu, S., Bao, X., Dickman, K. G., Sell, S. S., et al. (2020). Proximal tubular vacuolization and hypersensitivity to drug-induced nephrotoxicity in male mice with decreased expression of the NADPH-cytochrome P450 reductase. *Toxicol. Sci.* 173 (2), 362–372. doi: 10.1093/toxsci/kfz225

Elias, R. M., Correa-Costa, M., Barreto, C. R., Silva, R. C., Hayashida, C. Y., Castoldi, Â, et al. (2012). Oxidative stress and modification of renal vascular permeability are associated with acute kidney injury during p. *berghei ANKA Infection. PLoS One* 7 (8), e44004. doi: 10.1371/journal.pone.0044004

Franke-Fayard, B., Janse, C. J., Cunha-Rodrigues, M., Ramesar, J., Büscher, P., Que, I., et al. (2005). Murine malaria parasite sequestration: CD36 is the major receptor, but cerebral pathology is unlinked to sequestration. *Proc. Natl. Acad. Sci. U.S.A.* 102 (32), 11468–11473. doi: 10.1073/pnas.0503386102

Greka, A., and Mundel, P. (2012). Cell biology and pathology of podocytes. *Annu. Rev. Physiol.* 74, 299–323. doi: 10.1146/annurev-physiol-020911-153238

Huang, G., Bao, J., Shao, X., Zhou, W., Wu, B., Ni, Z., et al. (2020). Inhibiting pannexin-1 alleviates sepsis-induced acute kidney injury *via* decreasing NLRP3 inflammasome activation and cell apoptosis. *Life Sci.* 254, 117791. doi: 10.1016/j.lfs.2020.117791

Isik, B., Bayrak, R., Akcay, A., and Sogut, S. (2006). Erdosteine against acetaminophen induced renal toxicity. *Mol. Cell Biochem.* 287 (1–2), 185–191. doi: 10.1007/s11010-005-9110-6

Kambham, N., Nagarajan, S., Shah, S., Li, L., Salvatierra, O., and Sarwal, M. M. (2007). A novel, semiquantitative, clinically correlated calcineurin inhibitor toxicity score for renal allograft biopsies. *Clin. J. Am. Soc. Nephrol.* 2 (1), 135–142. doi: 10.2215/CJN.01320406

Katsoulis, O., Georgiadou, A., and Cunnington, A. J. (2021). Immunopathology of acute kidney injury in severe malaria. *Front. Immunol.* 12. doi: 10.3389/fimmu.2021.651739

Koopmans, L. C., Van Wolfswinkel, M. E., Hesselink, D. A., Hoorn, E. J., Koelewijn, R., Van Hellemond, J. J., et al. (2015). Acute kidney injury in imported plasmodium falciparum malaria. *Malar J.* 14 (1), 1–7. doi: 10.1186/s12936-015-1057-9

Kute, V. B., Trivedi, H. L., Vanikar, A. V., Shah, P. R., Gumber, M. R., and Kanodia, K. V. (2013). Collapsing glomerulopathy and hemolytic uremic syndrome associated with falciparum malaria: Completely reversible acute kidney injury. *J. Parasit Dis.* 37 (2), 286–290. doi: 10.1007/s12639-012-0164-6

Milner, D. A., Whitten, R. O., Kamiza, S., Carr, R., Liomba, G., Dzamalala, C., et al. (2014). The systemic pathology of cerebral malaria in African children. *Front. Cell Infect. Microbiol.* 4. doi: 10.3389/fcimb.2014.00104

Mishra, S. K., and Das, B. S. (2008). Malaria and acute kidney injury. *Semin. Nephrol.* 28 (4), 395–408. doi: 10.1016/j.semnephrol.2008.04.007

Morishita, Y., Matsuzaki, T., Hara-chikuma, M., Andoo, A., Shimono, M., Matsuki, A., et al. (2005). Disruption of aquaporin-11 produces polycystic kidneys following vacuolization of the proximal tubule. *Mol. Cell Biol.* 25 (17), 7770–7779. doi: 10.1128/mcb.25.17.7770-7779.2005

Nguansangiam, S., Day, N. P. J., Hien, T. T., Mai, N. T. H., Chaisri, U., Riganti, M., et al. (2007). A quantitative ultrastructural study of renal pathology in fatal plasmodium falciparum malaria. *Trop. Med. Int. Heal.* 12 (9), 1037–1050. doi: 10.1111/j.1365-3156.2007.01881.x

Niang, A., Niang, S. E., Ka, E. H. F., Ka, M. M., and Diouf, B. (2008). Collapsing glomerulopathy and haemophagocytic syndrome related to malaria: A case report. *Nephrol. Dial Transplant.* 23 (10), 3359–3361. doi: 10.1093/ndt/gfn427

Oshomah-Bello, E. O., Esezobor, C. I., Solarin, A. U., and Njokanma, F. O. (2020). Acute kidney injury in children with severe malaria is common and associated with adverse hospital outcomes. *J. Trop. Pediatr.* 66 (2), 218–225. doi: 10.1093/tropej/fmz057

Pham, T.-T., Verheijen, M., Vandermosten, L., Deroost, K., Knoops, S., Van den Eynde, K., et al. (2017). Pathogenic CD8+ T cells cause increased levels of VEGF-a in experimental malaria-associated acute respiratory distress syndrome, but therapeutic VEGFR inhibition is not effective. *Front. Cell Infect. Microbiol.* 7. doi: 10.3389/fcimb.2017.00416

Plewes, K., Royakkers, A. A., Hanson, J., Hasan, M. M. U., Alam, S., Ghose, A., et al. (2014). Correlation of biomarkers for parasite burden and immune activation with acute kidney injury in severe falciparum malaria. *Malar J.* 13 (1), 1–10. doi: 10.1186/1475-2875-13-91

Pollenus, E., Pham, T. T., Vandermosten, L., Possemiers, H., Knoops, S., Opdenakker, G., et al. (2021). CCR2 is dispensable for disease resolution but required for the restoration of leukocyte homeostasis upon experimental malaria-associated acute respiratory distress syndrome. *Front. Immunol.* 11. doi: 10.3389/fimmu.2020.628643

Possemiers, H., Pham, T. T., Coens, M., Pollenus, E., Knoops, S., Noppen, S., et al. (2021). Skeleton binding protein-1-mediated parasite sequestration inhibits spontaneous resolution of malaria-associated acute respiratory distress syndrome. *PLoS Pathog.* 17 (11), e1010114. doi: 10.1371/journal.ppat.1010114

Punsawad, C., and Viriyavejakul, P. (2017). Increased expression of kidney injury molecule-1 and matrix metalloproteinase-3 in severe plasmodium falciparum malaria with acute kidney injury. *Int. J. Clin. Exp. Pathol.* 10 (7), 7856–7864.

Ramos, S., Carlos, A. R., Sundaram, B., Jeney, V., Ribeiro, A., Gozzelino, R., et al. (2019). Renal control of disease tolerance to malaria. *Proc. Natl. Acad. Sci. U.S.A.* 116 (12), 5681–5686. doi: 10.1073/pnas.1822024116

Remuzzi, A., Gagliardini, E., Sangalli, F., Bonomelli, M., Piccinelli, M., Benigni, A., et al. (2006). ACE inhibition reduces glomerulosclerosis and regenerates glomerular tissue in a model of progressive renal disease. *Kidney Int.* 69 (7), 1124–1130. doi: 10.1038/sj.ki.5000060

Rosenberg, A. Z., and Kopp, J. B. (2017). Focal segmental glomerulosclerosis. *Clin. J. Am. Soc. Nephrol.* 12 (3), 502–517. doi: 10.2215/CJN.05960616

Scherf, A., Lopez-Rubio, J. J., and Riviere, L. (2008). Antigenic variation in plasmodium falciparum. *Annu. Rev. Microbiol.* 62, 445–470. doi: 10.1007/978-3-319-20819-0_3

Sehar, N., Gobran, E., and Elsayegh, S. (2015). Collapsing focal segmental glomerulosclerosis in a patient with acute malaria. *Case Rep. Med.* 2015, 420459. doi: 10.1155/2015/420459

Seki, M., Nakayama, M., Sakoh, T., Yoshitomi, R., Fukui, A., Katafuchi, E., et al. (2019). Blood urea nitrogen is independently associated with renal outcomes in Japanese patients with stage 3-5 chronic kidney disease: A prospective observational study. *BMC Nephrol.* 20 (1), 1–10. doi: 10.1186/s12882-019-1306-1

Silva, L. S., Peruchetti, D. B., Silva-Aguiar, R. P., Abreu, T. P., Dal-Cheri, B. K. A., Takiya, C. M., et al. (2018). The angiotensin II/AT1 receptor pathway mediates malaria-induced acute kidney injury. *PLoS One* 13 (9), 7–9. doi: 10.1371/journal.pone.0203836

Souza, M. C., Silva, J. D., Pádua, T. A., Torres, N. D., Antunes, M. A., Xisto, D. G., et al. (2015). Mesenchymal stromal cell therapy attenuated lung and kidney injury but not brain damage in experimental cerebral malaria. *Stem Cell Res. Ther.* 6 (1), 1–15. doi: 10.1186/s13287-015-0093-2

Srivastava, R. K., Muzaffar, S., Khan, J., Traylor, A. M., Zmijewski, J. W., Curtis, L. M., et al. (2020). Protective role of HO-1 against acute kidney injury caused by cutaneous exposure to arsenicals. *Ann. N Y Acad. Sci.* 1480 (1), 155–169. doi: 10.1111/nyas.14475

Tian, L., Shao, X., Xie, Y., Wang, Q., Che, X., Zhang, M., et al. (2017). Kidney injury molecule-1 is elevated in nephropathy and mediates macrophage activation *via* the mapk signalling pathway. *Cell Physiol. Biochem.* 41 (2), 769–783. doi: 10.1159/000458737

Trang, T., Phu, N. H., Vinh, H., Hien, T. T., Cuong, B. M., Chau, T. T., et al. (1992). Acute renal failure in patients with severe falciparum malaria. *Clin. Infect. Dis.* 15 (5), 874–880. doi: 10.1093/clind/15.5.874

Van den Steen, P. E., Geurts, N., Deroost, K., Van Aelst, I., Verhenne, S., Heremans, H., et al. (2010). Immunopathology and dexamethasone therapy in a new model for malaria-associated acute respiratory distress syndrome. *Am. J. Respir. Crit. Care Med.* 181 (9), 957–968. doi: 10.1164/rccm.200905-0786OC

Vandermosten, L., Pham, T. T., Knoops, S., De Geest, C., Lays, N., van der Molen, K., et al. (2018). Adrenal hormones mediate disease tolerance in malaria. *Nat. Commun.* 9 (1), 4525. doi: 10.1038/s41467-018-06986-5

Wang, S., Pan, Q., Xu, C., Li, J. J., Tang, H. X., Zou, T., et al. (2018). Massive proteinuria-induced injury of tubular epithelial cells in nephrotic syndrome is not exacerbated by furosemide. *Cell Physiol. Biochem.* 45 (4), 1700–1706. doi: 10.1159/000487776

Wen, Y., Shah, S., and Campbell, K. N. (2018). Molecular mechanisms of proteinuria in focal segmental glomerulosclerosis. *Front. Med.* 5. doi: 10.3389/fmed.2018.00098

Wharram, B. L., Goyal, M., Wiggins, J. E., Sanden, S. K., Hussain, S., Filipiak, W. E., et al. (2005). Podocyte depletion causes glomerulosclerosis: Diphtheria toxin-induced podocyte depletion in rats expressing human diphtheria toxin receptor transgene. *J. Am. Soc. Nephrol.* 16 (10), 2941–2952. doi: 10.1681/ASN.2005010055

World Health Organization (2021). (Geneva: World Health Organization)

Yang, Y., Yu, X., Zhang, Y., Ding, G., Zhu, C., Huang, S., et al. (2018). Hypoxia-inducible factor prolyl hydroxylase inhibitor roxadustat (FG-4592) protects against cisplatin-induced acute kidney injury. *Clin. Sci.* 132 (7), 825–838. doi: 10.1042/CS20171625

Yashima, A., Mizuno, M., Yuzawa, Y., Shimada, K., Suzuki, N., Tawada, H., et al. (2017). Mesangial proliferative glomerulonephritis in murine malaria parasite, plasmodium chabaudi AS, infected NC mice. *Clin. Exp. Nephrol.* 21 (4), 589–596. doi: 10.1007/s10157-016-1339-8

Zeuthen, T., Wu, B., Pavlovic-Djuranovic, S., Holm, L. M., Uzcategui, N. L., Duszenko, M., et al. (2006). Ammonia permeability of the aquaglyceroporins from plasmodium falciparum, toxoplasma gondii and trypansoma brucei. *Mol. Microbiol.* 61 (6), 1598–1608. doi: 10.1111/j.1365-2958.2006.05325.x

Zuk, A., and Bonventre, J. V. (2016). Acute kidney injury. *Annu. Rev. Med.* 67, 293–307. doi: 10.1146/annurev-med-050214-013407

Advantages of publishing in Frontiers

OPEN ACCESS
Articles are free to read for greatest visibility and readership

FAST PUBLICATION
Around 90 days from submission to decision

HIGH QUALITY PEER-REVIEW
Rigorous, collaborative, and constructive peer-review

TRANSPARENT PEER-REVIEW
Editors and reviewers acknowledged by name on published articles

Frontiers
Avenue du Tribunal-Fédéral 34
1005 Lausanne | Switzerland

Visit us: www.frontiersin.org
Contact us: frontiersin.org/about/contact

REPRODUCIBILITY OF RESEARCH
Support open data and methods to enhance research reproducibility

DIGITAL PUBLISHING
Articles designed for optimal readership across devices

FOLLOW US
@frontiersin

IMPACT METRICS
Advanced article metrics track visibility across digital media

EXTENSIVE PROMOTION
Marketing and promotion of impactful research

LOOP RESEARCH NETWORK
Our network increases your article's readership